

DISS. ETH Nr. 24424

Investigating the Chemistry and Biology of Danicalipin A and its Analogs

A thesis submitted to attain the degree

DOCTOR OF SCIENCES of ETH ZURICH

(Dr. sc. ETH Zurich)

presented by

JOHANNES BOSHKOW

Master of Science Chemistry ETH Zurich

born 11.04.1989

citizen of Germany

accepted on the recommendation of

Prof. Dr. Erick M. Carreira, examiner

Prof. Dr. Antonio Togni, co-examiner

2017

Acknowledgements

I am grateful to my supervisor ERICK M. CARREIRA for giving me the opportunity to work on these fascinating projects. His support and advice guided me through my doctoral studies and his constructive feedback helped me grow.

I would also like to thank my co-examiner ANTONIO TOGNI. Not only were his insights crucial to this thesis, he was also an important help during the last months of my doctoral studies.

The other members of the chlorosulfolipid team, STEFAN FISCHER, ADRIAN M. BAILEY, and SUSANNE WOLFRUM deserve a big “Thank you!”. The fruitful collaboration was only possible because of their valuable insights and hard work. I have really enjoyed working with them.

For their work on correcting this thesis, I would like to thank the above mentioned as well, but also MARCO BRANDSTÄTTER, ROBERT GILLESPIE, NICOLE HAUSER, MICHAEL IMHOF, ALBERTO KRAVINA, SIMON RÖSSLER, MICHAEL SCHNEIDER, ANDREJ SHEMET, PHILIPP SONDERMANN, MATTHIAS WESTPHAL, and HELENE WOLLEB. Their valuable input was vital to writing this thesis.

All of my students which I was allowed to supervise during my doctoral studies, EVA GLEISSNER, LEONARDO NANNINI, ARMIN SALIHOVIC and NIELS SIEVERTSEN, have to be thanked as well. It was a lot of fun working with you!

The CARREIRA GROUP as a whole, former and current members, has to be thanked for the pleasant working environment, the quick help with any encountered problems, the interesting discussions, and their general support in any situation.

A special thanks needs to go to STEFAN A. RUIDER. Especially in the beginning, his presence and input was incredibly helpful. But also after work or during our free time, I really appreciated having him as a friend.

My other labmates, RICCARDO CRIBIU, CORALIE DUCHEMIN, MAYUKO ISOMURA, MICHAEL SCHNEIDER, and RAFFAEL VORBERG certainly deserve my gratitude. Their positive attitudes, general openness, and ability to joke about anything made G330 a very funny and relaxed place to work.

Although I technically thanked all of them already, I would like to specifically thank, MARCO BRANDSTÄTTER, SIMON BREITLER, ERIK DA FUNDER, CHRISTIAN EBNER, STEFAN FISCHER, ROBERT GILLESPIE, NICOLE HAUSER, NIKOLAS HUWLYER, MICHAEL IMHOF, MATHIAS JACOBSON, ADRIEN JOLITON, LEONARDO NANNINI, TOBIAS SANDMEIER, MICHAEL SCHAFROTH, YESHUA SEMPERE, ANDREJ SHEMET, PHILIPP SONDERMANN, MATTHIAS WESTPHAL, BERND WOLFSTÄDTER, and HANNES ZIPFEL for all the fun that we had outside of the lab, eating, drinking, hiking, running, and skiing. All those trips were awesome!

For similar activities, I would like to thank all the members of the DIEDERICH GROUP, especially ELKE BRODBECK, CAGATAY DENGIZ, RAOUL DE GASPARO, CORNELIUS GROPP, NICOLAS KERISIT, BIRGIT LAUBER, TRISTAN REEKIE, CÉDRIC SCHAACK, GEOFFREY SCHWERTZ, and MICHAL TICHY. Good times.

Natürlich muss ich mich bei meinen Freunden JULIAN BLEICH, LUKAS BRAUN, DAVID HAHN, SEBASTIAN HARTWEG, KATHARINA KELLER, CARL PHILIPP ROSENAU und ERIK SCHRADER bedanken. Für nichts. Und für die fragwürdige Unterstützung in schwierigen Zeiten und ausreichend Ablenkung, wann auch immer ich welche brauchte.

Bei meinen Freunden ANNA BELTZUNG, VICTORIA CUSTODIS, LISA KAMBER, TOBIAS KÜMIN, KRIS MEIER, FRANZISKA REUST, GIN-WEI TRINH und ANNA WIEGAND möchte ich mich für den ganzen Spass ausserhalb der ETH bedanken. Wo auch immer wir uns getroffen haben.

ADRIAN HERRMANN verdient ein besonderes Dankeschön für die tolle Zeit, die wir zusammen verbracht haben. Meistens irgendwo draussen, aber auch drinnen war er sehr unterhaltsam. JULIA BARTH, MICHAEL MATSCHINER und JOSH SHARPE möchte ich für die Outdoorabenteuer danken, die wir erlebt haben.

Meinen Eltern ANTJE und MARCUS BOSHKOW bin ich unglaublich dankbar für alles, was sie für mich getan haben. Ausserdem will ich mich auch bei allen meinen Verwandten, besonders meinen Grosseltern, für ihre Unterstützung bedanken. Ohne euch wäre das alles nicht möglich gewesen.

Ich würde mich auch gerne bei ELISABETH und ROGER RIWAR, aber auch bei ROMAN-PASCAL RIWAR bedanken für die schönen Abende und Tage, die wir hatten.

Am allermeisten will ich mich aber bei meiner Freundin LESLIE-JOANA RIWAR bedanken! Für alles. Ich kann nicht in Worte fassen, wie wichtig es war, sie bei jedem Schritt dabei zu haben und wie sehr sie mir bei absolut allem geholfen hat.

Publications

J. Boshkow,[†] S. Fischer,[†] A. M. Bailey, S. Wolfrum, E. M. Carreira

“Stereochemistry and Biological Activity of Chlorinated Lipids: A Study of Danicalipin A and Selected Diastereomers”

Chem. Sci. **2017**, *8*, 6904-6910

Poster Presentations

J. Boshkow, S. Fischer, A. Bailey, S. Wolfrum, E. M. Carreira

“Danicalipin A – A Study on the Conformation and Biology of Diastereomers Enabled by Computation and Synthesis”

Workshop of the Competence Center for Computational Chemistry (C4)
at IBM Rüschlikon, January 2017

J. Boshkow, S. Fischer, A. Bailey, S. Wolfrum, E. M. Carreira

“Stereochemical Study of Chlorinated Lipids and the Impact of Configuration on Biological Activity”

Symposium by the Stipendienfonds der Schweizerischen Chemischen Industrie (SSCI)
at ETH Zurich, January 2017

Table of Contents

<i>Acknowledgments</i>	iii
<i>Publications and Presentations</i>	v
<i>Table of Content</i>	vi
<i>Abstract</i>	viii
<i>Zusammenfassung</i>	xi
<i>List of Abbreviations, Acronyms, and Symbols</i>	xiv
<i>General Remarks</i>	xviii
Part I: Introduction	1
1 Organohalogens	3
1.1 Halogenated Natural Products	3
1.2 Enzymatic Halogenation	6
1.2.1 Haloperoxidases	7
1.2.2 Flavin-Dependent Halogenases	9
1.2.3 Non-Heme Iron Halogenases	10
1.2.4 SAM-Dependent Halogenases	12
1.3 Summary	13
2 Chlorosulfolipids	14
2.1 Isolation and Discovery	14
2.2 Biosynthesis	17
2.3 Configurational and Conformational Analysis of Chlorosulfolipids	19
2.4 Strategies Used in the Total Syntheses of Chlorosulfolipids	21
2.4.1 CARREIRA's Synthesis of Mytilipin A	21
2.4.2 VANDERWAL's Synthesis of Danicalipin A, Malhamensilipin A, and Mytilipin A	24
2.4.3 YOSHIMITSU's Synthesis of Mytilipin A and Danicalipin A	28
2.4.4 UMEZAWA and MATSUDA's Synthesis of Danicalipin A	31
2.4.5 CARREIRA's Synthesis of Nominal Mytilipin B	33
2.4.6 CARREIRA's Synthesis of Danicalipin A	36
2.4.7 BURNS' Synthesis of Danicalipin A	38
2.5 Biological Activity	39
2.6 Summary	45
Part II: Configurational and Conformational Effects in Danicalipin A and its Analogs	47
3 Results and Discussion	49
3.1 Background	49
3.2 Project Outline	51
3.3 Target Selection	52
3.3.1 Conformations of Potential Diastereomers	52
3.3.2 Computational Analysis of Diastereomers	56
3.4 Synthesis of 11,15-di- <i>epi</i> -Danicalipin A	63
3.5 Biological Effects Exhibited by the Diastereomers	71
3.5.1 Membrane Permeability Enhancement	71
3.5.2 Toxicity	73
3.5.3 Rationalization of Bioactivity	74

4	Conclusions and Outlook	83
Part III:	Effect of Increasing Chlorination in Danicalipin A and its Analogs	87
5	Results and Discussion	89
5.1	Background	89
5.2	Project Outline	90
5.3	Synthesis of Trichloro-DDS	92
5.3.1	First Approach to Allylic Chlorohydrin 175	92
5.3.2	Second Approach to Allylic Chlorohydrin 175 and Conclusion of the Synthesis	94
5.4	Synthesis of Heptachloro-DDS	99
5.5	Biological Effects	102
5.5.1	Membrane Permeability Enhancement	102
5.5.2	Toxicity	105
6	Conclusions and Outlook	107
Part IV:	1,3-Sigmatropic Shifts in Allylic Chlorohydrins	111
7	Results and Discussion	113
7.1	Background	113
7.1.1	The WOODWARD–HOFFMANN Rules for Sigmatropic Rearrangements	113
7.1.2	Exceptions and Other Mechanistic Hypotheses	115
7.1.3	Sigmatropic Rearrangements of Chlorine	118
7.2	Project Outline	122
7.3	Elucidation and Preliminary Considerations	123
7.4	Studies on Optimization and Stereochemistry	127
7.5	Structural Studies on Other Allylic Chlorohydrins	134
8	Conclusions and Outlook	142
	General Conclusions	145
9	Final Remarks	147
	Experimental	151
10	General Considerations	153
9.1	Chemicals and Solvents	153
9.2	General Procedures	153
9.3	Analytics	154
9.4	Computational Details	155
9.5	Brine Shrimp Survival Assay	156
11	Experimental Details for Part II	158
12	Experimental Details for Part III	176
13	Experimental Details for Part IV	200
	Appendix	235
14	Computational Data	237
15	NMR Spectra	254
	<i>Curriculum Vitae</i>	345

Abstract

Chlorosulfolipids constitute an intriguing class of natural products, which have been isolated globally from freshwater microalgae and their consumers. Since initial reports on members of this family in the 1960's, they have sparked interest in the isolation and biochemical literature. Synthetic chemists joined the research on these compounds following stereochemical elucidation more than a decade ago. In particular danicalipin A (**I**) has been the topic of extensive discussion (Figure I). Yet, despite being the major polar component in the membrane of the golden-brown algae *Ochromonas danica*, the biological function of **I** remains unclear to date.

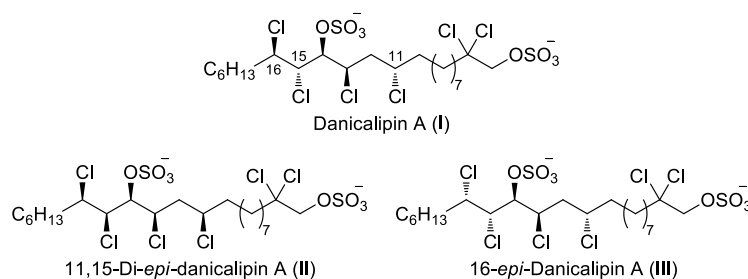


Figure I Structures of natural danicalipin A (**I**), and of unnatural diastereomers 11,15-di-*epi*-danicalipin A (**II**) and 16-*epi*-danicalipin A (**III**).

The first part of this thesis discusses the configurational and conformational effects in the complex chlorination pattern of danicalipin A (**I**) which was enabled by the synthesis of two diastereomers, 11,15-di-*epi*-danicalipin A (**II**) and 16-*epi*-danicalipin A (**III**) (Figure I). The selection of these targets was supported by a database/molecular modeling and MCOMM/DFT approach which predicted distinct conformations different from that of **I**. The synthesis of 11,15-di-*epi*-danicalipin A (**II**) was completed in 16 steps (12 steps longest linear sequence) and 3% overall yield, following a route comprised of enantioselective epoxidation, SHARPLESS' asymmetric dihydroxylation, epoxide openings, BROWN allylation, and cross-metathesis.

Biological investigations and comparison between the three diastereomers provided valuable insight into functions of the chlorinated array. Strikingly, diastereomers **I**, **II**, and **III** exhibited markedly different membrane permeability enhancement in bacteria and mammalian cells. These findings could not be fully explained by differences in configuration and conformation, therefore prompting us to take flexibility and molecular shape into account as well. MCOMM/DFT analysis

unearthed the high conformational stability of the singly-kinked structure of **I**, and allowed speculation about beneficial effects it may impart on fluidity and motility in *O. danica*. Furthermore, the same analysis attested **II** a higher flexibility and ill-defined molecular shape, as well as a singly-kinked, but flexible structure for **III**. These results correlated with biological activity, suggesting that the rigid, singly-kinked molecular structure of **I** was crucial for membrane behavior.

The second part of this thesis discloses contributions to a project aimed at uncovering the effects of varying degrees of chlorination in danicalipin A (**I**) and its analogs. To this end, the synthesis of chlorinated docosanedisulfates (DDS) **IV** and **V** were completed (Figure II). The synthesis of trichloro-DDS (**IV**) involved enantioselective α -chlorination, diastereoselective chloroallylation, BROWN allylation and cross-metathesis, culminating in the natural product after 11 steps (10 steps longest linear sequence) and 4% overall yield. Heptachloro-DDS (**V**) was accessed in 4 steps from known intermediates in 35% overall yield through cross-metathesis and dichlorination.

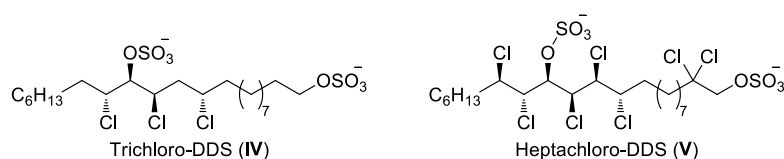
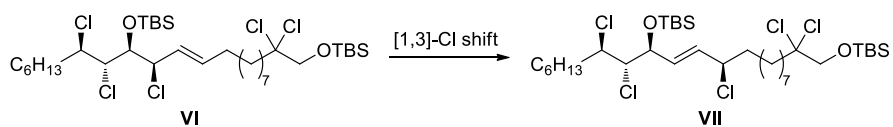


Figure II Structures of naturally-occurring trichloro-DDS (**IV**) and unnatural heptachloro-DDS (**V**).

The biological activities of **IV**, **V**, and other partially chlorinated analogs of danicalipin A (**I**) illustrated the advantages of the specific chlorination pattern in **I**. In cytotoxicity and membrane permeability enhancement assays, **I** demonstrated the most pronounced biological impact suggesting an intricate net of influences in the chlorination pattern. Unaccountable solely through molecular shape and flexibility arguments, these effects entailed conjecture of the superiority of **I** during competitive evolution.

The final part of this thesis covers the work based on an observation made during the synthesis of heptachloro-DDS (**V**). The allylic chlorine substituent in intermediate **VI** underwent [1,3]-allylic rearrangement, representing a rare example of a sigmatropic reaction involving a chlorine atom (Scheme I).



Scheme I Observed [1,3]-sigmatropic rearrangement of the allylic chlorine substituent in **VI**.

Further studies and extension of the methodology to other substrates established that the thermal reaction required polar medium as well as specific stereoelectronic prerequisites of the substrate. The driving force of this reaction is of an enthalpic nature with contributions from increased polarity and decreased steric hindrance of the product. The observations corroborated the hypothesis that the suprafacial shift proceeded through a polar transition state, reminiscent of a tight ion pair between an allyl cation and a chloride ion, and does not follow the WOODWARD–HOFFMANN rules but rather is under complementary subjacent-orbital control.

Zusammenfassung

Chlorosulfolipide stellen eine faszinierende Naturstoffklasse dar, welche weltweit aus Süßwassermikroalgen und deren Verzehrern isoliert wurde. Seit den ersten Berichten über Mitglieder dieser Familie in den 1960er Jahren weckten sie das Interesse in der Isolations- und biochemischen Literatur. Vor über einem Jahrzehnt begannen sich auch synthetische Chemiker an der Erforschung dieser Moleküle zu beteiligen, nachdem die Stereochemie aufgeklärt worden war. Insbesondere Danicalipin A (**I**) wurde ausgiebig diskutiert, da es den Hauptanteil der polaren Komponenten in der Membran der goldbraunen Alge *Ochromonas danica* bildet (Abbildung I). Trotzdem konnte die biologische Funktion bis heute nicht geklärt werden.

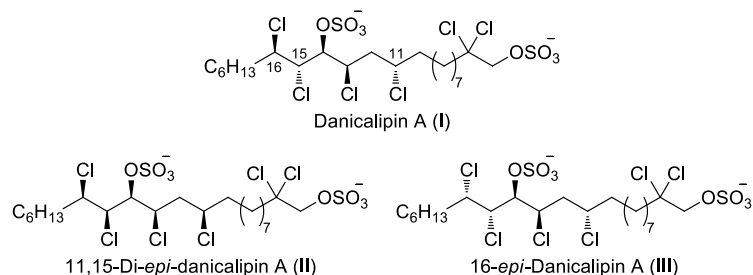


Abbildung I Struktur von natürlichem Danicalipin A (**I**) und den unnatürlichen Diastereomeren 11,15-Di-*epi*-danicalipin A (**II**) und 16-*epi*-Danicalipin A (**III**).

Im ersten Teil dieser Arbeit werden die Einflüsse von Konfiguration und Konformation im komplexen Chlorierungsmuster von Danicalipin A (**I**) behandelt. Diese Studie ist durch die Synthese zweier Diastereomere ermöglicht worden, 11,15-Di-*epi*-danicalipin A (**II**) und 16-*epi*-Danicalipin A (**III**) (Abbildung I). Die Auswahl dieser Zielmoleküle ist anhand eines Vorgehens getroffen worden, welches die Analyse aus Datenbanken und Molekularmodellierung mit MCMC und DFT Berechnungen kombinierte. Anhand dieses Ansatzes sind spezifische Konformationen für **II** und **III** prognostiziert worden, welche sich von **I** unterscheiden haben. Das synthetische Material, 11,15-Di-*epi*-danicalipin A (**II**), ist mit Hilfe von enantioselektiver Epoxidierung, SHARPLESS' asymmetrischer Dihydroxylierung, Epoxidöffnungen, BROWN Allylierung und Kreuzmetathese erhalten worden. Die Route ist in 16 Stufen (12 Stufen in der längsten linearen Sequenz) beendet worden, wobei die Gesamtausbeute 3% betrug.

Biologische Untersuchungen und der Vergleich der drei Diastereomere lieferten einen wertvollen Einblick in die Funktionen der chlorierten Domäne. Besonders markant war die unterschiedliche Membranpermeabilitätserhöhung durch **I**, **II** und **III** in Bakterien- und Säugetierzellen. Da diese Unterschiede nicht vollständig durch Unterschiede der Konfiguration und Konformation erklärt werden konnten, mussten zusätzlich noch die Flexibilität und Molekulargestalt berücksichtigt werden. MCMM und DFT Analysen ergaben eine hohe Konformationsstabilität der einfach gebeugten Struktur von **I** und erlaubten die Spekulation über die Vorteile dieser Eigenschaft auf die Fluidität und Motilität für *O. danica*. Außerdem bescheinigte dieselbe Analyse **II** eine höhere Flexibilität und unklare Molekulargestalt, während **III** eine einfach gebeugte aber flexible Molekulargestalt aufwies. Diese Erkenntnisse stimmten mit den biologischen Ergebnissen überein und wiesen darauf hin, dass die starre, einfach gebeugte Molekulargestalt von **I** für das Membranverhalten entscheidend war.

Der nachfolgende Teil dieser Arbeit war ein Beitrag zu einem Projekt, welches darauf abzielte, die Effekte variierender Chlorierungsgrade in Danicalipin A (**I**) und dessen Analoga zu bestimmen. Dazu wurden die Synthesen der beiden chlorierten Docosandisulfate (DDS) **IV** und **V** durchgeführt (Abbildung II). Die Synthese von Trichloro-DDS (**IV**) beinhaltete enantioselektive α -Chlorierung, diastereoselektive Chloroallylierung, BROWN Allylierung und Kreuzmetathese, was den Naturstoff in 11 Stufen (10 Stufen in der längsten linearen Sequenz) und 4% Gesamtausbeute ergab. Heptachloro-DDS (**V**) wurde durch Kreuzmetathese und Dichlorierung in 4 Stufen und 35% Gesamtausbeute aus bekannten Stoffen hergestellt.

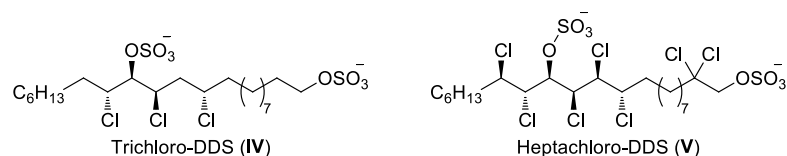
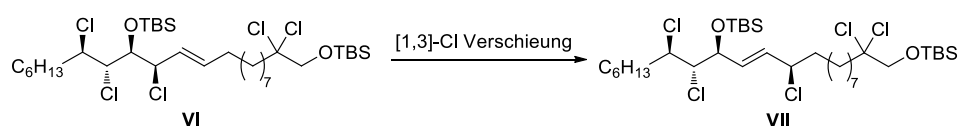


Abbildung II Strukturen des natürlich vorkommenden Trichloro-DDS (**IV**) und unnatürlichen Heptachloro-DDS (**V**).

Die biologischen Aktivitäten von **IV**, **V** und anderen teilchlorierten Analoga von Danicalipin A (**I**) hoben die Vorteile des spezifischen Chlorierungsmusters in **I** hervor. Sowohl die Cytotoxizität als auch die Membranpermeabilitätserhöhung von **I** waren am Höchsten, wodurch sich ein verzweigtes Netz aus verschiedenen Einflüssen

im Chlorierungsmuster andeutete. Diese Effekte gingen über Argumente der Molekulargestalt und Flexibilität hinaus. Aus ihnen ließen sich Schlussfolgerungen zur Überlegenheit von **I** während der kompetitiven Evolution ziehen.

Der letzte Teil dieser Arbeit befasst sich mit einer Entdeckung, welche im Rahmen der Synthese von Heptachloro-DDS (**V**) gemacht worden ist. Der allylische Chlorsubstituent in Zwischenprodukt **VI** hat eine [1,3]-sigmatrope Umlagerung begangen und dadurch ein Beispiel der seltenen, sigmatropen Reaktionen dargestellt, in welchen ein Chloratom beteiligt ist (Schema I).



Schema I Die beobachtete [1,3]-sigmatrope Umlagerung des allylischen Chlorsubstituenten in **VI**.

Durch zusätzliche Studien und die Erweiterung der Methodik auf andere Substrate wurde festgestellt, dass die thermische Reaktion eines polaren Mediums und konkreter stereoelektronischer Anforderungen bedurfte. Des Weiteren wurde die enthalpische Triebkraft der Umlagerung gefunden, zu welcher eine erhöhte Polarität und verringerte sterische Hinderung des Produkts beitragen. Die Beobachtungen bekräftigten die Hypothese, dass die suprafaciale Verschiebung durch einen polaren Übergangszustand verläuft, welcher einem engen Ionenpaar zwischen einem Allylkation und einem Chloridion gleicht, und nicht den Regeln von WOODWARD–HOFFMANN folgt, sondern vielmehr einer alternativen Kontrolle durch energetisch tiefer liegende Orbitale.

List of Abbreviations, Acronyms, and Symbols

2D	two dimensional
<i>a</i>	antarafacial
Å	Ångström
$[\alpha]_D^T$	optical rotation at temperature T at the sodium D line
A _{1,3}	allylic 1,3-strain
Ac	acetyl
AD	asymmetric dihydroxylation
approx.	approximately
aq.	aqueous
atm	atmosphere(s)
Bn	benzyl
brsm	by recovered starting material
Bu	butyl
c	concentration
°C	degrees celcius
cat.	catalytic
<i>cf.</i>	<i>confer</i> – compare
cm ⁻¹	inverse centimeter(s)
CoA	coenzyme A
COSY	homonuclear correlation spectroscopy
CSA	camphorsulfonic acid
Cy	cyclohexyl
Cys	cysteine
D	Debye
d	doublet
δ	chemical shift referenced to tetramethylsilane
DABCO	1,4-diazabicyclo[2.2.2]octane
DCC	<i>N,N'</i> -dicyclohexylcarbodiimide
DCE	1,3-dichloroethane
DDS	docosanedisulfate
DET	diethyltartrate
DFT	density functional theory
DIAD	diisopropyl azodicarboxylate
DMAP	4-dimethylaminopyridine
DMF	dimethylformamide
DMP	DESS–MARTIN periodinane
DMSO	dimethylsulfoxide
DNA	deoxyribonucleic acid
d.r.	diastereomeric ratio
ε	relative permittivity

<i>E. coli</i>	<i>Escherichia coli</i>
<i>ee</i>	enantiomeric excess
EI	electron ionization
<i>ent</i>	enantiomeric
<i>epi</i>	epimeric
ESI	electrospray ionization
equiv.	equivalents
Et	ethyl
<i>et al.</i>	<i>et alii</i> – and others
eV	electronvolt(s)
FAD	flavin adenine dinucleotide
FADH ₂	reduced, hydroquinone form of FAD
g	gram(s)
g+/-	clockwise/counterclockwise <i>gauche</i> conformation
<i>gem</i>	geminal
GLC-MS	gas liquid chromatography and mass spectrometry
h	hour(s)
HECADE	heteronuclear couplings from ASSCI-domain experiments with E.COSY-type cross peaks
His	histidine
HMBC	heteronuclear multiple bond correlation
HMDS	bis(trimethylsilyl)amide
HOMO	highest occupied molecular orbital
HRMS	high resolution mass spectrometry
HSQC	heteronuclear single quantum coherence
Hz	Hertz
<i>i</i>	<i>iso or</i> inversion
IC ₅₀	half maximal inhibitory concentration
Ipc	isopinocampheyl
IR	infrared
<i>J</i>	coupling constant
JBCA	<i>J</i> -based configuration analysis
l	large
LC ₅₀	lethal concentration for 50% of the organisms
LDA	lithium diisopropylamide
LUMO	lowest unoccupied molecular orbital
K	Kelvin
kcal	kilocalorie(s)
kg	kilogram(s)
m	medium <i>or</i> multiplet
μ	dipolar moment
MCMM	Monte Carlo molecular mechanics

<i>m</i> -CPBA	<i>meta</i> -chloroperbenzoic acid
Me	methyl
μg	microgram(s)
mg	milligram(s)
MHz	megahertz
min	minute(s)
μL	microliter(s)
mL	milliliter(s)
mM	millimolar
μM	micromolar
mM	millimolar
μmol	micromoles
mmol	millimole
mol	mole
<i>n</i>	normal
<i>v</i>	wavenumber
NAD(P)H	nicotinamide adenine dinucleotide (phosphate)
NCS	<i>N</i> -chlorosuccinimide
NME	<i>N</i> -methylephedrine
NMO	<i>N</i> -methylmorpholine <i>N</i> -oxide
NMR	nuclear magnetic resonance
NOE	nuclear Overhauser effect
Ns	4-nitrobenzenesulfonyl
<i>O.</i>	<i>Ochromonas</i>
<i>P.</i>	<i>Proterioochromonas</i>
p	page
PAPS	phosphoadenosine phosphosulfate
PC	propylene carbonate
PCP	peptidyl carrier protein
Ph	phenyl
PMB	<i>para</i> -methoxybenzyl
ppb	parts per billion
ppm	parts per million
Pr	propyl
quant.	quantitative
<i>r</i>	retention
ref.	reference
r.t.	room temperature
s	small <i>or</i> singlet
<i>s</i>	suprafacial
SAM	<i>S</i> -adenosyl methionine
sp.	species

t	triplet
<i>t</i>	<i>tert</i>
⤿	<i>trans</i> conformation
TBS	<i>tert</i> -butyldimethylsilyl
TBDPS	<i>tert</i> -butyldiphenylsilyl
TEMPO	(2,2,6,6-tetramethylpiperidin-1-yl)oxyl
TES	triethylsilyl
Tf	trifluoromethylsulfonyl
TFA	trifluoroacetic acid
TFAA	trifluoroacetic anhydride
THF	tetrahydrofuran
TLC	thin layer chromatography
TMP	2,2,6,6-tetramethylpiperidide
TMS	trimethylsilyl
TPAP	tetrapropylammonium perruthenate
Ts	<i>para</i> -toluenesulfonyl
UV	ultraviolet
<i>vic</i>	vicinal
X	halogen

General Remarks

Part I:

The theses by ROGER GEISSER,ⁱ CHRISTIAN NILEWSKI,ⁱⁱ NIKOLAS HUWYLER,ⁱⁱⁱ and MATHIAS J. JACOBSON^{iv} served as sources of some references and ideas.

Part II:

S. FISCHER devised database/molecular modeling approach and synthesized 16-*epi*-danicalipin A. The brine shrimp toxicity of 11,15-di-*epi*-danicalipin A and 16-*epi*-danicalipin A were performed with him. The membrane permeability enhancement assays and cytotoxicities were determined by DR. S. WOLFRUM and A. M. BAILEY. DR. STEFAN RUIDER advised on the computations and ensuing discussions. All of them are greatly acknowledged for their contributions and insights.

Parts of this chapter are published in: J. Boshkow, S. Fischer, A. M. Bailey, S. Wolfrum, E. M. Carreira *Chem. Sci.* **2017**, *8*, 6904-6910

Part III:

A M. BAILEY synthesized dichloro-, tetrachloro-, and pentachloro-DDS, as well as danicalipin A. He also provided the enantioenriched olefin required for the synthesis of heptachloro-DDS (see Chapter 12). S. FISCHER and F. GLATZ synthesized monochloro-DDS. The membrane permeability enhancement assays and cytotoxicities were determined by DR. S. WOLFRUM and A. M. BAILEY. The collaboration is greatly acknowledged.

Part IV:

No remarks need to be made.

ⁱ R. Geisser in “*Synthetic Investigations en route to Chlorosulfolipids*”, Dissertation ETH No. 19364, Zurich, **2010**.

ⁱⁱ C. Nilewski in “*Enabling Tactics and Strategies to Access Polychlorinated Hydrocarbons – Total Synthesis of Chlorosulfolipids and Insights into Their Chemistry*”, Dissertation ETH No. 19549, Zurich, **2011**.

ⁱⁱⁱ N. Huwyler in “*Total Synthesis of (±)-Gomerone C, (±)-Fluorodanicalipin A and Studies towards (+) and (-)-Merochlorin A*”, Dissertation ETH No. 22789, Zurich, **2015**.

^{iv} M. J. Jacobson in “*Towards a Structural Revision of Mytilipin B*”, Dissertation ETH No. 23251, Zurich, **2016**.

Part I

INTRODUCTION

1 Organohalogens

1.1 Halogenated Natural Products

In 1964, only 24 naturally occurring organohalogens were known.¹ Since then, the number has increased to over 5000, with around 100–200 new entries still being added every year.² Most organohalogens are isolated from marine sources due to the high content of halide ions in the oceans (Table 1).

Table 1 Distribution of halides in the biosphere. Values in mg/kg. Adapted with permission of Springer Nature from ref. 3, Copyright 2010 Springer-Verlag.

Halide	Oceans	Sedimentary rocks	Fungi	Wood pulp	Plants
F ⁻	1.4	270–740			
Cl ⁻	19,000	10–320		70–2100	200–10,000
Br ⁻	65	1.6–3	100		
I ⁻	0.05	0.3			

Although chloride is the most abundant halide in the biosphere, organochlorines (51%) and organobromines (45%) are almost equally abundant in nature, while only small fractions of organohalogens contain fluorine (1%) or iodine (3%).⁴ These differences can be rationalized by varying distributions, oxidation potentials, and enzymatic incorporation of the halides (*cf.* Chapter 1.2).

Simple organohalogens, such as chloroform or methyl bromide, can be found in emissions of volcanoes, minerals, soil, and even meteorites.⁵ More complex natural products are most often isolated from marine organisms, but also bacteria, fungi, terrestrial plants, insects, and higher animals. The biological function in these species is often associated with self-defense. Nevertheless, a great variety of promising

¹ G. W. Gribble *Chemosphere* **2003**, *52*, 289-297.

² G. W. Gribble *Environ. Chem.* **2015**, *12*, 396-405.

³ G. W. Gribble “*Naturally Occurring Organohalogen Compounds - A Comprehensive Update*”, Progress in the Chemistry of Organic Natural Products, Vol. 91, Springer Verlag, Wien, **2010**, p. 4.

⁴ G. W. Gribble *Am. Sci.* **2004**, *92*, 342-348.

⁵ G. W. Gribble *Acc. Chem. Res.* **1998**, *31*, 141-152.

biological activities can be exhibited by organohalogens.⁶ A few interesting examples of biologically active halogen-containing natural products are shown in Figure 1.

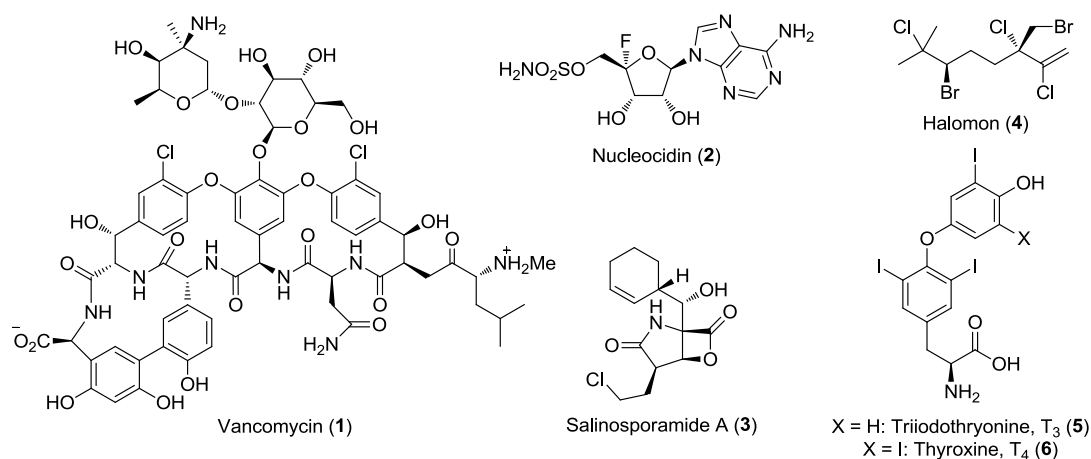


Figure 1 Examples of naturally occurring organohalogens with diverse biological activities.

Vancomycin (**1**) is a glycopeptide, isolated from the soil bacterium *Amycolatopsis orientalis*. It was commonly used as antibiotic against infections with Gram-positive bacteria but the emergence of vancomycin-resistant bacteria limits **1** to be used as drug of last resort against methicillin-resistant *Staphylococcus aureus* (MRSA) or in patients with serious allergies to β -lactam antibiotics.⁷ Nucleocidin (**2**) is one of the few organofluorines found in nature and was first isolated from the Indian soil bacterium *Streptomyces calvus* in 1957. Despite broad antibiotic activity, it was not considered for clinical use due to its high toxicity.⁸ Salinosporamide A (**3**) from marine bacteria *Salinospora tropica* and *Salinospora arenicola* is a potent inhibitor of the 20S proteasome.⁹ This activity renders **3** cytotoxic and the β -lactone is currently in clinical trials as treatment for multiple myeloma.¹⁰ The monoterpene halomon (**4**) was isolated from the marine red algae *Portieria hornemannii* and was in preclinical trials for its promising cytotoxicity against a variety of human cancer cell

⁶ G. W. Gribble *J. Chem. Educ.* **2004**, *81*, 1441-1449.

⁷ a) Centers for Disease Control and Prevention (CDC): *MMWR Recomm. Rep.* **1995**, Sep 22, *44* (RR12), 1-13; b) C. Liu, A. Bayer, S. E. Cosgrove, R. S. Daum, S. K. Fridkin, R. J. Gorwitz, S. L. Kaplan, A. W. Karchmer, D. P. Levine, B. E. Murray, M. J. Rybak, D. A. Talan, H. F. Chambers *Clin. Infect. Dis.* **2011**, *52*, 285-292.

⁸ D. O'Hagan, D. B. Harper *J. Fluor. Chem.* **1999**, *100*, 127-133.

⁹ R. H. Feling, G. O. Buchanan, T. J. Mincer, C. A. Kauffman, P. R. Jensen, W. Fenical *Angew. Chem. Int. Ed.* **2003**, *42*, 355-357.

¹⁰ D. Chauhan, L. Catley, G. Li, K. Podar, T. Hideshima, M. Velankar, C. Mitsiades, N. Mitsiades, H. Yasui, A. Letai, H. Ovaa, C. Berkers, B. Nicholson, T.-H. Chao, S. T. C. Neuteboom, P. Richardson, M. A. Palladino, K. C. Anderson *Cancer Cell* **2005**, *8*, 407-419.

lines.¹¹ The activity of **4** could arise from its inhibition of DNA methyltransferase-1.¹² The mammalian thyroid hormones T₃ (**5**) and T₄ (**6**), which are relevant for metabolism, belong to the rare class of organoiodine compounds. These essential hormones are ligands to DNA-binding transcription factors and can thereby regulate gene expression.¹³

The effects exhibited by halogen substitution can be manifold, but are often beneficial or even essential to biological function. Dechlorinated derivatives of vancomycin (**1**, Figure 1) were less effective in coordinating to the binding site in bacterial peptidoglycan. The chlorines are hypothesized to lock favorable positioning of the aromatic rings, imposing a more stable conformation of the antibiotic. In addition, one of the chlorines helps in shaping the binding pocket to allow more specific coordination.¹⁴ Dechlorination of salinosporamide A (**3**, Figure 1) attenuated activity by several orders of magnitude. The chlorine substituent was found to be directly involved in binding to the active site: after a threonine residue in the 20S proteasome opens the β -lactone, the resulting hydroxy group displaces the chlorine substituent to increase binding energy.¹⁵

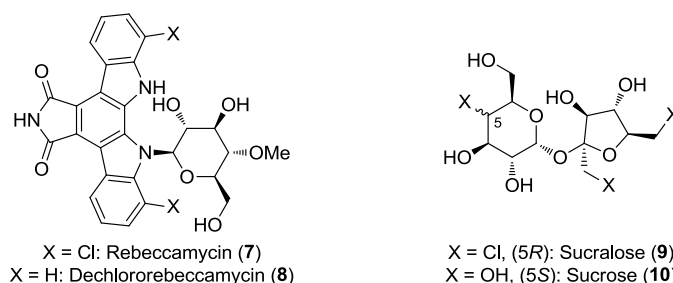


Figure 2 Examples of molecules with beneficial effects of chlorine on biological activity.

Rebeccamycin (**7**, Figure 2) inhibits topoisomerase I, but its dechlorinated analog **8** has been found to be more active. However, chlorine substituents increase

¹¹ a) R. W. Fuller, J. H. Cardellina II, Y. Kato, L. S. Brinen, J. Clardy, K. M. Snader, M. R. Boyd *J. Med. Chem.* **1992**, *35*, 3007-3011; b) M. J. Egorin, D. L. Sentz, D. M. Rosen, M. F. Ballesteros, C. M. Kearns, P. S. Callery, J. L. Eiseman *Cancer Chemother. Pharmacol.* **1996**, *39*, 51-60.

¹² E. H. Andrianasolo, D. France, S. Cornell-Kennon, W. H. Gerwick *J. Nat. Prod.* **2006**, *69*, 576-579.

¹³ Y. Wu, R. J. Koenig *TEM* **2000**, *11*, 207-211.

¹⁴ C. M. Harris, R. Kannan, H. Kopecka, T. M. Harris *J. Am. Chem. Soc.* **1985**, *107*, 6652-6658.

¹⁵ a) V. R. Macherla, S. S. Mitchell, R. R. Manam, K. A. Reed, T.-H. Chao, B. Nicholson, G. Deyanat-Yazdi, B. Mai, P. R. Jensen, W. F. Fenical, S. T. C. Neuteboom, K. S. Lam, M. A. Palladino, B. C. M. Potts *J. Med. Chem.* **2005**, *48*, 3684-3687; b) M. Groll, R. Huber, B. C. M. Potts *J. Am. Chem. Soc.* **2006**, *128*, 5136-5141.

lipophilicity, leading to better membrane permeability of **7**.¹⁶ Additionally, while **7** is active against Gram-positive bacteria, **8** is not.¹⁷ Beneficial increases in lipophilicity also account for the enhanced sweetness of sucralose (**9**), the main component of several artificial sweeteners, over sucrose (**10**) (Figure 2).¹⁸

While the organohalogens mentioned above exemplify the breadth of biological activities, as well as the diverse influences of halogenation, they do not present a complete picture. The plethora of natural products containing halogens gives rise to a vast number of intriguing compounds that have yet to be studied. This may lead to the understanding of their diverse inherent roles in nature.

1.2 Enzymatic Halogenation

Halogenating enzymes have been studied extensively and excellent reviews on this matter have been published.¹⁹ Such enzymes are categorized according to their co-factors, oxidants, and/or mechanisms. Most halogens are incorporated electrophilically (X^+) by oxidation of halide ions, but there are also enzymes that catalyze radical or anionic pathways (Table 2).

Table 2 Different types of halogenating enzymes, their co-factors, oxidants, and co-substrates. Adapted with permission from ref. 19a, Copyright 2006 American Chemical Society.

Enzyme type	Co-factor	Oxidant	Co-substrates
Haloperoxidases	heme iron <i>or</i> vanadium	H ₂ O ₂	halide
Flavin-dependent halogenases	FADH ₂	O ₂	halide
Non-heme iron halogenases	non-heme iron	O ₂	halide, α -ketoglutarate
SAM-dependent halogenases	SAM	-	halide

¹⁶ E. Rodrigues Pereira, L. Belin, M. Sancelme, M. Prudhomme, M. Ollier, M. Rapp, D. Sevère, J.-F. Riou, D. Fabbro, T. Meyer *J. Med. Chem.* **1996**, *39*, 4471-4477.

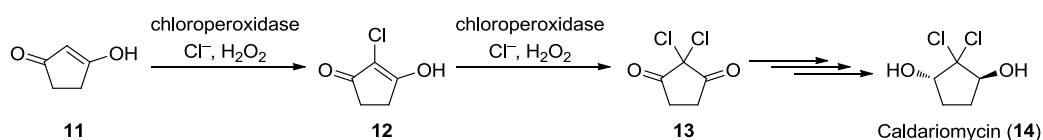
¹⁷ P. Moreau, F. Anizon, M. Sancelme, M. Prudhomme, C. Bailly, C. Carrasco, M. Ollier, D. Sevère, J.-F. Riou, D. Fabbro, T. Meyer, A.-M. Aubertin *J. Med. Chem.* **1998**, *41*, 1631-1640.

¹⁸ M. Mathlouthi, A.-M. Seuvre *Carbohydrate Research* **1986**, *152*, 47-61.

¹⁹ a) F. H. Vaillancourt, E. Yeh, D. A. Vosburg, S. Garneau-Tsodikova, C. T. Walsh *Chem. Rev.* **2006**, *106*, 3364-3378; b) C. S. Neumann, D. Galonić Fujimori, C. T. Walsh *Chem. Biol.* **2008**, *15*, 99-109; c) A. Butler, M. Sandy *Nature* **2009**, *460*, 848-854; d) V. Weichold, D. Milbredt, K.-H. van Pée *Angew. Chem. Int. Ed.* **2016**, *55*, 6374-6389.

1.2.1 Haloperoxidases

Haloperoxidases were found as the first enzymes, that were able to halogenate natural metabolites. By employing heme iron or vanadium co-factors and hydrogen peroxide, halide ions (Cl^- , Br^- , I^-) are oxidized to the corresponding hypohalous acids, which subsequently halogenate the substrate. These halogenations can essentially be regarded as chemical reactions between hypohalous acid ions (OX^-) and electron-rich, activated carbon-nucleophiles. Depending on the oxidation potential of the enzyme different halides can be oxidized. Consequently, chloroperoxidases are able to oxidize chloride, bromide, and iodide, bromoperoxidases can typically oxidize bromide and iodide, and iodoperoxidases can only oxidize iodide. To date, no fluoroperoxidase has been described, presumably due to the high oxidation potential of fluoride and the inherent instability of hypofluorous acid in aqueous media.

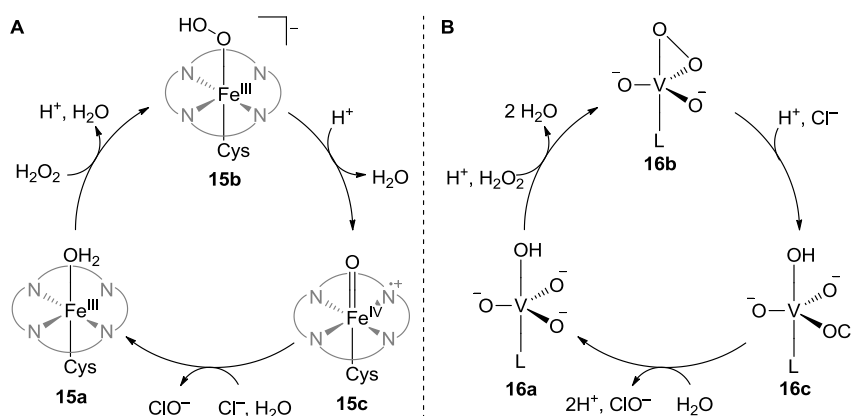


Scheme 1 Chloroperoxidases in the biosynthesis of caldariomycin (**14**).

The first haloperoxidase was isolated in 1959 from the fungus *Caldariomyces fumago* and is part of the biosynthetic path to caldariomycin (**14**, Scheme 1).²⁰ The enol form of cyclopentadienone (**11**) is converted to caldariomycin-precursor **13** via two subsequent chlorinations of **11** and **12** with a chloroperoxidase. The same enzyme from the fungus was also able to chlorinate, brominate, and iodinate β -keto acids, cyclic diketones, and substituted phenols, showcasing a lack of substrate specificity in the reaction of hypohalites in some haloperoxidases.²¹ Typical mechanisms for the oxidations by the metalloenzymes are depicted in Scheme 2.

²⁰ P. D. Shaw, L. P. Hager *J. Am. Chem. Soc.* **1959**, *81*, 1011-1012.

²¹ L. P. Hager, D. R. Morris, F. S. Brown, H. Eberwein *J. Biol. Chem.* **1966**, *241*, 1769-1777.



Scheme 2 Simplified mechanisms for the enzymatic oxidation of chloride to hypochlorite by haloperoxidases. **A:** Heme iron co-factor; **B:** Vanadium co-factor.

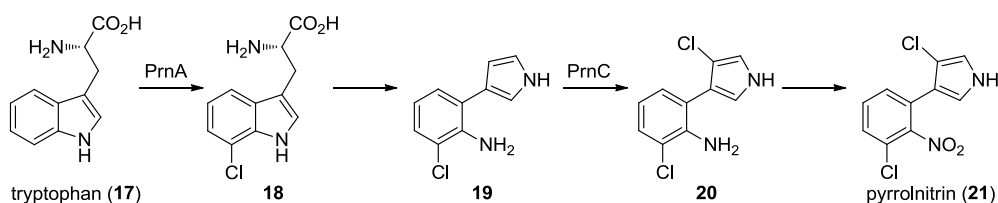
In the case of a heme iron co-factor (Scheme 2A), the resting state **15a** undergoes ligand exchange with hydrogen peroxide to form an iron(III)-hydroperoxo anion **15b**. The iron center is subsequently oxidized to oxidation state IV with concomitant oxidation of the porphyrin ligand to give the oxo-complex **15c**. Chloride ions can attack the oxo-ligand in **15c**, yielding hypochlorite ions and the metal complex returns to its initial resting state **15a**.²² In contrast, vanadium co-factors appear not to be redox-active catalysts, but LEWIS acids. In the catalytic cycle (Scheme 2B), two oxygen ligands on resting state **16a** are substituted by hydrogen peroxide to form peroxy complex **16b**. The peroxy ligand is forming a hydrogen bond to a positively charged lysine residue at the active site (not shown), activating the ligand towards oxidation. A chloride ion can attack this ligand, resulting in complex **16c**, which finally releases hypochlorite through ligand exchange.²³

²² K. Kühnel, W. Blankenfeldt, J. Turner, I. Schlichting *J. Biol. Chem.* **2006**, *281*, 23990-23998.

²³ a) W. Hemrika, R. Renirie, S. Macedo-Ribeiro, A. Messerschmidt, R. Wever *J. Biol. Chem.* **1999**, *274*, 23820-23827; b) A. Butler, J. N. Carter-Franklin *Nat. Prod. Rep.* **2004**, *21*, 180-188.

1.2.2 Flavin-Dependent Halogenases

A second class of halogenase enzymes, the flavin-dependent halogenases, also relies on an oxidative strategy to introduce halides into metabolites. As the name implies, they employ flavin as co-factor and molecular oxygen as oxidant. In contrast to haloperoxidases, the hypohalous acid equivalent does not dissociate from the active site but remains tightly bound to the enzyme. Thus, high substrate specificity is usually observed, since the binding to the active sites on the enzymes prearranges the metabolite. This prearrangement also determines the regioselectivity in such halogenations.²⁴ The flavin-dependent halogenases were discovered in the biosynthesis of the antifungal antibiotic pyrrolnitrin (**21**) from *Pseudomonas fluorescens* (Scheme 3).



Scheme 3 Simplified biosynthesis of pyrrolnitrin (**21**) from tryptophan.

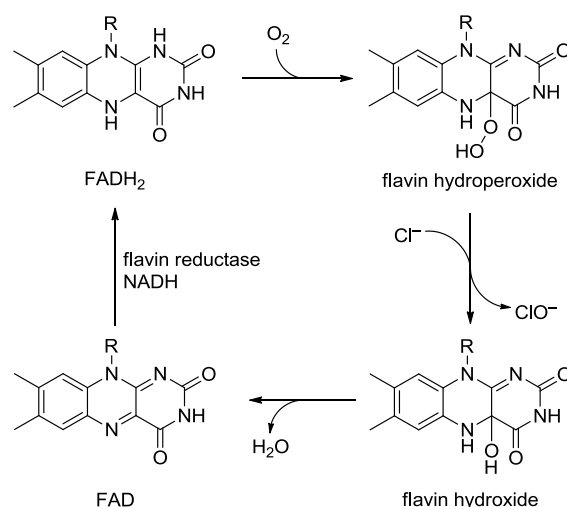
The isolated enzymes PrnA and PrnC displayed little structural similarity, but showed *in vitro* chlorination of their natural substrates tryptophan (**17**) and pyrrole **19**, respectively.²⁵ The presence of NADH was also found to be essential to the enzymatic activity although its function was initially not understood.²⁶ Both enzymes contain a nucleotide binding site, which was later explained by the need for flavin in the reaction. In the case of PrnA, a second enzyme was required, a flavin reductase, which explained the need for NADH as a reductant.²⁷ These findings, along with crystal structures of PrnA and other flavin-dependent enzymes, facilitated elucidation of the mechanism for this class of halogenases. A typical mechanism of a flavin-dependent halogenase is shown in Scheme 4.

²⁴ C. Dong, S. Flecks, S. Unversucht, C. Haupt, K.-H. van Pée, J. H. Naismith *Science* **2005**, *309*, 2216-2219.

²⁵ P. E. Hammer, D. S. Hill, S. T. Lam, K.-H. van Pée, J. M. Ligon *Appl. Environ. Microbiol.* **1997**, *63*, 2147-2154.

²⁶ K. Hohaus, A. Altmann, W. Burd, I. Fischer, P. E. Hammer, D. S. Hill, J. M. Ligon, K.-H. van Pée *Angew. Chem. Int. Ed. Engl.* **1997**, *36*, 2012-2013.

²⁷ S. Keller, K. Hohaus, M. Hölzer, E. Eichhorn, K.-H. van Pée *Angew. Chem. Int. Ed.* **2000**, *39*, 2300-2302.



Scheme 4 Mechanism for the generation of hypohalites in flavin-dependent halogenases.

Since flavin-dependent halogenases share several structural features with flavin monooxygenases,²⁸ their mechanisms are proposed to be similar. Initially, FADH₂ reacts with oxygen and forms flavin hydroperoxide. This flavin hydroperoxide is reduced to flavin hydroxide by a halide. The resulting hypohalous acid is delivered to the substrate by the enzyme. After flavin hydroxide eliminates water, it is reduced by NAD(P)H in the presence of a flavin reductase.²⁹

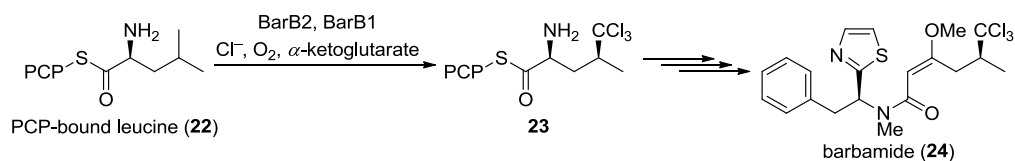
1.2.3 Non-Heme Iron Halogenases

The third class of halogenating enzymes, the non-heme iron halogenases, operate in a different fashion. Instead of functionalizing activated substrates with hypohalites, these enzymes cleave unactivated C–H bonds. The homolysis is catalyzed by a non-heme iron co-factor in the presence of sacrificial α -ketoglutarate and oxygen as the oxidant. A radical mechanism for halogenation was first suggested in the biosynthesis of barbamide (**24**) from the marine cyanobacterium *Lyngbya majuscula*, when it was found that the primary methyl group in a leucine residue was a direct precursor for the trichlorinated methyl in **23** (Scheme 5).³⁰

²⁸ B. Entsch, W. J. H. van Berkel *FASEB J.* **1995**, *9*, 476-483.

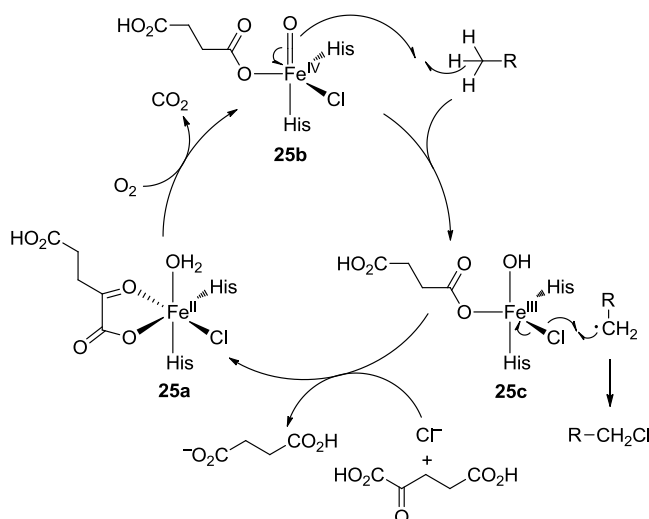
²⁹ E. Yeh, L. J. Cole, E. W. Barr, J. M. Bollinger, Jr., D. P. Ballou, C. T. Walsh *Biochemistry* **2006**, *45*, 7904-7912.

³⁰ a) N. Sitachitta, J. Rossi, M. A. Roberts, W. H. Gerwick, M. D. Fletcher, C. L. Willis *J. Am. Chem. Soc.* **1998**, *120*, 7131-7132; b) N. Sitachitta, B. L. Márquez, R. T. Williamson, J. Rossi, M. A. Roberts, W. H. Gerwick, V.-A. Nguyen, C. L. Willis *Tetrahedron* **2000**, *56*, 9103-9113.



Scheme 5 Halogenation of PCP-bound leucine in the biosynthesis of barbamide (**24**). PCP = peptidyl carrier protein.

Later comparisons of the halogenases involved in the halogenation *en route* to **24** (BarB1 and BarB2) with other enzymes from the biosyntheses of syringomycin (SyrB2 and SyrC) and coronatine (CmaA and CmaB) revealed similarities, that gave further insights into the mechanism by which these organochlorines are made.³¹ In particular SyrB2 resembled oxygenating enzymes, that depended on non-heme iron and α -ketoglutarate.³² All of these enzymes were identified as non-heme iron halogenases. Labeling studies and analyses of X-ray structures led to the elucidation of the proposed mechanisms, which proceeds *via* radical intermediates (Scheme 6).³³



Scheme 6 Simplified mechanism for the halogenation of unactivated carbons by a non-heme iron metalloenzyme.

The proposed catalytic cycle for this transformation starts from the resting state **25a**. A reaction with oxygen triggers release of carbon dioxide with concomitant oxidation of the iron(II) center to iron(IV). The oxo-ligand in **25b** is then able to abstract a hydrogen atom from the aliphatic substrate, reducing the metal center to the

³¹ Z. Chang, P. Flatt, W. H. Gerwick, V.-A. Nguyen, C. L. Willis, D. H. Sherman *Gene* **2002**, *296*, 235-247.

³² F. H. Vaillancourt, J. Yin, C. T. Walsh *Proc. Natl. Acad. Sci. USA* **2005**, *10*, 87-93.

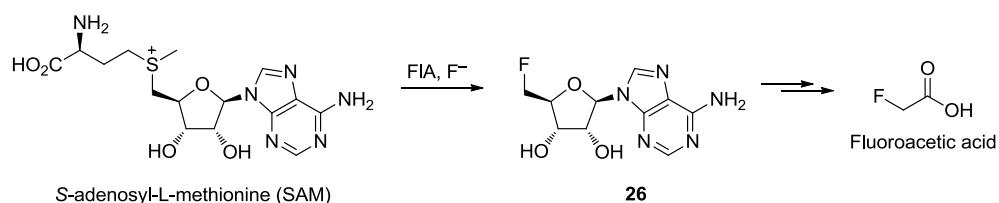
³³ L. C. Blasiak, F. H. Vaillancourt, C. T. Walsh, C. L. Drennan *Nature* **2006**, *440*, 368-371.

oxidation state III. The aliphatic radical reacts with the chloride ligand in **25c**, upon which iron(II) species **25a** is regenerated.³³

1.2.4 SAM-Dependent Halogenases

Another class of halogenases is particularly important for fluorinations, since all others are not able to synthesize organofluorines. The *S*-adenosyl-L-methionine (SAM)-dependent halogenases introduce halogens *via* nucleophilic displacement by halide ions (X^-). To overcome the barrier for displacement by hydrated halides in aqueous medium, the active sites contain amino acids (e.g. serine or threonine) that can displace water from the hydration sphere and render the halides more nucleophilic.

Such an enzyme is active during the biosynthesis of fluoroacetic acid in *Streptomyces cattleya* (Scheme 7).³⁴ The mechanism was established as an S_N2 displacement, through site-directed mutagenesis of halogenase FIA and further structural analysis, including X-ray crystallography. It was found that serine and threonine, displacing water in the hydration shell of fluoride at the active site, in combination with the positively charged methionine, were key to the reactivity of this enzyme.³⁵



Scheme 7 Fluorination of SAM by the halogenase FIA in the biosynthesis of fluoroacetic acid.

³⁴ D. O'Hagan, C. Schaffrath, S. L. Cobb, J. T. G. Hamilton, C. D. Murphy *Nature* **2002**, *416*, 279.

³⁵ X. Zhu, D. A. Robinson, A. R. McEwan, D. O'Hagan, J. H. Naismith *J. Am. Chem. Soc.* **2007**, *129*, 14597-14604.

1.3 Summary

Halogenated natural products span a vast range of biologically interesting compounds. More and more organohalogens are being isolated every year, mostly from marine sources, and will inspire biologists, chemists, and medicinal scientists to elucidate their functions and potential benefits. Several compounds reached clinical trials, promising an improvement in the way diseases can be tackled.

Nature's way of introducing halogens into metabolites is dominated by oxidative strategies. Chlorinations, brominations, and iodinations are either achieved by the formation of hypohalous acids in haloperoxidases or flavin-dependent halogenases, or by radical intermediates in non-heme iron halogenases. Non-oxidative strategies are exclusively employed in fluorinations, but also known for some chlorinations, brominations, and iodinations, where the halide anion displaces L-methionine nucleophilically in SAM-dependent halogenases. The diversity in biosynthetic pathways can give rise to yet undiscovered intriguing members of the organohalogens.

2 Chlorosulfolipids

The chlorosulfolipids are an intriguing class of halogenated lipids (Figure 3).³⁶ Over the past decades, they have been the subject of careful study by chemists and biologists, furnishing a number of interesting observations.³⁷

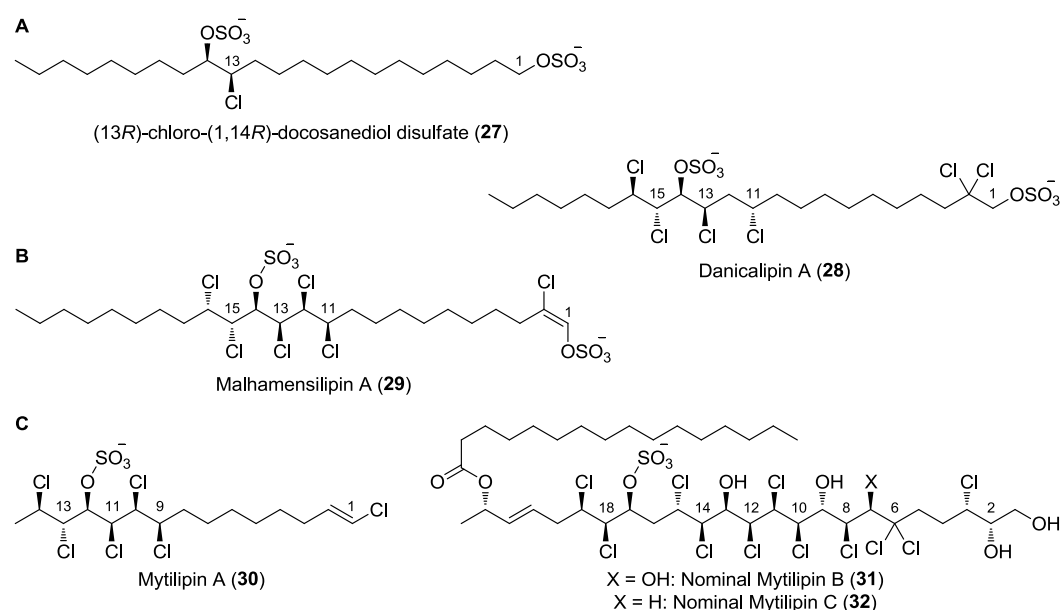


Figure 3 Representative examples of chlorosulfolipids. **A:** Selected chlorosulfolipids from *O. danica*. **B:** Malhamensilipin A, a chlorosulfolipid from *P. malhamensis*. **C:** Chlorosulfolipids from the digestive glands of *M. galloprovincialis*.

2.1 Isolation and Discovery

The first chlorosulfolipids were isolated by ELOVSON and VAGELOS in the 1960's when they investigated cell-free extracts from the golden-brown alga *Ochromonas danica* for their inhibitory activity of fatty acid synthesis.³⁸ After acid-hydrolysis of the ether-extract and TMS-derivatization, GLC-MS indicated the

³⁶ For reviews on chlorinated lipids and fatty acids, see: a) V. M. Dembitsky, M. Srebnik *Prog. Lipid Res.* **2002**, *41*, 315-367; b) C. M. Spickett *Pharmacology & Therapeutics* **2007**, *115*, 400-409.

³⁷ For reviews on chlorosulfolipids, see: a) D. K. Bedke, C. D. Vanderwal *Nat. Prod. Rep.* **2011**, *28*, 15-25; b) C. Nilewski, E. M. Carreira *Eur. J. Org. Chem.* **2012**, 1685-1698; c) T. Umezawa, F. Matsuda *Tetrahedron Lett.* **2014**, *55*, 3003-3012.

³⁸ J. Elovson, P. R. Vagelos *Proc. Natl. Acad. Sci. USA* **1969**, *62*, 957-963.

presence of several chlorinated docosane (C₂₂) and tetracosane (C₂₄) diols. Shortly after this report, HAINES and co-workers disclosed the structure of the second-most abundant of these compounds (24%) to be (13*R*)-chloro-(1,14*R*)-docosanediol disulfate (**27**, Figure 3).³⁹ The most-abundant lipid (34%) in the extract from *O. danica* was first characterized by ELOVSON and VAGELOS in 1970.⁴⁰ Through meticulous chemical degradation studies they correctly derived the structure to be 2,2,11,13,15,16-hexachloro-1,14-docosanediol disulfate (danicalipin A, **28**, Figure 3).⁴¹ No stereoinformation could be obtained at that time and it was only in 2009 that the configuration could be established (*cf.* Chapter 2.3).

In a later study on *O. danica*, HAINES and co-workers found that chlorosulfolipids constitute 91% of all polar lipids in the flagellar membrane and 81% in the membrane of the whole alga. Furthermore, no phospholipids could be detected.⁴² HAINES considered these results particularly puzzling as these chlorosulfolipids violate structural features present in lipids that form mono- or bilayer structures: *i*) chlorosulfolipids are partially water-soluble and, as detergents, can denature enzymes; *ii*) if both sulfate groups are at the hydrophilic surface of the membrane, the lipid would only form a relatively small hydrophobic region; or *iii*) if the C1-sulfate is at the hydrophilic surface, the hydrophobic region would contain the highly polar C14-sulfate. Possible reasons remain elusive to date and no explanation for the presence of **28** in the membrane of *O. danica* has been provided.

The occurrence of chlorosulfolipids is not limited to the microalgae *O. danica*. In the years following the discovery of danicalipin A (**28**), chlorosulfolipids were detected in other freshwater algae, namely *Poterioochromonas malhamensis*,⁴³ *Tribonema aequale*,⁴⁴ *Botrydium granulatum*, *Monodus subterraneus*, *Elakatothrix viridis*, and *Zygnema* sp.⁴⁵ Worthy of note is a detailed study by MERCER and DAVIES on the natural abundance of chlorosulfolipids.⁴⁶ When investigating different microalgae, chlorosulfolipids were found in 21 of 22 freshwater species, while,

³⁹ T. H. Haines, M. Pousada, B. Stern, G. L. Mayers *Biochem. J.* **1969**, *113*, 565-566.

⁴⁰ J. Elovson, P. R. Vagelos *Biochemistry* **1970**, *9*, 3110-3126.

⁴¹ Danicalipin A was later suggested as trivial name for this product and will be used in this thesis.

⁴² L. L. Chen, M. Pousada, T. H. Haines *J. Biol. Chem.* **1976**, *251*, 1835-1842.

⁴³ T. H. Haines *Annul. Rev. Microbiol.* **1973**, *27*, 403-412.

⁴⁴ E. I. Mercer, C. L. Davies *Phytochemistry* **1974**, *13*, 1607-1610.

⁴⁵ E. I. Mercer, C. L. Davies *Phytochemistry* **1975**, *14*, 1545-1548.

⁴⁶ E. I. Mercer, C. L. Davies *Phytochemistry* **1979**, *18*, 457-462.

somewhat surprising, none could be detected in the 8 marine species. Interestingly, both *Ochromonas* species contained the largest quantities of chlorosulfolipids (*O. danica*: 3%; *P. malhamensis*: 0.7% of dry weight), whereas all other species contained less (< 0.2%). The majority of chlorosulfolipids detected were in the docosane (C₂₂) family. In fact, only the *Ochromonas* species appear to produce the tetracosane (C₂₄) lipids. In *O. danica*, the total content of tetracosane chlorosulfolipids culminated in about 5% of the total chlorosulfolipids. On the other hand, the majority of chlorosulfolipids in *P. malhamensis* were tetracosanes.

The first complex tetracosane chlorosulfolipid was isolated by GERWICK, SLATE, and co-workers in 1994 during the search for a new pp60 protein tyrosine kinase inhibitor in *P. malhamensis*. The biologically active component was found to be malhamensilipin A (**29**, Figure 3).⁴⁷ In contrast to danicalipin A (**28**), the structure of **29** could be assigned by 2D-NMR techniques and mass spectrometry, albeit still without stereoinformation (*cf.* Chapter 2.3). The structure originally lacked the C14-sulfate and was later revised after a total synthesis (*cf.* Chapter 2.4.2).

The latest members of the chlorosulfolipids were added in 2001, 2002 and 2004, when CIMINIELLO, FATTORUSSO, and co-workers were trying to identify causative agents for diarrhetic shellfish poisoning in toxic mussels from the Adriatic sea.⁴⁸ The digestive glands of *Mytilus galloprovincialis* contained mytilipin A–C (**30–32**, Figure 3) which showed moderate cytotoxicity against several mammalian cell lines.⁴⁹ The structural information was obtained from NMR-based conformational analysis (*cf.* Chapter 2.3) but **31** appears to have been misassigned.⁵⁰ It was hypothesized that the mussel does not produce **30–32**, but merely accumulates these compounds by consuming the producer, presumably microalgae, through the continuous filter-feeding process. Hence, the primary organism which provides these

⁴⁷ J. L. Chen, P. J. Proteau, M. A. Roberts, W. H. Gerwick, D. L. Slate, R. H. Lee *J. Nat. Prod.* **1994**, *57*, 524–527.

⁴⁸ a) P. Ciminiello, E. Fattorusso, M. Forino, M. Di Rosa, A. Ianaro, R. Poletti *J. Org. Chem.* **2001**, *66*, 578–582; b) P. Ciminiello, C. Dell’Aversano, E. Fattorusso, M. Forino, S. Magno, M. Di Rosa, A. Ianaro, R. Poletti *J. Am. Chem. Soc.* **2002**, *124*, 13114–13120; c) P. Ciminiello, C. Dell’Aversano, E. Fattorusso, M. Forino, S. Magno, P. Di Meglio, A. Ianaro, R. Poletti *Tetrahedron* **2004**, *60*, 7093–7098.

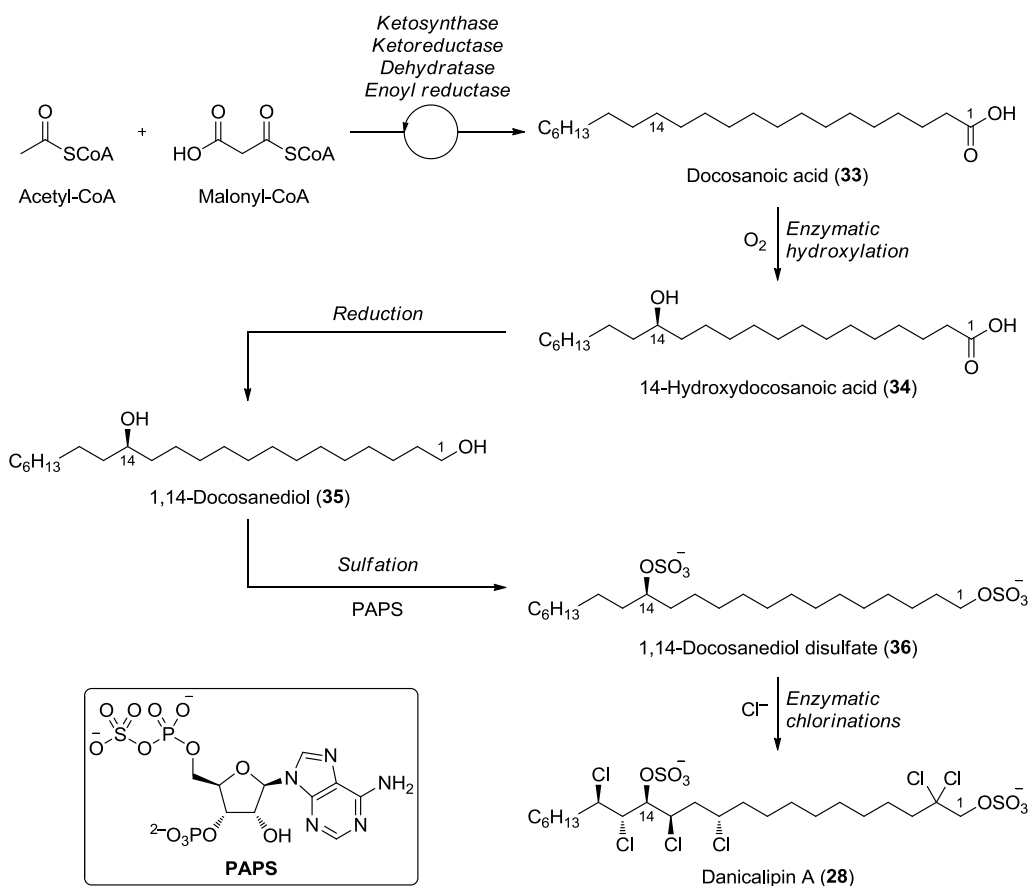
⁴⁹ Although the mussel has not been identified as the organism producing these compounds, the trivial names were given according to standard chlorosulfolipid nomenclature. The initial names were hexa- and undecachlorosulfolipids but will not be used in this thesis.

⁵⁰ M. Jacobson in “Towards a Structural Revision of Mytilipin B”, *Dissertation ETH No. 23251*, Zurich, **2016**.

chlorosulfolipids remains unknown. Mytilipin A (**30**) has also been isolated from the octocoral *Dedronephthya griffin* in the Taiwan Strait in 2010, highlighting the global presence of chlorosulfolipids and suggesting that the primary producer of these compounds serves as dietary source for other organisms.⁵¹

2.2 Biosynthesis

The structural features, in particular the complex chlorination pattern, of danicalipin A (**28**) inspired ELOVSON, HAINES, and MERCER to independently investigate the biosynthetic machinery involved in the formation of **28** (Scheme 8).



Scheme 8 Proposed biosynthetic route towards danicalipin A (**28**) in *O. danica*.

A first indication of the involved transformations was obtained by HAINES from feeding studies with ¹⁴C-labeled acetates, octanoates (C₈), laureates (C₁₂),

⁵¹ C.-H. Chao, H.-C. Huang, G.-H. Wang, Z.-H. Wen, W.-H. Wang, I.-M. Chen, J.-H. Sheu *Chem. Pharm. Bull.* **2010**, *58*, 944-946.

palmitates (C₁₆), oleates ((9Z)-C₁₈) and stearates (C₁₈). These were readily incorporated by *O. danica* into the chlorosulfolipid carbon chain.⁵² The incorporation of oleic acid suggested that the C14-hydroxy group is introduced into the unsaturated fatty acid by hydration of a double bond. MERCER noted later that the incorporation of unsaturated fatty acids (oleates and linoleates) is markedly less efficient when compared to the saturated fatty acids and excluded the presence of unsaturated fatty acid as biosynthetic intermediates.⁵³ Rather, a fatty acid synthase was invoked, which would produce docosanoic acid (**33**) as an intermediate (Scheme 8). ELOVSON was able to show that only the primary hydroxy group was ¹⁸O-enriched, when *O. danica* was grown in H₂¹⁸O.⁵⁴ This is consistent with an activated form of acid **33** being formed, e.g. a co-enzyme A (CoA) conjugate.⁵⁵ In the same study, ELOVSON reported that the C14-hydroxy group was derived from molecular oxygen, by growing the algae under an atmosphere of ¹⁸O₂. This would suggest an enzymatic hydroxylation of the saturated acid **33**, to give 14-hydroxydocosanoic acid (**34**). After reduction to diol **35**, sulfation with phosphoadenosine phosphosulfate (PAPS) would yield **36**.⁵⁶ Disulfate **36** was confirmed as a biosynthetic intermediate independently by both, MERCER⁵³ and HAINES⁵⁷, when ¹⁴C-labeled **36** was transformed to the corresponding ¹⁴C-labeled **28** in *O. danica*. This also indicated that sulfation precedes chlorination. MERCER gained some insight into the chlorinations by resubjecting partially chlorinated intermediates to the algae and reisolating molecules with more chlorines incorporated. This would be consistent with sequential, not necessarily ordered, chlorination events.⁵³ HAINES recognized the fact that unactivated carbons appear to be chlorinated and associated this observation with a free-radical mechanism for chlorination.⁵⁷

Given the discussion in Chapter 1.2, the hypothesis of a radical pathway is most likely in accordance with a non-heme iron halogenase, yet no investigations in this direction have been reported to date. The chlorination of unactivated carbons is conclusive with such an enzyme operating in the biosynthesis. Furthermore, an earlier

⁵² C. L. Mooney, E. M. Mahoney, M. Pousada, T. H. Haines *Biochemistry* **1972**, *11*, 4839-4844.

⁵³ G. Thomas, E. I. Mercer *Phytochemistry* **1974**, *13*, 797-805.

⁵⁴ J. Elovson *Biochemistry* **1974**, *13*, 2105-2109.

⁵⁵ S. R. Thorpe, C. C. Sweeley *Biochemistry* **1967**, *6*, 887-897.

⁵⁶ E. I. Mercer, G. Thomas, J. D. Harrison *Phytochemistry* **1974**, *13*, 1297-1302.

⁵⁷ C. L. Mooney, T. H. Haines *Biochemistry* **1973**, *12*, 4469-4472.

footnote in a review by HAINES hinted towards the formation of a brominated analogue of danicalipin A in the presence of bromide ions,⁴³ which agrees with the hypothesis of a non-heme iron halogenase. This brominated analog was isolated in 2016 by TSAI, VANDERWAL and co-workers.⁵⁸

2.3 Configurational and Conformational Analysis of Chlorosulfolipids

Gathering configurational information for chlorosulfolipids is no trivial task. The use of common methods, such as X-ray crystallography of the lipids or derivatives thereof, is hampered by their inability to form suitable crystals. Most of the isolated chlorosulfolipids were, in fact, oils and derivatization did not yield crystalline material either. In the earliest example, the relative configuration of the simplest member **27** (Figure 3) could be deduced by conversion to the *cis*-epoxide and its absolute configuration was obtained by comparison with known standards.³⁹ This approach is only applicable to very simple substrates and the more interesting chlorosulfolipids, such as **28–32** (Figure 3), cannot be elucidated in the same fashion.

A breakthrough was made when MURATA published his NMR-based method, named *J*-based configuration analysis (JBCA), to derive the relative configuration of polyoxygenated molecules in 1999.⁵⁹ The measurement of homo- and heteronuclear coupling constants ($^3J(\text{H,H})$, $^2J(\text{H,C})$, $^3J(\text{H,C})$) along a C–C bond gives rise to a characteristic pattern, which can be used to assign a conformation according to Table 3. The only exceptions are A-3 and B-3, which have the same coupling constant pattern. These can only be distinguished by the presence or absence of a NOE coupling between H(C1) and H(C4). The same method can be used to determine the conformation of *O*-substituted carbons to a neighboring methylene group by the same rules and the corresponding conformations are named C-1 to C-3 and D-1 to D-3, respectively.

⁵⁸ A. R. White, B. M. Duggan, S. C. Tsai, C. D. Vanderwal *Org. Lett.* **2016**, *18*, 1124-1127.

⁵⁹ N. Matsumori, D. Kaneno, M. Murata, H. Nakamura, K. Tachibana *J. Org. Chem.* **1999**, *64*, 866-876.

Table 3 *J*-based configuration analysis of *syn*- and *anti*-butanediol derivatives. The relative sizes of coupling constants obtained from 2D-NMR methods for the corresponding conformation of the substrates are given. Adapted with permission from ref. 59, Copyright 1999 American Chemical Society

	 <i>syn</i>			 <i>anti</i>		
$^3J(\text{H2},\text{H3})$	small	small	large	small	small	large
$^3J(\text{H2},\text{C4})$	small	large	small	large	small	small
$^3J(\text{C1},\text{H3})$	small	large	small	small	large	small
$^2J(\text{C2},\text{H3})$	small	large	large	large	small	large
$^2J(\text{C3},\text{H2})$	small	large	large	small	large	large

When CIMINIELLO and FATTORUSSO isolated mytilipin A (**30**), they realized the potential of MURATA's method.⁴⁸ Assuming similar sizes for the coupling constants in polyoxygenated and polychlorinated carbon chains, they applied JBCA to elucidate the correct relative configuration of **30**. The absolute configuration was established by MOSHER ester analysis,⁶⁰ thus allowing for the first time the configurational assignment of a complex chlorosulfolipid. In 2009, CARREIRA and co-workers undertook a systematic study on smaller polychlorinated fragments. They found that the values for coupling constants in polyoxygenated molecules had to be changed slightly for the polychlorinated analogs, but overall confirmed the initial assumption by CIMINIELLO and FATTORUSSO.⁶¹

In 2009, GERWICK, HAINES, and VANDERWAL used JBCA to elucidate the relative configuration of danicalipin A (**28**) almost 40 years after it had been first isolated.⁶² The absolute configuration was reported shortly thereafter by OKINO and co-workers.⁶³ In 2010, VANDERWAL and GERWICK collaborated once more and

⁶⁰ a) J. A. Dale, H. S. Mosher *J. Am. Chem. Soc.* **1973**, *95*, 512-519; b) G. R. Sullivan, J. A. Dale, H. S. Mosher *J. Org. Chem.* **1973**, *38*, 2143-2147; c) I. Ohtani, T. Kusumi, Y. Kashman, H. Kakisawa *J. Am. Chem. Soc.* **1991**, *113*, 4092-4096; d) T. R. Hoye, C. S. Jeffrey, F. Shao *Nature Protocols* **2007**, *2*, 2451-2458.

⁶¹ C. Nilewski, R. W. Geisser, M.-O. Ebert, E. M. Carreira *J. Am. Chem. Soc.* **2009**, *131*, 15866-15876.

⁶² D. K. Bedke, G. M. Shibuya, A. Pereira, W. H. Gerwick, T. H. Haines, C. D. Vanderwal *J. Am. Chem. Soc.* **2009**, *131*, 7570-7572.

⁶³ T. Kawahara, Y. Kumaki, T. Kamada, T. Ishii, T. Okino *J. Org. Chem.* **2009**, *74*, 6016-6024.

reported the absolute configuration of malhamensilipin A (**29**).⁶⁴ They revised the originally reported structure to include the C14-sulfate.

Unfortunately, when CIMINIELLO and FATTORUSSO attempted to determine the relative configurations of mytilipin B & C (**31** and **32**) by JBCA, the limits of the method became apparent. CARREIRA and co-workers succeeded in synthesizing nominal **31**, but the originally proposed structure appears to be misassigned (*cf.* Chapter 2.4.5).⁵⁰

2.4 Strategies Used in the Total Syntheses of Chlorosulfolipids

With no information on relative configuration, the synthesis of a chlorosulfolipid would necessitate synthesizing all possible diastereomers. Therefore, the chlorosulfolipids received little attention by synthetic organic chemists prior to their full structural elucidation. But since the characterization of the first chlorosulfolipids, synthetic organic chemists have developed a number of strategies to complete total syntheses of several members of this natural product family. The following chapter is meant to summarize key contributions and strategies in this field of research chronologically. Although there exist many other methods for the regio-, diastereo-, or enantioselective introduction of chlorine substituents, only transformations reported in the synthesis of chlorosulfolipids are going to be covered.⁶⁵

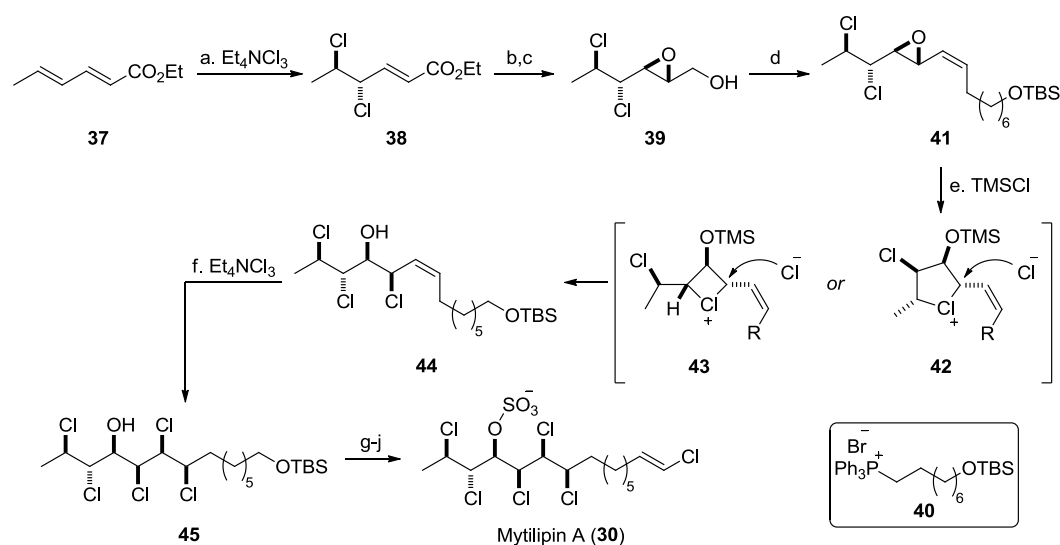
2.4.1 CARREIRA's Synthesis of Mytilipin A

In 2009, NILEWSKI, GEISSER, and CARREIRA were the first to report the total synthesis of a chlorosulfolipid.⁶⁶ Their strategy revolved around a series of selective dichlorinations and epoxide openings, and linking of two long fragments by a WITTIG reaction (Scheme 9).

⁶⁴ A. R. Pereira, T. Byrum, G. M. Shibuya, C. D. Vanderwal, W. H. Gerwick *J. Nat. Prod.* **2010**, *73*, 279-283.

⁶⁵ For a recent review on stereoselective halogenations in natural product synthesis, see: W.-j. Chung, C. D. Vanderwal *Angew. Chem. Int. Ed.* **2016**, *55*, 4396-4434.

⁶⁶ C. Nilewski, R. W. Geisser, E. M. Carreira *Nature* **2009**, *457*, 573-576.



Scheme 9 CARREIRA's total synthesis of mytilipin A (**30**). Reagents and conditions: a) Et_4NCl_3 , CH_2Cl_2 , 0°C , 68%; b) $(i\text{-Bu})_2\text{AlH}$, toluene, 0°C , 72%; c) $m\text{-CPBA}$, CH_2Cl_2 , 0°C to r.t., 95%, d.r. = 1:1; d) TPAP (5 mol%), NMO, 4 Å molecular sieves, CH_2Cl_2 , r.t., then **40**/ $n\text{-BuLi}$, THF, -78°C to r.t., 34% (56% brsm); e) TMSCl , $\text{EtOAc}/\text{CH}_2\text{Cl}_2$, r.t., 43% (73% brsm); f) Et_4NCl_3 , CH_2Cl_2 , -78°C , 93%, d.r. = 10:1; g) (+)-CSA (10 mol%), MeOH, r.t., 98%; h) $\text{PhI}(\text{OAc})_2$, TEMPO, CH_2Cl_2 , r.t.; i) CrCl_2 , CHCl_3 , THF, 65°C , 47% over 2 steps; j) SO_3 /pyridine, THF, r.t., 99%.

The synthesis commenced with dichlorination of ethyl sorbate (**37**). The use of MIOSKOWSKI's reagent (Et_4NCl_3) was particularly useful in selectively chlorinating the less electron-deficient olefin in **37**. MIOSKOWSKI's reagent had been developed in 1997 as a crystalline source of chlorine, which can be easily handled and stored.⁶⁷ Enoate **38** was reduced and epoxidized to give primary alcohol **39**. LEY–GRIFFITH oxidation⁶⁸ and WITTIG reaction⁶⁹ with **40**, resulted in *Z*-olefin **41**. An interesting observation was made, when the authors tried to open the epoxide. Initially, an opening of a *cis*-epoxide with TMSCl was attempted,⁷⁰ but JBCA revealed the major product of this reaction to have undergone opening with retention of configuration at the allylic position. Hence, the *trans*-epoxide **41** was opened, giving *syn*-chlorohydrin **44**. The selectivity was attributed to anchimeric assistance by the neighboring chloride *via* chloronium ions **42** or **43**. A systematic study by SHEMET *et al.* uncovered preferential pathways through the four-membered chloretanium ions (Scheme 10).⁷¹ When bishomoallylic chloroepoxide **46** was treated with trimethylsilyl chloride, a

⁶⁷ T. Schlama, K. Gabriel, V. Gouverneur, C. Mioskowski *Angew. Chem. Int. Ed.* **1997**, *36*, 2342-2344.

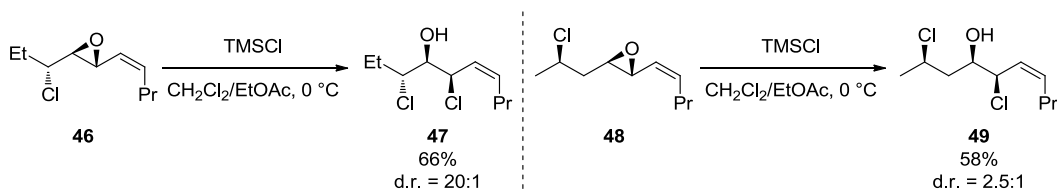
⁶⁸ W. P. Griffith, S. V. Ley, G. P. Whitcombe, A. D. White *J. Chem. Soc., Chem. Commun.* **1987**, 1625-1627.

⁶⁹ a) G. Wittig, U. Schöllkopf *Chem. Ber.* **1954**, *87*, 1318-1330; b) G. Wittig, W. Haag *Chem. Ber.* **1955**, *88*, 1654-1666.

⁷⁰ N. Daviu, A. Delgado, A. Llebaria *Synlett* **1999**, 1243-1244.

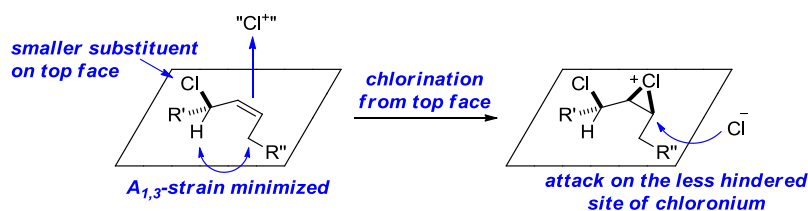
⁷¹ A. Shemet, D. Sarlah, E. M. Carreira *Org. Lett.* **2015**, *17*, 1878-1881.

high selectivity for stereoretention at the allylic position was observed. The selectivity for the opening of trishomoallylic epoxide **48** was lower, suggesting the four-membered intermediate to be operational.



Scheme 10 Stereoretentive epoxide opening, as investigated by SHEMET *et al.*⁷¹

CARREIRA's synthesis of **30** continued with the dichlorination of olefin **44** with MIOSKOWSKI's reagent. The high diastereoselectivity (10:1) for this reaction can be explained by the model in Scheme 11. After minimizing the allylic 1,3-strain, the initial attack onto the chlorine would occur with the less hindered face of the olefin, the one containing the chlorine substituent. The resulting chloronium would then be opened on the sterically less hindered site of the three membered ring, namely the one at the terminal end of the stereoheaxad. Similar selectivities had been observed by VANDERWAL during the dichlorination of allylic alcohol derivatives.⁷² The synthesis of **30** was accomplished in four further steps. Deprotection of the primary alcohol in **45** and oxidation to the aldehyde preceded TAKAI-UTIMOTO olefination⁷³ and sulfation with $\text{SO}_3 \cdot \text{pyridine}$.



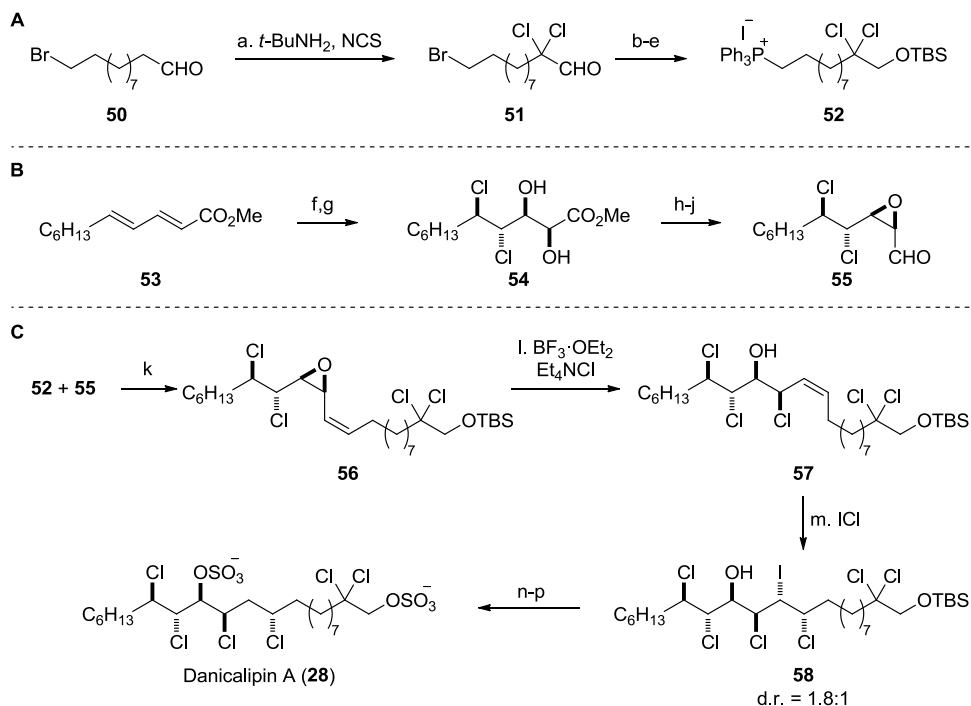
Scheme 11 Stereochemical model for the dichlorination of **44**.

⁷² G. M. Shibuya, J. S. Kanady, C. D. Vanderwal *J. Am. Chem. Soc.* **2008**, *130*, 12514-12518.

⁷³ K. Takai, K. Nitta, K. Utimoto *J. Am. Chem. Soc.* **1986**, *108*, 7408-7410.

2.4.2 VANDERWAL'S Synthesis of Danicalipin A, Malhamensilipin A, and Mytilipin A

Shortly after CARREIRA's synthesis of the first chlorosulfolipid, GERWICK, HAINES, and VANDERWAL published a synthesis of danicalipin A (**28**). Their synthesis also relied on epoxide openings, dihalogenations, and a WITTIG reaction to assemble the natural product (Scheme 12).⁶²



Scheme 12 VANDERWAL's total synthesis of danicalipin A (**28**). **A:** Synthesis of fragment **52**; **B:** Synthesis of fragment **55**; **C:** Joining of the fragments and completion of the synthesis. Reagents and conditions: a) i: *t*-BuNH₂, 10 °C; ii: NCS, CH₂Cl₂/CCl₄, r.t.; iii: aq. HCl, r.t.; b) NaBH₄, EtOH, 0 °C to r.t., 75% over 2 steps; c) TBSCl, imidazole, 0 °C to r.t., 95%; d) NaI, acetone, reflux, 95%; e) PPh₃, toluene, reflux, 95%; f) Et₄NCl₃, CH₂Cl₂, -78 °C; g) OsO₄ (4 mol%), NMO, *t*-BuOH/H₂O, 0 °C, 47% over 2 steps; h) NsCl, pyridine, 55 °C, 72%; i) K₂CO₃, MeOH, r.t., 80%; j) (*i*-Bu)₂AlH, toluene, -78 °C, 85%; k) **52**, KHMDS, THF, -78 to 0 °C, then **55**, -78 to 0 °C, *Z:E* = 2.5:1; l) BF₃·OEt₂, Et₄NCl, CH₂Cl₂, r.t., 30% over 2 steps; m) ICl, CH₂Cl₂, -78 °C to r.t.; d.r. = 1.8:1; n) Bu₃SnH, Et₃B, O₂, -78 °C, 30% over 2 steps; o) Et₃N·3HF, CH₂Cl₂, r.t., 87%; p) ClSO₃H, CH₂Cl₂, r.t., 66%.

The synthesis of fragment **52** commenced with a DE KIMPE α,α -dichlorination of 11-bromoundecanal (**50**, Scheme 12A).⁷⁴ Reduction of the aldehyde functionality, TBS-protection of the resulting primary alcohol, FINKELSTEIN reaction,⁷⁵ and phosphonium formation completed the synthesis of fragment **52**.

⁷⁴ R. Verhé, N. de Kimpe, L. de Buyck, N. Schamp *Synthesis* **1975**, 455-456.

⁷⁵ H. Finkelstein *Ber.* **1910**, *43*, 1528-1532.

Fragment **55** was synthesized from dienoic ester **53**. As in CARREIRA's synthesis of mytilipin A (**30**), dichlorination with MIOSKOWSKI's reagent⁶⁷ gave an *anti*-dichloroenoate (Scheme 12B). Dihydroxylation with catalytic OsO₄ gave **54**, whose stereoselectivity was in agreement with KISHI's model.⁷⁶ Following procedures by SHARPLESS and co-workers, the more reactive α -hydroxy group was converted to the nosylate, followed by formation of epoxide **55** under basic conditions.⁷⁷

The two fragments were combined in a WITTIG reaction⁶⁹ to give **56**, albeit in a relatively low *Z:E* ratio of 2.5:1 (Scheme 12C). In order to avoid stereoretentive epoxide opening of **56** (*cf.* Chapter 2.4.1), the authors used an excess of BF₃·OEt₂ and Et₄NCl to obtain **57** in 30% yield over both steps. Iodochlorination of the *Z*-olefin in **57** was achieved with ICl, but in contrast to the formation of **45** (Scheme 9) the reaction proved less selective, giving **58** as an inseparable mixture of diastereomers in a ratio of 1.8:1. Radical deiodination allowed separation of the diastereomers, with a yield of 30% over both steps. The synthesis of danicalipin A (**28**) was completed by deprotection of the primary TBS ether and sulfation with chlorosulfonic acid.

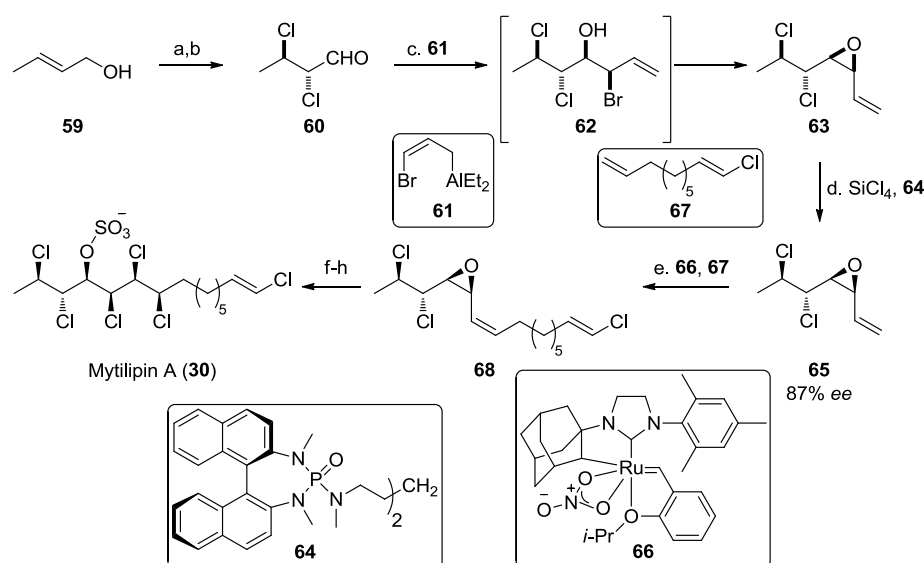
In 2010, VANDERWAL and co-workers reported a very similar strategy to synthesize malhamensilipin A (**29**) enantioselectively, but due to the close resemblance in strategy the route will not be discussed here.⁷⁸ In 2013, a revised approach was reported for the synthesis of mytilipin A (**30**) (Scheme 13).⁷⁹

⁷⁶ J. K. Cha, W. J. Christ, Y. Kishi *Tetrahedron* **1984**, *40*, 2247-2255.

⁷⁷ P. R. Fleming, K. B. Sharpless *J. Org. Chem.* **1991**, *56*, 2869-2875.

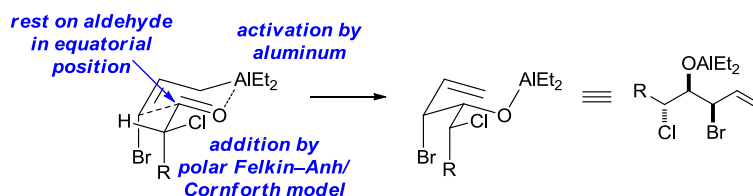
⁷⁸ D. K. Bedke, G. M. Shibuya, A. R. Pereira, W. H. Gerwick, C. D. Vanderwal *J. Am. Chem. Soc.* **2010**, *132*, 2542-2543.

⁷⁹ W.-j. Chung, J. S. Carlson, D. K. Bedke, C. D. Vanderwal *Angew. Chem. Int. Ed.* **2013**, *52*, 10052-10055.



Scheme 13 VANDERWAL's total synthesis of mytilipin A (**30**). Reagents and conditions: a) Cl_2 , Et_4NCl , CH_2Cl_2 , 0°C , 89%; b) DMP, NaHCO_3 , CH_2Cl_2 , 0°C to r.t.; c) **61**, -78°C , then aq. NaOH , Et_4NCl , 0°C , 52%, d.r. = 98:2; d) **64** (20 mol%), SiCl_4 , $i\text{-Pr}_2\text{NEt}$, CH_2Cl_2 , -78°C , 43%, 87% ee; e) **66** (30 mol%), **67**, $\text{CH}_2\text{Cl}_2/\text{DCE}$, r.t., 32%, $Z:E >20:1$; f) $\text{BF}_3 \cdot \text{OEt}_2$, Et_4NCl , CH_2Cl_2 , -78°C ; g) Et_4NCl_3 , CH_2Cl_2 , -78°C , 86%, d.r. = 97:3; h) $\text{SO}_3 \cdot \text{pyridine}$, THF, r.t., 94%.

In this synthesis, several steps are different and worth noting. The formation of bromohydrin **62** with allyl aluminum derivative **61** is a highly selective reaction. This type of reaction was pioneered by HOSOMI and co-workers in order to gain access to substituted *cis*-epoxides.⁸⁰ The high stereoselectivity of this reaction can be explained *via* a 6-membered transition state (Scheme 14). Coordination of the aluminum reagent activates the aldehyde for nucleophilic attack. The reaction proceeds through a chair-like transition state, in which the bromine resides in an axial position due to olefin geometry and the aliphatic residue on the aldehyde occupies the equatorial position. This ultimately yields a *syn*-bromohydrin. The α -stereocenter determines the *anti*-configuration of the resulting chlorohydrin, in accordance with the polar FELKIN–ANH and the CORNFORTH models.⁸¹



Scheme 14 Stereochemical model for the observed selectivity during the formation of **62**.

⁸⁰ A. Hosomi, S. Kohra, Y. Tominaga, M. Ando, H. Sakurai *Chem. Pharm. Bull.* **1987**, *35*, 3058-3061.

⁸¹ For a detailed discussion, see: V. J. Cee, C. J. Cramer, D. A. Evans *J. Am. Chem. Soc.* **2006**, *128*, 2920-2930.

Another noteworthy step is the kinetic resolution of chiral vinyl epoxide **63**, which gave enantioenriched **65** in 43% yield (87% *ee*). This method has been developed by DENMARK for the enantioselective opening of *meso*-epoxides.⁸² Phosphoramides, such as **64**, are hypothesized to displace a chloride on SiCl₄, rendering it more LEWIS acidic and allowing coordination of the epoxide. The activated epoxide is then opened to give an enantioenriched chlorohydrin. Non-linear effects during the reaction led to development of the dimeric catalyst **64**.⁸³

The *Z*-selective cross-metathesis⁸⁴ of **65** and **67** was implemented in order to replace the poorly selective WITTIG reaction in the syntheses of danicalipin A (**28**, Scheme 12) and malhamensilipin A (**30**). Despite the higher *Z:E* ratio (>20:1), the yield of olefin **68** remained low (32%), since no turnover of catalyst **66** could be achieved. Other vinyl epoxides performed better in this reaction, indicating an inherent and unresolved problem with the chlorinated vinyl epoxide **65**. In a later publication, VANDERWAL applied the same strategies to enantioselective syntheses of danicalipin A (**28**) and malhamensilipin A (**29**).⁸⁵

⁸² S. E. Denmark, P. A. Barsanti, K.-T. Wong, R. A. Stavenger *J. Org. Chem.* **1998**, *63*, 2428-2429.

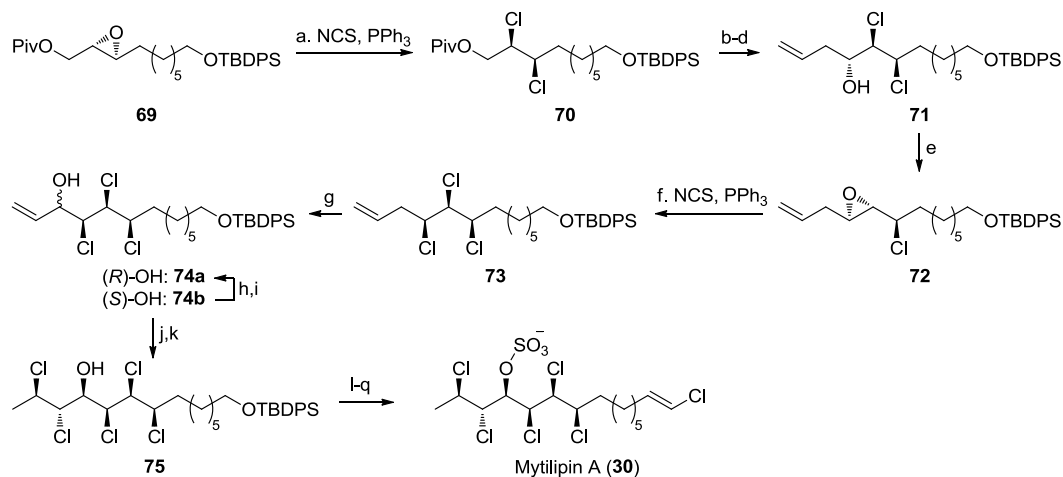
⁸³ S. E. Denmark, P. A. Barsanti, G. L. Beutner, T. W. Wilson *Adv. Synth. Catal.* **2007**, *349*, 567-582.

⁸⁴ a) K. Endo, R. H. Grubbs *J. Am. Chem. Soc.* **2011**, *133*, 8525-8527; b) B. K. Keitz, K. Endo, P. R. Patel, M. B. Herbert, R. H. Grubbs *J. Am. Chem. Soc.* **2012**, *134*, 693-699.

⁸⁵ W.-j. Chung, J. S. Carlson, C. D. Vanderwal *J. Org. Chem.* **2014**, *79*, 2226-2241.

2.4.3 YOSHIMITSU'S Synthesis of Mytilipin A and Danicalipin A

In 2010, YOSHIMITSU and co-workers published a synthetic route to mytilipin A (**30**) that utilized different disconnections. The synthesis relied on dichlorinative epoxide openings developed in their group (Scheme 15).⁸⁶



Scheme 15 YOSHIMITSU'S total synthesis of mytilipin A (**30**). Reagents and conditions: a) NCS, PPh₃, toluene, 90 °C, 85%; b) (*i*-Bu)₂AlH, CH₂Cl₂, -78 °C, 95%; c) DMP, NaHCO₃, CH₂Cl₂, r.t.; d) allyltrimethylsilane, BF₃·OEt₂, CH₂Cl₂, -78 to 0 °C, 72% over 2 steps, d.r. = 3.8:1; e) NaH, THF, 0 °C to r.t., 97%; f) NCS, PPh₃, DCE, 90 °C, 70%; g) SeO₂, *t*-BuOOH, salicylic acid (cat.), DCE, 49% (69% brsm), d.r. (**74a/74b**) = 3:5; h) DMP, NaHCO₃, CH₂Cl₂, r.t.; i) NaBH₄, CeCl₃·7H₂O, MeOH, 0 °C, 81% over 2 steps; j) GRUBBS' second generation catalyst, 2-butene, CH₂Cl₂, r.t., 93%; k) KMnO₄, BnEt₃NCl, TMSCl, CH₂Cl₂, -78 to 0 °C, 38% of **75**, d.r. = 3.8:1:2.6; l) Ac₂O, Et₃N, DMAP, CH₂Cl₂, r.t., quant.; m) aq. HF, pyridine, THF, r.t., 94%; n) DMP, CH₂Cl₂, r.t., 98%; o) CrCl₂, CHCl₃, THF, 65 °C, 75%; p) (*i*-Bu)₂AlH, CH₂Cl₂, -78 °C, 96%; q) SO₃, pyridine, DMF, r.t., 75%.

The synthesis commenced from epoxide **69**, which had been obtained from SHARPLESS' asymmetric epoxidation⁸⁷ and alcohol protection. The epoxide was opened with a combination of NCS and PPh₃ to give dichloride **70**. This method was developed by YOSHIMITSU as a substantial improvement on earlier reports of similar transformations. In 1972, ISAACS and KIRKPATRICK had reported that the same two-component system, that is used in the APPEL reaction⁸⁸ for the stereospecific displacement of primary and secondary alcohols (CCl₄ and PPh₃), is capable of opening epoxides stereospecifically to the *vic*-dichlorides.⁸⁹ However, this method did not find many applications, presumably due to low yields and many by-products.

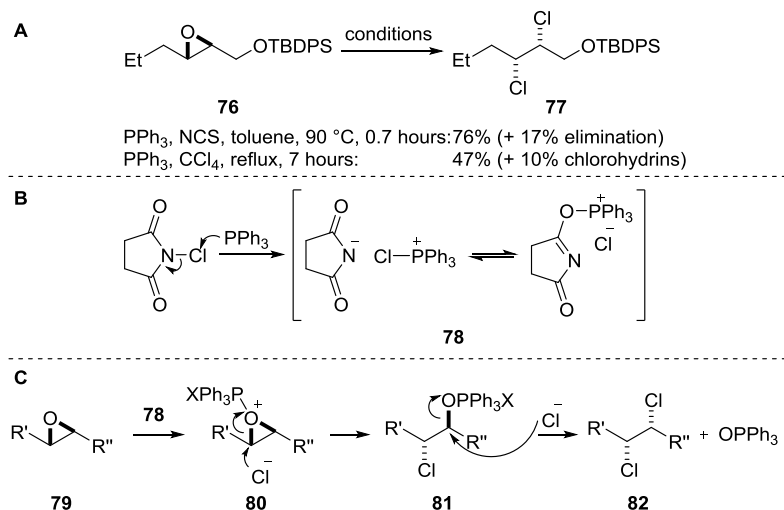
⁸⁶ T. Yoshimitsu, N. Fukumoto, R. Nakatani, N. Kojima, T. Tanaka *J. Org. Chem.* **2010**, *75*, 5425-5437.

⁸⁷ T. Katsuki, K. B. Sharpless *J. Am. Chem. Soc.* **1980**, *102*, 5974-5976.

⁸⁸ For an early review, see: R. Appel *Angew. Chem. Int. Ed.* **1975**, *14*, 801-811.

⁸⁹ N. S. Isaacs, D. Kirkpatrick *Tetrahedron Lett.* **1972**, *13*, 3869-3870.

YOSHIMITSU's conditions were found to be superior, generally delivering the dichloride in good yields with negligible by-product formation (Scheme 16A).⁹⁰



Scheme 16 Dichlorinative epoxide-opening reported by YOSHIMITSU. **A**: Comparison of APPEL's and YOSHIMITSU's conditions in the epoxide opening of **76**; **B**: Formation of the reactive intermediate **78**; **C**: Mechanism for the epoxide opening, X = succinimide anion or chloride.

The reaction is thought to proceed from a reactive intermediate, which is formed from PPh₃ and NCS, e.g. **78** (Scheme 16B). This reactive intermediate can then activate epoxide **79**. A chloride opens **80**, resulting in **81**, an intermediate that is also formed in the APPEL reaction. The alcohol is activated towards displacement by another chloride, leading to *vic*-dichloride **82** under expulsion of triphenylphosphine oxide (Scheme 16C).

YOSHIMITSU's synthesis of mytilipin A (**30**) then carries on with a sequence comprised of deprotection of the pivaloate, DESS–MARTIN oxidation⁹¹ of the resulting primary alcohol, and allylation. The selectivity of the allylation follows the same models as in VANDERWAL's synthesis of **30** (*cf.* Scheme 14). Chlorohydrin **71** is closed to epoxide **72**, setting the stage for another dichlorinative epoxide opening. Subsequently, modified RILEY oxidation⁹² gave a diastereomeric mixture (3:8) of allylic alcohols **74a** and **74b**. The major diastereomer **74b** could be converted to the desired allylic alcohol **74a** *via* oxidation and diastereoselective reduction. After cross-

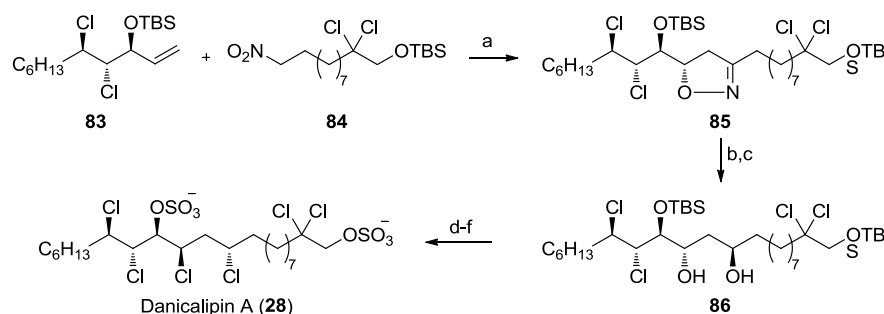
⁹⁰ T. Yoshimitsu, N. Fukumoto, T. Tanaka *J. Org. Chem.* **2009**, *74*, 696-702.

⁹¹ D. B. Dess, J. C. Martin *J. Org. Chem.* **1983**, *48*, 4155-4156.

⁹² H. L. Riley, J. F. Morley, N. A. C. Friend *J. Chem. Soc.* **1932**, 1875-1883.

metathesis with 2-butene⁹³ in the presence of GRUBBS' second generation catalyst,⁹⁴ the olefin was dichlorinated under MARKÓ–MAGUIRE conditions (KMnO₄, BnEt₃NCl, and TMSCl),⁹⁵ giving **75** in 38% yield with substantial formation of other diastereomers. The lack of selectivity was attributed to high conformational flexibility of the substrate, but protection with a trichloroacetate group⁷² led to preferential formation of undesired diastereomers. The synthesis of **30** was completed in a similar fashion to CARREIRA's synthesis (*cf.* Chapter 2.4.1).

In 2011, YOSHIMITSU published the synthesis of danicalipin A (**28**), following similar strategies to obtain intermediates **83** and **84** (Scheme 17).⁹⁶ The two fragments were joined by 1,3-dipolar cycloaddition between olefin **83** and a nitrile-oxide, generated *in situ* from **84** and an isocyanate,⁹⁷ followed by reduction of the dihydroisoxazoline in **85** with Mo(CO)₆.⁹⁸ The resulting β -hydroxyketone was reduced in an alkoxy-directed reduction with Me₄NBH(OAc)₃.⁹⁹ The diol was subjected to YOSHIMITSU's conditions (NCS and PPh₃), upon which both alcohols were displaced by chlorides in 38% yield. Deprotection and sulfation yielded danicalipin A (**28**).



Scheme 17 Final steps of YOSHIMITSU's total synthesis of danicalipin A (**28**). Reagents and conditions: a) PhNCO, Et₃N, toluene, 60%, d.r. = 7.3:1; b) Mo(CO)₆, MeCN/H₂O, 90 °C, 81%; c) Me₄NBH(OAc)₃, AcOH/MeCN/CH₂Cl₂, 0 °C, 84%, d.r. = 6:1; d) NCS, PPh₃, DCE, 90 °C, 38%; e) AcCl, MeOH, 80 °C, 97%; f) SO₃·pyridine, DMF, r.t., 94%.

⁹³ A. K. Chatterjee, T. L. Choi, D. P. Sanders, R. H. Grubbs *J. Am. Chem. Soc.* **2003**, *125*, 11360-11370.

⁹⁴ M. Scholl, S. Ding, C. W. Lee, R. H. Grubbs *Org. Lett.* **1999**, *1*, 953-956.

⁹⁵ I. E. Markó, P. R. Richardson, M. Bailey, A. R. Maguire, N. Coughlan *Tetrahedron Lett.* **1997**, *38*, 2339-2342.

⁹⁶ T. Yoshimitsu, R. Nakatani, A. Kobayashi, T. Tanaka *Org. Lett.* **2011**, *13*, 908-911.

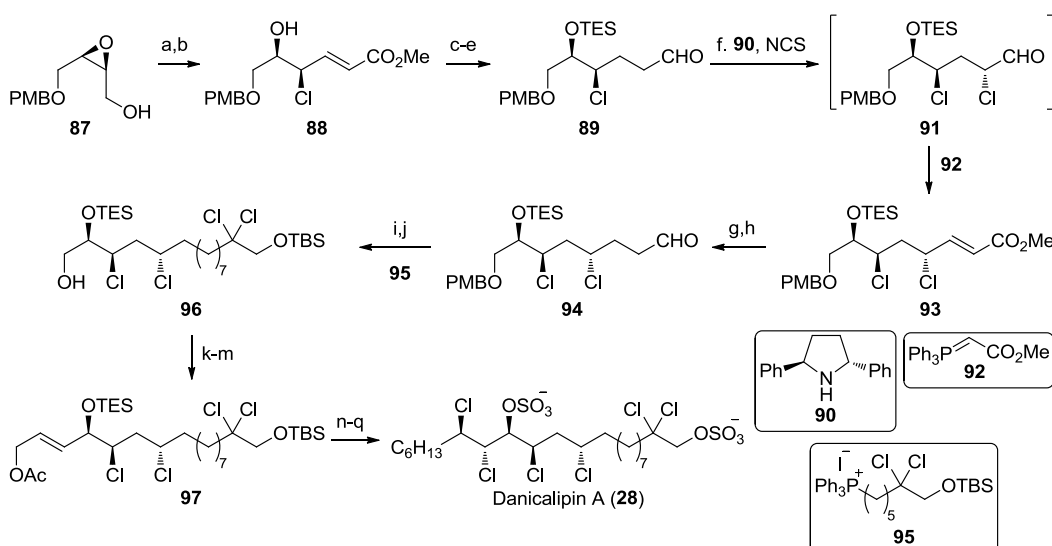
⁹⁷ T. Mukaiyama, T. Hoshino *J. Am. Chem. Soc.* **1960**, *82*, 5339-5342.

⁹⁸ P. G. Baraldi, A. Barco, S. Benetti, S. Manfredini, D. Simoni *Synthesis* **1987**, 276-278.

⁹⁹ D. A. Evans, K. T. Chapman, E. M. Carreira *J. Am. Chem. Soc.* **1988**, *110*, 3560-3578.

2.4.4 UMEZAWA and MATSUDA's Synthesis of Danicalipin A

In 2011, UMEZAWA and MATSUDA reported the total synthesis of danicalipin A (**28**). Their approach made use of several WITTIG reactions of stabilized ylides to introduce functionality to the molecule. Ultimately, their disconnections led them back to pseudo-symmetric epoxide **87** (Scheme 18).¹⁰⁰



Scheme 18 UMEZAWA and MATSUDA's total synthesis of danicalipin A (**28**). Reagents and conditions: a) TEMPO (10 mol%), PhI(OAc)₂, CH₂Cl₂, r.t., then **92**, 72%; b) SOCl₂, Et₂O, 0 °C, 96%; c) LiBH₄, THF, 0 °C; d) TESOTf, 2,6-lutidine, 0 °C, 85% over 2 steps; e) (COCl)₂, DMSO, CH₂Cl₂, -78 to -40 °C, then Et₃N, -40 °C to r.t., 89%; f) **90** (10 mol%), BrCH₂CO₂Et (10 mol%), NCS, DCE, 0 °C, then **92**, 85%; g) LiBH₄, THF/MeOH, r.t., 91%; h) TEMPO (20 mol%), PhI(OAc)₂, r.t., 87%; i) **95**, NaHMDS, THF, -78 °C, then **94**, -78 to 0 °C, 83%; j) Pd(OH)₂/C, H₂, CH₂Cl₂, r.t., 81%; k) TEMPO (20 mol%), PhI(OAc)₂, CH₂Cl₂, r.t., then MeO₂C(H)C=PBu₃, 86%; l) (*i*-Bu)₂AlH, CH₂Cl₂/toluene, 0 °C; m) Ac₂O, DMAP, CH₂Cl₂, r.t., 97% over 2 steps; n) *n*-C₅H₁₁MgBr, Li₂CuCl₄ (10 mol%), THF, 0 °C; o) Bu₄NF, AcOH, THF, r.t., 43% over 2 steps; p) KMnO₄, BnEt₃NCl, TMSCl, CH₂Cl₂, octane, 90 °C, 39%; q) ClSO₃H, CH₂Cl₂, r.t., 53%.

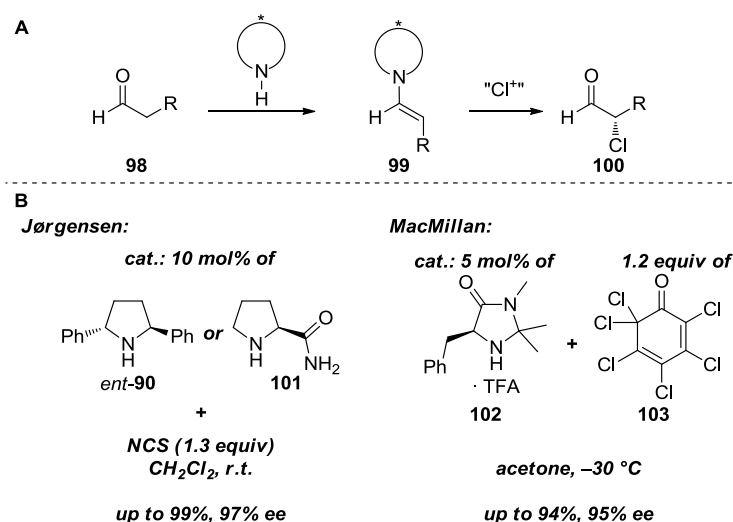
Enantioenriched epoxide **87**¹⁰¹ was converted to the α,β -unsaturated- γ,δ -epoxy ester, which was opened selectively at the more reactive site of the epoxide with thionyl chloride, resulting in chlorohydrin **88**. A three-step sequence then gave aldehyde **89**. The subsequent α -chlorination required the use of a chiral catalyst. Such transformations had been developed by the groups of JØRGENSEN¹⁰² and MACMILLAN¹⁰³ independently in 2004 (Scheme 19).

¹⁰⁰ T. Umezawa, M. Shibata, K. Kaneko, T. Okino, F. Matsuda *Org. Lett.* **2011**, *13*, 904-907.

¹⁰¹ B. M. Trost, S. T. Wroblewski, J. D. Chisholm, P. E. Harrington, M. Jung *J. Am. Chem. Soc.* **2005**, *127*, 13589-13597.

¹⁰² N. Halland, A. Braunton, S. Bachmann, M. Marigo, K. A. Jørgensen *J. Am. Chem. Soc.* **2004**, *126*, 4790-4791.

¹⁰³ M. P. Brochu, S. P. Brown, D. W. C. MacMillan *J. Am. Chem. Soc.* **2004**, *126*, 4108-4109.



Scheme 19 Enamine catalysis for the α -chlorination of aldehydes. **A** Simplified mechanism; **B** Comparison of the conditions developed in the groups of JØRGENSEN and MACMILLAN. Adapted with permission from ref. 50.

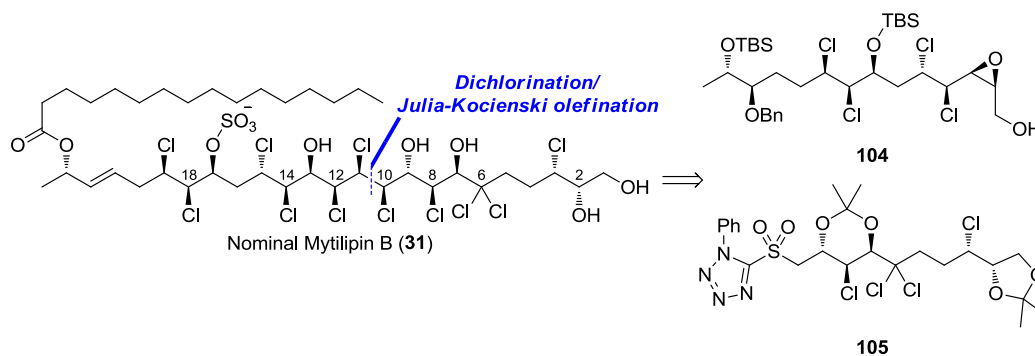
Both transformations employ organocatalysts that form an intermediate enamine **99** and thereby activate the α -position of aldehyde **98** (Scheme 19A). JØRGENSEN developed the reaction, using chiral pyrrolidine catalyst **90** or prolinamide (**101**) with NCS as the chlorinating agent. The pyrrolidine catalyst usually outperforms prolinamide in terms of enantioselectivity, but yields are better for **101**. MACMILLAN reported the use of imidazolidinone **102** as the chiral catalyst and **103** as the chlorinating agent.

In UMEZAWA and MATSUDA's synthesis of **28**, catalyst **90** in combination with NCS gave α -chloro aldehyde **91**, which underwent WITTIG reaction⁶⁹ with stabilized phosphonium ylide **92** to give γ -chloroenoate **93** in 85% yield. Through a sequence of reductions, oxidations, and WITTIG reactions **93** was elaborated to allylic acetate **97**. The primary allylic acetate in **97** was then displaced with an alkyl-GRIGNARD reagent under copper catalysis.¹⁰⁴ After deprotection of the secondary alcohol, the remaining olefin was dichlorinated under MARKÓ-MAGUIRE conditions (KMnO₄, BnEt₃NCl, TMSCl).⁹⁵ The dichlorination proceeded with 39% yield, but no indication about the diastereoselectivity of this dichlorination was made in this paper *vis-à-vis* the similar reaction by YOSHIMITSU (*cf.* Chapter 2.4.3). The synthesis of **28** was completed by sulfation with chlorosulfonic acid.

¹⁰⁴ J. E. Bäckvall, M. Sellen, B. Grant *J. Am. Chem. Soc.* **1990**, *112*, 6615-6621.

2.4.5 CARREIRA's Synthesis of Nominal Mytilipin B

Having gained some experience in the chemistry of chlorosulfolipids, CARREIRA and co-workers decided to synthesize the most complex member of this family, mytilipin B (**31**). In 2011, they published their route, noting that a structural revision would be necessary, since the assigned structure of **31** did not match the spectroscopic data of the isolated natural product.¹⁰⁵ The retrosynthetic approach is outlined in Scheme 20. A convergent synthesis was designed by tracing the C10–C11 bond back to an olefin, which was cleaved by a JULIA–KOCIENSKI coupling. The two fragments **104** and **105** were of similar complexity and allowed for an efficient synthesis.



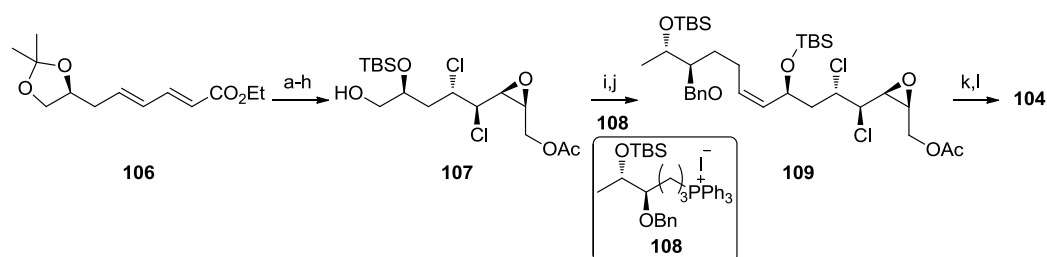
Scheme 20 Retrosynthetic analysis of CARREIRA's total synthesis of nominal mytilipin B (**31**).

The synthesis of fragment **104** began with the dichlorination of **106**¹⁰⁶ using MIOSKOWSKI's reagent⁶⁷ (Scheme 21) in 66% yield. The diastereoselectivity for this reaction was only 1.8:1, which could be expected, given that there are no strongly biasing stereochemical elements in the proximity of the olefin. After reduction of the ester and protection of the resulting primary alcohol as the acetate, the substrate was subjected to SHARPLESS' asymmetric dihydroxylation¹⁰⁷ in order to overcome the inherent preference of the enoate for *anti*-substitution (*cf.* Chapter 2.4.1). The *syn*-diol was closed to the *cis*-epoxide (*cf.* Chapter 2.4.2), followed by protecting group manipulations to give primary alcohol **107**. Oxidation of **107** preceded WITTIG reaction⁶⁹ with **108**, resulting in olefin **109**. Dichlorination with MIOSKOWSKI's

¹⁰⁵ C. Nilewski, N. R. Deprez, T. C. Fessard, D. B. Li, R. W. Geisser, E. M. Carreira *Angew. Chem. Int. Ed.* **2011**, *50*, 7940-7943.

¹⁰⁶ **106** was obtained from (*S*)-butanediol in 4 steps, see Supporting Information of ref. 105.

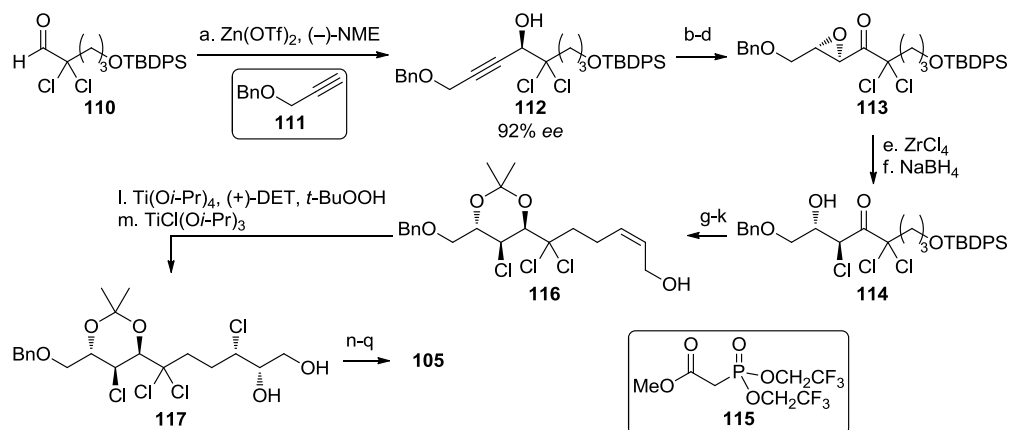
¹⁰⁷ For a comprehensive review, see: H. C. Kolb, M. S. VanNieuwenhze, K. B. Sharpless *Chem. Rev.* **1994**, *94*, 2483-2547.



Scheme 21 CARREIRA's synthesis of fragment **104**. Reagents and conditions: a) Et_4NCl_3 , CH_2Cl_2 , 0°C , 66%, d.r. = 1.8:1; b) $(i\text{-Bu})_2\text{AlH}$, toluene, 0°C , 43%; c) AcCl , DMAP (cat.), Et_3N , CH_2Cl_2 , 0°C , 81%; d) AD-mix β , MeSO_2NH_2 , $t\text{-BuOH}/\text{H}_2\text{O}$, 74%; e) DABCO, Tf_2O , CH_2Cl_2 , -78°C to r.t., 50%; f) CSA (cat.), MeOH , r.t., 72%; g) TBSOTf , 2,6-lutidine, CH_2Cl_2 , -78 to -15°C , 91%; h) HF-pyridine, pyridine, THF, 0 to 4°C , 40% (85% brsm); i) DMP, CH_2Cl_2 , r.t., 87%; j) **108**, KHMDs , THF, 0°C , then aldehyde, -78 to 0°C ; k) Et_4NCl_3 , CH_2Cl_2 , -78°C , 71%, d.r. = 5:1; l) K_2CO_3 , MeOH , 0°C , 98%.

reagent proceeded in 71% yield and 5:1 d.r., which completed the synthesis of **104** after hydrolysis of the primary acetate.

The synthesis of **105** is depicted in Scheme 22. An enantioselective zinc-mediated coupling of **110** and **111** provided propargylic alcohol **112** in 70% yield and 92% *ee*.¹⁰⁸ This method was later extended to other *gem*-dichloro aldehydes.¹⁰⁹



Scheme 22 CARREIRA's synthesis of fragment **105**. Reagents and conditions: a) **111**, $\text{Zn}(\text{OTf})_2$, $(-)\text{-}N$ -methylephedrine, Et_3N , toluene, r.t., 70%, 92% *ee*; b) $\text{NaAlH}_2(\text{OCH}_2\text{CH}_2\text{OCH}_3)_2$, THF, -78°C , 92%; c) $\text{VO}(\text{acac})_2$ (10 mol%), $t\text{-BuOOH}$, CH_2Cl_2 , 0°C to r.t., 62%; d) DMP, CH_2Cl_2 , 0°C to r.t., 95%; e) ZrCl_4 , CH_2Cl_2 , 0°C to r.t.; f) NaBH_4 , MeOH , -78°C , 36% over 2 steps; g) $\text{CH}_3\text{CH}(\text{OCH}_3)\text{CH}_2$, PPTS, CH_2Cl_2 , 0°C to r.t., 93%; h) Bu_4NF , AcOH , DMF, r.t., 95%; i) DMP, CH_2Cl_2 , 0°C to r.t.; j) **115**, KHMDs , THF, -78°C , 68%; k) $(i\text{-Bu})_2\text{AlH}$, THF, -78°C , 88%; l) $\text{Ti}(\text{O}i\text{-Pr})_4$, $(+)\text{-diethyl L-tartrate}$, $t\text{-BuOOH}$, CH_2Cl_2 , -20°C , 92%, d.r. = 9:1; m) $\text{TiCl}(\text{O}i\text{-Pr})_3$, benzene, r.t., 40%; n) CuSO_4 , TsOH , acetone, r.t., 83%; o) Pd/C , H_2 , EtOAc , r.t., 94%; p) DIAD, PPh₃, 1-phenyl-1*H*-tetrazole-5-thiol, THF, 0°C to r.t., 85%; q) *m*-CPBA, CH_2Cl_2 , 0 to 40°C , 61%.

¹⁰⁸ D. E. Frantz, R. Fässler, E. M. Carreira *J. Am. Chem. Soc.* **2000**, *122*, 1806-1807.

¹⁰⁹ Y. Sempere Molina, J. Ruchti, E. M. Carreira *Org. Lett.* **2017**, *19*, 743-745.

Semireduction of the alkyne with Red-Al, vanadium-catalyzed directed epoxidation of the resulting allylic alcohol,¹¹⁰ and DESS–MARTIN oxidation⁹¹ gave epoxyketone **113**. ZrCl₄ opened the epoxide at the more reactive α -position of the ketone,¹¹¹ giving chlorohydrin **114** in 36% yield after NaBH₄ reduction. Protection of the diol as acetonide, deprotection and oxidation of the primary alcohol set the stage for a STILL–GENNARI olefination¹¹² with **115** and subsequent DIBAL reduction. The obtained (*Z*)-olefin **116** was epoxidized using SHARPLESS' asymmetric epoxidation⁸⁷ in 92% yield and 9:1 d.r. The epoxide was subsequently opened regioselectively with TiCl(O*i*-Pr)₃ in 40% yield.¹¹³ The desired fragment **105** was obtained after protection of the diol as acetonide, deprotection of the benzyl ether, MITSUNOBU displacement¹¹⁴ with 1-phenyl-1*H*-tetrazole-5-thiol, and oxidation of the thioether.

The fragments could be joined after DESS–MARTIN oxidation of **104** by a JULIA–KOCIENSKI olefination (*Z/E* 3:1) in 67% yield (Scheme 23).¹¹⁵ The allylic epoxide in **118** was opened in the presence of Ph₃PCl₂ at the more reactive allylic site in 64% yield.¹¹⁶ Subsequent dichlorination of the *Z*-olefin in **119** with MIOSKOWSKI's reagent (70%) was followed by deprotection of the benzyl ether. Dehydration of the resulting alcohol with MARTIN sulfurane¹¹⁷ installed the C21–C22 olefin present in the natural product. The synthesis was completed by globally deprotecting all silyl groups in **120**, followed by esterification of the less hindered C23 alcohol, sulfation of the C17 alcohol, and, finally, deprotection of the acetonides.

Unfortunately, the obtained spectra did not match the data from the isolation report. Close analysis of several 2D NMR spectra of natural **31** suggested a misassignment of the C13–C14 relative configuration and led the CARREIRA group to attempt to revise the structure.⁵⁰ The structural revision by total synthesis is still ongoing.

¹¹⁰ E. D. Mihelich *Tetrahedron Lett.* **1979**, *20*, 4729-4732.

¹¹¹ F. Sarabia, A. Sánchez-Ruiz *Tetrahedron Lett.* **2005**, *46*, 1131-1135.

¹¹² W. C. Still, C. Gennari *Tetrahedron Lett.* **1983**, *24*, 4405-4408.

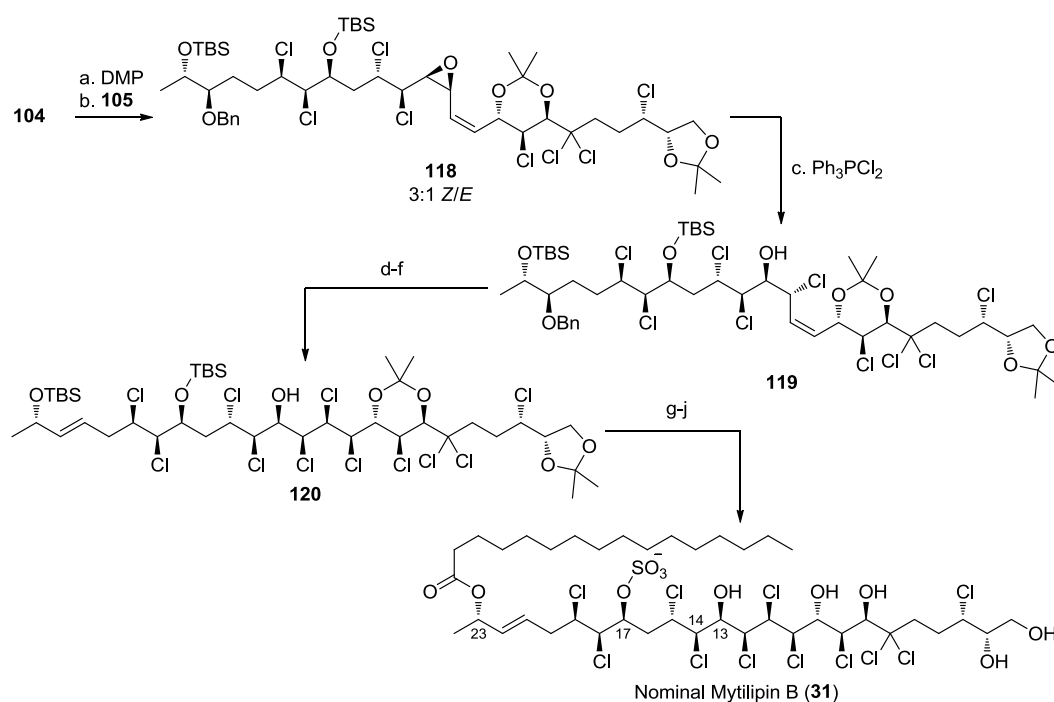
¹¹³ Y. E. Raifeld, A. A. Nikitenko, B. M. Arshava *Tetrahedron: Asymmetry* **1991**, *2*, 1083-1084.

¹¹⁴ O. Mitsunobu, M. Yamada *Bull. Chem. Soc. Jpn.* **1967**, *40*, 2380-2382.

¹¹⁵ P. R. Blakemore, W. J. Cole, P. J. Kociński, A. Morley *Synlett* **1998**, 26-28.

¹¹⁶ D. Díaz, T. Martín, V. S. Martín *J. Org. Chem.* **2001**, *66*, 7231-7233.

¹¹⁷ J. C. Martín, R. J. Arhart *J. Am. Chem. Soc.* **1971**, *93*, 4327-4329.



Scheme 23 Final steps in CARREIRA's synthesis of nominal mytilipin B (**31**). Reagents and conditions: a) DMP, CH_2Cl_2 , 0 °C to r.t., 95%; b) **105**, toluene, -78 °C, then NaHMDS, -78 °C to r.t., 67%, (*Z*:*E* = 3:1); c) Ph_3PCl_2 , CH_2Cl_2 , 0 °C, 64%; d) Et_4NCl_3 , CH_2Cl_2 , 0 to 4 °C, 70%; e) Pd/C (20 mol% Pd), H_2 , EtOAc, r.t., 79%; f) MARTIN sulfurane, benzene, r.t., 50%; g) HF-pyridine, pyridine, MeCN, 0 to 40 °C, quant.; h) palmitoyl chloride, pyridine, CH_2Cl_2 , -78 to -40 °C, 60%; i) SO_3 ·DMF, Na_2SO_4 , DMF/pyridine, 0 to 45 °C, 60%; j) TFA/ H_2O , 0 °C to r.t.

2.4.6 CARREIRA's Synthesis of Danicalipin A

In 2016, CARREIRA and co-workers published a synthesis of danicalipin A (**28**), that allowed for evaluation of biological properties of **28** (*cf.* Chapter 2.5). Since the authors required large quantities of the natural product for this study, an enantioselective synthesis was designed to circumvent steps that would involve low yields or selectivities (Scheme 24).¹¹⁸

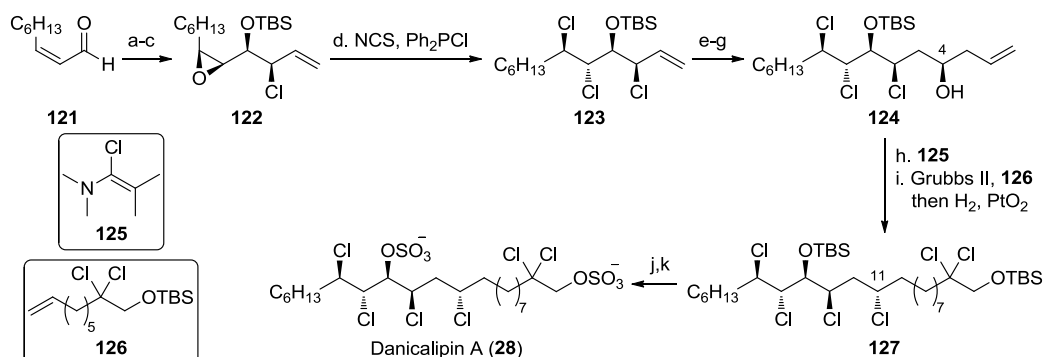
The synthesis began with an OEHSCHLAGER–BROWN chloroallylation of (*Z*)-nonenal (**121**).¹¹⁹ This transformation is the enantioselective equivalent of the bromoallylation with **61** (*cf.* Chapter 2.4.2), employing (-)-(Ipc)₂B(chloroallyl) as the enantiocontrolling reagent. The chlorohydrin was subjected to directed epoxidation with *m*-CPBA (d.r. = 11:1)¹²⁰ and TBS protection to give **122** in 30% yield over 3

¹¹⁸ A. M. Bailey, S. Wolfrum, E. M. Carreira *Angew. Chem. Int. Ed.* **2016**, *55*, 639-643.

¹¹⁹ S. Hu, S. Jayaraman, A. C. Oehlschlager *J. Org. Chem.* **1996**, *61*, 7513-7520.

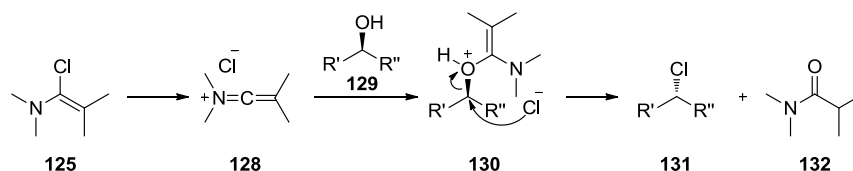
¹²⁰ H. B. Henbest, R. A. L. Wilson *J. Chem. Soc.* **1957**, 1958-1965.

steps. The epoxide was opened under YOSHIMITSU's modified conditions⁹⁰ in 44% yield.



Scheme 24 CARREIRA's synthesis of danicalipin A (**28**). Reagents and conditions: a) (–)-(Ipc)₂BOMe, allyl chloride, LiNCy₂, BF₃·OEt₂, Et₂O/THF, –78 °C to r.t.; b) *m*-CPBA, CH₂Cl₂, 0 °C to r.t., d.r. = 11:1; c) TBSCl, imidazole, DMAP, CH₂Cl₂, 0 to 40 °C, 30% over 3 steps; d) NCS, Ph₂PCL, CH₂Cl₂, 0 °C to r.t., 44%; e) Cy₂BH, THF, 0 °C to r.t., then NaBO₃·4H₂O, THF/H₂O, 0 °C to r.t., 75%; f) DMP, CH₂Cl₂, 0 °C to r.t., g) (+)-(Ipc)₂BCl, (allyl)MgBr, THF, –100 °C to r.t., 71%, d.r. = 8.3:1; h) **125**, CHCl₃, 0 °C to r.t., 93%; i) **126**, GRUBBS' second generation catalyst (10 mol%), CH₂Cl₂, 40 °C, then PtO₂, H₂, r.t., 77%; j) AcCl, MeOH, 0 to 80 °C, 89%; k) ClSO₃H, CH₂Cl₂, 0 °C to r.t., 92%.

With the stereotetrad of danicalipin A (**28**) completed efficiently, CARREIRA and co-workers needed to introduce the remaining chlorine substituent and the side chain. The work by others (*vide supra*) had shown that a substrate-controlled introduction of the remaining chlorine substituent can suffer from low selectivity and the authors relied on a BROWN allylation¹²¹ to introduce the C4-stereocenter. Thus, hydroboration/oxidation and DESS-MARTIN oxidation⁹¹ gave an aldehyde which was subjected to (+)-Ipc₂B(allyl), giving homoallylic alcohol **124** in 71% yield and 8.3:1 d.r. The alcohol was displaced with GHOSEZ's reagent (**125**).¹²² This reagent is thought to ionize *in situ* to the ketiminium chloride **128** (Scheme 25). Attack by alcohol **129**, formation of **130**, and displacement of the activated alcohol by chloride gives alkyl chloride **131** with inverted configuration and amide **132**.



Scheme 25 Mechanism for the displacement of secondary alcohols with GHOSEZ's reagent (**125**).

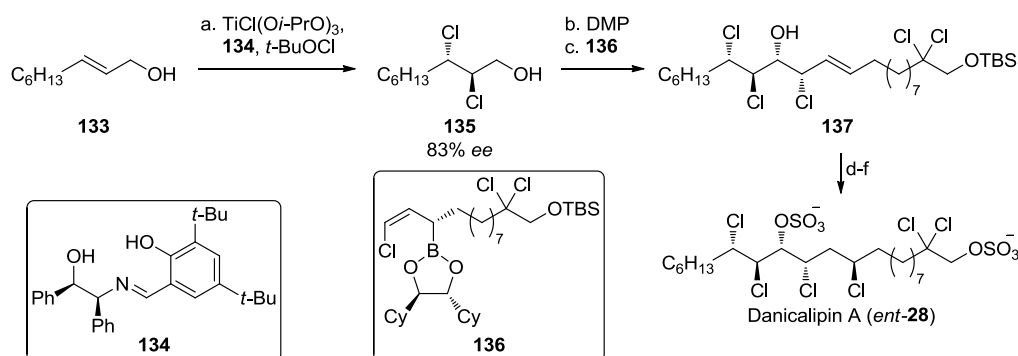
¹²¹ H. C. Brown, P. K. Jadhav *J. Am. Chem. Soc.* **1983**, *105*, 2092-2093.

¹²² F. Munyemana, A.-M. Frisque-Hesbain, A. Devos, L. Ghosez *Tetrahedron Lett.* **1989**, *30*, 3077-3080.

The terminal olefin in **124** conveniently set the stage for cross-metathesis, followed by a direct hydrogenation¹²³ of the resulting disubstituted olefin. This sequence completed the full carbon chain of **28** in 77% yield, which was more efficient than a coupling of fragments by WITTIG reaction (*vide supra*). The synthesis of danicalipin A (**28**) was completed after deprotection and sulfation.

2.4.7 BURNS' Synthesis of Danicalipin A

The latest synthesis of a chlorosulfolipid was published by BURNS and co-workers in 2016. Using an enantioselective dichlorination developed in their group, they accessed the unnatural enantiomer of danicalipin A (*ent*-**28**) (Scheme 26).¹²⁴



Scheme 26 BURNS' synthesis of danicalipin A (*ent*-**28**). Reagents and conditions: a) **134** (15 mol%), TiCl(O*i*-Pr)₃, *t*-BuOCl, hexane, -20 °C, 86%, 83% *ee*; b) DMP, NaHCO₃, CH₂Cl₂, 0 °C to r.t., 88%; c) **136**, *n*-BuLi, TFAA, THF, -78 °C, then aldehyde, -78 °C to r.t., 75%; d) CD₃OD, r.t., then concentrate, Me₄N(Cl₂Br), acetonitrile, r.t.; e) Bu₃SnH, Et₃B (20 mol%), air, toluene, -78 °C. 22% over 2 steps; f) ClSO₃H, CH₂Cl₂, r.t., 93%.

In a research program aimed at the enantioselective dihalogenation of allylic alcohols, BURNS developed a method using catalytic amounts of **134** and its derivatives in combination with TiCl(O*i*-Pr)₃ and an electrophilic halogen source.¹²⁵ In the most recent publication they employed this method in the first step of a chlorosulfolipid synthesis. While other examples of enantioselective dihalogenations have been reported previously,¹²⁶ this represents the only example where such a transformation was used in the context of chlorosulfolipids. Allylic alcohol **133** was

¹²³ J. Cossy, F. Bargiggia, S. BouzBouz *Org. Lett.* **2003**, *5*, 459-462.

¹²⁴ M. L. Landry, D. X. Hu, G. M. McKenna, N. Z. Burns *J. Am. Chem. Soc.* **2016**, *138*, 5150-5158.

¹²⁵ D. X. Hu, F. J. Seidl, C. Bucher, N. Z. Burns *J. Am. Chem. Soc.* **2015**, *137*, 3795-3798.

¹²⁶ See for example: a) S. A. Snyder, Z.-Y. Tang, R. Gupta *J. Am. Chem. Soc.* **2009**, *131*, 5744-5745; b) K. C. Nicolaou, N. L. Simmons, Y. Ying, P. M. Heretsch, J. S. Chen *J. Am. Chem. Soc.* **2011**, *133*, 8134-8137; c) D. X. Hu, G. M. Shibuya, N. Z. Burns *J. Am. Chem. Soc.* **2013**, *135*, 12960-12963.

treated with *t*-BuOCl and TiCl(*Oi*-Pr)₃ in the presence of catalytic amounts of **134** to give dichloride **135** in 86% yield and 83% *ee*. The primary alcohol was subsequently oxidized and treated with enantiopure chloroallylating reagent **136** (obtained by diastereoselective MATTESON rearrangement).¹²⁷ The synthesis of *ent*-**28** was completed after bromochlorination, debromination and sulfation.

2.5 Biological Activity

All of the above mentioned chlorosulfolipids were isolated during bioactivity-guided investigations (see Chapter 2.1.1). Hence, all identified chlorosulfolipids exhibit biological effects to some degree. Danicalipin A (**28**) is a fatty acid synthase inhibitor, malhamensilipin A (**29**) inhibits pp60 protein tyrosine kinase, and mytilipin A–C (**30–32**) were isolated in a search for causative agents of diarrhetic seafood poisoning (*vide supra*).

The only other studies on bioactivity directly published by an isolation group were performed on mytilipin A–C (**30–32**) by CIMINIELLO and FATTORUSSO.⁴⁸ In order to establish a biological profile of **30–32**, the authors tested cytotoxicity against several cell lines *in vitro*. Mytilipin A (**30**) was found cytotoxic against murine monocytes and macrophage cancer cell line J774 (IC₅₀ = 12.1 µg/mL), fibrosarcoma WEHI 164 (IC₅₀ = 16.3 µg/mL), and leukemia P338 (IC₅₀ = 10.4 µg/mL). Proliferative activity was also exhibited by mytilipin B (**31**) against murine fibrosarcoma WEHI 164 (IC₅₀ = 13.5 µg/mL), and monocyte and macrophage cancer cell line RAW 274.7 (IC₅₀ = 20 µg/mL). Mytilipin C (**32**) was cytotoxic towards murine fibrosarcoma WEHI 164 (IC₅₀ = 10.4 µg/mL), and monocytes and macrophage cancer cell line J774 (IC₅₀ > 20 µg/mL). No further studies on the toxicity or any other biological activity of **30–32** have been reported to date.

Some interesting observations regarding the toxicity of both *Ochromonas* species (*O. danica* and *P. malhamensis*) have been made, which might be related to the chlorosulfolipids function (*vide infra*). Early studies by REICH and SPIEGELSTEIN revealed that extracts from *O. danica* exhibited similar ichthyotoxicity as extracts from

¹²⁷ D. S. Matteson, K. M. Sadhu *J. Am. Chem. Soc.* **1983**, *105*, 2077-2078.

the golden alga *Prymnesium parvum*.¹²⁸ Extracts from *P. malhamensis* showed lower toxicity against fish, which would be in accordance with the lower concentration of malhamensilipin A (**29**) in the algae. Interestingly, the toxic compounds in *P. parvum*, prymnesins, have been suggested to compromise plasma membranes and cause ion leakage.¹²⁹ As these observations were made in 1964, no isolation of a chlorosulfolipid had been reported yet and no link could have been drawn.

Further investigations by HALEVY, SALITERNIK, and AVIVI reported the ichthyotoxicity of the *Ochromonas* sp. to arise from lipodial compounds, that were soluble in water and organic solvents, which fits properties displayed by danicalipin A (**28**) and malhamensilipin A (**29**).¹³⁰ They were not able to characterize the toxic compounds, but identified them *via* the formation of a red color with the cationic dye rhodamine 6G, possibly through ion exchange with the chlorosulfolipids **28** or **29**. Moreover, the authors found the same ichthyotoxins to be hemolysins of mammalian erythrocytes, although their toxic effects are counteracted in mammals.¹³¹

More studies on the toxicity of the *P. malhamensis* found the species to be toxic to rotifers *Branchionus angularis*¹³² and *Platyias* sp., as well as *Daphnia magna*.¹³³ While the above mentioned observations have not been linked to the chlorosulfolipid's present in the organisms, a relationship has not been excluded to the best of the author's knowledge. The possibility of the chlorosulfolipids to be part of a self-defense mechanism by the algae against predators and competitors remains.

More insight into the biological activity of danicalipin A (**28**) has been gained by OKINO and co-workers.⁶³ After isolating several partially chlorinated and sulfated analogs of danicalipin A (**27**, **138–143**), presumably biosynthetic intermediates or isolation artifacts (*cf.* Chapter 2.4.3), the authors tested the toxicity of **27**, **28**, and **138–143** towards the brine shrimp *Artemia salina* (Table 4).

¹²⁸ K. Reich, M. Spiegelstein *Isr. J. Zool.* **1964**, *13*, 141.

¹²⁹ S. R. Manning, J. W. La Claire, II *Mar. Drugs* **2010**, *8*, 678-704.

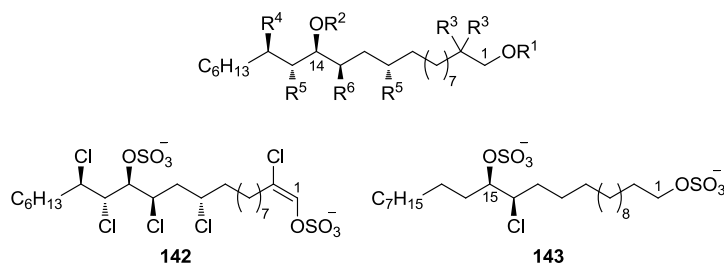
¹³⁰ S. Halevy, R. Saliternik, L. Avivi *Int. J. Biochem.* **1971**, *2*, 185-192.

¹³¹ A. Magazanik, S. Halevy *Experientia* **1973**, *29*, 310–311.

¹³² J. E. Boxhorn, D. A. Holen, M. E. Boraas *Hydrobiologia* **1998**, *387/388*, 283-287.

¹³³ J. Boenigk, P. Stadler *J. Plankton Res.* **2004**, *26*, 1507-1514.

Table 4 Brine shrimp toxicity of chlorosulfolipids **28** and **138–144** reported by KAWAHARA *et al.*⁶³ and the corresponding toxicities for **28**, **139**, **36**, **144**, **145** reported by CARREIRA and co-workers.^{118,134}



Compound number	R ¹	R ²	R ³	R ⁴	R ⁵	R ⁶	LC ₅₀ [μg/mL]	ref.
28	SO ₃ ⁻	SO ₃ ⁻	Cl	Cl	Cl	Cl	2.2 5.3	[63] [118]
138	SO ₃ ⁻	H	Cl	Cl	Cl	Cl	0.27	[63]
139	H	H	Cl	Cl	Cl	Cl	>30 141	[63] [118]
27	SO ₃ ⁻	SO ₃ ⁻	H	H	H	Cl	6.9	[63]
140	SO ₃ ⁻	SO ₃ ⁻	H	H	Cl	Cl	6.1	[63]
141	SO ₃ ⁻	SO ₃ ⁻	H	Cl	Cl	Cl	3.7	[63]
142	-	-	-	-	-	-	3.8	[63]
143	-	-	-	-	-	-	3.0	[63]
36	SO ₃ ⁻	SO ₃ ⁻	H	H	H	H	63.8	[118]
144	SO ₃ ⁻	SO ₃ ⁻	F	F	F	F	72.2	[134]
145	SO ₃ ⁻	SO ₃ ⁻	Br	Br	Br	Br	4.7	[134]

Given the toxicity of *O. danica* to aquatic organisms (*vide supra*), LC₅₀ values of brine shrimp cultures give a quantitative result and might help elucidating the natural role of danicalipin A (**28**). Indeed, **28** exhibits toxicity, albeit not as much as the C14 desulfated analog **138**. The C1 and C14 desulfated analog **139** was markedly less toxic, showing that the C1 sulfate is crucial to toxicity, while the C14 sulfate renders the compound less toxic. The partially chlorinated analogs **27**, **140**, and **141** all displayed similar toxicities as did **28**, but an increased chlorine content led to a slight increase in toxicity. Almost identical toxicities were observed for the C1–C2 olefin **142** and the monochloro-tetracosane disulfate **143**. The authors commented that the similarity in toxicities arise from complementary amphipathic shape of the compounds **28**, **27**, and **140–143**. This was further confirmed by CARREIRA and co-workers, who showed that the non-chlorinated docosane disulfate **36** had a significantly higher LC₅₀ than the chlorinated analogs (Table 4).¹¹⁸ UMEZAWA and MATSUDA observed that synthetic danicalipin A (**28**, LC₅₀ = 2.1 μg/mL) was as toxic

¹³⁴ S. Fischer, N. Huwyler, S. Wolfrum, E. M. Carreira *Angew. Chem. Int. Ed.* **2016**, *55*, 2555-2558.

as natural material, ruling out impurities in the isolation to be the causative toxin against brine shrimp.¹⁰⁰ The same authors also realized that the LC₅₀ values of racemic **28** and *ent*-**28** are almost identical to **28** (2.4 µg/mL and 2.4 µg/mL, respectively). This observation is consistent with a non-specific interaction leading to the brine shrimp toxicity of **28**. In a later study, CARREIRA and co-workers reported the syntheses of a fluorinated and a brominated analog of **28** (**144** and **145**) and the corresponding LC₅₀ values against brine shrimp (Table 4).¹³⁴ While the fluorinated analog **144** was about as toxic as the non-chlorinated disulfate **36**, the toxicity of bromosulfolipid **145** was comparable to that of danicalipin A (**28**). Furthermore, they were able to show that **144** and **145** had analogous conformations as **28**. This added support to OKINO's earlier hypothesis that amphiphilicity and toxicity were linked. An additional connection was drawn that correlates lipophilicity and toxicity. It seems that the C14 sulfate plays an important role. Potentially, the chlorine substituents in the vicinity of C14 shield its polarity by increasing the lipophilicity.¹³⁵ This would be consistent with the non-chlorinated analog **36** being an order of magnitude less toxic than the more lipophilic **28**, but equally toxic as fluorosulfolipid **144**. The latter effect can be caused by a less efficient shielding of the C14 sulfate by the smaller and more electronegative fluorine substituents.

It seems worth coming back to HAINES' hypothesis (*cf.* Chapter 2.1) that **28** would not be able to form stable membranes. His assumption was based on the presence of the polar C14 sulfate in the center of the molecule. If the chlorine atoms indeed had a shielding effect on the C14 sulfate, his argument would be invalid and **28** might aid in forming stable membranes.

With this idea in mind, CARREIRA and co-workers set out to investigate influences on membranes exhibited by danicalipin A (**28**) in several organisms, hoping that it would shed some light on natural function of **28** in the membranes of *O. danica*.¹¹⁸ When **28** was incubated with bacteria *E. coli* DH5α and the DNA stain Hoechst 33342,¹³⁶ an increase in fluorescence was noted (Figure 4). Particularly noteworthy is the result obtained at 125 µM concentrations of **28**, where the fluorescence is increased five-fold over the negative control, while maintaining >90%

¹³⁵ K. Naumann *J. Prakt. Chem.* **1999**, *341*, 417-435.

¹³⁶ M. J. Lydon, K. D. Keeler, D. B. Thomas *J. Cell. Physiol.* **1980**, *102*, 175-181.

viability of the bacteria. Hoechst 33342 on its own is not able to cross the bacterial membrane and should thus not stain the DNA of *E. coli*. The authors concluded that danicalipin A (**28**) compromises the bacterial membrane and allows the DNA stain to cross into the nuclei of the bacteria. Moreover, they found that both the non-chlorinated analog **36** and the C1,C14-diol **139** were not able to display the same membrane permeability enhancement.

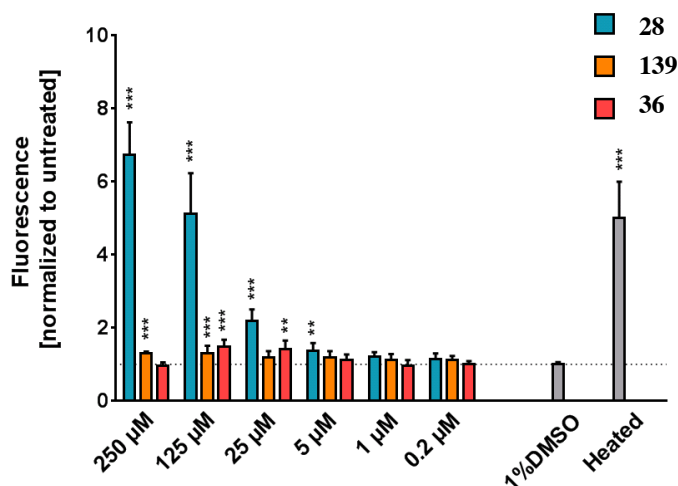
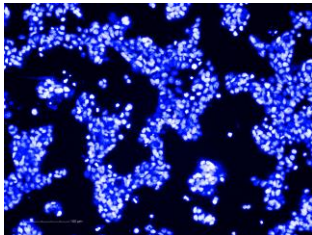
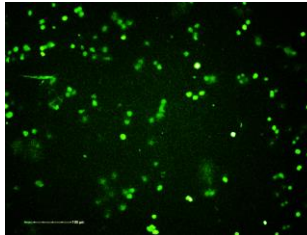
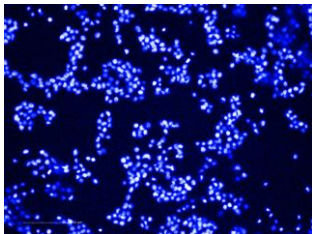
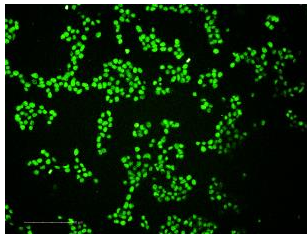
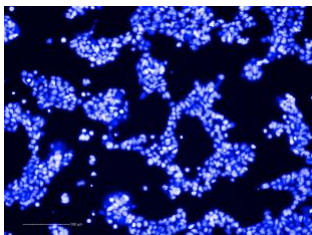
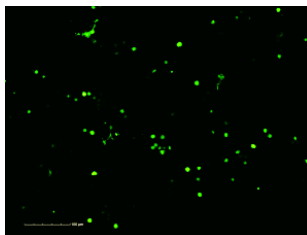
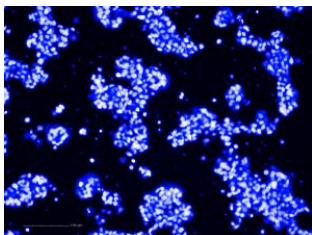
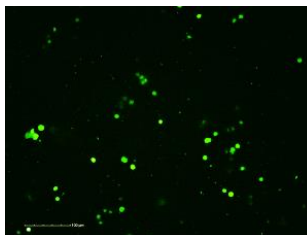
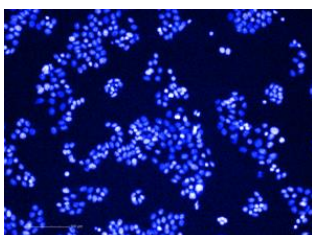
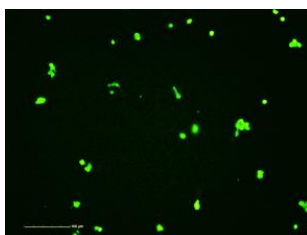
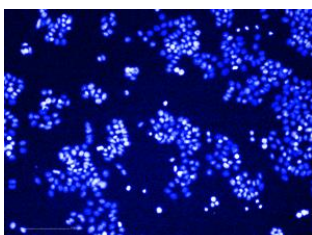
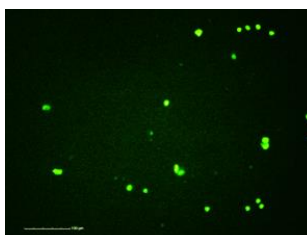


Figure 4 Increase in fluorescence by Hoechst 33342 in bacteria *E. coli* DH5 α after exposure to **28**, **139**, and **36** at varying concentrations. Negative (1% DMSO) and positive control (heated) are shown on the right. The data is normalized to the untreated results. The significance of each result vs. DMSO is shown above the bar: $p < 0.01 = **$; $p < 0.001 = ***$. Adapted with permission from ref. 118, Copyright 2016 John Wiley and Sons.

Furthermore, CARREIRA and co-workers used an assay with the DNA stains Hoechst 33342 and Sytox Green to corroborate the membrane permeability enhancing effects of danicalipin A (**28**) in other types of cell membranes. This assay relies on the ability of Hoechst 33342 to cross cellular membranes in combination with the ability of Sytox Green to only cross compromised cellular membranes.¹³⁷ The results of this assay on the human adenocarcinoma cells HT-29 can be seen in Table 5. At a concentration of 10 μM of **28**, the images of Hoechst 33342 and Sytox Green show the same stained material, while cellular viability remains >90%. Similar results were also obtained for the murine liver cell line Hepa 1-6 (not shown). Both the C1,C14-diol **139** and the non-chlorinated analog **36** did not exhibit similar activities. As was

¹³⁷ a) S. Langsrud, G. Sundheim *J. Appl. Bacteriol.* **1996**, *81*, 411-418; b) B. L. Roth, M. Poot, S. T. Yue, P. J. Millard *Appl. Environ. Microbiol.* **1997**, *63*, 2421-2431; c) M. P. Bova, D. Tam, G. MeMahon, M. N. Mattson *Toxicol. Lett.* **2005**, *155*, 41-50.

Table 5 Fluorescent images of HT-29 cells by Hoechst 33342 (all DNA in the sample) and Sytox Green (DNA of cells with compromised cellular membranes) at varying concentrations of **28**, **139**, and **36**. Adapted with permission from ref. 118, Copyright 2016 John Wiley and Sons.

Compound	Concentration	Hoechst 33342	Sytox Green
28	2 μ M		
	10 μ M		
139	2 μ M		
	10 μ M		
36	5 μ M		
	10 μ M		

the case of *E. coli* DH5 α , the authors explained this observation with the ability of **28** to compromise the cellular membrane. It was thus shown that danicalipin A (**28**) is able to interact with and compromise cellular and bacterial membranes at concentrations that are not toxic to the organisms.

In order to unravel the toxicological profile of danicalipin A (**28**), CARREIRA and co-workers further tested cytotoxicities of **28**, **36**, and **139** against various mammalian cell lines (Table 6). Danicalipin A (**28**) was more toxic to adenocarcinomic human lung cells A549, human colorectal cells HT-29, as well as murine liver cells Hepa 1-6 than were **139** and **36**. A clear trend cannot be drawn from this data, but a link between toxicity and permeability enhancement of these compounds seems possible. However, this is still a long way from fully understanding the natural function of **28** or other chlorosulfolipids.

Table 6 Cytotoxicity of **28**, **36**, and **139** towards several mammalian cell lines. EC₅₀ values are given in μM . Adapted with permission from ref. 118, Copyright 2016 John Wiley and Sons.

Toxicity (EC ₅₀)	A549	HT-29	Hepa 1-6
28	26.5 \pm 0.9	15.5 \pm 1.2	14.3 \pm 0.7
139	41.4 \pm 0.9	>166	17.3 \pm 0.1
36	69.3 \pm 1.2	84.4 \pm 0.7	39.1 \pm 0.2

2.6 Summary

The chlorosulfolipids are an intriguing class of naturally-occurring organohalogens. Although they have been isolated from various sources around the world, their numbers are still scarce. Members of this family are produced by microalgae but their natural function is still not understood. Some appear to serve an unspecified function in the membranes and others might be associated with self-defense mechanisms of the organisms that they are produced in.

Elucidation of their configuration by JBCA has inspired synthetic organic chemists to embark on several total syntheses and surprising chemical complexity has been observed. Furthermore, a number of methods have been developed in order to access this unusual class of natural products.

Future endeavours may reveal more of the chlorosulfolipids' enigmatic chemical and biological properties and help unravel their elusive natural function.

Part II

CONFIGURATIONAL AND CONFORMATIONAL EFFECTS IN DANICALIPIN A AND ITS DIASTEREOMERS

3 Results and Discussion

3.1 Background

The conformational bias of polychlorinated molecules originates from the interplay of several stereoelectronic features. Among them is the *gauche* effect which describes the preferential arrangement of two vicinal polar bonds *gauche* to each other.¹³⁸ This is particularly evident in 1,2-difluoroethane in which mixing¹³⁹ of $\sigma^*_{\text{C-F}}$ and $\sigma_{\text{C-H}}$ favors a low energy conformer in which the two fluorine substituents adopt a *gauche* conformation.¹⁴⁰ In 1,2-difluoroethane, this arrangement is favored by 0.6 kcal/mol over the *trans* conformer while in butane, the *trans* conformer is favored by 0.9 kcal/mol.¹⁴¹ The *gauche* effect becomes less pronounced as one moves down the periodic table: *trans* conformers are favored for 1,2-dichloro- (1.2 kcal/mol), dibromo- (1.7 kcal/mol), and diiodoethane (2.6 kcal/mol) in the gas phase.¹⁴² The picture becomes more complicated in solution. For example, depending on solvent polarity, the *gauche* conformer in 1,2-dichloroethane can be favored by 0.2 kcal/mol or disfavored by 0.7 kcal/mol.¹⁴³ The explanation for this variation lies in the minimization or maximization of dipole moments which signifies another important element capable of biasing conformations in polychlorinated molecules. The *trans* conformer of 1,2-dichloroethane has both dipoles of the C–Cl bonds counteracting each other, thereby minimizing the total dipolar moment of the molecule. In contrast, the overall dipole in the *gauche* conformer is maximized. In solvents of low polarity, the *trans* conformer, with its low dipole, is preferred whereas the *gauche* conformer is favored in polar solvents.

¹³⁸ For an early review, see: S. Wolfe *Acc. Chem. Res.* **1972**, *5*, 102-111.

¹³⁹ I. V. Alabugin, T. A. Zeidan *J. Am. Chem. Soc.* **2002**, *124*, 3175-3185.

¹⁴⁰ R. J. Abraham, R. H. Kemp *J. Chem. Soc. B* **1971**, 1240-1245.

¹⁴¹ D. A. C. Compton, S. Montero, W. F. Murphy *J. Phys. Chem.* **1980**, *84*, 3587-3591.

¹⁴² R. J. Abraham, K. Parry *J. Chem. Soc. B* **1970**, 539-545.

¹⁴³ K. B. Wiberg, T. A. Keith, M. J. Frisch, M. Murcko *J. Phys. Chem.* **1995**, *99*, 9072-9079.

While the *gauche* effect and dipole optimization are important in vicinal disubstituted systems, a major contributor to the conformation of more complex polychlorinated molecules is the minimization of *syn*-pentane interactions. *Syn*-pentane interactions arise when pentane assumes a g^+g^- conformer (Figure 5).

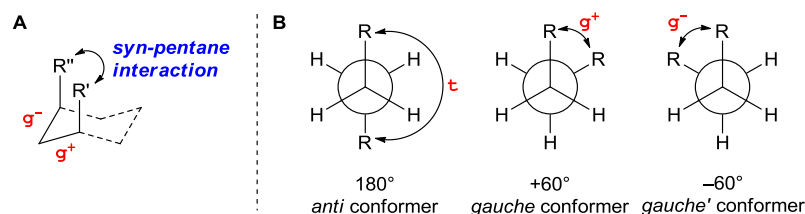


Figure 5 Conformational analysis of the *syn*-pentane interaction. **A:** 3D illustration of the *syn*-pentane interaction; **B:** Definition of τ , g^+ , and g^- letter codes to designate backbone conformations, presented in the Newman projections.

For pentane ($R' = R'' = \text{Me}$) this interaction is disfavored by 2.7 kcal/mol over the corresponding $\tau\tau$ conformer.¹⁴⁴ In fact, energetic penalties associated with such interactions are large by comparison to other conformational effects in acyclic molecules. Avoidance of these penalties has been suggested to be one of nature's most important biasing elements to control conformation in flexible molecules.¹⁴⁵

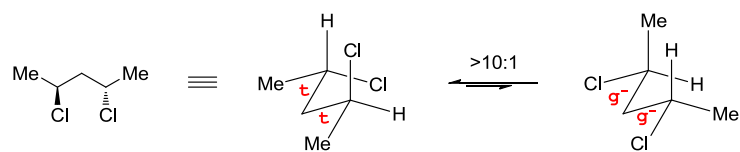
HOFFMANN *et al.* undertook a systematic investigation of 2,4-*anti*-disubstituted pentanes in order to determine equilibria between the various conformers.¹⁴⁶ The $\tau\tau$ and g^-g^- conformers were found to be the major contributors in the conformational equilibria, since *syn*-pentane interactions are avoided. For 2,4-*anti*-dichloropentane the equilibrium favored the $\tau\tau$ conformer with $K > 10$ (Scheme 27). This preference can be understood in terms of the *A* values, which assign an energetic preference to the equatorial positioning of a given substituent in cyclohexane. The smaller value for a chlorine substituent (0.6 kcal/mol) indicates its decreased steric demand when compared to a methyl group (1.7 kcal/mol) and explains why it is placed preferentially in the sterically hindered pseudoaxial position of the $\tau\tau$ conformer.¹⁴⁷

¹⁴⁴ S. Tsuzuki, L. Schäfer, H. Goto, E. D. Jemmis, H. Hosoya, K. Siam, K. Tanabe, E. Osawa *J. Am. Chem. Soc.* **1991**, *113*, 4665-4671.

¹⁴⁵ R. W. Hoffmann *Angew. Chem. Int. Ed.* **2000**, *39*, 2054-2070.

¹⁴⁶ R. W. Hoffmann, D. Stenkamp, T. Trieselmann, R. Göttlich *Eur. J. Org. Chem.* **1999**, 2915-2927.

¹⁴⁷ For a collection of *A*-values, see: E. L. Eliel, S. H. Wilen, L. N. Mander "Stereochemistry of Organic Compounds", Wiley, New York, **1994**, p. 696 f.



Scheme 27 Two major conformers of 2,4-*anti*-dichloropentane. The equilibrium between the *tt* and *g⁻g⁻* conformer lies in favor of the *tt* conformer with $K > 10$.¹⁴⁶

3.2 Project Outline

The question that we were interested in was: Does the configuration of chlorosulfolipids have an impact on their biological activity? As pointed out earlier, the biosynthetic pathway selectively introduces a complex stereodefined array of chlorines, which may have come about by coincidence or competitive evolution. To shed some light on the putative evolutionary advantages of the configuration in chlorosulfolipids, we set out to investigate configurational isomers for their bioactivity.

A comparison to methyl groups in natural products or materials is relevant here. Stereodefined methylated arrays impose a conformation onto otherwise flexible chains, giving those molecules a defined shape. It has been shown that the molecular shape is directly linked to the biological function or macroscopic physicochemical properties of such systems.¹⁴⁸

Similarly, OKINO and co-workers had suggested that the toxicity of danicalipin A (**28**) towards brine shrimp arises from its overall molecular shape (*cf.* Chapter 2.5).⁶³ They had determined the preferred conformation of **28** by JBCA, but lacked analogs with other conformations to back their hypothesis. The work by CARREIRA and co-workers raised some doubts as to whether this hypothesis is true. The fluorinated and non-chlorinated analogs **144** and **36**, respectively, were equally toxic despite the well-defined solution-state conformation of **144**.¹³⁴ Therefore, we envisioned that the synthesis of selected diastereomers of danicalipin A (**28**) would probe potential links between bioactivity and configuration, conformation, or other effects in **28**.

¹⁴⁸ M. Burns, S. Essafi, J. R. Bame, S. P. Bull, M. P. Webster, S. Balieu, J. W. Dale, C. P. Butts, J. N. Harvey, V. K. Aggarwal *Nature* **2014**, *513*, 183-188; and references therein.

3.3 Target Selection

3.3.1 Conformations of Potential Diastereomers

Given that there are five stereocenters in the complex chlorinated array of danicalipin A (**28**), sixteen diastereomers exist, not counting enantiomers. The individual synthesis of each one would be an enormous effort since not all diastereomers are easily accessed by common methods (*cf.* Chapter 2.4). A more sensible approach was the targeted selection of diastereomers which would display defined ground-state conformations different from **28**. The synthesis of such targets could be assessed for its feasibility and possibly entail the implementation of new methods.

In order to choose appropriate diastereomers, we divided the chlorinated array of danicalipin A (**28**) into two regions (Figure 6). The C11 to C13 region was represented by a 1,3-motif, which can be modeled in a similar fashion to HOFFMANN's analysis for 2,4-*anti*-dichloropentane (*cf.* Chapter 3.1).¹⁴⁶ The second fragment (C13 to C16) was significantly more complex. We assumed that the use of a database would allow for an assignment of conformations. Fortunately, although no database for chlorinated sulfates is available, one exists for 2,4,5-trichloro-1,3-hexanediols.⁶¹ In our experience, substituents on hydroxy groups, such as the C14-alcohol, do not change the solution-state conformation, as determined by JBCA.¹⁴⁹ Hence, we assumed that any structural assignment based on the hexanediol database would hold true for the corresponding disulfates.

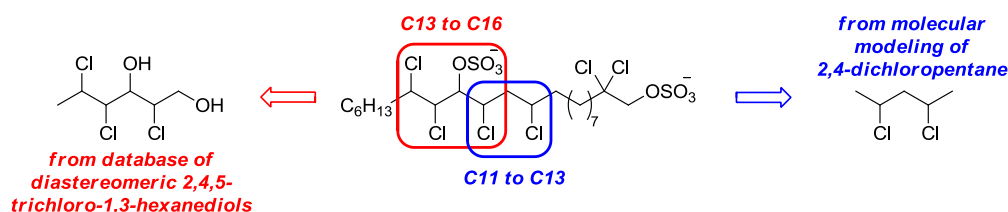


Figure 6 Fragment approach to identify diastereomers of danicalipin A (**28**) with defined ground-state conformations different from **28**. The C13 to C16 fragment was traced back to a database of 2,4,5-trichloro-1,3-hexanediols and the C11 to C13 fragment was derived from molecular modeling of 2,4-dichloropentane.

¹⁴⁹ See Supporting Information of refs. [63] and [134], and Chapter 3.5.3 of this thesis.

The analysis of the C11,C13 fragment was straightforward. As discussed in Chapter 3.1, HOFFMANN had already disclosed the lowest-energy conformer of 1,3-*anti*-dichloropentane as $\tau\tau$ (Figure 7A).¹⁴⁶ He also pointed out that the corresponding 1,3-*syn*-dichloropentane would have to assume a τg conformation, since minimization of *syn*-pentane interactions is otherwise not possible. However, in our case the pentane motif would be asymmetric, since both ends would contain different residues. A generalized analysis of the 1,3-*syn*-motif revealed that two conformers (τg^- and $g^+\tau$) would be energetically indistinguishable by molecular modeling of such systems (Figure 7B). For our purposes it is important to note that the 1,3-*anti*-motif would not impose any *gauche* interactions on the carbon backbone whereas the 1,3-*syn*-motif, regardless of which conformer is dominant, would lead to a single *gauche* conformation.

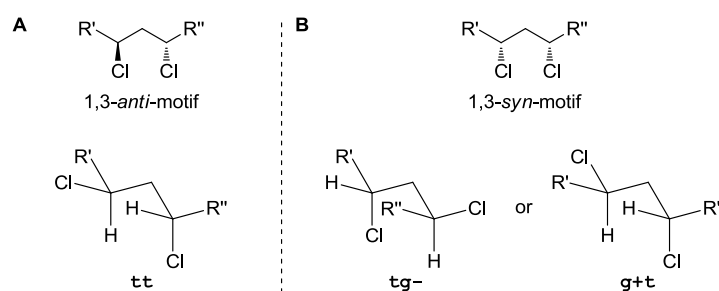


Figure 7 Molecular modeling of 1,3-dichloro-motif and possible low-energy conformers. **A:** The 1,3-*anti*-motif gives rise to one preferred conformer ($\tau\tau$); **B:** The 1,3-*syn*-motif has two possible low-energy conformers (τg^- and $g^+\tau$) if $R' \neq R''$. (Dihedral angles in the backbone: $\tau = 180^\circ$, $g^+ = +60^\circ$, $g^- = -60^\circ$).

The database of 2,4,5-trichloro-1,3-hexanediols was originally published to establish the values of coupling constants necessary for the JBCA of polychlorinated molecules.⁶¹ CARREIRA and co-workers synthesized all diastereomers in a divergent approach and investigated their solution-state conformation by JBCA, as well as their solid-state structures by X-ray crystallography (Figure 8).¹⁵⁰

¹⁵⁰ C. Nilewski in "Enabling Tactics and Strategies to Access Polychlorinated Hydrocarbons – Total Synthesis of Chlorosulfolipids and Insights into Their Chemistry", Dissertation ETH No. 19549, Zurich, 2011.

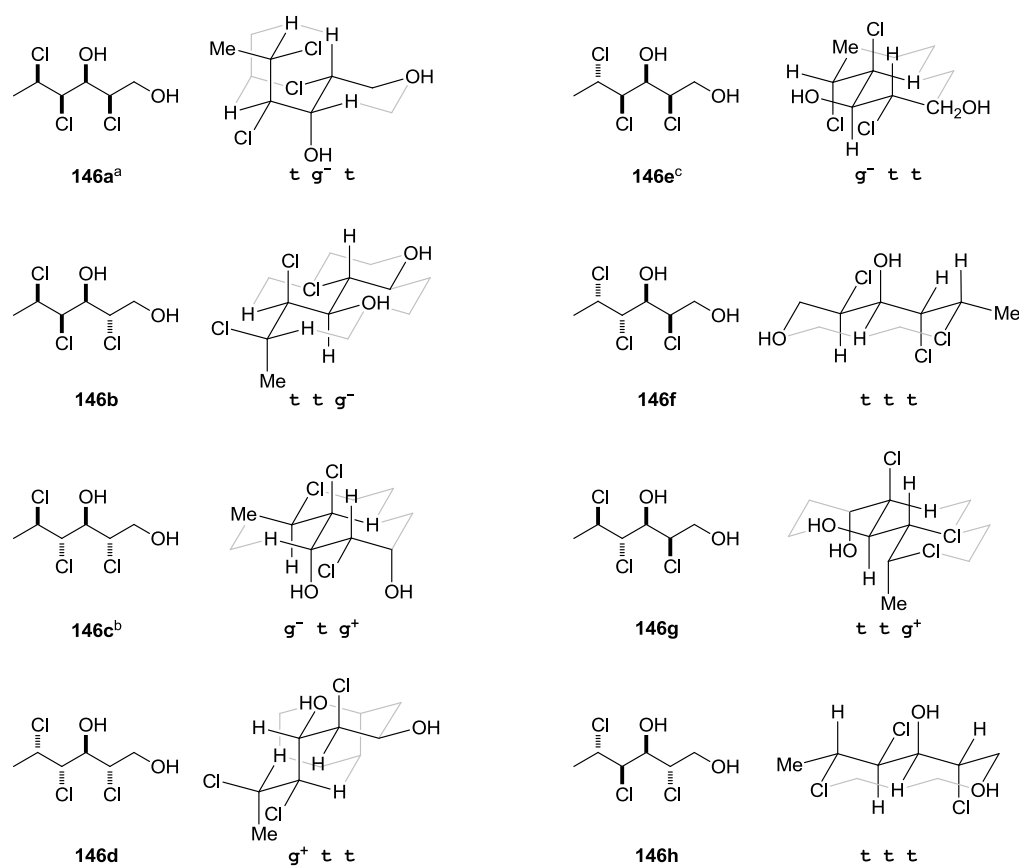


Figure 8 Possible diastereomers for 2,4,5-trichloro-1,3-hexanediols and their solution- and solid-state structures. a) In equilibrium with $t g^- g^-$; b) In equilibrium with $t t g^-$; c) Not in agreement with solid state structure ($t g^+ g^+$). The letter code order follows the numbering of the principle chain. (Dihedral angles in the backbone: $t = 180^\circ$, $g^+ = +60^\circ$, $g^- = -60^\circ$). Adapted with permission from ref. 150.

As described in Chapter 3.1, these conformations resulted from simple conformational considerations, such as avoidance of *syn*-pentane interactions, and no reason for deviation in more complex systems was apparent. Therefore, we became confident that the conformations of diastereomers of **28** could be predicted from the corresponding solution-state conformations of the diols **146a–f**.

Combination of the molecular modeling for the C11,C13 motif and the database analysis of the stereotetrad gave 24 conformers in total. The conformation corresponding to the chlorinated array of danicalipin A (**28**) was derived from the combination of the 1,3-*anti* motif ($t t$) and alcohol **146g** ($t t g^+$), giving a single *gauche* interaction between C15 and C16 ($t t t t g^+$, Figure 9). This analysis matched the solution-state structure reported by VANDERWAL and OKINO.^{62,63}

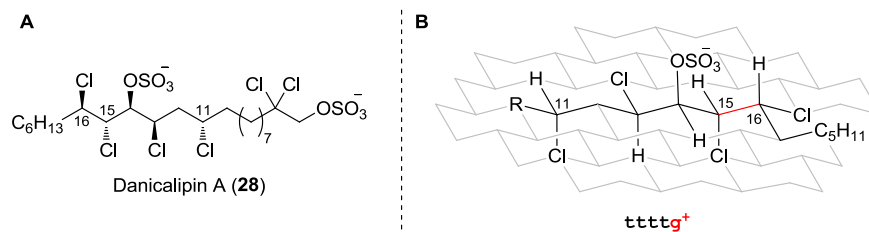


Figure 9 A: Chemical structure of danicalipin A (**28**); B: 3D representation of the solution-state conformation of **28**. The order of letter code follows the numbering of the principle chain. R = $(\text{CH}_2)_8\text{CCl}_2\text{CH}_2\text{OSO}_3^-$.

The analysis on the other possible diastereomers revealed that most of them would retain an overall singly-kinked molecular shape similar to **28**. Furthermore, a number of diastereomers would feature unavoidable *syn*-pentane interactions, rendering them unlikely to assume well-defined solution-state conformations. Since we were interested in diastereomers that would display defined solution-state structures different from **28**, diastereomers with a single bent or unavoidable *syn*-pentane interaction were excluded from further considerations.

Ultimately, this analysis generated two synthetically feasible structures which would be potentially interesting for our investigation. 11,15-Di-*epi*-danicalipin A (**147**) would have a *gauche* interaction between C14 and C15 (as opposed to C15–C16 in **28**) as suggested from the diol **146a** (Figure 10). Additionally, the C11,C13 *syn*-arrangement gives rise to an additional *gauche* interaction (*vide supra*). At this point, it was unclear, which of the two conformations along the C11–C13 motif would be preferred, $\text{tg}^- \text{tg}^- \text{t}$ or $\text{g}^+ \text{ttg}^- \text{t}$. However, with both having two *gauche* interactions in the carbon-backbone, they fit our criteria of having a defined solution-state structure different from **28**.

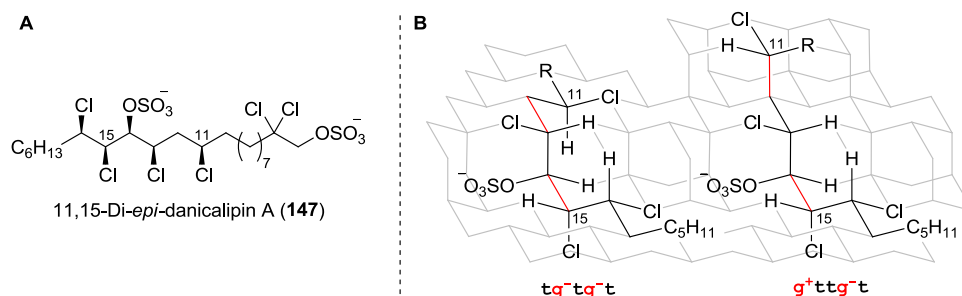


Figure 10 A: Chemical structure of 11,15-di-*epi*-danicalipin A (**147**); B: 3D representation of the potential solution-state conformations of **147**. The order of letter code follows the numbering of the principle chain. R = $(\text{CH}_2)_8\text{CCl}_2\text{CH}_2\text{OSO}_3^-$.

The second interesting structure was 16-*epi*-danicalipin A (**148**). The corresponding diol fragment **146f** had an all-*trans* arrangement. Given that the 1,3-*anti*-motif along C11,C13 would also have an all-*trans* conformation, **148** would be completely linear (Figure 11).

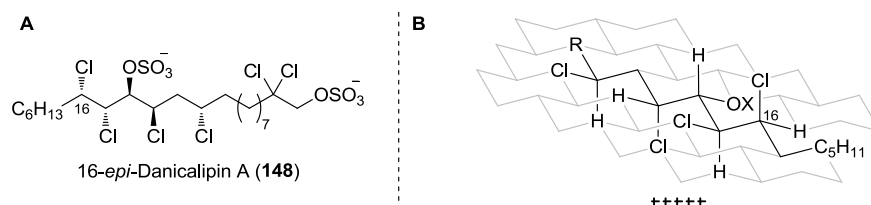


Figure 11 A: Chemical structure of 16-*epi*-danicalipin A (**148**); B: 3D representation of the predicted solution-state conformation of **148**. The order of letter code follows the numbering of the principle chain. R = (CH₂)₈CCl₂CH₂OSO₃⁻; X = OSO₃⁻.

We had obtained a set of three different diastereomers that varied in configuration and, if predicted correctly, molecular shape. We expected that **28**, **147**, and **148** would contain one, two, and zero *gauche* interactions, respectively, in the chlorinated array. The syntheses and biological activities of the two unnatural diastereomers **147** and **148** would give valuable insight into the influence of configuration, conformation, and molecular shape exhibited by danicalipin A (**28**) in nature.

3.3.2 Computational Analysis of Diastereomers

With the targets selected, we were interested to see if the conformations obtained by analysis of a database and molecular modeling would be supported by computational methods. For our purposes, the pre-selection of targets simplified the calculations significantly since optimizations of these large and flexible molecules are difficult to converge and therefore require long computational times. As pointed out earlier, we had no reason to assume different conformations for diols and disulfates and the disulfates would render the computations more challenging (*vide infra*). Therefore, we decided to use danicalipin A diol **139** with its known conformation as a benchmark for the optimization of the computational method.

A randomly generated starting geometry for **139** was optimized with Monte Carlo molecular mechanics (MCMM) simulations to find the lowest-energy geometry

of a given structure.¹⁵¹ The optimization of **139** was performed with the conformational search protocol, which retains optimized structures whose energies are within an adjustable energy-window of the lowest-energy conformer. The conformational search protocol was performed in an OPLS_2005 force field (Optimized Potentials for Liquid Simulations) in chloroform.¹⁵² Of the limited options, chloroform seemed to be ideally suited due to its medium polarity and common use as solvent for JBCA. To sample the conformational space adequately, a mixed torsional/low-mode sampling was employed.¹⁵³ This sampling method is particularly effective for large and flexible molecules, since it combines random torsions of all bonds with the sampling by low frequency molecular vibrations. During the MCMC optimization, structures within 2.01 kcal/mol of the one lowest in energy were retained, delivering 242 conformations, which were analyzed manually. We expected high flexibility in the unsubstituted carbon chain between C4 and C9, and C18 and C22, respectively, but considered it likely that the all-*trans* conformation would be energetically favored. For the purpose of further analysis, all conformers with *gauche* interactions in those regions were therefore omitted. At this point it was important not to omit any structures that exhibited a unique conformation in the C10 to C17 region. They were potentially important starting points for the subsequent optimizations by DFT calculations which might not be able to interconvert the different conformations of the chlorinated segment due to high rotational barriers. This limited the number of conformers to nine. With the goal of calculating the relative free energies, these structures were submitted to DFT calculations.

DFT calculations were performed using the hybrid Minnesota functional M06-2X due to its accurate performance in main group chemistry.¹⁵⁴ To account for the high number of chlorines in the region of interest, the Los Alamos National Laboratory effective core potential and basis set with diffuse and polarization functions (LANL2DZpd)¹⁵⁵ was employed for chlorine, while all other atoms were treated with a standard 6-31G+** basis set.¹⁵⁶ Since we were interested in the

¹⁵¹ G. Chang, W. C. Guida, W. C. Still *J. Am. Chem. Soc.* **1989**, *111*, 4379-4386.

¹⁵² W. L. Jorgensen, J. Tirado-Rives *J. Am. Chem. Soc.* **1988**, *110*, 1657-1666.

¹⁵³ I.-J. Chen, N. Foloppe *Bioorg. Med. Chem.* **2013**, *21*, 7898-7920.

¹⁵⁴ Y. Zhao, D. G. Truhlar, *Theor. Chem. Acc.* **2008**, *120*, 215-241.

¹⁵⁵ a) P. J. Hay, W. R. Wadt *J. Chem. Phys.* **1985**, *82*, 284-298; b) C. E. Check, T. O. Faust, J. M. Bailey, B. J. Wright, T. M. Gilbert, L. S. Sunderlin *J. Phys. Chem. A* **2001**, *105*, 8111-8116.

¹⁵⁶ M. J. Frisch, J. A. Pople, J. S. Binkley *J. Chem. Phys.* **1984**, *80*, 3265-3269.

solution-state structure of **139**, a self-consistent reaction field (SCRf) with the solvation model based on density (SMD) was implemented for chloroform.¹⁵⁷ We found that many structures failed to converge when the standard self-consistent field was used and thus changed to quadratical convergence.¹⁵⁸ In structures that still failed to converge, the conversion criterion had to be decreased. Through comparison between the different methods we made sure that changes to the convergence did not impact the final energy of the system.

With these methods we optimized the structures obtained from MCMM and calculated their frequencies. The structures obtained from the M06-2X/6-31+G**/LANL2DZpd(Cl)/SMD(chloroform) level of theory were submitted to single-point calculations with M06-2X/6-311++G**/LANL2DZpd(Cl)/SMD (chloroform) level of theory in order to get more accurate electronic energies E_{SP} . The final energies were then calculated according to $G^0_{final} = E_{SP} + G^0 - E$, where E_{SP} was obtained from the single-point calculations and G^0 and E were both obtained from the prior DFT optimization. The results of these calculations can be seen in Table 7. It should be pointed out that this protocol is not intended to find all possible structures but attempts to find the one lowest in energy, since it performs two independent optimizations. Therefore, the absence of certain conformers must not be misinterpreted as their being higher in energy than all shown conformers.

Table 7 Energy differences for different conformers of **139** obtained from DFT calculations.

Entry	ΔG^0 [kcal/mol]	conformation C10 to C17							conformation C1 to C3	
1	0.00	g ⁻	t	t	t	t	g ⁺	t	g ⁺ t	
2	1.12	t	t	t	t	t	g ⁺	t	g ⁻ t	
3	1.93	t	t	t	t	t	g ⁺	t	tt	
4	2.49	g ⁺	t	t	t	t	g ⁺	t	g ⁻ t	
5	2.88	g ⁻	t	t	t	t	g ⁺	t	tg ⁺	
6	3.43	g ⁺	t	t	t	t	g ⁺	t	tt	

It was interesting to see that all obtained structures had the correct conformation in the chlorinated array (ttttg⁺), as well as a *trans* conformer along C16–C17. The only differences came from the conformation at the C10–C11 bond

¹⁵⁷ A. V. Marenich, C. J. Cramer, D. G. Truhlar *J. Phys. Chem. B* **2009**, *113*, 6378-6396.

¹⁵⁸ G. B. Bacskay *Chem. Phys.* **1981**, *61*, 385-404.

and along C1 to C3. A difference in these regions might be expected, given that dipolar interactions become important for flexible links between polar segments. The lowest-energy structure of **139** is shown in Figure 12. Its two *gauche* interactions give it an overall U-shape.

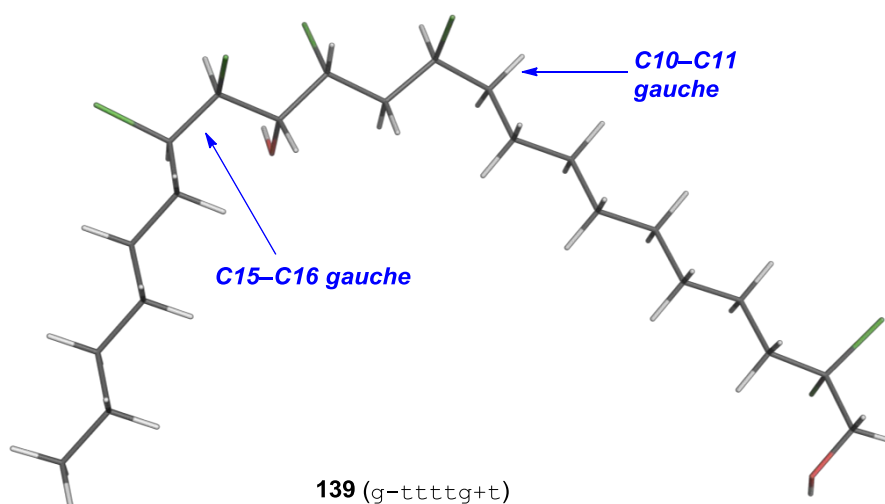


Figure 12 Lowest-energy conformer of **139** in a lines representation. The C10–C11 and C15–C16 *gauche* interactions are highlighted.

The combined MCMM/DFT approach worked for our test compound **139** and predicted the same conformation as the molecular modeling/database approach. Furthermore, it allowed for additional insight into regions not accessible by JBCA. Therefore, we attempted the same analysis for the diols of 11,15-di-*epi*-danicalipin A (**147**) and 16-*epi*-danicalipin A (**148**).

The results of the computational analysis for 11,15-di-*epi*-danicalipin A diol **149** are shown in Table 8. After MCMM conformational search, 274 structures were obtained of which 26 were retained. The higher number of low-energy conformations might point towards higher flexibility in this molecule. It is noteworthy that the computational method only found one of the two possible conformers (tg^-tg^-t), suggesting its preference over the other (g^+tg^-t , *cf.* Figure 10). In general, the obtained conformations were closer in energy. In particular, the C16–C17 bond was suggested to be more flexible (*cf.* Entries 1–6). Interestingly, additional *gauche* conformations along the C15–C16 bond were found in some structures but increased the overall energy significantly (Entries 15 & 16). Some conformations were assigned

imaginary frequencies, a problem sometimes encountered in Gaussian when low-mode vibrations are miscalculated (Entries 10 & 13). The small sizes (-35 and -21 cm^{-1}) point towards a real vibrational mode. Visualization with GaussView suggests them to be rocking vibrations of the carbon backbone. The lowest-energy conformer of **149** is shown in Figure 13. Despite the three *gauche* interactions in the chlorinated segment, **149** maintains an overall slight bent with a zig-zag shaped chlorinated array.

Table 8 Energy differences for different conformers of **149** obtained from DFT calculations.

Entry	ΔG^0 [kcal/mol]	conformation C10 to C17						conformation C1 to C3	
1	0.00	t	t	g ⁻	t	g ⁻	t	g ⁻	tt
2	0.07	t	t	g ⁻	t	g ⁻	t	t	g ⁻ t
3	0.29	t	t	g ⁻	t	g ⁻	t	t	g ⁻ g ⁻
4	0.57	t	t	g ⁻	t	g ⁻	t	g ⁻	tg ⁺
5	0.61	t	t	g ⁻	t	g ⁻	t	t	g ⁺ t
6	1.00 ^a	t	t	g ⁻	t	g ⁻	t	g ⁻	g ⁻ t
7	1.10 ^b	t	t	g ⁻	t	s ⁺	g ⁻	t	g ⁺ t
8	1.12	g ⁺	t	g ⁻	t	g ⁻	t	t	tt
9	1.35	t	t	g ⁻	t	g ⁻	t	t	tg ⁺
10	1.69	t	t	g ⁻	t	g ⁻	t	t	tt
11	2.35	g ⁻	t	g ⁻	t	g ⁻	t	g ⁻	tt
12	2.77	t	t	g ⁻	t	g ⁻	t	t	tg ⁻
13	3.00 ^c	g ⁻	t	g ⁻	t	g ⁻	t	t	tt
14	3.01	g ⁺	t	g ⁻	t	g ⁻	t	t	g ⁻ t
15	4.24	t	t	g ⁻	t	g ⁻	g ⁻	t	g ⁺ t
16	5.18	t	t	g ⁻	t	g ⁻	g ⁻	t	tt

a) imaginary frequency = -34.7 cm^{-1} ; b) s-conformation describes an angle that is significantly smaller than 60° and closer to a staggered conformation; c) imaginary frequency = -21.2 cm^{-1} .

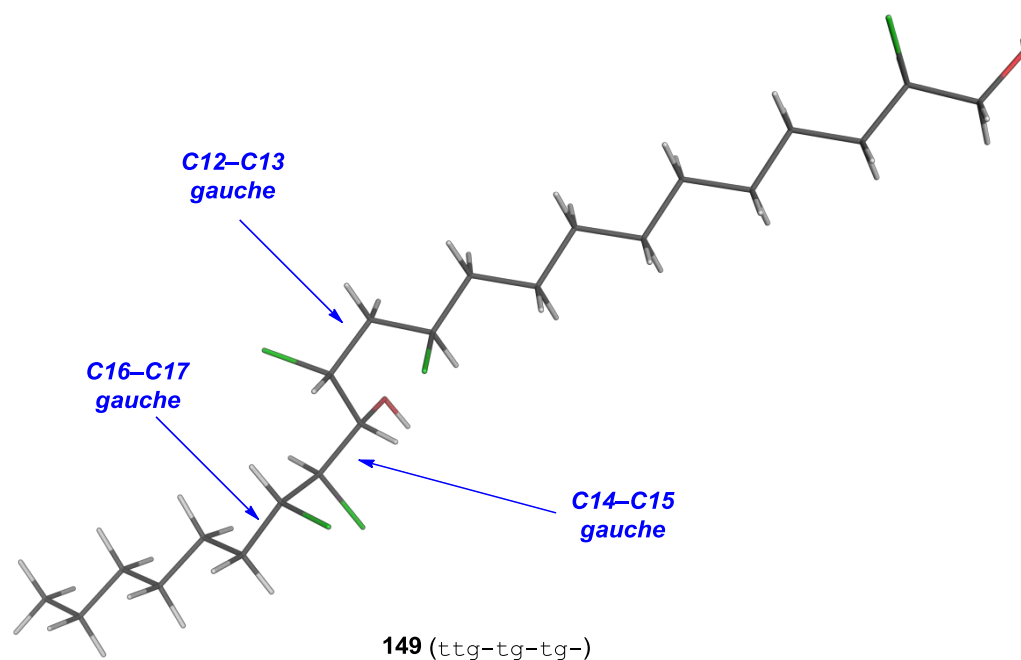


Figure 13 Lowest-energy conformer of **149** in a lines representation. The C12–C13, C14–C15, and C16–C17 *gauche* interactions are highlighted.

The low-energy conformations obtained for 16-*epi*-danicalipin A diol **150** are listed in Table 9. MCOMM gave 238 structures, 22 of which were analyzed by DFT calculations. As in the other examples, the computational analysis corroborated our analysis by molecular modeling/database approach.

Table 9 Energy differences for different conformers of **150** obtained from DFT calculations.

Entry	ΔG^0 [kcal/mol]		conformation C10 to C17						conformation C1 to C3	
1	0.00	g^+	t	t	t	t	t	t	g^+t	
2	0.31	t	t	t	t	t	t	t	g^-t	
3	0.45	t	t	t	t	t	t	g^+	tt	
4	0.47	g^-	t	t	t	t	t	t	g^-g^-	
5	0.88	g^-	t	t	t	t	t	t	g^-t	
6	0.93	t	t	t	t	t	t	t	g^+t	
7	1.64	t	t	t	t	t	t	t	tt	
8	1.67	g^-	t	t	t	t	t	t	tt	
9	1.81	g^-	t	t	t	t	t	t	tg^-	
10	2.18	g^-	t	t	t	t	t	g^+	tt	
11	2.50	g^+	t	t	t	t	t	t	tt	
12	3.03	t	t	t	t	t	t	t	tg^-	

The all-*trans* arrangement of the C11 to C16 region was the only one found. Small energy differences resulted from rotation around the C10–C11 and C16–C17 bonds, respectively and the more flexible bond appears to be C10–C11, as in danicalipin A diol **139**. Overall, the molecule should assume a singly-kinked structure, since four out of the six structures within 1 kcal/mol of the lowest one have a *gauche* interaction in the chlorinated segment (Entries 1,3–5). The lowest-energy structure with its single kink is shown in Figure 14.

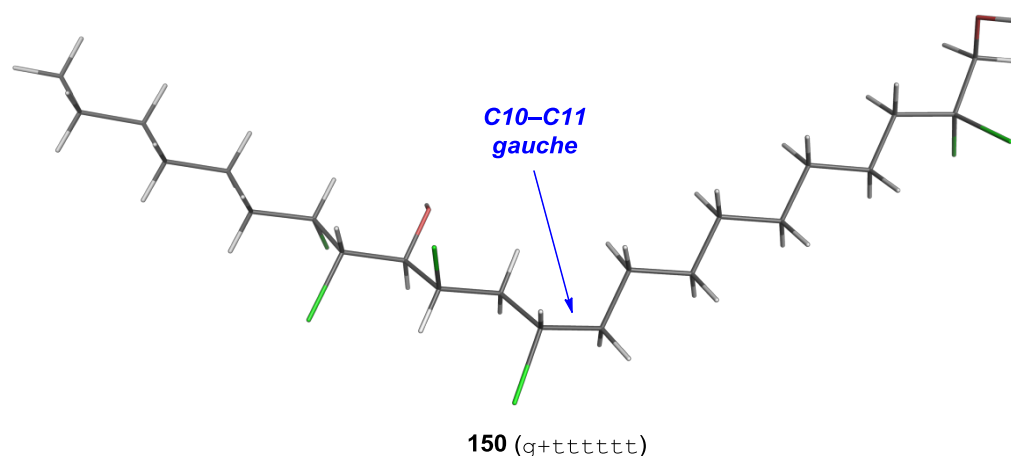


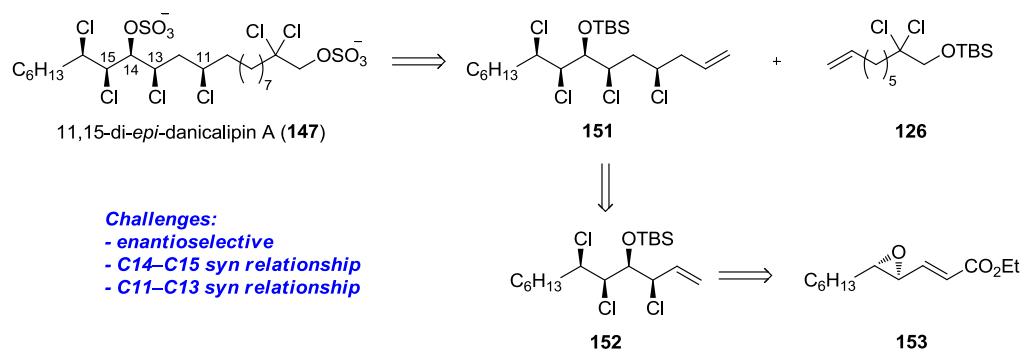
Figure 14 Lowest-energy conformer of **150** in a lines representation. The C10–C11 *gauche* interaction is highlighted.

Given that the computations arrived at the same conformations as did our molecular modeling/database approach, we were convinced that 11,15-di-*epi*- and 16-*epi*-danicalipin A (**147** & **148**) were suitable diastereomers to sample different molecular shapes, configurations, conformations, and flexibility. This would allow us to draw conclusions from their biological activity and potentially link the configuration of danicalipin A (**28**) to its unknown natural function.

3.4 Synthesis of 11,15-di-*epi*-Danicalipin A

During the planning of the route towards 11,15-di-*epi*-danicalipin A (**147**) our focus was on transformations that would allow for an efficient enantioselective synthesis. In particular, the C14–C15 *syn*-configuration was troublesome, since most known chlorosulfolipids carry a C14–C15 *anti*-motif, which is installed by the inherent selectivity of the substrate (*cf.* Chapter 2.4). Furthermore, we were wary of the C11,C13 *syn*-configuration, as this motif had only been previously described as a by-product.⁶²

We decided to follow similar disconnections as in CARREIRA's synthesis of danicalipin A (**28**, Scheme 28).¹¹⁷ Fragment **151** would be accessible by the highly diastereoselective BROWN allylation and displacement of the corresponding homoallylic hydroxy group. This strategy would lead us back to **152**, which is derived from the opening of a *cis*-vinyl epoxide, similar to CARREIRA's synthesis of mytilipin A (**30**, *cf.* Chapter 2.4.1).⁶⁶ The epoxide would result from SHARPLESS' dihydroxylation, followed by ring closure, as VANDERWAL had previously reported (*cf.* Chapter 2.4.2).⁶² The corresponding dichloroenoate had not been synthesized enantioselectively and methods to access this fragment in high *ee* have not been reported to date. However, we traced the dichloroenoate back to epoxide **153**.

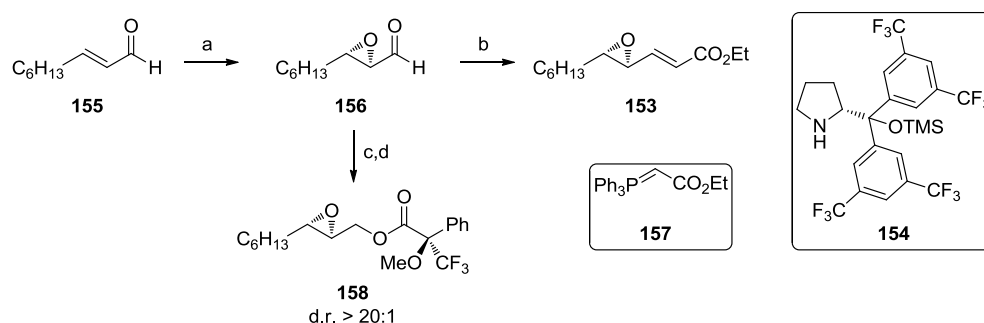


Scheme 28 Retrosynthetic analysis of 11,15-di-*epi*-danicalipin A (**147**) and the challenges associated with its synthesis.

Enantioenriched epoxides, such as **153**, can be synthesized from a variety of precursors. JØRGENSEN and co-workers had previously disclosed a method in which prolinol-derivative **154** was able to catalyze the enantioselective WEITZ–SCHEFFER

epoxidation¹⁵⁹ of α,β -unsaturated aldehydes.¹⁶⁰ Enolate **153** would follow from a WITTIG reaction.

To this end, (*E*)-nonenal (**155**) was subjected to 10 mol% **154** and aqueous H₂O₂ in CH₂Cl₂. The resulting epoxyaldehyde **156** was filtered through a pad of silica and directly treated with stabilized ylide **157** to give the desired epoxyenoate **153** in 61% yield (Scheme 29). The epoxidation proceeded in >95% *ee* as determined by formation of MOSHER ester derivative **158**.⁶⁰



Scheme 29 Synthesis of enoate **153**. Reagents and conditions: a) **154** (10 mol%), aq. H₂O₂, CH₂Cl₂, r.t.; b) **157**, CH₂Cl₂, 0 °C, 61% over 2 steps; c) NaBH₄, MeOH/THF, 0 °C; d) (*R*)-MOSHER acid, DCC, DMAP, CDCl₃, 44% over 3 steps, d.r. > 20:1.

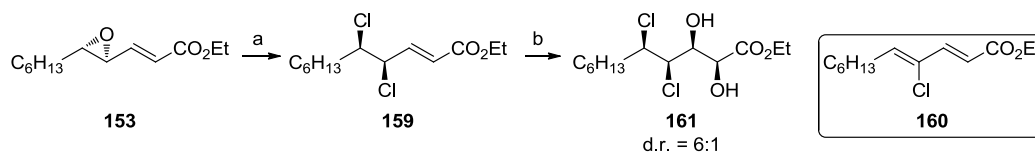
The synthesis continued with the reaction of **153** under YOSHIMITSU's conditions for the opening of vinyl epoxides (Ph₂PCI/NCS in CH₂Cl₂) to give dichloroenoate **159** in 45% yield (Scheme 30).⁹⁰ This reaction was hampered by the formation of **160** in 28%, presumably through elimination of the activated intermediate. The ideal reaction time was found to be five minutes, since longer exposure to the reaction conditions reduced the yields significantly. Any attempt to decrease the amount of elimination product proved to be in vain. The same results were obtained when the epoxide was added slowly or the temperature of the reaction was lowered to 18 °C.¹⁶¹ Enolate **159** was subsequently subjected to buffered SHARPLESS' dihydroxylation, giving diol **161** after 22 hours in 70% yield and 6:1 d.r.¹⁰⁷ Another elimination product was formed during the dihydroxylation and identified by the characteristic triplet in the olefinic region of the crude ¹H NMR

¹⁵⁹ E. Weitz, A. Scheffer *Chem. Ber.* **1921**, *54*, 2327-2344.

¹⁶⁰ M. Marigo, J. Franzen, T. B. Poulsen, W. Zhuang, K. A. Jørgensen *J. Am. Chem. Soc.* **2005**, *127*, 6964-6965.

¹⁶¹ The reaction did not yield any product at temperatures below 10 °C.

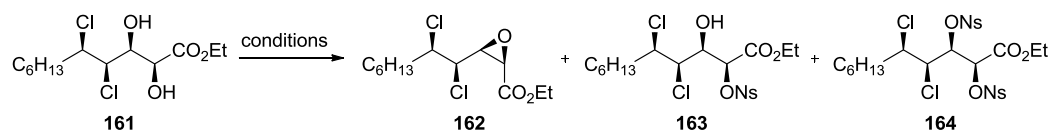
similar to a C5–H signal in **160**. Its yield increased with prolonged reaction times and required tedious chromatographic purification.



Scheme 30 Synthesis of diol **161**. Reagents and conditions: a) NCS, Ph_2PCl , CH_2Cl_2 , r.t., 45% of **159**, 28% of **160**; b) AD-mix β , NaHCO_3 , MeSO_3NH_2 , *t*-BuOH/ H_2O , 0 °C, 70%, d.r. = 6:1.

The next step was the formation of an epoxide similar to an intermediate in the synthesis of mytilipin B (**31**, *cf.* Chapter 2.4.5).¹⁰⁵ When **161** was subjected to Tf_2O and DABCO the desired epoxide was formed in 25% with substantial amounts of starting material recovered (Table 10, Entry 1). Purification of DABCO only decreased the yield further and since the amount of reagents could not be increased due to formation of bistriflated by-products, we anticipated a two-step procedure as reported by SHARPLESS.⁷⁷ To this end, diol **161** would be selectively nosylated at the α -hydroxy group and subsequently converted to the epoxide under basic conditions in methanol. We were surprised to find a complex mixture of products when diol **161** was treated with NsCl in pyridine at 0 °C (Entry 2). Subjecting diol **161** to NsCl and Et_3N in CH_2Cl_2 , yielded the primary *O*-nosyl derivative in 50% yield. We were delighted to find that epoxide **162** also formed in 40% yield during this reaction (Entry 3). However, when we attempted to close **163** under basic conditions (K_2CO_3 , EtOH) epoxide **162** was only obtained in 20% yield. Therefore, we decided to optimize the formation of epoxide **162** under the nosylating conditions. It proved sufficient to add more Et_3N to the reaction mixture after the reaction was completed to increase the yield of epoxide **162** to 74% yield on a 44 mg scale (Entry 4) and 58% yield on a 530 mg scale.

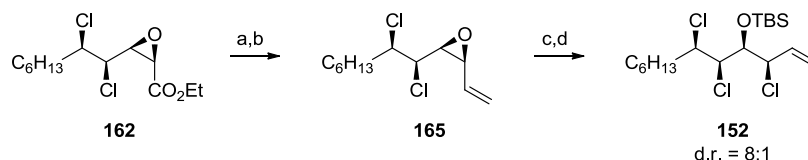
Table 10 Optimization studies for the formation of epoxide **162**.



Entry	Conditions	Yield 162	Yield 163
1	Tf ₂ O, DABCO, CH ₂ Cl ₂ , -78 °C	25% (68% brsm)	-
2	NsCl, pyridine, 0 °C	complex mixture (162 + 163 + 164 + others)	
3	NsCl, Et ₃ N, CH ₂ Cl ₂ , 0 °C	40%	50%
4	NsCl, Et ₃ N, CH ₂ Cl ₂ , 0 °C; then Et ₃ N	74%	n.d.

Reactions were performed on 50 mg scales. n.d. = not determined.

The synthesis continued with the reduction of the ester to an aldehyde, which was directly subjected to WITTIG reaction, giving vinyl epoxide **165** in 91% yield (Scheme 31).⁶⁹ Fortunately, since it was crucial that the epoxide opening would proceed with inversion of configuration, SHEMET *et al.* had reported that the opening of *cis*-epoxides that bear a *syn*-chloro substituent undergo opening under inversion (d.r. = 5:1).⁷¹ In our system the second chlorine substituent improved the diastereoselectivity to 8:1 and intermediate **152** was obtained in 76% yield after TBS protection.



Scheme 31 Synthesis of fragment **152**. Reagents and conditions: a) (*i*-Bu)₂AlH, toluene, -78 °C; b) KHMDS, MePPh₃Br, THF, -78 to 0 °C, then aldehyde, -78 to 0 °C, 91% over 2 steps; c) TMSCl, EtOAc/CH₂Cl₂, 0 °C to r.t., d.r. = 8:1; d) TBSOTf, Et₃N, CH₂Cl₂, r.t., 76% over 2 steps.

At this stage the relative configuration could be established by JBCA (Table 11).⁵⁹ The *gauche* conformation along the C4–C5 bond, which we expected for the final product, was already present in this intermediate, indicating that our initial conformational analysis was valid.

Table 11 JBCA for intermediate **152**.

152

C3–C4		C4–C5		C5–C6	
$^3J_{\text{H3-H4}}$	2.2 (s)	$^3J_{\text{H4-H5}}$	7.0 (l)	$^3J_{\text{H5-H6}}$	2.5 (s)
$^3J_{\text{H4-C2}}/{}^3J_{\text{C5-H3}}$	1.8 ^a (s)/1.1 (s)	$^3J_{\text{H5-C3}}/{}^3J_{\text{C6-H4}}$	1.5 (s)/2.5 (s)	$^3J_{\text{H6-C4}}/{}^3J_{\text{C7-H5}}$	0.9 (s)/1.2 (s)
$^2J_{\text{C4-H3}}/{}^2J_{\text{C3-H4}}$	-0.5 (s)/2.5 ^a (s)	$^2J_{\text{C5-H4}}/{}^2J_{\text{C4-H5}}$	-4.8 (l)/-5.6 (l)	$^2J_{\text{C6-H5}}/{}^2J_{\text{C5-H6}}$	n.d./n.d.

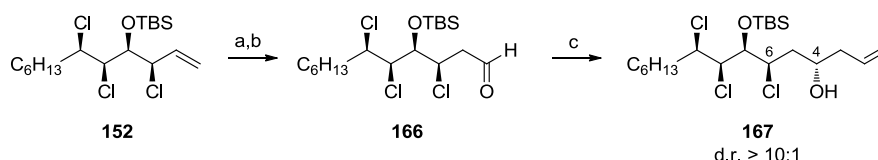
syn (A-1)

syn (A-3)^b

syn (A-1)

Coupling constants are reported in Hertz (Hz). All spectra were recorded in CDCl_3 . Heteronuclear coupling constants were determined in a HSQC-HECADE spectrum. a) determined in a phase sensitive-HMBC spectrum; b) NOE observed between H3 and H6. s = small, l = large; n.d. = not determined, due to weak peak intensity, overlap, or signal of higher order.

With the all-*syn* motif established, we followed the same reaction sequence as for the synthesis of danicalipin A (**28**).¹¹⁷ Hydroboration of the olefin with Cy_2BH preceded oxidation of the resulting alkylborane with NaBO_3 in 85% yield (Scheme 32). The primary alcohol was oxidized with DESS–MARTIN periodinane⁹¹ and subjected to BROWN allylation with $(-)\text{-(Ipc)}_2\text{B(allyl)}$,¹²¹ giving homoallylic alcohol **167** in 73% yield and d.r. > 10:1.

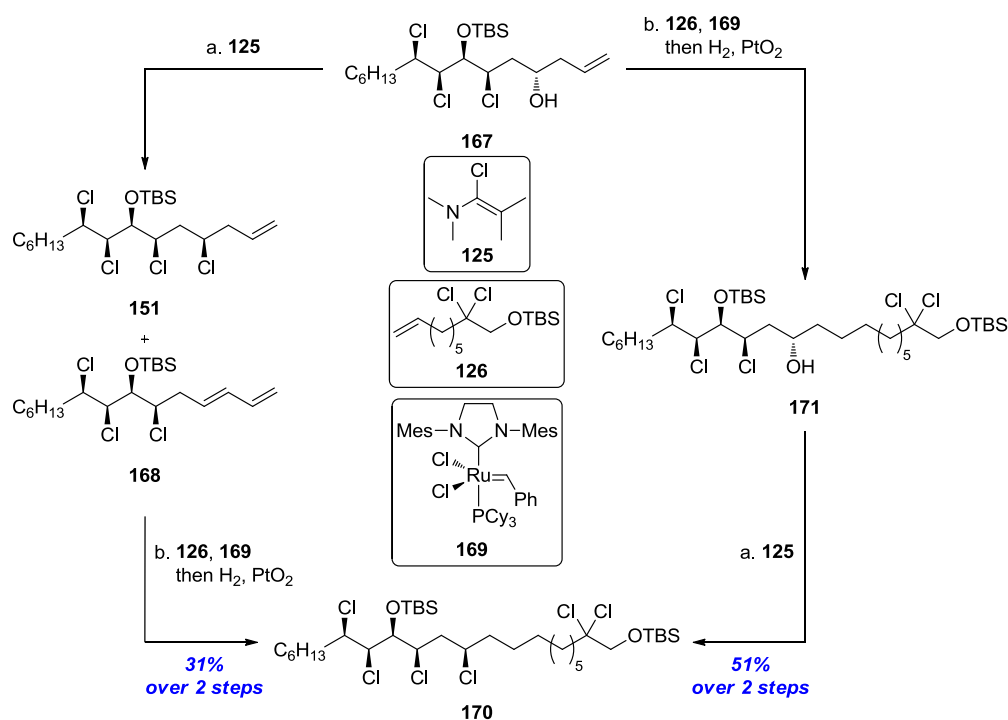


Scheme 32 Synthesis of homoallylic alcohol **167**. Reagents and conditions: a) Cy_2BH , THF, 0 °C to r.t., then $\text{NaBO}_3 \cdot 4\text{H}_2\text{O}$, THF/ H_2O , 0 °C to r.t., 85%; b) DMP, CH_2Cl_2 , 0 °C to r.t.; c) $(-)\text{-(Ipc)}_2\text{BCl}$, allylMgBr, THF, -78 °C to r.t., then **166**, -100 °C to r.t., 73% over 2 steps, d.r. > 10:1.

Unfortunately, when we tried to displace the homoallylic alcohol in **167** with GHOSEZ's reagent (**125**),¹²² we obtained an inseparable 1:1 mixture of **151** and conjugated diene **168** (Scheme 33). This problem had not been encountered for the 4,6-*syn* motif in **124** during the synthesis of danicalipin A (**28**), allowing the speculation that the distinct conformation of **167** or **151** sets intermediates up for elimination. Cross-metathesis of the mixture and **126** with GRUBBS' second generation catalyst (**169**)⁹⁴ was directly followed by addition of catalytic amounts of PtO_2 .^{93,123}

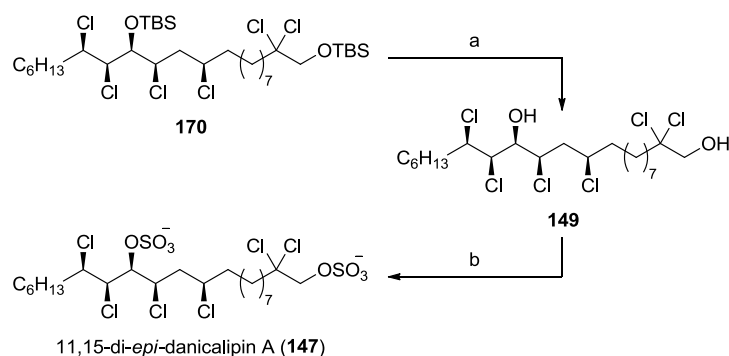
After the reaction had been set under an atmosphere of hydrogen, intermediate **170** was obtained in 31% yield over both steps.

The low yield prompted us to reinvestigate the order in which both reactions were conducted. Performing the cross-metathesis/reduction prior to the displacement with GHOSEZ's reagent (**125**) yielded a cleaner sample of hexachloride **170** in 51% overall yield.



Scheme 33 Synthesis of hexachloride **170**. Reagents and conditions: a) **125**, CHCl_3 , $0\text{ }^\circ\text{C}$ to r.t., for **171** to **170**: 78%; b) **126**, **169** (10 mol%), CH_2Cl_2 , $40\text{ }^\circ\text{C}$, then PtO_2 (10 mol%), H_2 (1 atm), r.t., for **151** to **170**: 31% over 2 steps, for **167** to **171**: 66%.

Diol **149** was obtained in 93% yield by refluxing **170** in acidified methanol (Scheme 34). Sulfation with $\text{SO}_3\cdot\text{pyridine}$ proceeded in less than five minutes and quantitative yield, completing the synthesis of 11,15-di-*epi*-danicalipin A (**147**). During the final sulfation, it was found important to stir the crude reaction mixture with aqueous NaHCO_3 to quench the excess of $\text{SO}_3\cdot\text{pyridine}$. Otherwise methylsulfuric acid formed under the column conditions ($\text{CH}_2\text{Cl}_2/\text{MeOH}$ 6:1, SiO_2) and was difficult to separate from the desired product.

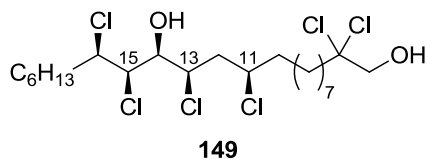


Scheme 34 Final steps of the synthesis of 11,15-di-*epi*-danicalipin A (**147**). Reagents and conditions: a) AcCl, MeOH, 0 to 80 °C, 93%; b) SO₃·pyridine, THF, r.t., quantitative.

The configuration could be established through JBCA of diol **149** (Table 12).⁵⁹ The all-*syn* structure was confirmed and the solution-state conformation was identical to the one obtained from computations, with *gauche* interactions along C12–C13 and C14–C15 (*tg*–*tg*–*t*, *vide supra*). Close inspection of the C11,C13 indicated that the predicted conformer is the major species in solution. But the medium coupling constants in $^3J_{\text{H}_{12}\text{H}_{11}}$ and $^3J_{\text{H}_{13}\text{H}_{12\text{h}}}$ suggest the presence of a minor conformer in that region (*vide infra*).

The conformation of 16-*epi*-danicalipin A diol **150** also supported our theoretical analysis. Accordingly, we had correctly predicted the solution-state conformation of two complex polychlorinated lipids. With the solution-state structures of the two diastereomers of danicalipin A (**28**) established, the biological impact of configuration and the resulting conformation could be investigated.

Table 12 JBCA for diol **149**.



C11–C12		C12–C13	
$^3J_{\text{H12h-H11}}/^3J_{\text{H12l-H11}}$	9.7 (l)/4.2 (m)	$^3J_{\text{H13-H12h}}/^3J_{\text{H13-H12l}}$	5.9 (m)/8.5 (l)
$^3J_{\text{H11-C13}}$	2.4 (s)	$^3J_{\text{H13-C11}}$	2.4 (s)
$^3J_{\text{C10-H12h}}/^3J_{\text{C10-H12l}}$	2.0 (s)/3.0 (s)	$^3J_{\text{C14-H12h}}/^3J_{\text{C14-H12l}}$	n.d./n.d.
$^2J_{\text{C11-H12h}}/^2J_{\text{C11-H12l}}$	n.d./n.d.	$^2J_{\text{C13-H12h}}/^2J_{\text{C13-H12l}}$	large ^a /large ^a

(D-1)

(D-3)

C11,C13-*syn* motif

C13–C14		C14–C15		C15–C16	
$^3J_{\text{H13-H14}}$	2.0 (s)	$^3J_{\text{H14-H15}}$	7.0 (l)	$^3J_{\text{H15-H16}}$	2.1 (s)
$^3J_{\text{H14-C12}}/^3J_{\text{C15-H13}}$	0.8 (s)/0.5 (s)	$^3J_{\text{H15-C13}}/^3J_{\text{C16-H14}}$	1.5 (s)/2.5 (s)	$^3J_{\text{H16-C14}}/^3J_{\text{C17-H15}}$	n.d./1.4 (s)
$^2J_{\text{C14-H13}}/^2J_{\text{C13-H14}}$	n.d./2.0 (s)	$^2J_{\text{C15-H14}}/^2J_{\text{C14-H15}}$	-4.8 (l)/-5.6 (l)	$^2J_{\text{C16-H15}}/^2J_{\text{C15-H16}}$	1.9 (s)/2.0 (s)

syn (A-1)

syn (A-3)^b

syn (A-1)

Coupling constants are reported in Hertz (Hz). All spectra were recorded in CDCl₃. Heteronuclear coupling constants were determined in a HSQC-HECADE spectrum. a) magnitude derived by comparing intensities in the phase sensitive-HMBC; b) NOE observed between H13 and H16. s = small, m = medium, l = large; n.d. = not determined, due to weak peak intensity, overlap, or signal of higher order.

3.5 Biological Effects Exhibited by the Diastereomers

3.5.1 Membrane Permeability Enhancement

One of the most interesting biological features of danicalipin A (**28**) is its ability to compromise bacterial and cellular membranes at non-toxic concentrations. When the organisms were incubated with danicalipin A (**28**) and a DNA stain, the fluorescence in the nuclei was consistent with the membranes of the organisms having become more permeable.¹¹⁷ This observation is intriguing, as **28**'s characteristic behavior in phospholipid-based membranes might shed light on its natural role in the membrane of *O. danica*.

In the experiment, incubation of *E. coli* DH5 α with 125 μ M concentrations of danicalipin A (**28**) led to a 5-fold increase in fluorescence of Hoechst 33342,¹³⁶ similar to positive control experiments, while the viability of the bacteria remained >90% (Figure 14). When the linear diastereomer 16-*epi*-danicalipin A (**148**) was used instead of **28**, the increase in fluorescence was just 3-fold at the same viability. Incubation with the zig-zag diastereomer 11,15-*di-epi*-danicalipin A (**147**) led to no

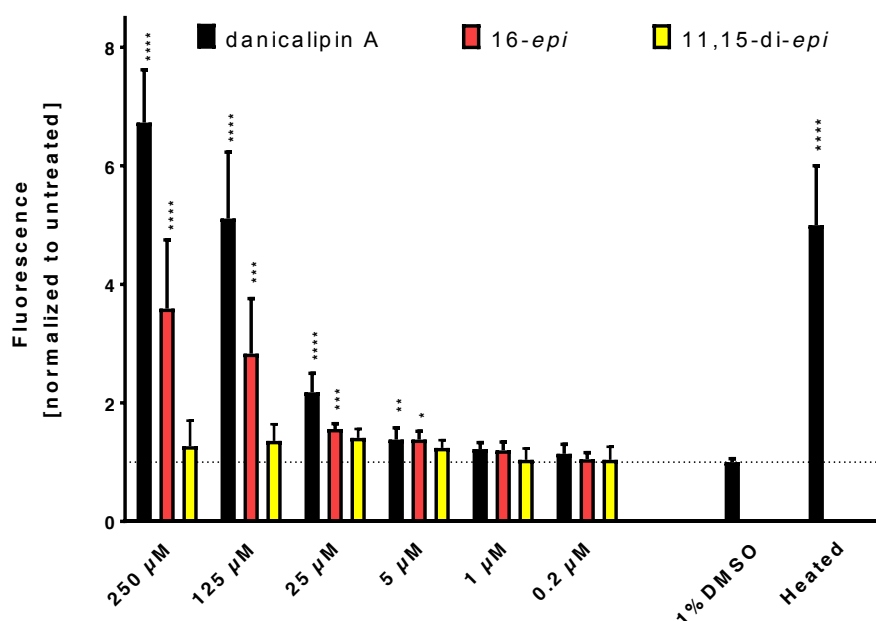
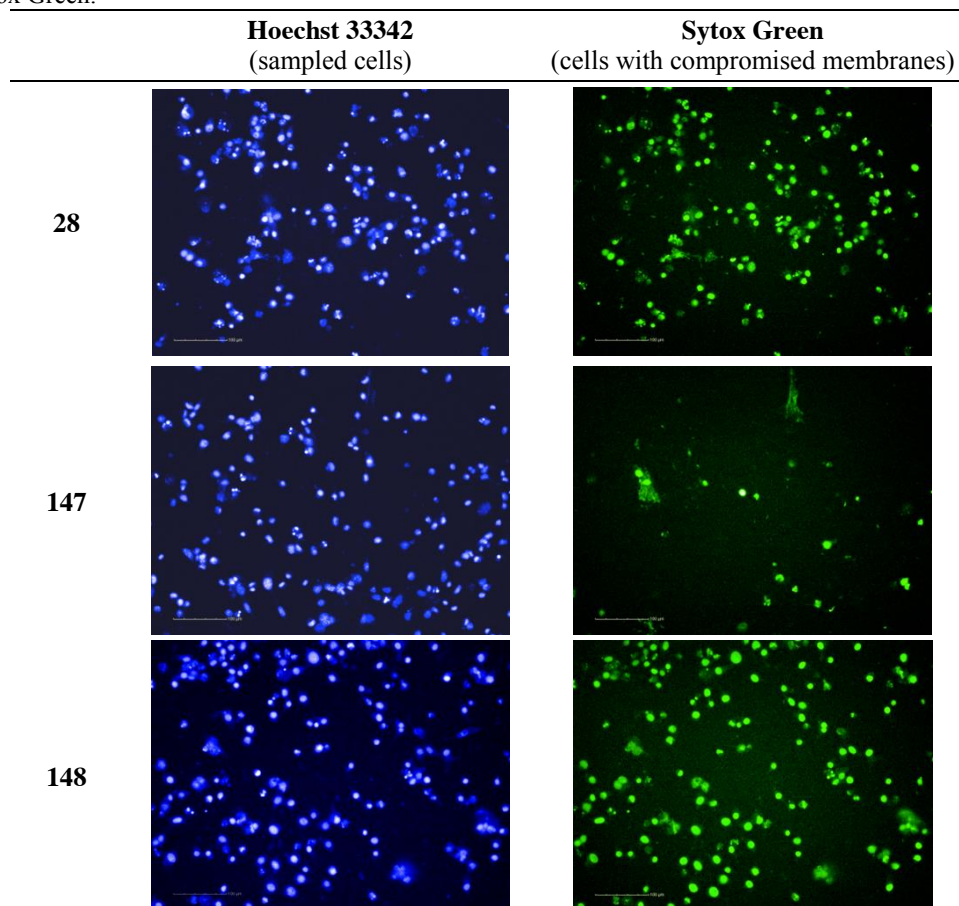


Figure 14 Membrane permeability enhancement in bacteria: Fluorescence response due to nuclear staining of *E. coli* DH5 α by Hoechst 33342 as a function of the concentration of **28**, **147**, or **148** as well as positive and negative control experiments. Data are normalized to the untreated results. The significance of each result vs. DMSO is shown above the bar: $p < 0.033 = *$; $p < 0.01 = **$; $p < 0.001 = ***$; $p < 0.0002 = ****$.

measurable increase in fluorescence even at toxic concentrations of 250 μM , at which point the viability dropped to 70%. Although we had anticipated differences in the membrane permeability enhancement of the diastereomers due to their distinct molecular shapes, the complete lack of this ability by **147** was surprising. We had attributed the membrane permeability enhancement to the amphipathic properties of **28**, which are also present in **147** and **148**.

In order to substantiate these observations we investigated the impact that the diastereomers had on the membrane of murine liver cancer cell line Hepa 1-6. The same trend as in the bacterial membranes was observed and is shown in Table 13. The Hoechst 33342/Sytox Green assay distinguishes between cells with intact and compromised membranes. The DNA stain Hoechst 33342 can permeate cellular membranes and stains all genetic material in the sample. Therefore, the blue spots in the pictures can be considered as all sampled cells. Sytox Green on the other hand is not able to cross cellular membranes, unless they are compromised.¹³⁷ Hence, green spots indicate cells whose membranes are more permeable. It can be clearly seen that all sampled cells had compromised cellular membranes when they were incubated with 25 μM concentrations of danicalipin A (**28**) or 16-*epi*-danicalipin A (**148**). However, minimal staining of Sytox Green was observed in samples that were incubated with 11,15-di-*epi*-danicalipin A (**147**), suggesting that **147** is not enhancing membrane permeability. It is worthy of note that the measurements with Hepa 1-6 cells were performed at concentrations close to the LC_{50} of compounds **28**, **147**, and **148** (*vide infra*) and the fact that **147** cannot compromise cellular membranes emphasizes that toxicity does not result from membrane permeability enhancement.

Table 13 Membrane permeability enhancement in mammalian cells: Fluorescent images of Hepa 1-6 cells after incubation with compounds **28**, **147**, and **148** at 25 μM concentration. Blue: Sampled cells, visualized with Hoechst 33342. Green: Cells with compromised cell membranes, visualized with Sytox Green.



3.5.2 Toxicity

The toxicological profile of danicalipin A (**28**) had been established in order to elucidate its potential link with self-defense mechanisms of *O. danica* (cf. Chapter 2.5). We were interested to see whether toxicity was linked to molecular shape and/or configuration. This might help in identifying the mode of action by which **28** is toxic and establish a starting point for the investigations of other chlorosulfolipids.

Given OKINO's hypothesis that the chlorosulfolipid's toxicity arises from their amphipathic shape, we started our investigations by measuring brine shrimp toxicity.⁶³ All of the three diastereomers **28**, **147**, and **148** displayed similar LC_{50} values, suggesting that configuration has no impact on toxicity (Table 14). These results were further corroborated by comparable cytotoxicities against several mammalian cell

lines. One exception is the increased toxicity of **147** against HT-29 cells. The zig-zag diastereomer **147** had already been a special case in the membrane permeability enhancement and its peculiar properties might be responsible for the increased toxicity against HT-29 cells (*vide infra*).

Table 14 Toxicity exhibited by **28**, **147**, and **148** against several organisms. The values correspond to the LC₅₀ value and are reported in μM . Brine shrimp *Artemia salina*; HT-29 human colorectal adenocarcinoma; A549 human alveolar adenocarcinoma; Hepa 1-6 murine liver cancer.

Toxicity (LC ₅₀) [μM]	Brine shrimp	HT-29 cells	A549 cells	Hepa 1-6 cells
28	2.5	14.7 \pm 0.4	32.2 \pm 0.4	14.7 \pm 0.1
147	4.5	3.7 \pm 0.6	36.0 \pm 0.8	10.2 \pm 0.1
148	5.7	10.9 \pm 0.1	42.6 \pm 1.3	13.3 \pm 0.1

In general, the configuration and/or conformation of danicalipin A (**28**) and its diastereomers does not seem to play a decisive role in their toxicology. It is possible that toxicity is linked to the amphiphilicity of these compounds. HAINES had already pointed out that danicalipin A (**28**) had detergent properties and was able to denature enzymes.⁴² The same properties would be present in diastereomers **147** and **148**, and could account for their overall toxicities. This hypothesis would render an explicit target unlikely, although more studies would be needed to completely rule out a specific mode of action.

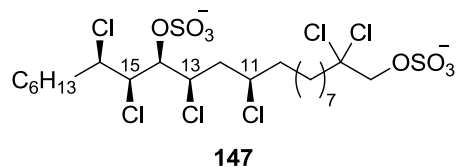
3.5.3 Rationalization of Bioactivity

Despite the fact that we expected an impact of configuration and conformation on bioactivity, we were surprised by the extent of our findings. Furthermore, we were not able to conclusively explain how the different number of *gauche* interactions would be this significant. Specifically, the reason why zero or one *gauche* conformations in 16-*epi*- and danicalipin A (**148** and **28**) would result in equal toxicity as two *gauche* conformations in 11,15-di-*epi*-danicalipin A (**147**), while the latter completely lacked the ability to compromise bacterial and cellular membranes, was exciting. Either solution-state conformation had nothing to do with bioactivity or there existed an additional level of complexity that we had not yet fully accounted for.

Given that our previous solution-state analysis was performed on the diols **139**, **149**, and **150**, a closer look was taken at the solution-state structure of disulfates **28**,

147, and **148**. In general, the spectra for these compounds suffered from peak overlap and ambiguous signal shapes, precluding full JBCA on the disulfates.⁵⁹ The JBCA of 11,15-di-*epi*-danicalipin A (**147**) is shown in Table 15.

Table 15 JBCA for 11,15-di-*epi*-danicalipin A **147**.



C11–C12		C12–C13			
$^3J_{\text{H12h-H11}}/^3J_{\text{H12l-H11}}$	9.7 (l)/4.0 (m)	$^3J_{\text{H13-H12h}}/^3J_{\text{H13-H12l}}$	5.6 (m)/8.7 (l)		
$^3J_{\text{H11-C13}}$	n.d.	$^3J_{\text{H13-C11}}$	2.0 (s) ^a		
$^3J_{\text{C10-H12h}}/^3J_{\text{C10-H12l}}$	n.d./n.d.	$^3J_{\text{C14-H12h}}/^3J_{\text{C14-H12l}}$	n.d./n.d.		
$^2J_{\text{C11-H12h}}/^2J_{\text{C11-H12l}}$	n.d./n.d.	$^2J_{\text{C13-H12h}}/^2J_{\text{C13-H12l}}$	n.d./-1.5 (m) ^a		
<p style="text-align: center;">(D-1)</p>		<p style="text-align: center;">(D-3)</p>			
C13–C14		C14–C15		C15–C16	
$^3J_{\text{H13-H14}}$	1.9 (s)	$^3J_{\text{H14-H15}}$	7.3 (l)	$^3J_{\text{H15-H16}}$	2.7 (s)
$^3J_{\text{H14-C12}}/^3J_{\text{C15-H13}}$	n.d./n.d.	$^3J_{\text{H15-C13}}/^3J_{\text{C16-H14}}$	n.d./n.d.	$^3J_{\text{H16-C14}}/^3J_{\text{C17-H15}}$	small ^b /small ^b
$^2J_{\text{C14-H13}}/^2J_{\text{C13-H14}}$	n.d./n.d.	$^2J_{\text{C15-H14}}/^2J_{\text{C14-H15}}$	-5.0 (l)/-5.4 (l)	$^2J_{\text{C16-H15}}/^2J_{\text{C15-H16}}$	n.d./n.d.
<p style="text-align: center;">A-1 (or A-2)</p>		<p style="text-align: center;">A-3</p>		<p style="text-align: center;">A-1</p>	

Coupling constants are reported in Hertz (Hz). All spectra were recorded in CD₃OD. Heteronuclear coupling constants were determined in a HSQC-HECADE spectrum. a) cross-peak was ambiguous, values approximated; b) values could not be determined but the peak intensity allowed approximation of coupling constant size. s = small, m = medium, l = large; n.d. = not determined, due to weak peak intensity, overlap, or signal of higher order.

Not even half of the required values could be measured, but all measured ones are within 0.2 Hz of the coupling constants for the diol **149** (*cf.* Table 12). Most of the bonds could therefore be assigned by comparison. A good example is the C13–C14 bond, where only one coupling constant could be measured. The size of that coupling constant by itself would suggest conformations A-1, A-2, B-1, or B-2, but since the relative *syn*-configuration was established on diol **149**, the *anti* configurations B-1 and B-2 could be excluded. The conformation of diol **149** and intermediate **152** was A-1

and we assumed the same conformation for disulfate **147**. All other bonds were not as ambiguous as C13–C14 and suggested the same solution-state structure of disulfate **147** and diol **149**. Similar results were obtained from the spectra of **28** and **148**. With configuration established on the diols, comparison led us to believe that the solution-state structures of the disulfates were in fact identical to those of the diols. As this had been our initial hypothesis, we were still not able to fully explain the differences in biological activity.

Therefore, we decided to undertake the more challenging computations on the solution-state structures of disulfates. The same protocol was used as in Chapter 3.3.2 with the exception that parameters for methanol were used in the SMD protocol.¹⁵⁷ Thus, M06-2X/6-311++G**/LANL2DZpd(Cl)/SMD(methanol)//M06-2X/6-31+G**/ LANL2DZpd(Cl)/SMD(methanol) level of theory for danicalipin A (**28**) gave the results shown in Table 16.

Table 16 Energy differences for different conformers for **28** obtained from DFT calculations.

Entry	ΔG^0 [kcal/mol]	conformation C10 to C17							conformation C1 to C3	
1	0.00	t	t	t	t	t	t	g ⁺	t	g ⁺ g ⁺
2	2.02	g ⁺	t	t	t	t	t	g ⁺	t	g ⁺ t
3	2.33	t	t	t	t	t	t	g ⁺	t	g ⁻ t
4	2.66 ^a	g ⁻	t	t	t	t	t	g ⁺	t	g ⁻ t
5	3.02	g ⁺	t	t	t	t	t	g ⁺	t	g ⁻ t
6	3.17	t	t	t	t	t	t	g ⁺	t	g ⁺ t
7	3.18	g ⁻	t	t	t	t	t	g ⁺	t	g ⁺ t

a) imaginary frequency = -10.3 cm^{-1} .

The results were comparable to the structures obtained for diol **139**, with the exception that the lowest-energy conformer did not show a *gauche* conformation at the C10–C11 olefin (Entry 1) and was 2 kcal/mol lower than the corresponding conformer with a *gauche* at C10–C11 (Entry 2). The lowest-energy structure therefore showed a singular kink at C15–C16 as depicted in Figure 15.

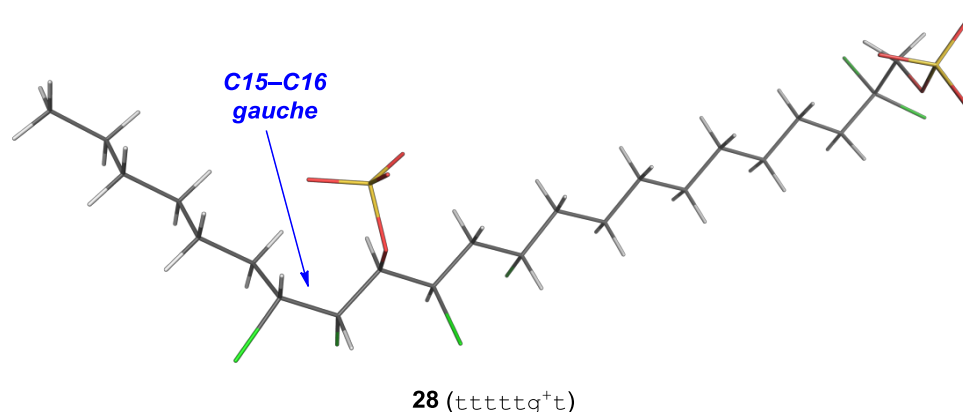


Figure 15 Lowest-energy conformer of danicalipin A (**28**) in a lines representation. The C15–C16 *gauche* interaction is highlighted.

This structure was in full agreement with the limited NMR data that was available for danicalipin A (**28**). Therefore, we were confident that this structure should be used to explain the bioactivity. The kink introduced a similar structural element to the carbon chain as would a (*Z*)-olefin, which could explain the natural function of danicalipin A (**28**) to some extent. In phospholipid-based membranes, the degree of (poly)unsaturated fatty acids determines a variety of functions, such as membrane fluidity, permeability, and fusion, as well as the binding properties of membrane-bound receptors and enzymes.¹⁶² For example, spermatozoa show an increased content of (poly)unsaturated fatty acid when compared to other cells and a higher content of these fatty acids in men,¹⁶³ boar,¹⁶⁴ and fish¹⁶⁵ leads to higher fertility, presumably by increasing membrane fluidity. In spermatozoa from the fish *Sparus aurata* membrane composition in the head and flagellum, respectively, were directly determined and correlated to the function of the domain.¹⁶⁶ The higher degree of (poly)unsaturated fatty acids in the flagellum correlated with higher sperm motility and viability. Accordingly, this might be relevant to the function that danicalipin A (**28**) fulfills in the flagellum of *O. danica*. The singular kink might help improve the flagellar beating in a similar fashion as unsaturated fatty acids in spermatozoa. The

¹⁶² T.-A. Hagve *Scand. J. Clin. Lab. Invest.* **1988**, *48*, 381-388.

¹⁶³ Y. Aksoy, H. Aksoy, K. Altınkaynak, H. R. Aydın, A. Özkan *Prostaglandins Leukot. Essent. Fatty Acids* **2006**, *75*, 75-79.

¹⁶⁴ N. Am-in, R. N. Kirkwood, M. Techakumphu, W. Tantasuparuk *Theriogenology* **2011**, *75*, 897-903.

¹⁶⁵ J. F. Asturiano, L. A. Sorbera, M. Carrillo, S. Zanuy, J. Ramos, J. C. Navarro, N. Bromage *Aquaculture* **2001**, *194*, 173-190.

¹⁶⁶ J. Beirão, L. Zilli, S. Vilella, E. Cabrita, C. Fernández-Díez, R. Schiavone, M. P. Herráez *J. Appl. Ichthyol.* **2012**, *28*, 1017-1019.

overall abundance in the membrane of the microalgae could be correlated to a requirement for fluidity.

With the notion that the analysis of solution-state structures obtained from calculation could possibly lead to explanations on the bioactivity, we attempted to compute the structure for the elusive 11,15-di-*epi*-danicalipin A (**147**). Unfortunately, the lowest-energy structure obtained from MCMM/DFT ($\tau g^- g^- \tau g^+$) did not match the limited spectroscopic data which we had obtained for **147** ($\tau g^- \tau g^- \tau$). This constitutes the only case in which the MCMM fails to give experimentally confirmed conformations in the chlorinated segment studied. The force field cannot fully account for the convoluted structural biases in **147** and this example showcases the limits of this method. Interestingly, the second-lowest structure ($\Delta G^0 = 0.16$ kcal/mol) from the calculations had a different conformation along the C11 to C13 region ($g^+ \tau g^- \tau g^+$), inspiring us to compare the energies for different conformations along C11 to C13. Since MCMM could not give satisfying results, we assumed similar solution-state conformations in the C13–C16 region as for 11,15-di-*epi*-danicalipin A diol **149**. Instead of obtaining them from MCMM, all possible structures were drawn manually and then optimized with Gaussian under the same level of theory as before. The results from this analysis can be seen in Table 17. It should be noted that the lowest-energy conformer obtained from manual analysis was 3.1 kcal/mol lower in energy than the one obtained from MCMM/DFT.

The lowest-energy conformer had the same conformation in the C11 to C16 region, which had been calculated for diol **149**. This conformation was in agreement with our limited spectroscopic data. Moreover, the lowest-energy structure containing a τg^- conformation was only favored by 0.12 kcal/mol over the lowest one containing $g^+ \tau$ (Entries 1 & 12). This helped us understand the medium coupling constants in the JBCA of 11,15-di-*epi*-danicalipin A (**147**) (*cf.* Table 15). The coupling constants along the C11–C12 and C12–C13 bonds are consistent with a major (D-1 and D-3, respectively; τg^-) and a minor conformer (D-3 and D-1, respectively; $g^+ \tau$). Specifically, coupling constants of 4.0 Hz or 5.6 Hz can be explained by mixing a small value from the major and a large value from the minor. On the other hand,

coupling constants of 8.7 Hz or 9.7 Hz are explained by the combination of a large value from the major and a small value from the minor conformer.

Table 17 Energy differences for different conformers for **147** obtained from DFT calculations.

Entry	ΔG^0 [kcal/mol]	conformation C10 to C17						C1 to C3	
1	0.00	t	t	g ⁻	t	g ⁻	t	t	g ⁺ t
2	0.27 ^a	t	t	g ⁻	t	g ⁻	t	t	g ⁻ t
3	0.30	g ⁺	t	g ⁻	t	g ⁻	t	g ⁻	g ⁺ t
4	0.76	g ⁺	t	g ⁻	t	g ⁻	t	t	g ⁻ t
5	1.01	g ⁺	t	g ⁻	t	g ⁻	t	g ⁻	g ⁻ t
6	1.10	g ⁻	t	g ⁻	t	g ⁻	t	g ⁻	g ⁻ t
7	1.22	g ⁻	t	g ⁻	t	g ⁻	t	g ⁻	g ⁺ t
8	1.67 ^b	t	t	g ⁻	t	g ⁻	t	g ⁻	g ⁺ t
9	2.04	g ⁺	t	g ⁻	t	g ⁻	t	t	g ⁺ t
10	2.44	g ⁻	t	g ⁻	t	g ⁻	t	t	g ⁺ t
11	2.72	g ⁻	t	g ⁻	t	g ⁻	t	t	g ⁻ t
12	0.12 ^c	g ⁺	g ⁺	t	t	g ⁻	t	t	g ⁺ t
13	1.53	g ⁺	g ⁺	t	t	g ⁻	t	t	g ⁻ t
14	1.64	t	g ⁺	t	t	g ⁻	t	t	g ⁺ t
15	1.98	g ⁺	g ⁺	t	t	g ⁻	t	g ⁻	g ⁺ t
16	2.82	g ⁻	g ⁺	t	t	g ⁻	t	g ⁻	g ⁻ t
17	3.28 ^d	t	g ⁺	t	t	g ⁻	t	g ⁻	g ⁺ t
18	3.47	t	g ⁺	t	t	g ⁻	t	t	g ⁻ t
19	3.64	g ⁻	g ⁺	t	t	g ⁻	t	t	g ⁺ t
20	3.95	g ⁺	g ⁺	t	t	g ⁻	t	g ⁻	g ⁻ t
21	4.12 ^e	g ⁻	g ⁺	t	t	g ⁻	t	g ⁻	g ⁺ t
22	6.19	g ⁻	g ⁺	t	t	g ⁻	t	t	g ⁻ t

a) imaginary frequency = -19 cm^{-1} ; b) imaginary frequency = -10 cm^{-1} ; c) imaginary frequency = -40 cm^{-1} ; d) imaginary frequency = -20 cm^{-1} ; e) imaginary frequency = -18 cm^{-1} .

While one has to be careful when correlating thermodynamic data to kinetic conclusions it stands to reason that the two conformers are in a dynamic equilibrium with each other. This would render the overall molecular shape of the molecule less ordered when compared to danicalipin A (**28**). The two lowest-energy conformers of 11,15-di-*epi*-danicalipin A (**147**) are depicted in Figure 16. It can be seen that the overall shapes of both conformers deviate significantly from each other.

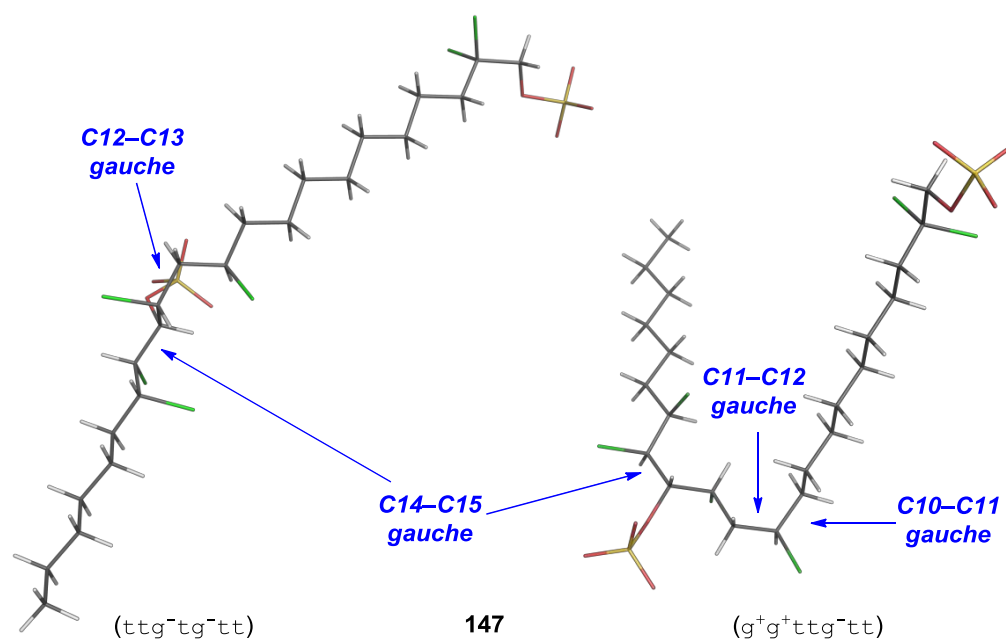


Figure 16 Lowest-energy conformers of 11,15-di-*epi*-danicalipin A (**147**) in lines representations. All *gauche* interactions are highlighted. The left-hand structure is 0.12 kcal/mol lower in energy than the right-hand one.

Given the differences in molecular shape of **28** and **147**, it became crucial to investigate the same properties for **148**. The structures obtained from MCMC were in accordance with JBCA. The results for the full MCMC/DFT analysis are shown in Table 18. The lowest-energy structure matched the one previously calculated and measured for diol **148** (Entry 1). This analysis represents another example in which additional conformers of the chlorinated region were found (Entries 5 & 6). Both of them have a *gauche* conformation in the C15–C16 bond but are too high in energy to be significantly populated.

Table 18 Energy differences for different conformers for **148** obtained from DFT calculations.

Entry	ΔG^0 [kcal/mol]	conformation C10 to C17							conformation C1 to C3	
1	0.00	<i>g</i> ⁻	<i>t</i>	<i>t</i>	<i>t</i>	<i>t</i>	<i>t</i>	<i>t</i>	<i>g</i> ⁺ <i>t</i>	
2	0.92	<i>t</i>	<i>t</i>	<i>t</i>	<i>t</i>	<i>t</i>	<i>t</i>	<i>g</i> ⁺	<i>g</i> ⁺ <i>t</i>	
3	1.15	<i>t</i>	<i>t</i>	<i>t</i>	<i>t</i>	<i>t</i>	<i>t</i>	<i>t</i>	<i>g</i> ⁺ <i>g</i> ⁺	
4	1.34	<i>t</i>	<i>t</i>	<i>t</i>	<i>t</i>	<i>t</i>	<i>t</i>	<i>t</i>	<i>g</i> ⁻ <i>t</i>	
5	4.85	<i>t</i>	<i>t</i>	<i>t</i>	<i>t</i>	<i>t</i>	<i>g</i> ⁻	<i>t</i>	<i>g</i> ⁺ <i>t</i>	
6	6.69	<i>t</i>	<i>t</i>	<i>t</i>	<i>t</i>	<i>t</i>	<i>g</i> ⁻	<i>g</i> ⁻	<i>g</i> ⁺ <i>t</i>	

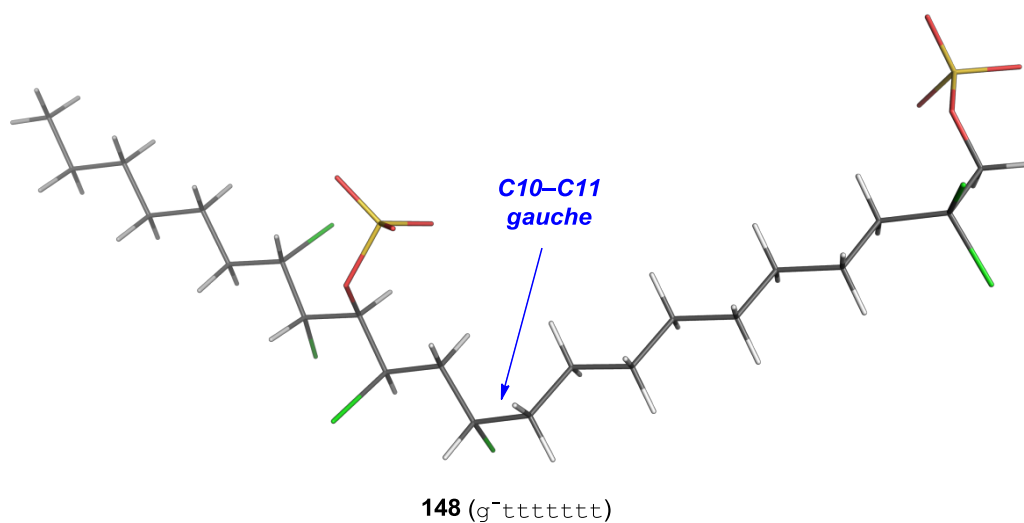


Figure 17 Lowest-energy conformer of 16-*epi*-danicalipin A (**148**) in a lines representation. The C10–C11 *gauche* interaction is highlighted.

The lowest-energy structure of **148** is depicted in Figure 17. While the C11 to C16 region is all-*trans*, as we had predicted earlier (*cf.* Figure 11), a *gauche* conformation in the C10–C11 bond gives the molecule an overall bent shape. Remarkably, when one compares the shape of **28** and **148** (*cf.* Figure 15), both look very similar. The major difference is that the kinks are on opposite sides of the C14-sulfate and that the energy differences to other conformers is larger in **28**.

Taking the gathered information on the solution-state structures of **28**, **147**, and **148** together, an interesting picture emerges. The membrane permeability enhancing properties are correlated to the molecular shape of the compound. Furthermore, the degree of flexibility determines the extent of this ability. Danicalipin A (**28**) was the most potent in compromising bacterial and cellular membranes, which could be explained by its kinked, non-flexible structure. The more-flexible 16-*epi*-danicalipin A (**148**) is still capable of compromising membranes with its kinked shape, albeit to a lesser extent. The ill-defined molecular shape and higher flexibility of 11,15-di-*epi*-danicalipin A (**147**) renders it completely incapable of compromising membranes.

This picture is in agreement with observations made in other systems. EWALD and SUNDIN reported that *anti*-9,10-dichlorostearic acid had a well-defined singly-kinked structure due to the *gauche* effect and was able to compromise cellular

membranes of mammalian tumor cells.¹⁶⁷ This effect was measured by ATP leakage and explained by the fatty acid's ability to increase membrane fluidity. Remarkably, the same effect was observed for oleic acid, albeit more pronounced. This exemplifies the similar behavior of a chlorinated segment and a (*Z*)-olefin, and gives credit to the hypothesis that the chlorinated segment in danicalipin A (**28**) acts in a similar fashion to an unsaturation in fatty acids.

¹⁶⁷ G. Ewald, P. Sundin *Pharmacol. Toxicol.* **1993**, 73, 159-162.

4 Conclusions and Outlook

In conclusion, we have studied diastereomers of danicalipin A (**28**), which exhibited diverse solution-state structures and biological activity. Selection of targets was achieved by an approach that combined a database analysis of trichlorinated hexanediols and molecular modeling of *syn*- and *anti*-2,4-dichloropentane, followed by MCMM and DFT calculations. The selected diastereomers, 11,15-di-*epi*-danicalipin A (**147**) and 16-*epi*-danicalipin A (**148**) contained zero and two *gauche* conformations, respectively, within the chlorinated C11 to C16 region, as opposed to a single one in danicalipin A (**28**).

The synthesis of 11,15-di-*epi*-danicalipin A (**28**) was achieved in 16 steps and 3% overall yield. The challenging C14–C15 *syn* relationship was established by JØRGENSEN's enantioselective epoxidation of enals, YOSHIMITSU's opening of the resulting epoxide to a dichloride, and subsequent asymmetric SHARPLESS' dihydroxylation. During this sequence, the propensity of the substrates to eliminate was noted and required careful optimization of reaction conditions and purification. The C11–C13 *syn* relationship was set by a diastereoselective BROWN allylation, followed by displacement of the resulting alcohol. While the homoallylic alcohol directly resulting from allylation could not be easily displaced due to competing elimination, it could be subjected to cross-metathesis/reduction and subsequent displacement to improve the overall yield of these steps. The synthesis of **147** and **148** allowed determination of their solution-state structures, which were in agreement with our earlier analysis. The JBCA of disulfates **28**, **147**, and **148** proved difficult and insufficient on their own, but conclusive in combination with JBCA of the corresponding diols **139**, **149**, and **150**.

The biological activity exhibited by the three diastereomers raised some questions. While **28** and **148** were able to compromise bacterial and cellular membranes, **147** was not. Furthermore, all compounds had similar toxicities towards

brine shrimp and mammalian cancer cell lines. The previously assumed link between toxicity and membrane permeability enhancement did not hold up to this test. Moreover, we were not able to fully rationalize the bioactivity with the different number of *gauche* conformations in solution. MCMM/DFT analysis of the disulfates revealed a high flexibility in the C11,C13 region of 11,15-di-*epi*-danicalipin A (**147**), explaining its peculiar properties. The flexibility and resulting ill-defined molecular shape prevents membrane permeability enhancement. In contrast, danicalipin A (**28**) and its C16-epimer **148** showed similar singly-kinked structures in their lowest-energy conformations, with the more flexible **148** being less efficient in compromising phospholipid-based membranes. This suggests that the toxicity arises from the amphiphilicity of these compounds and their detergent properties.

This project shed light on the polychlorinated array in danicalipin A (**28**) and its natural function. The C15–C16 *gauche* conformation introduces a kink to the molecule that resembles the effect a (*Z*)-olefin would impose in phospholipid-based membranes. Chlorosulfolipid **28** could be a substitute for unsaturated fatty acids in the membrane of *O. danica* and increase fluidity, thereby increasing the motility of the algae.

In future studies it would be interesting to see the effects exposure of the algae to diastereomers **147** and **148** has. It is known that when the algae are grown in a medium with low chloride concentrations, they can exist but are not as active or vital.³⁸ A lower concentration of danicalipin A (**28**) resulted from this starvation. Feeding these chloride-deprived organisms with the diastereomers would reveal how important the configuration is for the natural function of **28**. A quantitative investigation is inconceivable as the vitality is hard to measure, but qualitative analysis of algae movement could draw a telling picture. It would also be interesting to see if the algae would be able to complete the biosynthesis of partially chlorinated analogs of the diastereomers, e.g. missing the *gem*-dichloride at C2. Such an unspecific substrate binding would be unusual for a non-heme iron halogenase, making it interesting in biochemistry for the enzymatic halogenation of unactivated carbons.

Part III

EFFECT OF INCREASING CHLORINATION IN DANICALIPIN A AND ITS ANALOGS

5 Results and Discussion

5.1 Background

Beside the widespread use of halogenated hydrocarbons in pharmacological and medicinal applications (*cf.* Chapter 1.1), there exists an increasing number of harmful organohalogens of anthropogenic origin which accumulate in nature (Figure 18).¹⁶⁸

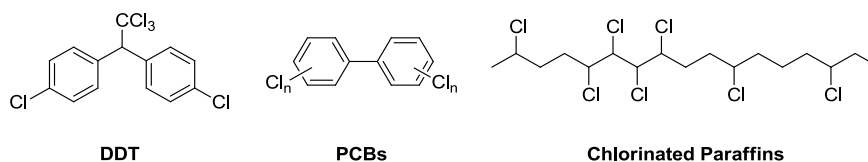


Figure 18 Examples of chlorinated persistent organic pollutants.

The discovery of dichlorodiphenyltrichloroethane (DDT) as an insecticide by MÜLLER was awarded the Nobel Prize in Physiology and Medicine in 1948.¹⁶⁹ But as carcinogen and endocrine disruptor in humans, along with its other detrimental effects on the environment, the molecule was placed on a list of banned organic compounds issued by the Stockholm Convention on Persistent Organic Pollutants in 2001.¹⁷⁰ Another entry from the same list addresses polychlorinated biphenyls (PCBs). Prior to their ban, they found extensive use as coolants, insulants, lubricants, and dielectric fluids, as well as plasticizers and additives to adhesives and paints.¹⁷¹ Toxicities exhibited by PCBs depend on the congeners, but span from carcinogenicity¹⁷² to

¹⁶⁸ M. Scheringer, S. Stempel, S. Hukari, C. A. Ng, M. Blepp, K. Hungerbühler *APR* **2012**, 3, 383-391.

¹⁶⁹ "The Nobel Prize in Physiology or Medicine 1948" Nobel Media AB 2014, retrieved 19 Apr 2017, <http://www.nobelprize.org/nobel_prizes/medicine/laureates/1948/>.

¹⁷⁰ Stockholm Convention, retrieved 19 Apr 2017, <<http://chm.pops.int/TheConvention/Overview/tabid/3351/Default.aspx>>.

¹⁷¹ M. Rossberg, W. Lendle, G. Pfeleiderer, A. Tögel, E.-L. Dreher, E. Langer, H. Rassaerts, P. Kleinschmidt, H. Strack, R. Cook, U. Beck, K.-A. Lipper, T. R. Torkelson, E. Löser, K. K. Beutel, T. Mann, "Chlorinated Hydrocarbons" in "Ullmann's Encyclopedia of Industrial Chemistry", Wiley-VCH, Weinheim, **2006**, p. 127.

¹⁷² B. Lauby-Secretan, D. Loomis, Y. Grosse, F. El Ghissassi, V. Bouvard, L. Benbrahim-Tallaa, N. Guha, R. Baan, H. Mattock, K. Straif *Lancet Oncol.* **2013**, 14, 287-288.

neurotoxicity.¹⁷³ Their longevity and bioaccumulation in fat tissue cause them to biomagnify¹⁷⁴ and PCBs have recently been isolated from amphipods in deep-sea trenches (>10,000 meters) at concentrations of 382 ppb dry weight.¹⁷⁵ Other recent studies have identified chlorinated paraffins as constituents of household dust in five different countries at concentrations of up to 700 ppm along with other anthropogenic organohalogenes.¹⁷⁶ Chlorinated paraffins can vary in chlorination degree and chain length and are commonly used in industry as plasticizers, flame retardants, and as additives in metal workings.¹⁷⁷ Some isomers have shown carcinogenicity in mice and rats,¹⁷⁸ while others were toxic to aquatic and avian organisms.¹⁷⁹

These and other anthropogenic organochlorines have been subject to intense scrutiny, and their toxicology and bioactivity is often linked to a specific chlorination pattern (*vide supra*). Chlorosulfolipids also display specific chlorinated arrays, allowing the conjecture that these arrays are tied to the biological functions of the polychlorinated natural products.

5.2 Project Outline

Our question was: To what extent does the degree of chlorination in danicalipin A (**28**) matter for its biological activities? More specifically, is the same dependence on chlorination observed for the toxicity of chlorosulfolipids as is the case for persistent organic pollutants (*cf.* Chapter 5.1)? The chlorination pattern does impart a defined molecular shape to the molecule and potentially enables its unspecified membrane function. However, the array between C11 and C16 seems to be too complex to simply introduce a stable kink to the molecule and we wanted to investigate whether the bioactivities further depend on all of the chlorine substituents, for example by increasing lipophilicity. To this end, we decided to synthesize a

¹⁷³ S. A. Roelens, V. Beck, G. Aerts, S. Clerens, G. Vanden Bergh, L. Arckens, V. M. Darras, S. van der Geyten *Ann. N.Y. Acad. Sci.* **2005**, *1040*, 454-456.

¹⁷⁴ W. J. Crinnion *Altern. Med. Rev.* **2011**, *16*, 5-13.

¹⁷⁵ A. J. Jamieson, T. Malkocs, S. B. Piertney, T. Fujii, Z. Zhang *Nat. Ecol. Evol.* **2017**, *1*, doi: 10.1038/s41559-016-0051.

¹⁷⁶ J. Pelley *ACS Cent. Sci.* **2017**, *3*, 5-9.

¹⁷⁷ ref. 171, p. 103 f.

¹⁷⁸ *IARC Monographs on the Evaluation of Carcinogenic Risks to Humans* **1990**, *48*, 55-72.

¹⁷⁹ J. R. Madeley, R. D. N. Birtley *Environ. Sci. Technol.* **1980**, *14*, 1215-1221.

variety of chlorinated docosanedisulfates (DDS), bearing one to seven chlorines (Table 19).

Table 19 Danicalipin A (**28**) and analogs thereof with varying degrees of chlorination.

Compound number	R ¹	R ²	R ³	R ⁴	R ⁵	R ⁶
27	Cl	H	H	H	H	H
171	H	Cl	H	H	H	H
140	Cl	Cl	H	H	H	H
141	Cl	Cl	Cl	H	H	H
172	Cl	Cl	Cl	Cl	H	H
28	Cl	Cl	Cl	Cl	Cl	H
173	Cl	Cl	Cl	Cl	Cl	Cl

The mono-, di-, tri-, and tetrachloro-DDS (**27**, **171**, **140**, and **141**) are proposed biosynthetic intermediates that have been isolated from *O. danica*.^{43,63} Concerning permeability enhancement, we would expect that tetrachloro-DDS **141** would have a similar shape to danicalipin A (**28**) and therefore display similar bioactivity. The same conformation as **28** should also be assumed by pentachloro-DDS **172**, since it is only lacking one of the two *gem*-dichlorines at C2. Another intriguing analog was heptachloro-DDS (**173**), since danicalipin A (**28**) is lacking a C12-chlorine when compared to other chlorosulfolipids (Figure 19). The bioactivity of such a heptachloro analog could reveal potential reasons for the absence of this chlorine in **28**.

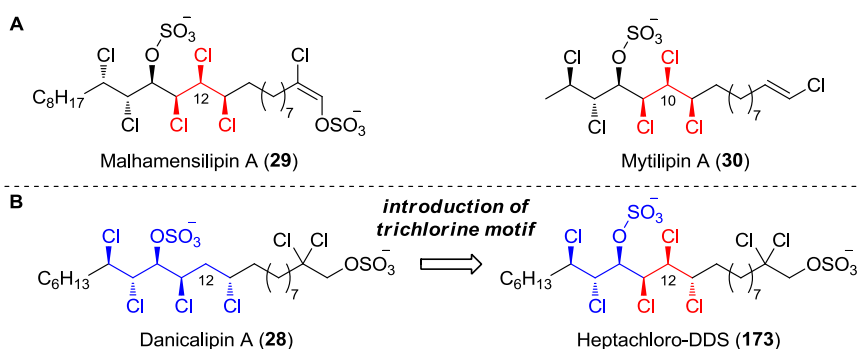
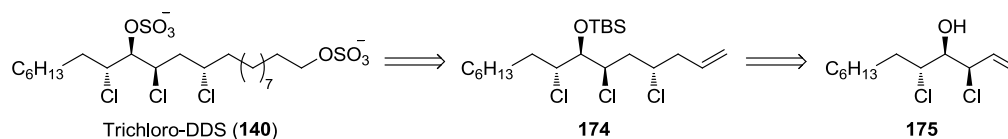


Figure 19 Rational for the design of a heptachloro-DDS analog. **A**: Malhamensilipin A (**29**) and mytilipin A (**30**) share a trichlorine motif vicinal to the sulfate group. **B**: The central chlorine of this motif is missing in danicalipin A (**28**) and led us to design heptachloro analog **173**.

We envisioned that the selected chlorosulfolipids **27**, **28**, **140**, **141**, and **171–173** would be suitable probes to investigate the chlorination pattern of danicalipin A (**28**) and raise the understanding of its potential function in the membrane of *O. danica* and/or its toxicological profile. Furthermore, such a systematic study could give valuable insights into the biology of other polychlorinated toxins.

5.3 Synthesis of Trichloro-DDS

The synthesis of trichloro-DDS (**140**) was envisaged to follow similar paths as the ones for danicalipin A (**28**) (*cf.* Chapter 2.4.6)¹¹⁷ or 11,15-di-*epi*-danicalipin A (**147**) (*cf.* Chapter 3.4). Retrosynthetic disconnection by cross-metathesis/reduction led us to trichloride **174** (Scheme 35). The homoallylic chlorine substituent could arise from BROWN allylation, oxidation, and hydroboration, suggesting allylic chlorohydrin **175** to be a suitable precursor.

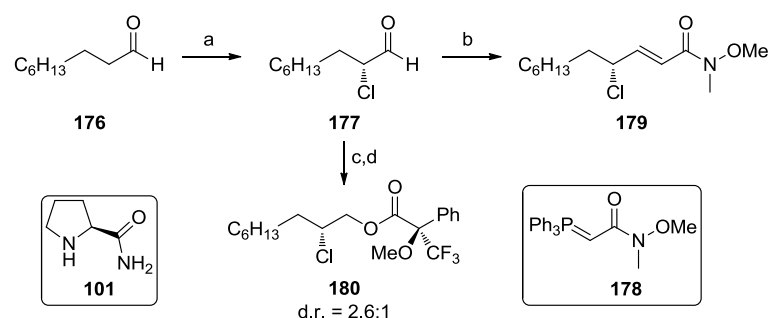


Scheme 35 Retrosynthetic analysis for trichloro-DDS (**140**).

5.3.1 First Approach to Allylic Chlorohydrin **175**

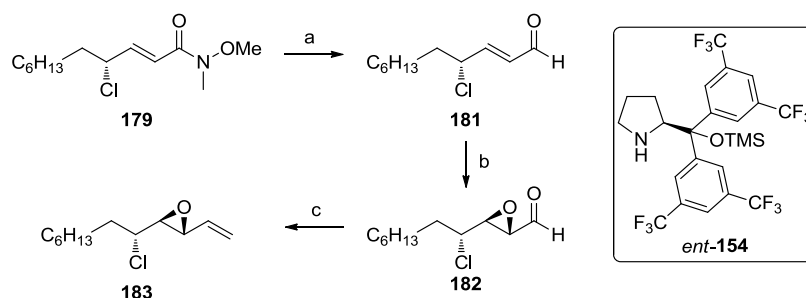
Following a similar strategy as in 11,15-di-*epi*-danicalipin A (**147**), the allylic chlorohydrin **175** would be accessed by the opening of a *trans*-vinyl epoxide. Such an epoxide, bearing a *cis*-substituent on the olefin, had previously been opened during a systematic study by CARREIRA and co-workers with retention of configuration at the allylic center in 20:1 d.r.⁷¹

The synthesis began with the α -chlorination of nonanal (**176**) as reported by JØRGENSEN and co-workers.¹⁰² The reaction proceeded with 10 mol% **101** and 1.1 equiv of NCS, followed by treatment with stabilized WITTIG reagent **178** (Scheme 36). The yield of this sequence was 76%, but the enantioselectivity was rather poor (44% *ee*) as determined by derivatization to MOSHER ester analog **180**.⁶⁰



Scheme 36 Synthesis of γ -chloroamide **179**. Reagents and conditions: a) **101** (10 mol%), NCS, CH_2Cl_2 , 0 °C to r.t.; b) **178**, CH_2Cl_2 , 0 °C to r.t., 75% over 2 steps; c) NaBH_4 , MeOH, 0 °C, 81% over 2 steps; d) (*R*)-MTPA, DCC, DMAP, CHCl_3 , quantitative, d.r. = 2.6:1.

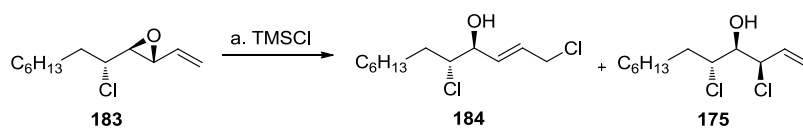
In order to overcome the low enantioenrichment of **179**, we employed a second diastereoselective reaction with a chiral catalyst. After DIBAL reduction of **179**, diastereoselective WEITZ–SCHEFFER epoxidation¹⁵⁹ with JØRGENSEN–HAYASHI catalyst *ent*-**154**¹⁸⁰ and aqueous H_2O_2 in CH_2Cl_2 gave epoxyaldehyde **182** (Scheme 37).¹⁶⁰ The aldehyde was converted to the terminal olefin by WITTIG reaction, giving the desired *trans*-vinyl epoxide **183** in 42% yield over 3 steps.



Scheme 37 Synthesis of vinyl epoxide **183**. Reagents and conditions: a) $(i\text{-Bu})_2\text{AlH}$, CH_2Cl_2 , -78 °C; b) *ent*-**154** (10 mol%), aq. H_2O_2 , CH_2Cl_2 , r.t.; c) MePPh_3Br , KHMDS, THF, -78 to 0 °C, then aldehyde, -78 to 0 °C, 42% over 3 steps.

Unfortunately, when vinyl epoxide **183** was treated with TMSCl in EtOAc , $\text{S}_{\text{N}}2'$ reaction dominated and **184** was formed in 26% yield together with small amounts (<5%) of $\text{S}_{\text{N}}2$ product **175** (Scheme 38).⁷¹ The stereoelectronic effects of a second substituent on the olefin must completely change the reactivity from $\text{S}_{\text{N}}2'$ to $\text{S}_{\text{N}}2$ displacement, as suggested by the different outcome in reports on 1,2-disubstituted olefins (*cf.* Chapter 2.4.1).

¹⁸⁰ a) Y. Hayashi, H. Gotoh, T. Hayashi, M. Shoji *Angew. Chem. Int. Ed.* **2005**, *44*, 4212-4215; b) J. Franzén, M. Marigo, D. Fielenbach, T. C. Wabnitz, A. Kjærsgaard, K. A. Jørgensen *J. Am. Chem. Soc.* **2005**, *127*, 18296-18304.

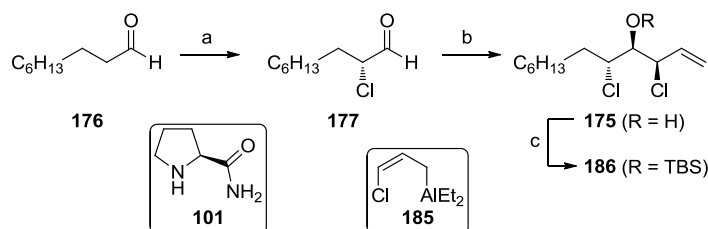


Scheme 38 Opening of vinyl epoxide **183**. Reagents and conditions: a) TMSCl, EtOAc, 0 °C to r.t., 26% of **184**, <5% of **175**.

Remarkably, the analogous reaction in the synthesis of 11,15-di-*epi*-danicalipin A (**147**) opened a *cis*-epoxide with a terminal vinyl group *via* S_N2 displacement exclusively (*cf.* Chapter 3.4).⁷¹ This accentuates the subtleties in vinyl epoxide reactivity encountered in chlorinated hydrocarbons. Circumvention of this stereoelectronic problem in the reaction from **183** to **175** would require several steps, e.g. by including the second olefin substituent, followed by oxidative cleavage and WITTIG reaction. As this seemed cumbersome, an alternative route had to be devised.

5.3.2 Second Approach to Allylic Chlorohydrin **175** and Conclusion of the Synthesis

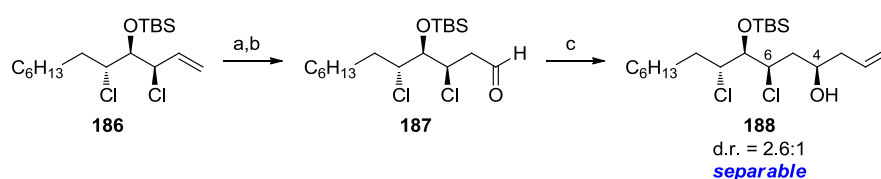
The second generation approach to allylic chlorohydrin **175** was inspired by VANDERWAL'S synthesis of mytilipin A (**30**) (*cf.* Chapter 2.4.2).⁷⁹ α -Chlorination of nonanal (**176**) and subsequent chloroallylation with *in situ* generated **185** gave allylic chlorohydrin **175**⁸⁰ which was protected as the TBS ether in 19% over 3 steps (Scheme 39). The chloroallylation nicely proceeded *via* a ZIMMERMAN–TRAXLER transition state,¹⁸¹ directed by the α -substituent through a polar FELKIN–ANH or CORNFORTH model,⁸¹ giving one diastereomer according to crude ¹H NMR analysis (*cf.* Scheme 14).



Scheme 39 Synthesis of protected allylic chlorohydrin **186**. Reagents and conditions: a) **101** (10 mol%), NCS, CH₂Cl₂, 0 °C to r.t.; b) LiTMP, allyl chloride, Et₂AlCl, THF, -78 °C, then **177**, -78 °C; c) TBSOTf, Et₃N, CH₂Cl₂, 0 °C to r.t., 19% over 3 steps.

¹⁸¹ H. E. Zimmerman, M. D. Traxler *J. Am. Chem. Soc.* **1957**, 79, 1920-1923.

With the low enantioenrichment of **186** in mind, we proceeded with the synthesis. Hydroboration with Cy_2BH followed by oxidation of the resulting alkylborane with NaBO_3 gave the primary alcohol in 80% yield (Scheme 40). Subsequent oxidation with DESS-MARTIN periodinane delivered aldehyde **187**⁹¹ which could be directly used in the next reaction. We envisioned that BROWN allylation could increase the enantioenrichment of **187** due to its high selectivities regardless of the configuration at the β -stereocenter of the aldehyde.¹²¹ In the case of danicalipin A (**28**), the 4,6-*syn* motif could be set in at least 8.3:1 d.r. (*cf.* Chapter 2.4.6)¹¹⁷ and the 4,6-*anti* motif was set in >10:1 d.r. during the synthesis of 11,15-di-*epi*-danicalipin A (**147**) (*cf.* Chapter 4.4). Indeed, when the BROWN allylation was performed with (+)-(Ipc)₂B(allyl) the homoallylic alcohol was obtained in a d.r. of 2.6:1, with no other detected diastereomers. This diastereomeric ratio matched the enantiomeric ratio determined for aldehyde **177** exactly. Moreover, the diastereomers were separable by careful column chromatography, allowing the isolation of **188** in 59% yield over two steps.



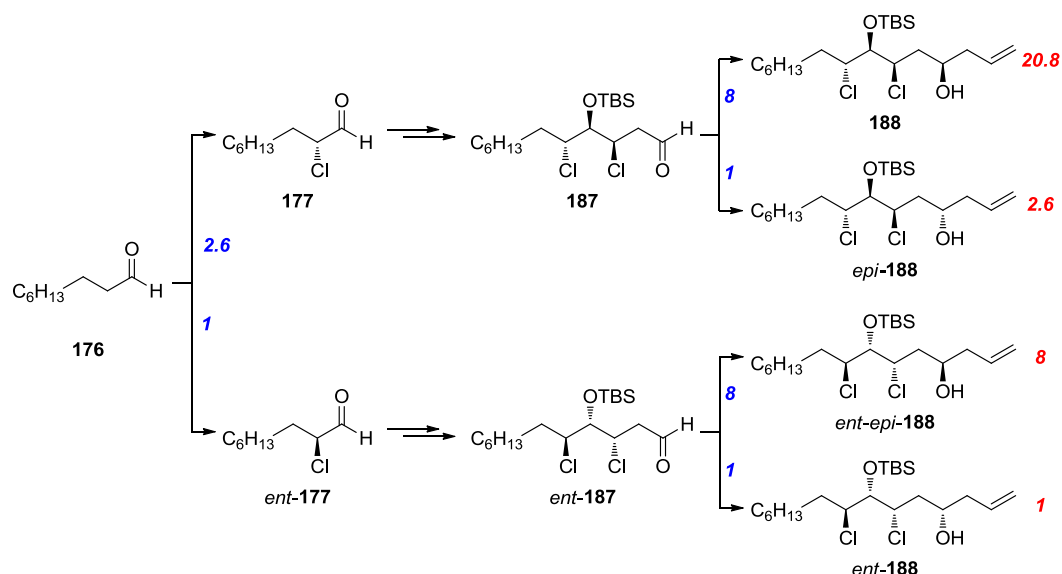
Scheme 40 Synthesis of homoallylic alcohol **188**. Reagents and conditions: a) Cy_2BH , THF, 0 °C to r.t., $\text{NaBO}_3 \cdot 4\text{H}_2\text{O}$, THF/ H_2O , 0 °C to r.t., 80%; b) DMP, CH_2Cl_2 , 0 °C to r.t.; c) (+)-(Ipc)₂B(allyl), allylMgBr, THF, -78 °C to r.t., then **187**, -100 °C to r.t., 59% of **188** over 2 steps, d.r. = 2.6:1.

The HOREAU principle suggests that the enantiomeric purity of the compound was greatly increased during this reaction (Scheme 41).¹⁸² If we assume a similar selectivity as for the analogous reaction in the synthesis of danicalipin A (**28**) of 8:1, statistical amplification would predict the product to be >90% *ee*. This is explained by the fact that the major **187** gives two epimeric products **188** and *epi*-**188** in a ratio of 8:1. The minor enantiomer *ent*-**187** also gives two epimeric products *ent-epi*-**188** and *ent*-**188**. Since the enantiomers *epi*-**188** and *ent-epi*-**188** are diastereomers of **188** and can be separated off, the final *ee* is determined by the ratio between **188** and *ent*-**188**. This ratio can be calculated by multiplying the selectivities for the reactions. Hence,

$$\frac{\mathbf{188}}{\mathit{ent}\text{-}\mathbf{188}} = \frac{2.6 \times 8}{1 \times 1} = \frac{20.8}{1} \cong 91\% \text{ } ee. \text{ This value could be a low estimation, since the d.r.}$$

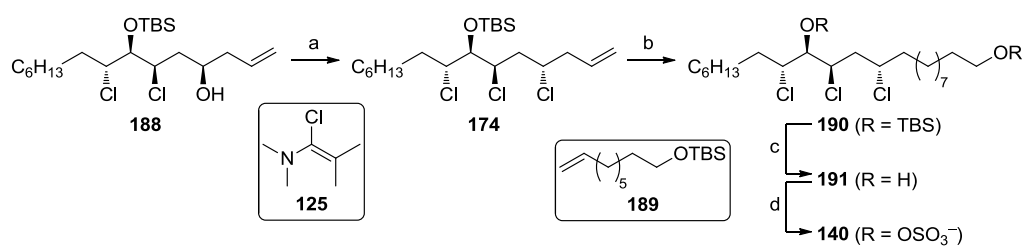
¹⁸² J. P. Vigneron, M. Dhaenens, A. Horeau *Tetrahedron* **1973**, 29, 1055-1059.

of 8.3:1 in the synthesis of **28** could have arisen on a similar basis and the true d.r. of this reaction might be much higher as suggested by the observed diastereomeric ratio of 2.6:1.



Scheme 41 Horeau principle: enantiomeric enrichment during the reaction from **187** to **188**. The numbers in blue represent selectivities. The number in red represents the final ratio of products.

The synthesis continued with the displacement of the homoallylic alcohol in **188** with GHOSEZ's reagent (**125**) in 79% yield (Scheme 42).¹²² One-pot cross-metathesis with **189** and reduction of the resulting olefin gave **190** in 68% yield.^{93,123} The TBS ethers were cleaved in refluxing acidified methanol in 91%, followed by sulfation with $\text{SO}_3 \cdot \text{pyridine}$ in 99% yield.



Scheme 42 Completion of the synthesis of trichloro-DDS (**140**). Reagents and conditions: a) **125**, CHCl_3 , 0 °C to r.t., 79%; b) GRUBBS' second generation catalyst (**169**, 10 mol%), **189**, CH_2Cl_2 , 45 °C, then PtO_2 (10 mol%), H_2 (1 atm), r.t., 68%; c) AcCl , MeOH , 0 to 80 °C, 91%; d) $\text{SO}_3 \cdot \text{pyridine}$, THF, r.t., 99%.

The spectroscopic data of the obtained material **140** was in agreement with the isolation literature (Tables 20 & 21).⁶³ In the ^1H spectrum the largest deviation in chemical shift was that of the protons on C1 with a $\Delta\delta$ of 0.04 ppm, possibly due to a

slight pH dependence on the primary sulfate (Table 20, Entry 5). Likewise, the ^{13}C resonance of C1 was the one with the largest $\Delta\delta$ of 0.2 ppm (Table 21, Entry 2). All other peaks match the isolation data within error.

Table 20 Comparison of ^1H resonances δ for synthetic and natural⁶³ trichloro-DDS (**140**).

Entry	synthetic [ppm]	multi-plicity	J [Hz]	natural [ppm]	multi-plicity	J [Hz]	$\Delta\delta$
1	4.94	dt	1.8, 11.3	4.93	dt	1.1, 11.4	0.01
2	4.43	dd	1.4, 9.4	4.41	dd	1.1, 9.6	0.02
3	4.21	dddd	2.1, 5.5, 7.6, 11.1	4.20	m	-	0.01
4	4.14	td	2.5, 9.8	4.12	dt	2.2, 9.6	0.02
5	4.02	t	6.5	3.98	t	6.6	0.04
6	2.54	ddd	2.1, 11.4, 15.5	2.53	t	2.0, 11.4, 15.6	0.01
7	2.32	m	-	2.32	m	-	0.00
8	2.08	ddd	2.1, 11.2, 15.5	2.07	ddd	2.0, 11.2, 15.6	0.01
9	1.79	m	-	1.76	m	-	0.03
10	1.68	ddt	5.9, 8.4, 12.8	1.68	m	-	0.00
11	0.89	t	6.8	0.90	t	7.0	-0.01

Spectra were recorded in CD_3OD and referenced to residual solvent signal (CD_2HOD : 3.31 ppm).

Table 21 Comparison of ^{13}C resonances δ for synthetic and natural⁶³ trichloro-DDS (**140**).

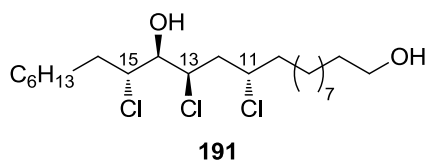
Entry	synthetic [ppm]	natural [ppm]	$\Delta\delta$	Entry	synthetic [ppm]	natural [ppm]	$\Delta\delta$
1	84.0	83.9	0.1	12	30.5	n.a.	-
2	69.4	69.2	0.2	13	30.4	n.a.	-
3	63.1	63.2	-0.1	14	30.3	n.a.	-
4	62.3	62.4	-0.1	15	30.3	n.a.	-
5	62.2	62.3	-0.1	16	30.1	n.a.	-
6	45.7	45.8	-0.1	17	30.1	n.a.	-
7	39.9	40.0	-0.1	18	27.6	27.6	0.0
8	34.9	34.9	0.0	19	27.4	27.5	-0.1
9	33.0	33.0	0.0	20	26.9	26.9	0.0
10	30.6	n.a.	-	21	23.7	23.7	0.0
11	30.6	n.a.	-	22	14.4	14.4	0.0

Spectra were recorded in CD_3OD and referenced to residual solvent signal (CD_3OD : 49.0 ppm).

Due to the poor quality of the spectra from the isolation, we decided to perform JBCA on trichlorodocosanediol **191**,⁵⁹ despite the accordance of the spectroscopic data. The obtained solution-state conformation confirmed the C11,C13-*anti* relationship as well as the C13-C14 *syn* and C14-C15 *anti* relative configurations

(Table 22). Furthermore, due to the missing C16 chlorine substituent, the chlorinated array is completely linear with a tttt conformation.

Table 22 JBCA for diol **191**.



C11-C12		C12-C13	
$^3J_{\text{H12h-H11}}/{}^3J_{\text{H12l-H11}}$	11.0 (l)/2.2 (s)	$^3J_{\text{H13-H12h}}/{}^3J_{\text{H13-H12l}}$	2.4 (s)/11.2 (l)
$^3J_{\text{H11-C13}}$	3.3 (s)	$^3J_{\text{H13-C11}}$	3.4 (s)
$^3J_{\text{C10-H12h}}/{}^3J_{\text{C10-H12l}}$	2.0 (s)/2.2 (s)	$^3J_{\text{C14-H12h}}/{}^3J_{\text{C14-H12l}}$	n.d./n.d.
$^2J_{\text{C11-H12h}}/{}^2J_{\text{C11-H12l}}$	-7.2 (l)/1.3 (s)	$^2J_{\text{C13-H12h}}/{}^2J_{\text{C13-H12l}}$	1.4 (s)/-7.4 (l)

(D-1)

(C-1)

C11,C13-*anti* motif

C13-C14		C14-C15	
$^3J_{\text{H13-H14}}$	1.4 (s)	$^3J_{\text{H14-H15}}$	9.3 (l)
$^3J_{\text{H14-C12}}/{}^3J_{\text{C15-H13}}$	small ^a /n.d.	$^3J_{\text{H15-C13}}/{}^3J_{\text{C16-H14}}$	n.d./1.8 (s)
$^2J_{\text{C14-H13}}/{}^2J_{\text{C13-H14}}$	small ^a /n.d.	$^2J_{\text{C15-H14}}/{}^2J_{\text{C14-H15}}$	-5.0 (l)/-4.1 (l)

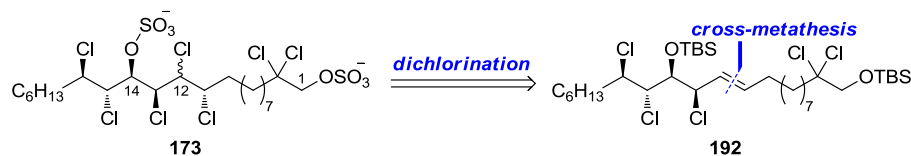
syn (A-1)

anti (B-3)^b

Coupling constants are reported in Hertz (Hz). All spectra were recorded in CDCl₃. Heteronuclear coupling constants were determined in a HSQC-HECADE spectrum. a) magnitude derived by comparing intensities in the phase sensitive-HMBC; b) no NOE observed between H13 and H16. s = small, m = medium, l = large; n.d. = not determined, due to weak peak intensity, overlap, or a signal of higher order.

5.4 Synthesis of Heptachloro-DDS

The synthesis of heptachloro-DDS (**173**) was envisioned to follow principal disconnections of VANDERWAL's synthesis of mytilipin A, in which the C11–C12 olefin is cleaved retrosynthetically with a cross-metathesis (*cf.* Chapter 2.4.2).⁷⁹ Subsequent dichlorination similar to CARREIRA's synthesis of mytilipin A (**30**) would give the heptachloro analog **173** (*cf.* Chapter 2.4.1).⁶⁶ The significant difference would be that a heptachloro analog of danicalipin A (**28**) would require a C11,C13 *anti* motif as opposed to *syn* in **30**. In principle, this can be achieved by using a *trans* instead of a *cis* olefin for dihalogenation (Scheme 43). The desired configuration at the C12 carbon was hard to predict. Given the results in Part II of this thesis, it was crucial to maintain the same solution-state conformation as danicalipin A (**28**). Molecular modeling could not give a clear answer as *syn*-pentane interactions cannot be avoided entirely in either of the C12 epimers. Ideally, both diastereomers would be accessed through dichlorination of either the free alcohol of **173** or the TBS ether (*cf.* Chapter 2.4).⁸⁵



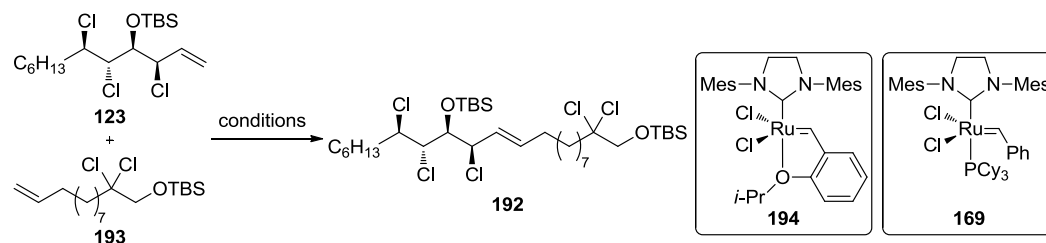
Scheme 43 Retrosynthetic analysis for heptachloro-DDS (**173**).

The synthesis commenced with the cross-metathesis of known olefins **123** and **193**. Earlier reports by VANDERWAL hinted at problems in the cross-metathesis of olefins such as **123** and we started our investigations by screening a variety of conditions for cross-metathesis with both GRUBBS' and GRUBBS-HOVEYDA second generation catalysts **169** and **194**, respectively (Table 23).^{85,94,183} In our case, the conditions reported by VANDERWAL (toluene, r.t., 40 h) resulted in low conversion of **123** (Entries 1 & 2). When the reaction was performed in refluxing CH₂Cl₂ for 16 hours the conversions improved with **169** outperforming **194** (Entries 4 & 5). When the reaction time was increased to 24 hours, the desired olefin **192** could be isolated in 82% yield (Entry 5). During flash column chromatography the formation of a by-

¹⁸³ a) S. B. Garber, J. S. Kingsbury, B. L. Gray, A. H. Hoveyda *J. Am. Chem. Soc.* **2000**, *122*, 8168-8179; b) S. Gessler, S. Randl, S. Blechert *Tetrahedron Lett.* **2000**, *41*, 9973-9976.

product was observed and thus quick purification was necessary. The by-product, its formation, and further studies are discussed in Part IV of this thesis.

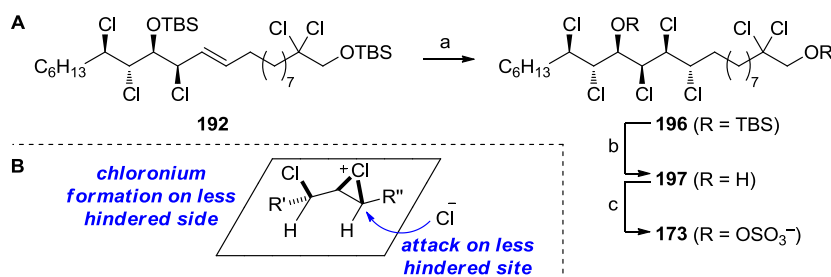
Table 23 Optimization for the cross-metathesis of **123** and **193**.



Entry	Catalyst ^a	Solvent	Temperature	Time	Conversion ^b	Yield
1	194	toluene	r.t.	40 h	ca. 25%	n.d.
2	169	toluene	r.t.	40 h	ca. 40%	~40% ^c
3	194	CH ₂ Cl ₂	40 °C	16 h	ca. 60%	59%
4	169	CH ₂ Cl ₂	40 °C	16 h	ca. 80%	27% ^d
5	169	CH ₂ Cl ₂	40 °C	24 h	ca. 90%	82%

a) 10 mol% catalyst was used; b) Conversion measured in crude ¹H NMR by integrating representative peaks of **123** and **192** and determining the ratio; c) Purity 90%; d) Yield low due to decomposition of **192** during careful flash column chromatography. n.d. = not determined.

The olefin in **192** was dichlorinated using excess MIOSKOWSKI's reagent (4.6 equiv) to give heptachloro compound **196** in 49% yield (Scheme 44A).⁶⁷ Crude ¹H NMR analysis indicates the diastereoselectivity to be greater than 5:1, but no other diastereomers could be isolated. The configuration of the product suggests the dichlorination to proceed through an intermediate such as the one depicted in Scheme 44B. Thus, formation of the chloronium on the less hindered side of the olefin, followed by opening at the less hindered site of the chloronium gives **196**. Both TBS groups in **196** were subsequently removed in refluxing acidified methanol, giving diol **197** in 87% yield. The final sulfation with SO₃·pyridine gave **173** quantitatively.



Scheme 44 A: Completion of the synthesis of heptachloro-DDS (**173**). Reagents and conditions: a) Et₄NCl₃, CH₂Cl₂, 0 °C to r.t., 49%; b) AcCl, MeOH, 0 to 80 °C, 87%; c) SO₃·pyridine, THF, r.t., quantitative. **B:** Stereochemical model for the selectivity of the dichlorination of **192**.

The configuration and conformation of the heptachloro analog of danicalipin A (**28**) could be established by JBCA of diol **197** (Table 24).⁵⁹ The C12 stereocenter was determined to have (*S*) absolute configuration through the C12–C13 *syn* and the C11–C12 *anti* relative configurations. Moreover, the conformation of the chlorinated segment matched the one from danicalipin A (**28**, ttttg^+) and we had thereby reached the required goal for a heptachloro analog of danicalipin A (**28**). This was particularly important, as other diastereomers of **197** could not be accessed. In light of other reports (*cf.* Chapter 2.4.2) a less selective dichlorination and access to other diastereomers would have been possible from a deprotected analog of **192**. Unfortunately, deprotection of **192** under our standard conditions (AcCl, MeOH, 0 to 80 °C) led to extensive decomposition, presumably due to the instability of the resulting allylic chlorohydrin (*cf.* Part IV).

Table 24 JBCA for diol **197**.

197

C11–C12		C12–C13			
$^3J_{\text{H12-H11}}$	9.6 (l)	$^3J_{\text{H12-H13}}$	2.1 (s)		
$^3J_{\text{H12-C10}}/^3J_{\text{C13-H11}}$	2.2 (s)/2.2 (s)	$^3J_{\text{H13-C11}}/^3J_{\text{C14-H12}}$	1.7 (s)/1.7 ^b (s)		
$^2J_{\text{C12-H11}}/^2J_{\text{C11-H12}}$	–5.0 (l)/–4.0 (l)	$^2J_{\text{C14-H13}}/^2J_{\text{C13-H14}}$	2.0 ^b (s)/–1.5 (s)		
<p><i>anti</i> (B-3)^a</p>		<p><i>syn</i> (A-1)</p>			
C13–C14		C14–C15		C15–C16	
$^3J_{\text{H13-H14}}$	2.0 (s)	$^3J_{\text{H14-H15}}$	8.5 (l)	$^3J_{\text{H15-H16}}$	3.3 (s)
$^3J_{\text{H14-C12}}/^3J_{\text{C15-H13}}$	0.2 (s)/1.7 ^b (s)	$^3J_{\text{H15-C13}}/^3J_{\text{C16-H14}}$	3.1 ^b (s)/1.6 (s)	$^3J_{\text{H16-C14}}/^3J_{\text{C17-H15}}$	1.5 (s)/3.8 (m)
$^2J_{\text{C14-H13}}/^2J_{\text{C13-H14}}$	–2.5 (m)/2.1 (s)	$^2J_{\text{C15-H14}}/^2J_{\text{C14-H15}}$	–4.1 (l)/–4.2 (l)	$^2J_{\text{C16-H15}}/^2J_{\text{C15-H16}}$	–3.9 (l)/0.6 (s)
<p><i>syn</i> (A-1)</p>		<p><i>anti</i> (B-3)^c</p>		<p><i>anti</i> (B-2)</p>	

Coupling constants are reported in Hertz (Hz). All spectra were recorded in CDCl₃. Heteronuclear coupling constants were determined in a HSQC-HECADE spectrum. a) no NOE observed between H10 and H13; b) obtained from phase sensitive-HMBC; a) no NOE observed between H13 and H16; s = small, m = medium, l = large; n.d. = not determined, due to weak peak intensity, overlap, or a signal of higher order.

5.5 Biological Effects

5.5.1 Membrane Permeability Enhancement

With all analogs in hand, we were interested in their membrane permeability enhancing abilities. As before, we started our investigations with the bacterial membrane of *E. coli* DH5 α .¹¹⁷ The fluorescence response of Hoechst 33342 as a result of incubation with analogs **27**, **28**, **140**, **141**, or **171–173** is shown in Figure 20.¹³⁶ At 125 μ M concentrations of danicalipin A (**28**) the fluorescence is increased five-fold over the negative control, maintaining >90% viability. Mono- and dichloro-DDS (**27** & **171**) compromised bacterial membranes at 125 μ M barely over the negative control and tri- and tetrachloro-DDS (**140** & **141**) also showed only a slight increase in fluorescence at reliable viabilities.

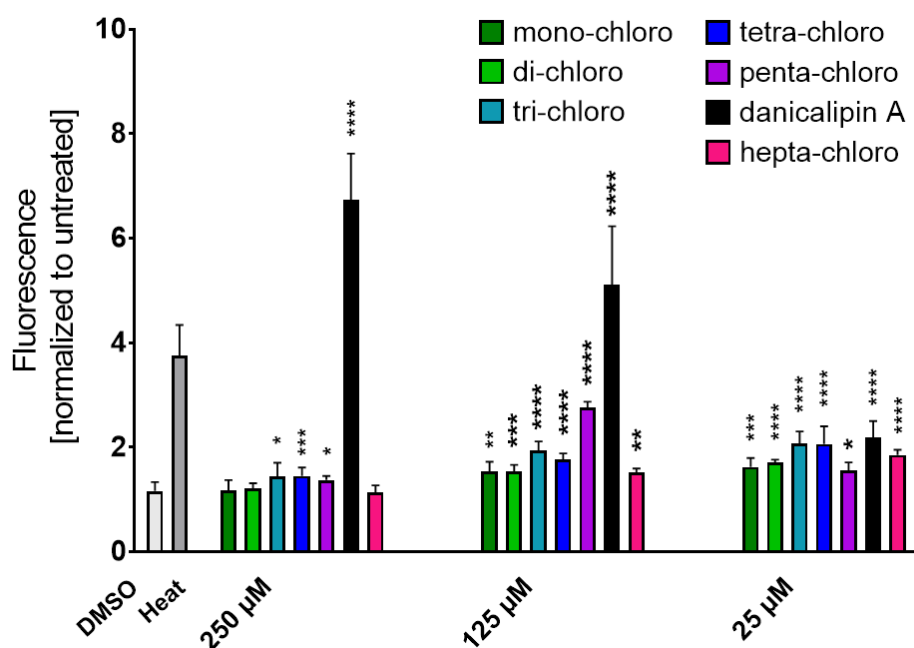


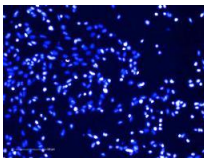
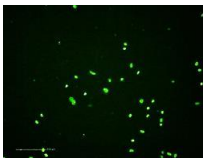
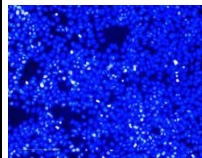
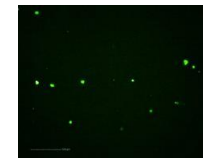
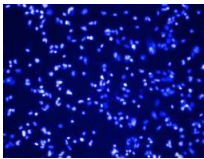
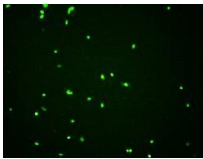
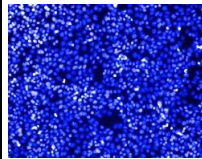
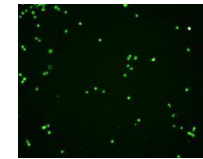
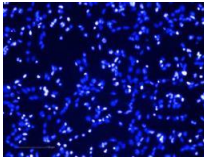
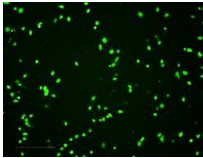
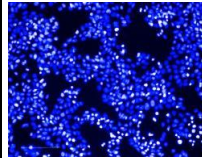
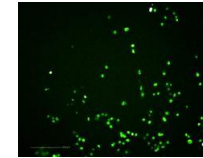
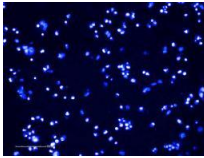
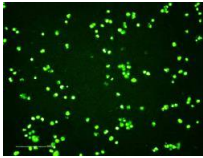
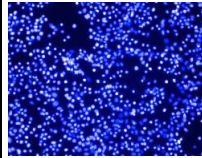
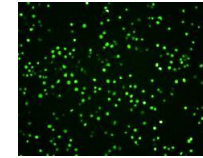
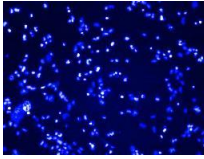
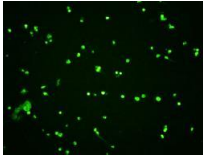
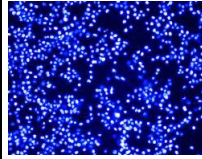
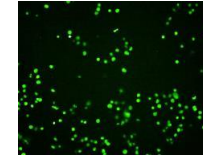

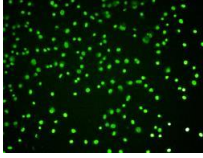

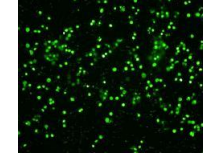
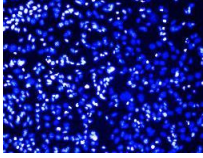
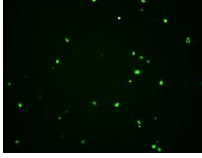
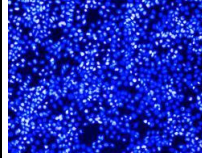
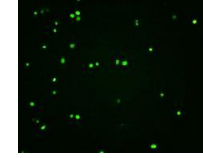
Figure 20 Membrane permeability enhancement in bacteria: Fluorescence response due to nuclear staining of *E. coli* DH5 α by Hoechst 33342 as a function of the concentration of **27** (mono-chloro), **171** (di-chloro), **140** (tri-chloro), **141** (tetra-chloro), **172** (penta-chloro), **28** (danicalipin A), or **173** (hepta-chloro) as well as positive and negative control experiments. Data are normalized to the untreated results. The significance of each result vs. DMSO is shown above the bar: $p < 0.033 = *$; $p < 0.01 = **$; $p < 0.001 = ***$; $p < 0.0002 = ****$.

However, the membrane permeability enhancement is evident in pentachloro-DDS (**172**), whose presence increased fluorescence of Hoechst 33342 three-fold, albeit not as much as in positive control experiments. Strikingly, heptachloro-DDS (**173**) was incapable of compromising bacterial membranes, even at a toxic concentration of 250 μM .

These results were in line with data from the membrane permeability enhancement of mammalian cell lines (Table 25). When murine liver cancer cells Hepa 1-6 or human colorectal adenocarcinoma cells HT-29 were incubated with **27**, **28**, **140**, **141**, or **171–173** in a Hoechst 33342/Sytox Green assay,¹³⁷ the results were consistent with trichloro-DDS (**140**), tetrachloro-DDS (**141**) and pentachloro-DDS (**172**) being able to slightly compromise mammalian cellular membranes. The extent of their ability is not as dramatic as for **28**, as it can be seen that not all sampled cells have compromised membranes, but the general trend observed in the bacterial membrane permeability enhancement is corroborated.

These observations broaden the conclusions drawn in Chapter 3.5.3. The single kink in the molecular structure of danicalipin A (**28**), although important, is by no means sufficient for its ability to compromise phospholipid-based membranes. The C2-*gem*-dichlorine is as important as the kink. This can be seen from the increase in bacterial membrane permeability enhancement from tetrachloro- (**141**) to pentachloro-DDS (**172**) to danicalipin A (**28**), where the two chlorine substituents at C2 are added sequentially. Furthermore, the inability of heptachloro-DDS (**173**) to compromise membranes reveals an even more complex interplay within the chlorination pattern of danicalipin A (**28**). The striking influence imparted by the C12-chlorine substituent could result from too much steric hindrance around the C14-sulfate to fulfill its unspecified role or could indicate the requirement for some conformational flexibility within the chlorinated segment. As mentioned before, the behavior of danicalipin A (**28**) in phospholipid-based membranes could relate to its elusive role in the membrane of *O. danica*. These results point towards the chlorination pattern of danicalipin A (**28**) to be a consequence of competitive evolution, as no analogs were able to fully compete with the bioactivity of **28**.

Table 25 Membrane permeability enhancement in mammalian cells: Fluorescent images of Hepa 1-6 cells and HT-29 cells after incubation with compounds **27** (Cl₁-DDS), **171** (Cl₂-DDS), **140** (Cl₃-DDS), **141** (Cl₄-DDS), **172** (Cl₅-DDS), **28** (danicalipin A, Cl₆-DDS), or **173** (Cl₇-DDS) at 25 μM concentration. Blue: Sampled cells, visualized with Hoechst 33342. Green: Cells with compromised cell membranes, visualized with Sytox Green.

Compound	Hepa 1-6		HT-29	
	Hoechst 33342 (sampled cells)	Sytox Green (cells with compromised membranes)	Hoechst 33342 (sampled cells)	Sytox Green (cells with compromised membranes)
Cl ₁ -DDS (27)				
Cl ₂ -DDS (171)				
Cl ₃ -DDS (140)				
Cl ₄ -DDS (141)				
Cl ₅ -DDS (172)				
Cl ₆ -DDS (28)				
Cl ₇ -DDS (173)				

5.5.2 Toxicology

A direct link between toxicity and permeability enhancement was previously refuted (*cf.* Chapter 3.5). Nevertheless, the toxicities of analogs with varying degrees of chlorination against brine shrimp had shown a similar trend as our results from membrane permeability enhancement (*cf.* Chapter 2.5).⁶³ Hence, the toxicology of analogs **27**, **28**, **140**, **141**, and **171–173** against a variety of mammalian cancer cell lines was tested (Table 26). In human colorectal adenocarcinoma cell line HT-29 the same trend as for brine shrimp is observed, namely that increasing chlorination degree and thereby lipophilicity leads to an increase in toxicity. The only exceptions are a decrease in toxicity from tri- to tetrachloro-DDS (**140** → **141**) and from danicalipin A to heptachloro-DDS (**28** → **173**). In human alveolar adenocarcinoma cell line A549 the same trend is not observed. Both mono- and dichloro-DDS (**27** & **171**) are equally toxic, but significantly less toxic than all other analogs. A similar observation is made in murine liver cancer cell line Hepa 1-6. Most of the compounds have similar LC₅₀ values with the exception of **171**. Combination of all results speaks to an unspecified mode of action since no consistent trend can be noted. The target and/or mode of action can vary for different cell lines as signified by the varying orders of magnitude and no discernable trend within the series. Overall, the toxicity might arise from the detergent properties of the chlorosulfolipids and their ability to denature enzymes.

Table 26 Toxicity exhibited by **27**, **28**, **140**, **141**, and **171–173** against several mammalian cell lines. The values correspond to the LC₅₀ and are reported in μM. HT-29 human colorectal adenocarcinoma; A549 human alveolar adenocarcinoma; Hepa 1-6 murine liver cancer.

Toxicity (LC ₅₀) [μM]	HT-29 cells	A549 cells	Hepa 1-6 cells
Monochloro-DDS (27)	264.3 ± 4.3	104 ± 1.0	40.1 ± 0.5
Dichloro-DDS (171)	151.8 ± 5.2	104 ± 1.0	72.0 ± 2.0
Trichloro-DDS (140)	67.5 ± 1.0	39.5 ± 0.7	24.2 ± 0.3
Tetrachloro-DDS (141)	82.9 ± 4.8	36.7 ± 1.5	29.6 ± 0.6
Pentachloro-DDS (172)	27.3 ± 0.2	42.8 ± 0.9	23.6 ± 0.1
Danicalipin A (28)	15.5 ± 1.2	24.1 ± 0.2	14.3 ± 0.7
Heptachloro-DDS (173)	31.4 ± 0.2	26.8 ± 0.4	24.8 ± 0.2

It is worth noting that danicalipin A (**28**) is the most toxic of the chlorinated analogs, further supporting its advantageous biological activity. Due to the possible connection between the self-defense mechanisms of *O. danica* and the presence of **28** in this organism, the high toxicity of **28** is therefore also consistent with its structure

having come about by competitive evolution. However, a specific cellular target and the mode of action against competitors and predators of *O. danica* are still unresolved.

6 Conclusions and Outlook

In conclusion, we have completed the synthesis of two chlorosulfolipids, one natural and one unnatural, as part of a project that aimed at establishing the effect that varying degrees of chlorination have on bioactivity. Furthermore, this helped gaining insight into advantageous biological properties exhibited by danicalipin A (**28**).

The synthesis of natural trichlorodocosanedisulfate **140** was completed in eleven steps and 4.3% overall yield from nonanal. The enantioselectivity of the route could be increased by employing two independent chiral reagent-controlled transformations according to the HOREAU principle. Unnatural heptachlorodocosanedisulfate **173** was synthesized in four steps and 35% overall yield from known intermediates. Its configuration was established by JBCA, also revealing its singly-kinked molecular shape, which was important in order to assure the comparability with danicalipin A (**28**).

In combination with the biological activity of other partially chlorinated analogs of danicalipin A (**28**), the membrane permeability enhancement and toxicology of **140** and **173**, respectively, advanced our understanding of the necessity for a specific chlorination pattern for the natural function of **28** significantly. Despite the lack of C16-chlorine substituent in **140**, which is responsible for the kink in **28**, the trichloro analog exhibited a similar membrane permeability enhancement as did the C16-chlorine containing tetrachlorodocosanedisulfate **141**. The two analogs **140** and **141** also showed comparable cytotoxicities against various mammalian cell lines. On the other hand, the heptachloro analog **173** displayed no ability to compromise bacterial or cellular membranes, even though it adopts the same conformation as danicalipin A (**28**). The additional C12-chlorine substituent in **173** also leads to a slight decrease in cytotoxicity when compared to **28**. The obtained biological data supports the picture that the chlorination pattern fulfills very specific requirements, which lead to the bioactivity and potentially natural role of danicalipin A (**28**). In

addition to the chlorinated array (C11 to C16), the C2-*gem* dichlorine is necessary for membrane functions. On the other hand, the missing C12 chlorine is not necessary for membrane functions of **28**, but rather detrimental. Ultimately, the chlorination pattern of **28** appears to exhibit an intricate net of influences, where shielding of the C14-sulfate, lipophilicity, rigidity, and flexibility counterbalance each other, resulting in **28**'s unique biological properties.

This study promotes the understanding of polychlorinated organic molecules by emphasizing that biological activity is not a direct consequence of increasing chlorination. Furthermore, the degree of chlorination does not influence all biological activities of organohalogenes to the same extent. For example, with increasing chlorination the cytotoxicity can rise while at the same time the detrimental effects on membranes can cease to exist. This study also confirms the observation previously made in the PCBs that a particular chlorination pattern and degree can lead to distinctly pronounced biological effects. The insights gained herein may help approaching the biological activity of other acyclic polychlorinated hydrocarbons, such as the chlorinated paraffins.

The results gathered in this project can serve as a benchmark for the study of other chlorosulfolipids. For example, the biological function of the closely related malhamensilipin A (**29**) has not been determined yet and it remains to see if it also compromises phospholipid-based membranes. Possibly being associated with self-defense mechanisms, it might also show cytotoxicities comparable to those of danicalipin A (**28**). Systematic studies on other chlorination patterns in chlorosulfolipids might reveal even more perplexing bioactivities by members of this intriguing natural product family.

Part IV

1,3-SIGMATROPIC SHIFTS IN ALLYLIC CHLOROHYDRINS

7 Results and Discussion

7.1 Background

7.1.1 The WOODWARD–HOFFMANN Rules for Sigmatropic Rearrangements

In their seminal publications from 1965, WOODWARD and HOFFMANN devised rules that determine whether a given pericyclic reaction is allowed.¹⁸⁴ More specifically, these rules state that orbital symmetry must be conserved for a concerted reaction.¹⁸⁵ This means that bonding states in the starting materials correspond to bonding states of the same symmetry in the products. It can be shown that any concerted thermal pericyclic reaction is allowed if the number of $(4q+2)_s$ and $(4r)_a$ components is odd ($q, r \in \mathbb{N}$). The subscript refers to suprafacial (s) or antarafacial (a) reactivity of the component and the number in parentheses refers to the total number of participating electrons. In the [1,3]-sigmatropic rearrangement of a hydrogen atom in propene for example, two different possibilities emerge (Figure 21). The hydrogen atom can only react suprafacially since the s-orbital contains no node while the π -system can participate either supra- or antarafacially. If one considers the hydrogen atom to migrate on the same face of the allyl fragment (suprafacial) the reaction can be regarded as $[\sigma_s^2 + \pi_s^2]$. That is to say that the σ_{C-H} bond with its two electrons reacts with the π -system, also containing two electrons, in a suprafacial-suprafacial manner. As shown on the left side in Figure 21, one bonding orbital in the starting material ($\sigma + \pi$) corresponds to a bonding orbital in the product ($\sigma + \pi$), but the other bonding orbital ($\sigma - \pi$) corresponds to an antibonding one in the product ($\sigma^* + \pi^*$). The WOODWARD–HOFFMANN rules state that this reaction would be symmetry forbidden since the number of $(4q+2)_s$ components is two and thereby even.

¹⁸⁴ a) R. B. Woodward, R. Hoffmann *J. Am. Chem. Soc.* **1965**, *87*, 395-397; b) R. Hoffmann, R. B. Woodward *J. Am. Chem. Soc.* **1965**, *87*, 2046-2048; c) R. B. Woodward, R. Hoffmann *J. Am. Chem. Soc.* **1965**, *87*, 2511-2513.

¹⁸⁵ R. B. Woodward, R. Hoffmann *Angew. Chem. Int. Ed.* **1969**, *8*, 781-853.

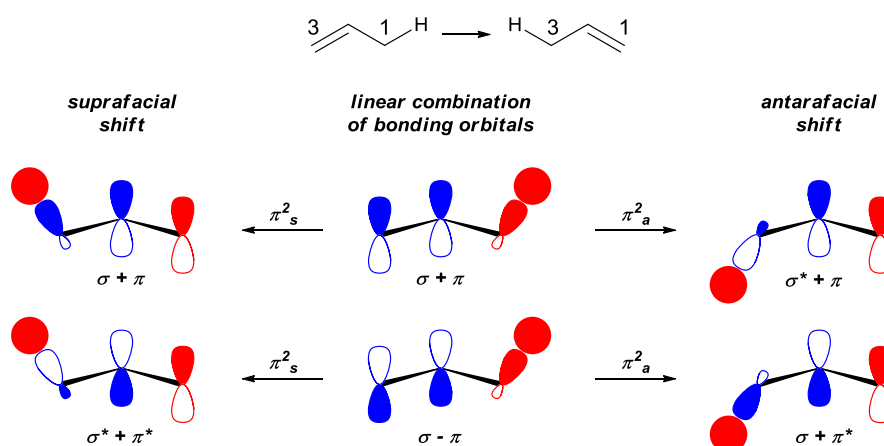


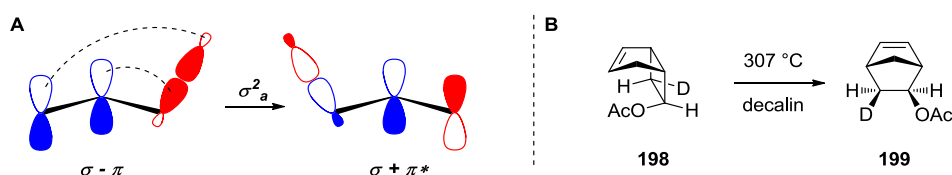
Figure 21 [1,3]-Sigmatropic shifts in propene. *Middle*: linear combinations of the bonding orbitals in propene; *left*: resulting orbitals from a suprafacial shift; *right*: resulting orbitals from an antarafacial shift. The combination at the bottom in the suprafacial shift leads to a fully antibonding combination, whereas both linear combinations lead to bonding orbitals in the antarafacial shift.

The antarafacial migration of hydrogen would result in an overall $[\sigma_s^2 + \pi_a^2]$ reaction and thus, is allowed. Both linear combinations of bonding orbitals lead to bonding orbitals of the same symmetry in the products (Figure 21, right). However, the steric requirements for such a transition state cannot be met since the allyl fragment would need to distort significantly to allow antarafacial migration of hydrogen. Therefore, the concerted reaction does not take place and *ab initio* calculations suggested the activation energy for this allowed reaction to be higher than the corresponding dissociation energy.¹⁸⁶

When one considers migrating atoms or groups other than hydrogen, two more possibilities become available. Due to the partial p-orbital character of the σ -bond, this orbital can also undergo an antarafacial reaction. Hence, the $[\sigma_a^2 + \pi_s^2]$ and $[\sigma_a^2 + \pi_a^2]$ reactions have to be taken into account. According to WOODWARD and HOFFMANN, only the $[\sigma_a^2 + \pi_s^2]$ reaction is thermally allowed, because the linear combination of bonding orbitals that previously led to an antibonding orbital combination can now lead to a bonding one (Scheme 45A). This reaction is preferred due to the decreased steric requirements for the suprafacial shift. In order for the σ -bond to react antarafacially the migrating atom has to undergo inversion of

¹⁸⁶ W. R. Rodwell, W. J. Bouma, L. Radom *Int. J. Quant. Chem.* **1980**, *18*, 107-116.

configuration. This reactivity has been observed by BERSON and NELSON during the vinylcyclobutane rearrangement of **198** (Scheme 45B).¹⁸⁷



Scheme 45 A: Orbitals for the $[\sigma_a^2 + \pi_s^2]$ reaction, a bonding orbital ensues. B: Vinylcyclobutane rearrangement of **198**.¹⁸⁷ Inversion of configuration is observed at the migrating methylene.

Structural restraints favor the suprafacial shift along the allyl fragment and, according to the WOODWARD–HOFFMANN rules, inversion of configuration at the chiral methylene had to occur. When **198** was heated, norbornene **199** was formed in a diastereomeric ratio of 19:1.¹⁸⁸ The authors claimed that the high specificity of this reaction is a clear indication of a concerted mechanism and showcases the steric implications imposed by orbital-symmetry arguments.

7.1.2 Exceptions and Other Mechanistic Hypotheses

BERSON and NELSON were interested in testing the limits of orbital-symmetry allowed reactions and the predictive power of the WOODWARD–HOFFMANN rules.¹⁸⁹ An interesting observation was made while studying substituted bicycloheptenes (Scheme 46).¹⁹⁰ The *exo*-methyl compound **200** underwent suprafacial (*s*) migration with inversion (*i*) of configuration at the migrating methine. In contrast, the *endo*-isomer **202** migrated suprafacially with retention of configuration (*sr*). Furthermore, the authors were able to show that the rate of *sr* rearrangement of **202** exceeded the rate of racemization from **202** to **200** by a factor of 1.5.¹⁹¹

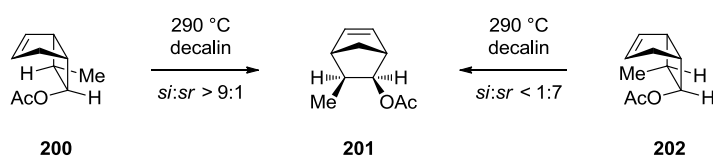
¹⁸⁷ J. A. Berson, G. L. Nelson *J. Am. Chem. Soc.* **1967**, *89*, 5503-5504.

¹⁸⁸ J. A. Berson *Acc. Chem. Res.* **1968**, *1*, 152-160.

¹⁸⁹ J. A. Berson *Acc. Chem. Res.* **1972**, *5*, 406-414.

¹⁹⁰ J. A. Berson, G. L. Nelson *J. Am. Chem. Soc.* **1970**, *92*, 1096-1097.

¹⁹¹ For a more recent review on vinylcyclobutane rearrangements, see: P. A. Leber, J. E. Baldwin *Acc. Chem. Res.* **2002**, *35*, 279-287.



Scheme 46 Vinylcyclobutane rearrangements of bicycloheptenes **200** and **202**. The *exo*-isomer **201** undergoes preferential migration with inversion while the *endo*-isomer **202** prefers a retentive pathway. (*s* = suprafacial, *i* = inversion, *r* = retention).

In 1970, the authors surmised that the rearrangement of **200** followed the WOODWARD–HOFFMANN rules and underwent a concerted shift, while the steric encumbrance involved in the rotation of the *endo*-methyl group in **202** disfavored the same pathway during migration. Instead, they suggested **202** to react through a diradical, although it was unclear why a diradical would entail such a high stereospecificity. A computational study by CARPENTER in 1995 contradicted the previous assumption and suggested dynamic effects¹⁹² to be responsible for the configurational outcome of the rearrangements of **200** and **202**.¹⁹³ Based on PM3 calculations, CARPENTER concluded that both reactions proceeded through a diradical and that the stereospecificity of this reaction arose from dynamics that were passed to the migrating group during bond-breaking. Specifically, based on the substitution pattern, the vibrational mode responsible for bond-breaking imparted a clockwise rotation (as in **200**) or a counterclockwise rotation (as in **202**) onto the migrating center. The same “torquoselectivity” was found independently by HOUK and co-workers, and DAVIDSON and GAJEWSKI to be operative in vinylcyclopropane rearrangements.¹⁹⁴ In 1999, HOUK and co-workers performed DFT calculations on a B3LYP/6-31G* level of theory to establish the potential energy surface for the parent bicyclo[3.2.0]hept-2-ene to norbornene rearrangement.¹⁹⁵ They found that, although this process was allowed by orbital symmetry, a diradical is predicted as the lowest-energy transition state. Furthermore, the transition state region was characterized by a flat plateau with no bonding interactions between both radicals. It was unclear to them how the non-statistical product distributions observed in such reactions would come about but suggested CARPENTER’s dynamic effects to be operational. Quasiclassical

¹⁹² For a review on Carpenter’s “dynamic matching” in organic mechanisms, see: B. K. Carpenter *Angew. Chem. Int. Ed.* **1998**, *37*, 3340-3350.

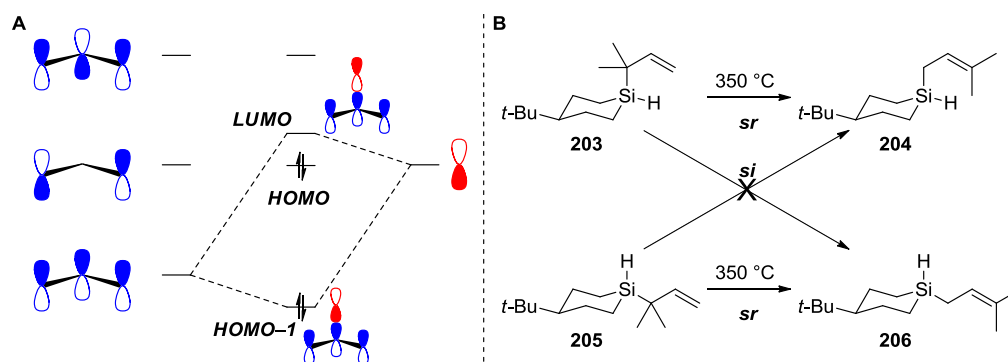
¹⁹³ B. K. Carpenter *J. Am. Chem. Soc.* **1995**, *117*, 6336-6344.

¹⁹⁴ a) K. N. Houk, M. Nendel, O. Wiest, J. W. Storer *J. Am. Chem. Soc.* **1997**, *119*, 10545-10546; b) E. R. Davidson, J. J. Gajewski *J. Am. Chem. Soc.* **1997**, *119*, 10543-10544.

¹⁹⁵ B. R. Beno, S. Wilsey, K. N. Houk *J. Am. Chem. Soc.* **1999**, *121*, 4816-4826.

trajectory calculations by DOUBLEDAY in 2001 pointed towards a more complex picture.¹⁹⁶ The vinylcyclopropane rearrangement proceeded through a flat plateau of a diradical transition state, but followed different paths over this plateau, depending on the dynamics and lifetimes of the diradicals, thereby causing non-statistical product-distributions. This overall picture of a diradical transition state in which dynamic factors determine the product ratio was consistent with the mechanistic description of “continuous diradicals” as already proposed in mechanisms for [1,3]-alkyl migrations in the 1970’s by DOERING¹⁹⁷ and KLÄRNER.¹⁹⁸

Another mechanistic explanation for the observed preference of *sr* products was given early on by BERSON.¹⁸⁹ Considering frontier molecular orbital (FMO) analysis¹⁹⁹ for the *sr* shift unveiled a stabilizing interaction in the transition state. An orbital of the migrating group or atom could interact with the subjacent orbital (HOMO–1) of the allyl moiety, culminating in an overall stabilization of a bonding interaction and destabilization of an antibonding one (Scheme 47A).



Scheme 47 Subjacent orbital control in sigmatropic rearrangements. **A:** Illustration of the stabilizing interaction between the subjacent orbital in the allyl system in the transition state.¹⁸⁹ **B:** Sigatropic rearrangement with retention of configuration at silicon as reported by KIRA and co-workers.²⁰⁴

Although this mechanistic hypothesis was not operational for the systems investigated by BERSON (*vide supra*), computational studies suggested subjacent-orbital interactions to control the stereospecificity in rearrangements of allylsilanes. Initially discovered by KWART and co-workers in 1972,²⁰⁰ these rearrangements were

¹⁹⁶ C. Doubleday *J. Phys. Chem. A* **2001**, *105*, 6333-6341.

¹⁹⁷ a) W. v. E. Doering, K. Sachdev *J. Am. Chem. Soc.* **1974**, *96*, 1168-1187; b) W. v. E. Doering, K. Sachdev *J. Am. Chem. Soc.* **1975**, *97*, 5512-5520.

¹⁹⁸ F.-G. Klärner, S. Yaslak, M. Wette *Chem. Ber.* **1979**, *112*, 1168-1188.

¹⁹⁹ K. Fukui *Acc. Chem. Res.* **1971**, *4*, 57-64.

²⁰⁰ H. Kwart, J. Slutsky *J. Am. Chem. Soc.* **1972**, *94*, 2515-2516.

suggested to react *via* the *si* pathway as shown by comparing optical rotations of the product allylsilanes.²⁰¹ In 1997, KIRA²⁰² and YAMABE²⁰³ independently disclosed *ab initio* calculations that suggested that the transition state for the *sr* pathway was lower in energy than the corresponding one for *si* by 9 and 10 kcal/mol, respectively. Both groups suggested that the penalty for rehybridization of the migrating silicon atom in combination with the steric hindrance involved in the inversion transition state were responsible for the overall preference of the *sr* pathway. Additionally, they realized that the HOMO–1 stabilized the transition state in the *sr* pathway, which was consistent with subjacent-orbital control. In 1999, KIRA and co-workers were able to show retention of configuration in the migration of silacyclohexanes **203** and **205**, respectively (Scheme 47B).²⁰⁴ Both compounds underwent *sr* sigmatropic rearrangement specifically. The replacement of the hydride substituent by aryls diminished this selectivity. This gave further credit to the energetic nuances deciding the configurational outcome of [1,3]-sigmatropic rearrangements.

7.1.3 Sigmatropic Rearrangements of Chlorine

The first report on a sigmatropic chlorine shift dates back to 1937, when BERGMANN and BLUM-BERGMANN found a [1,5]-shift in dichlorodihydroanthracene **207** upon melting (Scheme 48A).²⁰⁵ The sigmatropic reaction proceeded in 90% yield and they proposed an anionotropic [1,5]-shift of chloride through intermediate **208**, followed by loss of HCl.²⁰⁶

²⁰¹ J. Slutsky, H. Kwart *J. Am. Chem. Soc.* **1973**, *95*, 8678-8685.

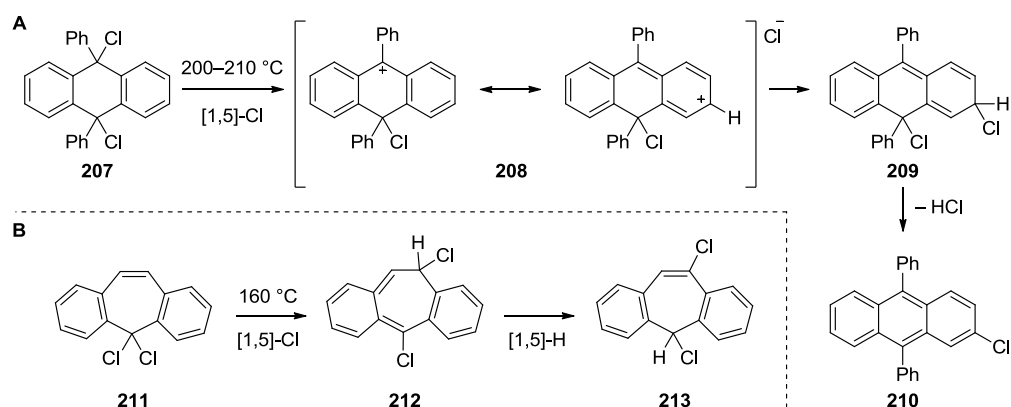
²⁰² M. Takahashi, M. Kira *J. Am. Chem. Soc.* **1997**, *119*, 1948-1953.

²⁰³ T. Yamabe, K. Nakamura, Y. Shiota, K. Yoshizawa, S. Kawauchi, M. Ishikawa *J. Am. Chem. Soc.* **1997**, *119*, 807-815.

²⁰⁴ L. C. Zhang, C. Kabuto, M. Kira *J. Am. Chem. Soc.* **1999**, *121*, 2925-2926.

²⁰⁵ E. Bergmann, O. Blum-Bergmann *J. Am. Chem. Soc.* **1937**, *59*, 1439-1441.

²⁰⁶ G. M. Badger, M. E. Mitchell *Aust. J. Chem.* **1965**, *18*, 919-921.



Scheme 48 [1,5]-Chlorine shifts in aromatic systems. **A**: Anionotropic rearrangement proposed by BERGMANN and BLUM-BERGMANN;²⁰⁵ **B**: Sequential sigmatropic rearrangements reported by LOOKER.²⁰⁷

A similar rearrangement was observed by LOOKER in dibenzocycloheptene **211** in 70% yield (Scheme 48B).²⁰⁷ He suggested steric release at the *gem*-disubstituted carbon as driving force of this reaction and proposed a sequence comprised of [1,5]-chlorine shift of **211** and [1,5]-hydrogen shift of **212** which were both allowed by the WOODWARD–HOFFMANN rules.²⁰⁸

The [1,5]-chlorine rearrangement was studied more carefully by DUSHENKO and co-workers.²⁰⁹ Through careful NMR analysis of several substituted chlorocyclopentadienes they determined the energy barriers for the sigmatropic [1,5]-chlorine shift to be 26.0 – 27.3 kcal/mol. In a DFT analysis on the B3LYP/6-311+G** level of theory, OKAJIMA and IMAFUKU later found the thermal [1,5]-chlorine shift to easily occur suprafacially in substituted chlorocyclopentadienes according to the WOODWARD–HOFFMANN rules.²¹⁰ More interestingly, they also studied substituted chlorocycloheptatrienes and found that the [1,7]-chlorine shift also occurs suprafacially and with a lower barrier than the [1,5]-rearrangement. Their computations suggested that the forbidden [1,7]-shift does not follow orbital-symmetry control but rather goes through a polar intermediate, in which the chlorine atom accumulates partial negative charge. The seven-membered ring becomes partially positive, reminiscent of a tropylium ion, thereby stabilizing the transition state

²⁰⁷ J. J. Looker *J. Org. Chem.* **1966**, *31*, 3599-3601.

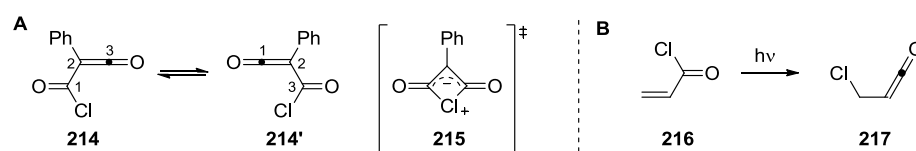
²⁰⁸ J. J. Looker *J. Org. Chem.* **1972**, *37*, 1059-1060.

²⁰⁹ I. E. Mikhailov, G. A. Dushenko, A. V. Kisin, C. Mügge, A. Zschunkem, V. I. Minkin *Mendeleev Commun.* **1994**, *4*, 85-88.

²¹⁰ T. Okajima, K. Imafuku *J. Org. Chem.* **2002**, *67*, 625-632.

through coulombic interactions. This reaction would therefore classify as an anionotropic shift, similar to the earliest reports by BERGMANN and BLUM-BERGMANN.

By comparison, [1,3]-sigmatropic reactions of chlorine remain rare curiosities. The shift of chlorine has been reported in α -chloro isocyanates,²¹¹ vinylsulfur reagents,²¹² polymers of trichlorobutadiene,²¹³ and vinylgermanes.²¹⁴ A more detailed study by WENTRUP is worthy of note, in which chlorocarbonyl(phenyl)ketene (**214**) undergoes rapid [1,3] migration at room temperature (Scheme 49A).²¹⁵ Based on earlier studies,²¹⁶ WENTRUP and co-workers recorded the ¹³C NMR spectrum of **214** at various temperatures and found that the single carbonyl signal at room temperature coalesced at -30 °C and split into two signals at -60 °C. Computations on the B3LYP/6-31G* level of theory suggested these peaks to arise from the equilibrium between **214** and **214'**, and the transition state energy between the two as 10.0 kcal/mol. Furthermore, they suggested a symmetric, planar transition state **215** which would result from the interaction between a lone pair on chlorine and the ketene-LUMO ($n_{\text{Cl}} \rightarrow \text{LUMO}_{\text{ketene}}$). Therefore, this reaction appears to follow the WOODWARD–HOFFMANN rules, because a non-bonding orbital in the starting material (n_{Cl}) would correspond to a bonding orbital in the product ($\sigma_{\text{C-Cl}}$) and *vice versa*.



Scheme 49 [1,3]-Chlorine shifts. **A**: Rapid equilibrium between **214** and **214'** via transition state **215**;²¹⁵ **B**: Rearrangement of **216** as reported by AYCARD and co-workers.²¹⁷

Another [1,3]-sigmatropic reaction of chlorine was reported by AYCARD and co-workers.²¹⁷ Acryloyl chloride (**216**) underwent rearrangement to **217** upon UV-irradiation in a frozen Argon matrix at 10 K (Scheme 49B). According to MP2/6-

²¹¹ K.-H. König, K.-H. Feuerherd, V. M. Schwendemann, H.-G. Oeser *Angew. Chem. Int. Ed.* **1981**, *20*, 883.

²¹² V. Y. Popkova, V. M. Anisimov, G. N. Dolenko, M. N. Semenenko, V. M. Fedoseev *J. Chem. Soc. Perkin Trans. 2* **1995**, 1375-1379.

²¹³ T. L. Lebedeva, I. I. Vointseva, L. M. Gil'man, P. V. Petrovskii, T. A. Larina *Russ. Chem. Bull.* **1997**, *46*, 732-738.

²¹⁴ G. Nemes, J. Escudié, I. Silaghi-Dumitrescu, H. Ranaivonjatovo, L. Silaghi-Dumitrescu, H. Gornitzka *Organometallics* **2007**, *26*, 5136-5139.

²¹⁵ J. Finnerty, J. Andraos, Y. Yamamoto, M. W. Wong, C. Wentrup *J. Am. Chem. Soc.* **1998**, *120*, 1701-1704.

²¹⁶ R. Koch, M. W. Wong, C. Wentrup *J. Org. Chem.* **1996**, *61*, 6809-6813.

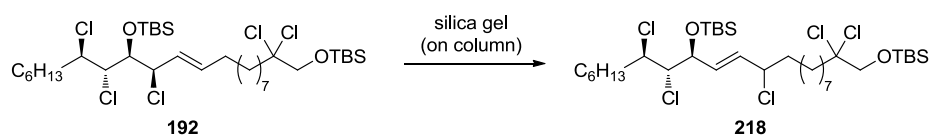
²¹⁷ N. Piétri, M. Monnier, J.-P. Aycard *J. Org. Chem.* **1998**, *63*, 2462-2468.

31G* calculations, the light was only required for the initial excitation of the system and the sigmatropic rearrangement took place from a ground state electronic configuration. Therefore, the ground state WOODWARD–HOFFMANN rule would need to apply and the reaction would take place with inversion on chlorine. However, later computations on the B3LYP/cc-pVDZ level of theory by SU and co-workers indicated that the reaction proceeds stepwise from the ground state through a diradical intermediate rather than in a concerted pericyclic reaction.²¹⁸

²¹⁸ W. Wu, K. Liu, C. Yang, H. Zhao, H. Wang, Y. Yu, H. Su *J. Phys. Chem. A* **2009**, *113*, 13892-13900.

7.2 Project Outline

As mentioned in Chapter 5.4, we were interested in the synthesis of **192** in order to gain access to a heptachloro analog of danicalipin A (**28**). After cross-metathesis, crude ^1H NMR suggested formation of **192** with 80% conversion. We were surprised to isolate 27% of **192** after chromatographic purification (hexane/toluene 50:1 to 10:1), along with 43% of a second product, which had not been present in the crude reaction mixture (Scheme 50). The second product was identified as **218** through 2D NMR analysis (*vide infra*).



Scheme 50 Formation of by-product **218** during flash column chromatography of **192** (hexane/toluene 50:1 to 10:1).

The by-product **218** arises from a [1,3]-sigmatropic rearrangement of the allylic chlorine substituent and its yield was improved to 62% by leaving **192** on silica for 30 minutes prior to elution. It is noteworthy that only one diastereomer of **218** could be detected, implying a highly stereospecific reaction, albeit without information on relative configuration.

In their report on the second generation approaches towards danicalipin A (**28**) and malhamensilipin A (**29**), VANDERWAL and co-workers had pointed towards the complex behavior of chlorinated vinyl epoxides and other allylic chlorines during cross-metathesis (*cf.* Chapter 2.4.2).⁸⁵ Although they never reported any isolated by-products, their comments and low yields indicated substantial problems with cross-metathesis. They concluded that these compounds suffered from unidentified influences which hampered cross-metathesis.

We became intrigued by our observation of a [1,3]-chlorine shift, which might account for troublesome reactions in prior syntheses. In particular the questions of configuration, mechanism, and general prerequisites were appealing to us. As this field of research was relatively unexplored (*cf.* Chapter 7.1.3), we anticipated an insight into [1,3]-sigmatropic chlorine migrations.

7.3 Elucidation and Preliminary Considerations

When we first performed the cross-metathesis, we were surprised to isolate a second product that we found to be isomeric to the desired product **192** according to NMR analysis. Careful structural analysis by 2D NMR uncovered the different substitution patterns. Assignment of the structure of **192** proved difficult. Although the allylic H13 was well resolved, the signals for H14, H15, and H16 overlapped in the ^1H NMR spectrum and impeded full elucidation of the C14 to C16 region (Figure 22). However, cross-peaks in the COSY spectrum allowed elucidation of the region from C13 to C10 and unveiled **192** as the desired allylic chlorine. The full elucidation ensued after functionalization of the double bond and dichlorination of the C11–C12 olefin (*cf.* Chapter 5.4).

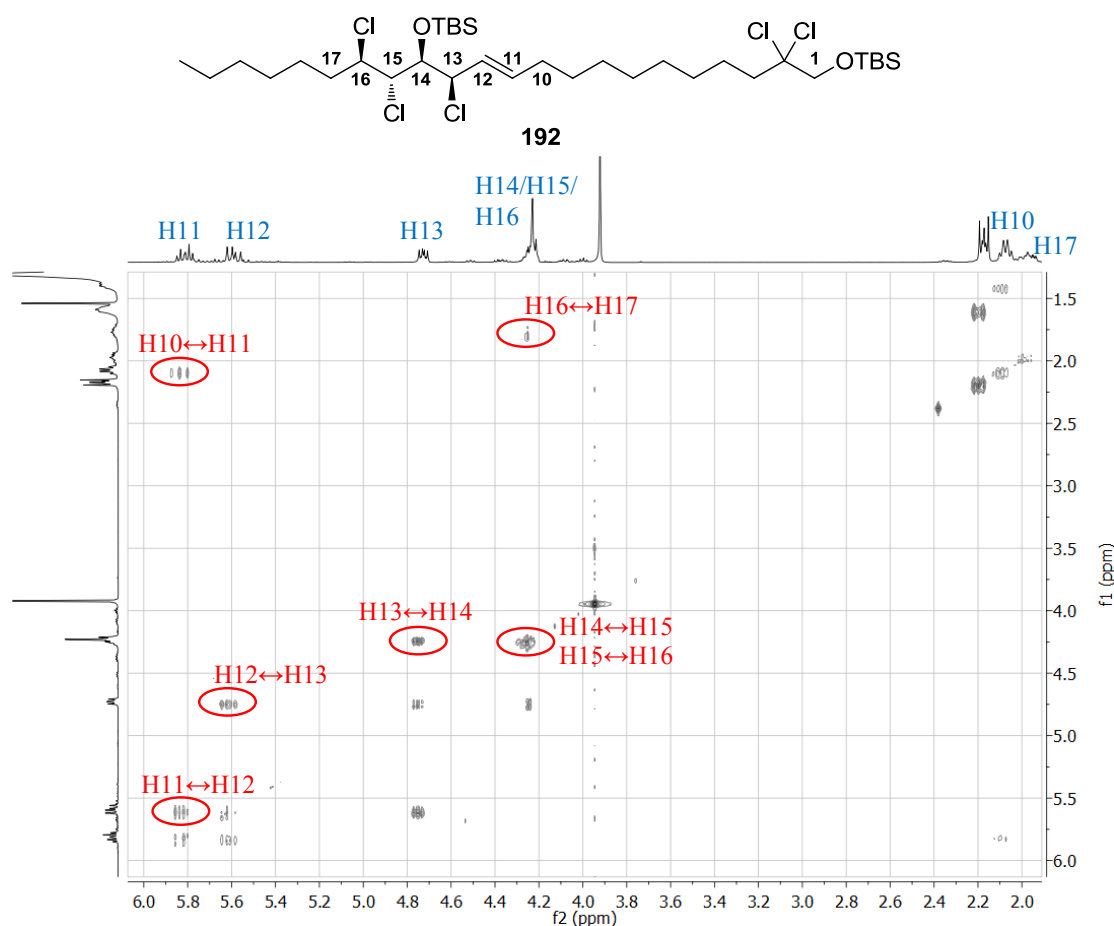


Figure 22 COSY spectrum of **192** at 600 MHz. Important signals for the structural elucidation are marked in the spectrum. Spectrum was recorded in CDCl_3 .

The spectrum of **218** was better resolved and allowed conclusive assignment of the C10 to C17 region (Figure 23). It became immediately apparent that two protons, H11 and H14, were shifted downfield into the region of heteroatom-substituted, allylic methines. The COSY spectrum of **218** showed cross-peaks which suggested that the olefin was located between C12–C13 instead of the desired C11–C12 and that the C13 chlorine substituent had shifted to C11.

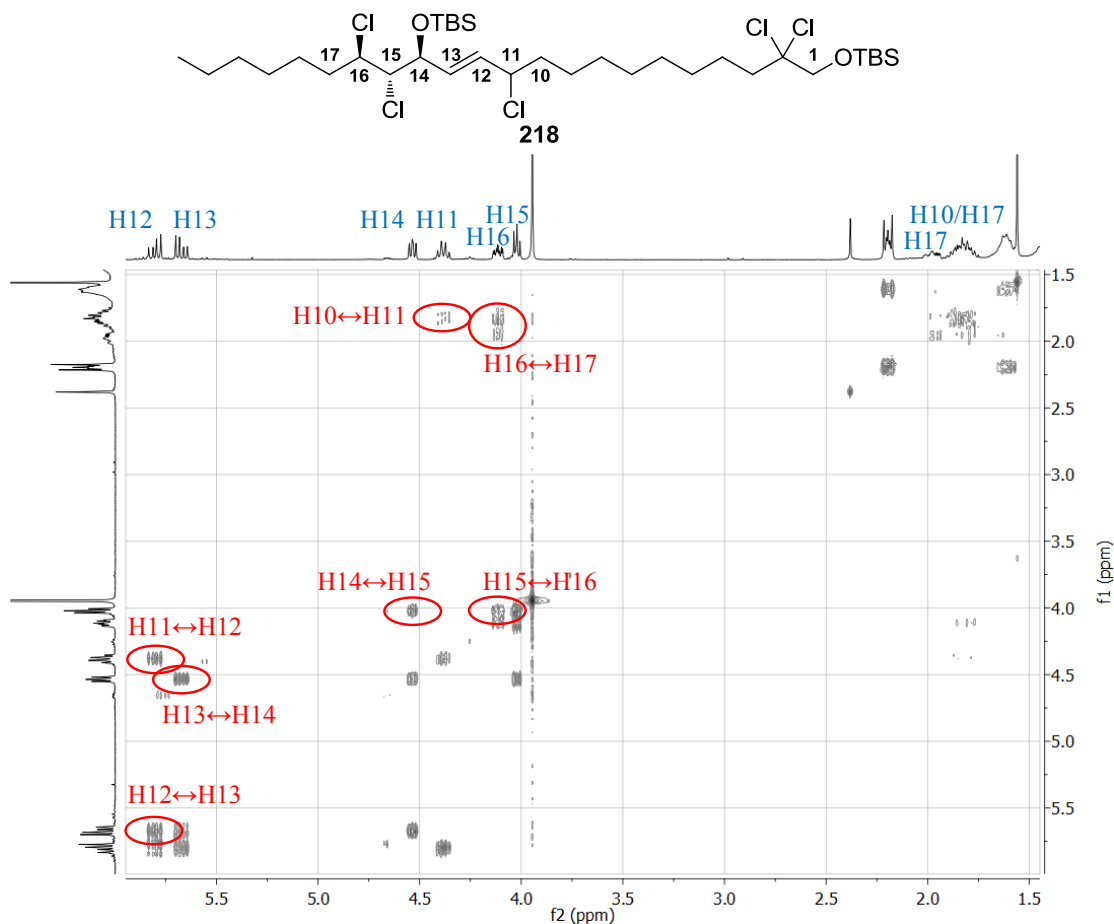


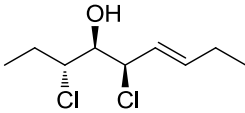
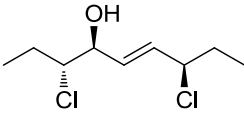
Figure 23 COSY spectrum of **218** at 600 MHz. Important signals for the structural elucidation are marked in the spectrum. Spectrum was recorded in CDCl_3 .

As **192** and **218** are structurally related and **218** was only present in the reaction mixture after column chromatography, we wanted to investigate the conditions under which **218** was formed. Addition of silica gel (ca. 1000% w/w) to the reaction mixture after completion of the cross-metathesis yielded no **218**, suggesting that silica gel did not catalyze this reaction. However, 2D TLC experiments of **192** showed that **218** was formed directly from **192** on silica gel. In the first dimension, the spot whose R_f corresponds to the less polar **192** changed its R_f to the one

corresponding to **218** in the second dimension, giving an off-diagonal spot. Furthermore, depending on the time between running the two dimensions, the conversion of **192** to **218** could be varied. Indeed, when chromatographic purification was performed in less than five minutes, **192** could be isolated in 82% yield. When the material was left on the column for 30 minutes prior to elution, **218** was isolated in 62% yield with no remaining **192** detectable. Despite the fact that silica gel might not be a catalyst for this reaction, the rearrangement occurred on silica gel.

In order to extract more details of this reaction, we decided to perform DFT calculations on the M06-2X/6-311++G**/LANL2DZpd(Cl)/SMD(hexane)//M06-2X/6-31+G**/LANL2DZpd(Cl)/SMD(hexane) level of theory on a simplified model system after MCMM optimization. Such DFT calculations had helped us previously in gaining valuable insights into the structure and flexibility of danicalipin A (**28**) and its diastereomers **147** and **148** (*cf.* Chapter 3). The results obtained for the simplified models **219** and **220** can be seen in Table 27. We assumed the more common suprafacial shift for the chlorine substituent in **220**.

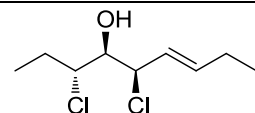
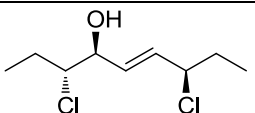
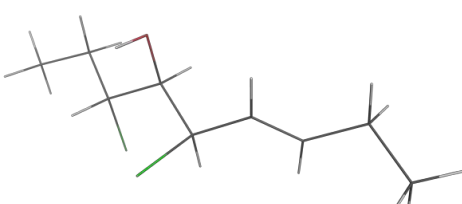
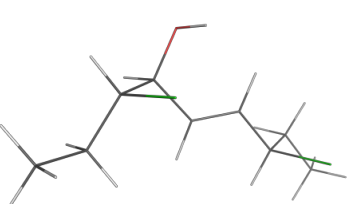
Table 27 Comparison of results for **219** and **220** obtained from DFT calculations in hexane. Lowest energy conformers of **219** and **220**, respectively, are shown in a sticks representation.

	219	220
		
# Found structures ^a	20	36
G^0	-287'015.39 kcal/mol	-287'015.61 kcal/mol
H^0	-286'977.35 kcal/mol	-286'978.25 kcal/mol
S	127.6 cal/mol/K	125.3 cal/mol/K
Dipole moment	1.68 D	2.52 D
Average dipole ^b	2.08 D	3.05 D
ΔG^0	0.23 kcal/mol (in favor of 220)	

a) Represents the number of individual structures obtained from MCMM in octanol and optimized with DFT calculations; b) dipole moment was calculated with energy-weighted average of the dipoles of all structures, according to $\mu_{avg} = \frac{\sum_i \mu_i * \exp(-\Delta G_i)}{\sum_i \exp(-\Delta G_i)}$

Interestingly, the lowest-energy structure for the rearranged model **220** appears to be favored by $\Delta G^0 = 0.23$ kcal/mol. The energetic preference is of enthalpic nature, while entropy favors the lowest-energy structure of starting material model **219**. Additional analysis confirmed that **219** would be less polar than **220**, as had been indicated by R_f values of **192** and **218** on TLC. The lowest-energy structure of **219** had a dipole moment of 1.68 D, whereas the lowest-energy structure of **220** had one of 2.52 D. An energy-weighted average of dipoles of all analyzed structures revealed that the overall difference is even larger with **219** having an average of 2.08 D and **220** having 3.05 D. Due to the high polarity of the medium on which the reaction of **192** to **218** took place, namely silica gel, we suspected that the higher dipole moment and polarity favored **218** and thus performed the same calculations in a polar solvent. Acetonitrile seemed appropriate due to its common use as aprotic organic solvent and its high polarity. The results of the computations are shown in Table 28.

Table 28 Comparison of results for **219** and **220** obtained from DFT calculations in acetonitrile. Lowest energy conformers of **219** and **220**, respectively, are shown in a sticks representation.

		
	219	220
		
# found structures^a	14	26
G^0	-287'018.86 kcal/mol	-287'019.99 kcal/mol
H^0	-286'980.49 kcal/mol	-286'982.40 kcal/mol
S	128.7 cal/mol/K	126.1 cal/mol/K
dipole moment	2.33 D	5.77 D
average dipole^b	3.31 D	4.42 D
ΔG^0	1.14 kcal/mol (in favor of 220)	

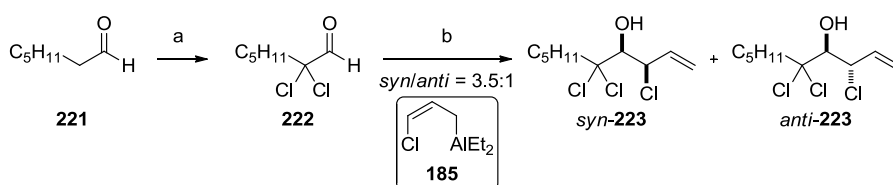
a) Represents the number of individual structures obtained from MCMM in chloroform and optimized with DFT calculations; b) dipole moment was calculated with energy-weighted average of the dipoles of all structures, according to $\mu_{avg} = \frac{\sum_i \mu_i * \exp(-\Delta G_i)}{\sum_i \exp(-\Delta G_i)}$

The rearranged model **220** is favored by 1.14 kcal/mol in acetonitrile due to an increased enthalpic contribution. Additionally, the dipole moment for the lowest-energy structure of **220** increased to 5.77 D and the energy-weighted average of all structures to 4.42 D. In contrast, the lowest-energy structure of **219** did not change dramatically. This had been anticipated given the rigidity of its trichlorinated segment due to the avoidance of *syn*-pentane interactions (*cf.* Chapter 3.1). While the dipole moment of the lowest-energy structure was similar as in hexane (2.33 D vs. 1.68 D in hexane), the averaged dipole moment increased to 3.31 D. This change in overall dipole moment was not as pronounced as in **220** and, consequently, an increased polarity of the medium should favor the rearranged product **220** more significantly.

As the computational analysis of **219** and **220** indicated that the [1,3]-chlorine shift might not be limited to our initial substrate **192**, we set out to investigate this reaction. In particular, we were interested to see if the thermal sigmatropic rearrangement was possible and the final configuration could be elucidated.

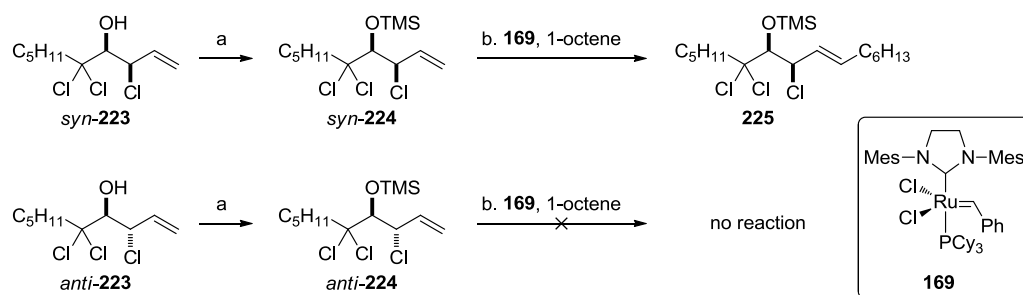
7.4 Studies on Optimization and Configuration

Since the material needed for the synthesis of **192** was required in the syntheses of danicalipin A (**28**) and other analogs, and its synthesis involved the use of valuable reagents, we devised a simpler substrate, assuming that any discoveries would be of a general nature. To this end, we decided to synthesize allylic chlorohydrin **225** which had similar stereoelectronic influences to **192**, but would allow access to both diastereomers. The synthesis of **225** commenced with α,α -dichlorination of heptanal (**221**), followed by chloroallylation,⁸⁰ giving a 3.5:1 mixture of *syn*- and the *anti*-chlorohydrins **223** (Scheme 51).



Scheme 51 Synthesis of allylic chlorohydrin **223**. Reagents and conditions: a) DL-proline (50 mol%), NCS, CH₂Cl₂, 0 °C to r.t.; b) LiTMP, allyl chloride, Et₂AlCl, THF, -78 °C, then **222**, -78 °C, 30% over 2 steps, d.r. = 3.5:1.

Through careful chromatographic purification, *syn*- and *anti*-**223** were separable and could be taken forward individually. Before cross-metathesis, the introduction of a silyl protecting group was required. Attempts to protect the alcohol as TBS ether were unfruitful, presumably due to steric encumbrance, but TMS protection of *syn*- and *anti*-**223** delivered *syn*- and *anti*-**224**, respectively (Scheme 52). This set the stage for cross-metathesis of **224** with 1-octene.⁹³ The internal olefin **225** was isolated in 71% yield from *syn*-**224**. Unfortunately, the same reaction did not yield any product from *anti*-**224**, but only starting material could be recovered.



Scheme 52 Synthesis of protected allylic chlorohydrin **225**. Reagents and conditions: a) TMSOTf, Et₃N, CH₂Cl₂, 0 °C to r.t., *syn*-**224**: quantitative, *anti*-**224**: 96%; b) **169** (10 mol%), 1-octene, CH₂Cl₂, 40 °C, 71%.

Nevertheless, the possibility of a [1,3]-sigmatropic shift in **225** could be investigated (Table 29). We began with the previously established conditions and were delighted to isolate the rearranged product **226** in 51% yield and in 3:1 d.r. (Entry 1). Since a 2D TLC of **225** suggested significant decomposition on silica gel, we decided to attempt a thermal rearrangement in solution. When **225** was refluxed in heptane (b.p. 98 °C, $\epsilon = 1.92$)²¹⁹ for 24 hours, no product formation could be observed by ¹H NMR analysis (Entry 2). Although earlier calculations had indicated that the more polar compound would be more stable, the reaction did not proceed in the apolar solvent. In contrast, when **225** was refluxed in acetonitrile (b.p. 82 °C, $\epsilon = 35.9$)²¹⁹ for 24 hours, the rearranged product was detected (Entry 3). Refluxing for five days gave 10% conversion, indicating that the thermal rearrangement in solution was feasible (Entry 4).

²¹⁹ C. Reichardt "Solvents and Solvent Effects in Organic Chemistry", 2nd edition, VCH, Weinheim, 1990, pp. 408 ff.

Table 29 Optimization for the thermal rearrangement of **225** to **226**.

Entry	Conditions	Time	Conversion ^a	Yield
1	silica gel (on column), hexane/toluene 50:1	30 min	n.d.	51%
2	heptane ^b , reflux	1 d	0%	-
3	acetonitrile ^b , reflux	1 d	<5%	-
4	acetonitrile ^b , reflux	5 d	10%	-
5	DMF ^b , reflux	1 d	decomposition	-

Reactions were performed on a 5 mg scale. a) Determined from crude ¹H NMR spectrum by integrating representative peaks; b) Reaction was run at a 0.014 mM concentration. n.d. = not determined.

To increase the rate of the thermal rearrangement in solution, we intended to increase the reaction temperature. Unfortunately, in refluxing DMF (b.p. 153 °C, $\epsilon = 36.7$),²¹⁹ only decomposition was observed (Entry 5). However, the reaction could be performed in a microwave reactor,²²⁰ allowing increased reaction temperatures with acetonitrile as solvent. When the reaction was run at 150 °C in d₃-acetonitrile, its progress could be monitored by ¹H NMR and is depicted in Figure 24.

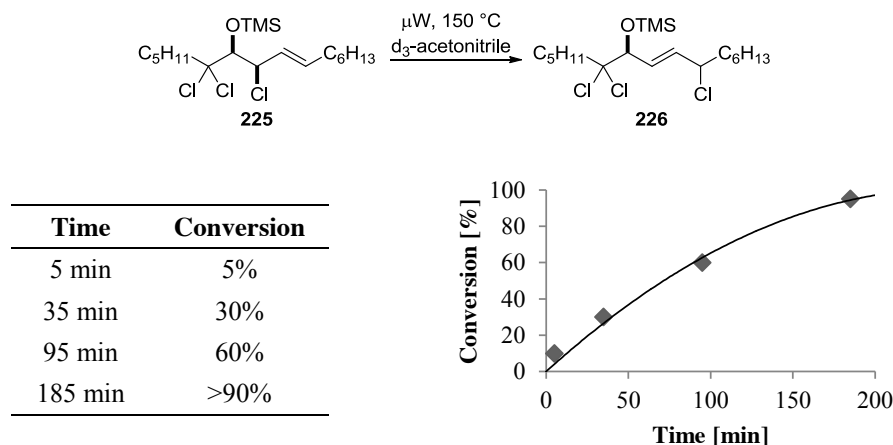


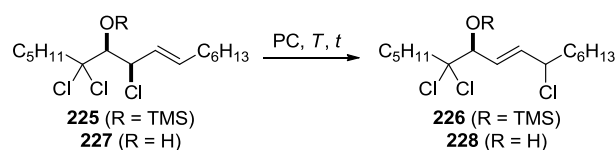
Figure 24 Rearrangement of **225** to **226** in deuterated acetonitrile at 150 °C. The conversions were determined by comparison of the integrals for representative signals in the ¹H NMR spectrum to each other and the residual solvent signal. The conversion *versus* time plot is shown on the right. Reaction was performed on a 2 mg scale at 0.02 mM.

The [1,3]-chlorine migration took place in a polar medium at elevated temperatures which was consistent with our earlier calculations. However, due to the

²²⁰ The microwave reactor belonged to the group of Prof. Dr. Pablo Rivera-Fuentes at ETH Zürich and was used with the assistance of Dr. Giovanni Bassolino. Their help was greatly appreciated.

propensity of acetonitrile to form hydrogen cyanide at elevated temperatures,²²¹ we were interested in other solvents that would facilitate the [1,3]-sigmatropic reaction. Propylene carbonate (PC) with its high boiling point (242 °C) and dielectric constant ($\epsilon = 64.9$) appeared to be an excellent choice. Indeed, when **225** was heated in PC at 100 °C, the rearranged product **226** could be isolated in 53% and 3:1 d.r. (Table 30, Entry 1). Furthermore, when deprotected **227**²²² was used, the rearranged product **228** could be isolated in 42% and 2:1 d.r. (Entry 3). Even more surprising, the reaction temperature for free alcohol **227** could be lowered to 70 °C, giving **228** in 69% yield and 2:1 d.r. (Entry 4). The lowering of the reaction temperature was considered an advantage as the calculations indicated an entropic preference for the starting material. Therefore a lower temperature should increase the yield of the rearrangement. Satisfyingly, heating the initial substrate for the [1,3]-chlorine migration **192** at 100 °C in PC gave rearranged **218** in an improved yield of 83% (Entry 5).

Table 30 Optimization of the thermal sigmatropic [1,3]-chlorine shift in propylene carbonate.



Entry	Compound	Product	Temperature	Time	Yield	d.r.
1	225	226	100 °C	4 days	53%	3:1
2	225	226	70 °C	1 week	20%	3:1
3	227	228	100 °C	1 hour	42%	2:1
4	227	228	70 °C	17 hours	69%	2:1
5	192	218	100 °C	30 hours	83%	>10:1

Reactions were performed on a 10 mg scale at a concentration of 0.05 mM.

We were surprised to see that the rearrangement of **225** or **227** gave two diastereomers, as this had not been the case when **192** rearranged. To further analyze the diastereomeric ratio during the reaction, we decided to run the rearrangement of **227** for varying times. The results are shown in Figure 25. When the product was exposed to the reaction conditions for prolonged times, the diastereomeric ratio decreased markedly. While the ratio was 2.3:1 after twelve hours, it decayed to 1.4:1 after one week. The plot on the right in Figure 25 also shows that the decline was

²²¹ T. W. Asmus, T. J. Houser *J. Phys. Chem.* **1969**, *73*, 2555-2558.

²²² **227** was obtained from treatment of **226** with catalytic amounts of AcOH in MeOH or cross-metathesis of *syn*-**223** with 1-octene.

steeper at the beginning than for the rest of the reaction, hence the diastereomeric ratio decreased faster at the beginning of the reaction. Additionally, the diastereomeric ratio appears to be approaching a value close to 1:1 towards infinity which is suggestive of an equilibrium mixture. A possible explanation for this decay of the diastereomeric ratio was the epimerization at the allylic site after rearrangement. A common observation made in sigmatropic rearrangements is that the substrates can undergo epimerization at similar rates as rearrangement.²²³ Accordingly, the intramolecular epimerization of **228** could be possible. Alternatively, the allylic chlorine substituent in **228** could be subject to substitution with chloride ions which might be present in the reaction mixture due to partial decomposition or elimination of **227** or **228**. In fact, stirring **228** (2:1 d.r.) with five equivalents of LiCl in PC at 70 °C for 24 hours allowed reisolated **228** in 91% yield and a diastereomeric ratio of 1:1 which would be in support of a possible substitution mechanisms. Whatever the mechanism for the epimerization might be, it appears to be absent in **218** (*vide infra*).

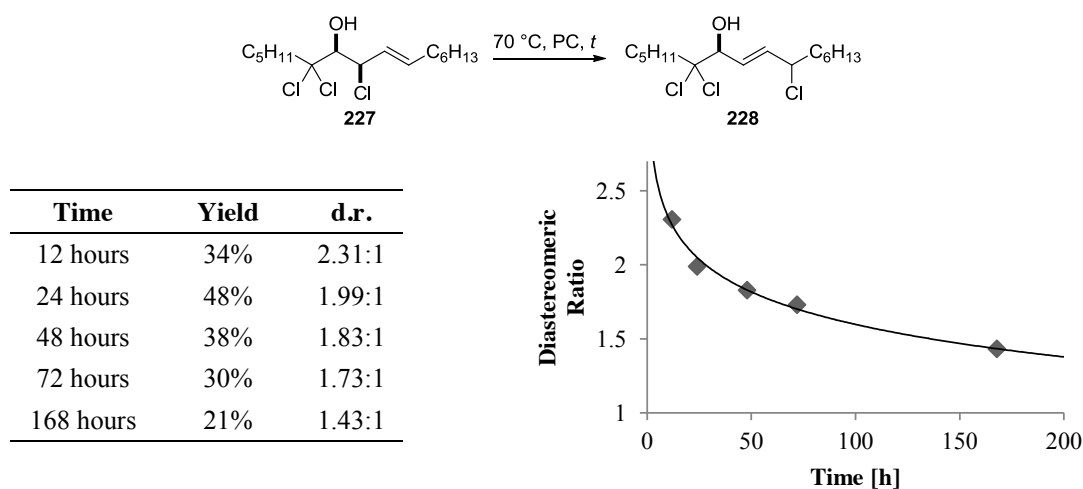
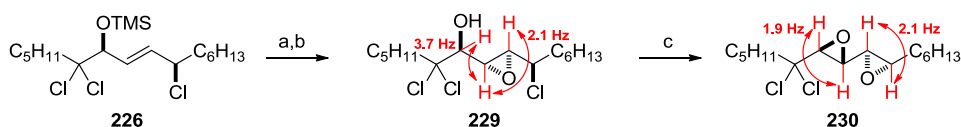


Figure 25 Rearrangement of **227** to **228** in propylene carbonate at 70 °C. The isolated yields and diastereomeric ratios were determined after different reaction times and are shown on the left. The diastereomeric ratios were determined by comparison of the integrals for representative signals in the ¹³C NMR spectrum. The diastereomeric ratio *versus* time plot is shown on the right. Reactions were performed on a 5 mg scale at 0.05 mM concentrations.

²²³ See for example: X. S. Bogle, P. A. Leber, L. A. McCullough, D. C. Powers *J. Org. Chem.* **2005**, *70*, 8913-8918.

In order to elucidate which relative configuration corresponded to the major diastereomer of the rearrangement, we set out to functionalize **226** (Scheme 53). After deprotection of the TMS group in **226** (d.r. = 3:1), **227** was obtained in 83% yield and 5:1 d.r. The material was subjected to epoxidation with *m*-CPBA, giving epoxyalcohol **229**. The configuration of this epoxidation was found to give a *trans*-epoxide *anti* to the alcohol, as determined by the coupling constants from the ^1H NMR spectrum.¹¹⁰ When this epoxyalcohol was treated with K_2CO_3 in methanol, PAYNE rearrangement²²⁴ gave bis-epoxide **230**. Again, the small coupling constants are indicative of two *trans*-epoxides.²²⁵ Ultimately, this would suggest a *syn*-relative configuration in **226** and therefore a suprafacial shift of the chlorine.



Scheme 53 Functionalization of **226**. The numbers in red represent the corresponding coupling constants in the ^1H NMR spectra and allow the configurational elucidation of the intermediates. The conclusion of this functionalization is the relative *syn*-configuration in **226**. Reagents and conditions: a) AcOH, MeOH, r.t., 83%, d.r. = 5:1; b) *m*-CPBA, CH_2Cl_2 , 0 °C to r.t.; c) K_2CO_3 , MeOH, r.t., 50% over 2 steps.

Having established that the chlorine undergoes a suprafacial shift, we were interested in knowing whether this reaction proceeded intramolecularly. Since we suspected the allylic chlorine to undergo displacement reactions, labeling studies would not have been feasible and we had to rely on another method. For example, in the allylic rearrangement of phenylthioethers reported by KWART and co-workers, a strong dependence of concentration on reaction rate was found.²²⁶ This behavior was attributed to the competition between an intramolecular and a bimolecular mechanism. In our case, when the rearrangement of **227** was run at a 10-fold dilution, identical reaction time and outcome were observed (*cf.* Table 30, Entry 4).²²⁷ This would be consistent with an intramolecular reaction, as alternative mechanisms, such as $\text{S}_{\text{N}}2'$ or other bimolecular reactions, should be slower at lower concentrations. Furthermore,

²²⁴ G. B. Payne *J. Org. Chem.* **1962**, *27*, 3819-3822.

²²⁵ E. Pretsch, P. Bühlmann, M. Badertscher "Spektroskopische Daten zur Strukturaufklärung organischer Verbindungen", 5th edition, Springer, Heidelberg, **2010**, p. 206.

²²⁶ H. Kwart, N. Johnson *J. Am. Chem. Soc.* **1970**, *92*, 6064-6066.

²²⁷ The reaction was run on a 10 mg scale at 0.005 M. After stirring for 20 hours, **228** was isolated in approximately 70% yield and 2:1 d.r.

an intermolecular reaction on silica gel would require free mobility of chloride ions or radicals, which is unlikely given the apolar nature of the eluent.

At this point it seems worth commenting on the mechanism of the [1,3]-sigmatropic rearrangement of chlorine. Given the hypothesis of an intramolecular, suprafacial shift, we need to differentiate between three possible mechanisms. The first option would be a diradical as transition state or intermediate. The second possible mechanism is a concerted pericyclic rearrangement with inversion of configuration according to the WOODWARD–HOFFMANN rules. And a third alternative is a transition state with retention at chlorine under subjacent-orbital control. The most important detail for this appears to be the solvent required for the reaction. In principle, the reaction should be proceeding in both apolar and polar media, since the rearranged product was calculated to be more stable regardless of the solvent (*cf.* Chapter 7.3). However, no reaction was observed in heptane at elevated temperatures. The reaction proceeds in acetonitrile or propylene carbonate and, furthermore, the more polar the solvent the lower the required reaction temperature. This can be explained by a polar transition state which is stabilized and thereby lowered energetically in a solvent of high polarity. However, a transition state that involves a diradical would be apolar in nature as no charge accumulates on either component. The same would be true for a reaction following the WOODWARD–HOFFMANN rules, as the HOMO of the transition state would have nodes at the sp^2 -hybridized chlorine atom and the allyl fragment, and should therefore distribute the charge evenly. In fact, these rearrangements are typically performed in apolar solvents. Consequently, we hypothesize that the polar transition state is under subjacent-orbital control and characterized by charge accumulation on the components. In 1973, EPIOTIS had suggested that subjacent-orbital control would be preferred in systems where both components have different ionization potentials, due to the more favorable interaction between the orbital of the migrating component and the HOMO–1.²²⁸ The ionization potential for an allyl radical (9.05 eV)²²⁹ is smaller than for a chlorine atom (12.97 eV)²³⁰ and would suggest that the energy of the orbital on

²²⁸ N. D. Epiotis *J. Am. Chem. Soc.* **1973**, *95*, 1206-1214.

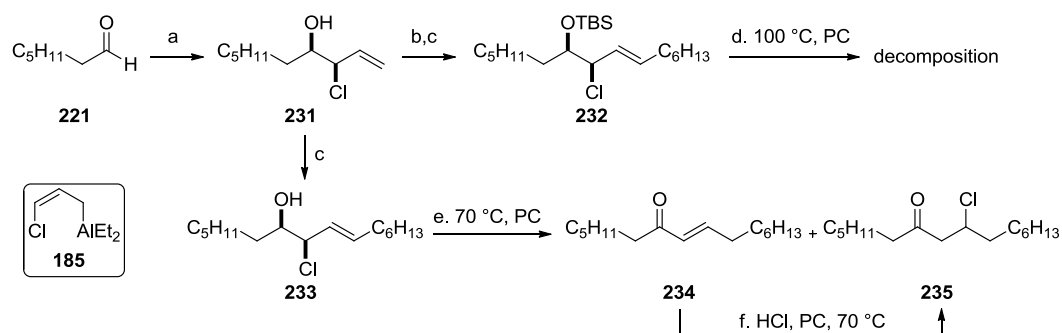
²²⁹ M. G. Evans, M. Szwarc *J. Chem. Phys.* **1951**, *19*, 1322-1323.

²³⁰ W. M. Haynes “*CRC Handbook of Chemistry and Physics*”, 97th edition, CRC Press/Taylor & Francis, Boca Raton, **2017**, p. 10–197.

chlorine is lower than the one of the π -system. Accordingly, the HOMO-1 of the transition state would be mostly located on the chlorine atom and lead to a partial negative charge on chlorine (*cf.* Scheme 45). This would result in a polar transition state which is reminiscent of a tight ion-pair between an allyl cation and a chloride ion. A similar hypothesis had been made for the [1,7]-sigmatropic rearrangement in chlorocycloheptatrienes and supported by calculations (*cf.* Chapter 7.1.3).

7.5 Structural Studies on Other Allylic Chlorohydrins

With optimized conditions and a basic understanding of this reaction in hand, we wanted to probe additional effects, such as the required stereoelectronic prerequisites. The rearrangement of a substrate lacking the *gem*-dichlorine was considered interesting as it would contain minimal stereoelectronic biases. To this end, heptanal (**221**) was treated with chloroallyl reagent **185**,⁸⁰ protected, and then subjected to cross-metathesis with 1-octene (Scheme 54).⁹³ Unfortunately, when **232** was heated at 100 °C in PC, no rearrangement but only decomposition could be observed.²³¹



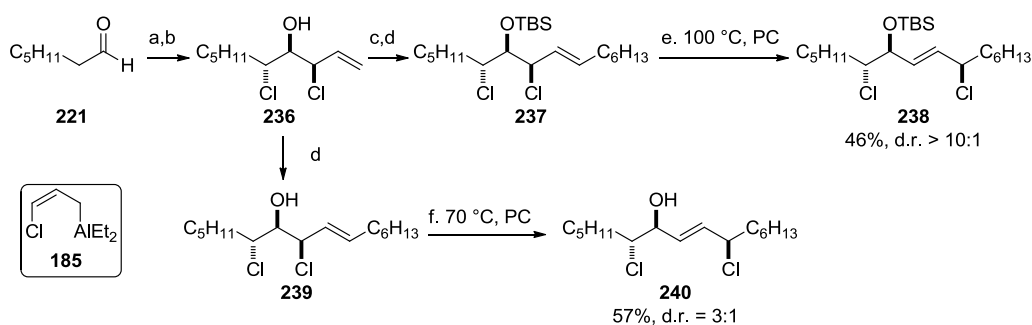
Scheme 54 Synthesis and attempted rearrangements of **232** and **233**. Reagents and conditions: a) LiTMP, allyl chloride, Et_2AlCl , THF, $-78\text{ }^\circ\text{C}$, then **221**, $-78\text{ }^\circ\text{C}$, 79%, d.r. > 10:1; b) TBSCl, imidazole, DMAP, CH_2Cl_2 , r.t., 34% (57% brsm); c) **185** (10 mol%), 1-octene, CH_2Cl_2 , $40\text{ }^\circ\text{C}$, ca. 60% for **232**, 56% for **233**; d) propylene carbonate, $100\text{ }^\circ\text{C}$; e) propylene carbonate, $70\text{ }^\circ\text{C}$, 21% of **234** and 29% of **235**; f) HCl, propylene carbonate, $70\text{ }^\circ\text{C}$, 46%.

When allylic chlorohydrin **231** was directly subjected to cross-metathesis, **233** was obtained in 56% yield. This material underwent elimination and isomerization when heated to $70\text{ }^\circ\text{C}$ in PC, giving enone **234** and β -chloroketone **235**. The

²³¹ The only material obtained after flash column chromatography of the crude mixture consisted of apolar compounds that had several different olefins and appeared to be lacking any heteroatoms according to ^1H and ^{13}C NMR analysis.

elimination product **234** could be the primary product of this reaction, as it was converted to **235** under modified reaction conditions (HCl, PC, 70 °C) and the reverse reaction could not be observed (**235** \nrightarrow **234**). The fact that neither **232** nor **233** underwent sigmatropic rearrangement was important as this result suggested that the correct stereoelectronic requirements had to be met in order to suppress side reactions, such as elimination.

According to these results, we decided to access an analog that would carry one chlorine substituent instead of the *gem*-dichlorine in **225** and **227**. Such a substrate would also resemble **219** and **220**, for which the calculations in Chapter 7.3 had been performed. α -Chlorination and subsequent chloroallylation gave **236** which was subjected to TBS protection and cross-metathesis with 1-octene,^{80,93,102} resulting in protected chlorohydrin **237** (Scheme 55). When **237** was heated in PC at 100 °C, rearranged **238** was obtained in 45% yield and >10:1 d.r. The diastereoselectivity of this reaction was as high as the one observed for **192** which indicated that the increased shielding of the larger TBS-group slowed or inhibited the epimerization of the allylic chlorine. Furthermore, the deprotected analog **239** also underwent rearrangement in PC at 70 °C and **240** was obtained in 57% yield and 3:1 d.r. Therefore, one can conclude that the single additional chlorine substituent is sufficient to fulfill the stereoelectronic requirements for the [1,3]-chlorine shift.

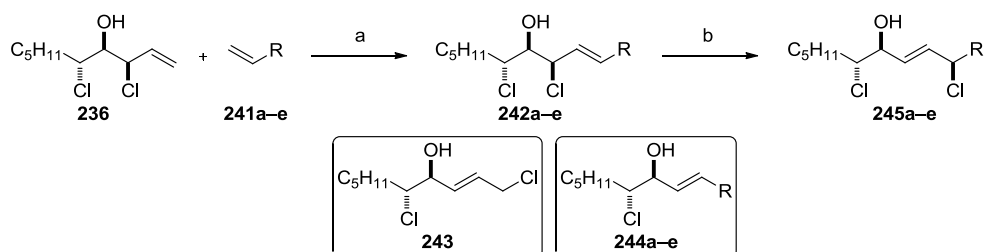


Scheme 55 Synthesis and rearrangements of **237** and **239**. Reagents and conditions: a) DL-proline (10 mol%), NCS, CH₂Cl₂, 0 °C to r.t.; b) LiTMP, allyl chloride, Et₂AlCl, THF, -78 °C, then aldehyde, -78 °C, 37% over 2 steps, d.r. = 9:1; c) TBSOTf, Et₃N, CH₂Cl₂, 0 °C to r.t., 45%; d) **185** (10 mol%), 1-octene, CH₂Cl₂, 40 °C, 67% for **237**, 51% for **239**; e) propylene carbonate, 100 °C, 46%, d.r. > 10:1; f) propylene carbonate, 70 °C, 57%, d.r. = 3:1.

With these results in hand, we investigated the partners that could be employed in cross-metathesis, giving rise to other substrates for rearrangement. The data is shown in Table 31. When vinylcyclohexane (**241a**) was used as cross-metathesis

partner, **242a** was isolated in 27% along with another compound **244a** (Entry 1). The by-product **244a** was lacking the allylic chloromethine, presumably through rearrangement of the starting material **236** or the intermediate **242a**, followed by cross-metathesis of **241a** with the resulting internal olefin. Gratifyingly, the sigmatropic rearrangement of cyclohexyl-derivative **242a** was observed in PC at 70 °C, giving **245a** in 33% yield and 4:1 d.r., although this reaction appeared to stop at approximately 60% conversion.²³² The increased steric hindrance at the allylic site could disfavor the rearranged product and lead to a reduced energetic difference between **242a** and **245a**. This suggests a steric influence in the driving force of the rearrangement, similar to what had been observed in other chlorine migrations (*cf.* Chapter 7.1.3). The steric hindrance can also explain the higher diastereomic ratio in **245a** when compared to **240**. The second displacement or epimerization could be slower in **245a** due to steric effects introduced by the larger cyclohexyl group.

Table 31 Synthesis and attempted rearrangements of **242a–e**. Reagents and conditions: a) **169** (10 mol%), olefin **241a–e**, CH₂Cl₂, 40 °C; b) propylene carbonate, 70 °C.



Entry	R	Yields of cross-metathesis			Yield of rearrangement	d.r.
		242	243	244		
1		27% (242a)	n.d.	22% (244a)	33% ^a (245a)	4:1
2		18% (242b)	n.d.	16% (244b)	30% (245b)	>10:1
3		42% (242c)		16% (243)	n.r.	-
4		29% ^b (242d)	29% (243)	11% (244d)	n.r.	-
5		51% ^b (242e)	n.d.	n.d.	n.r.	-

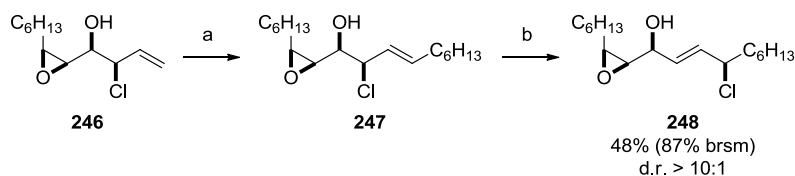
a) Reaction stopped at approx. 60% conversion (TLC); b) isolated as a 1:3 mixture with homodimer of olefin **241**. n.d. = not determined; n.r. = no reaction.

²³² Approximation by TLC analysis

Cross-metathesis of **236** with hex-4-en-2-one (**241b**) gave **242b** in 18% yield along with 16% of the shorter **244b** (Entry 2). Subjecting **242b** to 70 °C in PC led to chlorine migration and **245b** was isolated in 30% yield and >10:1 d.r. The rearrangement of **242b** displayed a very high diastereospecificity, similar to what had been observed in **192**. The electron-poor nature of the appendage could decelerate the epimerization by decreasing electron-density at the associated carbon atom.

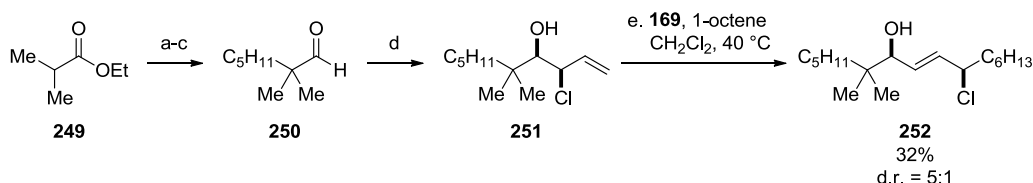
When we attempted to rearrange electron-poor substrates **242c–d**, no reaction was observed and only starting material was recovered (Entries 3–5). Even at 100 °C these substrates failed to undergo rearrangement and increasing the temperature to 130 °C led to extensive decomposition to several unidentifiable by-products. This indicated that the substrates for rearrangement should not be too electron-poor as this hampers the rearrangement.

To test whether the stereoelectronic requirements can only be met by a chlorine substituent in the vicinity of the chlorohydrin, or if it can be replaced by other functional groups, we decided to employ an epoxide instead of the *vic*-dichlorine motif in **192**. As we had access to epoxide **246** from the synthesis of danicalipin A (**28**),¹¹⁷ this seemed to be the ideal substrate (*cf.* Chapter 2.4.6). Cross-metathesis of **246** with 1-octene gave allylic chlorohydrin **247** in 85% yield (Scheme 56). The rearrangement of **247** only proceeded to 50% completion²³² and rearranged product **248** was isolated in 48% yield and >10:1 d.r. along with 45% of **247**. As in other examples before, the low conversion was indicative of an equilibrium mixture of **247** and **248** with no decisive energetic preference for either substrate. Nevertheless, the rearrangement proceeded with the epoxide, which suggested that the nature of the additional substituent adjacent to the chlorohydrin can be varied.



Scheme 56 Synthesis and rearrangement of **247**. Reagents and conditions: a) **169** (10 mol%), 1-octene, CH₂Cl₂, 40 °C, 85%; b) propylene carbonate, 70 °C, 48% (87% brsm), d.r. > 10:1.

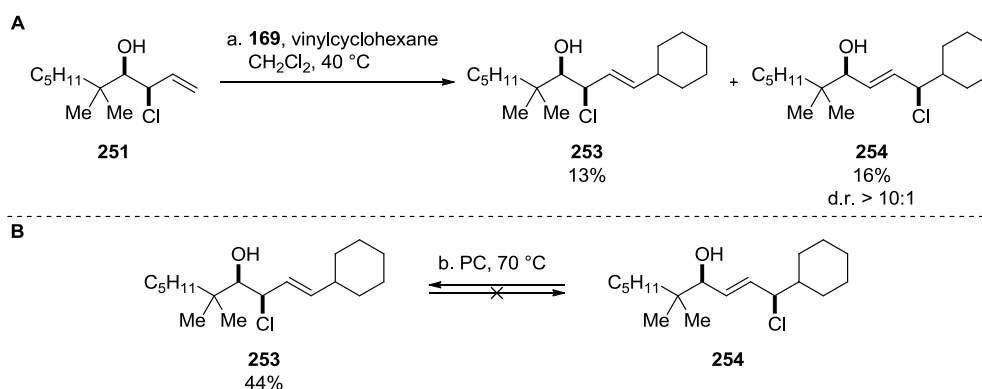
This prompted us to study whether the nature of the additional substitution had to be electron-poor or if there were other stereoelectronic requirements to this side of the allylic chlorohydrin. We anticipated a *gem*-dimethyl analog to display the same steric effects as the *gem*-dichloro but reversed electronic influences. The dimethyl analog was accessed by alkylation of ethyl isobutyrate (**249**),²³³ followed by reduction of the ester to the primary alcohol and oxidation to aldehyde **250** (Scheme 57). Chloroallylation of **250** gave allylic chlorohydrin **251** in 30% yield over four steps and in 6.5:1 d.r. Surprisingly, when this material was subjected to cross-metathesis conditions with 1-octene, the rearranged product **252** was isolated in 32% and 5:1 d.r. exclusively. This observation allowed for several speculations. First, the additional substituents can shield the carbinol proton from elimination and favor rearrangement by releasing the *syn*-pentane interactions. Second, the more facile reaction of the electron-rich substrate could indicate that an electron-rich allylic chlorine is more prone to rearrange, possibly due to better stabilization of the decreased charge density of the allylic fragment in the polar transition state (*cf.* Chapter 7.4).



Scheme 57 Synthesis and *in situ* rearrangement of **252**. Reagents and conditions: a) LDA, 1-bromopentene, THF, -78°C , 81%; b) $(i\text{-Bu})_2\text{AlH}$, CH_2Cl_2 , -78°C , 91%; c) DMP, NaHCO_3 , CH_2Cl_2 , 0°C ; d) LiTMP, allyl chloride, Et_2AlCl , THF, -78°C , then **250**, -78°C , 41% over 2 steps, d.r. = 6.5:1; e) **169** (10 mol%), 1-octene, CH_2Cl_2 , 40°C , 32%, d.r. = 5:1.

A similar observation was made during cross-metathesis of **251** and vinylcyclohexane (Scheme 58A). Both, the cross-coupled product **253** and the rearranged product **254**, were obtained in low yields. The shift already occurred during cross-metathesis which emphasized the beneficial effects that the *gem*-dimethyl substituents exhibited on the rearrangement.

²³³ R. Mueller, J. Yang, C. Duan, E. Pop, O. J. Geoffroy, L. H. Zhang, T.-B. Huang, S. Denisenko, B. H. McCosar, D. C. Oniciu, C. L. Bisgaier, M. E. Pape, C. Delaney Freiman, B. Goetz, C. T. Cramer, K. L. Hopson, J.-L. H. Dasseux *J. Med. Chem.* **2004**, *47*, 6082-6099.



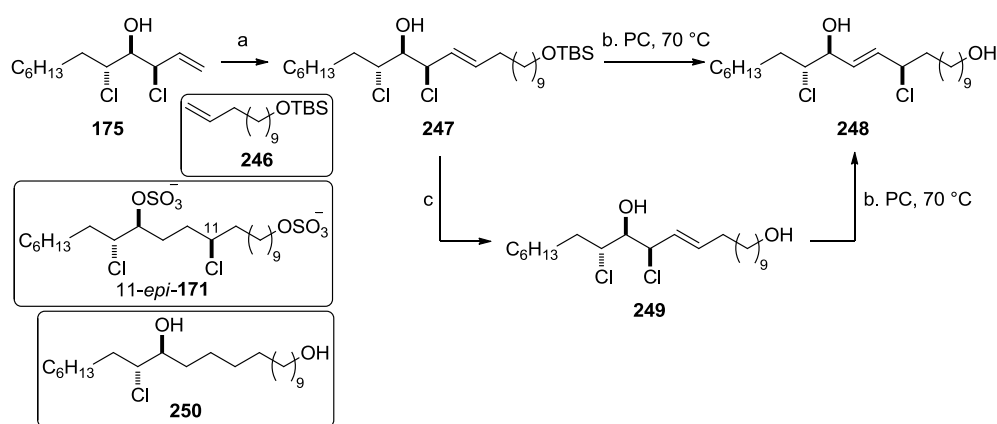
Scheme 58 A: Synthesis and *in situ* rearrangement of **253**. **B:** Rearrangement of **254** to **253**. Reagents and conditions: a) **169** (10 mol%), vinylcyclohexane, CH_2Cl_2 , 40 °C, 13% (**253**), 16 %, d.r. = 5:1 (**254**); b) propylene carbonate, 70 °C, 44%.

Interestingly, this represents the only example in which the rearranged product **254** was less polar on TLC than the allylic chlorohydrin **253**. When we attempted to interconvert the two compounds under the standard conditions, we found that **253** does not rearrange to give **254** but the other way around. Heating **254** in PC at 70 °C for seven hours gave **253** in 44% yield (Scheme 58B). This observation led us to hypothesize that the driving force of the reaction is two-fold. Besides the release of steric strain during the rearrangement there exists a polarity component, namely that the more polar product is preferred in the rearrangement. This might be the dominant effect in the equilibrium between **253** and **254**, as steric requirements are similar in both products.

It also seems worth noting that the conditions for cross-metathesis gave both **253** and **254** although the latter is converted to the former in PC. Hence, the different polarities of CH_2Cl_2 and PC appear to shift the equilibrium. Furthermore, the thermal rearrangement of **254** or **253** did not take place in CH_2Cl_2 at 40 °C in the absence of other reagents, indicating that the sigmatropic rearrangement can be catalyzed by a ruthenium-complex during the cross-metathesis.²³⁴ This observation gave us an idea as to how products, such as **244**, may be formed since rearrangement must take place during cross-metathesis (*cf.* Table 31).

²³⁴ Such rearrangements are known to be catalyzed by transition metals, see: a) G. Heinrich-Olivé, S. Olivé *J. Organomet. Chem.* **1971**, 29, 307-311; b) W. Strohmeier, E. Eder *Z. Naturforsch. B* **1974**, 29, 280-282.

At this point, the accumulated data encouraged us to attempt the implementation of the [1,3]-sigmatropic rearrangement in a short synthesis. During the work on the project discussed in Part III of this thesis, we were interested in partially chlorinated docosanedisulfates. As part of this project, we accessed a dichlorinated docosanedisulfate (**171**), a proposed intermediate of the biosynthesis of danicalipin A (**28**). The synthesis of intermediate **175** had already been described in the synthesis of trichloro-DDS (**140**) and we envisaged the [1,3]-chlorine rearrangement to enable easy access to 11-*epi*-**171** (Scheme 59).



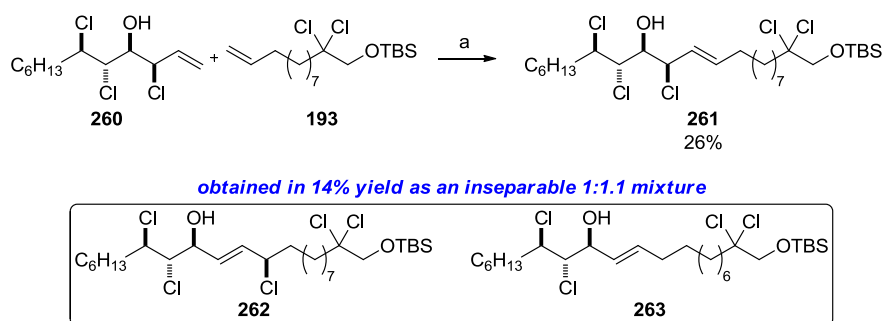
Scheme 59 Synthesis and rearrangements of **247** and **249**. Reagents and conditions: a) **169** (10 mol%), **246**, CH₂Cl₂, 40 °C, 45%; b) propylene carbonate, 70 °C, from **247**: 27%, d.r. = 2:1; from **249**: 41% (59% brsm), d.r. = 2.5:1; c) AcOH, MeOH, r.t., 80%.

Cross-metathesis of **175** with **246** gave allylic chlorohydrin **247** in 45% yield. When **247** was heated in PC at 70 °C, deprotection occurred *in situ* and rearrangement product **248** was isolated in 27% yield and 2:1 d.r. along with other unidentified products. When chlorohydrin **247** was deprotected prior to the rearrangement, **248** was isolated in 41% yield and 2.5:1 d.r. along with 31% of recovered **249**. As in previous examples, the reaction did not proceed past this conversion,²³² potentially due to attainment of the equilibrium. The higher diastereomeric ratio in the rearrangement of **249** *vis-à-vis* **247** can be explained by the prolonged reaction times required for the reaction of **247** (120 hours *vs.* 58 hours). Unfortunately, attempts to reduce the olefin in **248** heterogeneously (H₂, Pd/C) or homogeneously (H₂, WILKINSON's catalyst)²³⁵ also resulted in reduction of the allylic chlorine, giving **250** exclusively. The instability of the C–Cl bond, which led to the epimerization during

²³⁵ a) J. F. Young, J. A. Osborn, F. H. Jardine, G. Wilkinson *Chem. Commun.* **1965**, 131-132; b) J. A. Osborn, F. H. Jardine, J. F. Young, G. Wilkinson *J. Chem. Soc. A* **1966**, 1711-1732.

the rearrangement, rendered reduction of the olefin without concomitant reduction of the allylic chlorine impossible. This method was therefore not suited to efficiently access an epimeric **171**.

As pointed out in Chapter 7.2, earlier reports by VANDERWAL and co-workers omitted any mention of this rearrangement,⁸⁵ despite the fact that similar substrates which should have been capable of undergoing sigmatropic shifts, were synthesized and handled. The only indicators that problems were encountered with these substrates are the low yields of cross-metathesis and the avoidance of substrates that carried the chlorinated allylic chlorohydrin. With the knowledge we had gained we set out trying to unravel the problems encountered by others. As these reports had attempted cross-metathesis of free alcohols, which we knew to be more reactive towards rearrangement, the unprotected analog **260** was employed (Scheme 60).



Scheme 60 Synthesis of **261** and *in situ* rearrangement. Reagents and conditions: a) **169** (10 mol%), CH₂Cl₂, 40 °C, 26% of **261**, 14% of a 1:1.1 mixture of **262** and **263**.

To our surprise, the cross-metathesis yielded the desired allylic chlorohydrin **261** in 26% yield along with an inseparable 1:1.1 mixture of two compounds in 14% yield. Through careful 2D NMR analysis we were able to identify these two molecules as **262**, which arose from *in situ* rearrangement of **261**, and **263**, which missed the allylic chloromethine. Although we were able to assign **262** and **263** based on our gathered knowledge of these reactions, a small amount of an inseparable mixture of these two unlikely compounds might have been dismissed as undesired by-products if this reaction had been attempted on its own.

8 Conclusions and Outlook

The final part of this thesis has covered our work on the sigmatropic shift of allylic chlorines. The reaction was initially discovered during the synthesis of a heptachloro-DDS analog of danicalipin A (**28**). Intermediate **192**, a protected allylic chlorohydrin, underwent diastereospecific sigmatropic rearrangement during purification and the structure of rearranged product **218** was elucidated by 2D NMR analysis.

Computations on models **219** and **220** suggested that the rearranged product is favored energetically, especially in polar environments. The optimization of the rearrangement was performed on substrates **225** and **227** and revealed that the reaction cannot be performed in apolar solvents but only in polar ones. Especially the use of propylene carbonate, a highly polar, aprotic solvent, was found beneficial in promoting the thermal rearrangement. This led us to believe that the mechanism involves a polar intermediate, reminiscent of a tight ion pair between an allyl cation and a chloride ion, and is under subjacent-orbital control.

Applying the same conditions to other allylic chlorohydrins proved less efficient. Additional substituents vicinal to the chlorohydrin were found crucial to shield the carbinol proton from elimination and contribute to the release of steric congestion as driving force to the reaction. Furthermore, steric shielding or electron-withdrawing substituents were found advantageous to increase the diastereospecificity of the rearrangement, as they decelerate epimerization of the allylic chlorine substituent in the product. Interestingly, a reverse rearrangement was observed in the case where the allylic chlorohydrin was more polar than the rearranged product and suggested polarity as an additional driving force in this reaction.

Future studies could focus on the identification of a catalyst for this reaction. Early indications suggest a transition metal which could displace the chlorine substituent and form a π -allyl complex, thereby serving as viable intermediate and

promoting the sigmatropic rearrangement. Such a catalyst could allow for the use of a variety of solvents, which could be important in steering the reaction outcome. The subtle stereoelectronic effects in these rearrangements requires a fine tuning of the reaction conditions in order to increase yield and diastereospecificity, and the right choice of catalyst and solvent might go a long way to improve the generality and broaden the substrate scope of the rearrangement.

Ultimately, the [1,3]-sigmatropic shift of chlorine signifies yet another example in which synthetic work on the chlorosulfolipids uncovered unprecedented reactivity. Despite extensive research in this area, the chemical diversity hidden in the chlorinated arrays never ceases to amaze, and inspires future endeavors aimed at unearthing new chemical and biological secrets of the chlorosulfolipids.

GENERAL CONCLUSIONS

9 Final Remarks

As a whole, the projects described in this thesis have significantly expanded the understanding of the chemical and biological roles of the chlorinated natural product danicalipin A, and perhaps the chlorosulfolipids in general. Prior to this work, the extent of the uniqueness of the particular chlorination pattern in danicalipin A could not be fully appreciated. Earlier studies had focussed on the advantages to lipophilic properties and the impact on toxicity. A considerable advance was made when it was found that the natural product interacted with and compromised phospholipid-based membranes, as this pointed towards its unclear role in the membrane of *O. danica*. Although the complete picture did not emerge at that point, it has now become clear that danicalipin A contains several previously unidentified features that make it exceptional.

Comparing danicalipin A to two unnatural diastereomers revealed the importance of the molecular shape on membrane functions, but also disproved the previous assumption that these membrane functions were linked to the toxicity of the natural product. Thus, a crucial indication for the importance of the chlorinated array, beyond mere lipophilicity arguments, was given. This allowed not only speculation about the mode-of-action of the observed membrane permeability enhancement in phospholipid-based membranes but also about the significance of the molecular shape for the unidentified membrane functions in the natural organism. By drawing analogies to studies on the membranes of various spermatozoa, the work presented in this thesis proposed similar beneficial effects exhibited by the presence of danicalipin A in a membrane. While these conclusions correlate with the observations made in several bioassays, impeccably proving this hypothesis will require studying danicalipin A in the membrane of *O. danica* or models thereof.

Although the molecular shape of danicalipin A was found to be vital to its biological activities, its particular uniqueness became more apparent when investigating analogs with varying degrees of chlorination. The complete chlorination

pattern in danicalipin A had to be present to significantly exhibit membrane functions and the highest toxicity. Moreover, an additional chlorine substituent, while not perturbing the molecular shape, suppressed any membrane function and led to decreased toxicity. Given these observations, the advantageous influence of the chlorinated array in the natural product was obvious and a heretofore inconceivable development of danicalipin A by competitive evolution became reasonable. The specific effects imposed by the chlorination pattern, a combination of stereoelectronics, lipophilicity, molecular shape, flexibility, and possibly yet indeterminate properties, are key to its natural function, regardless of whether every subtle detail can be understood. This conclusion gives appreciation for the uniqueness of a seemingly random motif and constitutes another example in which nature has hidden complex forces in an inconspicuous pattern.

Throughout the projects of this thesis, the chemical diversity exhibited by the chlorosulfolipid intermediates accentuated their complex reactivity in cases that are not commonly encountered in organic synthesis. Small differences in steric or stereoelectronic biases drastically changed the reactivity of a previously established reaction and opened the possibility to explore and discover unprecedented pathways. The [1,3]-sigmatropic rearrangements of allylic chlorides is an example of such a pathway but only a part of what can be found by studying this rare class of natural products.

EXPERIMENTAL

10 General Considerations

10.1 Chemicals and Solvents:

All chemicals and solvents were purchased from ABCR, ACROS, ALFA-AESAR, APOLLO, J. T. BAKER, COMBI-BLOCKS, FLUKA, FLUOROCHEM, MERCK, TCI, SIGMA-ALDRICH, STREM or LANCASTER and were used as received without further purification unless otherwise noted. THF, Et₂O, CH₂Cl₂, MeCN, and toluene were dried over two 4" × 36" columns of anhydrous neutral A-2 alumina (MACHEREY & NAGEL; activated over night at 300 °C under a flow of N₂) under an atmosphere of Ar (H₂O content < 30 ppm, KARL-FISCHER titration)²³⁶. Pyridine and Et₃N were distilled from KOH under an atmosphere of dry N₂. Deuterated solvents for NMR spectroscopy were obtained from ARMAR CHEMICALS, Döttingen, Switzerland.

10.2 General Procedures:

All non-aqueous reactions were performed under an inert atmosphere of dry argon in oven-dried glassware unless otherwise noted. Argon was dried by passage over CaCl₂ prior to use. Reactions were monitored by thin layer chromatography using MERCK Silica Gel F²⁵⁴ TLC alumina plates cerium ammonium molybdate (CAM) [0.5 g Ce(NH₄)₂(NO₃)₆, 24 g (NH₄)₆Mo₇O₂₄·4H₂O, 1 L H₂O, 28 mL conc. H₂SO₄] or aqueous potassium permanganate (KMnO₄) [1.5 g KMnO₄, 10 g K₂CO₃, 200 mL H₂O, 1.25 mL 10% aq. NaOH] for staining. Concentration *in vacuo* was performed on a rotatory evaporator at 40 °C at the appropriate pressure. Flash column chromatography²³⁷ was performed on SILACYCLE SiliaFlash® P60 (230-400 mesh) or SIGMA-ALDRICH high-purity grade (230-400 mesh) silica gel at 0.4-0.5 bar over-

²³⁶ A. B. Pangborn, M. A. Giardello, R. H. Grubbs, R. K. Rosen, F. J. Timmers *Organometallics* **1996**, *15*, 1518-1520.

²³⁷ W. C. Still, M. Kahn, A. J. Mitra *J. Org. Chem.* **1978**, *43*, 2923-2925.

pressure. Purified compounds were dried further under high vacuum (0.1 torr). Yields refer to the purified compound.

10.3 Analytics

Nuclear Magnetic Resonance (NMR): NMR data was recorded on VARIAN Mercury (300 MHz), BRUKER AV or DRX (400 MHz), BRUKER DRX or DRXII (500 MHz) or BRUKER AVIII (600 MHz; cryoprobe) spectrometers. Measurements were carried out at ambient temperature (*ca.* 22 °C). Chemical shifts (δ) are reported in ppm with the residual solvent signal as internal standard (chloroform at 7.26 and 77.16 ppm, methanol-d₄ at 3.31 and 49.0 ppm). The data is reported as (s = singlet, d = doublet, t = triplet, q = quartet, m = multiplet or unresolved, coupling constant(s) in Hz, integration). ¹³C NMR spectra were recorded with broadband ¹H-decoupling. Service measurements were performed by the NMR service team of the LABORATORIUM FÜR ORGANISCHE CHEMIE at ETH ZÜRICH by Mr. RENÉ ARNOLD, Mr. RAINER FRANKENSTEIN, Mr. STEPHAN BURKHARDT and Mr. PHILIPP ZUMBRUNNEN under the direction of Dr. MARC-OLIVIER EBERT.

Infrared (IR): IR data was recorded on a PERKIN ELMER *Spectrum TWO FT-IR (UATR)* instrument as thin films. Absorptions are given in wavenumbers (cm⁻¹).

High Resolution Mass Spectrometry (HRMS): HRMS analyses were performed as EI measurements on a WATERS MICROMASS *AutoSpec Ultima* instrument at 70 eV or as ESI measurements on a BRUKER DALTONICS *maXis ESI-QTOF* instrument or as ESI/MALDI measurements on a BRUKER DALTONICS *solariX* instrument by the mass spectrometry service of the LABORATORIUM FÜR ORGANISCHE CHEMIE at ETH ZÜRICH by Mr. LOUIS BERTSCHI, Mr. OSWALD GRETER and Mr. ROLF HÄFLIGER under direction of Dr. XIANGYANG ZHANG.

Optical Rotations: Optical Rotations were measured on a Jasco *DIP-2000* polarimeter at the sodium D line in 10 cm path length cells with 2 mL of volume, and are reported as $[\alpha]_D^T$ (concentration in g/100 mL, solvent).

10.4 Computational Details:

Conformational Search: All conformational searches were performed using the Monte Carlo Multiple Minimum (MCMM)²³⁸ search protocol as implemented by MacroModel²³⁹ 9.9 with an implicit solvation model in CHCl₃ or octanol and an OPLS-2005 force field. Conformational spaces were generated employing a Polak-Ribière Conjugate gradient (PRCG) method with a convergence criteria of 0.005 and a maximum of 5000 iterations. All conformations obtained from mixed torsional/low mode sampling (maximum of 5000 steps, 1000 steps per rotatable bond) within 2 kcal of the lowest energy conformer were retained to verify sufficient sampling of the conformational space. The results of these conformational searches were manually analyzed. Duplicated structures were deleted and all retained conformations were considered for further optimization at the DFT level.

DFT calculations: All DFT calculations were performed using the Gaussian 09 program package,²⁴⁰ and the M06-2X hybrid functional.²⁴¹ All calculations were performed using an SMD solvation model²⁴² unless otherwise noted. Previously obtained structures were optimized with the Los Alamos National Laboratory 2 double ζ (LANL2DZ) Effective Core Potential and associated basis set²⁴³ augmented with diffuse and polarization functions for Cl (= LANL2DZpd),²⁴⁴ and a standard 6-31+G**²⁴⁵ for the remaining elements. Geometry optimizations were carried out

²³⁸ G. Chang, W. C. Guida, W. C. Still *J. Am. Chem. Soc.* **1989**, *111*, 4379.

²³⁹ MacroModel, Version 9.9, Schrödinger, LLC, New York, NY, **2014**.

²⁴⁰ Gaussian 09, Revision A.02, M. J. Frisch, G. W. Trucks, H. B. Schlegel, G. E. Scuseria, M. A. Robb, J. R. Cheeseman, G. Scalmani, V. Barone, B. Mennucci, G. A. Petersson, H. Nakatsuji, M. Caricato, X. Li, H. P. Hratchian, A. F. Izmaylov, J. Bloino, G. Zheng, J. L. Sonnenberg, M. Hada, M. Ehara, K. Toyota, R. Fukuda, J. Hasegawa, M. Ishida, T. Nakajima, Y. Honda, O. Kitao, H. Nakai, T. Vreven, J. A. Montgomery, Jr., J. E. Peralta, F. Ogliaro, M. Bearpark, J. J. Heyd, E. Brothers, K. N. Kudin, V. N. Staroverov, R. Kobayashi, J. Normand, K. Raghavachari, A. Rendell, J. C. Burant, S. S. Iyengar, J. Tomasi, M. Cossi, N. Rega, J. M. Millam, M. Klene, J. E. Knox, J. B. Cross, V. Bakken, C. Adamo, J. Jaramillo, R. Gomperts, R. E. Stratmann, O. Yazyev, A. J. Austin, R. Cammi, C. Pomelli, J. W. Ochterski, R. L. Martin, K. Morokuma, V. G. Zakrzewski, G. A. Voth, P. Salvador, J. J. Dannenberg, S. Dapprich, A. D. Daniels, O. Farkas, J. B. Foresman, J. V. Ortiz, J. Cioslowski, D. J. Fox, Gaussian, Inc., Wallingford CT, **2009**.

²⁴¹ Y. Zhao and D. G. Truhlar, *Theor. Chem. Acc.* **2008**, *120*, 215.

²⁴² A. V. Marenich, C. J. Cramer, D. G. Truhlar, *J. Phys. Chem. B* **2009**, *113*, 6378.

²⁴³ P. J. Hay and W. R. Wadt, *J. Chem. Phys.* **1985**, *82*, 270; P. J. Hay and W. R. Wadt, *J. Chem. Phys.* **1985**, *82*, 284; P. J. Hay and W. R. Wadt, *J. Chem. Phys.* **1985**, *82*, 299.

²⁴⁴ C. E. Check, T. O. Faust, J. M. Bailey, B. J. Wright, T. M. Gilbert, L. S. Sunderlin, *J. Phys. Chem. A* **2001**, *105*, 8111.

²⁴⁵ R. Ditchfield, W. J. Hehre, J. A. Pople, *J. Chem. Phys.* **1971**, *54*, 724; W. J. Hehre, R. Ditchfield, J. A. Pople, *ibid.* **1972**, *56*, 2257; P. C. Hariharan, J. A. Pople, *Theor. Chem. Acc.* **1973**, *28* 213; P. C. Hariharan, J. A. Pople, *Mol. Phys.* **1974**, *27*, 209; M. S. Gordon, *Chem. Phys. Lett.* **1980**, *76*, 163; M.

without any constraints. In case that the structures did not converge, the convergence criterion had to be set to 10^{-7} (subsequent reoptimization with the standard convergence criterion on structures generated by a reduced convergence criterion had the same energies as reported herein). Ground state minima were confirmed by frequency calculations, yielding no imaginary frequency unless otherwise noted. Electronic energies obtained, E , were converted to relative free energies G^0 at 298.15 K and 1 atm by using zero point energy and thermal energy corrections obtained in the frequency calculation. Optimized geometries for each conformer were then subjected to single point calculations at a M06-2X/6-311++G**/LANL2DZpd(Cl)/SMD level of theory. The free energy values discussed in the manuscript were derived from the electronic energy values obtained at the M06-2X/6-311++G**/LANL2DZpd(Cl)/SMD//M06-2X/6-311++G**/LANL2DZpd(Cl)/SMD level, E_{SP} , according to the following equation: $G_{final}^0 = E_{SP} + G^0 - E$. All energies are reported in hartrees/particle, unless otherwise noted.

10.5 Brine Shrimp Survival Assay

Brine Shrimp: The brine shrimp eggs, hatchery, and artemia salt were purchased from a pet store (Qualipet) and distributed by Hobby. Dry baker's yeast was manufactured and distributed by Patissier and purchased from Migros.

Sample preparation: Samples were prepared by dissolving 10 mg of **1**, **2**, and **3** in 1 mL DMSO yielding a 10 mg/mL stock solution which was then used to prepare the following dilutions: 1:1 with DMSO (5 mg/mL), 1:4 with DMSO (2.5 mg/mL), 1:10 with DMSO (1 mg/mL). The resulting solutions were further diluted with DMSO to the following concentrations: 0.5 mg/mL, 0.25 mg/mL, 0.1 mg/mL and 0.01 mg/mL.

Hatching the brine shrimp: The brine shrimp eggs were hatched using a brine shrimp hatchery which is a round container that is completely covered except for a hole containing a microsieve in the center. Since the *Artemia nauplii* are attracted to

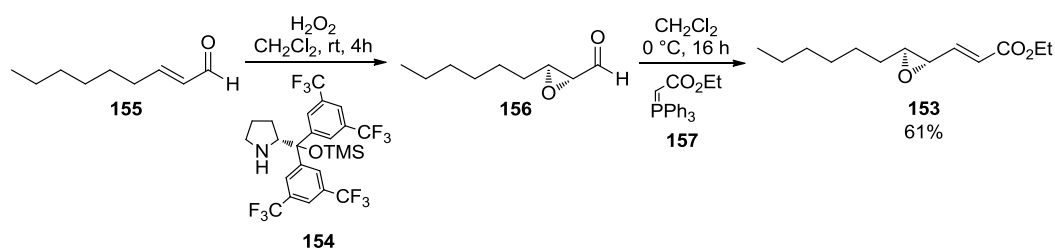
M. Francl, W. J. Pietro, W. J. Hehre, J. S. Binkley, D. J. DeFrees, J. A. Pople, M. S. Gordon, *J. Chem. Phys.* **1982**, *77*, 3654; R. C. Binning Jr. and L. A. Curtiss, *J. Comp. Chem.* **1990**, *11*, 1206; J.-P. Blaudeau, M. P. McGrath, L. A. Curtiss, L. Radom, *J. Chem. Phys.* **1997**, *107*, 5016; V. A. Rassolov, J. A. Pople, M. A. Ratner, T. L. Windus, *ibid.* **1998**, *109*, 1223; V. A. Rassolov, M. A. Ratner, J. A. Pople, P. C. Redfern, L. A. Curtiss, *J. Comp. Chem.* **2001**, *22*, 976; G. A. Petersson, A. Bennett, T. G. Tensfeldt, M. A. Al-Laham, W. A. Shirley, J. Mantzaris, *J. Chem. Phys.* **1988**, *89*, 2193; G. A. Petersson, M. A. Al-Laham, *ibid.* **1991**, *94*, 6081.

light, they slowly migrated through a series of baffles toward the center leaving their egg shell behind. This set-up naturally separates the shell from the newly hatched *Artemia* nauplii. The dish-like device was filled with artificial sea water prepared with artemia salt before *ca.* 0.4g eggs were added to the outer ring of the hatchery. After 48 hours the phototropic nauplii were collected from the microsieve by pipette.

Brine shrimp bioassay: Approximately ten shrimp (9 – 16) were transferred to a 24 well tissue culture plate in 2 mL of artificial sea water. The nauplii were counted using a microscope set to 1.25x magnification. 20 μ L of the series dilutions of **1**, **2**, and **3** (see above) were added to give final concentrations of 100, 50, 10, 5, 2.5, 1 or 0.1 μ g/mL of the respective compound per well. Each condition was tested in triplicate. 20 μ L of DMSO was added to three control wells to ascertain that the solvent alone had no toxic effect while three untreated wells served to determine the natural death rate of the shrimp during the time of the treatment. A suspension of dry baker's yeast (22 μ L; 3mg/5mL in artificial sea water) was added to each well as food supply. The plates were kept in a room with a normal dark-light cycle and survivors were counted under the microscope after 24 hours.

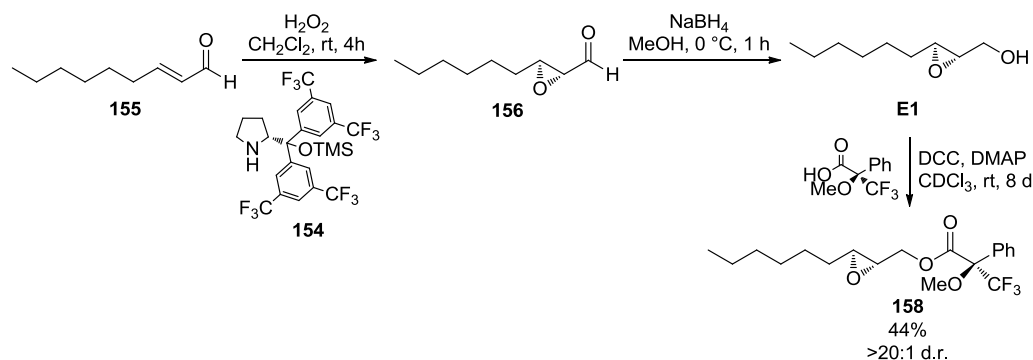
LC₅₀ determination: LC₅₀ values were determined from the 24 hour live vs. dead counts by transferring mg to μ M concentrations and plotting the ln[concentration in μ M] against the number of live shrimp (see below). Subsequent non-linear curve fitting with Graph Pad Prism 6 yielded the values presented in Table 1.

11 Experimental Details for Part II



(*E*)-ethyl 3-((2*S*,3*S*)-3-hexyloxiran-2-yl)acrylate (153**):** To a solution of enal **155** (3.55 mL, 21.4 mmol, 1.00 equiv) in CH_2Cl_2 (42.8 mL) (*R*)-Jørgensen-Hayashi-catalyst **154** (1.28 g, 2.14 mmol, 10.0 mol%). The solution was stirred and aqueous hydrogen peroxide (30%, 2.84 mL, 27.8 mmol, 1.30 equiv) was added. After stirring for 4 hours, the reaction was filtered through a silica gel plug, eluting with CH_2Cl_2 . After concentration, the residue was taken up in CH_2Cl_2 (120 mL) and cooled to 0 °C in an ice bath. Ethyl 2-(triphenylphosphoranylidene)acetate (**157**, 7.45 g, 21.4 mmol, 1.00 equiv) was added and the reaction was stirred at 0 °C for 16 hours. After concentration, flash column chromatography (pentane/ Et_2O 9:1, SiO_2) gave the desired product **153** as colorless oil (2.93 g, 13.0 mmol, 61%).

$^1\text{H NMR}$ (400 MHz, CDCl_3) δ 6.68 (dd, $J = 15.7, 7.1$ Hz, 1H), 6.12 (d, $J = 15.7$ Hz, 1H), 4.20 (q, $J = 7.1$ Hz, 2H), 3.20 (dd, $J = 7.1, 2.0$ Hz, 1H), 2.88 (td, $J = 5.6, 2.0$ Hz, 1H), 1.68 – 1.54 (m, 2H), 1.51 – 1.39 (m, 2H), 1.39 – 1.20 (m, 9H), 0.89 (t, $J = 6.8$ Hz, 3H); $^{13}\text{C NMR}$ (101 MHz, CDCl_3) δ 165.9, 145.0, 123.7, 61.7, 60.7, 56.5, 32.1, 31.8, 29.2, 25.9, 22.7, 14.4, 14.2; **HRMS** (EI+) exact mass for $\text{C}_{11}\text{H}_{17}\text{O}_2$ [$\text{M}-\text{C}_2\text{H}_5\text{O}$] $^+$, calculated 118.1223, found 181.1223; **IR** (thin film, cm^{-1}) ν 2958, 2930, 2859, 1721, 1567, 1466, 1369, 1344, 1303, 1278, 1259, 1180, 1139, 1039, 977, 853; $[\alpha]_{\text{D}}^{23\text{ }^\circ\text{C}} = -9.5$ ($c = 0.57, \text{CHCl}_3$).



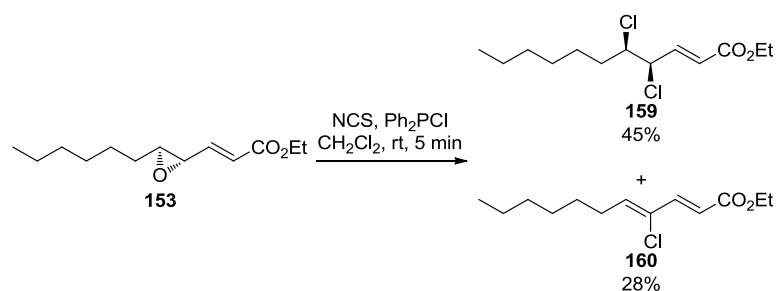
(R)-((2*S*,3*S*)-3-hexyloxiran-2-yl)methyl-3,3,3-trifluoro-2-methoxy-2-phenylpropanoate (158**):** To a solution of enal **155** (0.59 mL, 3.57 mmol, 1.00 equiv) in CH₂Cl₂ (7.1 mL) (*R*)-Jørgensen-Hayashi-catalyst **154** (0.213 g, 0.357 mmol, 10.0 mol%). The solution was stirred and aqueous hydrogen peroxide (30%, 0.473 mL, 4.64 mmol, 1.30 equiv) was added. After stirring for 4 hours, the reaction was filtered through a silica gel plug, eluting with DCM. After concentration, a crude mixture of epoxyaldehyde **156** was obtained (0.629 g, 113%).

Of this mixture, an aliquot (34.1 mg, 5.4% of total amount) was dissolved in THF (0.96 mL) and MeOH (0.96 mL) and cooled to 0 °C. Sodium borohydride (10.9 mg, 0.288 mmol, ca. 1.50 equiv) was added and the reaction was stirred at 0 °C for 1 hour. Sat. aq. NaHCO₃ was added and the mixture was extracted three times with CH₂Cl₂. Combined organic phases were dried over Na₂SO₄, filtered, and concentrated. Flash column chromatography (hexanes/EtOAc 3:1, SiO₂) gave alcohol **E1** as white solid.

Alcohol **E1** was taken up in CDCl₃ (1.5 mL) and (*R*)-Mosher-acid (24.8 mg, 0.106 mmol, ca. 0.55 equiv), DCC (21.8 mg, 0.106 mmol, ca. 0.55 equiv), and DMAP (12.9 mg, 0.106 mmol, ca. 0.55 equiv) were added. After stirring overnight, the reaction was concentrated and resuspended in CDCl₃ (0.6 mL). After 4 days, the reaction was filtered and concentrated. The residue was taken up in CDCl₃ (0.6 mL) and (*R*)-Mosher-acid (24.8 mg, 0.106 mmol, ca. 0.55 equiv), DCC (21.8 mg, 0.106 mmol, ca. 0.55 equiv), and DMAP (12.9 mg, 0.106 mmol, ca. 0.55 equiv) were added. After another 4 days, the reaction was filtered, concentrated and analyzed by crude ¹⁹F NMR, to show a d.r. of >20:1. Flash column chromatography (pentane/Et₂O 10:1, SiO₂) gave product **158** as colorless oil (31.8 mg, 0.085 mmol, 44% over 3 steps).

Experimental

$^1\text{H NMR}$ (400 MHz, CDCl_3) δ 7.59 – 7.49 (m, 2H), 7.48 – 7.36 (m, 3H), 4.53 (dd, $J = 12.0, 3.5$ Hz, 1H), 4.23 (dd, $J = 12.0, 6.1$ Hz, 1H), 3.57 (d, $J = 1.2$ Hz, 3H), 2.99 (ddd, $J = 5.9, 3.5, 2.1$ Hz, 1H), 2.83 (td, $J = 5.6, 2.1$ Hz, 1H), 1.65 – 1.47 (m, 2H), 1.47 – 1.35 (m, 2H), 1.35 – 1.19 (m, 6H), 0.96 – 0.80 (m, 3H); $^{19}\text{F NMR}$ (377 MHz, CDCl_3) δ -71.74; $^{13}\text{C NMR}$ (101 MHz, CDCl_3) δ 166.5, 132.2, 129.8, 128.6, 127.4 (app d, $J = 1.4$ Hz), 123.3 (q, $J = 288.5$ Hz), 84.8 (q, $J = 27.9$ Hz), 66.4, 56.9, 55.7 (app d, $J = 1.6$ Hz), 54.7, 31.8, 31.6, 29.1, 25.9, 22.7, 14.2; **HRMS** (EI) exact mass for $\text{C}_{19}\text{H}_{25}\text{F}_3\text{O}_4$ $[\text{M}]^+$, calculated 174.1705, found 374.1700; **IR** (thin film, cm^{-1}) ν 2931, 1858, 1753, 1452, 1271, 1243, 1169, 1122, 1081, 1022, 765, 719; $[\alpha]_{\text{D}}^{25\text{ }^\circ\text{C}} = +22.8$ ($c = 1.02, \text{CHCl}_3$).



(4*R*,5*R*,*E*)-ethyl 4,5-dichloroundec-2-enoate (159): To a solution of *N*-chlorosuccinimide (2.91 g, 21.8 mmol, 3.50 equiv) in CH_2Cl_2 (75 mL) in a water bath was added chlorodiphenylphosphin (3.45 mL, 18.7 mmol, 3.00 equiv). The water bath was removed and the reaction was stirred for 5 minutes. Epoxide **153** (1.41 g, 6.23 mmol, 1.00 equiv) in CH_2Cl_2 (50 mL) was added rapidly *via* two syringes. After 3 minutes, sat. aq. NaHCO_3 was added and the reaction was extracted three times with Et_2O . Combined organic layers were filtered through a silica gel plug, eluting with Et_2O , and finally concentrated. Flash column chromatography (hexanes/ Et_2O 100:1, SiO_2) gave dichloride **159** as colorless oil (0.79 g, 2.81 mmol, 45%) and the elimination product **160** (0.43 g, 1.76 mmol, 28%).

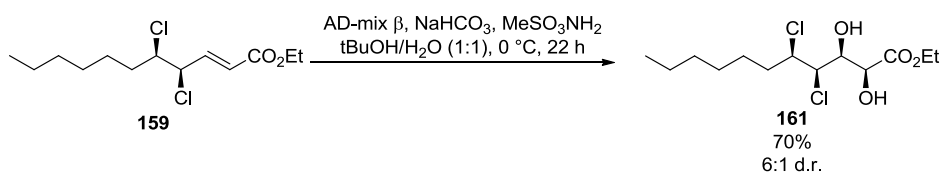
Analytical data for **159**:

$^1\text{H NMR}$ (400 MHz, CDCl_3) δ 7.02 (dd, $J = 15.4, 7.2$ Hz, 1H), 6.17 (dd, $J = 15.4, 1.3$ Hz, 1H), 4.73 (ddd, $J = 7.2, 3.7, 1.3$ Hz, 1H), 4.26 (q, $J = 7.1$ Hz, 2H), 4.11 (dt, $J = 10.1, 3.6$ Hz, 1H), 1.99 (dddd, $J = 13.8, 9.6, 5.7, 3.5$ Hz, 1H), 1.79 – 1.64 (m, 1H), 1.47 – 1.19 (m, 11H), 0.91 (m, 3H); $^{13}\text{C NMR}$ (101 MHz, CDCl_3) δ 165.6,

141.7, 125.5, 64.2, 62.7, 61.1, 33.8, 31.7, 29.9, 28.7, 22.7, 14.3, 14.2; **HRMS** (EI) exact mass for $C_{11}H_{17}Cl_2O$ $[M-C_2H_5O]^+$, calculated 235.0651, found 235.0651; **IR** (thin film, cm^{-1}) ν 2928, 2859, 1721, 1661, 1466, 1368, 1309, 1270, 1168, 1039, 976, 864, 768, 726, 661; $[\alpha]_D^{24\text{ }^\circ C} = +53.4$ ($c = 2.0$, $CHCl_3$).

Analytical data for 160:

1H NMR (400 MHz, $CDCl_3$) δ 7.62 (dd, $J = 14.8, 0.7$ Hz, 1H), 6.31 (d, $J = 14.8$ Hz, 1H), 6.13 (t, $J = 8.1$ Hz, 1H), 4.24 (q, $J = 7.1$ Hz, 2H), 2.39 – 2.24 (m, 2H), 1.51 – 1.40 (m, 2H), 1.37 – 1.20 (m, 6H), 1.32 (t, $J = 7.1$ Hz, 3H), 0.97 – 0.80 (m, 3H); **^{13}C NMR (101 MHz, $CDCl_3$)** δ 166.8, 139.7, 135.9, 128.4, 122.2, 60.7, 31.6, 29.1, 28.9, 28.8, 22.5, 14.3, 14.0; **HRMS** (EI) exact mass for $C_{13}H_{21}ClO_2$ $[M]^+$, calculated 244.1230, found 244.1225; **IR** (cm^{-1}) ν 2928, 2858, 1717, 1632, 1465, 1367, 1304, 1265, 1176, 1095, 1036, 964, 869, 728, 691.



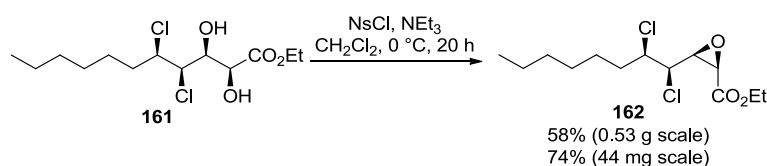
(2S,3S,4R,5R)-ethyl 4,5-dichloro-2,3-dihydroxyundecanoate (161):

AD-mix β (4.18 g), methanesulfonamide (0.282 g, 2.97 mmol, 1.00 equiv), and sodium bicarbonate (0.748 g, 8.91 mmol, 1.00 equiv) were dissolved in *t*BuOH (14.9 mL) and water (14.9 mL). After cooling to 0 °C, olefin **159** (0.835 g, 2.97 mmol, 1.00 equiv) was added, rinsing with little *t*BuOH. After stirring for 22 hours at 0 °C, sodium sulfite (4.49 g, 35.6 mmol, 12.0 equiv) was added and the reaction was allowed to warm to 25 °C. After 1 hour at 25 °C, the mixture was diluted with water and extracted three times with EtOAc. Combined organic phases were dried over Na_2SO_4 , filtered, and concentrated. Flash column chromatography (pentane/ Et_2O 100:1, then toluene/acetone 20:1, SiO_2), gave the product **161** as pale yellow oil (0.652 g, 2.07 mmol, 70%) as 6:1 mixture of diastereomers (as determined by ^{13}C NMR of the purified product).

1H NMR (600 MHz, $CDCl_3$) δ 4.40 – 4.37 (m, 1H), 4.35 – 4.28 (m, 2H), 4.27 (d, $J = 1.7$ Hz, 2H), 4.24 (ddd, $J = 8.4, 5.4, 1.6$ Hz, 1H), 3.20 (d, $J = 5.7$ Hz, 1H), 2.52 (s, 1H), 2.00 – 1.92 (m, 1H), 1.88 (ddt, $J = 14.1, 10.1, 5.5$ Hz, 1H), 1.52 (dddd, $J =$

Experimental

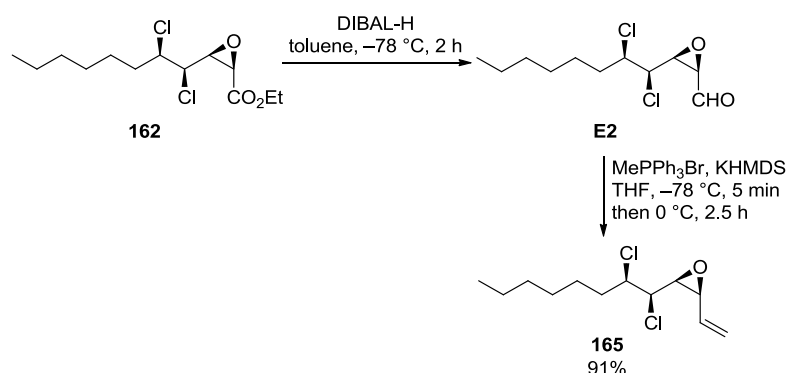
19.2, 9.9, 7.2, 5.0 Hz, 1H), 1.44 – 1.36 (m, 1H), 1.33 (t, $J = 7.1$ Hz, 3H), 1.36 – 1.28 (m, 6H), 0.91 – 0.85 (m, 3H); ^{13}C NMR (151 MHz, CDCl_3) δ 172.3, 74.8, 70.2, 68.3, 62.7, 61.6, 36.8, 31.7, 28.7, 26.4, 22.7, 14.3, 14.2; HRMS (ESI) exact mass for $\text{C}_{13}\text{H}_{24}\text{Cl}_2\text{NaO}_4$ $[\text{M}+\text{Na}]^+$, calculated 337.0944, found 337.0948; IR (thin film, cm^{-1}) ν 3461, 2957, 2858, 1740, 1466, 1377, 1277, 1223, 1118, 1064, 1022; $[\alpha]_{\text{D}}^{23}$ $^{\circ}\text{C} = +16.3$ ($c = 0.67$, CHCl_3).



(2R,3S)-ethyl 3-((1R,2R)-1,2-dichlorooctyl)oxirane-2-carboxylate (162): To a solution of diol **161** (0.527 g, 1.67 mmol, 1.00 equiv) in CH_2Cl_2 (16.7 mL) was added triethylamine (0.35 mL, 2.51 mmol, 1.50 equiv). The solution was cooled to 0 $^{\circ}\text{C}$ and after 30 minutes *p*-nitrobenzenesulfonyl chloride (0.389 g, 1.75 mmol, 1.05 equiv) was added. After stirring for 12 hours at 0 $^{\circ}\text{C}$, triethylamine (0.23 mL, 1.67 mmol, 1.00 equiv) was added and the reaction was stirred for another 8 hours at 0 $^{\circ}\text{C}$. The reaction was concentrated and the residue applied to a column with hexanes. Flash column chromatography (hexanes/EtOAc 1:0, 100:1, then 50:1, SiO_2) gave epoxide **162** as colorless oil (0.286 g, 0.962 mmol, 58%).

The same procedure on a 44.0 mg scale of diol **X8** produced epoxide **X9** in 74% yield.

^1H NMR (500 MHz, CDCl_3) δ 4.37 – 4.20 (m, 3H), 3.92 (ddd, $J = 9.3, 4.8, 2.9$ Hz, 1H), 3.67 (d, $J = 4.2$ Hz, 1H), 3.57 (dd, $J = 8.6, 4.3$ Hz, 1H), 2.02 – 1.92 (m, 1H), 1.79 (dtd, $J = 14.2, 9.4, 4.9$ Hz, 1H), 1.52 – 1.44 (m, 1H), 1.32 (t, $J = 7.2$ Hz, 3H), 1.41 – 1.20 (m, 7H), 0.92 – 0.84 (m, 3H); ^{13}C NMR (151 MHz, CDCl_3) δ 167.5, 62.3, 62.3, 61.0, 58.7, 54.4, 34.7, 31.7, 28.6, 26.5, 22.7, 14.3, 14.2; HRMS (ESI) exact mass for $\text{C}_{13}\text{H}_{22}\text{Cl}_2\text{NaO}_3$ $[\text{M}+\text{Na}]^+$, calculated 319.0838, found 319.0839; IR (thin film, cm^{-1}) ν 2957, 2929, 2859, 1748, 1466, 1380, 1202, 1109, 1027, 850, 807, 702; $[\alpha]_{\text{D}}^{23}$ $^{\circ}\text{C} = +40.0$ ($c = 0.33$, CHCl_3).



(2S,3S)-2-((1R,2R)-1,2-dichlorooctyl)-3-vinyloxirane (165): To a solution of ester **162** (0.316 g, 1.06 mmol, 1.00 equiv) in toluene at $-78\text{ }^{\circ}\text{C}$ was added DIBAL-H dropwise (1.0 M in CH_2Cl_2 , 1.60 mL, 1.60 mmol, 1.50 equiv). After stirring at $-78\text{ }^{\circ}\text{C}$ for 2 hours, methanol (1.5 mL) was added and the cooling bath was removed. Then sat. aq. sodium potassium tartrate was added and the mixture was stirred vigorously until both phases were clear. The mixture was then poured into water and EtOAc. Phases were separated and the aqueous phase was extracted twice with water. Combined organic phases were dried over Na_2SO_4 , filtered and concentrated. The crude aldehyde **E2** was then taken up in THF (8.5 mL) and used in the next reaction as was.

Crude analysis of aldehyde **E2**:

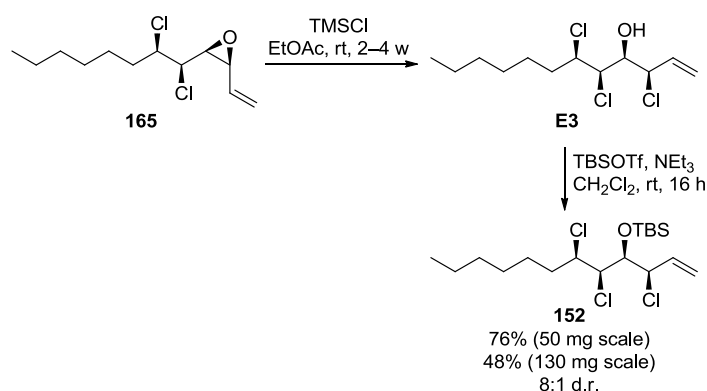
$^1\text{H NMR}$ (300 MHz, CDCl_3) δ 9.60 – 9.56 (m, 1H), 4.10 – 4.03 (m, 1H), 3.97 (dt, $J = 9.8, 3.5$ Hz, 1H), 3.72 – 3.63 (m, 2H), 2.12 – 1.97 (m, 1H), 1.85 – 1.69 (m, 1H), 1.64 – 1.45 (m, 1H), 1.29 (m, 7H), 0.93 – 0.86 (m, 3H).

In a separate flask, methyltriphenylphosphonium bromide (0.759 g, 2.13 mmol, 2.00 equiv) was suspended in THF (12.8 mL). After cooling to $-78\text{ }^{\circ}\text{C}$, KHMDS (0.5 M in toluene, 3.20 mL, 1.60 mmol, 1.50 equiv) was added dropwise. The yellow suspension was placed in an ice bath after 5 minutes and stirred for 20 minutes. After cooling back down to $-78\text{ }^{\circ}\text{C}$, the solution of aldehyde **E2**, obtained in the first section, was added dropwise to the reaction (the flask was rinsed with 0.5 mL THF twice). The dark yellow suspension was then placed in an ice bath after 5 minutes and stirred for 2.5 hours. The reaction was then quenched through the addition of sat. aq. NH_4Cl and separated between water and EtOAc. Phases were separated and the aqueous phase extracted three times with pentane. Combined organic layers were washed with water

Experimental

and brine, dried over Na_2SO_4 , filtered, and concentrated. Flash column chromatography (hexanes/ Et_2O gradient 100:1 to 50:1, SiO_2) gave olefin **165** as colorless oil (0.242 g, 0.963 mmol, 91%).

$^1\text{H NMR}$ (600 MHz, CDCl_3) δ 5.74 (ddd, $J = 17.2, 10.6, 6.3$ Hz, 1H), 5.56 (dt, $J = 17.2, 1.2$ Hz, 1H), 5.43 (ddd, $J = 10.6, 1.3, 0.9$ Hz, 1H), 3.99 (ddd, $J = 8.8, 5.3, 2.8$ Hz, 1H), 3.86 (dd, $J = 8.8, 2.8$ Hz, 1H), 3.66 (ddt, $J = 6.2, 4.1, 0.9$ Hz, 1H), 3.50 (dd, $J = 8.8, 4.2$ Hz, 1H), 1.94 – 1.78 (m, 2H), 1.52 – 1.42 (m, 1H), 1.40 – 1.20 (m, 7H), 0.94 – 0.84 (m, 3H); $^{13}\text{C NMR}$ (151 MHz, CDCl_3) δ 130.9, 121.6, 62.9, 62.4, 60.2, 59.0, 35.4, 31.7, 28.7, 26.4, 22.7, 14.2; HRMS (EI) exact mass for $\text{C}_{12}\text{H}_{20}\text{ClO}$ [$\text{M}-\text{Cl}$] $^+$, calculated 215.1197, found 215.1198; IR (thin film, cm^{-1}) ν 2956, 2929, 2859, 1467, 1254, 985, 933, 823, 772, 662; $[\alpha]_D^{23}$ = +82.3 ($c = 0.55, \text{CHCl}_3$).



tert-butyl dimethyl(((3*R*,4*S*,5*R*,6*R*)-3,5,6-trichlorododec-1-en-4-yl)oxy) silane (152**):** To a solution of epoxide **165** (50.0 mg, 0.199 mmol, 1.00 equiv) in EtOAc (6.5 mL) at 0 °C was added TMSCl (63.0 μL , 0.498 mmol, 2.50 equiv) in CH_2Cl_2 (184 μL) dropwise. The reaction was allowed to warm to 23 °C and was stirred for 2 weeks. The reaction was quenched with pH 7 buffer solution and extracted three times with EtOAc. Combined organic phases were dried over Na_2SO_4 , filtered, and concentrated to give crude alcohol **E3** with a diastereomeric ratio of 8:1 (as determined from crude $^1\text{H NMR}$).

Crude analysis of alcohol **E3**:

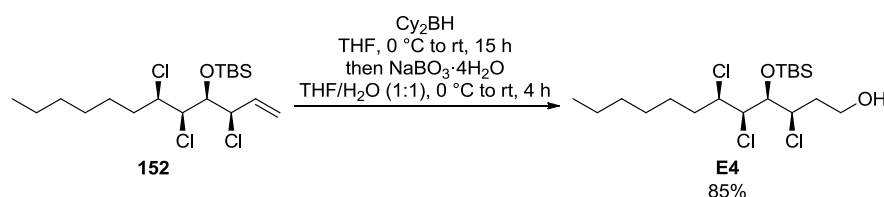
$^1\text{H NMR}$ (300 MHz, CDCl_3) δ 5.93 (ddd, $J = 17.1, 10.1, 8.4$ Hz, 1H), 5.40 (dt, $J = 16.7, 0.8$ Hz, 1H), 5.27 (dt, $J = 10.3, 0.8$ Hz, 1H), 4.54 (dd, $J = 8.5, 4.8$ Hz, 1H),

4.18 – 4.09 (m, 2H), 4.02 (q, $J = 5.0$ Hz, 1H), 2.42 (d, $J = 4.9$ Hz, 1H), 1.99 – 1.72 (m, 2H), 1.41 – 1.14 (m, 8H), 0.89 – 0.72 (m, 3H).

The residue was taken up in CH_2Cl_2 (2.0 mL). Triethylamine (0.111 mL, 0.796 mmol, 4.00 equiv) and TBSOTf (0.137 mL, 0.597 mmol, 3.00 equiv) were added and the reaction was stirred for 16 hours. The solution was then poured into water and extracted three times with CH_2Cl_2 . Combined organic phases were dried over Na_2SO_4 , filtered, and concentrated. Flash column chromatography (hexanes, SiO_2) gave compound **152** as colorless oil (60.8 mg, 0.151 mmol, 76%).

The same conditions (syring epoxide opening for 1 month) on a 130 mg scale, gave trichloride **152** in 48% yield.

$^1\text{H NMR}$ (600 MHz, CDCl_3) δ 6.00 (ddd, $J = 16.9, 10.2, 7.7$ Hz, 1H), 5.38 (dt, $J = 17.0, 1.0$ Hz, 1H), 5.25 (dt, $J = 10.2, 0.9$ Hz, 1H), 4.61 (ddt, $J = 7.7, 2.1, 1.0$ Hz, 1H), 4.26 (ddd, $J = 8.1, 5.8, 2.5$ Hz, 1H), 4.13 (dd, $J = 7.0, 2.5$ Hz, 1H), 4.10 (dd, $J = 7.0, 2.2$ Hz, 1H), 1.98 – 1.82 (m, 2H), 1.52 – 1.44 (m, 1H), 1.44 – 1.37 (m, 1H), 1.37 – 1.23 (m, 6H), 0.94 (s, 9H), 0.92 – 0.86 (m, 3H), 0.19 (d, $J = 0.4$ Hz, 3H), 0.11 (d, $J = 0.4$ Hz, 3H); $^{13}\text{C NMR}$ (151 MHz, CDCl_3) δ 135.8, 118.5, 78.0, 68.1, 63.8, 62.4, 36.8, 31.7, 28.8, 26.3, 26.3, 22.7, 18.8, 14.2, -3.0, -3.3; **HRMS** (EI) exact mass for $\text{C}_{14}\text{H}_{26}\text{Cl}_3\text{OSi} [\text{M}-\text{C}_4\text{H}_9]^+$, calculated 343.0813, found 343.0813; **IR** (thin film, cm^{-1}) ν 2957, 2929, 2858, 1472, 1464, 1362, 1256, 1134, 991, 929, 861, 838, 805, 778, 707; $[\alpha]_{\text{D}}^{23\text{ }^\circ\text{C}} = +30.0$ ($c = 0.50, \text{CHCl}_3$).



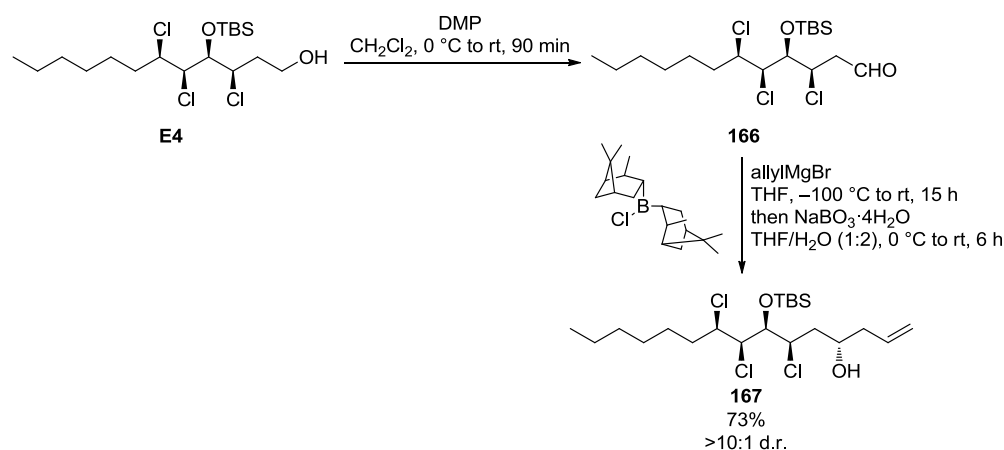
(3*R*,4*S*,5*R*,6*R*)-4-((*tert*-butyldimethylsilyl)oxy)-3,5,6-trichlorododecan-1-ol

(E4): Dicyclohexylborane (111 mg, 0.621 mmol, 2.40 equiv) was suspended in THF (1.5 mL) and cooled to 0 °C. To the suspension was added olefin **152** (104 mg, 0.259 mmol, 1.00 equiv) in THF (0.8 mL), rinsing with THF (2x 0.1 mL). The reaction was allowed to warm to 25 °C during 15 hours. Subsequently it was cooled to 0 °C and water (2.2 mL) was added, followed by $\text{NaBO}_3 \cdot 4\text{H}_2\text{O}$ (1.19 g, 7.76 mmol,

Experimental

30.0 equiv). Cooling was removed and the reaction was stirred for 4 hours before being separated between water and EtOAc. Phases were separated and the aqueous phase was extracted with EtOAc twice. Combined organic phases were washed with brine, dried over Na₂SO₄, filtered, and concentrated. Flash column chromatography (hexanes/Et₂O 5:1, SiO₂) gave alcohol **E4** as colorless oil (92.0 mg, 0.219 mmol, 85%).

¹H NMR (400 MHz, CDCl₃) δ 4.39 (ddd, *J* = 10.0, 3.5, 1.7 Hz, 1H), 4.26 (ddd, *J* = 8.0, 5.9, 2.1 Hz, 1H), 4.21 (dd, *J* = 7.2, 2.1 Hz, 1H), 4.06 (dd, *J* = 7.1, 1.7 Hz, 1H), 3.86 (ddd, *J* = 7.9, 5.2, 3.8 Hz, 2H), 2.08 (ddt, *J* = 14.5, 10.2, 4.4 Hz, 1H), 2.03 – 1.95 (m, 1H), 1.90 (dddd, *J* = 17.6, 9.3, 6.9, 4.4 Hz, 2H), 1.43 (t, *J* = 5.1 Hz, 1H), 1.53 – 1.21 (m, 8H), 0.94 (s, 9H), 0.91 – 0.85 (m, 3H), 0.22 (s, 3H), 0.14 (s, 3H); **¹³C NMR (101 MHz, CDCl₃)** δ 77.9, 68.2, 62.3, 59.9, 59.5, 38.4, 37.0, 31.7, 28.8, 26.4, 26.3, 22.7, 18.8, 14.2, -3.0, -3.3; **HRMS (ESI)** exact mass for C₁₈H₃₇Cl₃NaO₂Si [M+Na]⁺, calculated 441.1521, found 441.1521; **IR (thin film, cm⁻¹)** ν 3326, 2956, 2929, 2858, 1472, 1254, 1125, 1055, 835, 778, 685, 617; **[α]_D²³** = +27.8 (*c* = 1.0, CHCl₃).



(4*S*,6*R*,7*S*,8*R*,9*R*)-7-((*tert*-butyldimethylsilyl)oxy)-6,8,9-trichloropentadec-1-en-4-ol (167): To a solution of alcohol **E4** (92.0 mg, 0.219 mmol, 1.00 equiv) in CH₂Cl₂ (2.2 mL) at 0 °C was added Dess–Martin Periodinane (112 mg, 0.263 mmol, 1.20 equiv). Cooling was removed after 15 minutes and the reaction was stirred for another 75 minutes. Sat. aq. Na₂S₂O₃ was added, followed by sat. aq. NaHCO₃. The aqueous phase was extracted with Et₂O three times. Combined organic phases were

washed with sat. aq. NaHCO₃ and brine, dried over Na₂SO₄, filtered, and concentrated. Crude aldehyde **166** was used as is.

Crude analysis of aldehyde **166**:

¹H NMR (300 MHz, CDCl₃) δ 9.78 (d, *J* = 2.1 Hz, 1H), 4.63 (ddd, *J* = 9.3, 4.0, 2.1 Hz, 1H), 4.29 – 4.22 (m, 1H), 4.20 (dd, *J* = 6.8, 2.2 Hz, 1H), 4.12 (dd, *J* = 6.7, 2.0 Hz, 1H), 3.11 (ddd, *J* = 17.9, 9.3, 1.6 Hz, 1H), 2.97 – 2.81 (m, 1H), 1.90 (ddd, *J* = 10.5, 6.1, 2.0 Hz, 2H), 1.49 – 1.19 (m, 8H), 0.95 (s, 9H), 0.89 (td, *J* = 6.8, 6.2, 3.1 Hz, 3H), 0.22 (s, 3H), 0.14 (s, 3H).

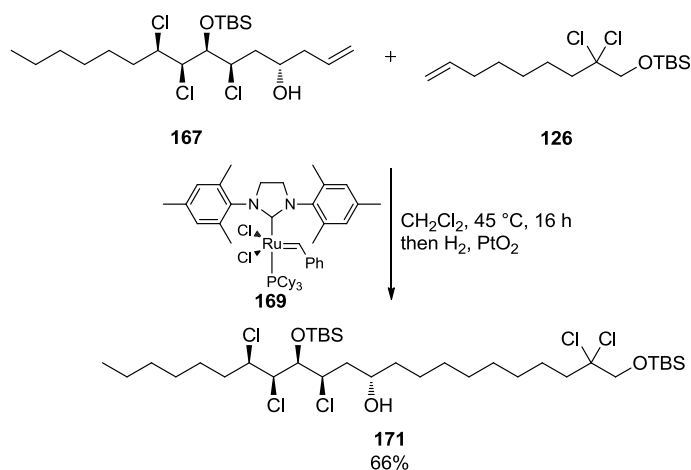
To a solution of (–)-DIP-Chloride (140 mg, 0.438 mmol, 2.00 equiv) in THF (3.7 mL) at –78 °C was added allylmagnesium bromide (1.0 M in Et₂O, 0.33 mL, 0.33 mmol, 1.5 equiv) dropwise. After stirring 1 hour at –78 °C and 30 minutes without cooling, the reaction was cooled to –100 °C. Crude aldehyde **166** in THF (0.7 mL) was added slowly, rinsing with THF (2x 0.1 mL). The reaction was allowed to warm to 24 °C for 15 hours, before being cooled to 0 °C. Water (8 mL) and NaBO₃·4H₂O (1.01 g, 6.57 mmol, 30.0 equiv) was added and the reaction was stirred at 0 °C for 1 hour. After another 5 hours without cooling, the reaction was filtered into water, rinsing with EtOAc. Phases were separated and the aqueous phase was extracted with EtOAc twice. Combined organic phases were washed with brine, dried over Na₂SO₄, filtered, and concentrated. Flash column chromatography (hexanes/EtOAc 10:1, SiO₂) gave the homoallylic alcohol **167** as colorless oil (73.8 mg, 0.16 mmol, 73% over both steps) in a diastereomeric ratio of >10:1 (as determined from ¹H NMR of the purified product).

Employing the same reaction conditions on a 5.0 mg scale, gave product **167** in 92% yield.

¹H NMR (400 MHz, CDCl₃) δ 5.81 (dddd, *J* = 16.4, 10.9, 7.8, 6.7 Hz, 1H), 5.19 (s, 1H), 5.17 – 5.11 (m, 1H), 4.49 (dt, *J* = 10.8, 2.0 Hz, 1H), 4.27 (ddd, *J* = 7.9, 6.1, 2.0 Hz, 1H), 4.20 (dd, *J* = 7.3, 2.0 Hz, 1H), 4.03 (dd, *J* = 7.4, 1.6 Hz, 1H), 3.97 (dtt, *J* = 9.5, 4.7, 2.2 Hz, 1H), 2.39 – 2.29 (m, 1H), 2.28 – 2.18 (m, 1H), 2.09 – 1.99 (m, 1H), 1.97 – 1.81 (m, 2H), 1.71 – 1.67 (m, 1H), 1.67 – 1.60 (m, 1H), 1.53 – 1.15 (m, 8H), 0.94 (s, 9H), 0.91 – 0.83 (m, 3H), 0.22 (s, 3H), 0.12 (s, 3H); ¹³C NMR (101 MHz, CDCl₃) δ 134.0, 119.1, 78.4, 68.3, 67.1, 62.1, 60.4, 43.1, 42.6, 37.0, 31.7, 28.8, 26.4, 26.3, 22.7, 18.9, 14.2, –3.0, –3.3; HRMS (EI) exact mass for C₂₁H₄₁Cl₃O₂Si [M-

Experimental

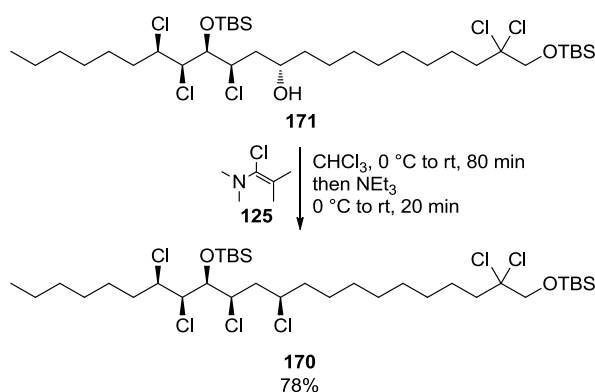
$C_4H_9]^+$, calculated 401.1232, found 401.1232; IR (thin film, cm^{-1}) ν 3362, 2957, 2929, 2858, 1472, 1464, 1255, 1140, 1114, 1071, 995, 919, 836, 778, ; $[\alpha]_D^{23\text{ }^\circ C} = +35.1$ ($c = 0.5$, $CHCl_3$).



(5*S*,6*R*,8*S*)-6,17,17-trichloro-5-((1*R*,2*R*)-1,2-dichlorooctyl)-2,2,3,3,20,20,21,21-octamethyl-4,19-dioxo-3,20-disiladocosan-8-ol (171): Homoallylic alcohol **167** (41.0 mg, 89.0 μ mol, 1.00 equiv) and olefin **126** (87.0 mg, 0.267 mmol, 3.00 equiv) were dissolved in CH_2Cl_2 (4.5 mL, previously spraged with argon for 20 minutes). Grubbs' 2nd Generation Catalyst (**169**, 7.6 mg, 8.9 μ mol, 10 mol%) was added and the reaction was stirred at 45 $^\circ C$ under argon for 16 hours. The mixture was allowed to cool to 24 $^\circ C$ and PtO_2 (2.0 mg, 8.9 μ mol, 10 mol%) was added. The reaction was placed under an atmosphere of hydrogen (5 backfills) and stirred for 6 hours before it was filtered through a plug of silica, eluting with CH_2Cl_2 . Solvent was removed and the residue was purified by flash column chromatography (hexanes/EtOAc 30:1, SiO_2) to give alcohol **171** as colorless oil (44.8 mg, 59.0 μ mol, 66%).

1H NMR (400 MHz, $CDCl_3$) δ 4.48 (dt, $J = 10.7, 2.0$ Hz, 1H), 4.27 (ddd, $J = 7.9, 6.0, 2.1$ Hz, 1H), 4.21 (dd, $J = 7.4, 2.0$ Hz, 1H), 4.02 (dd, $J = 7.3, 1.6$ Hz, 1H), 3.92 (s, 2H), 3.94 – 3.85 (m, 1H), 2.23 – 2.12 (m, 2H), 2.03 (ddd, $J = 13.5, 10.9, 2.2$ Hz, 1H), 1.90 (dddd, $J = 16.3, 14.0, 8.4, 4.3$ Hz, 2H), 1.66 – 1.56 (m, 3H), 1.55 – 1.21 (m, 21H), 0.94 (s, 9H), 0.91 (s, 9H), 0.91 – 0.86 (m, 3H), 0.22 (s, 3H), 0.13 (s, 3H), 0.11 (s, 6H); ^{13}C NMR (101 MHz, $CDCl_3$) δ 93.7, 78.4, 72.3, 68.4, 68.3, 62.2, 60.5, 43.7, 43.5, 38.2, 37.0, 31.7, 29.6, 29.5, 29.4, 29.2, 28.8, 26.4, 26.3, 25.9, 25.7, 24.9,

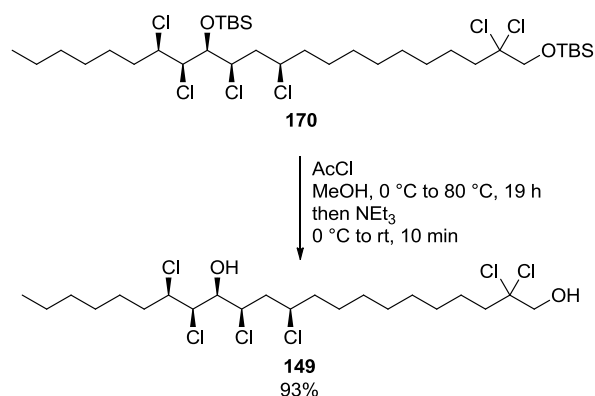
22.7, 18.9, 18.4, 14.2, -3.0, -3.3, -5.2; **HRMS** (ESI) exact mass for $C_{34}H_{70}Cl_5O_3Si_2$ $[M+H]^+$, calculated 757.3301, found 757.3198 (high error presumably due to minimal amounts of residual olefin in the sample); **IR** (**thin film, cm^{-1}**) ν 3353, 2955, 2929, 2857, 1472, 1463, 1255, 1118, 836, 778, 694; $[\alpha]_D^{23\text{ }^\circ C} = +17.8$ ($c = 1.0$, $CHCl_3$).



(5S,6R,8R)-6,8,17,17-tetrachloro-5-((1R,2R)-1,2-dichlorooctyl)-2,2,3,3,20,20,21,21-octamethyl-4,19-dioxo-3,20-disiladocosane (170): To a solution of alcohol **171** (44.5 mg, 59.0 μmol , 1.00 equiv) in $CHCl_3$ (1.2 mL, previously filtered through activated basic alumina) at 0 $^\circ\text{C}$ was added Ghosez' reagent (**125**, 25 μL , 0.18 mmol, 3.0 equiv). Cooling was removed and the reaction was stirred for 75 minutes. After cooling to 0 $^\circ\text{C}$ again, triethylamine (33 μL , 0.23 mmol, 4.0 equiv) were added. Cooling was removed and the reaction was stirred for 20 minutes before celite was added and solvent removed. The solid was applied to a column and purified by repeated column chromatography (hexanes, SiO_2) to give the title compound **170** as colorless oil (35.5 mg, 46.0 μmol , 78%).

$^1\text{H NMR}$ (400 MHz, $CDCl_3$) δ 4.34 (ddd, $J = 7.7, 6.2, 1.5$ Hz, 1H), 4.24 (ddd, $J = 7.8, 6.0, 2.0$ Hz, 1H), 4.15 (dd, $J = 7.2, 2.0$ Hz, 1H), 4.08 (dd, $J = 7.2, 1.5$ Hz, 1H), 4.05 – 3.99 (m, 1H), 3.92 (s, 2H), 2.34 (dt, $J = 14.9, 7.5$ Hz, 1H), 2.29 – 2.20 (m, 1H), 2.20 – 2.12 (m, 2H), 1.99 – 1.83 (m, 2H), 1.76 (m, 1H), 1.72 – 1.65 (m, 1H), 1.65 – 1.55 (m, 3H), 1.52 – 1.19 (m, 17zH), 0.94 (s, 9H), 0.92 (s, 9H), 0.98 – 0.83 (m, 3H), 0.24 (s, 3H), 0.14 (s, 3H), 0.11 (s, 6H); **$^{13}\text{C NMR}$ (101 MHz, $CDCl_3$)** δ 93.6, 77.1, 72.3, 68.3, 62.0, 59.6, 59.5, 44.0, 43.7, 37.3, 37.0, 31.7, 29.5, 29.4, 29.2, 29.1, 28.8, 26.4, 26.3, 26.1, 25.9, 24.9, 22.7, 18.9, 18.4, 14.2, -2.8, -3.5, -5.2; **HRMS** (ESI) exact mass for $C_{34}H_{72}Cl_4NO_2Si_2$ $[M+NH_4]^+$, calculated 792.3227, found 792.3219; **IR** (**thin**

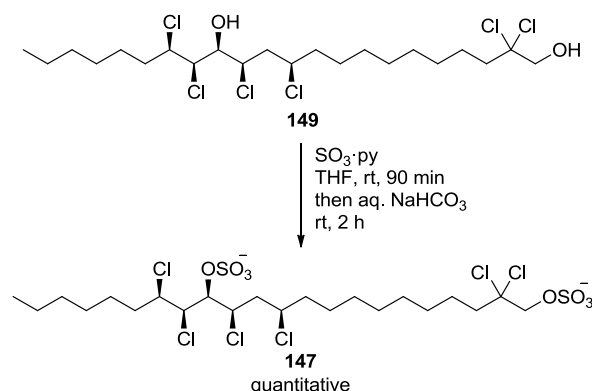
film, cm^{-1}) ν 2954, 2929, 2857, 1463, 1255, 1120, 837, 778, 696; $[\alpha]_{\text{D}}^{23\text{ }^\circ\text{C}} = +13.4$ ($c = 0.5$, CHCl_3).



(11R,13R,14S,15R,16R)-2,2,11,13,15,16-hexachlorodocosane-1,14-diol

(149): To a solution of disilylether **170** (7.9 mg, 10.2 μmol , 1.00 equiv) in MeOH (1.0 mL) at 0 °C was added acetyl chloride (36 μL , 0.51 mmol, 50 equiv) and cooling was removed. The reaction was heated at 80 °C for 19 hours before being cooled back to 0 °C. Triethylamine (71 μL , 0.51 mmol, 50 equiv) was added and cooling was removed. After 10 minutes, celite was added and solvent was removed. The solid was purified by flash column chromatography (hexanes/EtOAc gradient from 10:1 to 5:1, SiO_2) to give diol **149** as colorless oil (5.2 mg, 9.5 μmol , 93%).

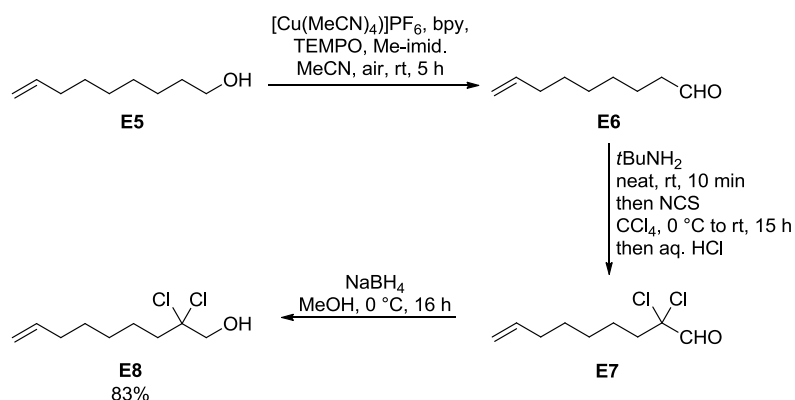
^1H NMR (600 MHz, CDCl_3) δ 4.45 (ddd, $J = 8.5, 6.0, 1.9$ Hz, 1H), 4.29 (dd, $J = 7.8, 2.2$ Hz, 1H), 4.22 (ddd, $J = 8.0, 5.9, 2.1$ Hz, 1H), 4.12 (ddd, $J = 7.5, 4.9, 2.1$ Hz, 1H), 4.02 – 3.97 (m, 1H), 3.90 (d, $J = 7.5$ Hz, 2H), 2.49 (ddd, $J = 14.3, 8.6, 4.2$ Hz, 1H), 2.45 (dd, $J = 5.0, 1.1$ Hz, 1H), 2.32 (t, $J = 7.5$ Hz, 1H), 2.29 (ddd, $J = 14.4, 9.7, 5.9$ Hz, 1H), 2.24 – 2.19 (m, 2H), 2.03 – 1.84 (m, 2H), 1.82 – 1.69 (m, 2H), 1.68 – 1.60 (m, 3H), 1.56 – 1.17 (m, 17H), 0.89 (t, $J = 7.0$ Hz, 3H); **^{13}C NMR (101 MHz, CD_3OD)** δ 91.3, 81.4, 75.5, 66.4, 63.0, 61.2, 59.5, 45.1, 45.0, 39.0, 37.4, 32.8, 30.4, 30.4, 30.0, 30.0, 29.7, 27.3, 27.0, 25.8, 23.6, 14.4; **HRMS** (ESI) exact mass for $\text{C}_{22}\text{H}_{44}\text{Cl}_6\text{NO}_2$ $[\text{M}+\text{NH}_4]^+$, calculated 564.1498, found 564.1497; **IR (thin film, cm^{-1})** ν 3409, 2928, 2856, 1465, 1378, 1278, 1073, 707, 603; $[\alpha]_{\text{D}}^{21\text{ }^\circ\text{C}} = +2.8$ ($c = 0.25$, CHCl_3).



(11R,13R,14S,15R,16R)-2,2,11,13,15,16-hexachlorodocosane-1,14-diyl

bis(sulfate) disulfate salt (147): Diol **149** (9.1 mg, 17 μmol , 1.0 equiv) was dissolved in THF and $\text{SO}_3 \cdot \text{pyridine}$ complex (10.8 mg, 68.0 μmol , 4.1 equiv) was added. After 90 minutes of stirring $\text{SO}_3 \cdot \text{pyridine}$ complex (5.4 mg, 34 μmol , 2.0 equiv) was added. After another 15 minutes, sat. aq. NaHCO_3 was added and the suspension stirred for 2 hours. The mixture was filtered through a silica plug, eluting with $\text{CH}_2\text{Cl}_2/\text{MeOH}$ 3:1. The residue was concentrated and applied to a column. Flash column chromatography ($\text{CH}_2\text{Cl}_2/\text{MeOH}$ gradient from 8:1 to 6:1, SiO_2) gave the title compound as white solid (12.7 mg, 18 μmol , quantitative).

$^1\text{H NMR}$ (400 MHz, CD_3OD) δ 4.96 (dd, $J = 7.3, 1.9$ Hz, 1H), 4.65 (ddd, $J = 8.8, 5.5, 1.9$ Hz, 1H), 4.42 (dd, $J = 7.3, 2.6$ Hz, 1H), 4.35 (dd, $J = 7.5, 2.5$ Hz, 1H), 4.32 (s, 2H), 4.23 (dtd, $J = 10.5, 6.3, 5.2, 2.5$ Hz, 1H), 2.84 – 2.72 (m, 1H), 2.30 – 2.22 (m, 2H), 2.23 – 2.12 (m, 1H), 2.01 – 1.94 (m, 2H), 1.83 (ddt, $J = 9.6, 6.1, 3.7$ Hz, 1H), 1.66 (m, 3H), 1.60 – 1.20 (m, 18H), 0.92 (t, $J = 6.7$ Hz, 3H); $^{13}\text{C NMR}$ (101 MHz, CD_3OD) δ 91.3, 81.3, 75.5, 66.4, 63.0, 61.2, 59.5, 45.1, 45.0, 39.0, 37.4, 32.8, 30.4, 30.4, 30.1, 30.0, 29.7, 27.3, 27.0, 25.8, 23.6, 14.4; **HRMS** (ESI) exact mass for $\text{C}_{22}\text{H}_{42}\text{Cl}_6\text{NNa}_2\text{O}_8\text{S}_2$ $[\text{M}+\text{NH}_4]^+$, calculated 724.0634, found 724.0635; **IR** (thin film, cm^{-1}) ν 3439, 2928, 2857, 1625, 1459, 1227, 1083, 1004, 836, 709; $[\alpha]_{\text{D}}^{22\text{ }^\circ\text{C}} = +8.0$ ($c = 1.0$, MeOH).



2,2-dichloronon-8-en-1-ol (E8): Procedure from *Angew. Chem. Int. Ed.* **2016**, *55* (2), 639-643 was followed.

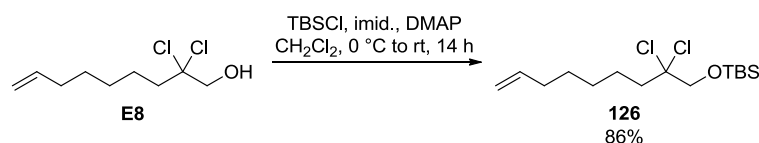
To a stirred solution of non-8-en-1-ol (**E5**, 0.50 g, 3.52 mmol, 1.0 eq.) in MeCN (3.5 mL) open to air were added the following solutions in this order: (1) tetrakis(acetonitrile)copper (I) tetrafluoroborate (0.111 g, 0.352 mmol, 10.0 mol%) in MeCN (3.5 mL), (2) 2,2'-bipyridine (0.055 g, 0.35 mmol, 10 mol%) in MeCN (3.5 mL), (3) TEMPO (0.055 g, 0.35 mmol, 10 mol%) in MeCN (3.5 mL), and (4) 1-methylimidazole (28 μL , 0.35 mmol, 10 mol%). The dark brown solution was allowed to stir for 5 hours. The reaction was then diluted with H₂O and pentane. Phases were separated and the aqueous phase was extracted twice with pentane. Combined organic phases were washed with brine, dried over Na₂SO₄, filtered, and concentrated. Crude aldehyde **E6** was used as is in the next reaction.

To crude aldehyde **E6** was added *tert*-butylamine (0.391 mL, 3.69 mmol, 1.05 eq.) and this mixture was stirred for 10 minutes. The mixture was then diluted with CH₂Cl₂ and dried over Na₂SO₄, filtered, and concentrated. The crude imine was dissolved in CCl₄ (3.5 mL) and the stirred solution was cooled to 0 °C. A reflux condenser was attached and the fume hood light was turned off. *N*-chlorosuccinimide (0.986 g, 7.38 mmol, 2.10 eq.) was added portionwise (5 portions) during 10 minutes. After 1 hour the cold bath was removed and the reaction was allowed to stir in the dark for 14 hours. The reaction was diluted with hexanes and filtered through a celite pad, rinsing with hexane. The filtrate was concentrated. To this mixture was added H₂O (3.5 mL), followed by conc. aq. HCl (1.8 mL). After 4 hours the reaction was diluted with H₂O and extracted three times with CH₂Cl₂. Combined organic phases

were dried over Na_2SO_4 , filtered, and concentrated. The crude dichloroaldehyde **E7** was used as is in the next reaction.

A stirred solution of crude aldehyde **E7** in MeOH (35 mL) was cooled to 0 °C. Sodium borohydride (0.666 g, 17.6 mmol, 5.00 eq.) was added carefully. The reaction was stirred at 0 °C for 14h and subsequently diluted with Et_2O . The mixture was poured into brine and phases were separated. The aqueous phase was extracted twice with Et_2O . Combined organic phases were dried over Na_2SO_4 , filtered, and concentrated. Flash column chromatography (hexanes/ EtOAc 8:1, SiO_2) gave alcohol **E8** as colorless liquid (607 mg, 2.88 mmol, 82% over 3 steps).

$^1\text{H NMR}$ (400 MHz, CDCl_3) δ 5.81 (ddt, $J = 16.9, 10.1, 6.7$ Hz, 1H), 5.01 (dq, $J = 17.1, 1.7$ Hz, 1H), 4.95 (ddt, $J = 10.3, 2.5, 1.3$ Hz, 1H), 3.90 (d, $J = 7.5$ Hz, 2H), 2.30 (td, $J = 7.5, 1.6$ Hz, 1H), 2.26 – 2.17 (m, 2H), 2.13 – 2.01 (m, 2H), 1.71 – 1.60 (m, 2H), 1.50 – 1.33 (m, 4H); $^{13}\text{C NMR}$ (101 MHz, CDCl_3) δ 138.9, 114.7, 94.8, 72.3, 43.7, 33.7, 28.7, 28.6, 24.8.¹¹⁸



tert-butyl((2,2-dichloronon-8-en-1-yl)oxy)dimethylsilane (126): Procedure from *Angew. Chem. Int. Ed.* **2016**, 55 (2), 639-643 was followed.

To a solution of alcohol **E8** (0.600 g, 2.84 mmol, 1.00 equiv) in CH_2Cl_2 at 0 °C were added TBSCl (0.642 g, 4.26 mmol, 1.50 equiv), imidazole (0.580 g, 8.53 mmol, 3.00 equiv), and 4-dimethylaminopyridine (35 mg, 0.28 mmol, 0.1 equiv) sequentially. The reaction was allowed to warm to 24 °C during 14 hours. H_2O was added and the mixture was poured into sat. aq. NH_4Cl . The aqueous phase was extracted three times with CH_2Cl_2 . Combined organic phases were dried over Na_2SO_4 , filtered, and concentrated. Flash column chromatography (hexanes, SiO_2) gave the title compound as colorless liquid (0.795 g, 2.44 mmol, 86%).

$^1\text{H NMR}$ (400 MHz, CDCl_3) δ 5.83 (ddt, $J = 16.9, 10.2, 6.7$ Hz, 1H), 5.03 (dq, $J = 17.1, 1.7$ Hz, 1H), 4.97 (ddt, $J = 10.2, 2.3, 1.2$ Hz, 1H), 3.95 (s, 2H), 2.25 – 2.17 (m, 2H), 2.09 (tdd, $J = 8.2, 6.1, 1.5$ Hz, 2H), 1.70 – 1.57 (m, 2H), 1.52 – 1.34 (m, 4H),

Experimental

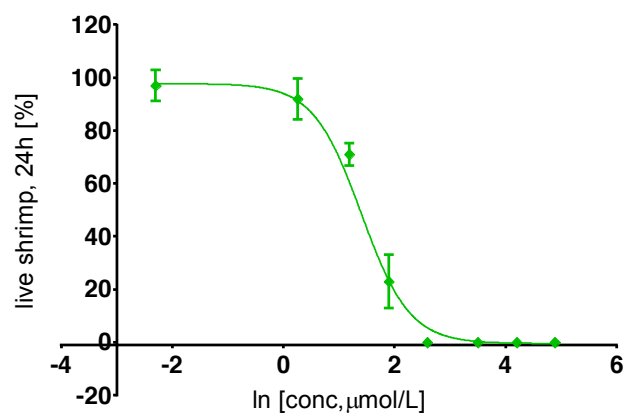
0.94 (s, 9H), 0.14 (s, 6H); ^{13}C NMR (101 MHz, CDCl_3) δ 139.0, 114.6, 93.6, 72.3, 43.6, 33.7, 28.8, 28.7, 25.9, 24.8, 18.4, -5.2.¹¹⁸

Brine shrimp toxicity

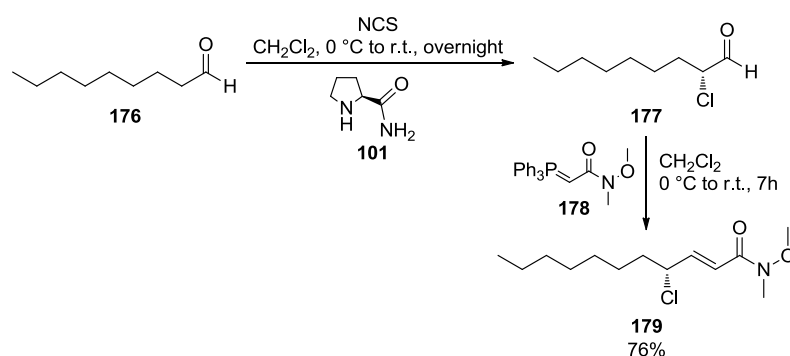
Blanks						
well	live shrimps (t = 0)	live shrimps (t = 24 h)	alive	average [%]	conditions	s.d.
A1	12	12	100%			
A2	13	13	100%	100%	20 μL DMSO	0.0%
A3	12	12	100%			
A4	11	10	91%			
A5	13	12	92%	90%	blank	7.7%
A6	16	13	81%			
A3*	13	13	100%			

* = data from another well

11,15-di- <i>epi</i> -Danicalipin A							
well	live shrimps (t = 0)	live shrimps (t = 24 h)	alive	average [%]	final concentration of 3 per well [μ M]	s.d.	
A1	14	0	0%	0%	133.0	0.0%	
A2	14	0	0%	0%			
A4	11	0	0%		66.5	0.0%	
A5	12	0	0%	0%			
A6	11	0	0%				
B1	12	0	0%		33.0	0.0%	
B2	11	0	0%	0%			
B3	15	0	0%				
B4	15	0	0%		13.3	0.0%	
B5	14	0	0%	0%			
B6	15	0	0%				
C1	9	3	33%		6.7	10.0%	
C2	15	2	13%	23%			
C3	13	3	23%				
C4	10	7	70%		3.3	4.2%	
C5	12	8	67%	71%			
C6	12	9	75%				
D1	9	9	100%		1.3	7.7%	
D2	13	12	92%	92%			
D3	13	11	85%				
D4	10	9	90%		0.1	5.8%	
D5	10	10	100%	97%			
D6	13	13	100%				



12 Experimental Details for Part III

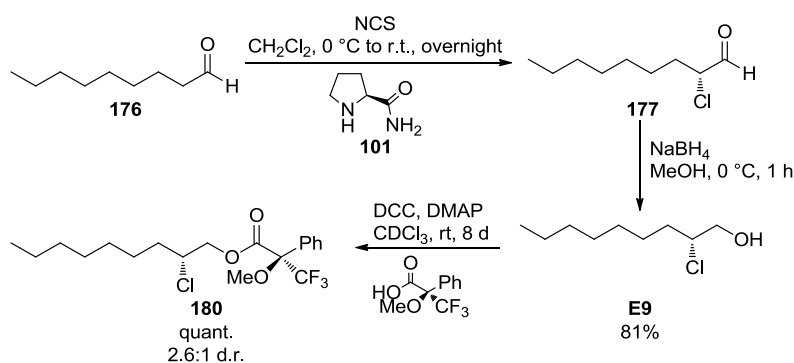


(*R,E*)-4-chloro-*N*-methoxy-*N*-methylundec-2-enamide (179**):** To a solution of nonanal (**176**, 0.61 mL, 3.52 mmol, 1.00 equiv) in CH_2Cl_2 (7.0 mL) at $0\text{ }^\circ\text{C}$ were added L-prolinamide (**101**, 40.0 mg, 0.352 mmol, 10.0 mol%) and *N*-chlorosuccinimide (0.61 g, 4.52 mmol, 1.30 equiv). After stirring for 24 hours, pentane was added to the reaction and the precipitate filtered off. After concentration *in vacuo*, the residue was taken up into pentane again and the filtration repeated. After concentration *in vacuo*, aldehyde **177** was obtained as pale yellow liquid, and used crude for the next reaction.

Analysis of crude aldehyde **177**: $^1\text{H NMR}$ (400 MHz, CDCl_3) δ 9.49 (d, $J = 2.5$ Hz, 1H), 4.15 (ddd, $J = 8.1, 5.5, 2.5$ Hz, 1H), 1.98 (ddt, $J = 14.2, 9.9, 5.7$ Hz, 1H), 1.91 – 1.70 (m, 1H), 1.57 – 1.38 (m, 1H), 1.37 – 1.20 (m, 9H), 0.92 – 0.84 (m, 3H).

Crude aldehyde **177** was dissolved in CH_2Cl_2 (35 mL) and cooled to $0\text{ }^\circ\text{C}$. *N*-methoxy-*N*-methyl-2-(triphenylphosphoranylidene)acetamide (**178**, 1.28 g, 3.52 mmol, 1.00 equiv) was added and cooling was removed. After stirring for 7 hours, celite was added to the reaction mixture and solvent was removed *in vacuo*. The solid was then subjected to flash column chromatography (hexanes/EtOAc 2:1, SiO_2) to give Weinreb amide **179** as clear liquid (0.70 g, 2.68 mmol, 76%).

$^1\text{H NMR}$ (400 MHz, CDCl_3) δ 6.92 (dd, $J = 15.1, 7.7$ Hz, 1H), 6.60 (dd, $J = 15.2, 1.1$ Hz, 1H), 4.53 (dtd, $J = 7.8, 6.8, 1.1$ Hz, 1H), 3.71 (s, 3H), 3.25 (s, 3H), 1.92 – 1.79 (m, 2H), 1.54 – 1.38 (m, 2H), 1.36 – 1.16 (m, 8H), 0.92 – 0.83 (m, 3H); $^{13}\text{C NMR}$ (101 MHz, CDCl_3) δ 166.0, 145.2, 120.0, 62.0, 60.8, 38.1, 32.5, 31.9, 29.2, 29.1, 26.4, 22.7, 14.2; **HRMS** (ESI) exact mass for $\text{C}_{13}\text{H}_{25}\text{ClNO}_2$ $[\text{M}+\text{H}]^+$, calculated 262.1568, found 262.1569; **IR** (thin film, cm^{-1}) ν 2929, 2857, 1668, 1633, 1463, 1416, 1382, 1178, 1000, 979, 737; $[\alpha]_{\text{D}}^{23\text{ }^\circ\text{C}} = -19.1$ ($c = 1.0, \text{CHCl}_3$).



(R)-2-chlorononan-1-ol (E9): Crude **177** was prepared as mentioned before.

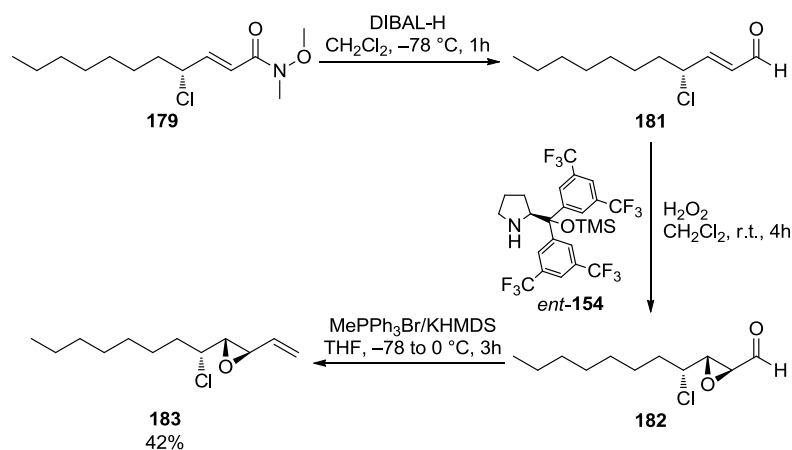
Crude aldehyde (**177**) (73. mg, 0.413 mmol, 1.00 equiv) was dissolved in MeOH (4.1 mL) and cooled to 0 °C. Sodium borohydride (23.5 mg, 0.620 mmol, 1.50 equiv) was added and the reaction was stirred at 0 °C for 1 hour. Water and sat. aq. NaHCO_3 was added and the mixture was extracted three times with EtOAc. Combined organic phases were washed with brine, dried over Na_2SO_4 , filtered, and concentrated. Flash column chromatography (hexanes/EtOAc 5:1, SiO_2) gave alcohol **E9** as colorless oil (60.0 mg, 0.336 mmol, 81% over 2 steps).

$^1\text{H NMR}$ (400 MHz, CDCl_3) δ 4.10 – 3.97 (m, 1H), 3.79 (ddd, $J = 11.8, 8.0, 3.7$ Hz, 1H), 3.66 (ddd, $J = 12.1, 7.1, 5.3$ Hz, 1H), 2.02 (ddt, $J = 8.0, 5.0, 2.3$ Hz, 1H), 1.86 – 1.64 (m, 2H), 1.59 – 1.47 (m, 1H), 1.41 (mz, 1H), 1.29 (m, 8H), 0.92 – 0.84 (m, 3H); $^{13}\text{C NMR}$ (101 MHz, CDCl_3) δ 67.2, 65.6, 34.4, 31.9, 29.2, 29.2, 26.5, 22.8, 14.2; **HRMS** (EI) exact mass for $\text{C}_9\text{H}_{18}\text{Cl}$ $[\text{M}-\text{OH}]^+$, calculated 161.1097, found 161.1093; **IR** (thin film, cm^{-1}) ν 3359, 2926, 2857, 1465, 1379, 1081, 1039, 724, 682, 617; $[\alpha]_{\text{D}}^{21\text{ }^\circ\text{C}} = +7.1$ ($c = 1.0, \text{CHCl}_3$).

(*R,R*)-2-chlorononyl-3,3,3-trifluoro-2-methoxy-2-phenylpropanoate (180):

Alcohol **E9** (3.9 mg, 22 μ mol, 1.00 equiv) was taken up in CHCl_3 (0.5 mL) and (*R*)-Mosher-acid (15.8 mg, 0.086 mmol, 3.10 equiv), DCC (14.0 mg, 0.068 mmol, 3.10 equiv), and DMAP (8.3 mg, 0.086 mmol, 3.10 equiv) were added. After stirring for 30 minutes, the reaction was filtered and concentrated. Flash column chromatography (pentane/ Et_2O 30:1, SiO_2) gave product **180** in 2.6:1 d.r. as colorless oil (9.0 mg, 22 μ mol, quantitative).

Only Peaks corresponding to major compound reported: $^1\text{H NMR}$ (400 MHz, CDCl_3) δ 7.61 – 7.49 (m, 2H), 7.48 – 7.33 (m, 3H), 4.56 – 4.35 (m, 2H), 4.15 – 4.01 (m, 1H), 3.58 (p, $J = 1.2$ Hz, 3H), 1.81 – 1.61 (m, 2H), 1.60 – 1.46 (m, 1H), 1.39 (m, 1H), 1.33 – 1.17 (m, 8kH), 0.94 – 0.76 (m, 3H); $^{19}\text{F NMR}$ (377 MHz, CDCl_3) δ -71.7; $^{13}\text{C NMR}$ (101 MHz, CDCl_3) δ 166.4, 132.1, 129.9, 128.6, 127.5, 69.3, 58.5, 55.8, 34.6, 31.8, 29.2, 29.1, 26.0, 22.8, 14.2; **HRMS** (ESI) exact mass for $\text{C}_{19}\text{H}_{26}\text{ClF}_3\text{NaO}_3$ $[\text{M}+\text{Na}]^+$, calculated 417.1415, found 417.1416; **IR** (thin film, cm^{-1}) ν 2929, 2856, 2119, 1754, 1452, 1241, 1170, 1123, 1081, 1024, 765, 720, 697; $[\alpha]_{\text{D}}^{21\text{ }^\circ\text{C}} = +41.7$ ($c = 0.5$, CHCl_3).



(*2S,3R*)-2-((*R*)-1-chlorooctyl)-3-vinyloxirane (183): To a solution of Weinreb amide **179** (0.69 g, 2.64 mmol, 1.00 equiv) in CH_2Cl_2 (26.4 mL) at -78 $^\circ\text{C}$ was added DIBAL-H (1.0 M in CH_2Cl_2 , 3.4 mL, 3.4 mmol, 1.3 equiv) dropwise. After stirring for 1 hour, MeOH (ca. 1 mL) was added dropwise, followed by sat. aq. Rochelle's salt (ca. 75 mL). Cooling was removed and the mixture was stirred until a clear organic phase had formed. The reaction was then pouted into water and extracted three times with

CH₂Cl₂. Combined organic phases were dried over Na₂SO₄, filtered, and concentrated *in vacuo*. Crude enal **181** was directly used in the next reaction.

Analysis of crude enal **181**: ¹H NMR (300 MHz, CDCl₃) δ 9.60 (d, *J* = 7.6 Hz, 1H), 6.75 (dd, *J* = 15.5, 7.6 Hz, 1H), 6.24 (ddd, *J* = 15.6, 7.7, 1.1 Hz, 1H), 4.54 (q, *J* = 7.5, 7.0 Hz, 1H), 1.95 – 1.83 (m, 2H), 1.70 – 1.18 (m, 10H), 0.93 – 0.83 (m, 3H).

Crude aldehyde **181** was dissolved in CH₂Cl₂ (35 mL) and Jørgensen-Hayashi catalyst (*ent*-**154**, 158 mg, 0.264 mmol, 10.0 mol%) was added, followed by addition of H₂O₂ (30% in water, 0.55 mL, 5.4 mmol, 2.0 equiv). After stirring for 4 hours, the reaction was directly subjected to flash column chromatography (hexanes/EtOAc 3:1, SiO₂) to give epoxyaldehyde **182**. The epoxyaldehyde was used crude in the following reaction.

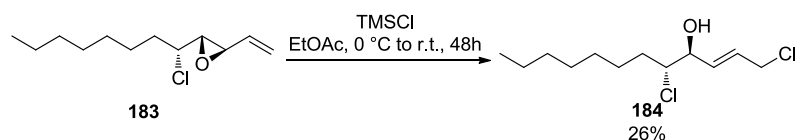
Analysis of crude epoxyaldehyde **182**: ¹H NMR (300 MHz, CDCl₃) δ 9.23 (d, *J* = 5.9 Hz, 1H), 4.27 (q, *J* = 7.1 Hz, 1H), 3.74 (ddd, *J* = 8.8, 7.3, 4.8 Hz, 1H), 3.60 – 3.47 (m, 1H), 2.16 – 1.89 (m, 2H), 1.53 – 1.37 (m, 10H), 1.10 – 0.96 (m, 3H).

In a separate flask, methyltriphenylphosphonium bromide (1.23 g, 3.43 mmol, 1.30 equiv) was suspended in THF (21 mL). After cooling to –78 °C, KHMDS (0.5 M in toluene, 5.3 mL, 2.6 mmol, 1.0 equiv) was added dropwise. The yellow suspension was placed in an ice bath after 5 minutes and stirred for 20 minutes. After cooling back down to –78 °C, the solution of epoxyaldehyde crude **182** in THF (14 mL) was added dropwise to the reaction (the flask was rinsed with 1 mL THF twice). The dark yellow suspension was then placed in an ice bath after 5 minutes and stirred for 2.5 hours. The reaction was then quenched through the addition of sat. aq. NH₄Cl and separated between water and EtOAc. Phases were separated and the aqueous phase extracted three times with pentane. Combined organic layers were washed with water and brine, dried over Na₂SO₄, filtered, and concentrated. Flash column chromatography (hexanes/EtOAc gradient 70:1 to 50:1, SiO₂) gave olefin **183** as colorless oil (0.24 g, 1.1 mmol, 42%).

¹H NMR (400 MHz, CDCl₃) δ 5.60 (ddd, *J* = 17.0, 9.9, 7.0 Hz, 1H), 5.51 (dd, *J* = 17.2, 1.8 Hz, 1H), 5.36 – 5.28 (m, 1H), 3.53 (ddd, *J* = 8.7, 7.6, 4.4 Hz, 1H), 3.32 (dd, *J* = 6.9, 2.0 Hz, 1H), 3.01 (dd, *J* = 7.7, 2.0 Hz, 1H), 1.95 (dddd, *J* = 14.5, 10.3, 5.8, 4.4 Hz, 1H), 1.79 (dddd, *J* = 14.0, 10.2, 8.7, 4.8 Hz, 1H), 1.64 – 1.51 (m, 1H), 1.52 – 1.40 (m, 1H), 1.38 – 1.20 (m, 8H), 0.93 – 0.84 (m, 3H); ¹³C NMR (101 MHz,

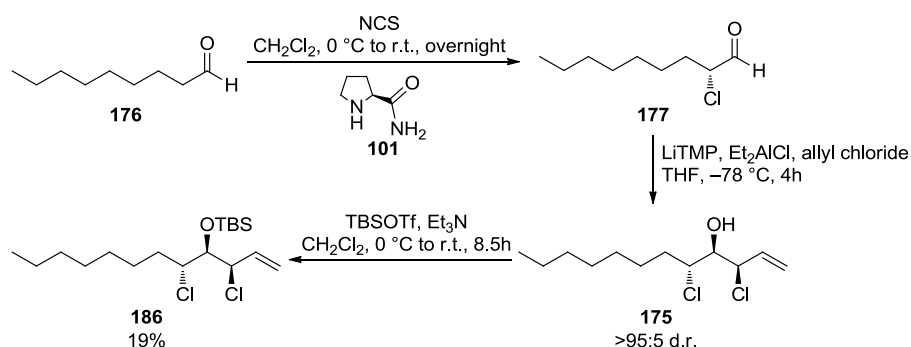
Experimental

CDCl₃) δ 134.3, 120.3, 62.5, 61.8, 58.9, 35.9, 31.9, 29.2, 29.2, 26.0, 22.8, 14.2.;
HRMS (EI) exact mass for C₁₂H₂₁O [M-Cl]⁺, calculated 181.1587, found 181.1587;
IR (thin film, cm⁻¹) ν 2956, 2928, 2857, 1461, 984, 926, 889, 796, 724, 690; [α]_D^{22 °C}
= +1.5 (c = 1.0, CHCl₃).



(4S,5R,E)-1,5-dichlorododec-2-en-4-ol (X7): Epoxide **183** (73.0 mg, 0.337 mmol, 1.00 equiv) was dissolved in EtOAc (11 mL) and cooled to 0 °C. Trimethylsilylchloride (85 μ L, 0.67 mmol, 2.0 equiv) in CH₂Cl₂ (0.22 mL) was added dropwise. The reaction was stirred at 0 °C for 20 hours before being warmed to room temperature. After stirring at room temperature for a further 28 hours, the reaction was quenched with pH 7 buffer and extracted three times with CH₂Cl₂. Combined organic phases were dried over Na₂SO₄, filtered, and concentrated *in vacuo*. Crude ¹H NMR analysis showed approximately 30% conversion. Flash column chromatography (hexanes/EtOAc gradient 9:1 to 7:1, SiO₂) gave the title compound (22.2 mg, 0.088 mmol, 26%), along with both S_N2 products (<5%).

¹H NMR (400 MHz, CDCl₃) δ 5.89 (dtd, J = 11.0, 7.9, 1.2 Hz, 1H), 5.73 (dd, J = 11.0, 8.2 Hz, 1H), 4.56 (dddd, J = 7.9, 6.5, 4.0, 1.2 Hz, 1H), 4.16 (dd, J = 7.8, 1.0 Hz, 2H), 4.05 (dt, J = 9.8, 4.0 Hz, 1H), 2.18 (d, J = 6.5 Hz, 1H), 1.80 – 1.63 (m, 2H), 1.63 – 1.53 (m, 1H), 1.45 – 1.16 (m, 9H), 0.95 – 0.80 (m, 3H).; **¹³C NMR (101 MHz, CDCl₃)** δ 131.6, 130.1, 70.3, 67.9, 39.3, 33.3, 31.9, 29.2, 29.1, 26.7, 22.8, 14.2.;
HRMS (EI) exact mass for C₁₂H₂₂ClO [M-Cl]⁺, calculated 217.1354, found 217.1354;
IR (thin film, cm⁻¹) ν 3394, 2955, 2926, 2857, 1457, 1379, 1254, 1028, 783, 724, 618; [α]_D^{21 °C} = +4.7 (c = 1.0, CHCl₃).



tert-butyl(((3R,4R,5R)-3,5-dichlorododec-1-en-4-yl)oxy)dimethylsilane

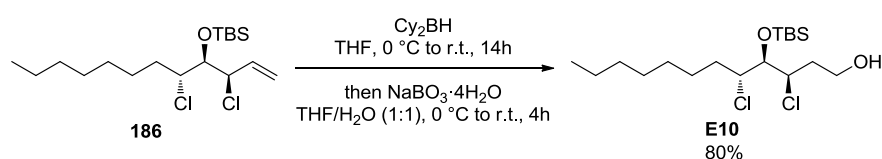
(186): Crude aldehyde **177** was prepared as before.

To a solution of 2,2,6,6-tetramethylpiperidine (0.634 mL, 3.74 mmol, 2.20 equiv) in THF (7.6 mL) at $-78\text{ }^\circ\text{C}$ was added butyl lithium (1.6 M in hexanes, 2.16 mL, 3.57 mmol, 2.10 equiv) dropwise. After 30 minutes, the solution was transferred to another flask, containing allyl chloride (0.291 mL, 3.57 mmol, 2.10 equiv) and diethylaluminum chloride (1.0 M in hexanes, 6.79 mL, 6.79 mmol, 4.0 equiv) in THF (15.2 mL) at $-78\text{ }^\circ\text{C}$, via canula transfer. After another 30 minutes, crude aldehyde **177** (theoretical: 0.3 g, 1.70 mmol, 1.00 equiv) in THF (1.5 mL) was added dropwise. After stirring for 4 hours at $-78\text{ }^\circ\text{C}$, sat. aq. NH_4Cl and sat. aq. Rochelle's salt were added and the reaction was allowed to warm to room temperature. The reaction was stirred vigorously until two clear phases formed (ca. 1h), before being extracted with Et_2O three times. Combined organic phases were dried over Na_2SO_4 , filtered, and concentrated. Flash column chromatography (hexanes/ EtOAc 20:1, SiO_2) gave product **175** and starting material **177** as an inseparable mixture (177 mg, 3:1 mixture).

The crude material was dissolved in CH_2Cl_2 and cooled to $0\text{ }^\circ\text{C}$. Et_3N (195 μL , 1.34 mmol, 0.79 equiv) and TBSOTf (241 μL , 1.05 mmol, 0.62 equiv) were added and the reaction was stirred for 30 minutes before cooling was removed. After another 4 hours, the reaction was quenched through the addition of water and extracted with CH_2Cl_2 three times. Combined organic phases were dried over Na_2SO_4 , filtered, and concentrated. Flash column chromatography (hexanes, SiO_2) gave the title compound **186** as colorless oil (117 mg, 0.319 mmol, 19% over 3 steps).

$^1\text{H NMR}$ (400 MHz, CDCl_3) δ 5.94 (ddd, $J = 17.0, 10.2, 8.5$ Hz, 1H), 5.34 (dt, $J = 17.0, 1.1$ Hz, 1H), 5.23 (dt, $J = 10.3, 1.0$ Hz, 1H), 4.62 (ddt, $J = 8.5, 4.8, 1.0$ Hz,

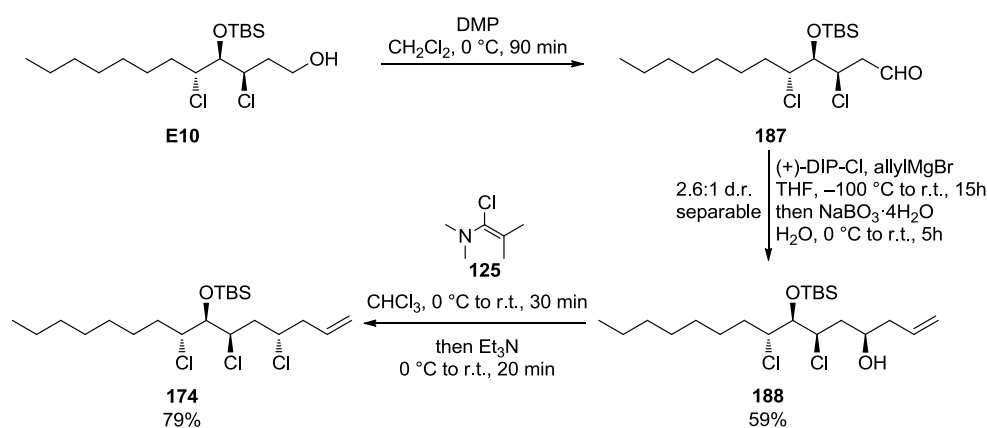
1H), 4.05 (ddd, $J = 10.5, 4.8, 2.5$ Hz, 1H), 3.95 (t, $J = 4.8$ Hz, 1H), 1.90 – 1.75 (m, 1H), 1.69 – 1.46 (m, 2H), 1.41 – 1.19 (m, 9H), 0.94 (s, 9H), 0.88 (t, $J = 6.8$ Hz, 3H), 0.15 (s, 3H), 0.14 (s, 3H); ^{13}C NMR (101 MHz, 101 MHz) δ 135.7, 118.4, 79.9, 65.2, 63.9, 32.7, 31.9, 29.3, 29.1, 26.7, 26.2, 22.8, 18.7, 14.2, -3.6, -3.6; HRMS (ESI) exact mass for $\text{C}_{18}\text{H}_{37}\text{Cl}_2\text{OSi}$ $[\text{M}+\text{H}]^+$, calculated 367.1985, found 367.1988; IR (thin film, cm^{-1}) ν 2956, 2928, 2857, 1464, 1362, 1255, 1112, 990, 929, 836, 777, 710, 676; $[\alpha]_{\text{D}}^{21\text{ }^\circ\text{C}} = +39.9$ ($c = 1.0, \text{CHCl}_3$).



(3R,4R,5R)-4-((tert-butyldimethylsilyl)oxy)-3,5-dichlorododecan-1-ol

(E10): To a suspension of dicyclohexylborane (98.0 mg, 0.551 mmol, 2.40 equiv) in THF (1.4 mL) at 0 °C was added olefin **186** (84.4 mg, 0.230 mmol, 1.00 equiv) in THF (0.7 mL + 2 x 0.2 mL rinse) dropwise. The reaction was allowed to warm to room temperature during 14 hours, before it was cooled back to 0 °C. THF (0.5 mL) and water (2 mL) were added, shortly followed by $\text{NaBO}_3 \cdot 4\text{H}_2\text{O}$ (1.06 g, 6.89 mmol, 30.0 equiv). The reaction was allowed to warm to room temperature during 4 hours, before it was poured into water/EtOAc and phases were separated. The aqueous phase was extracted twice with EtOAc and combined organic phases were dried over Na_2SO_4 , filtered, and concentrated. Flash column chromatography (hexanes/Et₂O, gradient 5:1 to 3:1, SiO₂) gave alcohol **E10** as colorless oil (71.0 mg, 0.184 mmol, 80%).

^1H NMR (400 MHz, CDCl_3) δ 4.52 (ddd, $J = 9.7, 4.3, 2.6$ Hz, 1H), 4.11 (ddd, $J = 10.7, 6.6, 2.4$ Hz, 1H), 3.86 (m, 3H), 2.01 – 1.90 (m, 3H), 1.70 – 1.18 (m, 12H), 0.93 (s, 9H), 0.91 – 0.85 (m, 3H), 0.15 (s, 3H), 0.13 (s, 3H); ^{13}C NMR (101 MHz, CDCl_3) δ 79.3, 63.9, 61.3, 60.0, 37.9, 33.9, 31.9, 29.3, 29.2, 26.8, 26.2, 22.8, 18.6, 14.2, -3.3, -3.5; HRMS (ESI) exact mass for $\text{C}_{18}\text{H}_{38}\text{Cl}_2\text{NaO}_2\text{Si}$ $[\text{M}+\text{Na}]^+$, calculated 407.1910, found 407.1910; IR (thin film, cm^{-1}) ν 3330, 2956, 2928, 2857, 1464, 1362, 1255, 1120, 1065, 939, 835, 776, 685; $[\alpha]_{\text{D}}^{22\text{ }^\circ\text{C}} = +20.0$ ($c = 1.0, \text{CHCl}_3$).



***tert*-butyldimethyl(((4*S*,6*R*,7*R*,8*R*)-4,6,8-trichloropentadec-1-en-7-yl)oxy)silane (174):** To a solution of alcohol **E10** (71.0 mg, 0.184 mmol, 1.00 equiv) in CH_2Cl_2 (1.8 mL) at 0 °C was added DMP (94.0 mg, 0.221, 1.20 equiv). After 15 minutes, cooling was removed and the reaction was stirred for another 90 minutes. Sat. aq. $\text{Na}_2\text{S}_2\text{O}_3$ was added and the mixture was stirred for 5 minutes before it was poured into sat. aq. NaHCO_3 and Et_2O . Phases were separated and the aqueous phase extracted twice with Et_2O . Combined organic phases were washed with sat. aq. NaHCO_3 and brine, dried over Na_2SO_4 , filtered, and concentrated. The obtained aldehyde **187** (66.9 mg) was used as is.

Crude analysis of aldehyde **187**: $^1\text{H NMR}$ (300 MHz, CDCl_3) δ 9.77 (dd, $J = 2.0, 1.0$ Hz, 1H), 4.83 (ddd, $J = 9.5, 4.5, 2.4$ Hz, 1H), 4.07 (ddd, $J = 10.6, 6.7, 2.4$ Hz, 1H), 3.90 (dd, $J = 6.7, 2.4$ Hz, 1H), 2.97 (ddd, $J = 17.4, 9.5, 2.0$ Hz, 1H), 2.82 (ddd, $J = 17.5, 4.4, 1.0$ Hz, 1H), 2.01 – 1.87 (m, 1H), 1.68 – 1.45 (m, 2H), 1.27 (d, $J = 10.9$ Hz, 9H), 0.94 (s, 9H), 0.92 – 0.84 (m, 3H), 0.15 (s, 3H), 0.12 (s, 3H).

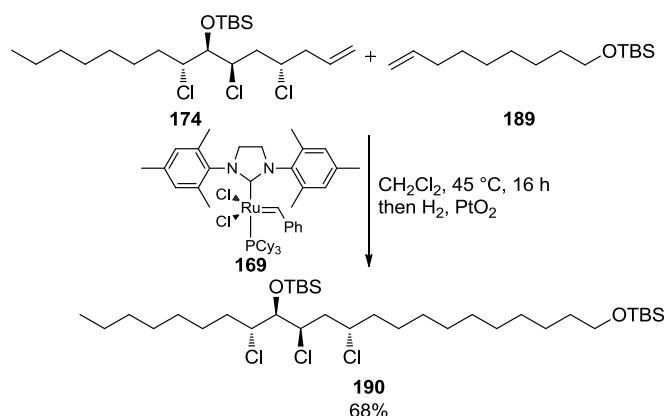
(+)-*B*-Chlorodiisopinocampheylborane (118 mg, 0.368 mmol, 2.00 equiv) was dissolved in THF (3.1 mL) and cooled to -78 °C. Allylmagnesium bromide (1.0 M in Et_2O , 0.276 mL, 0.276 mmol, 1.50 equiv) was added and the reaction was stirred at -78 °C for 1 hour and room temperature for 45 minutes. The reaction was then cooled to -100 °C (THF/LN_2) and crude aldehyde **187** was added dropwise. The reaction was allowed to warm to room temperature during 15 hours. The reaction was then cooled to 0 °C and water (ca. 6.5 mL) was added, followed by $\text{NaBO}_3\cdot 4\text{H}_2\text{O}$ (0.849 g, 5.52 mmol, 30.0 equiv). The mixture was stirred at 0 °C for 1 hour and room temperature for 4 hours. The reaction was then filtered through a plug of celite, eluting with EtOAc and separated between EtOAc and water. Phases were separated

and the aqueous phase extracted twice with EtOAc. Combined organic phases were washed with brine, dried over Na₂SO₄, filtered, and concentrated. Flash column chromatography (hexanes/EtOAc 9:1, SiO₂) gave the product as diastereomeric mixture (2.6:1). Repeated flash column chromatography (toluene/EtOAc 100:1, SiO₂) increased gave allylic alcohol **188** (46.0 mg, 0.108 mmol, 59% over 2 steps) as a diastereomeric mixture of >7:1.

Crude analysis of allylic alcohol **188**: **¹H NMR (400 MHz, CDCl₃)** δ 5.94 – 5.74 (m, 1H), 5.19 (d, *J* = 1.3 Hz, 1H), 5.18 – 5.13 (m, 1H), 4.43 (ddd, *J* = 9.3, 4.6, 2.6 Hz, 1H), 4.09 (ddd, *J* = 10.6, 6.5, 2.4 Hz, 1H), 3.92 (m, 1H), 3.87 (dd, *J* = 6.4, 2.6 Hz, 1H), 2.42 – 2.37 (m, 1H), 2.19 (dddd, *J* = 14.1, 7.8, 6.8, 1.1 Hz, 1H), 2.10 – 1.87 (m, 3H), 1.70 – 1.47 (m, 2H), 1.42 – 1.23 (m, 10H), 0.93 (s, 9H), 0.91 – 0.85 (m, 3H), 0.15 (s, 3H), 0.13 (s, 3H).

Alcohol **188** (46.0 mg, 0.108 mmol, 1.00 equiv) was dissolved in CHCl₃ (1.2 mL, previously filtered through basic alumina) and cooled to 0 °C. Ghosez' reagent (**125**, 43 μL, 0.31 mmol, 3.00 equiv) was added and cooling removed. The reaction was stirred for 30 minutes, before it was cooled to 0 °C and Et₃N (57 μL, 0.41 mmol, 4.00 equiv) was added. Cooling was removed and the reaction was stirred for 20 minutes before celite was added and solvent removed. The residue was subjected to flash column chromatography (hexanes, SiO₂) to give homoallylic chloride **174** (35.7 mg, 0.080 mmol, 79%).

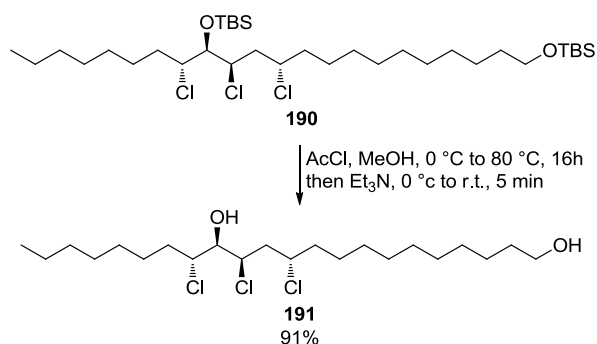
¹H NMR (300 MHz, CDCl₃) δ 5.84 (ddt, *J* = 18.6, 9.5, 7.0 Hz, 1H), 5.17 (s, 1H), 5.16 – 5.09 (m, 1H), 4.66 (dt, *J* = 11.5, 2.2 Hz, 1H), 4.28 (dtd, *J* = 11.0, 6.3, 2.0 Hz, 1H), 4.08 (ddd, *J* = 10.6, 6.6, 2.4 Hz, 1H), 3.83 (dd, *J* = 6.6, 2.5 Hz, 1H), 2.56 (tdd, *J* = 6.2, 3.1, 1.4 Hz, 2H), 2.16 (ddd, *J* = 14.8, 11.5, 2.1 Hz, 1H), 1.96 (ddt, *J* = 7.8, 6.2, 3.3 Hz, 1H), 1.85 (ddd, *J* = 14.7, 11.1, 1.9 Hz, 1H), 1.71 – 1.44 (m, 2H), 1.29 (q, *J* = 5.5, 4.8 Hz, 9H), 0.92 (s, 9H), 0.87 (m, 3H), 0.14 (s, 3H), 0.10 (s, 3H); **¹³C NMR (CDCl₃, 75 MHz)** δ 137.1, 122.3, 82.7, 67.2, 65.4, 62.8, 47.1, 46.8, 37.4, 35.4, 32.8, 32.7, 30.3, 29.7, 26.3, 22.1, 17.8, 0.2, 0.0; **HRMS (ESI)** exact mass for C₂₁H₄₂Cl₃OSi [M+H]⁺, calculated 443.2062, found 443.2062; **IR (thin film, cm⁻¹)** ν 2956, 2929, 2858, 1464, 1362, 1334, 1256, 1136, 1109, 1006, 993, 940, 922, 836, 776, 689, 616; **[α]_D^{22 °C}** = +49.7 (c = 1.0, CHCl₃).



(5*R*,6*R*,8*S*)-6,8-dichloro-5-((*R*)-1-chlorooctyl)-2,2,3,3,20,20,21,21-

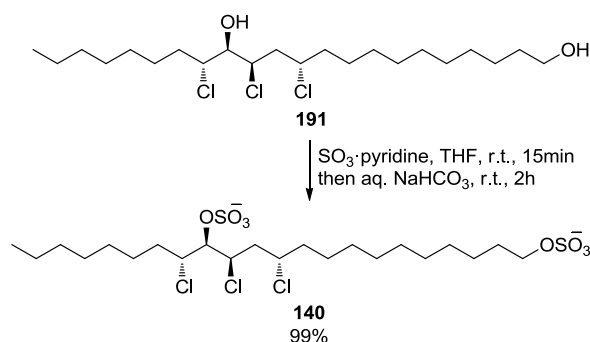
octamethyl-4,19-dioxa-3,20-disiladocosane (190): Homoallylic chloride **174** (34.0 mg, 77.6 μmol , 1.00 equiv) and olefin **189** (58.9 mg, 0.230 mmol, 3.00 equiv) were dissolved in CH_2Cl_2 (3.8 mL, previously sparged with argon for 15 min). Grubbs' 2nd Generation Catalyst (**169**, 6.5 mg, 7.7 μmol , 10 mol%) was added and the reaction heated at 45 $^\circ\text{C}$ for 13 hours. The mixture was allowed to cool to room temperature and platinum dioxide (1.7 mg, 7.7 μmol , 10 mol%) was added. The reaction was placed under hydrogen atmosphere (balloon) by carefully evacuating the flask and refilling with hydrogen (5 cycles). The reaction was then stirred for 6 hours under hydrogen atmosphere before it was put under argon atmosphere (evacuate – backfill with argon, 5 cycles). The mixture was then filtered through a plug of celite, eluting with CH_2Cl_2 and solvent was removed. Flash column chromatography (hexanes/ Et_2O 100:1, SiO_2) was followed by flash column chromatography (hexanes/toluene 6:1, SiO_2) to give the title compound (35.0 mg, 52.0 μmol , 68%).

$^1\text{H NMR}$ (400 MHz, CDCl_3) δ 4.65 (dt, $J = 11.5, 2.2$ Hz, 1H), 4.19 (dddd, $J = 10.2, 7.5, 5.2, 2.0$ Hz, 1H), 4.09 (ddd, $J = 10.6, 6.3, 2.3$ Hz, 1H), 3.86 (dd, $J = 6.3, 2.6$ Hz, 1H), 3.60 (t, $J = 6.6$ Hz, 2H), 2.12 (ddd, $J = 14.6, 11.4, 2.1$ Hz, 1H), 2.02 – 1.85 (m, 2H), 1.75 (m, 2H), 1.52 (m, 4H), 1.64 – 1.17 (m, 23H), 0.93 (s, 9H), 0.90 (m, 12H), 0.15 (s, 3H), 0.12 (s, 3H), 0.05 (s, 6H); $^{13}\text{C NMR}$ (101 MHz, CDCl_3) δ 79.3, 63.7, 63.5, 62.1, 60.9, 44.3, 39.1, 33.9, 33.0, 31.9, 29.7, 29.6, 29.6, 29.6, 29.3, 29.2, 29.2, 26.8, 26.6, 26.2, 26.0, 22.8, 18.6, 18.5, 14.2, -3.4, -3.5, -5.1; **HRMS** (ESI) exact mass for $\text{C}_{34}\text{H}_{72}\text{Cl}_3\text{O}_2\text{Si}_2$ $[\text{M}+\text{H}]^+$, calculated 673.4131, found 673.4124; **IR** (thin film, cm^{-1}) ν 2927, 2856, 1463, 1389, 1361, 1255, 1101, 1006, 938, 835, 814, 775, 689, 616; $[\alpha]_{\text{D}}^{22\text{ }^\circ\text{C}} = +27.2$ ($c = 1.0, \text{CHCl}_3$).



(11*S*,13*R*,14*R*,15*R*)-11,13,15-trichlorodocosane-1,14-diol (191): Disilylether **190** (35.0 mg, 52.0 μmol , 1.00 equiv) was dissolved in MeOH (5.2 mL) and cooled to 0 °C. Acetyl chloride (185 μL , 2.59 mmol, 50.0 equiv) was added dropwise and the reaction was heated to 80 °C for 16 hours. The reaction was then cooled back to 0 °C and triethylamine (362 μL , 2.59 mmol, 50.0 equiv) was added. After removal of cooling and stirring for 5 minutes, celite was added and the residue dried *in vacuo*. The solid was then subjected to flash column chromatography (hexanes/EtOAc, gradient 4:1 to 2:1, SiO₂) to give diol **191** as a white solid (21.1 mg, 47.0 μmol , 91%).

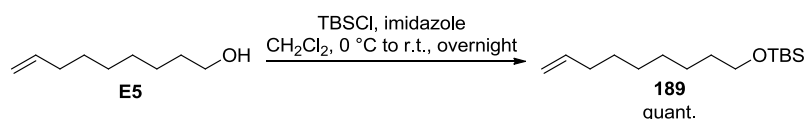
¹H NMR (600 MHz, CDCl₃) δ 5.00 (ddd, $J = 11.2, 2.4, 1.4$ Hz, 1H), 4.17 (dddd, $J = 11.0, 7.6, 5.3, 2.1$ Hz, 1H), 3.93 (td, $J = 9.3, 2.7$ Hz, 1H), 3.64 (t, $J = 6.6$ Hz, 2H), 3.56 (ddd, $J = 10.7, 9.2, 1.4$ Hz, 1H), 2.33 (ddd, $J = 15.1, 11.2, 2.2$ Hz, 1H), 2.11 (dddd, $J = 14.1, 10.4, 5.6, 2.7$ Hz, 1H), 2.05 (d, $J = 11.1$ Hz, 1H), 1.97 (ddd, $J = 15.1, 11.0, 2.4$ Hz, 1H), 1.77 (m, 2H), 1.72 – 1.65 (m, 1H), 1.64 – 1.49 (m, 5H), 1.49 – 1.40 (m, 2H), 1.39 – 1.19 (m, 20H), 0.91 – 0.86 (t, $J = 7.0$ Hz, 3H); **¹³C NMR (151 MHz, CDCl₃)** δ 77.3, 63.3, 63.2, 62.6, 60.8, 44.6, 38.9, 33.9, 32.9, 31.9, 29.6, 29.5, 29.5, 29.3, 29.3, 29.1, 26.4, 25.9, 25.9, 25.8, 22.8, 14.2; **HRMS (ESI)** exact mass for C₂₂H₄₃Cl₃NaO₂ [M+Na]⁺, calculated 467.2218, found 467.2218; **IR (thin film, cm⁻¹)** ν 3299, 2921, 2852, 1467, 1432, 1291, 1253, 1059, 935, 724, 689, 615; **[α]_D^{22 °C}** = +24.2 (c = 0.5, CHCl₃).



(11S,13R,14R,15R)-11,13,15-trichlorodocosane-1,14-diyl bis(sulfate)

disodium salt (140): To a solution of diol **191** (12.0 mg, 27.0 μmol , 1.00 equiv) in THF (0.5 mL) was added sulfur trioxide pyridine complex (17.6 mg, 0.110 mmol, 4.1 equiv). The reaction was stirred for 15 minutes before sat. aq. NaHCO_3 was added and the mixture stirred for 2 hours. The mixture was then filtered through a plug of silica, eluting with 2:1 $\text{CH}_2\text{Cl}_2/\text{MeOH}$. The resulting solution was concentrated and subjected to flash column chromatography ($\text{CH}_2\text{Cl}_2/\text{MeOH}$, gradient 6:1 to 4:1) to give disulfate **140** (17.3 mg, 27.0 μmol , 99%) as a colorless solid.

$^1\text{H NMR}$ (400 MHz, CD_3OD) δ 4.94 (dt, $J = 11.3, 1.8$ Hz, 1H), 4.43 (dd, $J = 9.4, 1.4$ Hz, 1H), 4.21 (dddd, $J = 11.1, 7.6, 5.5, 2.1$ Hz, 1H), 4.14 (td, $J = 9.8, 2.5$ Hz, 1H), 4.02 (t, $J = 6.5$ Hz, 2H), 2.54 (ddd, $J = 15.5, 11.4, 2.1$ Hz, 1H), 2.32 (m, 1H), 2.08 (ddd, $J = 15.5, 11.2, 2.1$ Hz, 1H), 1.84 – 1.75 (m, 2H), 1.68 (ddt, $J = 12.7, 8.4, 5.9$ Hz, 4H), 1.56 – 1.24 (m, 23H), 0.94 – 0.87 (t, $J = 6.8$ Hz, 3H); **$^{13}\text{C NMR}$ (101 MHz, CD_3OD)** δ 84.0, 69.4, 63.1, 62.3, 62.2, 45.7, 39.9, 34.9, 33.0, 30.6, 30.5, 30.5, 30.4, 30.3, 30.3, 30.1, 30.1, 27.6, 27.4, 26.9, 23.7, 14.4; **HRMS** (ESI) exact mass for $\text{C}_{22}\text{H}_{41}\text{Cl}_3\text{NaO}_8\text{S}_2$ [$\text{M}-\text{Na}$], calculated 625.1212, found 625.1221; **IR (thin film, cm^{-1})** ν 3435, 2926, 2855, 1632, 1466, 1219, 1083, 974, 828, 724, 683, 630, 575; **$[\alpha]_D^{22}$** = +25.4 ($c = 0.5$, MeOH).

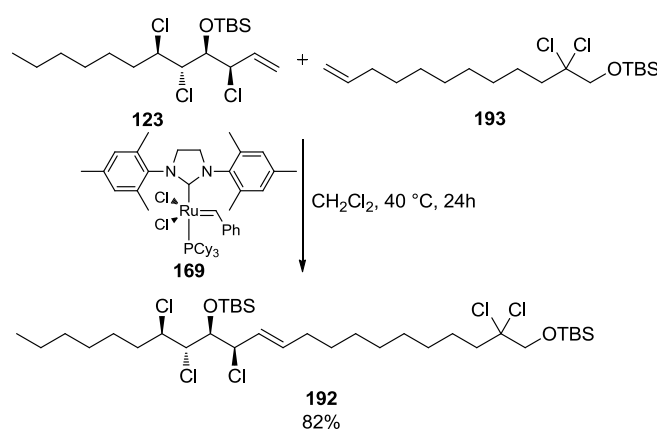


tert-butyldimethyl(non-8-en-1-yloxy)silane (189): To a solution of non-8-enol **E5** (1.77 mL, 10.6 mmol, 1.00 equiv) in CH_2Cl_2 at 0 °C were added *tert*-butyldimethylsilylchloride (1.91 g, 12.7 mmol, 1.20 equiv) and imidazole (1.08 g,

Experimental

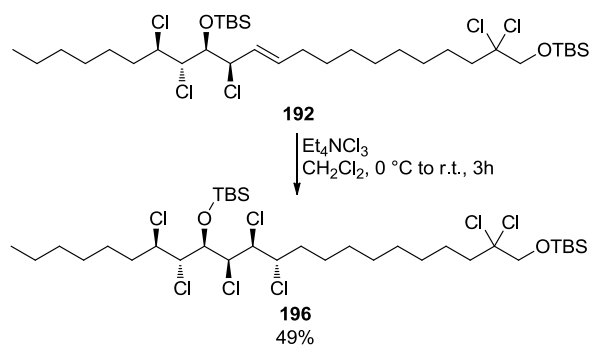
15.8 mmol, 1.50 equiv). The reaction was allowed to warm to room temperature during 14 hours. Sat. aq. NH_4Cl was added and the mixture was poured into water. The aqueous phase was extracted three times with CH_2Cl_2 . Combined organic phases were dried over Na_2SO_4 , filtered, and concentrated. Flash column chromatography (hexanes/EtOAc gradient 1:0 to 9:1, SiO_2) gave the title compound as colorless liquid (2.72 g, 10.6 mmol, quantitative).

$^1\text{H NMR}$ (400 MHz, CDCl_3) δ 5.81 (ddt, $J = 16.9, 10.1, 6.7$ Hz, 1H), 5.01 (dq, $J = 17.2, 1.6$ Hz, 1H), 4.93 (ddd, $J = 10.3, 2.3, 1.2$ Hz, 1H), 3.60 (t, $J = 6.6$ Hz, 2H), 2.11 – 1.96 (m, 2H), 1.51 (ddt, $J = 14.0, 7.8, 4.6$ Hz, 2H), 1.41 – 1.34 (m, 2H), 1.34 – 1.25 (m, 6H), 0.89 (s, 9H), 0.05 (s, 6H); $^{13}\text{C NMR}$ (101 MHz, CDCl_3) δ 139.4, 114.3, 63.5, 33.9, 33.0, 29.4, 29.3, 29.0, 26.1, 25.9, 18.5, -5.1.; **HRMS** (EI) exact mass for $\text{C}_{11}\text{H}_{23}\text{OSi}$ $[\text{M}-\text{C}_4\text{H}_9]^+$, calculated 199.1513, found 199.1513; **IR** (thin film, cm^{-1}) ν 2928, 2857, 1641, 1472, 1463, 1388, 1361, 1254, 1098, 1006, 992, 939, 909, 833, 773, 712, 661.



(5*S*,6*R*,*E*)-6,17,17-trichloro-5-((1*S*,2*R*)-1,2-dichlorooctyl)-2,2,3,3,20,20,21,21-octamethyl-4,19-dioxo-3,20-disiladocos-7-ene (192): To a solution of a solution of allylic chloride **123** (50.0 mg, 0.124 mmol, 1.00 equiv) and olefin **193** (137 mg, 0.373 mmol, 3.00 equiv) in CH_2Cl_2 (6.2 mL, previously sparged with argon for 15 minutes) was added Grubbs' 2nd Generation Catalyst (**169**, 10.6 mg, 12.0 μmol , 10.0 mol%). The reaction was filtered through a plug of silica, eluting with CH_2Cl_2 . The solution was concentrated. Flash column chromatography (hexanes/toluene 30:1, SiO_2) gave the product as colorless oil (76.0 mg, 0.103 mmol, 82%).

¹H NMR (400 MHz, CDCl₃) δ 5.81 (dt, *J* = 15.3, 6.7 Hz, 1H), 5.59 (ddt, *J* = 15.3, 9.6, 1.5 Hz, 1H), 4.76 – 4.70 (m, 1H), 4.28 – 4.19 (m, 3H), 3.92 (s, 2H), 2.21 – 2.14 (m, 2H), 2.12 – 2.04 (m, 2H), 2.03 – 1.91 (m, 1H), 1.84 – 1.69 (m, 1H), 1.67 – 1.53 (m, 4H), 1.46 – 1.23 (m, 16H), 0.94 (s, 9H), 0.92 (s, 9H), 0.91 – 0.88 (m, 3H), 0.17 (s, 3H), 0.14 (s, 3H), 0.11 (s, 6H); **¹³C NMR (CDCl₃, 101 MHz)** δ 136.7, 127.0, 93.6, 77.7, 72.3, 68.1, 65.6, 62.0, 43.7, 34.4, 32.3, 31.8, 29.5, 29.4, 29.3, 29.2, 28.9, 28.8, 26.1, 26.0, 25.9, 24.9, 22.7, 18.6, 18.4, 14.2, -3.9, -3.9, -5.2; **HRMS (ESI)** exact mass for C₃₄H₇₁Cl₅NO₂Si₂ [M+NH₄]⁺, calculated 756.3460, found 756.3445; **IR (thin film, cm⁻¹)** ν 2953, 2928, 2856, 1463, 1362, 1255, 1119, 1006, 971, 939, 837, 778, 696, 603; **[α]_D^{22 °C}** = +25.6 (*c* = 1.0, CHCl₃).

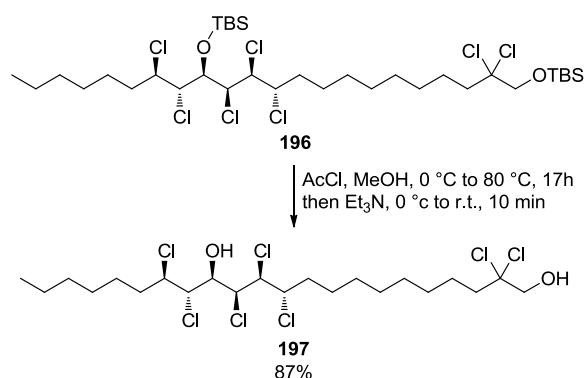


(5*R*,6*S*,7*S*,8*S*)-6,7,8,17,17-pentachloro-5-((1*S*,2*R*)-1,2-dichlorooctyl)-2,2,3,3,20,20,21,21-octamethyl-4,19-dioxo-3,20-disiladocosane (196): To a solution of allylic chloride **192** (61.0 mg, 82.0 μmol, 1.00 equiv) in CH₂Cl₂ (0.8 mL) at 0 °C was added tetraethylammonium trichloride (45.0 mg, 0.190 mmol, 2.30 equiv). Cooling was removed and the reaction was stirred for 1 hour. tetraethylammonium trichloride trichloride (45.0 mg, 0.190 mmol, 2.30 equiv) was added again and the reaction was stirred for another 2 hours. The mixture was quenched with sat. aq. NaHCO₃ and sat. aq. Na₂S₂O₃ and extracted three times with CH₂Cl₂. Combined organic phases were dried over Na₂SO₄, filtered, and concentrated. Flash column chromatography (hexanes/toluene 50:1, SiO₂) gave the product as colorless oil (33.0 mg, 41.0 μmol, 49%).

¹H NMR (400 MHz, CDCl) δ 5.06 (dd, *J* = 8.0, 1.7 Hz, 1H), 4.48 (d, *J* = 8.0 Hz, 1H), 4.29 – 4.15 (m, 4H), 3.92 (s, 2H), 2.28 – 2.08 (m, 4H), 1.84 – 1.69 (m, 2H), 1.59 (m, 4H), 1.47 (m, 2H), 1.40 – 1.23 (m, 14H), 0.95 (s, 9H), 0.92 (s, 9H), 0.91 –

Experimental

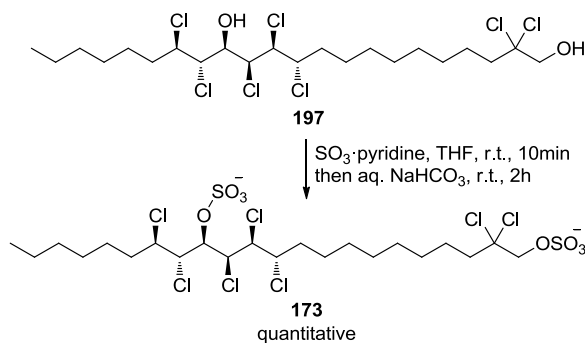
0.88 (m, 3H), 0.23 (s, 3H), 0.20 (s, 3H), 0.11 (s, 6H); ^{13}C NMR (101 MHz, CDCl_3) δ 93.6, 80.6, 72.3, 66.8, 65.2, 64.3, 62.8, 60.4, 43.7, 35.5, 34.6, 31.7, 29.4, 29.4, 29.2, 29.1, 28.6, 26.3, 25.9, 25.5, 25.2, 24.9, 22.7, 18.8, 18.4, 14.2, -3.8, -4.2, -5.2; ; HRMS (ESI) exact mass for $\text{C}_{34}\text{H}_{68}\text{Cl}_7\text{O}_2\text{Si}_2$ $[\text{M}+\text{H}]^+$, calculated 809.2572, found 809.2580; IR (thin film, cm^{-1}) ν 2953, 2928, 2857, 1463, 1377, 1362, 1256, 1122, 1006, 838, 780, 671; $[\alpha]_{\text{D}}^{22\text{ }^\circ\text{C}} = -3.0$ ($c = 0.5$, CHCl_3).



(11S,12S,13S,14R,15S,16R)-2,2,11,12,13,15,16-heptachlorodocosane-1,14-diol (197): Disilylether **196** (33.0 mg, 41.0 μmol , 1.00 equiv) was dissolved in MeOH (4.1 mL) and cooled to 0 °C. Acetyl chloride (145 μL , 2.03 mmol, 50.0 equiv) was added dropwise and the reaction was heated to 80 °C for 17 hours. The reaction was then cooled back to 0 °C and triethylamine (283 μL , 2.03 mmol, 50.0 equiv) was added. After removal of cooling and stirring for 10 minutes, celite was added and the residue dried *in vacuo*. The solid was then subjected to flash column chromatography (hexanes/EtOAc 5:1, SiO_2) to give diol **197** as a colorless oil (20.7 mg, 35.0 μmol , 87%).

^1H NMR (600 MHz, CDCl_3) δ 5.39 (t, $J = 2.1$ Hz, 1H), 4.50 (dt, $J = 10.0$, 3.3 Hz, 1H), 4.27 (dd, $J = 8.6$, 3.4 Hz, 1H), 4.23 (dd, $J = 9.5$, 2.2 Hz, 1H), 4.16 (td, $J = 9.2$, 2.5 Hz, 1H), 4.07 (ddd, $J = 8.3$, 6.0, 2.0 Hz, 1H), 3.91 (d, $J = 7.2$ Hz, 2H), 2.75 (d, $J = 6.0$ Hz, 1H), 2.32 (t, $J = 7.5$ Hz, 1H), 2.25 – 2.19 (m, 2H), 2.15 (dddd, $J = 14.4$, 10.5, 5.6, 2.5 Hz, 1H), 1.92 – 1.75 (m, 3H), 1.70 – 1.54 (m, 5H), 1.47 (m, 1H), 1.42 – 1.23 (m, 14H), 0.89 (t, $J = 6.9$ Hz, 3H); ^{13}C NMR (151 MHz, CDCl_3) δ 94.8, 75.5, 72.3, 67.4, 66.8, 63.1, 62.4, 62.0, 43.7, 34.2, 32.6, 31.8, 29.4, 29.3, 29.1, 29.0, 28.8, 26.5, 25.3, 24.9, 22.7, 14.2; HRMS (ESI) exact mass for $\text{C}_{22}\text{H}_{43}\text{Cl}_7\text{NO}_2$ $[\text{M}+\text{NH}_4]^+$,

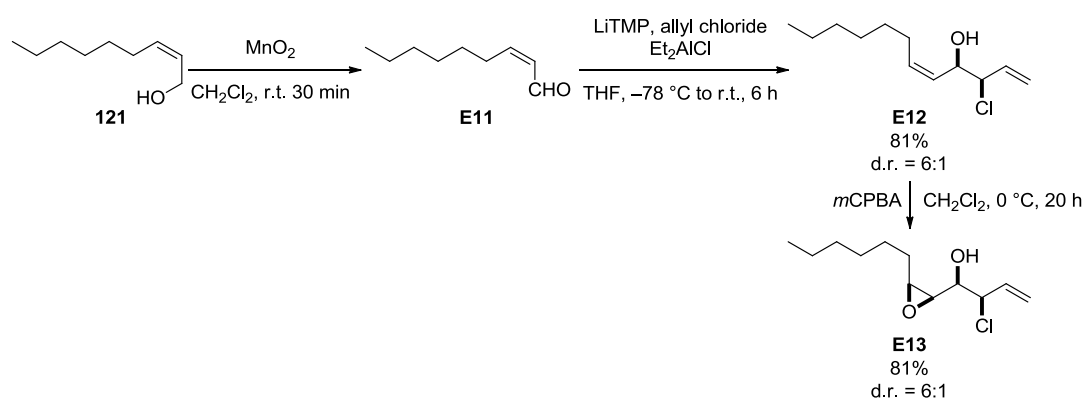
calculated 598.1098, found 598.1098; **IR** (thin film, cm^{-1}) ν 3566, 3411, 2929, 2857, 1465, 1379, 1266, 1191, 1068, 933, 159, 706, 657, 602; $[\alpha]_{\text{D}}^{22} = -0.4$ ($c = 0.5$, CHCl_3).



(11S,13R,14R,15R)-11,13,15-trichlorodocosane-1,14-diyl bis(sulfate)

disodium salt (173): To a solution of diol **197** (19.8 mg, 34.0 μmol , 1.00 equiv) in THF (0.7 mL) was added sulfur trioxide pyridine complex (22.1 mg, 0.139 mmol, 4.1 equiv). The reaction was stirred for 10 minutes before sat. aq. NaHCO_3 was added and the mixture stirred for 2 hours. The mixture was then filtered through a plug of silica, eluting with 3:1 $\text{CH}_2\text{Cl}_2/\text{MeOH}$. The resulting solution was concentrated and subjected to flash column chromatography ($\text{CH}_2\text{Cl}_2/\text{MeOH}$, gradient 8:1 to 4:1) to give disulfate **173** (27.0 mg, 34.0 μmol , quantitative) as a white solid.

$^1\text{H NMR}$ (400 MHz, CD_3OD) δ 4.88 (dd, $J = 7.7, 2.1$ Hz, 1H), 4.77 (m, 1H), 4.74 (dd, $J = 8.6, 2.2$ Hz, 1H), 4.70 – 4.61 (m, 2H), 4.52 (dd, $J = 8.8, 3.0$ Hz, 1H), 4.31 (s, 2H), 2.30 – 2.19 (m, 2H), 2.02 (dddd, $J = 14.0, 10.7, 5.3, 2.1$ Hz, 1H), 1.95 – 1.25 (m, 23H), 0.91 (t, $J = 6.8$ Hz, 3H); **$^{13}\text{C NMR}$ (101 MHz, CD_3OD)** δ 91.3, 78.0, 75.6, 69.2, 68.3, 65.4, 62.8, 62.5, 45.1, 33.9, 32.9, 32.7, 30.4, 30.1, 30.1, 29.7, 27.4, 26.7, 25.8, 23.7, 14.5; **HRMS** (ESI) exact mass for $\text{C}_{22}\text{H}_{38}\text{Cl}_7\text{O}_8\text{S}_2$ $[\text{M}-2\text{Na}+\text{H}]^+$, calculated 738.9833, found 738.9831; **IR** (thin film, cm^{-1}) ν 3429, 2927, 2856, 1628, 1464, 1229, 1075, 1005, 833, 578; $[\alpha]_{\text{D}}^{22} = +10.5$ ($c = 1.0$, MeOH).



2-chloro-1-(3-hexyloxiran-2-yl)but-3-en-1-ol (E13): Procedure adapted from enantioselective synthesis: A. M. Bailey, S. Wolfrum, E. M. Carreira *Angew. Chem. Int. Ed.* **2016**, *55*, 639-643.

To a solution of (*Z*)-non-2-enal (**121**, 1.2 mL, 7.1 mmol, 1.0 equiv) in CH₂Cl₂ (36 mL) was added manganese dioxide (15.5 g, 178 mmol, 25.0 equiv). The reaction was stirred vigorously for 30 minutes and filtered through celite, eluting with CH₂Cl₂. Concentration gave crude aldehyde **E11** (1.13 g).

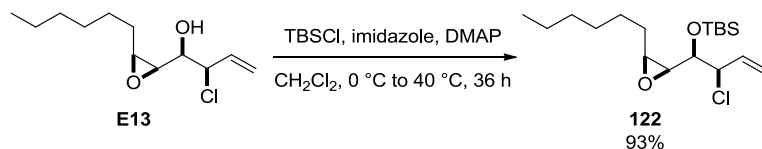
According to General Procedure 3 (see Chapter 12), LiTMP was prepared from tetramethylpiperidine (2.66 mL, 15.7 mmol, 2.20 equiv) and *n*-BuLi (1.6 M in hexanes, 9.4 mL, 15 mmol, 2.1 equiv) in THF (32 mL) and added to a solution of allyl chloride (1.2 mL, 15 mmol, 2.1 equiv) and diethylaluminum chloride (1.0 M in hexanes, 29 mL, 29 mmol, 4.0 equiv) in THF (64 mL). Crude **E11** (1.13 g) in THF (6.4 mL) was added. After 5 hours, the reaction was worked up and purified by flash column chromatography (hexanes/Et₂O gradient 7:1 to 5:1, SiO₂) to give **E12** (1.3 g, 5.8 mmol, 81%, d.r. = 6:1).

¹H NMR (CDCl₃, 400 MHz) δ (only peaks for major diastereomer reported) 5.91 (ddd, *J* = 16.9, 10.2, 8.3 Hz, 1H), 5.66 (dtd, *J* = 11.1, 7.5, 1.0 Hz, 1H), 5.42 – 5.33 (m, 2H), 5.29 – 5.22 (m, 1H), 4.54 – 4.45 (m, 1H), 4.38 – 4.30 (m, 1H), 2.23 (d, *J* = 4.4 Hz, 1H), 2.18 – 2.02 (m, 2H), 1.41 – 1.22 (m, 8H), 0.93 – 0.85 (m, 3H); ¹³C NMR (CDCl₃, 101 MHz) δ 136.1, 134.6, 127.0, 119.3, 70.7, 68.4, 31.8, 29.5, 29.1, 28.3, 22.7, 14.2.¹¹⁸

The material was taken up into CH₂Cl₂ (58 mL) and cooled to 0 °C. Dried *m*CPBA (1.10 g, 6.37 mmol, 1.10 equiv) was added and the reaction was allowed to warm to r.t. during 20 hours. Sat. aq. Na₂S₂O₃ was added and the reaction was stirred

for another 45 minutes. The mixture was then poured into sat. aq. NaHCO_3 and extracted three times with CH_2Cl_2 . Combined organic phases were washed with sat. aq. NaHCO_3 and brine, dried over Na_2SO_4 , filtered, and concentrated. Flash column chromatography (hexanes/ Et_2O gradient 6:1 to 4:1, SiO_2) gave **E13** (1.1 g, 4.7 mmol, 81%, d.r. = 6:1).

$^1\text{H NMR}$ (CDCl_3 , 400 MHz) δ (only peaks for major diastereomer reported) 6.03 (ddd, $J = 16.9, 10.2, 8.1$ Hz, 1H), 5.47 (dt, $J = 16.9, 1.1$ Hz, 1H), 5.35 (dt, $J = 10.3, 1.0$ Hz, 1H), 4.50 (ddt, $J = 8.2, 4.7, 1.0$ Hz, 1H), 3.79 (td, $J = 5.8, 4.7$ Hz, 1H), 3.15 (dd, $J = 5.7, 4.2$ Hz, 1H), 3.07 (dt, $J = 6.9, 4.4$ Hz, 1H), 2.52 – 2.44 (m, 1H), 1.76 – 1.63 (m, 1H), 1.62 – 1.44 (m, 3H), 1.45 – 1.22 (m, 6H), 0.94 – 0.89 (m, 3H); $^{13}\text{C NMR}$ (CDCl_3 , 101 MHz) δ 133.9, 119.8, 71.0, 64.8, 57.9, 57.1, 31.8, 29.2, 28.2, 26.9, 22.7, 14.2.¹¹⁸

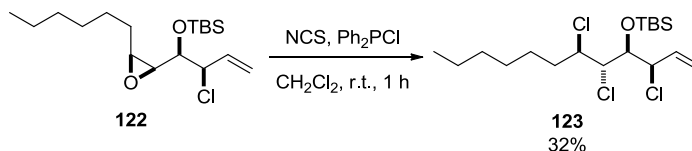


tert-butyl((2-chloro-1-(3-hexyloxiran-2-yl)but-3-en-1-yl)oxy)dimethylsilane (122): To a solution of alcohol **E13** (200 mg, 0.859 mmol, 1.00 equiv, d.r. = 6:1) in CH_2Cl_2 (5.7 mL) at 0 °C was added imidazole (117 mg, 1.72 mmol, 2.0 equiv). After 10 minutes, *tert*-butyldimethylsilyl chloride (155 mg, 1.03 mmol, 1.50 equiv) and 4-dimethylaminopyridine (10.5 mg, 86.0 μmol , 10.0 mol%) were added and the reaction was allowed to warm to room temperature during 24 hours. More *tert*-butyldimethylsilyl chloride (13 mg, 86 μmol , 0.10 equiv) was added and the reaction was heated at 40 °C for 12 hours. Sat. aq. NH_4Cl was added and the mixture extracted three times with CH_2Cl_2 . Combined organic phases were dried over Na_2SO_4 , filtered, and concentrated. Flash column chromatography (hexanes/ Et_2O 50:1, SiO_2) gave **122** (278 mg, 0.801 mmol, 93%, d.r. = 6:1).

$^1\text{H NMR}$ (CDCl_3 , 400 MHz) δ 6.00 (ddd, $J = 17.0, 10.3, 7.9$ Hz, 1H), 5.35 (dt, $J = 16.9, 1.2$ Hz, 1H), 5.24 (dt, $J = 10.3, 1.1$ Hz, 1H), 4.35 (ddt, $J = 7.9, 4.6, 1.1$ Hz, 1H), 3.60 (dd, $J = 8.0, 4.6$ Hz, 1H), 3.09 – 2.91 (m, 2H), 1.76 – 1.63 (m, 1H), 1.63 – 1.43 (m, 2H), 1.43 – 1.21 (m, 7H), 0.92 (s, 9H), 0.94 – 0.82 (m, 3H), 0.15 (s, 3H),

Experimental

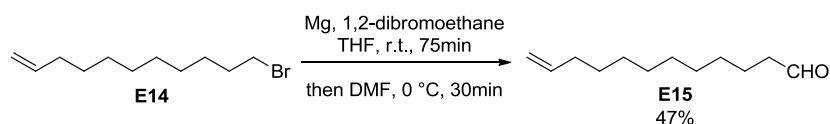
0.10 (s, 3H); ^{13}C NMR (CDCl_3 , 101 MHz) δ 134.8, 118.4, 74.3, 64.3, 58.7, 58.1, 31.8, 29.2, 29.2, 27.1, 26.0, 22.7, 18.4, 14.2, -4.1, -4.9.¹¹⁸



tert-butyldimethyl((3,5,6-trichlorododec-1-en-4-yl)oxy)silane (123): To a solution of alcohol *N*-chlorosuccinimide (374 mg, 2.80 mmol, 3.50 equiv) in CH_2Cl_2 (9.6 mL) was added diphenylchlorophosphine (440 μL , 2.4 mmol, 3.0 equiv). After 5 minutes, **122** (278 mg, 0.801 mmol, 1.00 equiv, d.r. = 6:1) was quickly added and the reaction was stirred for 1 hour. Sat. aq. NaHCO_3 was added and the mixture extracted three times with Et_2O . Combined organic phases were filtered through a plug of silica, eluting with Et_2O , and subsequently concentrated. Flash column chromatography (hexanes, SiO_2) gave **123** as an inseparable mixture of diastereomers (0.10 g, 0.26 mmol, 32%, d.r. = 6:1).

^1H NMR (CDCl_3 , 400 MHz) δ 5.98 (ddd, J = 17.0, 10.1, 8.8 Hz, 1H), 5.42 (dt, J = 17.0, 1.0 Hz, 1H), 5.29 (dt, J = 10.1, 0.9 Hz, 1H), 4.77 (dd, J = 8.8, 5.5 Hz, 1H), 4.33 – 4.20 (m, 3H), 2.00 – 1.89 (m, 1H), 1.89 – 1.71 (m, 1H), 1.61 (ddt, J = 9.0, 6.8, 4.2 Hz, 1H), 1.42 – 1.21 (m, 7H), 0.94 (s, 9H), 0.91 – 0.86 (m, 3H), 0.17 (s, 3H), 0.14 (s, 3H); ^{13}C NMR (CDCl_3 , 101 MHz) δ 135.0, 119.7, 77.4, 67.9, 65.2, 62.0, 34.2, 31.8, 29.0, 26.1, 26.0, 22.7, 18.6, 14.2, -3.8, -3.9.¹¹⁸

Enantiomerically pure material was synthesized and supplied by A. M. Bailey.

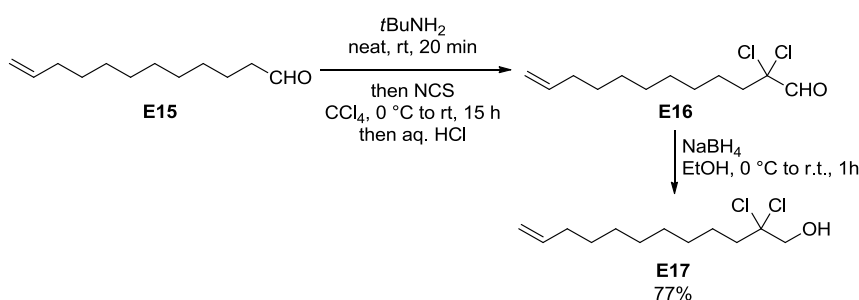


dodec-11-enal (E15): Procedure from *J. Org. Chem.* **2014**, 79, 2226-2241 was followed.

To a suspension of magnesium turnings (0.485 g, 19.9 mmol, 3.10 equiv) in THF (1.4 mL) was added 1,2-dibromoethane (39 μL , 0.45 mmol, 7.0 mol%). The reaction started to reflux and was diluted with THF (9.9 mL). 11-Bromoundec-1-ene

(**E14**, 1.41 mL, 6.43 mmol, 1.00 equiv) in THF (2.8 mL) was added dropwise during 15 minutes. The reaction was stirred for 1 hour and subsequently cooled to 0 °C. The mixture was then cannulated into a flask containing DMF (7.5 mL) and THF (7.5 mL) at 0 °C. After the cannula transfer, the reaction was stirred for 30 minutes before being diluted with hexanes. The mixture was then poured into 1M HCl. The phases were separated and the aqueous phase was extracted hexanes three times. Combined organic phases were washed with brine, dried over Na₂SO₄, filtered, and concentrated. Flash column chromatography (hexanes/EtOAc 20:1, SiO₂) gave the title compound as colorless oil (554 mg, 3.04 mmol, 47%)

¹H NMR (400 MHz, CDCl₃) δ 9.76 (t, *J* = 1.9 Hz, 1H), 5.81 (ddt, *J* = 16.9, 10.2, 6.7 Hz, 1H), 4.99 (dq, *J* = 17.2, 1.8 Hz, 1H), 4.93 (ddt, *J* = 10.1, 2.3, 1.3 Hz, 1H), 2.41 (td, *J* = 7.4, 1.9 Hz, 2H), 2.09 – 1.97 (m, 2H), 1.62 (p, *J* = 7.4 Hz, 2H), 1.41 – 1.20 (m, 12H); ¹³C NMR (101 MHz, CDCl₃) δ 203.1, 139.3, 114.3, 44.1, 33.9, 29.5, 29.5, 29.5, 29.3, 29.2, 29.1, 22.2.⁸⁵



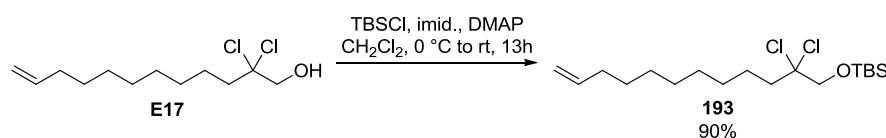
2,2-dichlorododec-1-en-1-ol (E17): To aldehyde **E15** (554 mg, 3.04 mmol, 1.00 equiv) was added *tert*-butylamine (0.338 mL, 3.19 mmol, 1.05 eq.) and this mixture was stirred for 20 minutes. The mixture was then diluted with CH₂Cl₂ and dried over Na₂SO₄, filtered, and concentrated. The crude imine was dissolved in CCl₄ (3.0 mL) and the stirred solution was cooled to 0 °C. A reflux condenser was attached and the fume hood light was turned off. *N*-chlorosuccinimide (0.852 g, 6.38 mmol, 2.10 eq.) was added portionwise (3 portions) during 5 minutes. After 90 minutes the cold bath was removed and the reaction was allowed to stir in the dark for 14 hours. The reaction was diluted with hexanes and filtered through a celite pad, rinsing with hexane. The filtrate was concentrated. To this mixture was added H₂O (3.0 mL), followed by conc. aq. HCl (1.5 mL). After 4 hours the reaction was diluted with H₂O

Experimental

and extracted three times with CH₂Cl₂. Combined organic phases were dried over Na₂SO₄, filtered, and concentrated. The crude dichloroaldehyde **E16** was used as is in the next reaction.

A stirred solution of crude aldehyde **E16** in EtOH (20 mL) was cooled to 0 °C. Sodium borohydride (0.225 g, 5.96 mmol, 2.00 eq.) was added carefully. The reaction was stirred at 0 °C for 30 minutes and at room temperature for 30 minutes. The reaction was then quenched through the addition of sat. aq. NH₄Cl and extracted three times with EtOAc. Combined organic phases were dried over Na₂SO₄, filtered, and concentrated. Flash column chromatography (pentanes/CH₂Cl₂, gradient 1:1 to 1:2, SiO₂) gave alcohol **E17** as colorless liquid (584 mg, 2.31 mmol, 77% over 2 steps).

¹H NMR (400 MHz, CDCl₃) δ 5.81 (ddt, *J* = 16.9, 10.1, 6.7 Hz, 1H), 5.00 (dq, *J* = 17.1, 1.7 Hz, 1H), 4.93 (ddt, *J* = 10.2, 2.2, 1.2 Hz, 1H), 3.90 (d, *J* = 7.6 Hz, 2H), 2.29 (t, *J* = 7.5 Hz, 1H), 2.25 – 2.17 (m, 2H), 2.04 (tdd, *J* = 6.6, 5.2, 1.4 Hz, 2H), 1.64 (ddt, *J* = 10.6, 7.8, 6.1 Hz, 2H), 1.45 – 1.19 (m, 10H).; **¹³C NMR (101 MHz, CDCl₃)** δ 139.3, 114.3, 94.9, 72.3, 43.7, 33.9, 29.5, 29.5, 29.2, 29.2, 29.0, 25.0.⁸⁵



tert-butyl((2,2-dichlorododec-11-en-1-yl)oxy)dimethylsilane (193): To a solution of alcohol **E17** (0.580 g, 2.29 mmol, 1.00 equiv) in CH₂Cl₂ (12 mL) at 0 °C were added TBSCl (0.518 g, 3.44 mmol, 1.50 equiv), imidazole (0.468 g, 6.87 mmol, 2.00 equiv), and 4-dimethylaminopyridine (28.0 mg, 0.229 mmol, 0.10 equiv) sequentially. The reaction was allowed to warm to room temperature during 13 hours. The reaction was quenched through the addition of sat. aq. NH₄Cl. The aqueous phase was extracted three times with CH₂Cl₂. Combined organic phases were dried over Na₂SO₄, filtered, and concentrated. Flash column chromatography (hexanes, SiO₂) gave the title compound as colorless liquid (0.757 g, 2.06 mmol, 90%).

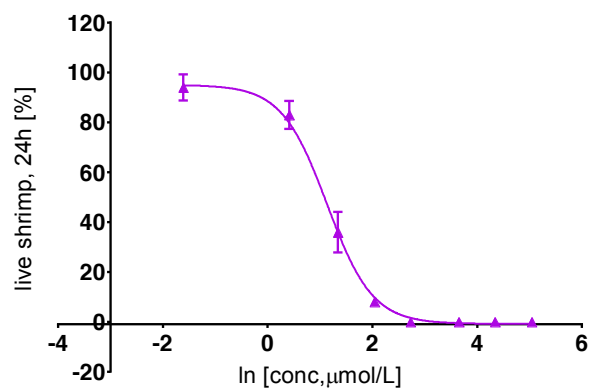
¹H NMR (400 MHz, CDCl₃) δ 5.81 (ddt, *J* = 16.9, 10.1, 6.6 Hz, 1H), 5.00 (dq, *J* = 17.1, 1.9 Hz, 1H), 4.93 (dt, *J* = 10.2, 1.7 Hz, 1H), 3.92 (s, 2H), 2.23 – 2.14 (m, 2H), 2.04 (q, *J* = 7.7, 7.1 Hz, 2H), 1.58 (m, 2H), 1.47 – 1.15 (m, 10H), 0.92 (s, 9H),

0.11 (s, 6H); ^{13}C NMR (101 MHz, CDCl_3) δ 139.3, 114.3, 93.7, 72.3, 43.7, 34.0, 29.5, 29.5, 29.2, 29.2, 29.1, 25.9, 24.9, 18.4, -5.2.⁸⁵

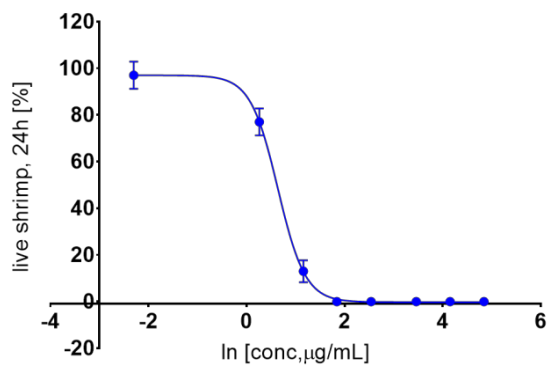
Brine shrimp toxicity

Blanks					
well	live shrimps (t = 0)	live shrimps (t = 24 h)	alive	average [%]	conditions
A1	10	8	80%		
A2	12	11	92%	85%	20 μL DMSO
A3	12	10	83%		
A4	13	13	100%		
A5	13	12	92%	95%	blank
A6	12	11	92%		

Trichloro-DDS					
well	live shrimps (t = 0)	live shrimps (t = 24 h)	alive	average [%]	conditions [μM]
A1	10	0	0%		
A2	14	0		0%	154.0
A3	11	0	0%		
A4	14	0	0%		
A5	10	0	0%	0%	76.9
A6	11	0	0%		
B1	14	0	0%		
B2	9	0	0%	0%	38.5
B3	14	0	0%		
B4	11	0	0%		
B5	9	0	0%	0%	15.4
B6	10	0	0%		
C1	12	1	8%		
C2	15	1	7%	8%	7.7
C3	13	1	8%		
C4	10	3	30%		
C5	12	4	33%	36%	3.8
C6	11	5	45%		
D1	9	7	78%		
D2	12	10	83%	83%	1.5
D3	18	16	89%		
D4	9	9	100%		
D5	10	9	90%	94%	0.2
D6	14	13	93%		



Heptachloro-DDS						
well	live shrimps (t = 0)	live shrimps (t = 24 h)	alive	average [%]	conditions [μM]	sd [%]
A1	11	0	0%			
A2	12	0	0%	0%	126.9	0.0%
A3	10	0	0%			
A4	10	0	0%			
A5	13	0	0%	0%	63.5	0.0%
A6	14	0	0%			
B1	11	0	0%			
B2	12	0	0%	0%	31.7	0.0%
B3	13	0	0%			
B4	10	0	0%			
B5	10	0	0%	0%	12.7	0.0%
B6	10	0	0%			
C1	11	0	0%			
C2	10	0	0%	0%	6.3	0.0%
C3	10	0	0%			
C4	11	2	18%			
C5	10	1	10%	13%	3.2	4.7%
C6	10	1	10%			
D1	10	7	70%			
D2	10	8	80%	77%	1.3	5.8%
D3	10	8	80%			
D4	10	9	90%			
D5	11	11	100%	97%	0.1	5.8%
D6	10	10	100%			



13 Experimental Details for Part IV

General Procedure 1: Thermal [1,3]-Sigmatropic Rearrangement of Allylic Chlorohydrins

In a representative example, protected allylic chlorohydrin **192** (4.8 mg, 6.5 μmol , 1.0 equiv) was placed in a small vial and dissolved in propylene carbonate (0.13 mL). The vial was purged with argon and sealed with a teflon cap. The vial was then placed in an aluminum block and heated to 100 °C. After TLC showed >90% consumption of starting material (30 hours), the vial was removed from the block and allowed to cool to room temperature. The material was directly applied to a column and product **218** eluted via flash column chromatography (gradient hexanes/toluene 50:1 to 10:1, SiO_2).

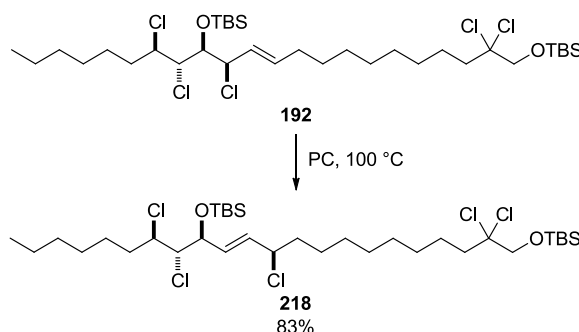
General Procedure 2: Cross-Metathesis of Allylic Chlorohydrins and Olefins

In a representative example, protected allylic chlorohydrin **123** (14 mg, 49 μmol , 1.0 equiv) and olefin **193** (54 mg, 150 μmol , 3.0 equiv) were placed in a flask equipped with a reflux condenser and put under argon. The substrates were dissolved in CH_2Cl_2 (2.4 mL, previously sparged 15 min with argon) and Grubbs' 2nd generation catalyst (**169**, 4.1 mg, 4.9 μmol , 10 mol%) was added. The reaction was heated at 40 °C for 24 h before solvent was removed. Conversion was checked by crude ^1H NMR and the material purified by quick flash column chromatography (hexanes/toluene 30:1, SiO_2) to give allylic chlorohydrin **192**.

General Procedure 3: Addition of Allyl Chloride to Aldehydes

In a representative example, to a solution of 2,2,6,6-tetramethylpiperidine (0.634 mL, 3.74 mmol, 2.20 equiv) in THF (7.6 mL) at -78 °C was added butyl lithium (1.6 M in hexanes, 2.16 mL, 3.57 mmol 2.10 equiv) dropwise. After

30 minutes, the solution was transferred to another flask, containing allyl chloride (0.291 mL, 3.57 mmol, 2.10 equiv) and diethylaluminum chloride (1.0 M in hexanes, 6.79 mL, 6.79 mmol, 4.0 equiv) in THF (15.2 mL) at $-78\text{ }^{\circ}\text{C}$, via canula transfer. After another 30 minutes, crude aldehyde **177** (theoretical: 0.3 g, 1.70 mmol, 1.00 equiv) in THF (1.5 mL) was added dropwise. After stirring for 4 hours at $-78\text{ }^{\circ}\text{C}$, sat. aq. NH_4Cl and sat. aq. Rochelle's salt were added and the reaction was allowed to warm to room temperature. The reaction was stirred vigorously until two clear phases formed (ca. 1h), before being extracted with Et_2O three times. Combined organic phases were dried over Na_2SO_4 , filtered, and concentrated. Flash column chromatography (hexanes/ EtOAc 20:1, SiO_2) gave product **175**.

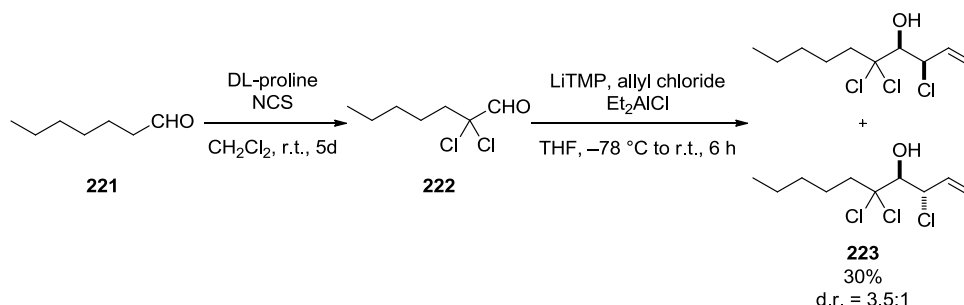


8,17,17-trichloro-5-1,2-dichlorooctyl)-2,2,3,3,20,20,21,21-octamethyl-4,19-dioxa-3,20-disiladocos-6-ene (218): According to General Procedure 1, protected allylic chlorohydrin **192** (4.8 mg, 6.5 μmol , 1.0 equiv) was stirred for 30 hours at $100\text{ }^{\circ}\text{C}$ in propylene carbonate (0.13 mL). Purification by flash column chromatography (hexanes/toluene gradient 50:1 to 10:1, SiO_2) gave **218** as colorless oil (4.0 mg, 5.4 μmol , 83%).

$^1\text{H NMR}$ (CDCl_3 , 400 MHz) δ 5.78 (dd, $J = 15.3, 8.6$ Hz, 1H), 5.65 (dd, $J = 15.4, 7.4$ Hz, 1H), 4.51 (dd, $J = 7.3, 5.7$ Hz, 1H), 4.36 (dt, $J = 8.6, 7.0$ Hz, 1H), 4.09 (ddd, $J = 9.8, 6.3, 2.5$ Hz, 1H), 4.00 (t, $J = 6.0$ Hz, 1H), 3.92 (s, 2H), 2.22 – 2.13 (m, 2H), 2.01 – 1.89 (m, 1H), 1.89 – 1.70 (m, 2H), 1.67 – 1.52 (m, 5H), 1.38 – 1.27 (m, 16H), 0.92 (s, 9H), 0.90 (s, 9H), 0.93 – 0.86 (m, 3H), 0.11 (s, 6H), 0.10 (s, 3H), 0.08 (s, 3H); $^{13}\text{C NMR}$ (CDCl_3 , 101 MHz) δ 135.2, 130.7, 93.6, 74.0, 72.3, 69.5, 62.4, 61.9, 43.7, 38.7, 33.5, 31.8, 29.9, 29.5, 29.4, 29.2, 29.1, 29.0, 26.6, 26.1, 25.9, 25.9, 24.9, 22.7, 14.3, 14.2, -3.7, -4.7, -5.2; **HRMS** (ESI) exact mass for $\text{C}_{34}\text{H}_{71}\text{Cl}_5\text{NO}_2\text{Si}_2$

Experimental

$[M+NH_4]^+$, calculated 756.3460, found 756.3448; **IR (thin film, cm^{-1})** ν 2954, 2929, 2857, 1463, 1257, 1118, 970, 838, 778, 697.



3,5,5-trichlorodec-1-en-4-ol (223): To a solution of heptanal (1.22 mL, 8.76 mmol, 1.00 equiv) in CH_2Cl_2 (17.5 mL) at $0\text{ }^\circ\text{C}$ was added DL-proline (0.500 g, 4.38 mmol, 0.500 mol%). After 10 minutes, *N*-chlorosuccinimide (2.92 g, 21.9 mmol, 2.50 equiv) was added and cooling was removed. After 5 days, pentane was added and the reaction was filtered through a plug of silica, eluting with pentane/ CH_2Cl_2 1:1. The solution was concentrated and the residue filtered through a plug of silica, eluting with pentane/ Et_2O 10:1. The solution was concentrated and crude aldehyde **222** (1.03 g) directly used in the next reaction.

According to General Procedure 3, LiTMP was prepared from tetramethylpiperidine (2.37 mL, 13.9 mmol, 2.20 equiv) and *n*-BuLi (1.6 M in hexanes, 8.3 mL, 13 mmol, 2.1 equiv) in THF (28 mL) and added to a solution of allyl chloride (1.1 mL, 13 mmol, 2.1 equiv) and diethylaluminum chloride (25% in toluene, 14 mL, 25 mmol, 4.0 equiv) in THF (57 mL). Crude aldehyde **222** (1.16 g) in THF (5.7 mL) was added. After 6 hours, the reaction was worked up and purified by flash column chromatography (hexanes/ Et_2O 15:1, SiO_2) to give **223** (0.77 g, 3.0 mmol, 30%, d.r. = 3.5:1).

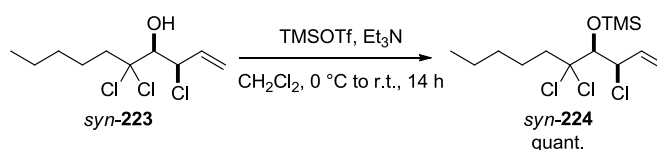
Spectroscopic data for *syn*-**223** (major):

1H NMR (400 MHz, $CDCl_3$) δ 6.09 (ddd, $J = 16.9, 10.1, 8.5$ Hz, 1H), 5.48 – 5.37 (m, 1H), 5.28 (dd, $J = 10.1, 0.9$ Hz, 1H), 5.18 – 5.11 (m, 1H), 4.00 (dd, $J = 9.7, 2.2$ Hz, 1H), 2.98 (d, $J = 9.7$ Hz, 1H), 2.43 – 2.16 (m, 2H), 1.78 – 1.63 (m, 2H), 1.43 – 1.27 (m, 4H), 0.98 – 0.90 (m, 3H); **^{13}C NMR ($CDCl_3, 101$ MHz)** δ 136.3, 118.1, 96.0, 79.3, 63.2, 44.6, 31.4, 24.5, 22.6, 14.1; **HRMS (ESI)** exact mass for $C_{34}H_{71}Cl_5NO_2Si_2$

$[M+NH_4]^+$, calculated 756.3460, found 756.3445; **IR (thin film, cm^{-1})** ν 3828, 2958, 2932, 2873, 1467, 1421, 1380, 1244, 1107, 1083, 987, 931, 858, 788, 731, 622.

Spectroscopic data for *anti*-**223** (minor), analytical sample obtained from repeated flash column chromatography:

1H NMR (400 MHz, $CDCl_3$) δ 6.22 (ddd, $J = 17.0, 10.2, 8.8$ Hz, 1H), 5.48 (dt, $J = 17.0, 1.1$ Hz, 1H), 5.38 (dd, $J = 10.3, 1.0$ Hz, 1H), 5.11 (dd, $J = 8.8, 2.3$ Hz, 1H), 4.34 (dd, $J = 7.0, 2.2$ Hz, 1H), 2.66 (d, $J = 7.0$ Hz, 1H), 2.33 – 2.16 (m, 2H), 1.77 – 1.65 (m, 2H), 1.44 – 1.26 (m, 5H), 0.97 – 0.90 (m, 3H); **^{13}C NMR ($CDCl_3, 101$ MHz)** δ 133.3, 120.5, 95.8, 82.4, 62.4, 44.2, 31.3, 24.6, 22.6, 14.1; **HRMS (ESI)** exact mass for $C_{34}H_{71}Cl_5NO_2Si_2$ $[M+NH_4]^+$, calculated 756.3460, found 756.3445; **IR (thin film, cm^{-1})** ν 3522, 2957, 2930, 2872, 2860, 1467, 1423, 1380, 1311, 1243, 1107, 1080, 1016, 989, 932, 859, 799, 731, 702, 662, 620.



((2-chloro-1-(3-hexyloxiran-2-yl)but-3-en-1-yl)oxy)trimethylsilane

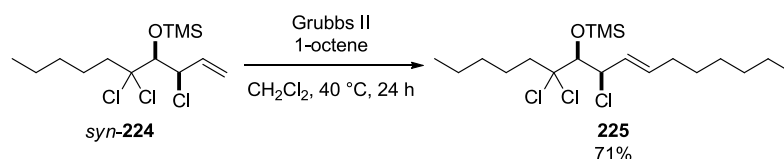
(*syn*-224): To a solution of alcohol *syn*-**223** (50 mg, 0.19 mmol, 1.0 equiv) in CH_2Cl_2 (1.9 mL) at 0 °C was added triethylamine (140 μ L, 0.96 mmol, 5.0 equiv) and trimethylsilyl trifluoromethanesulfonate (110 μ L, 0.58 mmol, 3.0 equiv). The reaction was allowed to warm to room temperature during 14 hours. Sat. aq. $NaHCO_3$ was added and the mixture extracted three times with CH_2Cl_2 . Combined organic phases were dried over Na_2SO_4 , filtered, and concentrated. Filtration through a silica plug, eluting with hexanes/ CH_2Cl_2 1:1, gave *syn*-**224** (66 mg, 0.19 mmol, quant.).

1H NMR ($CDCl_3, 400$ MHz) δ 5.97 (ddd, $J = 16.8, 10.1, 8.1$ Hz, 1H), 5.37 (dt, $J = 16.8, 1.0$ Hz, 1H), 5.23 (dt, $J = 10.0, 0.9$ Hz, 1H), 4.95 (dd, $J = 8.2, 2.7$ Hz, 1H), 4.18 (d, $J = 2.7$ Hz, 1H), 2.37 – 2.18 (m, 2H), 1.73 (dddd, $J = 9.4, 7.8, 6.5, 4.7$ Hz, 2H), 1.41 – 1.29 (m, 4H), 0.96 – 0.87 (m, 3H), 0.22 (s, 9H); **^{13}C NMR ($CDCl_3, 101$ MHz)** δ 136.8, 117.7, 97.5, 83.7, 62.9, 42.3, 31.5, 24.8, 22.7, 14.1, 0.8; **HRMS (EI+)** exact mass for $C_{12}H_{22}Cl_3OSi$ $[M-CH_3]^+$, calculated 315.0500, found 315.0547; exact mass for $C_{10}H_{21}Cl_2OSi$ $[M-C_3H_4Cl]^+$, calculated 255.0734, found 255.0736; **IR (thin**

film, cm⁻¹) ν 2958, 2934, 2860, 2874, 1467, 1252, 1152, 1031, 988, 929, 873, 843, 756, 702, 640.

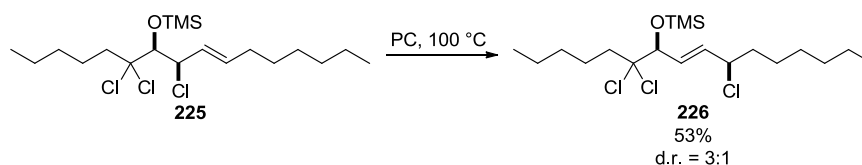
The same procedure for *anti*-**223** (20.0 mg, 77.0 μ mol, 1.00 equiv) gave *anti*-**224** (24.5 mg, 74.0 μ mol, 96%).

¹H NMR (CDCl₃, 400 MHz) δ 6.15 (ddd, J = 17.2, 10.1, 9.1 Hz, 1H), 5.35 (dt, J = 17.7, 1.0 Hz, 1H), 5.24 (dd, J = 10.0, 1.4 Hz, 1H), 5.14 – 5.08 (m, 1H), 4.43 (d, J = 1.3 Hz, 1H), 2.10 – 2.01 (m, 2H), 1.68 (dddd, J = 11.0, 7.3, 5.5, 3.8 Hz, 2H), 1.40 – 1.21 (m, 4H), 0.91 (t, J = 6.9 Hz, 3H), 0.26 (s, 9H); **¹³C NMR (CDCl₃, 101 MHz)** δ 134.7, 119.3, 96.4, 85.7, 63.2, 42.3, 31.4, 24.5, 22.6, 14.1, 0.6; **HRMS (EI+)** exact mass for C₁₂H₂₂Cl₃OSi [M-CH₃]⁺, calculated 315.0500, found 315.0521; exact mass for C₁₀H₂₁Cl₂OSi [M-C₃H₄Cl]⁺, calculated 255.0734, found 255.0741; **IR (thin film, cm⁻¹)** ν 2959, 2927, 1857, 1466, 1423, 1252, 1144, 1010, 992, 930, 902, 845, 755.



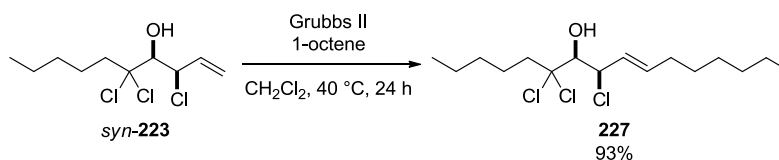
trimethyl((6,6,8-trichlorohexadec-9-en-7-yl)oxy)silane (225): According to General Procedure 2, protected allylic chlorohydrin *syn*-**224** (69.8 mg, 210 μ mol, 1.00 equiv) and 1-octene (99 μ L, 630 μ mol, 3.0 equiv) were dissolved in CH₂Cl₂ (10.5 mL). Grubbs' second generation catalyst (**169**, 18.0 mg, 21.0 μ mol, 10.0 mol%) was added. Purification by flash column chromatography (hexanes, SiO₂) gave **225** (62.0 mg, 149 μ mol, 71%).

¹H NMR (CDCl₃, 400 MHz) δ 5.76 (dt, J = 15.2, 6.6 Hz, 1H), 5.60 (ddt, J = 15.1, 8.9, 1.4 Hz, 1H), 4.90 (dd, J = 8.9, 3.1 Hz, 1H), 4.15 (d, J = 3.2 Hz, 1H), 2.35 – 2.17 (m, 2H), 2.11 – 2.01 (m, 2H), 1.78 – 1.66 (m, 2H), 1.43 – 1.21 (m, 12H), 0.92 (t, J = 6.9 Hz, 3H), 0.93 – 0.84 (m, 3H), 0.23 (s, 9H); **¹³C NMR (CDCl₃, 101 MHz)** δ 134.5, 128.9, 97.5, 84.2, 63.4, 42.4, 32.1, 31.8, 31.5, 29.1, 28.8, 24.8, 22.7, 22.7, 14.2, 14.1, 0.8; **HRMS (EI+)** exact mass for C₁₈H₃₄Cl₃OSi [M-CH₃]⁺, calculated 399.1445, found 399.1477; **IR (thin film, cm⁻¹)** ν 2957, 2927, 2856, 1466, 1379, 1252, 1151, 967, 937, 875, 843, 755, 687, 624.



trimethyl((6,6,10-trichlorohexadec-8-en-7-yl)oxy)silane (226): According to General Procedure 1, protected allylic chlorohydrin **225** (15.0 mg, 36.0 μmol , 1.00 equiv) was stirred for 4 days at 100 °C in propylene carbonate (0.13 mL). Extracting 10 times with hexanes was followed by concentration *in vacuo*. The residue was purified by flash column chromatography (hexanes, SiO_2) gave **226** as an inseparable mixture of diastereomers (7.9 mg, 19 μmol , 53%, d.r. = 3:1).

$^1\text{H NMR}$ (CDCl_3 , 400 MHz) δ 5.98 – 5.75 (m, 2H), 4.47 – 4.29 (m, 2H), 2.16 – 2.01 (m, 2H), 1.94 – 1.74 (m, 2H), 1.73 – 1.62 (m, 2H), 1.50 – 1.21 (m, 14H), 0.90 (m, 7H), 0.17 (s, 9H); $^{13}\text{C NMR}$ (CDCl_3 , 101 MHz) δ (only peaks of major diastereomer reported) 135.9, 129.7, 96.6, 80.5, 62.0, 42.8, 38.7, 31.8, 31.5, 28.8, 26.6, 24.4, 22.7, 22.7, 14.2, 14.1, 0.5; **HRMS** (EI+) exact mass for $\text{C}_{18}\text{H}_{34}\text{Cl}_3\text{OSi}$ [$\text{M}-\text{CH}_3$] $^+$, calculated 399.1445, found 399.1439; **IR** (thin film, cm^{-1}) ν 2957, 2930, 2860, 1467, 1252, 1129, 1099, 970, 883, 843, 752.



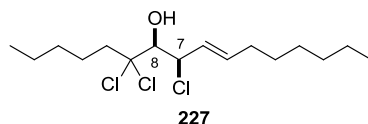
6,6,8-trichlorohexadec-9-en-7-ol (227): According to General Procedure 2, allylic chlorohydrin *syn*-**223** (8.3 mg, 320 μmol , 1.0 equiv) and 1-octene (15 μL , 96 μmol , 3.0 equiv) were dissolved in CH_2Cl_2 (1.6 mL). Grubbs' second generation catalyst (2.7 mg, 3.2 μmol , 10 mol%) was added. Purification by flash column chromatography (hexanes/ Et_2O 50:1, SiO_2) gave **227** (10.2 mg, 30.0 μmol , 93%).

$^1\text{H NMR}$ (CDCl_3 , 400 MHz) δ 5.82 (dt, $J = 15.2, 6.5$ Hz, 1H), 5.70 (ddt, $J = 15.2, 9.0, 1.3$ Hz, 1H), 5.09 (dd, $J = 9.0, 2.6$ Hz, 1H), 3.95 (dd, $J = 9.3, 2.6$ Hz, 1H), 2.97 (d, $J = 9.2$ Hz, 1H), 2.41 – 2.15 (m, 2H), 2.13 – 2.02 (m, 2H), 1.75 – 1.62 (m, 2H), 1.46 – 1.21 (m, 12H), 0.92 (t, $J = 6.3$ Hz, 3H), 0.88 (t, $J = 6.3$ Hz, 3H); $^{13}\text{C NMR}$ (CDCl_3 , 101 MHz) δ 135.4, 128.4, 96.0, 79.7, 64.1, 44.7, 32.1, 31.8, 31.4, 29.0, 28.7,

Experimental

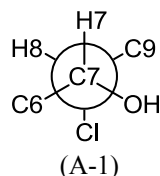
24.5, 22.7, 22.6, 14.2, 14.1; **HRMS** (ESI) exact mass for $C_{16}H_{29}Cl_3NaO$ $[M+Na]^+$, calculated 365.1176, found 365.1168; **IR** (thin film, cm^{-1}) ν 3526, 2957, 2927, 2872, 2857, 1664, 1467, 1379, 1271, 1252, 1228, 1108, 1078, 1012, 966, 917, 857, 784, 730, 702, 666, 611, 563.

JBCA for diol **227**:

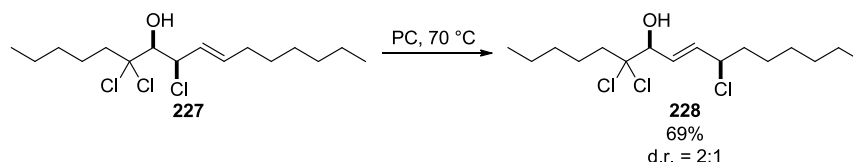


C11-C12

$^3J_{H7-H8}$	2.6 (s)
$^3J_{H7-C9}/^3J_{C6-H8}$	2.8 (s)/n.d.
$^2J_{C7-H8}/^2J_{C8-H7}$	-1.7 (m)/0.6 (s)



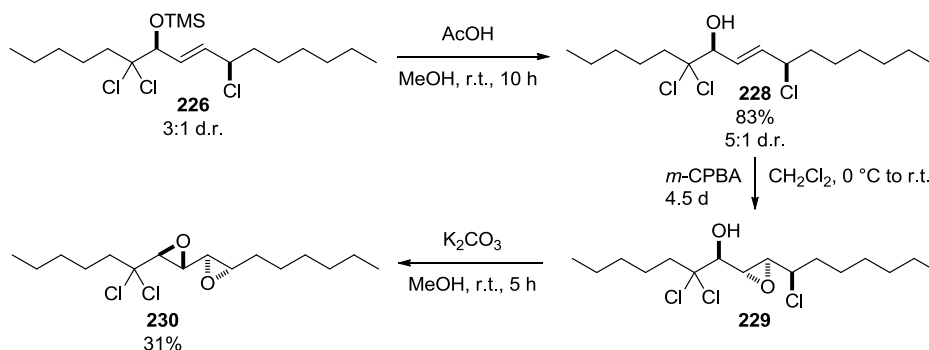
Coupling constants are reported in Hertz (Hz). All spectra were recorded in $CDCl_3$. Heteronuclear coupling constants were determined in a HSQC-HECADE spectrum. n.d. = not determined, due to weak peak intensity, overlap, or a signal of higher order. s = small, m = medium, l = large.



6,6,10-trichlorohexadec-8-en-7-ol (28): According to General Procedure 1, allylic chlorohydrin **227** (10.0 mg, 29.0 μ mol, 1.00 equiv) was stirred for 48 hours at 70 $^{\circ}C$ in propylene carbonate (0.58 mL). Extracting 10 times with hexanes was followed by concentration *in vacuo*. The residue was purified by flash column chromatography (hexanes/ Et_2O 9:1, SiO_2) gave **228** as an inseparable mixture of diastereomers (6.9 mg, 20 μ mol, 69%, d.r. = 2:1).

1H NMR ($CDCl_3$, 400 MHz) δ 6.05 – 5.91 (m, 2H), 4.42 (m, 2H), [major: 2.45 (d, J = 6.9 Hz, 1H), minor: 2.46 (d, J = 6.9 Hz, 1H)], 2.31 – 2.07 (m, 2H), 1.92 – 1.79 (m, 2H), 1.79 – 1.65 (m, 2H), 1.43 – 1.21 (m, 12H), 1.01 – 0.84 (m, 6H); ^{13}C NMR ($CDCl_3$, 101 MHz) δ (only peaks for major diastereomer reported) δ 136.6, 128.0, 97.7, 79.1, 61.8, 43.4, 38.6, 31.8, 31.4, 28.8, 26.5, 24.5, 22.7, 22.6, 14.2, 14.1; **HRMS**

(EI+) base peak: exact mass for $C_{10}H_{18}ClO$ $[M-C_6H_{11}Cl_2]^+$, calculated 189.1046, found 189.1032 (other unassignable peaks: 270.1809, 234.1978, 153.1268, 135.1167); **IR (thin film, cm^{-1})** ν 3419, 2956, 2930, 2859, 1654, 1597, 1466, 1379, 1243, 1125, 1057, 969, 858, 779, 729, 641.



3-(1,1-dichlorohexyl)-3'-hexyl-2,2'-bioxirane (230): Silyl ether **226** (7.9 mg, 19 μ mol, 1.0 equiv) was dissolved in MeOH (0.25 ml) and AcOH (10 μ L, 0.18 mmol, 8.5 equiv) was added. After 10 hours, toluene was added and solvent removed. Flash column chromatography (hexanes/ Et_2O 9:1, SiO_2) gave **7** (5.9 mg, 17 μ mol, 90%, d.r. = 5:1).

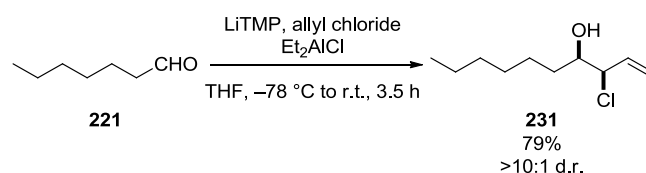
Alcohol **228** (5.9 mg, 17 μ mol, 1.0 equiv) was dissolved in CH_2Cl_2 and cooled to 0 $^{\circ}C$. *meta*-Chloroperbenzoic acid (4.6 mg, 21 μ mol, 1.2) was added and cooling removed. After 48 h, more *meta*-chloroperbenzoic acid (2.7 mg, 12 μ mol, 0.7 equiv) was added. After another 48 h, more *meta*-chloroperbenzoic acid (1.2 mg, 5.2 μ mol, 0.3 equiv) was added. After 8 more hours, sat. aq. $Na_2S_2O_3$ was added and the reaction stirred for another 15 minutes. The mixture was then poured into sat. aq. $NaHCO_3$ and extracted three times with Et_2O . Combined organic phases were dried over Na_2SO_4 , filtered, and concentrated. Flash column chromatography (hexanes/ Et_2O 9:1) gave an inconclusive 2:1 mixture containing **229** as the major product (3.8 mg).

The crude material of **229** (3.8 mg) was taken up into MeOH (1.0 mL). Potassium carbonate (4.4 mg, 32 μ mol, ca. 3 equiv) was added and the reaction was stirred for 5 hours. The mixture was filtered through a silica plug, eluting with CH_2Cl_2 . Flash column chromatography (hexanes/ Et_2O) gave an inseparable mixture of

Experimental

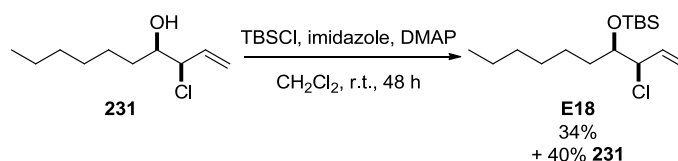
compounds, with **230** as the major. Repeated flash column chromatography (cyclohexane/toluene 3:1, SiO₂) gave **X35** (1.7 mg, 5.3 μmol, 50%).

¹H NMR (CDCl₃, 400 MHz) δ 3.38 (d, *J* = 1.9 Hz, 1H), 3.36 (dd, *J* = 3.9, 1.9 Hz, 1H), 2.90 (ddd, *J* = 6.0, 5.2, 2.1 Hz, 1H), 2.84 (dd, *J* = 3.9, 2.1 Hz, 1H), 2.24 – 2.13 (m, 2H), 1.74 – 1.64 (m, 2H), 1.63 – 1.51 (m, 2H), 1.49 – 1.40 (m, 2H), 1.39 – 1.21 (m, 10H), 0.91 (t, *J* = 7.0 Hz, 3H), 0.89 (t, *J* = 7.0 Hz, 3H); **¹³C NMR (CDCl₃, 101 MHz)** δ 90.2, 61.8, 57.6, 56.3, 54.9, 45.4, 31.8, 31.6, 31.3, 29.1, 25.9, 24.4, 22.7, 22.5, 14.2, 14.1; **HRMS (EI+)** exact mass for C₁₆H₂₇O₂ [M-HCl-Cl]⁺, calculated 251.2011, found 251.2004; exact mass for C₁₀H₁₇O₂ [M-C₆H₁₁Cl₂]⁺, calculated 169.1229, found 169.1224; **IR (thin film, cm⁻¹)** ν 2956, 2928, 2858, 1466, 1379, 1124, 917, 898, 858, 815, 778, 731, 610.



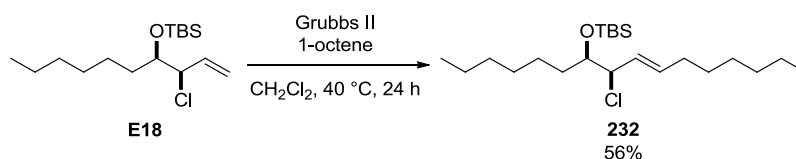
3-chlorodec-1-en-4-ol (231): According to General Procedure 3, LiTMP was prepared from tetramethylpiperidine (0.98 mL, 5.8 mmol, 2.2 equiv) and *n*-BuLi (1.6 M in hexanes, 3.5 mL, 5.5 mmol, 2.1 equiv) in THF (12 mL) and added to a solution of allyl chloride (0.45 mL, 5.5 mmol, 2.1 equiv) and diethylaluminum chloride (25% in toluene, 5.7 mL, 11 mmol, 4.0 equiv) in THF (24 mL). Heptanal (**221**, 0.37 mL, 2.6 mmol, 1.0 equiv) was added. After 3.5 hours, the reaction was worked up and purified by flash column chromatography (hexanes/Et₂O 4:1, SiO₂) to give **231** (0.34 g, 2.1 mmol, 79%, d.r. = 10:1).

¹H NMR (CDCl₃, 400 MHz) δ 5.95 (ddd, *J* = 16.9, 10.1, 8.6 Hz, 1H), 5.37 (dd, *J* = 17.1, 1.2 Hz, 1H), 5.26 (dd, *J* = 10.2, 0.8 Hz, 1H), 4.33 (dd, *J* = 8.7, 5.7 Hz, 1H), 3.66 (dtd, *J* = 7.9, 5.7, 3.7 Hz, 1H), 2.10 (d, *J* = 5.6 Hz, 1H), 1.67 – 1.18 (m, 10H), 0.93 – 0.84 (m, 3H); **¹³C NMR (CDCl₃, 101 MHz)** δ 135.5, 119.1, 74.4, 69.2, 33.9, 31.9, 29.3, 25.6, 22.7, 14.2; **HRMS (EI+)** exact mass for C₁₀H₁₉O [M-Cl]⁺, calculated 155.1436, found 155.1421; **IR (thin film, cm⁻¹)** ν 3402, 2955, 2927, 2858, 1466, 1421, 1379, 1146, 1069, 988, 928, 763, 725.



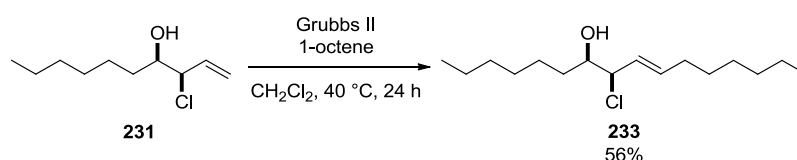
tert-butyl((3-chlorodec-1-en-4-yl)oxy)dimethylsilane (E18): To a solution of alcohol **231** (0.10 g, 0.52 mmol, 1.0 equiv, d.r. > 10:1) in CH₂Cl₂ (5.2 mL) were added imidazole (71 mg, 1.1 mmol, 2.0 equiv) and *tert*-butyldimethylsilyl chloride (119 mg, 0.787 mmol, 1.50 equiv). The reaction was stirred for 24 hours before 4-dimethylaminopyridine (6.4 mg, 52 μmol, 10 mol%) were added. The reaction was stirred for another 24 hours, after which water was added and the mixture extracted three times with CH₂Cl₂. Combined organic phases were dried over Na₂SO₄, filtered, and concentrated. Flash column chromatography (hexanes followed by hexanes/Et₂O 4:1, SiO₂) gave **E18** (55 mg, 0.18 mmol, 34%) and **231** (40 mg, 0.21 mmol, 40%, d.r. > 10:1).

¹H NMR (CDCl₃, 400 MHz) δ 5.96 (ddd, *J* = 17.0, 10.3, 7.8 Hz, 1H), 5.32 (dt, *J* = 17.0, 1.3 Hz, 1H), 5.21 (dt, *J* = 10.2, 1.1 Hz, 1H), 4.33 (ddt, *J* = 7.8, 4.7, 1.0 Hz, 1H), 3.78 (dt, *J* = 7.2, 4.4 Hz, 1H), 1.78 – 1.59 (m, 1H), 1.47 – 1.20 (m, 9H), 0.90 (s, 9H), 0.91 – 0.86 (m, 3H), 0.09 (s, 3H), 0.08 (s, 3H); ¹³C NMR (CDCl₃, 101 MHz) δ 135.1, 118.1, 75.6, 65.8, 32.9, 31.9, 29.5, 26.0, 25.3, 22.8, 18.3, 14.2, -4.2, -4.3; HRMS (EI⁺) exact mass for C₁₂H₂₄ClOSi [M-C₄H₉]⁺, calculated 247.1280, found 247.1284; IR (thin film, cm⁻¹) ν 2955, 2929, 2858, 1463, 1362, 1101, 1057, 1005, 988, 924, 898, 834, 774, 705, 663.



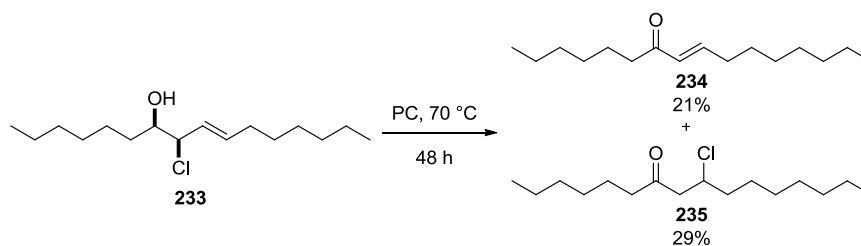
tert-butyl((8-chlorohexadec-9-en-7-yl)oxy)dimethylsilane (232): According to General Procedure 2, allylic chlorohydrin **E18** (0.194 g, 0.636 mmol, 1.00 equiv) and 1-octene (0.30 mL, 1.9 mmol, 3.0 equiv) were dissolved in CH₂Cl₂ (31.8 mL). Grubbs' second generation catalyst (**169**, 54.0 mg, 64.0 μmol, 10.0 mol%) was added. Purification by flash column chromatography (hexanes, SiO₂) gave **232** as an inseparable 1.9:1 mixture with **E18** (148 mg, ca. 50%).

^1H NMR (CDCl_3 , 400 MHz) δ (only peaks for **XX36** reported) 5.70 (dt, $J = 15.2, 6.7$ Hz, 1H), 5.59 – 5.50 (m, 1H), 4.30 (dd, $J = 8.8, 4.9$ Hz, 1H), 3.79 – 3.70 (m, 1H), 2.05 (dddd, $J = 12.8, 7.0, 3.9, 2.0$ Hz, 2H), 1.73 – 1.59 (m, 2H), 1.43 – 1.22 (m, 16H), 0.91 – 0.89 (m, 15H), 0.11 – 0.06 (m, 6H); ^{13}C NMR (CDCl_3 , 101 MHz) δ (only peaks for **XX36** reported) 135.3, 127.3, 75.8, 66.5, 33.2, 32.3, 31.9, 31.8, 29.5, 29.0, 28.9, 26.1, 26.0, 26.0, 22.8, 18.3, 14.2, -4.2, -4.3; HRMS (EI+) exact mass for $\text{C}_{18}\text{H}_{36}\text{ClOSi} [\text{M}-\text{C}_4\text{H}_9]^+$, calculated 331.2219, found 331.2211; IR (thin film, cm^{-1}) ν 2956, 2928, 1857, 1463, 1379, 1362, 1255, 1105, 1005, 965, 925, 897, 835, 775, 723.



8-chlorohexadec-9-en-7-ol (233): According to General Procedure 2, allylic chlorohydrin **231** (10.0 mg, 52 μmol , 1.0 equiv) and 1-octene (24 μL , 0.16 mmol, 3.0 equiv) were dissolved in CH_2Cl_2 (2.6 mL). Grubbs' second generation catalyst (**169**, 4.5 mg, 5.2 μmol , 10 mol%) was added. Purification by flash column chromatography (hexanes/ Et_2O 8:1, SiO_2) gave **233** (13 mg, 48 μmol , 91%, d.r. > 10:1).

^1H NMR (CDCl_3 , 400 MHz) δ 5.78 (dt, $J = 15.3, 6.7$ Hz, 1H), 5.56 (ddt, $J = 15.2, 9.3, 1.5$ Hz, 1H), 4.32 (dd, $J = 9.3, 6.3$ Hz, 1H), 3.74 – 3.52 (m, 1H), 2.15 (d, $J = 5.3$ Hz, 1H), 2.10 – 2.01 (m, 2H), 1.63 – 1.19 (m, 18H), 0.92 – 0.84 (m, 6H); ^{13}C NMR (CDCl_3 , 101 MHz) δ 136.5, 127.5, 74.8, 70.2, 33.9, 32.3, 31.9, 31.8, 29.4, 28.9, 28.9, 25.6, 22.7 (2C), 14.2 (2C); HRMS (EI+) exact mass for $\text{C}_{16}\text{H}_{31}\text{O} [\text{M}-\text{Cl}]^+$, calculated 239.2375, found 239.2368; IR (thin film, cm^{-1}) ν 3428, 2956, 2927, 2857, 1665, 1466, 1379, 1127, 1067, 967, 724.



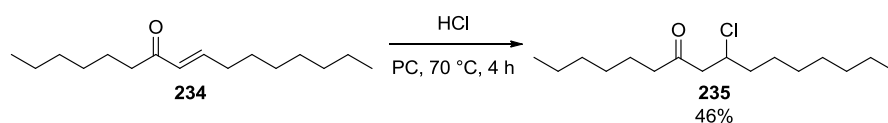
hexadec-8-en-7-one (234) & 9-chlorohexadecan-7-one (235): According to General Procedure 1, allylic chlorohydrin **233** (10 mg, 36 μmol , 1.0 equiv) was dissolved in propylene carbonate (0.73 mL). The reaction was stirred for 48 hours at 70 °C before being extracted ten times with hexanes. Purification by flash column chromatography (hexanes/Et₂O gradient 100:1 to 50:1, SiO₂) gave **234** (1.8 mg, 7.6 μmol , 21%) and **235** (2.9 mg, 11 μmol , 29%).

Spectroscopic data for **234**:

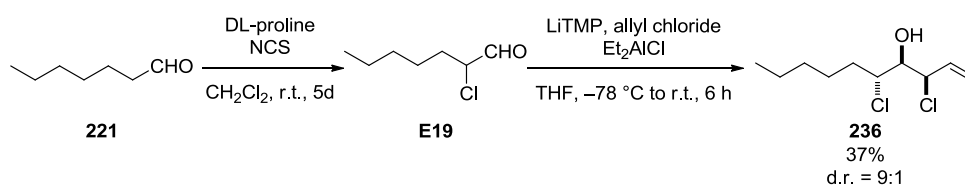
¹H NMR (CDCl₃, 400 MHz) δ 6.82 (dt, $J = 15.9, 6.9$ Hz, 1H), 6.08 (dt, $J = 15.9, 1.5$ Hz, 1H), 2.63 – 2.45 (m, 2H), 2.20 (qd, $J = 7.1, 1.5$ Hz, 2H), 1.65 – 1.57 (m, 2H), 1.51 – 1.39 (m, 4H), 1.36 – 1.20 (m, 12H), 0.92 – 0.84 (m, 6H); **¹³C NMR (CDCl₃, 101 MHz)** δ 201.2, 147.5, 130.5, 40.3, 32.6, 31.9, 31.8, 29.3, 29.2, 29.2, 28.3, 24.5, 22.8, 22.7, 14.2, 14.2; **HRMS (EI+)** exact mass for C₁₆H₃₀O [M]⁺, calculated 238.2292, found 238.2287; **IR (thin film, cm⁻¹)** ν 2956, 2927, 2856, 1698, 1675, 1631, 1466, 1378, 977, 724, 498.

Spectroscopic data for **235**:

¹H NMR (CDCl₃, 400 MHz) δ 4.34 (tt, $J = 8.3, 4.9$ Hz, 1H), 2.92 (dd, $J = 16.7, 8.3$ Hz, 1H), 2.71 (dd, $J = 16.7, 5.1$ Hz, 1H), 2.49 – 2.37 (m, 2H), 1.77 – 1.66 (m, 2H), 1.59 (td, $J = 7.4, 6.0$ Hz, 2H), 1.52 – 1.37 (m, 2H), 1.37 – 1.16 (m, 14H), 0.90 – 0.85 (m, 6H); **¹³C NMR (CDCl₃, 101 MHz)** δ 207.9, 57.7, 51.1, 44.0, 38.4, 31.9, 31.7, 29.3, 29.1, 29.0, 26.5, 23.6, 22.8, 22.6, 14.2, 14.2; **HRMS (EI+)** exact mass for C₁₆H₃₁O [M-Cl]⁺, calculated 239.2375, found 239.2371; **IR (thin film, cm⁻¹)** ν 2956, 2928, 2857, 1718, 1466, 1408, 1377, 1130, 1083, 724, 620, 498.



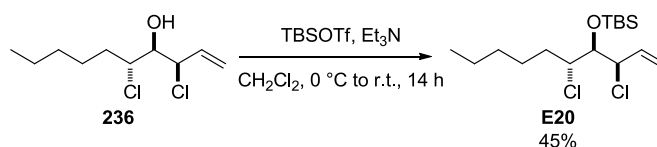
Reaction of 234 to 235: Allylic chlorohydrin **234** (1.5 mg, 6.3 μmol , 1.0 equiv) was dissolved in propylene carbonate (130 μL) and hydrogen chloride (4 M in dioxane, 5.0 μL , 19 μmol , 3.0 equiv) was added. The reaction was stirred for 4 hours at 70 $^\circ\text{C}$ and then filtered through a plug of silica, eluting with hexanes/ CH_2Cl_2 1:1. Purification by flash column chromatography (hexanes/ Et_2O gradient 100:1 to 50:1, SiO_2) gave **235** (0.8 mg, 2.9 μmol , 46%).



3,5-dichlorodec-1-en-4-ol (236): To a solution of heptanal (1.72 mL, 13.1 mmol, 1.00 equiv) in CH_2Cl_2 (26.3 mL) at 0 $^\circ\text{C}$ was added DL-proline (0.151 g, 1.31 mmol, 10.0 mol%). After 10 minutes, *N*-chlorosuccinimide (2.11 g, 15.8 mmol, 1.20 equiv) was added and cooling was removed. After 16 hours, pentane was added and the reaction was filtered through a plug of silica, eluting with pentane/ CH_2Cl_2 1:1. The solution was concentrated and the residue filtered through a plug of silica, eluting with pentane/ Et_2O 7:1. The solution was concentrated and crude aldehyde **E19** (1.7 g) directly used in the next reaction.

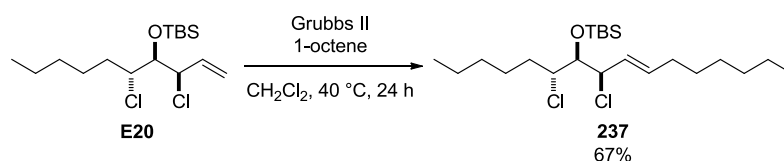
According to General Procedure 3, LiTMP was prepared from tetramethylpiperidine (4.0 mL, 24 mmol, 2.2 equiv) and *n*-BuLi (1.6 M in hexanes, 14 mL, 23 mmol, 2.1 equiv) in THF (48 mL) and added to a solution of allyl chloride (1.8 mL, 23 mmol, 2.1 equiv) and diethylaluminum chloride (1.0 M in hexanes, 43 mL, 43 mmol, 4.0 equiv) in THF (96 mL). Crude aldehyde **E19** (1.7 g) in THF (9.6 mL) was added. After 6 hours, the reaction was worked up and purified by flash column chromatography (hexanes/ Et_2O 10:1, SiO_2) to give **236** (1.1 g, 4.9 mmol, 37%, d.r. = 9:1).

¹H NMR (400 MHz, CDCl₃) δ 6.04 (ddd, *J* = 16.9, 10.2, 7.8 Hz, 1H), 5.45 (dt, *J* = 17.2, 1.2 Hz, 1H), 5.31 (d, *J* = 10.2 Hz, 1H), 5.09 – 5.00 (m, 1H), 3.98 – 3.89 (m, 1H), 3.70 (td, *J* = 8.9, 2.4 Hz, 1H), 2.12 (dd, *J* = 9.3, 1.4 Hz, 1H), 2.10 – 2.00 (m, 1H), 1.77 – 1.67 (m, 1H), 1.61 (dtd, *J* = 10.5, 4.2, 1.8 Hz, 1H), 1.49 – 1.21 (m, 5H), 0.90 (t, *J* = 6.9 Hz, 3H); **¹³C NMR (CDCl₃, 101 MHz)** δ 135.2, 119.3, 76.9, 65.3, 62.8, 33.4, 31.5, 25.7, 22.7, 14.1; **HRMS (EI+)** exact mass for C₇H₁₄ClO [M-C₃H₄Cl]⁺, calculated 149.0733, found 149.0730; exact mass for C₄H₆ClO [M-C₆H₁₂Cl]⁺, calculated 105.0107, found 105.0103; **IR (thin film, cm⁻¹)** ν 3437, 2957, 2929, 2861, 1467, 1421, 1379, 1281, 1255, 1087, 988, 933, 905, 852, 790, 776, 729, 701, 687, 497.



***tert*-butyl((3,5-dichlorodec-1-en-4-yl)oxy)dimethylsilane (E20):** To a solution of alcohol **236** (30 mg, 0.13 mmol, 1.0 equiv) in CH₂Cl₂ (1.3 mL) at 0 °C was added triethylamine (37 μL, 0.27 mmol, 2.0 equiv) and *tert*-butyldimethylsilyl trifluoromethanesulfonate (46 μL, 0.20 mmol, 1.5 equiv). The reaction was allowed to warm to room temperature during 14 hours. Water was added and the mixture extracted three times with CH₂Cl₂. Combined organic phases were dried over Na₂SO₄, filtered, and concentrated. Flash column chromatography (hexanes, SiO₂) gave **E20** (20 mg, 60 μmol, 45%, d.r. > 10:1).

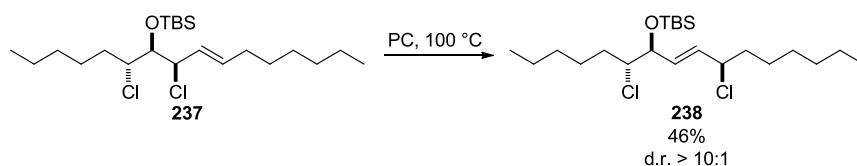
¹H NMR (CDCl₃, 400 MHz) δ 5.94 (ddd, *J* = 17.0, 10.2, 8.4 Hz, 1H), 5.34 (dt, *J* = 16.8, 1.1 Hz, 1H), 5.23 (dt, *J* = 10.2, 0.9 Hz, 1H), 4.61 (ddt, *J* = 8.5, 4.7, 0.9 Hz, 1H), 4.05 (ddd, *J* = 10.5, 4.8, 2.5 Hz, 1H), 3.95 (t, *J* = 4.8 Hz, 1H), 1.90 – 1.76 (m, 1H), 1.61 (dddd, *J* = 16.9, 10.6, 8.9, 4.3 Hz, 2H), 1.39 – 1.21 (m, 5H), 0.94 (s, 9H), 0.92 – 0.86 (m, 3H), 0.15 (s, 3H), 0.13 (s, 3H); **¹³C NMR (CDCl₃, 101 MHz)** δ 135.7, 118.4, 79.9, 65.2, 63.9, 32.7, 31.3, 26.4, 26.2, 22.7, 18.7, 14.1, -3.6, -3.6; **HRMS (EI+)** exact mass for C₁₆H₃₂Cl₂OSi [M-C₄H₉]⁺, calculated 281.0890, found 281.0901; **IR (thin film, cm⁻¹)** ν 2957, 2930, 1859, 1472, 1464, 1256, 1135, 1109, 990, 929, 836, 777, 709, 676.



***tert*-butyl((6,8-dichlorohexadec-9-en-7-yl)oxy)dimethylsilane (237):**

According to General Procedure 2, protected allylic chlorohydrin **X16** (20.0 mg, 59.0 μmol , 1.00 equiv) and 1-octene (28 μL , 180 μmol , 3.0 equiv) were dissolved in CH_2Cl_2 (2.9 mL). Grubbs' second generation catalyst (**169**, 5.0 mg, 5.9 μmol , 10 mol%) was added. Purification by flash column chromatography (hexanes, SiO_2) gave **237** (16.6 mg, 39.0 μmol , 67%, d.r. = 9:1).

$^1\text{H NMR}$ (CDCl_3 , 400 MHz) δ 5.73 (dt, $J = 14.9, 6.7$ Hz, 1H), 5.54 (ddt, $J = 15.2, 9.4, 1.5$ Hz, 1H), 4.55 (dd, $J = 9.3, 5.2$ Hz, 1H), 4.04 (ddd, $J = 10.5, 4.4, 2.5$ Hz, 1H), 3.96 – 3.86 (m, 1H), 2.13 – 1.99 (m, 2H), 1.87 – 1.70 (m, 1H), 1.69 – 1.52 (m, 2H), 1.41 – 1.20 (m, 13H), 0.94 (s, 9H), 0.92 – 0.86 (m, 6H), 0.15 (s, 3H), 0.14 (s, 3H); $^{13}\text{C NMR}$ (CDCl_3 , 101 MHz) δ 135.5, 127.7, 80.4, 65.7, 64.2, 32.4, 32.3, 31.8, 31.4, 29.1, 28.9, 26.5, 26.3, 22.7, 22.7, 18.7, 14.2, 14.2, -3.6, -3.7; **HRMS** (ESI) exact mass for $\text{C}_{22}\text{H}_{44}\text{ClOSi}$ $[\text{M}-\text{Cl}]^+$, calculated 387.2844, found 387.2841; **IR** (thin film, cm^{-1}) ν 2956, 2928, 2857, 1463, 1379, 1362, 1254, 1137, 1006, 969, 939, 836, 777, 680, 620.

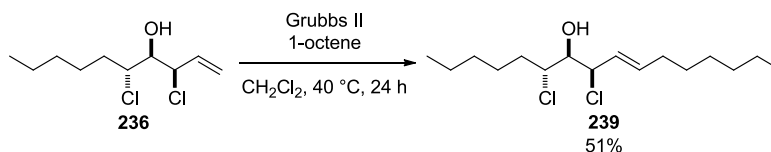


***tert*-butyl((6,10-dichlorohexadec-8-en-7-yl)oxy)dimethylsilane (238):**

According to General Procedure 1, protected allylic chlorohydrin **237** (8.0 mg, 19 μmol , 1.00 equiv) was stirred for 26 h at 100 $^\circ\text{C}$ in propylene carbonate (0.38 mL). Purification by flash column chromatography (hexanes, SiO_2) gave **238** as an inseparable mixture of diastereomers (3.7 mg, 8.7 μmol , 46%, d.r. > 10:1).

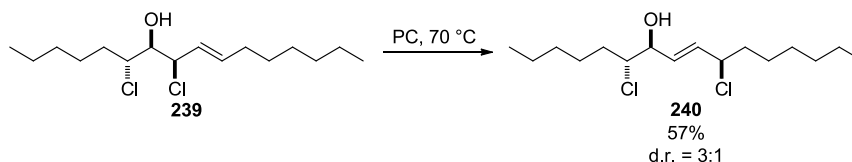
$^1\text{H NMR}$ (CDCl_3 , 400 MHz) δ 5.79 – 5.61 (m, 2H), 4.36 (q, $J = 7.2$ Hz, 1H), 4.17 (t, $J = 5.6$ Hz, 1H), 3.74 (ddd, $J = 9.5, 5.4, 3.1$ Hz, 1H), 1.90 – 1.71 (m, 3H), 1.66 – 1.51 (m, 3H), 1.48 – 1.15 (m, 12H), 0.94 – 0.78 (m, 6H), 0.90 (s, 9H) 0.09 (s, 3H),

0.05 (s, 3H); ^{13}C NMR (CDCl_3 , 101 MHz) δ 133.7, 132.3, 76.4, 66.5, 62.3, 38.8, 33.1, 31.8, 31.5, 28.8, 26.6, 26.1, 26.0, 22.7, 22.7, 18.3, 14.2, 14.2, -3.9, -4.7; HRMS (ESI) exact mass for $\text{C}_{22}\text{H}_{44}\text{Cl}_2\text{NaOSi}$ $[\text{M}+\text{Na}]^+$, calculated 445.2431, found 445.2421; IR (thin film, cm^{-1}) ν 2956, 2929, 2858, 1463, 1379, 1362, 1254, 1083, 1006, 968, 939, 836, 777, 727, 683.



6,8-dichlorohexadec-9-en-7-ol (239): According to General Procedure 2, allylic chlorohydrin **236** (24.0 mg, 107 μmol , 1.00 equiv, d.r. = 9:1) and 1-octene (45 μL , 280 μmol , 2.7 equiv) were dissolved in CH_2Cl_2 (4.0 mL). Grubbs' second generation catalyst (8.5 mg, 10 μmol , 9.4 mol%) was added. Purification by flash column chromatography (hexanes/ Et_2O 12:1, SiO_2) gave **239** (17 mg, 55 μmol , 51%).

^1H NMR (CDCl_3 , 400 MHz) δ 5.87 (dt, J = 15.3, 6.7 Hz, 1H), 5.68 (ddt, J = 15.2, 8.8, 1.4 Hz, 1H), 5.00 (dd, J = 8.9, 2.9 Hz, 1H), 3.93 (ddd, J = 9.6, 8.0, 2.7 Hz, 1H), 3.67 (ddd, J = 8.8, 8.1, 2.9 Hz, 1H), 2.18 (d, J = 9.0 Hz, 1H), 2.07 (td, J = 8.0, 7.4, 6.0 Hz, 2H), 2.04 – 1.94 (m, 1H), 1.78 – 1.67 (m, 1H), 1.66 – 1.55 (m, 1H), 1.48 – 1.22 (m, 13H), 0.93 – 0.85 (m, 6H); ^{13}C NMR (CDCl_3 , 101 MHz) δ 136.7, 127.1, 77.4, 66.1, 63.0, 33.1, 32.3, 31.8, 31.5, 29.0, 28.9, 25.8, 22.7, 22.7, 14.2, 14.2; HRMS (ESI) exact mass for $\text{C}_{16}\text{H}_{30}\text{Cl}_2\text{NaO}$ $[\text{M}+\text{Na}]^+$, calculated 331.1566, found 331.1562; IR (thin film, cm^{-1}) ν 3441, 2957, 2927, 2858, 1664, 1467, 1379, 1272, 1079, 967, 910, 852, 774, 728, 686, 611, 497.

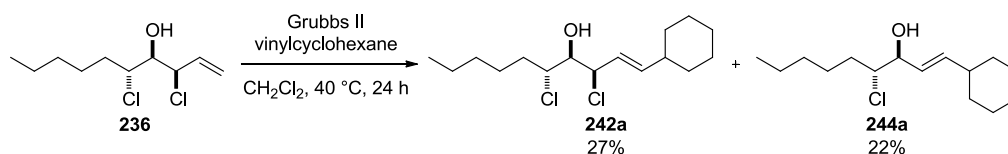


6,10-dichlorohexadec-8-en-7-ol (240): According to General Procedure 1, allylic chlorohydrin **239** (8.6 mg, 28 μmol , 1.0 equiv) was stirred for 48 h at 70 °C in propylene carbonate (0.55 mL). Purification by flash column chromatography

Experimental

(hexanes/Et₂O 7:1, SiO₂) gave **240** as an inseparable mixture of diastereomers (4.9 mg, 16 μmol, 57%, d.r. = 3:1).

¹H NMR (CDCl₃, 400 MHz) δ (only peaks for major diastereomer reported) 5.91 – 5.80 (m, 1H), 5.76 (dd, *J* = 15.3, 6.0 Hz, 1H), 4.38 (q, *J* = 7.2 Hz, 1H), 4.32 – 4.22 (m, 1H), 4.02 (dt, *J* = 9.7, 3.9 Hz, 1H), 2.15 (d, *J* = 6.4 Hz, 1H), 1.92 – 1.56 (m, 5H), 1.47 – 1.21 (m, 13H), 0.89 (td, *J* = 6.9, 4.6 Hz, 6H); **¹³C NMR (CDCl₃, 101 MHz)** δ (only peaks for major diastereomer reported) 134.8, 129.7, 74.6, 67.7, 62.0, 38.6, 33.3, 31.8, 31.4, 28.8, 26.6, 26.4, 22.7, 22.6, 14.2, 14.1; **HRMS (ESI)** exact mass for C₁₆H₃₀Cl₂NaO [M+Na]⁺, calculated 331.1566, found 331.1569; **IR (thin film, cm⁻¹)** ν 3400, 2956, 2929, 2859, 1466, 1379, 1234, 1128, 1038, 969, 853, 727.



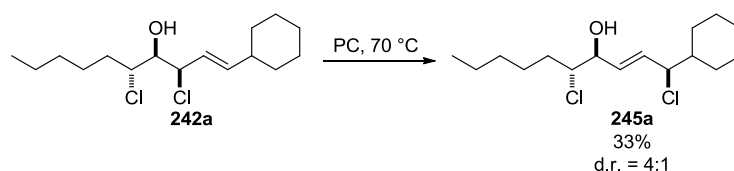
3,5-dichloro-1-cyclohexyldec-1-en-4-ol (242a): According to General Procedure 2, allylic chlorohydrin **236** (23.5 mg, 104 μmol, 1.00 equiv, d.r. = 9:1) and vinylcyclohexane (43 μL, 310 μmol, 3.0 equiv) were dissolved in CH₂Cl₂ (5.2 mL). Grubbs' second generation catalyst (**169**, 8.9 mg, 10 μmol, 10 mol%) was added. Purification by flash column chromatography (hexanes/Et₂O 10:1, SiO₂) gave **242a** (8.5 mg, 28 μmol, 27%) and **244a** (6.0 mg, 23 μmol, 22%).

Spectroscopic data for **242a**:

¹H NMR (CDCl₃, 400 MHz) δ 5.80 (ddd, *J* = 15.4, 6.6, 0.7 Hz, 1H), 5.63 (ddd, *J* = 15.4, 8.9, 1.3 Hz, 1H), 4.97 (dd, *J* = 8.8, 3.0 Hz, 1H), 3.93 (ddd, *J* = 9.6, 7.9, 2.7 Hz, 1H), 3.67 (ddd, *J* = 8.8, 7.9, 3.1 Hz, 1H), 2.19 (d, *J* = 8.9 Hz, 1H), 2.01 (dddd, *J* = 14.2, 10.0, 5.7, 2.6 Hz, 2H), 1.79 – 1.56 (m, 7H), 1.47 – 1.03 (m, 9H), 0.90 (t, *J* = 6.9 Hz, 3H), 0.88 – 0.79 (m, 1H); **¹³C NMR (CDCl₃, 101 MHz)** δ 142.1, 124.8, 77.4, 66.4, 63.1, 40.4, 33.1, 32.6 (2C), 31.5, 26.2, 26.0 (2C), 25.8, 22.7, 14.2; **HRMS (ESI)** exact mass for C₁₆H₂₈Cl₂NaO [M+Na]⁺, calculated 329.1409, found 329.1411; **IR (thin film, cm⁻¹)** ν 3440, 2926, 2853, 1449, 1379, 1081, 969.

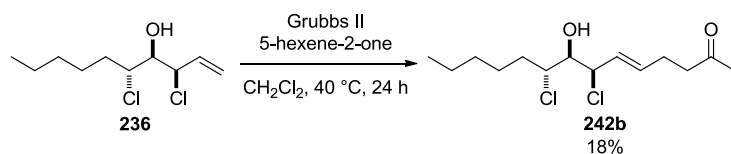
Spectroscopic data for **244a**:

$^1\text{H NMR}$ (CDCl_3 , 400 MHz) δ 5.71 (ddd, $J = 15.6, 6.6, 0.9$ Hz, 1H), 5.49 (ddd, $J = 15.6, 7.0, 1.3$ Hz, 1H), 4.23 – 4.15 (m, 1H), 4.03 (dt, $J = 9.5, 3.9$ Hz, 1H), 2.06 (d, $J = 6.3$ Hz, 1H), 2.02 – 1.82 (m, 1H), 1.80 – 1.46 (m, 5H), 1.45 – 1.04 (m, 13H), 0.93 – 0.80 (m, 3H); $^{13}\text{C NMR}$ (CDCl_3 , 101 MHz) δ 141.4, 124.9, 75.8, 68.7, 40.6, 33.4, 32.9, 32.8, 31.4, 26.4, 26.3, 26.1 (2C), 22.6, 14.1; **HRMS** (EI+) exact mass for $\text{C}_{10}\text{H}_{16}\text{ClO}$ [$\text{M}-\text{C}_5\text{H}_{11}$] $^+$, calculated 187.0890, found 187.0892; exact mass for $\text{C}_9\text{H}_{15}\text{O}$ [$\text{M}-\text{C}_6\text{H}_{13}\text{Cl}$] $^+$, calculated 139.1123, found 139.1121; **IR** (thin film, cm^{-1}) ν 3392, 2925, 1853, 1449, 1379, 1146, 1036, 970, 728.



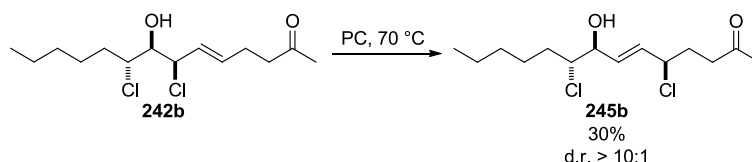
1,5-dichloro-1-cyclohexyldec-2-en-4-ol (245a): According to General Procedure 1, allylic chlorohydrin **242a** (4.2 mg, 14 μmol , 1.0 equiv) was stirred for 48 h at 70 $^{\circ}\text{C}$ in propylene carbonate (0.27 mL). According to TLC, the reaction appeared to have stopped when **242a** was consumed by approx. 60%. Purification by flash column chromatography (hexanes/ Et_2O 7:1, SiO_2) gave **245a** as an inseparable mixture of diastereomers (1.4 mg, 4.6 μmol , 33%, d.r. = 4:1).

$^1\text{H NMR}$ (CDCl_3 , 400 MHz) δ (only peaks for major diastereomer reported) 5.85 (ddd, $J = 15.3, 8.7, 1.1$ Hz, 1H), 5.73 (ddd, $J = 15.3, 6.3, 0.6$ Hz, 1H), 4.28 (tdd, $J = 6.2, 4.0, 1.0$ Hz, 1H), 4.21 (dd, $J = 8.7, 6.4$ Hz, 1H), 4.02 (dt, $J = 9.5, 4.0$ Hz, 1H), 2.13 (d, $J = 6.3$ Hz, 1H), 1.93 (d, $J = 12.5$ Hz, 1H), 1.84 – 1.71 (m, 4H), 1.71 – 1.56 (m, 4H), 1.42 – 0.98 (m, 10H), 0.90 (t, $J = 6.9$ Hz, 3H); $^{13}\text{C NMR}$ (CDCl_3 , 101 MHz) δ (only peaks for major diastereomer reported) 133.3, 130.4, 74.7, 67.8, 67.7, 44.7, 33.4, 31.4, 29.9, 29.7, 26.3, 26.3, 26.1, 26.0, 22.6, 14.1; **HRMS** (EI+) no molecular peak found, two highest peaks reported: exact mass for $\text{C}_{10}\text{H}_{16}\text{ClO}$ [$\text{M}-\text{C}_6\text{H}_{12}\text{Cl}$] $^+$, calculated 187.0890, found 187.0886; exact mass for $\text{C}_{10}\text{H}_{15}\text{O}$ [$\text{M}-\text{C}_6\text{H}_{12}\text{Cl}-\text{HCl}$] $^+$, calculated 151.1123, found 151.1122; **IR** (thin film, cm^{-1}) ν 3402, 2929, 2855, 1451, 1379, 1302, 1038, 970, 894, 850, 729.



7,9-dichloro-8-hydroxytetradec-5-en-2-one (242b): According to General Procedure 2, allylic chlorohydrin **236** (43 mg, 0.19 mmol, 1.0 equiv, d.r. = 9:1) and 5-hexene-2-one (66 μ L, 0.57 mmol, 3.0 equiv) were dissolved in CH_2Cl_2 (9.5 mL). Grubbs' second generation catalyst (**169**, 16 mg, 19 μ mol, 10 mol%) was added. Purification by flash column chromatography (hexanes/ Et_2O gradient 3:1 to 1:1, SiO_2) gave **242b** (10.0 mg, 34.0 μ mol, 18%).

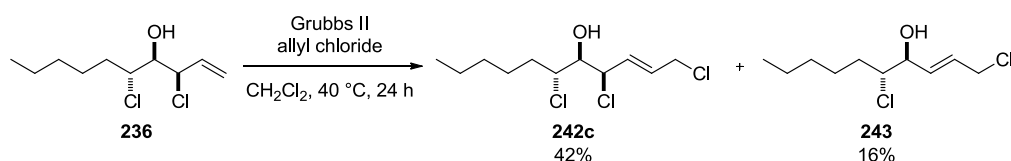
$^1\text{H NMR}$ (CDCl_3 , 400 MHz) δ 5.86 (dt, $J = 15.3, 6.5$ Hz, 1H), 5.72 (ddt, $J = 15.2, 8.5, 1.3$ Hz, 1H), 5.00 (dd, $J = 8.5, 2.5$ Hz, 1H), 3.91 (ddd, $J = 9.4, 8.4, 2.7$ Hz, 1H), 3.64 (dd, $J = 8.4, 2.6$ Hz, 1H), 2.55 (t, $J = 7.2$ Hz, 2H), 2.35 (qd, $J = 7.6, 7.2, 1.2$ Hz, 2H), 2.15 (s, 3H), 2.03 (dddd, $J = 14.0, 10.0, 5.6, 2.6$ Hz, 1H), 1.75 – 1.54 (m, 3H), 1.46 – 1.22 (m, 7H), 0.90 (t, $J = 6.9$ Hz, 3H); $^{13}\text{C NMR}$ (CDCl_3 , 101 MHz) δ 207.7, 134.3, 128.3, 77.2, 65.4, 62.8, 42.5, 33.3, 31.4, 30.2, 26.2, 25.7, 22.7, 14.1; **HRMS** (ESI) exact mass for $\text{C}_{14}\text{H}_{24}\text{Cl}_2\text{NaO}_2$ [$\text{M}+\text{Na}$] $^+$, calculated 317.1046, found 317.1049; **IR** (thin film, cm^{-1}) ν 3426, 2956, 2929, 2860, 1714, 1630, 1457, 1409, 1367, 1234, 1187, 1163, 1097, 1055, 971, 913, 853, 729, 686.



5,9-Dichloro-8-hydroxytetradec-6-en-2-one (245b): According to General Procedure 1, allylic chlorohydrin **242b** (5.0 mg, 17 μ mol, 1.0 equiv) was stirred for 48 h at 70 $^\circ\text{C}$ in propylene carbonate (0.34 mL). Purification by flash column chromatography (hexanes/ Et_2O 2:1, SiO_2) gave **245b** (1.5 mg, 5.1 μ mol, 30%, d.r. > 10:1).

$^1\text{H NMR}$ (CDCl_3 , 400 MHz) δ 5.87 (ddd, $J = 15.3, 7.3, 0.7$ Hz, 1H), 5.80 (dd, $J = 15.4, 5.5$ Hz, 1H), 4.47 (ddd, $J = 8.5, 7.3, 5.2$ Hz, 1H), 4.27 (q, $J = 5.0$ Hz, 1H), 4.01 (dt, $J = 9.7, 3.9$ Hz, 1H), 2.65 (t, $J = 7.1$ Hz, 2H), 2.17 (s, 3H), 2.15 – 1.95 (m,

2H), 1.78 – 1.51 (m, 3H), 1.36 – 1.22 (m, 6H), 0.90 (t, $J = 6.9$ Hz, 3H); ^{13}C NMR (CDCl₃, 101 MHz) δ 207.5 (obtained from HMBC), 133.9, 130.3, 74.5, 67.6, 61.0, 40.1, 33.3, 32.0, 31.4, 30.3, 26.3, 22.6, 14.1; HRMS (ESI) exact mass for C₁₄H₂₄Cl₂NaO₂ [M+Na]⁺, calculated 317.1046, found 317.1044; IR (thin film, cm⁻¹) ν 3421, 2956, 2928, 2860, 1714, 1457, 1410, 1366, 1261, 1163, 1098, 1033, 971, 911, 853, 803, 729, 697, 607.



1,4,6-trichloroundec-2-en-5-ol (242c): According to General Procedure 2, allylic chlorohydrin **236** (25.6 mg, 114 μmol , 1.00 equiv) and allyl chloride (46 μL , 0.57 mmol, 3.0 equiv) were dissolved in CH₂Cl₂ (5.7 mL). Grubbs' second generation catalyst (**169**, 9.7 mg, 11 μmol , 10 mol%) was added. Purification by flash column chromatography (hexanes/Et₂O gradient 6:1 to 5:1, SiO₂) gave **242c** (13 mg, 48 μmol , 42%) and **243** (4.2 mg, 19 μmol , 16%).

Spectroscopic data for **242c**:

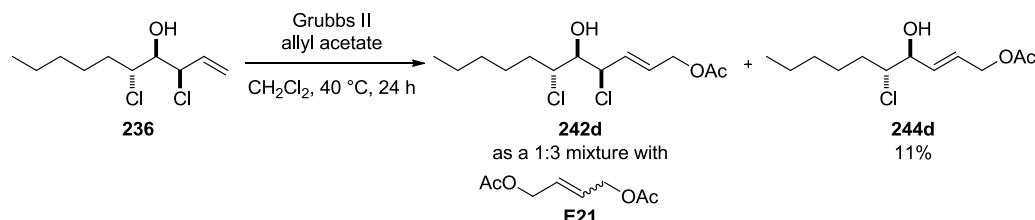
^1H NMR (CDCl₃, 400 MHz) δ 6.06 – 5.98 (m, 2H), 5.09 (dq, $J = 3.5, 2.1$ Hz, 1H), 4.10 – 4.07 (m, 2H), 3.92 (td, $J = 9.2, 2.7$ Hz, 1H), 3.69 (ddd, $J = 9.8, 8.6, 2.3$ Hz, 1H), 2.10 (d, $J = 9.9$ Hz, 1H), 2.14 – 2.00 (m, 1H), 1.75 – 1.56 (m, 3H), 1.48 – 1.23 (m, 4H), 0.95 – 0.86 (m, 3H); ^{13}C NMR (CDCl₃, 101 MHz) δ 131.3, 130.5, 76.8 (under CDCl₃ signal), 63.8, 62.6, 43.6, 33.4, 31.4, 25.7, 22.7, 14.1; HRMS (EI+) exact mass for C₅H₇Cl₂O [M-C₅H₁₁]⁺, calculated 152.9874, found 152.9880; exact mass for C₄H₆ClO [M-C₆H₁₂Cl]⁺, calculated 105.0107, found 105.0094; IR (thin film, cm⁻¹) ν 3443, 2957, 2929, 2860, 1467, 1380, 1259, 1088, 968, 913, 852, 728, 687, 608.

Spectroscopic data for **243**:

^1H NMR (CDCl₃, 400 MHz) δ 5.97 (dtd, $J = 15.3, 6.4, 1.0$ Hz, 1H), 5.87 (ddt, $J = 15.3, 5.9, 0.9$ Hz, 1H), 4.34 – 4.26 (m, 1H), 4.09 (dt, $J = 6.5, 0.8$ Hz, 2H), 4.04 (dt, $J = 9.6, 3.9$ Hz, 1H), 2.16 (d, $J = 6.7$ Hz, 1H), 1.77 – 1.50 (m, 3H), 1.45 – 1.20 (m, 5H), 0.93 – 0.86 (m, 3H); ^{13}C NMR (CDCl₃, 101 MHz) δ 131.9, 129.7, 74.5, 67.9, 44.2, 33.2, 31.4, 26.4, 22.6, 14.1; HRMS (EI+) exact mass for C₅H₇Cl₂O [M-

Experimental

$C_6H_{12}Cl]^+$, calculated 152.9874, found 152.9865; exact mass for $C_7H_{14}ClO$ [$M-C_4H_5Cl_2]^+$, calculated 149.0733, found 149.0720; **IR** (thin film, cm^{-1}) ν 3399, 2956, 2930, 2861, 1467, 1380, 1251, 1126, 1081, 1038, 969, 694.



4,6-dichloro-5-hydroxyundec-2-en-1-yl acetate (242d): According to General Procedure 2, allylic chlorohydrin **236** (24.5 mg, 109 μmol , 1.00 equiv) and allyl acetate (35 μL , 0.33 mmol, 3.0 equiv) were dissolved in CH_2Cl_2 (5.4 mL). Grubbs' second generation catalyst (**236**, 9.2 mg, 11 μmol , 10 mol%) was added. Purification by flash column chromatography (hexanes/ Et_2O gradient 3:1 to 2:1, SiO_2) gave **242d** as an inseparable 1:3 mixture with **E21** (26 mg), **243** (7.1 mg, 32 μmol , 29%) and **244d** (3.0 mg, 12 μmol , 11%).

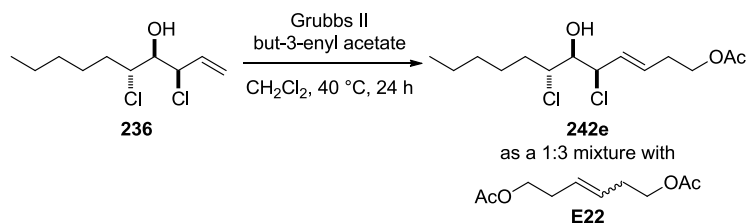
Spectroscopic data for **242d**:

1H NMR ($CDCl_3$, 400 MHz) δ (only signals for **242d** reported, assigned by COSY&HSQC) 5.97 (dd, $J = 5.5, 3.6$ Hz, 2H), 5.09 (dt, $J = 6.4, 1.9$ Hz, 1H), 4.63 – 4.57 (m, 1H), 3.92 (td, $J = 9.1, 2.7$ Hz, 1H), 3.74 – 3.63 (m, 1H), 2.17 (dd, $J = 9.7, 1.4$ Hz, 1H), 2.08 (s, 3H), 1.76 – 1.63 (m, 2H), 1.48 – 1.21 (m, 7H), 0.90 (t, $J = 6.9$ Hz, 3H); **^{13}C NMR** ($CDCl_3$, 101 MHz) δ (only signals for **242d** reported, assigned by HSQC and HMBC) 170.7, 130.8, 129.0, 76.8 (shoulder in $CDCl_3$ signal), 64.1, 63.6, 62.6, 33.4, 31.4, 25.6, 22.7, 21.0, 14.1; **HRMS** (ESI) exact mass for $C_{13}H_{22}Cl_2NaO_3$ [$M+Na]^+$, calculated 319.0838, found 319.0845; **IR** (thin film, cm^{-1}) ν 3474, 2954, 1736, 1444, 1380, 1365, 1220, 1083, 1025, 967, 836, 607, 486.

Spectroscopic data for **244d**:

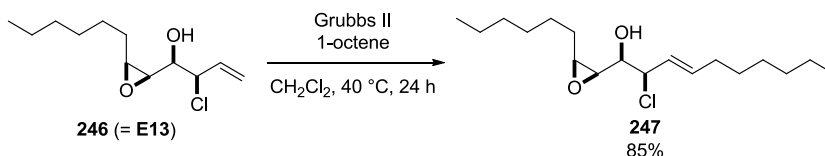
1H NMR ($CDCl_3$, 400 MHz) δ 5.96 – 5.79 (m, 2H), 4.60 (dd, $J = 5.3, 1.1$ Hz, 2H), 4.33 – 4.26 (m, 1H), 4.03 (dt, $J = 9.6, 3.9$ Hz, 1H), 2.16 (d, $J = 6.6$ Hz, 1H), 2.08 (s, 3H), 1.78 – 1.59 (m, 3H), 1.44 – 1.22 (m, 5H), 0.90 (t, $J = 6.9$ Hz, 3H); **^{13}C NMR** ($CDCl_3$, 101 MHz) δ 170.8, 131.5, 128.1, 74.7, 67.9, 64.1, 33.2, 31.4, 26.4, 22.6, 21.1,

14.1; **HRMS** (ESI) exact mass for $C_{12}H_{21}ClNaO_3$ $[M+Na]^+$, calculated 271.1071, found 271.1078; **IR** (thin film, cm^{-1}) ν 3451, 2955, 2930, 2861, 1741, 1457, 1381, 1365, 1239, 1028, 970, 851, 772, 729, 606.



5,7-dichloro-6-hydroxydodec-3-en-1-yl acetate (242e): According to General Procedure 2, allylic chlorohydrin **236** (21.9 mg, 95.0 μmol , 1.00 equiv) and allyl acetate (36 μL , 0.28 mmol, 3.0 equiv) were dissolved in CH_2Cl_2 (4.7 mL). Grubbs' second generation catalyst (**169**, 9.0 mg, 9.5 μmol , 10 mol%) was added. Purification by flash column chromatography (hexanes/ Et_2O gradient 3:1 to 2.5:1, SiO_2) gave **242e** as an inseparable 1:3 mixture with **E22** (31 mg).

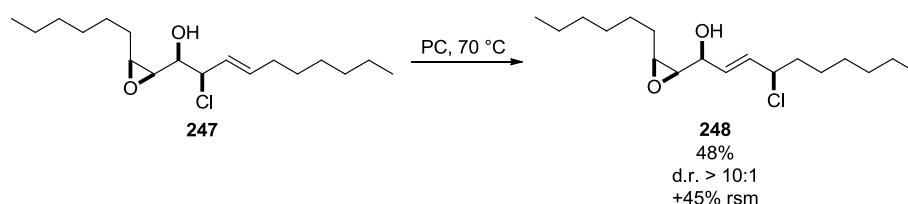
$^1\text{H NMR}$ (CDCl_3 , 400 MHz) δ (only signals for **242e** reported, assigned by COSY&HSQC) 5.94 – 5.76 (m, 1H), 5.05 (dd, $J = 7.7, 2.5$ Hz, 1H), 4.15 (td, $J = 6.6, 2.8$ Hz, 2H), 3.94 (td, $J = 9.1, 2.7$ Hz, 1H), 3.68 (td, $J = 9.0, 2.5$ Hz, 1H), 2.47 – 2.39 (under peak from **E22**, 1H), 2.24 – 2.18 (m, 1H), 2.12 – 2.03 (under peak from **E22**, 4H), m, 1.78 – 1.58 (m, 2H), 1.50 – 1.18 (m, 7H), 0.95 – 0.88 (m, 3H); $^{13}\text{C NMR}$ (CDCl_3 , 101 MHz) δ (only signals for **242d** reported, assigned by HSQC and HMBC) δ 171.1, 131.2, 130.1, 77.2 (under CDCl_3 signal), 65.2, 63.1, 62.8, 33.3, 31.7, 31.4, 25.7, 22.7, 21.1, 14.1; **HRMS** (ESI) exact mass for $C_{14}H_{24}Cl_2NaO_3$ $[M+Na]^+$, calculated 333.0995, found 333.0999; **IR** (thin film, cm^{-1}) ν 3563, 2958, 1861, 1736, 1457, 1432, 1384, 1365, 1230, 1032, 970, 895, 853, 776, 731, 686, 635, 606.



2-chloro-1-(3-hexyloxiran-2-yl)dec-3-en-1-ol (247): According to General Procedure 2, allylic chlorohydrin **246** (20 mg, 86 μmol , 1.0 equiv, d.d. = 6:1) and

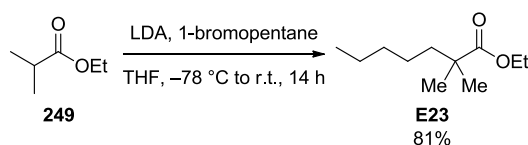
1-octene (41 μL , 0.26 mmol, 3.0 equiv) were dissolved in CH_2Cl_2 (4.3 mL). Grubbs' second generation catalyst (**169**, 7.3 mg, 8.6 μmol , 10 mol%) was added. Purification by flash column chromatography (hexanes/ Et_2O gradient 6:1 to 3:1, SiO_2) gave **247** (23 mg, 73 μmol , 85%, d.r. = 6:1).

$^1\text{H NMR}$ (CDCl_3 , 400 MHz) δ (only peaks for major diastereomer reported) 5.85 (dt, $J = 15.4, 6.7$ Hz, 1H), 5.61 (ddt, $J = 15.1, 9.0, 1.4$ Hz, 1H), 4.45 (dd, $J = 9.0, 5.3$ Hz, 1H), 3.71 (q, $J = 5.7$ Hz, 1H), 3.10 (dd, $J = 5.8, 4.3$ Hz, 1H), 3.02 (dt, $J = 7.2, 4.4$ Hz, 1H), 2.44 (d, $J = 5.9$ Hz, 1H), 2.14 – 2.03 (m, 2H), 1.70 – 1.60 (m, 2H), 1.54 – 1.18 (m, 16H), 0.93 – 0.82 (m, 6H); $^{13}\text{C NMR}$ (CDCl_3 , 101 MHz) δ 137.3, 125.9, 71.5, 65.5, 57.9, 57.3, 32.3, 31.9, 31.8, 29.2, 29.0, 28.9, 28.3, 26.9, 22.7, 22.7, 14.2, 14.2; HRMS (ESI) exact mass for $\text{C}_{18}\text{H}_{33}\text{ClNaO}_2$ $[\text{M}+\text{Na}]^+$, calculated 339.2061, found 339.2063; IR (thin film, cm^{-1}) ν 3438, 2956, 2926, 2856, 1665, 1626, 1466, 1379, 1267, 1110, 1064, 967, 889, 846, 724, 618.



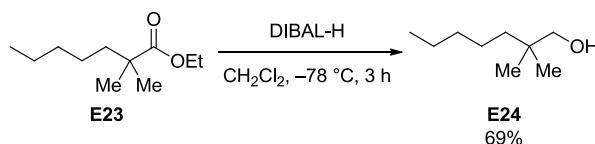
4-Chloro-1-(cis-3-hexyloxiran-2-yl)dec-2-en-1-ol (248): According to General Procedure 1, allylic chlorohydrin **247** (5.5 mg, 17 μmol , 1.0 equiv) was stirred for 48 h at 70 $^{\circ}\text{C}$ in propylene carbonate (0.32 mL). Purification by flash column chromatography (hexanes/ Et_2O gradient 6:1 to 2:1, SiO_2) gave **248** (2.5 mg, 7.9 μmol , 48%) and **247** (2.7 mg, 8.5 μmol , 45%, d.r. = 1.6:1).

$^1\text{H NMR}$ (CDCl_3 , 400 MHz) δ (only peaks for major diastereomer reported) 5.90 (ddd, $J = 15.4, 8.1, 1.4$ Hz, 1H), 5.75 (dd, $J = 15.4, 5.5$ Hz, 1H), 4.38 (q, $J = 7.3$ Hz, 1H), 4.08 – 4.02 (m, 1H), 3.09 – 3.03 (m, 1H), 2.95 (dd, $J = 7.8, 4.3$ Hz, 1H), 2.06 (d, $J = 3.3$ Hz, 1H), 1.82 (m, 2H), 1.64 – 1.18 (m, 18H), 0.92 – 0.86 (m, 6H); $^{13}\text{C NMR}$ (CDCl_3 , 101 MHz) δ 133.3, 129.5, 70.1, 61.9, 59.8, 57.8, 38.4, 31.7, 31.6, 30.3, 29.7, 29.1, 28.7, 28.3, 26.8, 26.4, 22.6, 14.0; HRMS (ESI) exact mass for $\text{C}_{18}\text{H}_{34}\text{ClO}_2$ $[\text{M}+\text{H}]^+$, calculated 317.2242, found 317.2240; IR (thin film, cm^{-1}) ν 3428, 2956, 2927, 2858, 1692, 1460, 1378, 1264, 1084, 1023, 969, 855, 725.



ethyl 2,2-dimethylheptanoate (E23): To a solution of diisopropylamine (1.0 mL, 7.2 mmol, 2.5 equiv) in THF (7.7 mL) at 0 °C was added *n*-butyl lithium (1.6 M in hexanes, 4.1 mL, 6.6 mmol, 2.3 equiv) and the reaction was stirred for 30 minutes before it was cooled to -78 °C. The solution was then transferred to a flask containing ethyl isobutyrate (**249**, 1.1 mL, 8.6 mmol, 3.0 equiv) in THF (7.7 mL) and stirred for 1 hour. 1-Bromopentane (0.36 mL, 2.9 mmol, 1.0 equiv) in THF (3.8 mL) was added dropwise and the reaction was allowed to warm to room temperature during 14 hours. Sat. aq. NH_4Cl was added and the mixture extracted three times with Et_2O . Combined organic phases were dried over Na_2SO_4 , filtered, and concentrated. Flash column chromatography (hexanes/ Et_2O 20:1, SiO_2) gave **E23** (0.43 g, 2.3 mmol, 81%).

^1H NMR (CDCl_3 , 400 MHz) δ 4.11 (q, $J = 7.2$ Hz, 2H), 1.52 – 1.46 (m, 2H), 1.34 – 1.18 (m, 6H), 1.24 (t, $J = 7.1$ Hz, 3H), 1.15 (s, 6H) 0.87 (t, $J = 7.0$ Hz, 3H); ^{13}C NMR (CDCl_3 , 101 MHz) δ 178.3, 60.3, 42.3, 40.9, 32.4, 25.3, 24.7, 22.6, 14.4, 14.2; HRMS (EI⁺) exact mass for $\text{C}_{11}\text{H}_{22}\text{O}_2$ $[\text{M}]^+$, calculated 186.1615, found 186.1614; exact mass for $\text{C}_9\text{H}_{17}\text{O}$ $[\text{M}-\text{C}_2\text{H}_5\text{O}]^+$, calculated 141.1274, found 141.1270; exact mass for $\text{C}_7\text{H}_{13}\text{O}_2$ $[\text{M}-\text{C}_4\text{H}_9]^+$, calculated 129.0910, found 129.0912; IR (thin film, cm^{-1}) ν 2959, 2933, 2862, 1729, 1473, 1386, 1365, 1293, 1264, 1191, 1146, 1101, 1029, 863, 772, 726.

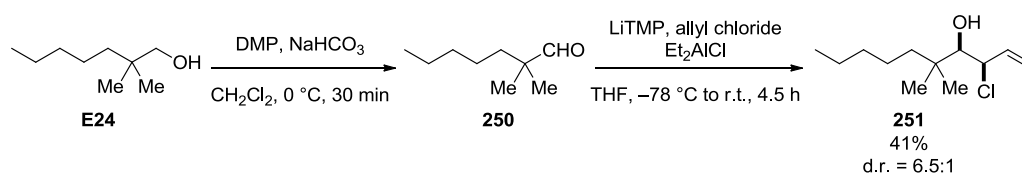


2,2-dimethylheptan-1-ol (E24): To a solution of ester **E23** (0.15 g, 0.81 mmol, 1.0 equiv) in CH_2Cl_2 (8.1 mL) at -78 °C was added diisobutylaluminum hydride (1.0 M in CH_2Cl_2 , 1.7 mL, 1.7 mmol, 2.1 equiv) and the reaction was stirred for 3 hours. Sat. aq. sodium potassium tartrate was added and the mixture was stirred until

Experimental

two clear phases had formed (2 hours). The mixture was poured into water and extracted three times with CH₂Cl₂. Combined organic phases were dried over Na₂SO₄, filtered, and concentrated. Flash column chromatography (hexanes/Et₂O gradient 4:1 to 3:1, SiO₂) gave **E24** (110 mg, 0.76 mmol, 91%).

¹H NMR (CDCl₃, 400 MHz) δ 3.31 (s, 2H), 1.37 – 1.16 (m, 9H), 0.88 (t, *J* = 6.9 Hz, 3H), 0.86 (s, 6H); **¹³C NMR (CDCl₃, 101 MHz)** δ 72.2, 38.8, 35.2, 33.0, 24.0, 23.7, 22.8, 14.2; **HRMS (EI⁺)** exact mass for C₈H₁₇ [M-CH₂OH]⁺, calculated 113.1325, found 113.1324; **IR (thin film, cm⁻¹)** ν 3343, 2956, 2929, 2861, 1469, 1380, 1364, 1040, 902, 725.

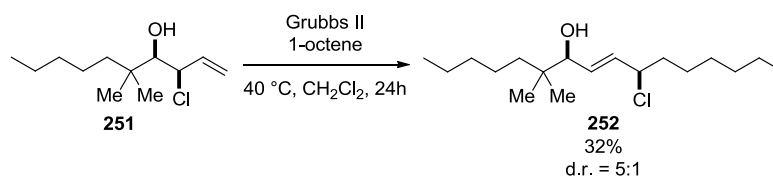


3-chloro-5,5-dimethyldec-1-en-4-ol (251): To a solution of alcohol **E24** (0.106 mg, 0.74 mmol, 1.0 equiv) in CH₂Cl₂ (7.3 mL) at 0 °C was added Dess–Martin Periodinane (374 mg, 0.882 mmol, 1.20 equiv) and NaHCO₃ (154 mg, 1.84 mmol, 2.5 equiv). The reaction was stirred for 30 minutes before sat. aq. Na₂S₂O₃ was added and the mixture was stirred for 10 minutes, poured into sat. aq. NaHCO₃ and extracted three times with Et₂O. Combined organic phases were dried over Na₂SO₄, filtered, and carefully (>450 mbar) concentrated. Crude aldehyde **250** (68 mg, 0.48 mmol, 65%) was directly in the next step.

According to General Procedure 3, LiTMP was prepared from tetramethylpiperidine (0.18 mL, 1.1 mmol, 2.2 equiv) and *n*-BuLi (1.6 M in hexanes, 0.63 mL, 1.0 mmol, 2.1 equiv) in THF (2.2 mL) and added to a solution of allyl chloride (82 μL, 1.0 mmol, 2.1 equiv) and diethylaluminum chloride (1.0 M in hexanes, 1.9 mL, 1.9 mmol, 4.0 equiv) in THF (4.4 mL). Crude aldehyde **250** (68 mg) in THF (0.5 mL) was added. After 4.5 hours, the reaction was worked up and purified by flash column chromatography (hexanes/Et₂O 30:1, SiO₂) to give **251** as an inseparable mixture of diastereomers (43 mg, 0.19 mmol, 41%, d.r. = 6.5:1).

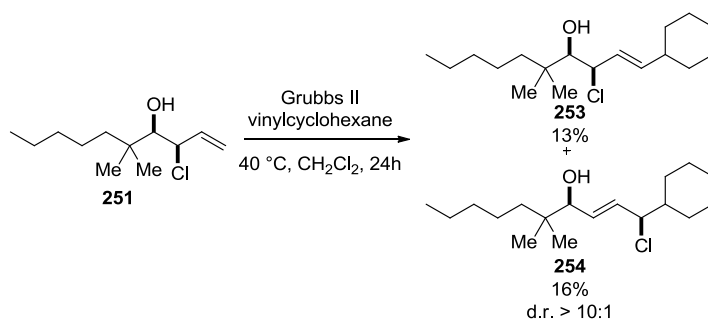
¹H NMR (CDCl₃, 400 MHz) δ 6.06 (ddd, *J* = 17.0, 10.0, 8.8 Hz, 1H), 5.30 (dt, *J* = 17.0, 1.0 Hz, 1H), 5.24 – 5.12 (m, 1H), 4.65 (dd, *J* = 8.8, 3.7 Hz, 1H), 3.43 (dd, *J*

= 7.9, 3.6 Hz, 1H), 2.20 (d, $J = 7.9$ Hz, 1H), 1.60 – 1.18 (m, 8H), 0.97 (s, 3H), 0.95 (s, 3H), 0.89 (t, $J = 6.9$ Hz, 3H); ^{13}C NMR (CDCl_3 , 101 MHz) δ 137.7, 117.1, 79.1, 66.5, 40.2, 38.3, 32.9, 24.1, 23.9, 23.5, 22.8, 14.2; HRMS (EI+) exact mass for $\text{C}_8\text{H}_{17} [\text{M}-\text{CH}_2\text{OH}]^+$, calculated 113.1325, found 113.1324; IR (thin film, cm^{-1}) ν 3343, 2956, 2929, 2861, 1469, 1380, 1364, 1040, 902, 725.



10-chloro-6,6-dimethylhexadec-8-en-7-ol (252): According to General Procedure 2, allylic chlorohydrin **251** (13.2 mg, 60 μmol , 1.0 equiv) and 1-hexene (28 μL , 180 μmol , 3.0 equiv) were dissolved in CH_2Cl_2 (3.0 mL). Grubbs' second generation catalyst (**169**, 5.1 mg, 6.0 μmol , 10 mol%) was added. Purification by flash column chromatography (hexanes/ Et_2O 15:1, SiO_2) gave **252** as an inseparable mixture of diastereomers (5.8 mg, 19 μmol , 32%, d.r. = 5:1).

^1H NMR (CDCl_3 , 400 MHz) δ 5.82 – 5.67 (m, 2H), 4.37 (q, $J = 7.0$ Hz, 1H), 3.83 (dd, $J = 6.0, 4.0$ Hz, 1H), 1.70 – 1.90 (m, 2H), 1.48 – 1.13 (m, 17H), 0.88 (t, $J = 7.0$ Hz, 6H), 0.88 (s, 3H), 0.84 (s, 3H); ^{13}C NMR (CDCl_3 , 101 MHz) δ 133.1, 132.2, 78.7, 62.6, 38.9, 38.7, 37.5, 32.8, 31.7, 28.7, 26.5, 23.3, 22.8 (2C), 22.7, 22.6, 14.1, 14.0; HRMS (ESI) exact mass for $\text{C}_{18}\text{H}_{35}\text{ClNaO} [\text{M}+\text{Na}]^+$, calculated 325.2269, found 325.2274; IR (thin film, cm^{-1}) ν 3436, 2957, 2929, 2859, 1467, 1379, 1365, 1262, 1091, 1000, 970, 802, 725.



Cross-metathesis of allylic chlorohydrin **251 with vinylcyclohexane – 3-chloro-1-cyclohexyl-5,5-dimethyldec-1-en-4-ol (**253**) and 1-chloro-1-cyclohexyl-5,5-dimethyldec-2-en-4-ol (**254**):** According to General Procedure 2, allylic chlorohydrin **251** (13 mg, 59 μ mol, 1.0 equiv, d.r. = 6.5:1) and vinylcyclohexane (41 μ L, 300 μ mol, 5.0 equiv) were dissolved in CH₂Cl₂ (3.0 mL). Grubbs' second generation catalyst (**169**, 5.0 mg, 5.9 μ mol, 10 mol%) was added. Purification by flash column chromatography (hexanes/Et₂O gradient 50:1 to 10:1, SiO₂) gave **253** (2.9 mg, 9.6 μ mol, 16%, d.r. = 6.5:1) and **254** as an inseparable mixture of diastereomers (2.3 mg, 7.6 μ mol, 13%, d.r. > 10:1).

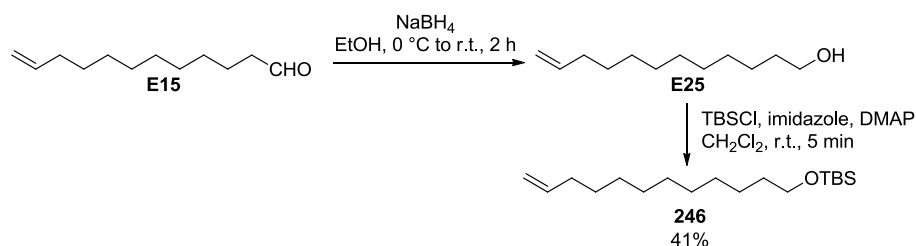
Spectroscopic data for **253:**

¹H NMR (CDCl₃, 400 MHz) δ 5.76 – 5.69 (m, 2H), 4.25 – 4.16 (m, 1H), 3.84 (br, 1H), 1.93 (d, J = 12.4 Hz, 1H), 1.83 – 1.71 (m, 3H), 1.71 – 1.56 (m, 3H), 1.48 – 1.40 (m, 1H), 1.36 – 1.11 (m, 8H), 1.13 – 0.98 (m, 3H), 0.93 – 0.84 (m, 7H), 0.84 (s, 3H); **¹³C NMR (CDCl₃, 101 MHz)** δ 132.8, 131.7, 78.8, 68.5, 44.7, 39.0, 37.4, 32.8, 29.8, 29.7, 26.2, 26.0, 25.9, 23.3, 22.9, 22.8, 22.7, 14.1; **HRMS (ESI)** exact mass for C₁₈H₃₃O [M-Cl]⁺, calculated 265.2531, found 265.2516; exact mass for C₁₀H₁₆ClO [M-C₈H₁₇]⁺, calculated 187.0890, found 187.0893; exact mass for C₁₀H₁₆O [M-C₈H₁₇-Cl]⁺, calculated 152.1201, found 152.1198; **IR (thin film, cm⁻¹)** ν 3436, 2929, 2855, 1468, 1450, 1379, 1365, 1301, 1201, 1001, 972, 894, 714, 617, 479.

Spectroscopic data for **254:**

¹H NMR (CDCl₃, 400 MHz) δ 5.79 – 5.60 (m, 2H), 4.63 (dd, J = 10.2, 7.1 Hz, 1H), 4.16 (d, J = 9.1 Hz, 1H), 2.02 (d, J = 13.0 Hz, 1H), 1.84 – 1.63 (m, 5H), 1.64 – 1.40 (m, 4H), 1.40 – 1.10 (m, 13H), 1.09 – 1.00 (m, 2H), 0.93 – 0.84 (m, 3H), 0.90 (s, 3H), 0.84 (s, 3H); **¹³C NMR (CDCl₃, 101 MHz)** δ 132.5, 131.9, 73.8, 62.6, 44.8, 38.9, 37.4, 33.0, 30.2, 29.8, 26.3, 26.2, 26.0, 23.5, 22.8, 22.7, 22.5, 14.3; **HRMS (EI+)**

exact mass for $C_{10}H_{16}O$ $[M-C_8H_{17}-Cl]^+$, calculated 152.1201, found 152.1206; exact mass for C_8H_{17} $[M-C_{10}H_{16}-ClO]^+$, calculated 113.1330, found 113.1335; **IR** (thin film, cm^{-1}) ν 3453, 2956, 2929, 2855, 1467, 1451, 1379, 1365, 1301, 1214, 1029, 990, 893, 807, 726, 549, 487, 454.



tert-butyl(dodec-11-en-1-yloxy)dimethylsilane (246): Procedure adapted from *J. Org. Chem.* 2014, 79, 2226-2241.

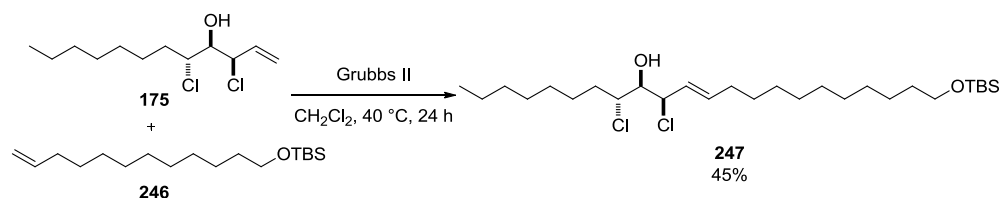
A stirred solution of crude aldehyde **E15** (0.776 g) in EtOH (21 mL) was cooled to 0 °C. Sodium borohydride (0.32 g, 8.5 mmol, 2.0 eq.) was added carefully. The reaction was stirred at 0 °C for 1 hour and at room temperature for 1 hour. The reaction was then quenched through the addition of sat. aq. NH_4Cl and extracted three times with EtOAc. Combined organic phases were dried over Na_2SO_4 , filtered, and concentrated. Alcohol **E25** (0.718 g) was used directly in the next step.

To a solution of alcohol **E25** (0.718) in CH_2Cl_2 (39 mL) was added imidazole (0.80 g, 12 mmol, 3.0 equiv). After 10 minutes, *tert*-butyldimethylsilyl chloride (0.88 mg, 5.8 mmol, 1.5 equiv) and 4-dimethylaminopyridine (48 mg, 0.39 mmol, 10 mol%) were added and the reaction was stirred for 5 minutes. Sat. aq. NH_4Cl was added and the mixture extracted three times with CH_2Cl_2 . Combined organic phases were dried over Na_2SO_4 , filtered, and concentrated. Flash column chromatography (hexanes, SiO_2) gave **246** (0.55 g, 1.8 mmol, 41%).

1H NMR ($CDCl_3$, 400 MHz) δ 5.81 (ddt, $J = 16.9, 10.1, 6.7$ Hz, 1H), 4.99 (dq, $J = 17.2, 1.7$ Hz, 1H), 4.93 (ddt, $J = 10.2, 2.3, 1.2$ Hz, 1H), 3.60 (t, $J = 6.6$ Hz, 2H), 2.04 (tdd, $J = 6.6, 5.3, 1.5$ Hz, 2H), 1.51 (p, $J = 7.2, 6.8$ Hz, 2H), 1.42 – 1.21 (m, 14H), 0.89 (s, 9H), 0.05 (s, 6H); **^{13}C NMR** ($CDCl_3$, 101 MHz) δ 139.4, 114.2, 63.5, 34.0, 33.1, 29.8, 29.7, 29.6, 29.6, 29.3, 29.1, 26.2, 26.0, 18.5, -5.1; **HRMS** (EI+) exact mass for C_8H_{17} $[M-CH_2OH]^+$, calculated 113.1325, found 113.1324; **IR** (thin film, cm^{-1}) ν

Experimental

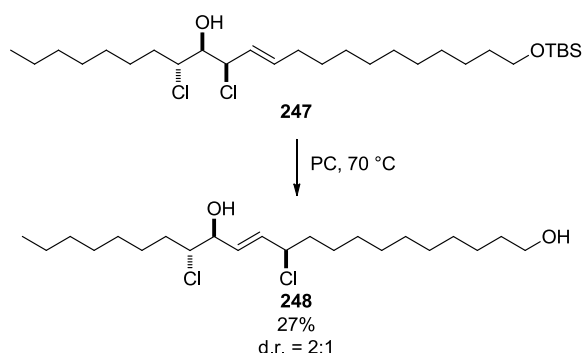
2926, 2855, 1642, 1472, 1463, 1388, 1361, 1255, 1099, 1006, 992, 939, 909, 835, 774, 722, 661.



22-((*tert*-butyldimethylsilyl)oxy)-8,10-dichlorodocos-11-en-9-ol (**247**):

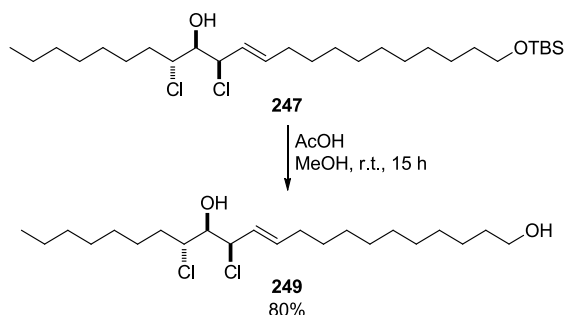
According to General Procedure 2, allylic chlorohydrin **175** (50.0 mg, 0.197 mmol, 1.00 equiv) and olefin **246** (177 mg, 0.592 mmol, 3.00 equiv) were dissolved in CH_2Cl_2 (9.9 mL). Grubbs' second generation catalyst (**169**, 16.8 mg, $19.7\text{ }\mu\text{mol}$, 10.0 mol%) was added. Purification by flash column chromatography (hexanes/ Et_2O gradient 30:1 to 20:1, SiO_2) gave **247** (46.6 mg, $89.0\text{ }\mu\text{mol}$, 45%).

$^1\text{H NMR}$ (CDCl_3 , 400 MHz) δ 5.86 (dt, $J = 15.3, 6.7\text{ Hz}$, 1H), 5.68 (ddt, $J = 15.2, 8.9, 1.4\text{ Hz}$, 1H), 4.99 (dd, $J = 8.8, 2.9\text{ Hz}$, 1H), 3.92 (ddd, $J = 9.6, 8.0, 2.7\text{ Hz}$, 1H), 3.67 (ddd, $J = 9.0, 8.0, 3.0\text{ Hz}$, 1H), 3.60 (t, $J = 6.6\text{ Hz}$, 2H), 2.18 (d, $J = 9.0\text{ Hz}$, 1H), 2.07 (q, $J = 6.7\text{ Hz}$, 2H), 2.03 – 1.95 (m, 1H), 1.70 (dtd, $J = 14.2, 9.7, 4.5\text{ Hz}$, 1H), 1.64 – 1.56 (m, 1H), 1.53 – 1.46 (m, 2H), 1.44 – 1.20 (m, 23H), 0.89 (s, 9H), 0.91 – 0.85 (m, 3H), 0.05 (s, 6H); $^{13}\text{C NMR}$ (CDCl_3 , 101 MHz) δ 136.7, 127.1, 77.4, 66.1, 63.5, 63.0, 33.2, 33.1, 32.3, 31.9, 29.8, 29.7, 29.6, 29.6, 29.3 (2C), 29.3, 28.9, 26.2, 26.1, 26.0, 22.8, 18.5, 14.2, -5.1; HRMS (ESI) exact mass for $\text{C}_{28}\text{H}_{56}\text{Cl}_2\text{NaO}_2\text{Si}$ $[\text{M}+\text{Na}]^+$, calculated 545.3319, found 545.3313; IR (thin film, cm^{-1}) ν 3552, 2926, 2855, 1664, 1463, 1387, 1361, 1255, 1097, 1006, 968, 938, 835, 813, 775, 723, 686, 662, 608.



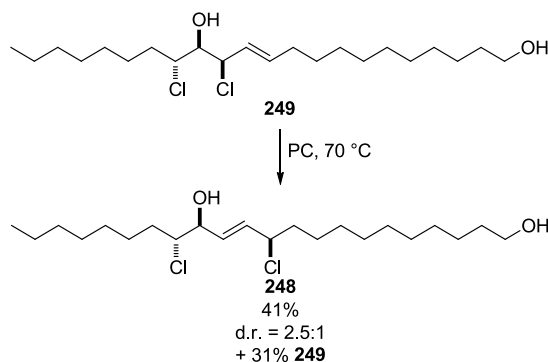
11,15-dichlorodocos-12-ene-1,14-diol (248): According to General Procedure 1, allylic chlorohydrin **247** (13.5 mg, 26 μmol , 1.0 equiv) was stirred for 4 days at 70 °C in propylene carbonate (0.52 mL). Purification by flash column chromatography (hexanes/EtOAc 2:1, SiO₂) gave a complex mixture, which was redissolved in propylene carbonate (0.52 mL) and stirred at 70 °C for 3 days. Purification by flash column chromatography (hex/Et₂O gradient 3:1 to 1:1) gave **248** as an inseparable mixture of diastereomers (1.2 mg, 2.9 μmol , 24%, d.r. = 2:1).

¹H NMR (CDCl₃, 400 MHz) δ (only peaks for major diastereomer reported) 5.92 – 5.78 (m, 1H), 5.76 (dd, $J = 15.4, 6.1$ Hz, 1H), 4.38 (q, $J = 7.2$ Hz, 1H), 4.32 – 4.22 (m, 1H), 4.02 (dt, $J = 9.7, 3.9$ Hz, 1H), 3.69 – 3.59 (m, 2H), 2.18 (d, $J = 6.4$ Hz, 1H), 1.88 – 1.50 (m, 8H), 1.48 – 1.08 (m, 23H), 0.94 – 0.85 (m, 3H); ¹³C NMR (CDCl₃, 101 MHz) δ (only peaks for major diastereomer reported) 134.7, 129.8, 74.6, 67.7, 63.2, 62.0, 38.6, 33.3, 32.9, 31.4, 29.7, 29.6, 29.5, 29.5, 29.1, 29.1, 26.6, 26.3, 25.9, 25.9, 22.6, 14.1; HRMS (EI⁺) exact mass for C₁₄H₂₆ClO₂ [M-C₈H₁₆Cl]⁺, calculated 261.1621, found 261.1621; exact mass for C₁₄H₂₄ClO [M-C₈H₁₆Cl-H₂O]⁺, calculated 243.1516, found 243.1515; exact mass for C₁₄H₂₅O₂ [M-C₈H₁₆Cl-HCl]⁺, calculated 225.1855, found 225.1850; IR (thin film, cm⁻¹) ν 3364, 2927, 2856, 1745, 1465, 1379, 1264, 1053, 970, 727.



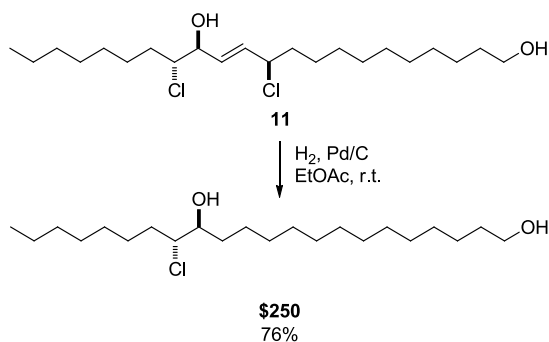
13,15-dichlorodocos-11-ene-1,14-diol (249): Allylic chlorohydrin **247** (48.6 mg, 93.0 μmol , 1.00 equiv) was dissolved in MeOH (1.9 mL). Acetic acid (27 μL , 0.46 mmol, 5.0 equiv) was added and the reaction was stirred for 15 hours. Toluene was added and solvent removed. Flash column chromatography (hexanes/EtOAc 3:1, SiO₂) gave **249** (30.5 mg, 74.0 μmol , 80%).

¹H NMR (CDCl₃, 400 MHz) δ 5.86 (dt, $J = 15.2, 6.7$ Hz, 1H), 5.68 (ddt, $J = 15.0, 8.7, 1.3$ Hz, 1H), 5.00 (dd, $J = 8.8, 2.9$ Hz, 1H), 3.93 (ddd, $J = 9.7, 8.1, 2.7$ Hz, 1H), 3.72 – 3.65 (br, 1H), 3.64 (t, $J = 6.6$ Hz, 2H), 2.28 – 2.14 (br, 1H), 2.07 (dd, $J = 13.8, 7.0$ Hz, 2H), 2.02 (m, 1H), 1.70 (dtd, $J = 14.1, 9.7, 4.3$ Hz, 1H), 1.64 – 1.51 (m, 3H), 1.44 – 1.20 (m, 24H), 0.90 (t, $J = 6.9$ Hz, 3H); ¹³C NMR (CDCl₃, 101 MHz) δ 136.6, 127.1, 77.4, 66.1, 63.3, 63.0, 33.2, 33.0, 32.2, 31.5, 29.7, 29.6, 29.5, 29.5, 29.2, 29.2, 28.9, 28.9, 25.9, 25.8, 22.7, 14.2; HRMS (EI+) exact mass for C₂₈H₅₆Cl₂NaO₂Si [M-C₈H₁₆Cl]⁺, calculated 261.1621, found 261.1619; IR (thin film, cm⁻¹) ν 3363, 2926, 2855, 1664, 1466, 1379, 1282, 1058, 969, 911, 851, 726, 684, 617.



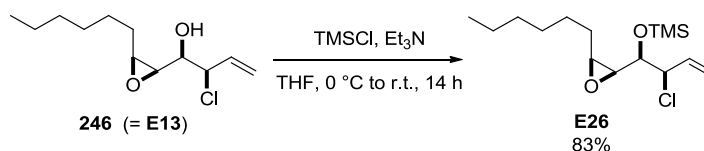
11,15-dichlorodocos-12-ene-1,14-diol (248): According to General Procedure 1, allylic chlorohydrin **249** (4.2 mg, 10 μmol , 1.0 equiv) was stirred for 52 h at 70 °C in propylene carbonate (0.20 mL). Purification by flash column chromatography

(hexanes/Et₂O gradient 2:1 to 1:1, SiO₂) gave **248** as an inseparable mixture of diastereomers (1.7 mg, 4.2 μmol, 41%, d.r. = 2.5:1) and **249** (1.3 mg, 3.2 μmol, 31%).



15-chlorodocosane-1,14-diol (\$250): To a solution of olefin **11** (4.0 mg, 9.8 μmol, 1.0 equiv) in EtOAc (1.0 mL) was added Pd/C (10% Pd, 1.0 mg, 0.97 μmol, 10 mol%). The reaction was put under an atmosphere with a hydrogen balloon (5 cycles) and stirred for 15 hours. The reaction was filtered through a plug of silica gel, eluting with DCM and subsequently concentrated. Flash column chromatography (hexanes/Et₂O gradient 2:1 to 1.5:1, SiO₂) gave **\$250** as a colorless oil (2.8 mg, 7.4 μmol, 76%).

¹H NMR (CDCl₃, 400 MHz) δ 4.00 (dt, *J* = 8.6, 3.8 Hz, 1H), 3.74 (q, *J* = 4.8, 3.8 Hz, 1H), 3.64 (td, *J* = 6.6, 5.4 Hz, 2H), 1.91 (d, *J* = 6.4 Hz, 1H), 1.79 – 1.67 (m, 2H), 1.54 (s, 4H), 1.43 – 1.17 (m, 31H), 0.88 (d, *J* = 7.0 Hz, 3H); HRMS (EI+) exact mass for C₂₂H₄₄O₂ [M-HCl]⁺, calculated 340.3341, found 340.3314; exact mass for C₁₄H₂₉O₂ [M-C₈H₁₆Cl]⁺, calculated 229.2168, found 229.2159; IR (thin film, cm⁻¹) ν 3324, 2920, 2851, 1716, 1629, 1467, 1261, 1062, 723.



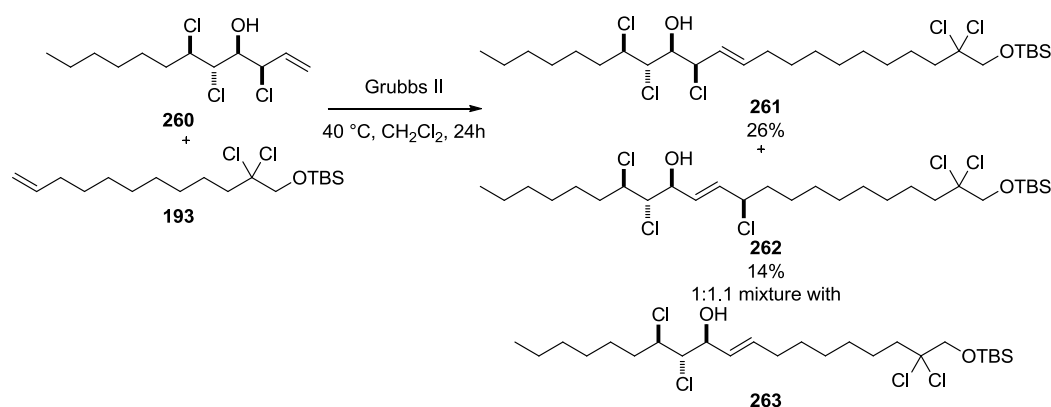
((2-chloro-1-(3-hexyloxiran-2-yl)but-3-en-1-yl)oxy)trimethylsilane (E26): To a solution of alcohol **246** (22.2 mg, 95.0 μmol, 1.00 equiv, d.r. = 6:1) in THF (0.95 mL) at 0 °C was added triethylamine (20 μL, 0.14 mmol, 1.5 equiv) and trimethylsilyl chloride (13 μL, 0.11 mmol, 1.1 equiv). The reaction was allowed to

Experimental

warm to room temperature during 14 hours. Water was added and the mixture extracted three times with CH_2Cl_2 . Combined organic phases were dried over Na_2SO_4 , filtered, and concentrated. Flash column chromatography (hexanes/ Et_2O 20:1, SiO_2) gave **E26** (24 mg, 79 μmol , 83%, d.r. = 6:1).

$^1\text{H NMR}$ (CDCl_3 , 400 MHz) δ 5.97 (ddd, $J = 16.9, 10.2, 8.2$ Hz, 1H), 5.36 (dt, $J = 17.0, 1.1$ Hz, 1H), 5.24 (dt, $J = 10.1, 1.0$ Hz, 1H), 4.34 (ddt, $J = 8.2, 5.0, 0.9$ Hz, 1H), 3.58 (dd, $J = 7.9, 4.9$ Hz, 1H), 3.03 – 2.96 (m, 2H), 1.68 (dddd, $J = 12.9, 9.0, 5.6, 3.2$ Hz, 1H), 1.62 – 1.44 (m, 2H), 1.44 – 1.24 (m, 7H), 0.94 – 0.86 (m, 3H), 0.18 (s, 9H); $^{13}\text{C NMR}$ (CDCl_3 , 101 MHz) δ 134.8, 118.5, 74.3, 64.4, 58.6, 58.2, 31.8, 29.2, 29.1, 27.1, 22.7, 14.2, 0.4; HRMS (EI+) exact mass for $\text{C}_{14}\text{H}_{26}\text{ClO}_2\text{Si}$ $[\text{M}-\text{CH}_3]^+$, calculated 289.1386.1621, found 289.1382; IR (thin film, cm^{-1}) ν 2957, 2928, 2859, 1459, 1251, 1120, 1098, 990, 929, 877, 842, 755, 708.

Treating **E26** (23.0 mg, 75.0 μmol , 1.0 equiv) in the same way as **122** gave **260** (9.8 mg, 34 μmol , 45%), which was in accordance with literature data.



Cross-metathesis of allylic chlorohydrin 260 with olefin 193 - 22-((tert-butyl dimethylsilyl)oxy)-7,8,10,21,21-pentachlorodocos-11-en-9-ol (261) and 22-((tert-butyl dimethylsilyl)oxy)-7,8,12,21,21-pentachlorodocos-10-en-9-ol (263): According to General Procedure 2, allylic chlorohydrin **260** (14 mg, 49 μmol , 1.0 equiv) and olefin **193** (54 mg, 150 μmol , 3.0 equiv) were dissolved in CH_2Cl_2 (2.4 mL). Grubbs' second generation catalyst (**169**, 4.1 mg, 4.9 μmol , 10 mol%) was added. Purification by flash column chromatography (hexanes/ Et_2O 5:1, SiO_2) gave

261 contaminated with an unidentified impurity (7.9 mg, 13 μmol , 26%) and **262** as an inseparable 1:1.1 mixture with **263** (4.3 mg, 6.9 μmol , ca. 14%).

Spectroscopic data for 261 (analytical sample obtained from cross-metathesis of TMS-X13 with X14, followed by deprotection with AcOH/MeOH):

^1H NMR (CDCl₃, 400 MHz) δ 5.90 (dt, $J = 15.3, 6.7$ Hz, 1H), 5.70 (ddt, $J = 15.2, 8.6, 1.4$ Hz, 1H), 5.05 (dd, $J = 8.5, 1.0$ Hz, 1H), 4.50 (dt, $J = 10.2, 3.0$ Hz, 1H), 4.28 (dd, $J = 9.2, 2.9$ Hz, 1H), 3.92 (s, 2H), 3.84 (ddd, $J = 10.0, 9.2, 2.0$ Hz, 1H), 2.27 (d, $J = 10.0$ Hz, 1H), 2.21 – 2.13 (m, 2H), 2.08 (q, $J = 6.9$ Hz, 2H), 1.94 – 1.73 (m, 2H), 1.69 – 1.51 (m, 3H), 1.48 – 1.21 (m, 17H), 0.91 (s, 9H), 0.93 – 0.79 (m, 3H) 0.11 (s, 6H); **^{13}C NMR (CDCl₃, 101 MHz)** δ 137.0, 126.6, 93.7, 75.2, 72.3, 66.9, 65.9, 62.6, 43.7, 32.6, 32.2, 31.8, 29.4, 29.4, 29.3, 29.2, 28.8, 28.8, 26.7, 25.9, 24.9, 22.7, 18.4, 14.2, -5.2; **HRMS (ESI)** exact mass for C₂₈H₅₇Cl₅NO₂Si [M+NH₄]⁺, calculated 642.2596, found 642.2594; **IR (thin film, cm⁻¹)** ν 3457, 2928, 2856, 1667, 1626, 1463, 1378, 1362, 1257, 1188, 1006, 969, 939, 922, 839, 816, 779, 724, 696, 673, 602.

Spectroscopic data for 262 (1:1.1 mixture with 263):

^1H NMR (CDCl₃, 400 MHz) δ 6.00 – 5.76 (m, 2H (minor) + 1H (major)), 5.56 (dd, $J = 15.5, 7.5$ Hz, 1H(major)), 4.74 (q, $J = 6.6$ Hz, 1H(minor)), 4.67 (q, $J = 6.9, 6.3$ Hz, 1H(major)), 4.40 (q, $J = 7.2$ Hz, 1H(minor)), 4.19 (dt, $J = 8.7, 4.3$ Hz, 1H(major + minor)), 3.95 (s, 3H(major+minor)), 3.93 – 3.88 (m, 1H(major+minor)), 2.24 – 2.16 (m, 2H), 2.16 – 2.05 (m, 3H(major) + 2H(minor)), 2.00 (d, $J = 7.8$ Hz, 1H), 1.93 – 1.77 (m, 2H(major) + 3H(minor)), 1.72 – 1.56 (m, 4H), 1.56 – 1.20 (m, 14H), 0.94 (s, 9H), 0.93 – 0.88 (m, 3H), 0.13 (s, 6H); **^{13}C NMR (CDCl₃, 101 MHz)** δ 137.1, 136.0, 128.2, 126.0, 93.5, 93.5, 77.3, 77.2, 77.0, 76.7, 72.9, 72.2, 72.1, 72.0, 69.7, 69.1, 62.0, 61.9, 61.6, 43.5, 43.5, 38.4, 34.5, 32.4, 31.6, 31.6, 29.3, 29.3, 29.0, 29.0, 28.9, 28.7, 28.6, 26.4, 25.7, 25.7, 25.4, 25.3, 24.8, 22.6, 18.3, 14.1, 1.0, -5.3; **HRMS (ESI)** exact mass for C₂₈H₅₇Cl₅NO₂Si [M+NH₄]⁺, calculated 642.2596, found 642.22604; **IR (thin film, cm⁻¹)** ν 3385, 2928, 2856, 2062, 1997, 1671, 1463, 1379, 1362, 1257, 1188, 1154, 1119, 1029, 1007, 971, 939, 839, 815, 779, 724, 696, 667, 602, 572.

APPENDIX

14 Computational Data

Data for lowest-energy structure of 139:

Data from optimization:
 Electronic energy = -1102.06278729
 Zero-point correction = 0.603287
 Thermal correction to Energy = 0.641168
 Thermal correction to Enthalpy = 0.642112
 Thermal correction to Gibbs Free Energy = 0.524596
 Sum of electronic and zero-point Energies = -1101.459500
 Sum of electronic and thermal Energies = -1101.421620
 Sum of electronic and thermal Enthalpies = -1101.420676
 Sum of electronic and thermal Free Energies = -1101.538191

Electronic energy from single point calculation = -1102.29561221

Cartesian coordinates for lowest-energy conformer of 139:

C	6.03180400	6.47711100	0.37302600
C	6.61196500	5.19736600	-0.22690400
C	6.68337000	7.73776300	-0.18970300
C	5.97308200	3.92669200	0.32984900
C	6.55838800	2.65211500	-0.27609200
C	5.90464100	1.39285800	0.29019900
C	6.37929200	0.10718500	-0.36781500
C	5.62931000	-1.16611100	0.02753400
Cl	8.15023800	-0.14801700	-0.05916400
Cl	5.71485700	-1.45350100	1.80539400
C	4.14773700	-1.11981500	-0.39792200
O	4.04624100	-0.70448600	-1.74061900
C	3.38628200	-2.42557100	-0.14530600
Cl	4.14038500	-3.75493500	-1.13761400
C	1.91253800	-2.28555500	-0.49599600
C	1.06608400	-3.52830000	-0.26948200
C	-0.37832800	-3.37561500	-0.73108400
Cl	1.10646300	-3.97478700	1.50349700
C	-1.13901300	-2.18219900	-0.15600900
C	-2.62207100	-2.22331000	-0.52247100
C	-3.40609300	-1.03001600	0.01912500
C	-4.89407000	-1.08705500	-0.32182700
C	-5.68110200	0.09625800	0.23716800
C	-7.16844600	0.03564600	-0.11018200
C	-7.92426500	1.22064400	0.48233900
C	-9.41863100	1.28570900	0.20752600
Cl	-9.72408500	1.35182900	-1.57626700
Cl	-10.25679900	-0.16589700	0.86526500
C	-10.09458200	2.50983900	0.84415200
O	-9.52042800	3.71147600	0.40115600
H	4.95060300	6.50597100	0.18415200
H	6.15677800	6.45277300	1.46352100
H	7.69499400	5.17003300	-0.04146300

H	6.48436300	5.21971700	-1.31856600
H	6.25608400	8.64374400	0.25134600
H	6.54646700	7.79780900	-1.27521800
H	7.76062200	7.74440000	0.01034800
H	4.88988800	3.95444400	0.14557600
H	6.10409100	3.90232900	1.42069100
H	7.63834000	2.62510300	-0.08888900
H	6.42393000	2.66973400	-1.36656200
H	4.82146500	1.45756000	0.12164800
H	6.06334100	1.33257400	1.37289600
H	6.30088400	0.19194300	-1.45387000
H	6.12362900	-2.02471500	-0.43387100
H	3.63526200	-0.35557300	0.19797100
H	4.36051600	-1.41425100	-2.32305900
H	3.51184200	-2.74132900	0.89142000
H	1.80997200	-2.00124200	-1.55045300
H	1.51936600	-1.45819000	0.10720400
H	1.51599800	-4.39147400	-0.76286400
H	-0.34581600	-3.29884200	-1.82660200
H	-0.91181600	-4.30398900	-0.49675700
H	-1.03717000	-2.17172600	0.93711500
H	-0.70374700	-1.24508500	-0.52634500
H	-2.72752800	-2.26285000	-1.61590500
H	-3.06139800	-3.15218100	-0.13347800
H	-3.28635600	-0.98460300	1.11074400
H	-2.97744700	-0.10001700	-0.38014100
H	-5.01647000	-1.12205400	-1.41344200
H	-5.31912900	-2.02189500	0.06925500
H	-5.56250700	0.12633400	1.32917200
H	-5.25541400	1.03254900	-0.14949300
H	-7.28775000	0.02763900	-1.20014500
H	-7.59186000	-0.90290700	0.26730200
H	-7.81476300	1.22590000	1.57453500
H	-7.50524200	2.16311000	0.11163000
H	-9.92599100	2.44866900	1.92362600
H	-11.17221800	2.46854400	0.64963400
H	-9.84767200	3.91255000	-0.48661300

Data for lowest-energy structure of 149:

Data from optimization:

Electronic energy = -1101.537497

Zero-point correction = 0.603791

Thermal correction to Energy = 0.641532

Thermal correction to Enthalpy = 0.642476

Thermal correction to Gibbs Free Energy = 0.525714

Sum of electronic and zero-point Energies = -1101.459420

Sum of electronic and thermal Energies = -1101.421679

Sum of electronic and thermal Enthalpies = -1101.420734

Sum of electronic and thermal Free Energies = -1101.537497

Electronic energy from single point calculation = -1102.29621674

Cartesian coordinates for lowest energy conformer of 149:

C	12.07151000	-0.07794800	0.48094400
C	10.60594500	0.33997900	0.58868100
C	9.64831200	-0.66964500	-0.04061300
C	8.18239500	-0.25195600	0.07037500
C	7.24937600	-1.27965300	-0.57430900
C	5.81392000	-0.78149800	-0.68620500

C	5.17681900	-0.33881900	0.62443400
C	13.02297100	0.94892300	1.08981000
C	3.70729200	0.10053300	0.54981100
Cl	5.28920000	-1.64785900	1.87243400
Cl	4.79791100	-2.04957200	-1.49352400
C	3.43512800	1.13249600	-0.54327500
C	2.01573800	1.69341400	-0.49083600
Cl	4.58765300	2.53264000	-0.41593400
C	0.91723200	0.63886700	-0.48111700
C	-0.47408500	1.25479400	-0.47915500
Cl	1.10902600	-0.44560600	-1.94077600
C	-1.60515100	0.24489400	-0.29989800
C	-2.98274300	0.90448600	-0.26821700
C	-4.11473800	-0.10437400	-0.07939800
C	-5.50082000	0.53708900	-0.07221200
C	-6.62655700	-0.48091400	0.10314000
C	-8.01268700	0.16280800	0.09584200
C	-9.11389100	-0.88701800	0.21758100
C	-10.54702700	-0.37223300	0.26164400
Cl	-10.78607700	0.67127800	1.72461200
Cl	-10.90818500	0.62271000	-1.19242000
C	-11.55564200	-1.52402600	0.33920500
O	-12.89503000	-1.12146600	0.36647300
O	3.28631900	0.65444300	1.77434600
H	12.20675800	-1.04734400	0.97812300
H	12.32423600	-0.23343200	-0.57610500
H	10.47169100	1.31770800	0.10436800
H	10.34603000	0.47958100	1.64752300
H	9.78218100	-1.64895400	0.43949100
H	9.90704300	-0.80318700	-1.09993400
H	8.04438000	0.72712900	-0.41015100
H	7.92896900	-0.12572300	1.13120000
H	7.26823200	-2.21820400	-0.01007400
H	7.59631100	-1.50308800	-1.58930500
H	5.78480800	0.07869000	-1.36187000
H	5.76741400	0.48844000	1.02579200
H	14.06652500	0.62963600	1.00700900
H	12.92777000	1.91732600	0.58606900
H	12.80418600	1.10477000	2.15206500
H	3.10497500	-0.78150900	0.28703900
H	3.63349200	0.68639600	-1.51930500
H	1.90392500	2.27942100	0.42709200
H	1.87181300	2.36386900	-1.34481000
H	1.02960300	-0.03396900	0.37343700
H	-0.61313900	1.82792300	-1.40478600
H	-0.49488300	1.97365400	0.35143200
H	-1.44510800	-0.31131400	0.63434500
H	-1.57557300	-0.48928000	-1.11417400
H	-3.14141800	1.45620900	-1.20529700
H	-3.01783200	1.64686300	0.54145300
H	-3.96145700	-0.64839000	0.86337500
H	-4.06687500	-0.85374500	-0.88202600
H	-5.65212200	1.08390000	-1.01333900
H	-5.55560200	1.28230300	0.73366700
H	-6.48086000	-1.02580400	1.04620400
H	-6.56670000	-1.22659600	-0.70191500
H	-8.14519400	0.72805000	-0.83361300
H	-8.08873100	0.87990700	0.92210100
H	-8.96551200	-1.47847000	1.12999600
H	-9.06022600	-1.57926400	-0.63260700
H	-11.42160600	-2.13452000	-0.55856500
H	-11.28873700	-2.12689700	1.21747900
H	-13.08224000	-0.68245600	1.20800800
H	3.32139300	-0.02569200	2.46198200

Data for lowest-energy structure of 150:

Data from optimization:

Electronic energy = -1102.06376784

Zero-point correction = 0.603139

Thermal correction to Energy = 0.641276

Thermal correction to Enthalpy = 0.642112

Thermal correction to Gibbs Free Energy = 0.642220

Sum of electronic and zero-point Energies = -1101.460629

Sum of electronic and thermal Energies = -1101.422492

Sum of electronic and thermal Enthalpies = -1101.421548

Sum of electronic and thermal Free Energies = -1101.539638

Electronic energy from single point calculation = -1102.29618796

Cartesian coordinates for lowest-energy conformer of 150:

C	-11.91144300	-2.72431700	-0.05935800
C	-10.43035800	-2.85315100	-0.41139500
C	-9.59355500	-1.67651500	0.08589700
C	-8.11068100	-1.80247400	-0.25972000
C	-7.30721700	-0.60641700	0.24466400
C	-5.83207000	-0.64876400	-0.12650000
C	-5.09530500	0.66449500	0.12077900
C	-12.74166300	-3.90171300	-0.56312300
C	-3.62334900	0.63523500	-0.32345100
Cl	-5.20084100	1.16231400	1.84894500
Cl	-5.00793800	-2.01828100	0.73321000
C	-2.87396600	1.95576100	-0.12915800
C	-1.41122700	1.82932300	-0.52514300
Cl	-3.68243900	3.25014100	-1.12870000
C	-0.57329700	3.08488800	-0.34116100
C	0.86023300	2.93984600	-0.83819000
Cl	-0.56956100	3.55833600	1.42547500
C	1.64404000	1.75765100	-0.27061000
C	3.12197900	1.81907800	-0.65419000
C	3.92313400	0.62201600	-0.14694200
C	5.40945400	0.71040300	-0.48823700
C	6.20691900	-0.49836900	-0.00343700
C	7.70104700	-0.38152200	-0.30467300
C	8.45273000	-1.63764600	0.14236500
C	9.97206800	-1.53082700	0.06612200
Cl	10.67948800	-3.14205300	0.50771400
Cl	10.57509000	-0.33187600	1.26516200
C	10.48555800	-1.15449300	-1.32595400
O	-3.55374200	0.18305000	-1.65695500
O	11.88004800	-1.10472000	-1.43171700
H	-12.30238600	-1.78956900	-0.48231700
H	-12.01578100	-2.63929500	1.03027000
H	-10.03630000	-3.78633600	0.01522600
H	-10.32386700	-2.94139600	-1.50200600
H	-9.98923700	-0.74449300	-0.34186600
H	-9.70316400	-1.58897200	1.17578100
H	-7.99360700	-1.88888700	-1.34882400
H	-7.71197100	-2.72646900	0.17648400
H	-7.40753900	-0.51498500	1.33193700
H	-7.71464400	0.31548500	-0.19397000
H	-5.70964900	-0.87877000	-1.18809700
H	-5.63243500	1.43546300	-0.44166900
H	-12.38386700	-4.84463600	-0.13483100
H	-13.79780900	-3.79331900	-0.29739600
H	-12.67873600	-3.98761600	-1.65369700

H	-3.09362500	-0.10920700	0.28247000
H	-2.96871900	2.29727800	0.90214100
H	-0.99055900	1.01434000	0.07638200
H	-1.33782600	1.53116200	-1.57812100
H	-1.04551400	3.93568200	-0.83537400
H	1.39152000	3.87496700	-0.62637200
H	0.80120000	2.85181600	-1.93176300
H	1.21684600	0.81464500	-0.63516700
H	1.55511500	1.74641200	0.82359300
H	3.55787700	2.74431600	-0.25278600
H	3.21329600	1.88065900	-1.74792600
H	3.50637500	-0.30188300	-0.57223600
H	3.80636300	0.54313000	0.94293300
H	5.82895300	1.62370200	-0.04372600
H	5.52745200	0.81118600	-1.57633000
H	5.80866500	-1.40951700	-0.47137200
H	6.06747600	-0.61692800	1.07967500
H	8.10594300	0.50056600	0.20648000
H	7.83917200	-0.22259100	-1.38137700
H	8.16081500	-2.48730000	-0.48619500
H	8.18539000	-1.88965100	1.17426500
H	10.11618700	-0.15219500	-1.55719000
H	10.04159700	-1.86560700	-2.03679100
H	-3.87755500	0.88015400	-2.24920500
H	12.24132000	-1.99878800	-1.35388100

Data for lowest-energy structure of 28

Data from optimization:

Electronic energy = -2348.61120273

Zero-point correction = 0.609842

Thermal correction to Energy = 0.654584

Thermal correction to Enthalpy = 0.655528

Thermal correction to Gibbs Free Energy = 0.520675

Sum of electronic and zero-point Energies = -2348.001361

Sum of electronic and thermal Energies = -2347.956619

Sum of electronic and thermal Enthalpies = -2347.955675

Sum of electronic and thermal Free Energies = -2348.090528

Electronic energy from single point calculation = -2349.03248929

Cartesian coordinates for lowest energy conformer of 28:

C	-10.97968200	3.38083100	-2.69614600
C	-10.60130600	2.69085200	-1.38673100
C	-12.04688600	4.45576800	-2.50720100
C	-9.51361600	1.63236900	-1.55726200
C	-9.13517800	0.94942800	-0.24442700
C	-8.04646900	-0.10407500	-0.44061700
C	-7.54213000	-0.70128500	0.86361500
C	-6.29217600	-1.57565300	0.78022400
C1	-8.86706600	-1.68477500	1.64129900
C	-5.00530800	-0.77736400	0.48672000
C1	-6.50292900	-2.87079900	-0.46080600
C	-3.75900000	-1.64847400	0.30411200
C	-2.50312000	-0.82551200	0.07537700
C1	-3.53641000	-2.73181100	1.74726700
C	-1.23494200	-1.62135900	-0.19199500
C	-0.03242500	-0.71760900	-0.41286100
C1	-1.48704500	-2.68650500	-1.66331700

Appendix

C	1.29022100	-1.45148200	-0.61584700
C	2.48244900	-0.49722700	-0.66005300
C	3.81104200	-1.21514400	-0.88935200
C	5.01022600	-0.26912200	-0.90252800
C	6.34055700	-0.99386700	-1.09584000
C	7.53571200	-0.04109700	-1.10714700
C	8.85219500	-0.81299200	-1.19197600
C	10.08845500	0.06873200	-1.31527600
C	10.18868800	1.17402100	-0.26923300
Cl	10.12597500	0.89063800	-2.91943000
Cl	11.55895000	-0.97630900	-1.19927200
O	10.08615600	0.54403400	1.00446600
S	9.69300100	1.54019900	2.25322100
O	9.74293900	0.61275000	3.38851700
O	10.73187100	2.58272200	2.25529900
O	8.34978500	2.05176000	1.93453600
O	-4.81111500	0.08843200	1.60800500
S	-4.81794200	1.72474900	1.35822200
O	-6.18821200	2.04905000	0.93283300
O	-3.81244900	1.97457100	0.31611600
O	-4.45840100	2.20330300	2.69715400
H	-10.08060700	3.82934000	-3.13913900
H	-11.33731700	2.62836300	-3.41156900
H	-11.49719300	2.22695100	-0.94968000
H	-10.25934200	3.44724900	-0.66592600
H	-12.30290500	4.94055700	-3.45488900
H	-12.96635600	4.02758700	-2.09185300
H	-11.70045700	5.23297600	-1.81666100
H	-8.61888200	2.09964100	-1.99239000
H	-9.85266300	0.87426700	-2.27756800
H	-10.02663700	0.48330600	0.19372700
H	-8.78261400	1.70286100	0.47244900
H	-7.18911500	0.36421900	-0.94047900
H	-8.40520700	-0.90490900	-1.09686700
H	-7.33221900	0.08700700	1.58884300
H	-6.15725500	-2.09798300	1.72903000
H	-5.11077400	-0.19844800	-0.44034500
H	-3.92581000	-2.32746400	-0.53169100
H	-2.69705000	-0.16036100	-0.77468800
H	-2.31348000	-0.19309500	0.95020000
H	-1.03585000	-2.33128000	0.61399200
H	0.03811700	-0.08759200	0.48444700
H	-0.23421000	-0.04821700	-1.25911400
H	1.25356400	-2.02889300	-1.54774800
H	1.43091200	-2.17466000	0.19982200
H	2.32672900	0.24360600	-1.45693800
H	2.53253800	0.06478500	0.28296900
H	3.76878200	-1.76309900	-1.84129400
H	3.95453900	-1.96883700	-0.10211300
H	5.04019400	0.29069100	0.04274300
H	4.88004800	0.47435200	-1.70154400
H	6.31832300	-1.56001300	-2.03720100
H	6.47152400	-1.72914300	-0.28987900
H	7.52118400	0.56206600	-0.19069500
H	7.44391500	0.65120600	-1.95378700
H	8.84246300	-1.50403500	-2.04174300
H	8.98078900	-1.40964000	-0.28243500
H	9.35775900	1.87222100	-0.42003400
H	11.14010800	1.70639200	-0.35936600

Data for lowest-energy structures of 147 obtained from MCMC Conformational Search

Data from optimization (lowest-energy conformer):

Electronic energy = -2348.60330854

Zero-point correction = 0.610872

Thermal correction to Energy = 0.655372

Thermal correction to Enthalpy = 0.656316

Thermal correction to Gibbs Free Energy = 0.522160

Sum of electronic and zero-point Energies = -2347.992436

Sum of electronic and thermal Energies = -2347.947937

Sum of electronic and thermal Enthalpies = -2347.946993

Sum of electronic and thermal Free Energies = -2348.081149

Electronic energy from single point calculation = -2349.02520049

Cartesian coordinates for lowest energy conformer of 147:

C	-10.37425200	3.10878800	2.51476600
C	-9.02506400	3.07362200	1.79923700
C	-8.93755200	1.97411600	0.74354900
C	-7.58320400	1.92329100	0.03794300
C	-7.54613600	0.82007800	-1.01696400
C	-6.27702100	0.73998600	-1.86476100
C	-4.96734800	0.65684300	-1.06952200
C	-10.45842200	4.21603900	3.56179100
C	-4.95314000	-0.54575200	-0.11693700
Cl	-3.57886600	0.55411300	-2.22774300
Cl	-6.21355300	2.20766400	-2.94376800
C	-3.86356500	-0.57848600	0.97303100
C	-2.38737500	-0.52185100	0.59084800
Cl	-4.20045400	0.79973500	2.10841400
C	-1.90493000	-1.67275800	-0.28741900
C	-0.47225800	-1.50223700	-0.77356800
Cl	-2.06949300	-3.24200600	0.64611500
C	0.59153300	-1.27305300	0.29791400
C	1.99114700	-1.21701200	-0.31328800
C	3.09859200	-0.99317300	0.71441400
C	4.48582600	-0.93528700	0.07750800
C	5.61298100	-0.73825300	1.08909800
C	6.98734200	-0.69094000	0.42210300
C	8.10199200	-0.49490800	1.44966900
C	9.50636500	-0.57648800	0.86421300
Cl	10.70143600	-0.15399900	2.15129900
Cl	9.86797700	-2.25592000	0.31417200
C	9.75016900	0.32208500	-0.34369600
O	9.40732900	1.64709200	0.05192900
S	-5.89196700	-2.96670400	-0.53012500
O	-5.34792100	-4.05216800	-1.35180400
O	-7.21430700	-2.47615500	-0.95267800
O	-5.78435100	-3.16396300	0.92410700
O	-4.84622300	-1.74157500	-0.88958500
S	9.17858400	2.70939700	-1.18307800
O	8.96475300	3.96165400	-0.44993200
O	7.99913300	2.21109200	-1.90960700
O	10.41970500	2.65321000	-1.97328500
H	-10.55265600	2.13605900	2.99158600
H	-11.17238800	3.24275600	1.77271100
H	-8.84097500	4.04847700	1.32546300
H	-8.22613400	2.93143700	2.54105900
H	-9.72823600	2.12516300	-0.00466300
H	-9.13506900	1.00103500	1.21489300
H	-6.79792400	1.76016700	0.78828400

H	-7.37892600	2.89466600	-0.43076700
H	-8.38194300	0.94569000	-1.71472200
H	-7.69404700	-0.15821500	-0.54754300
H	-6.33921800	-0.10733900	-2.55166500
H	-4.80677200	1.57493900	-0.49910200
H	-10.32334700	5.20160600	3.10181200
H	-11.42726100	4.21582000	4.07156700
H	-9.68022900	4.09552500	4.32405300
H	-5.90812100	-0.53442600	0.42261900
H	-4.05950700	-1.47846100	1.55943200
H	-2.16021700	0.41609200	0.07382300
H	-1.81462500	-0.52259400	1.52356700
H	-2.56209800	-1.82285500	-1.14097600
H	-0.48727500	-0.64508100	-1.46206100
H	-0.20930000	-2.38085200	-1.37431600
H	0.54957500	-2.08058600	1.04099200
H	0.39421100	-0.33505600	0.83267700
H	2.02600200	-0.41371900	-1.06301400
H	2.18479800	-2.15489600	-0.85280400
H	3.07214400	-1.80149500	1.45902300
H	2.90812900	-0.05795400	1.25973100
H	4.51306700	-0.11841600	-0.65740400
H	4.66453600	-1.86448100	-0.48218900
H	5.59288600	-1.55595200	1.82271700
H	5.44606500	0.19285200	1.64817000
H	7.00647600	0.13117300	-0.30458500
H	7.14907300	-1.62219700	-0.13554100
H	8.02564000	-1.24034600	2.24875400
H	8.00623000	0.49385800	1.91092200
H	10.79770100	0.27251300	-0.65431500
H	9.10503700	-0.01240000	-1.16395800

Data from optimization (second lowest-energy conformer):

Electronic energy = -2348.60200348

Zero-point correction = 0.609981

Thermal correction to Energy = 0.654869

Thermal correction to Enthalpy = 0.655813

Thermal correction to Gibbs Free Energy = 0.520141

Sum of electronic and zero-point Energies = -2347.992023

Sum of electronic and thermal Energies = -2347.947135

Sum of electronic and thermal Enthalpies = -2347.946191

Sum of electronic and thermal Free Energies = -2348.081863

Electronic energy from single point calculation = -2349.02293057

Cartesian coordinates for second lowest energy conformer of 147:

C	-9.92402600	5.01891000	-1.69438700
C	-9.91775300	3.70363800	-0.91789300
C	-8.72159800	2.81377700	-1.24928200
C	-8.72352600	1.50097800	-0.46836600
C	-7.54169200	0.61031400	-0.85020500
C	-7.40161600	-0.62826000	0.03222900
C	-6.14930800	-1.46213900	-0.27877000
C	-11.13299500	5.89055600	-1.36380800
C	-4.86442700	-0.67718600	0.01858700
Cl	-6.16583900	-2.99199600	0.68510800
Cl	-8.88168800	-1.65876200	-0.21298500
C	-3.54452100	-1.19972400	-0.57400500
C	-3.09032500	-2.59139100	-0.15789900
Cl	-3.66663100	-1.09243500	-2.38374400
C	-1.63393100	-2.87120300	-0.52767200
C	-0.61810100	-2.03863900	0.23743800
Cl	-1.33685300	-4.64733500	-0.20205300
C	0.83774100	-2.28373100	-0.15367000

C	1.78226800	-1.27664700	0.50024600
C	3.24645500	-1.48719200	0.12001600
C	4.17410100	-0.43927000	0.73210600
C	5.63454300	-0.60783300	0.31876100
C	6.53856100	0.46959400	0.91725100
C	7.97620600	0.32765000	0.42847100
C	8.98061700	1.32725500	0.98353800
Cl	8.46303900	3.01857200	0.61915000
Cl	9.12022800	1.16441800	2.77536500
C	10.39318700	1.12654600	0.43591200
O	10.34562200	1.29699800	-0.97864800
S	-4.49506100	0.94525500	2.03404300
O	-4.31251300	0.66657700	3.46088400
O	-5.74082400	1.65131100	1.69207100
O	-3.30985300	1.48166300	1.34516100
O	-4.69157200	-0.58015100	1.43177600
S	11.13970800	0.16369500	-1.86576900
O	10.87371400	0.62910200	-3.23120100
O	10.50962200	-1.12039800	-1.51662900
O	12.54661400	0.25846900	-1.44040400
H	-9.91034500	4.80159000	-2.77072300
H	-9.00081600	5.57201700	-1.47629800
H	-9.92207700	3.91917500	0.16014300
H	-10.84718500	3.15572400	-1.12970900
H	-7.79122400	3.35975000	-1.03890000
H	-8.72039100	2.59556300	-2.32673200
H	-9.66738800	0.97310900	-0.64751700
H	-8.67503800	1.71502300	0.60871600
H	-6.63398100	1.21273600	-0.75243100
H	-7.61382700	0.29621500	-1.89950500
H	-7.41400700	-0.35882800	1.09181500
H	-6.15936200	-1.76658800	-1.32847800
H	-11.15353900	6.14246100	-0.29743600
H	-11.12024300	6.82828400	-1.92855300
H	-12.06780400	5.37020400	-1.60155800
H	-4.99244900	0.32214300	-0.40691900
H	-2.80062400	-0.44893000	-0.30356900
H	-3.20426300	-2.66893200	0.93024200
H	-3.73463500	-3.34441500	-0.61818300
H	-1.48070800	-2.77353700	-1.60560900
H	-0.76206600	-2.19674700	1.31435000
H	-0.85209100	-0.98501600	0.03529800
H	0.93293100	-2.21610400	-1.24657200
H	1.13495700	-3.30096100	0.12890100
H	1.67732100	-1.33570900	1.59281000
H	1.47908400	-0.26000700	0.21289800
H	3.34291400	-1.45832400	-0.97467100
H	3.56711700	-2.49008500	0.43563000
H	4.09828700	-0.48051000	1.82793300
H	3.83091500	0.56138000	0.43344000
H	5.70701700	-0.57335400	-0.77717700
H	5.99247900	-1.59987500	0.62671300
H	6.50529500	0.40690900	2.01190800
H	6.15201400	1.45702100	0.63825800
H	8.01138500	0.42755900	-0.66275200
H	8.36755900	-0.66803200	0.67458900
H	11.08363600	1.85653700	0.86597600
H	10.71279500	0.11292300	0.70134600

Data for lowest-energy structures of 147 obtained from Manual Conformational Analysis

Data from optimization (lowest-energy conformer Table 17):

Electronic energy = -2348.60852270

Zero-point correction = 0.609853

Thermal correction to Energy = 0.654616

Thermal correction to Enthalpy = 0.655560

Thermal correction to Gibbs Free Energy = 0.521862

Sum of electronic and zero-point Energies = -2347.998669

Sum of electronic and thermal Energies = -2347.953907

Sum of electronic and thermal Enthalpies = -2347.952962

Sum of electronic and thermal Free Energies = -2348.086661

Electronic energy from single point calculation = -2349.02992430

Cartesian coordinates for lowest energy conformer (Table 17) of 147:

C	-12.89344400	2.75258100	-0.25026000
C	-11.42275200	2.65350700	-0.65065500
C	-10.62668000	1.67424100	0.20966400
C	-9.16389100	1.56825700	-0.21733300
C	-8.37088200	0.60645600	0.66394200
C	-6.94502600	0.38353500	0.18281900
C	-6.21651900	-0.75500500	0.88740200
C	-13.67436600	3.73614100	-1.11804300
C	-4.78312700	-1.02076500	0.40775600
Cl	-6.17569600	-0.50116300	2.67367000
Cl	-5.98037500	1.91946400	0.30727100
C	-4.65020800	-1.13091300	-1.11334900
C	-3.26218500	-1.55607900	-1.57928100
Cl	-5.83952300	-2.34637600	-1.76044400
C	-2.13066800	-0.61792200	-1.17926400
C	-0.77844600	-1.13538700	-1.64299400
Cl	-2.44294000	1.04010800	-1.89859000
C	0.40911900	-0.29297700	-1.18618900
C	1.74738000	-0.96908500	-1.47960300
C	2.94475100	-0.10942700	-1.07976700
C	4.28697200	-0.80591100	-1.29527100
C	5.47806100	0.06662600	-0.90497100
C	6.81822100	-0.64999100	-1.06605000
C	7.98082300	0.26668700	-0.69897900
C	9.36663400	-0.36262400	-0.69581000
Cl	9.45177100	-1.68514900	0.53017300
Cl	9.75197800	-1.07247500	-2.30934500
C	10.48200700	0.64095800	-0.41438500
O	10.20109100	1.24074300	0.84658400
O	-4.36474200	-2.23878300	1.01554600
S	-3.00381700	-2.30580800	1.95567100
O	-1.97546800	-2.89381500	1.08168300
O	-2.71485700	-0.91980300	2.35250400
O	-3.43307100	-3.19174900	3.04506000
H	-13.35310000	1.75759200	-0.31811800
H	-12.96154400	3.05647700	0.80272800
H	-10.96219700	3.64975600	-0.58578400
H	-11.35584300	2.34738200	-1.70463100
H	-11.09399500	0.68082700	0.15716100
H	-10.67668200	1.98961200	1.26138400
H	-8.70463100	2.56410200	-0.18166100
H	-9.11189800	1.23018000	-1.26149900
H	-8.85350800	-0.38115300	0.65571600
H	-8.36290000	0.95629100	1.70179200

H	-6.96573200	0.14987100	-0.88554200
H	-6.81355700	-1.65946700	0.74180600
H	-14.72688100	3.78607100	-0.82094500
H	-13.25599700	4.74606800	-1.03950900
H	-13.63880600	3.44183000	-2.17326100
H	-4.14313300	-0.19322200	0.73474700
H	-4.93280100	-0.18072600	-1.57165800
H	-3.03153200	-2.53880900	-1.15426400
H	-3.27534000	-1.65280500	-2.66974100
H	-2.10663000	-0.43538900	-0.10214500
H	-0.78441700	-1.23857900	-2.73581200
H	-0.68527100	-2.14607000	-1.22342000
H	0.32411700	-0.10943300	-0.10570500
H	0.37993200	0.68706700	-1.67844600
H	1.81039200	-1.20587700	-2.55126200
H	1.79253300	-1.92749000	-0.94365200
H	2.85054600	0.16976500	-0.02068500
H	2.92491400	0.82862800	-1.65233100
H	4.38116800	-1.10057000	-2.35011700
H	4.31009600	-1.73466700	-0.70798100
H	5.36463400	0.38834000	0.13953800
H	5.47573100	0.98012100	-1.51570000
H	6.92763500	-0.99360400	-2.10163500
H	6.83025200	-1.54120500	-0.42694400
H	7.82880100	0.68037100	0.30441600
H	8.02743700	1.11433200	-1.39457500
H	11.45262200	0.13546600	-0.39354400
H	10.46736100	1.40034600	-1.20445100
S	11.31867500	2.32293100	1.37841700
O	10.72669800	2.74482300	2.65211900
O	11.36808100	3.36754500	0.34269000
O	12.57066600	1.55881900	1.50476100

Data from optimization (second lowest-energy conformer Table 17):

Electronic energy = -2348.60649509

Zero-point correction = 0.609425

Thermal correction to Energy = 0.653670

Thermal correction to Enthalpy = 0.654614

Thermal correction to Gibbs Free Energy = 0.520209

Sum of electronic and zero-point Energies = -2347.997071

Sum of electronic and thermal Energies = -2347.952825

Sum of electronic and thermal Enthalpies = -2347.951881

Sum of electronic and thermal Free Energies = -2348.086286

Electronic energy from single point calculation = -2349.02807379

Cartesian coordinates for second-lowest energy conformer (Table 17) of 147:

C	-2.67777900	7.96184300	-0.45896800
C	-2.44687900	6.47481100	-0.72130900
C	-3.44302100	5.57520600	0.00652700
C	-3.19398200	4.08807800	-0.23763800
C	-4.20404000	3.21262500	0.49911300
C	-4.00284800	1.72231800	0.26790400
C	-5.16759400	0.85417600	0.72942000
C	-4.97303700	-0.65819100	0.57661500
C	-4.46431800	-1.08834000	-0.79901300
C	-4.33338000	-2.60188300	-0.88939100
C	-3.75320200	-3.08320100	-2.21665000
C	-2.43640100	-2.44346600	-2.63642000
C1	-5.56974300	-0.47258200	-2.10623800
C1	-3.54848900	-4.89689000	-2.08488200
C1	-5.58739800	1.18218900	2.45416100
C1	-2.45120500	1.17070400	1.04464800
C	-0.05513500	-1.78006600	-2.11067500

Appendix

C	1.08676200	-1.78596400	-1.09726600
C	2.33154900	-1.05790000	-1.60003800
C	3.47435400	-1.04931200	-0.58753200
C	4.70178700	-0.29477900	-1.09671100
C	5.82282300	-0.29052100	-0.06252000
C	7.07937700	0.48427500	-0.43298000
C	8.13902800	0.48169300	0.66661900
Cl	7.81135300	-0.17820600	-1.94266100
Cl	6.68935200	2.22360800	-0.72067200
C	-1.31239300	-2.48473800	-1.60372000
O	8.46774900	-0.87711200	0.94159900
S	9.88165200	-1.10363200	1.74914300
O	9.85304400	-2.55125600	1.98553100
O	10.93644900	-0.65281100	0.82640500
O	9.76795300	-0.27349000	2.96013800
C	-1.68215400	8.85216700	-1.19749400
O	-6.23177800	-1.27094600	0.83181700
S	-6.41632500	-2.38697300	2.04114900
O	-7.58651100	-1.88203700	2.77113600
O	-5.15787600	-2.37087400	2.80142800
O	-6.66792800	-3.64683600	1.32332400
H	-2.61096900	8.15147300	0.62058500
H	-3.70054500	8.22698700	-0.75828200
H	-2.50650700	6.28403500	-1.80248500
H	-1.42542300	6.20808200	-0.41431800
H	-3.39202700	5.77636700	1.08590100
H	-4.46365000	5.83135800	-0.31085500
H	-3.24625100	3.87689100	-1.31453000
H	-2.17720500	3.83465400	0.08808200
H	-4.17651100	3.42322000	1.57358700
H	-5.21812700	3.44882700	0.14791400
H	-3.86132000	1.54043900	-0.80196200
H	-6.04559200	1.16374900	0.15541500
H	-4.23028200	-1.00465800	1.30364600
H	-3.50180900	-0.60758700	-0.98705300
H	-5.31174600	-3.06272500	-0.72728700
H	-3.67922600	-2.91160900	-0.06451200
H	-4.48844000	-2.96608300	-3.01425600
H	-2.10489300	-2.91704300	-3.56787700
H	-2.66204400	-1.39856800	-2.89420100
H	-0.30499700	-0.74031600	-2.36659000
H	0.28045300	-2.25870900	-3.04150800
H	1.34664800	-2.82429300	-0.84758100
H	0.74431000	-1.31676500	-0.16367300
H	2.06607300	-0.02157000	-1.85285300
H	2.67613300	-1.52761000	-2.53229700
H	3.75464900	-2.08327200	-0.34353600
H	3.12695400	-0.58913000	0.34797000
H	4.41568700	0.73577100	-1.33971500
H	5.05532600	-0.75877200	-2.02548800
H	6.14107600	-1.31737500	0.15206600
H	5.46348700	0.14149000	0.88039600
H	9.02266100	1.03677900	0.33478300
H	7.71399500	0.95054600	1.56060700
H	-1.63346100	-2.00599900	-0.66848000
H	-1.07520500	-3.52791700	-1.35730900
H	-1.86145900	9.91234900	-0.99186700
H	-1.75342300	8.70469400	-2.28117400
H	-0.65327900	8.62186800	-0.89823900

Data for lowest-energy structure of 148

Data from optimization:

Electronic energy = -2348.60985052

Zero-point correction = 0.610011

Thermal correction to Energy = 0.654857

Thermal correction to Enthalpy = 0.655801
 Thermal correction to Gibbs Free Energy = 0.520640
 Sum of electronic and zero-point Energies = -2347.999839
 Sum of electronic and thermal Energies = -2347.954994
 Sum of electronic and thermal Enthalpies = -2347.954049
 Sum of electronic and thermal Free Energies = -2348.089211

Electronic energy from single point calculation = -2349.03095035

Cartesian coordinates for lowest energy conformer of 148:

C	-12.17268900	3.67447700	0.02938000
C	-10.65085100	3.60586100	0.14140300
C	-10.08603500	2.22285200	-0.17542900
C	-8.56507100	2.15670100	-0.04922400
C	-8.01895200	0.78037600	-0.42011300
C	-6.51849600	0.63714200	-0.21826500
C	-6.00794200	-0.79177400	-0.37229300
C	-12.72281900	5.06692900	0.32679800
C	-4.50944400	-0.94227100	-0.08492400
Cl	-6.37428600	-1.45074200	-2.01013600
Cl	-5.61959100	1.75696200	-1.33421400
C	-3.93645900	-2.34837200	-0.25308100
C	-2.47052900	-2.39623600	0.14873500
Cl	-4.89866600	-3.54225200	0.72657900
C	-1.78697600	-3.74109000	-0.03122200
C	-0.35796900	-3.76917900	0.49561300
Cl	-1.80571000	-4.20100300	-1.80725700
C	0.57085100	-2.68137900	-0.03944800
C	2.00902100	-2.87683400	0.43793200
C	2.95950500	-1.79408300	-0.06856400
C	4.39725900	-1.99186800	0.40690900
C	5.35228600	-0.91483800	-0.10331600
C	6.78525500	-1.12290400	0.38554100
C	7.71731100	-0.03633400	-0.14087800
C	9.17734600	-0.13815500	0.27548500
Cl	9.89443500	-1.69819400	-0.28018700
Cl	9.32958600	-0.06446700	2.07302500
C	10.05457200	0.95452100	-0.33119200
O	-4.33260700	-0.53425300	1.27056600
S	9.86398900	3.48910400	-0.85453700
O	9.35266800	4.60271700	-0.04843800
O	11.32313000	3.48441300	-1.05505100
O	9.10355500	3.22412500	-2.08755300
O	9.55938500	2.20934900	0.12941000
S	-3.33461600	0.72688200	1.66422500
O	-4.24676900	1.84639400	1.94170500
O	-2.46362200	0.92847800	0.49734300
O	-2.65210500	0.20687700	2.85661500
H	-12.47386500	3.36806500	-0.98130000
H	-12.61784500	2.94714900	0.72098700
H	-10.34943500	3.89862300	1.15745300
H	-10.20477100	4.34387200	-0.54042500
H	-10.37670600	1.93892200	-1.19689100
H	-10.53986700	1.48111200	0.49675900
H	-8.27015300	2.40125400	0.98047500
H	-8.11581400	2.91786200	-0.69897700
H	-8.27562700	0.54028600	-1.45818500
H	-8.48917700	0.01758500	0.21631700
H	-6.23543400	0.96676900	0.78559100
H	-6.57571200	-1.40817700	0.33027900
H	-13.81479500	5.09299500	0.25301200
H	-12.44832100	5.38896600	1.33788300
H	-12.32221000	5.80483900	-0.37754600
H	-3.93961600	-0.29430100	-0.76073600

H	-4.06341300	-2.66624600	-1.28885500
H	-1.95254400	-1.63212600	-0.44307800
H	-2.36757400	-2.12040900	1.20617800
H	-2.36431900	-4.53565600	0.44403100
H	-0.43635300	-3.67958500	1.58792900
H	0.06633700	-4.75901700	0.29096900
H	0.54990800	-2.68342000	-1.13761200
H	0.21709200	-1.69418000	0.28492900
H	2.02844500	-2.89127200	1.53698200
H	2.36986500	-3.86054800	0.10592800
H	2.93849300	-1.77942800	-1.16759200
H	2.59907900	-0.81040600	0.26375800
H	4.41769600	-2.00193500	1.50592700
H	4.75566100	-2.97794100	0.07882500
H	5.33845300	-0.90729500	-1.20204400
H	4.99566500	0.07202700	0.22237400
H	6.79704400	-1.12242000	1.48219600
H	7.13962600	-2.10785300	0.05844300
H	7.71050300	-0.03261500	-1.23861300
H	7.36943700	0.94945600	0.18837000
H	9.97108400	0.88143100	-1.42154500
H	11.09699700	0.82661300	-0.02582100

Data for lowest-energy structure of 219 in hexane:

Data from optimization:

Electronic energy = -457.48245066

Zero-point correction = 0.239089

Thermal correction to Energy = 0.254156

Thermal correction to Enthalpy = 0.255101

Thermal correction to Gibbs Free Energy = 0.194488

Sum of electronic and zero-point Energies = -457.243362

Sum of electronic and thermal Energies = -457.228294

Sum of electronic and thermal Enthalpies = -457.227350

Sum of electronic and thermal Free Energies = -457.287963

Electronic energy from single point calculation = -457.58262618

Cartesian coordinates for lowest energy conformer:

C	4.54115400	-0.08933200	0.39059800
C	3.15985700	-0.00786600	1.03142100
C	2.01838700	-0.01467100	0.02482600
C	0.64468800	0.16484900	0.69241100
Cl	2.01424100	-1.58482400	-0.88786800
C	-0.54824000	0.14606600	-0.27344200
O	0.64411900	1.33389400	1.47904400
C	-1.86087100	0.19741100	0.43317600
Cl	-0.39708300	1.60583400	-1.38107300
C	-2.83514300	-0.68399500	0.19705100
C	-4.16908100	-0.69329400	0.88152200
C	-5.31555700	-0.49963500	-0.11628500
H	4.68475500	-1.03725700	-0.13436500
H	4.68812100	0.72254300	-0.32992800
H	5.32026800	-0.00474500	1.15300600
H	3.06578000	0.92260200	1.60085500
H	3.01354700	-0.83296500	1.73927500
H	2.17008800	0.75557200	-0.73767900
H	0.49063600	-0.67148200	1.38646700
H	-0.49268600	-0.71513400	-0.93903900
H	0.58348200	2.10196500	0.89141000
H	-1.98361900	0.98281200	1.17775500
H	-2.67821800	-1.45136800	-0.56446200

H	-4.19667000	0.08953800	1.64719200
H	-4.30106600	-1.65341400	1.39623500
H	-6.28440400	-0.54282100	0.38929800
H	-5.30248300	-1.27970900	-0.88469200
H	-5.23333900	0.46835200	-0.61936000

Data for lowest-energy structure of 220 in hexane:

Data from optimization:
 Electronic energy = -457.48359459
 Zero-point correction = 0.239221
 Thermal correction to Energy = 0.254117
 Thermal correction to Enthalpy = 0.255061
 Thermal correction to Gibbs Free Energy = 0.195509
 Sum of electronic and zero-point Energies = -457.244373
 Sum of electronic and thermal Energies = -457.229478
 Sum of electronic and thermal Enthalpies = -457.228533
 Sum of electronic and thermal Free Energies = -457.288086

Electronic energy from single point calculation = -457.58400899

Cartesian coordinates for lowest energy conformer:

C	3.11197000	2.25343900	-0.15424100
C	2.04656300	1.23396200	0.23389900
C	2.17480200	-0.09511500	-0.49286700
C	1.06517400	-1.11082200	-0.16184800
C1	3.76720100	-0.88300700	-0.07311000
C	-0.25956600	-0.58405700	-0.63730900
O	0.99446800	-1.37464800	1.21813400
C	-1.29076000	-0.31531900	0.16165300
C	-2.59135300	0.21868200	-0.34382900
C	-3.80745900	-0.54615200	0.16491700
C1	-2.73408700	1.96544500	0.18818600
C	-3.79503200	-1.99540200	-0.31846500
H	4.11151400	1.91750300	0.13396600
H	2.92199400	3.20883100	0.34203900
H	3.11254400	2.43271800	-1.23501800
H	1.05202500	1.62767000	-0.00873400
H	2.05573600	1.04992600	1.31300200
H	2.22018100	0.05012700	-1.57630600
H	1.29003200	-2.03366100	-0.71880300
H	-0.33754900	-0.40903300	-1.71081300
H	1.84387000	-1.73974500	1.50027700
H	-1.20870900	-0.48169000	1.23477400
H	-2.59088600	0.26551800	-1.43602700
H	-3.81392100	-0.50805900	1.26023300
H	-4.71171200	-0.03746600	-0.18322000
H	-4.70139000	-2.51261100	0.00749900
H	-3.75490500	-2.04760600	-1.41192200
H	-2.93354000	-2.54198800	0.07622500

Data for lowest-energy structure of 219 in acetonitrile:

Data from optimization:
 Electronic energy = -457.48703969
 Zero-point correction = 0.238737
 Thermal correction to Energy = 0.253810
 Thermal correction to Enthalpy = 0.254755
 Thermal correction to Gibbs Free Energy = 0.193612

Sum of electronic and zero-point Energies = -457.248302
Sum of electronic and thermal Energies = -457.233229
Sum of electronic and thermal Enthalpies = -457.232285
Sum of electronic and thermal Free Energies = -457.293428

Electronic energy from single point calculation = -457.58727651

Cartesian coordinates for lowest energy conformer:

C	4.52135100	-0.19566700	0.53130900
C	3.11040700	-0.25490000	1.10552600
C	2.02036300	0.00130200	0.07576000
C	0.62184400	0.05836500	0.71114000
Cl	2.05128300	-1.30792500	-1.18888000
C	-0.55256600	0.15700000	-0.27030900
O	0.58781100	1.10489500	1.65755400
C	-1.87398200	0.19472500	0.42121100
Cl	-0.34943500	1.69331000	-1.26325100
C	-2.84221000	-0.68733200	0.15906000
C	-4.17729500	-0.71630700	0.84095300
C	-5.32593100	-0.54259700	-0.15675800
H	4.69596100	-0.99873700	-0.19051900
H	4.69559300	0.76073400	0.02609100
H	5.26132800	-0.29494800	1.33032200
H	2.99411500	0.51520200	1.87570900
H	2.92574800	-1.22321200	1.58601800
H	2.22165700	0.92440000	-0.47633900
H	0.45963600	-0.86934400	1.27475700
H	-0.51717600	-0.65519400	-0.99626700
H	0.66681700	1.95386200	1.19409900
H	-2.00961300	0.96419300	1.18015100
H	-2.67442300	-1.44254100	-0.61219000
H	-4.21665400	0.06611700	1.60680500
H	-4.29471600	-1.68016800	1.35272600
H	-5.29630100	-1.32289100	-0.92494300
H	-5.26420000	0.42877200	-0.65788400
H	-6.29355800	-0.60448500	0.34990600

Data for lowest-energy structure of 220 in acetonitrile:

Data from optimization:

Electronic energy = -457.48967356

Zero-point correction = 0.238676

Thermal correction to Energy = 0.253608

Thermal correction to Enthalpy = 0.254553

Thermal correction to Gibbs Free Energy = 0.194642

Sum of electronic and zero-point Energies = -457.250998

Sum of electronic and thermal Energies = -457.236065

Sum of electronic and thermal Enthalpies = -457.235121

Sum of electronic and thermal Free Energies = -457.295031

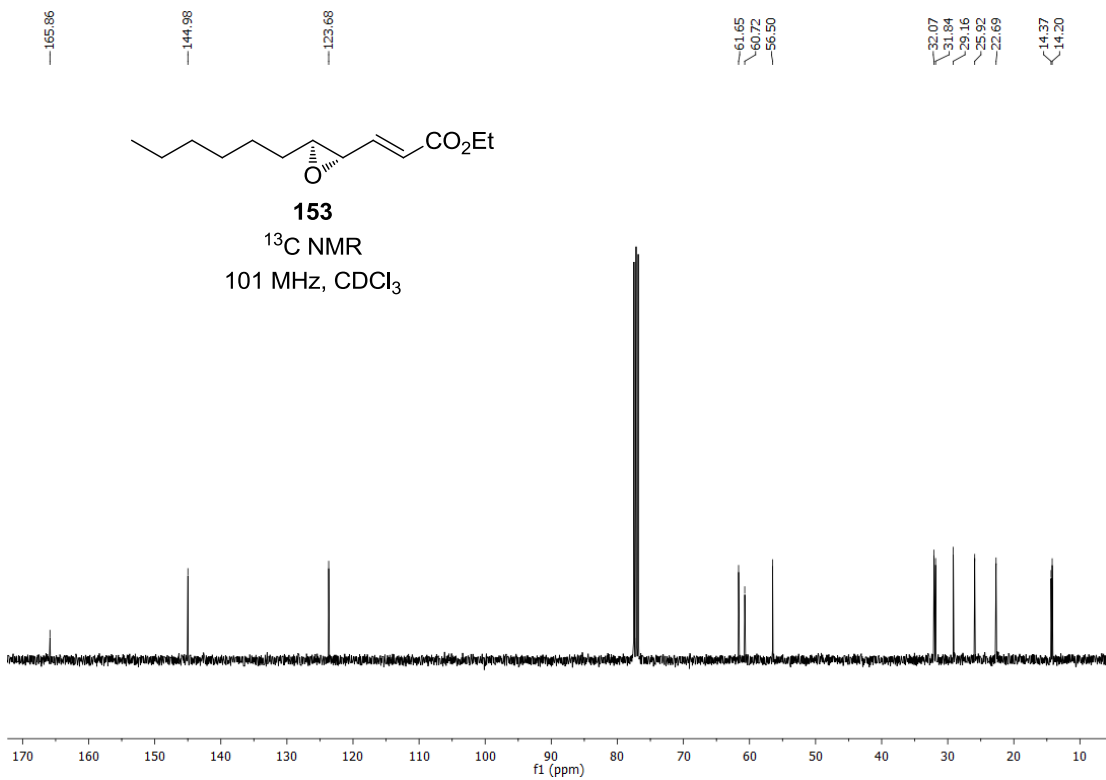
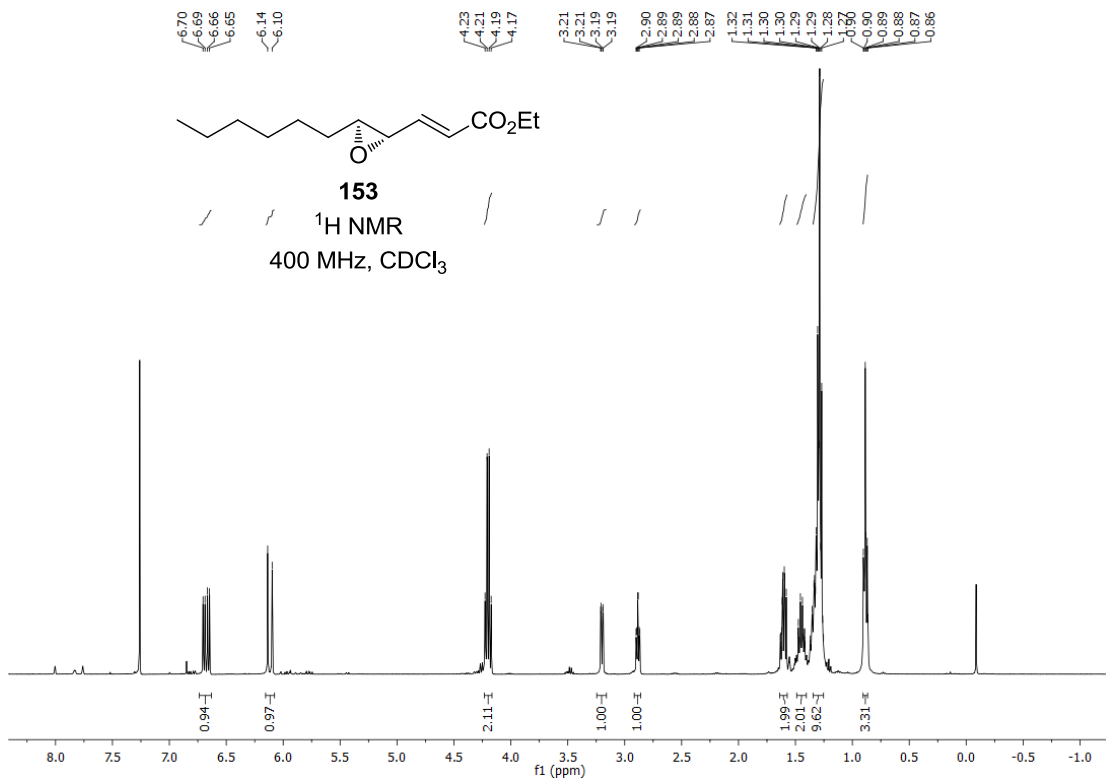
Electronic energy from single point calculation = -457.59011838

Cartesian coordinates for lowest energy conformer:

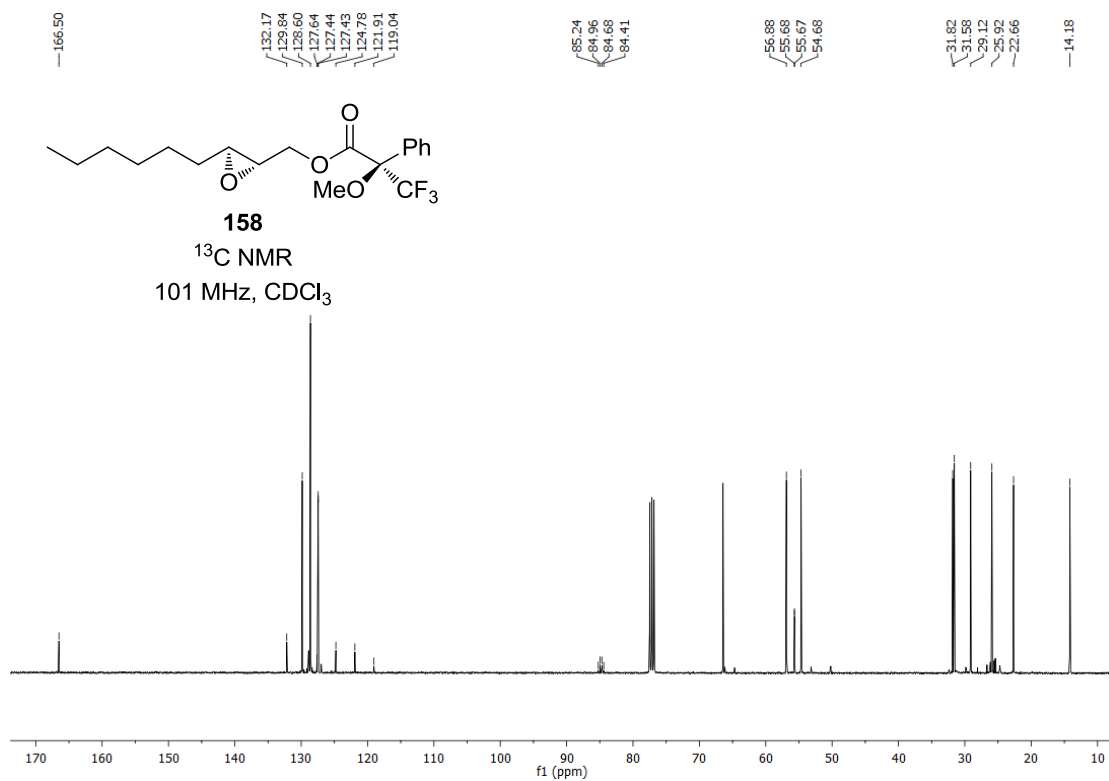
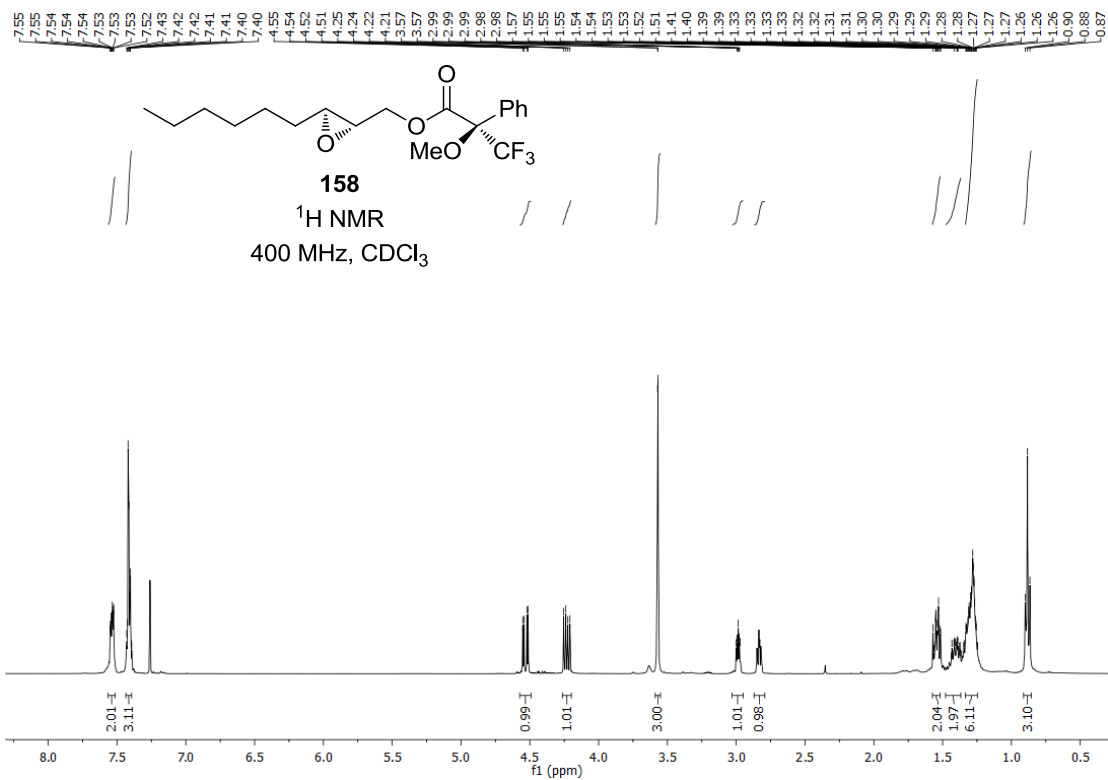
C	-4.28575800	0.31679700	1.58774200
C	-2.92749300	-0.33399300	1.34665900
C	-2.56102400	-0.43140400	-0.12507500
C	-1.32520400	-1.28934600	-0.43311800
Cl	-2.29691700	1.23993600	-0.82163200
C	-0.07946100	-0.79773300	0.25594100

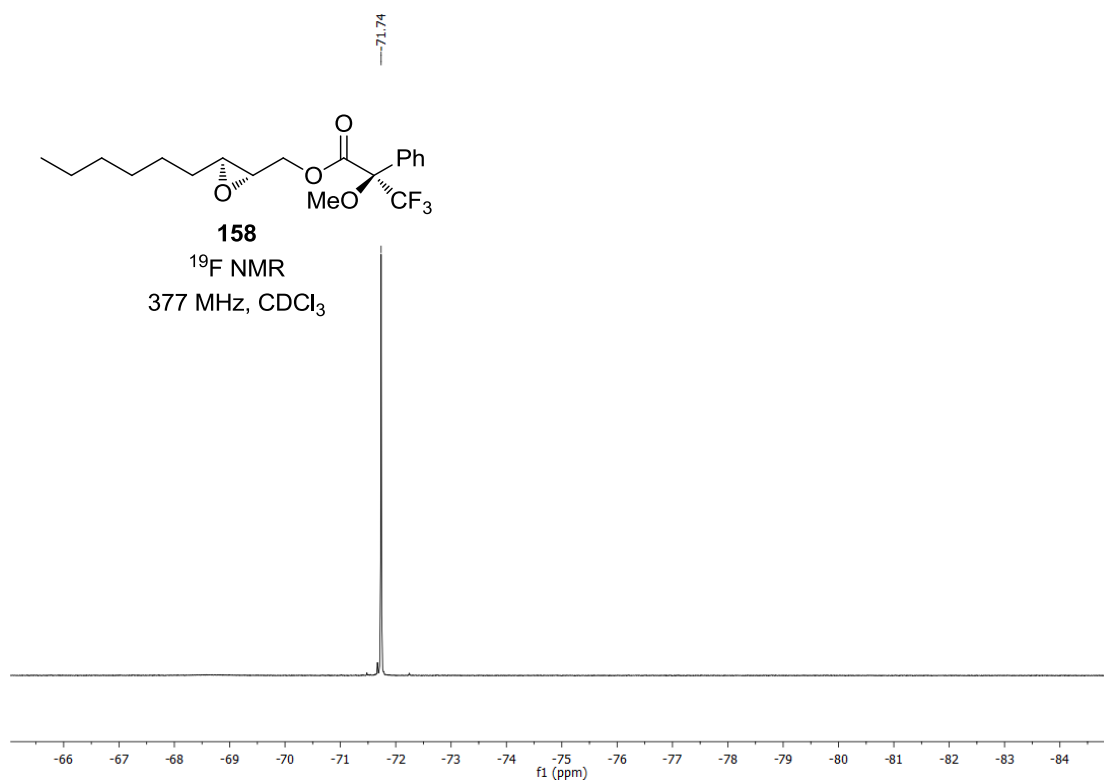
O	-1.16233200	-1.46156100	-1.82258100
C	1.07595100	-0.54757800	-0.36056900
C	2.29438800	-0.08804300	0.37132400
C	3.51173400	-0.96585400	0.12043000
Cl	2.66043500	1.63384000	-0.18155800
C	4.75663000	-0.54539100	0.89310500
H	-4.28929900	1.36112400	1.26176300
H	-5.07537800	-0.21382300	1.04537300
H	-4.53391700	0.29694300	2.65248300
H	-2.93744700	-1.36281600	1.72974500
H	-2.14640800	0.20621700	1.89128100
H	-3.39758900	-0.83087100	-0.70394100
H	-1.57181800	-2.28455700	-0.03829700
H	-0.15292200	-0.65431600	1.33369500
H	-0.97266100	-0.59785200	-2.22136200
H	1.18819500	-0.69481300	-1.43458100
H	2.09581700	0.01326100	1.44105100
H	3.21382300	-1.97818900	0.42191900
H	3.71195600	-0.99799400	-0.95713800
H	5.12159900	0.43077500	0.56179400
H	4.54708800	-0.48608500	1.96665800
H	5.55923300	-1.27344600	0.74580400

15NMR Spectra

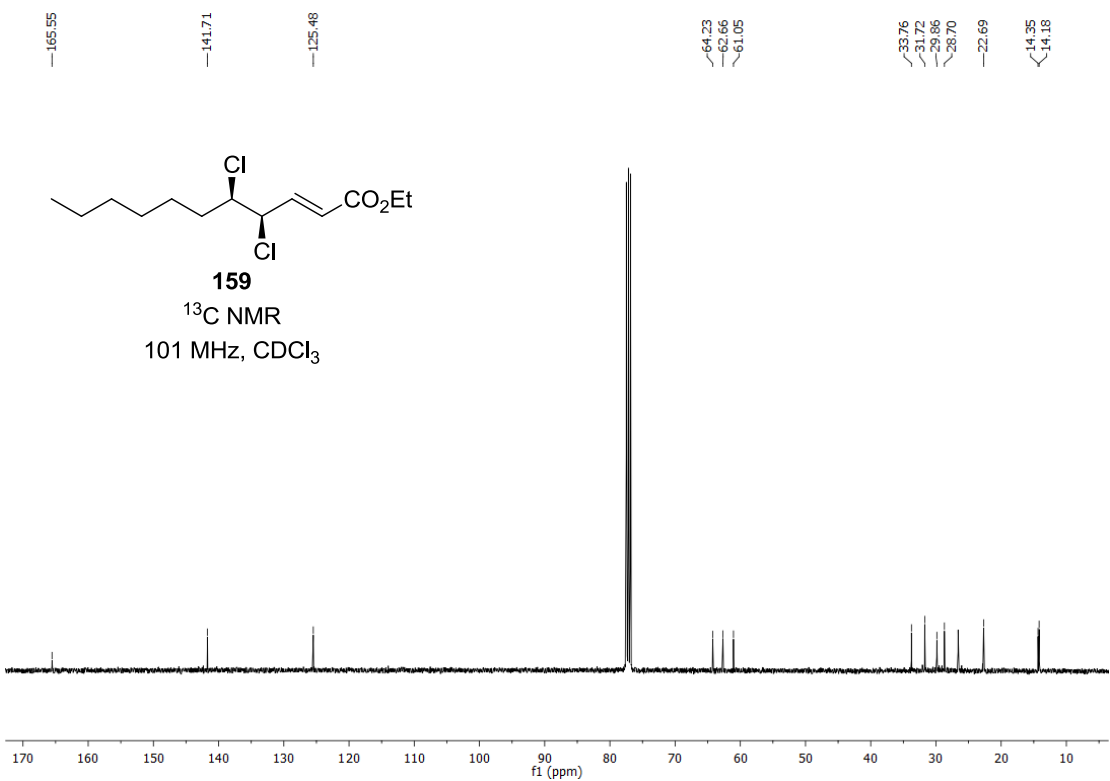
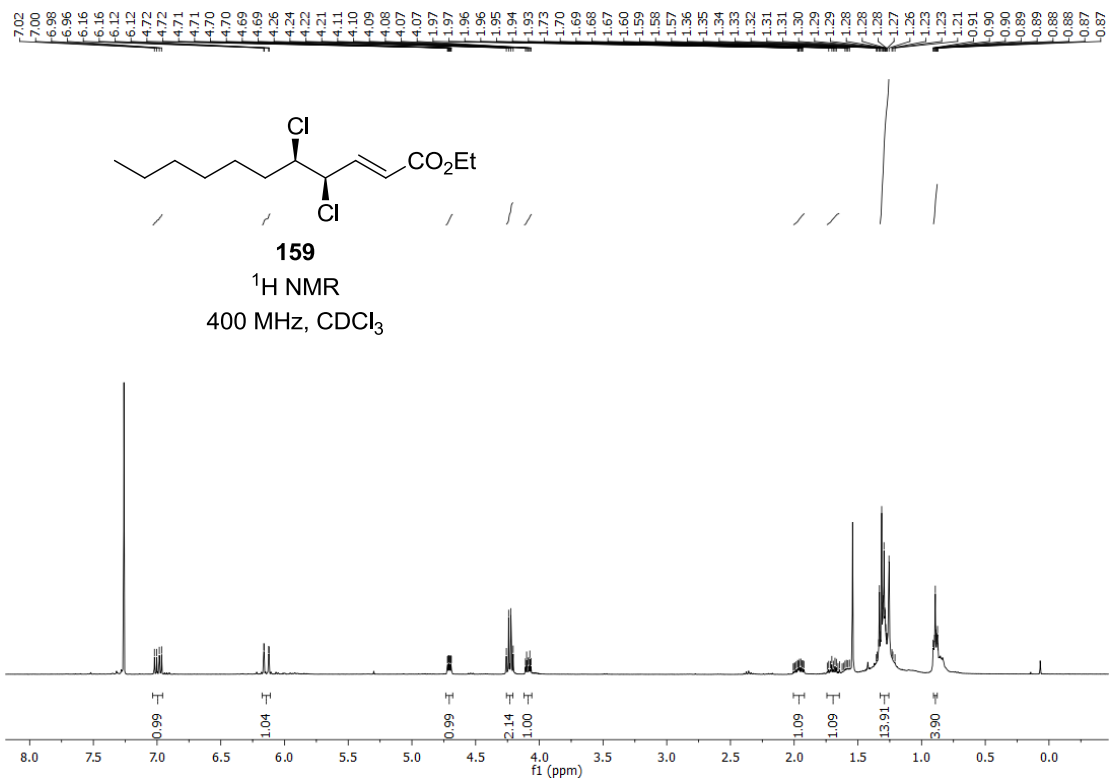


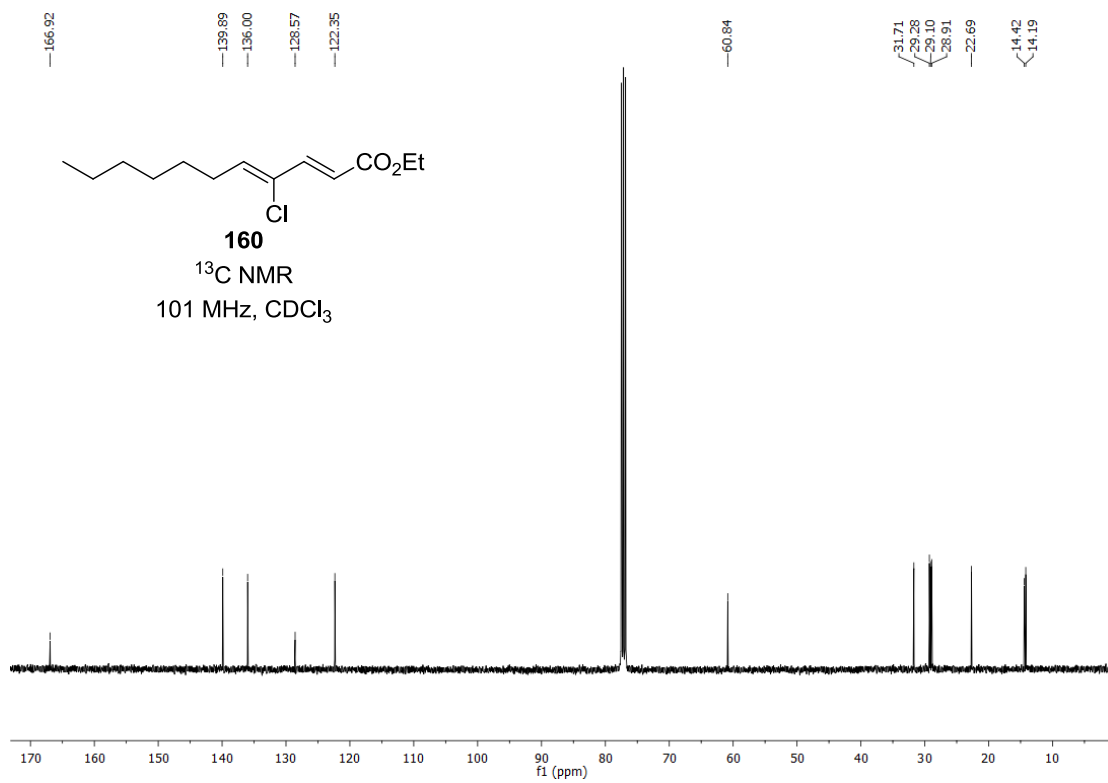
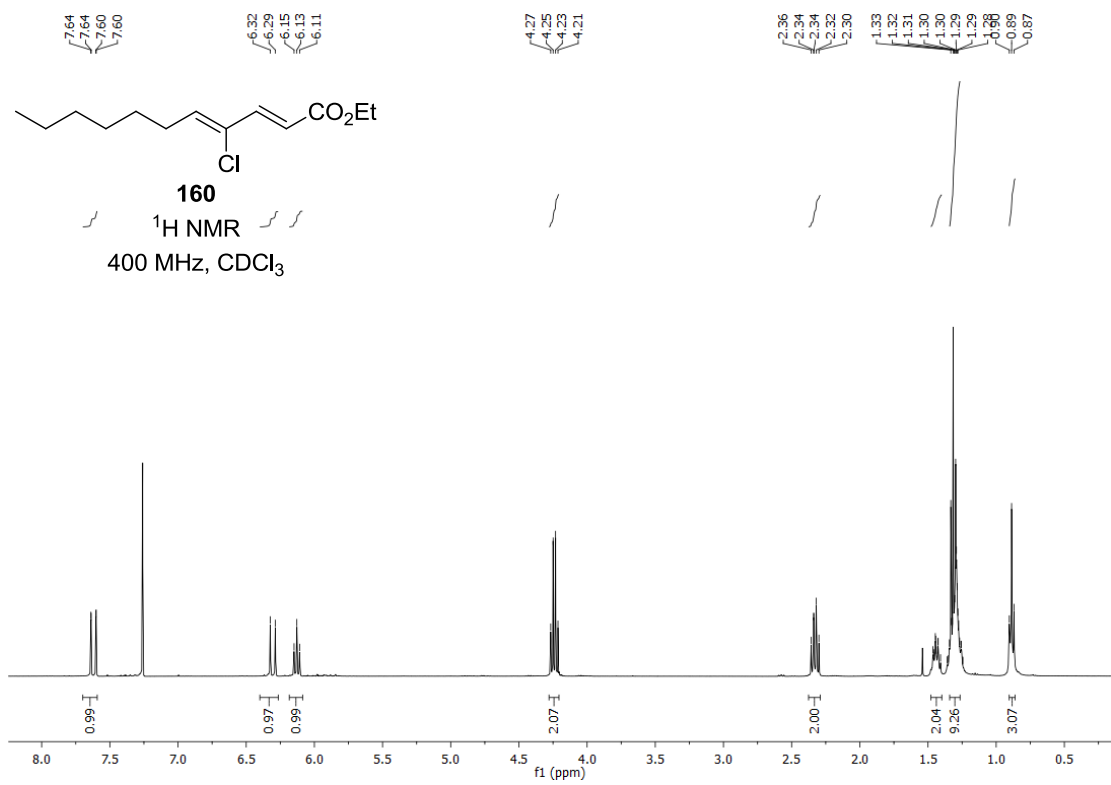
Appendix



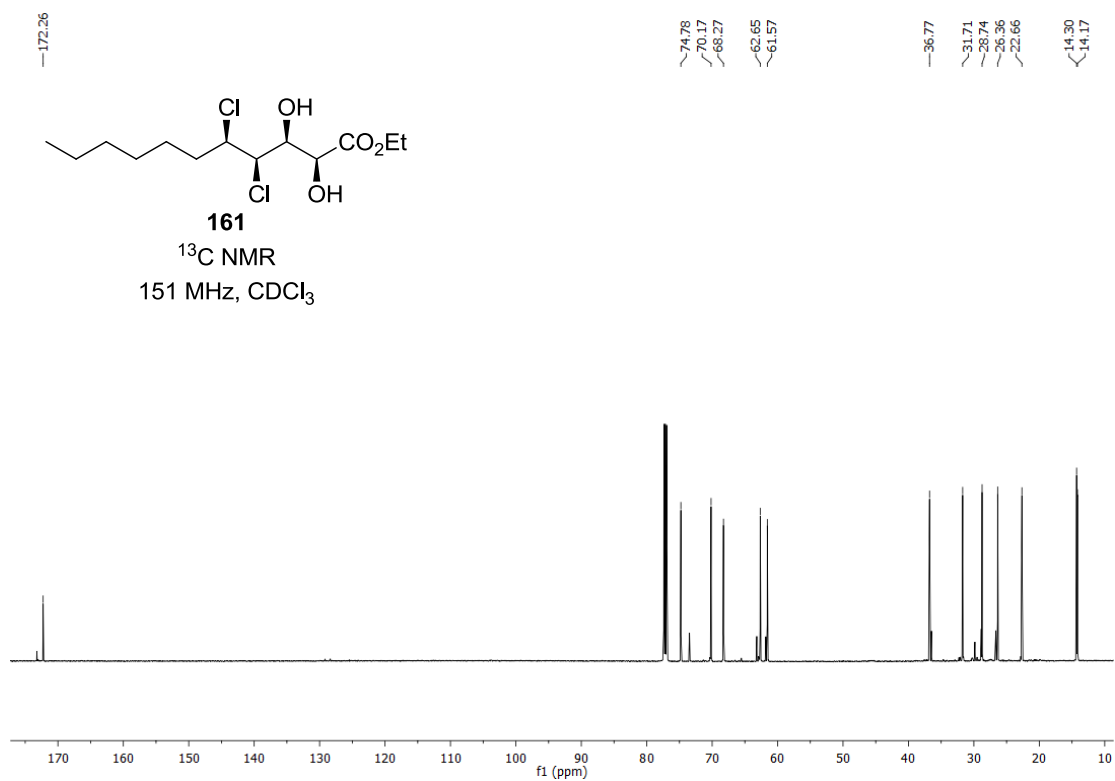
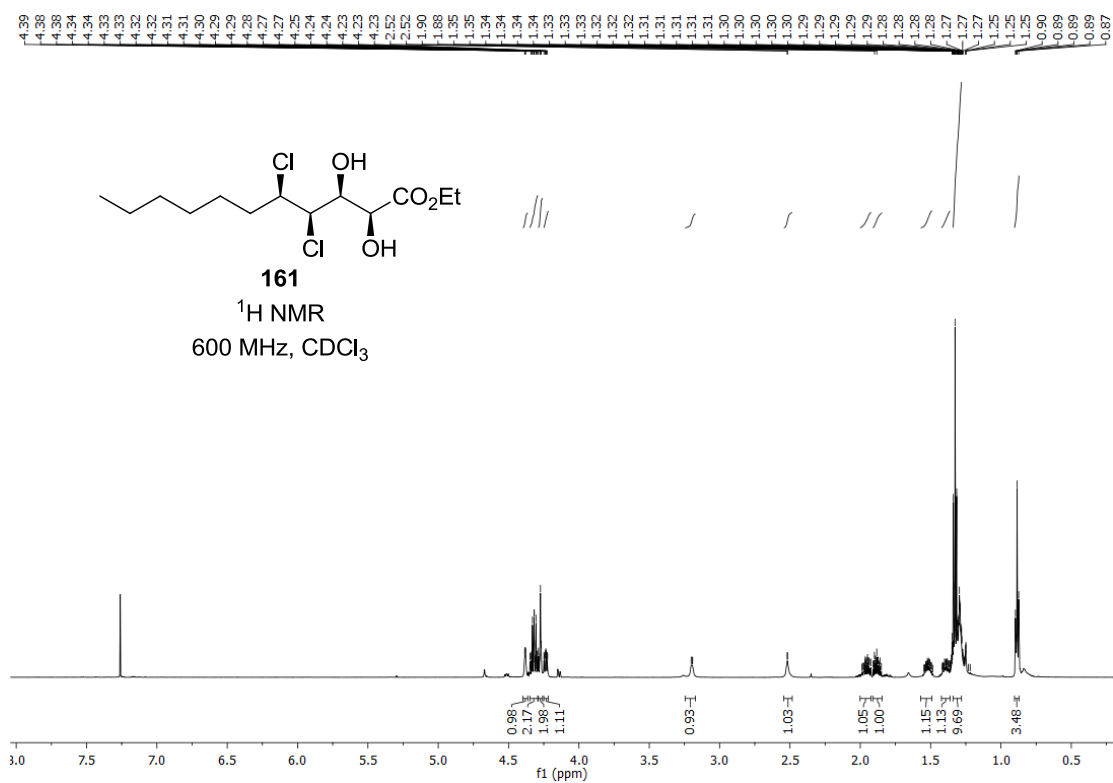


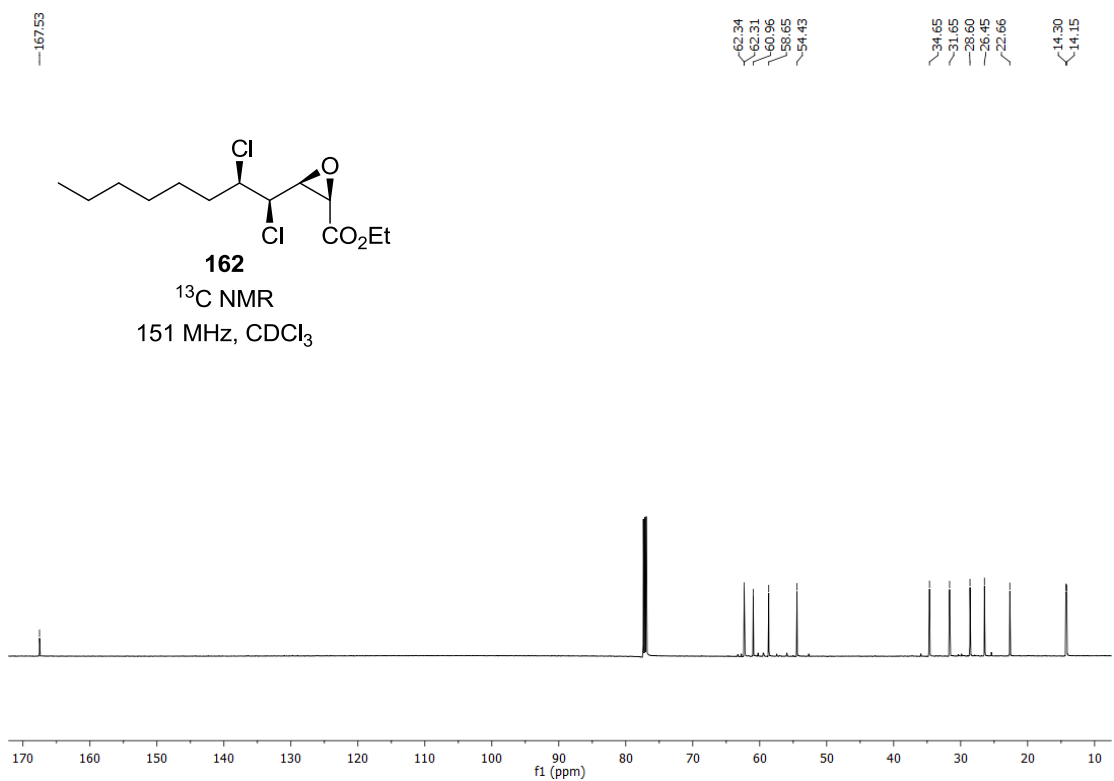
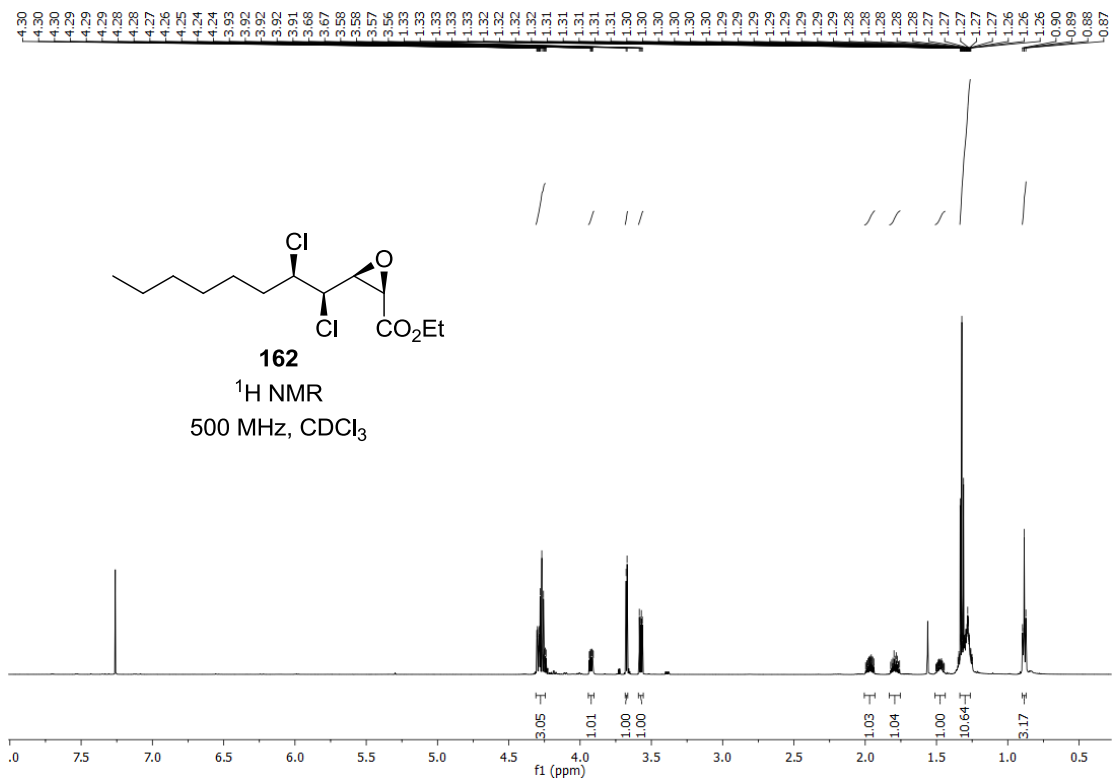
Appendix



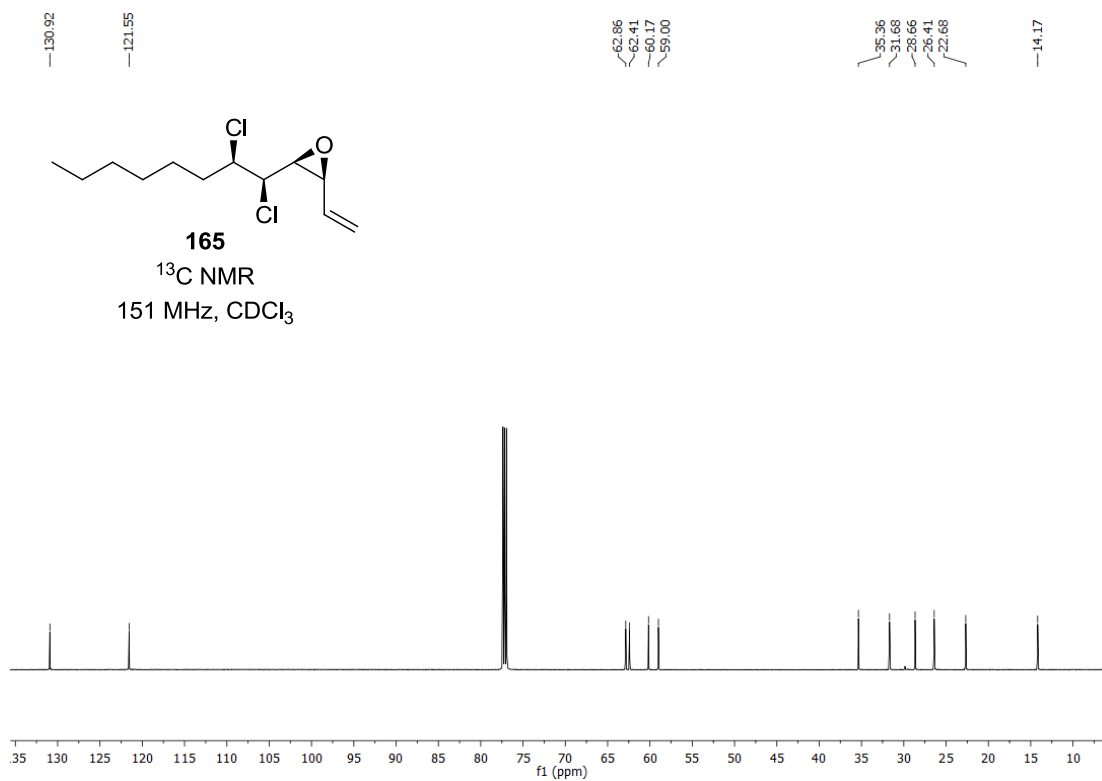
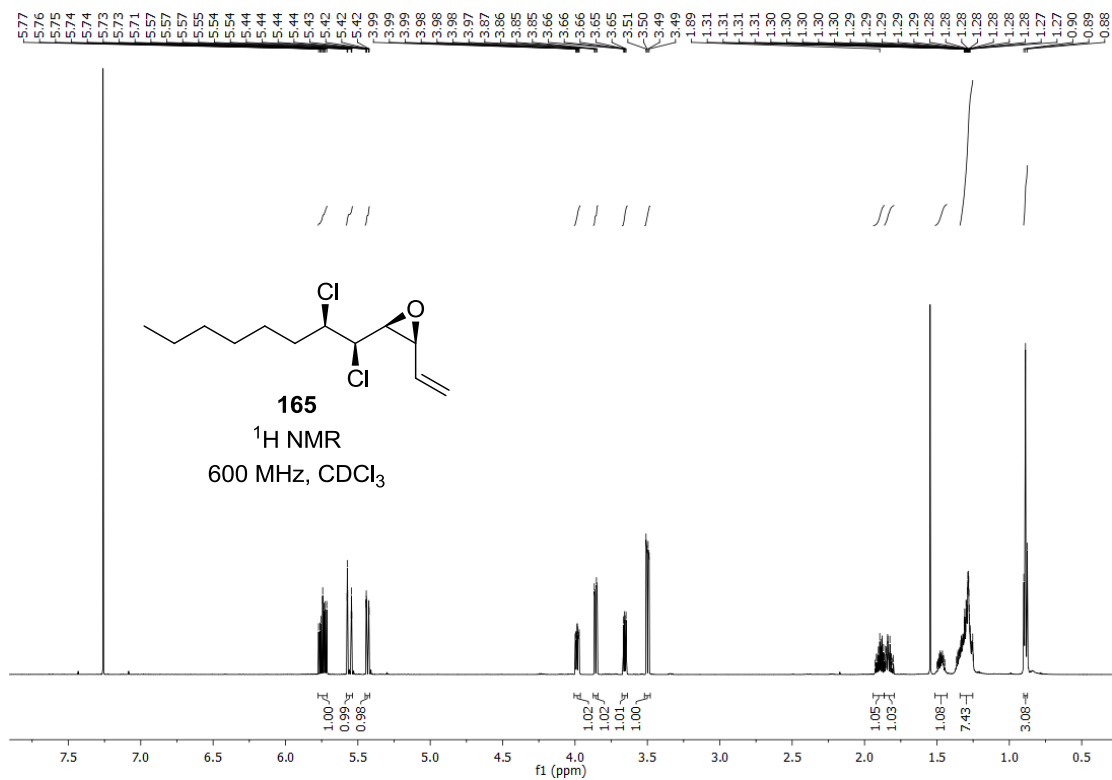


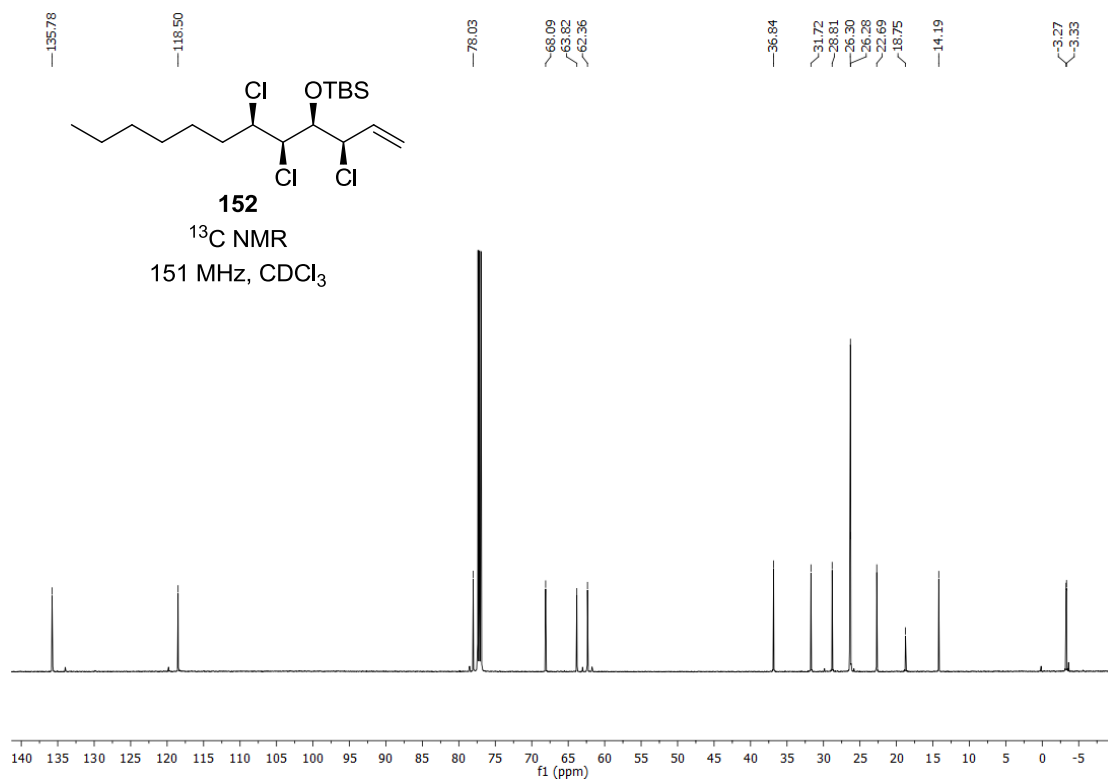
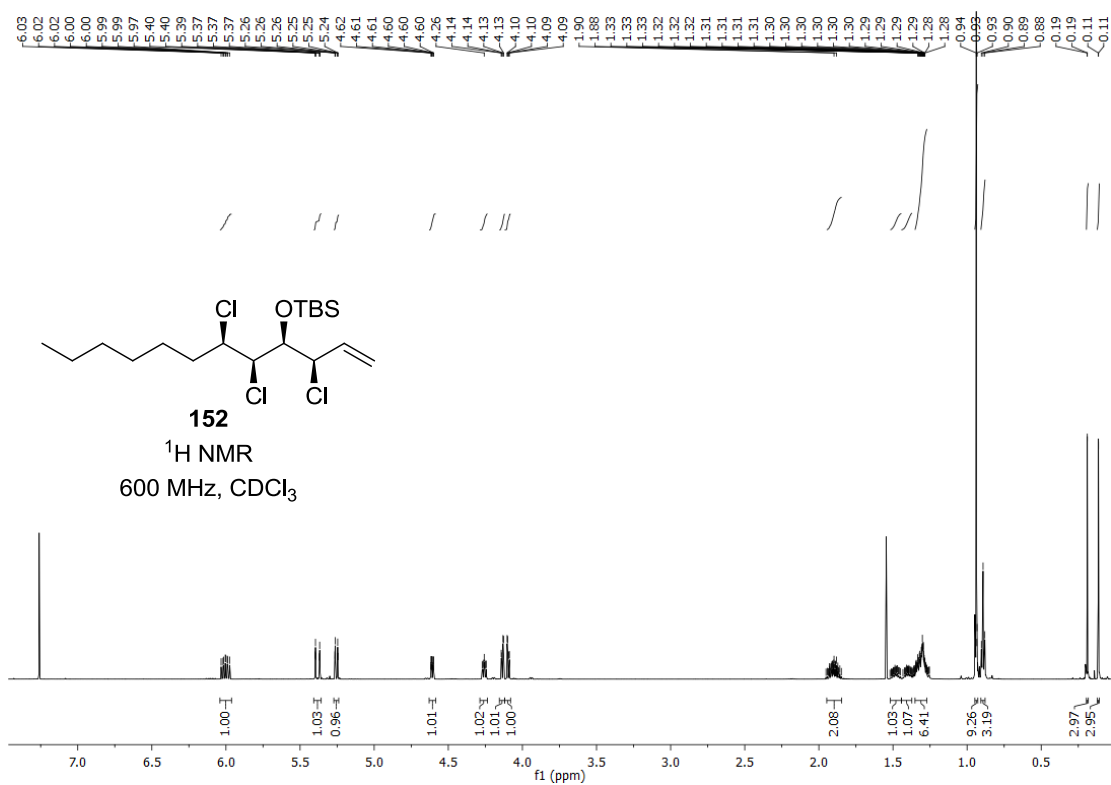
Appendix



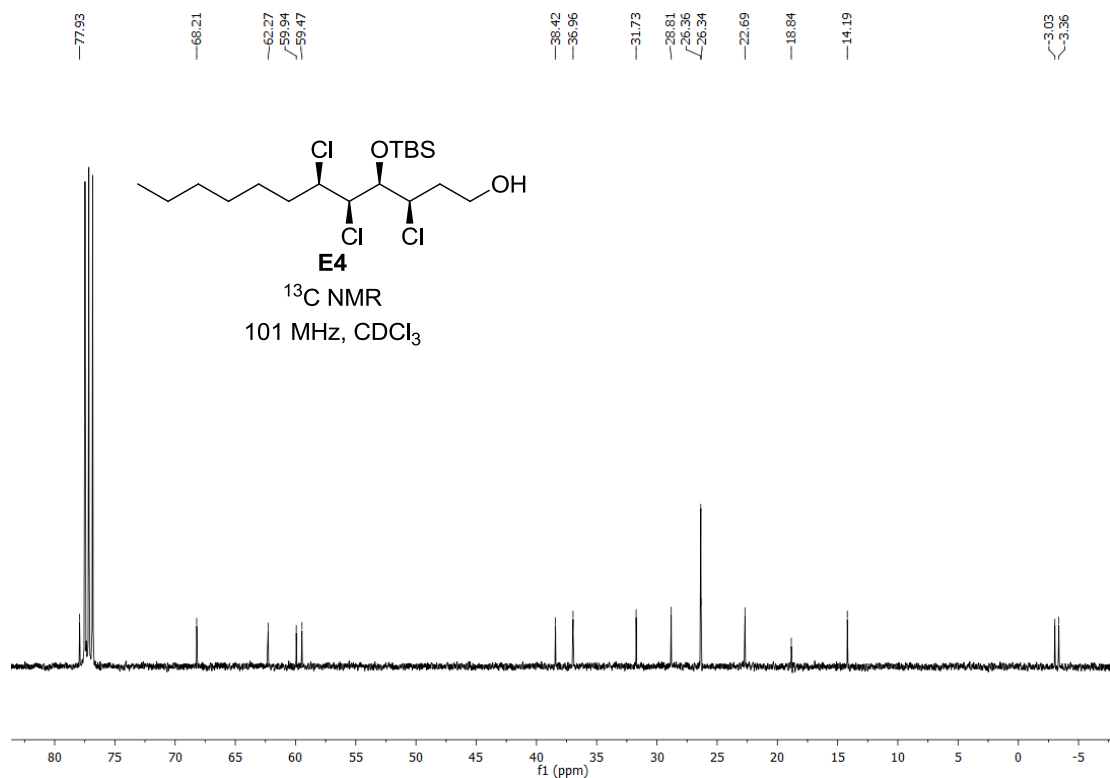
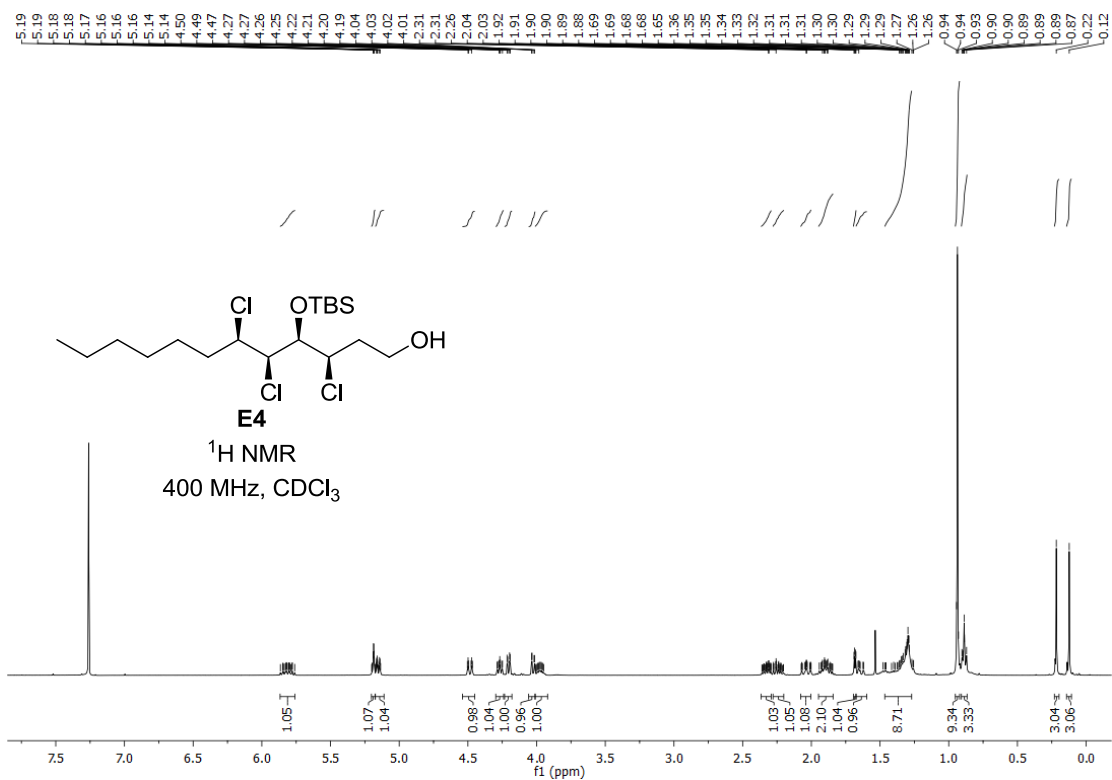


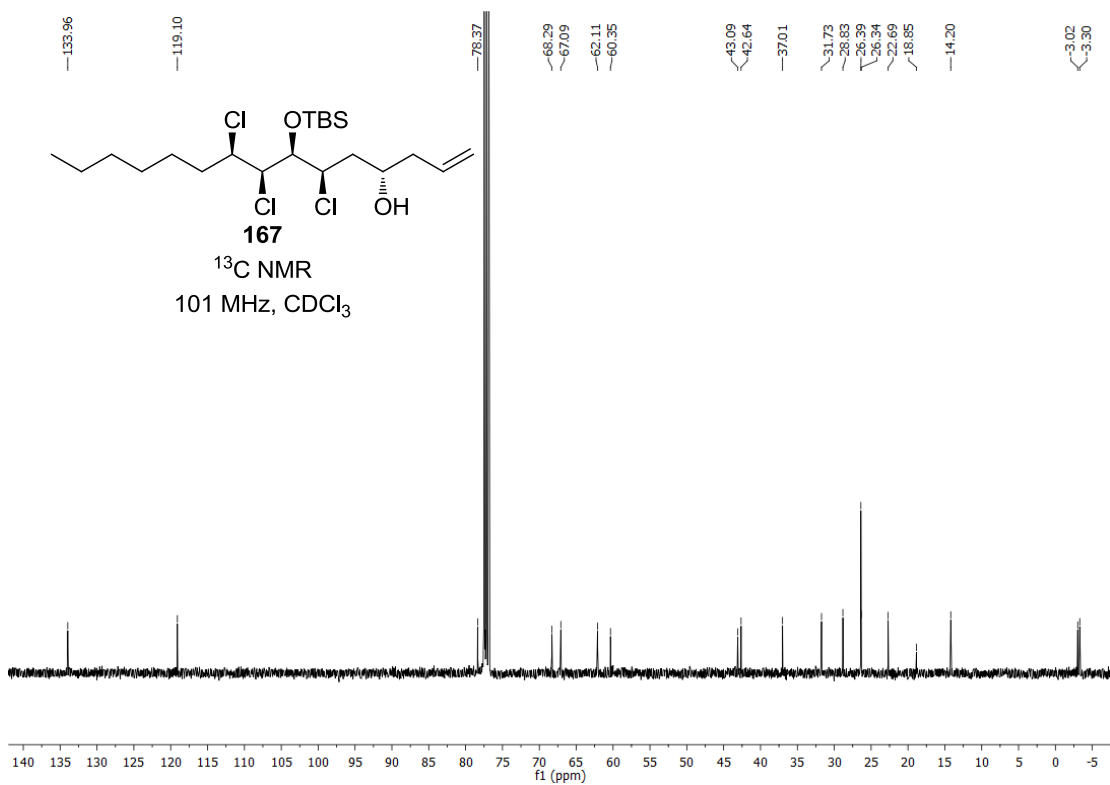
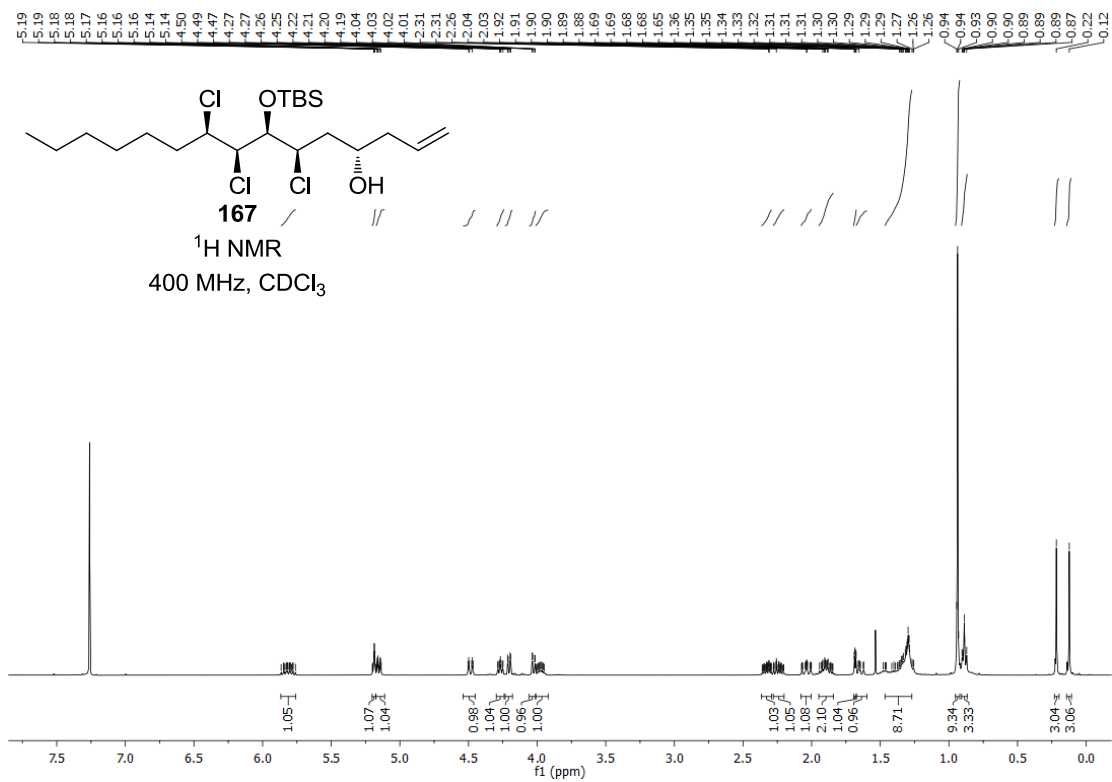
Appendix



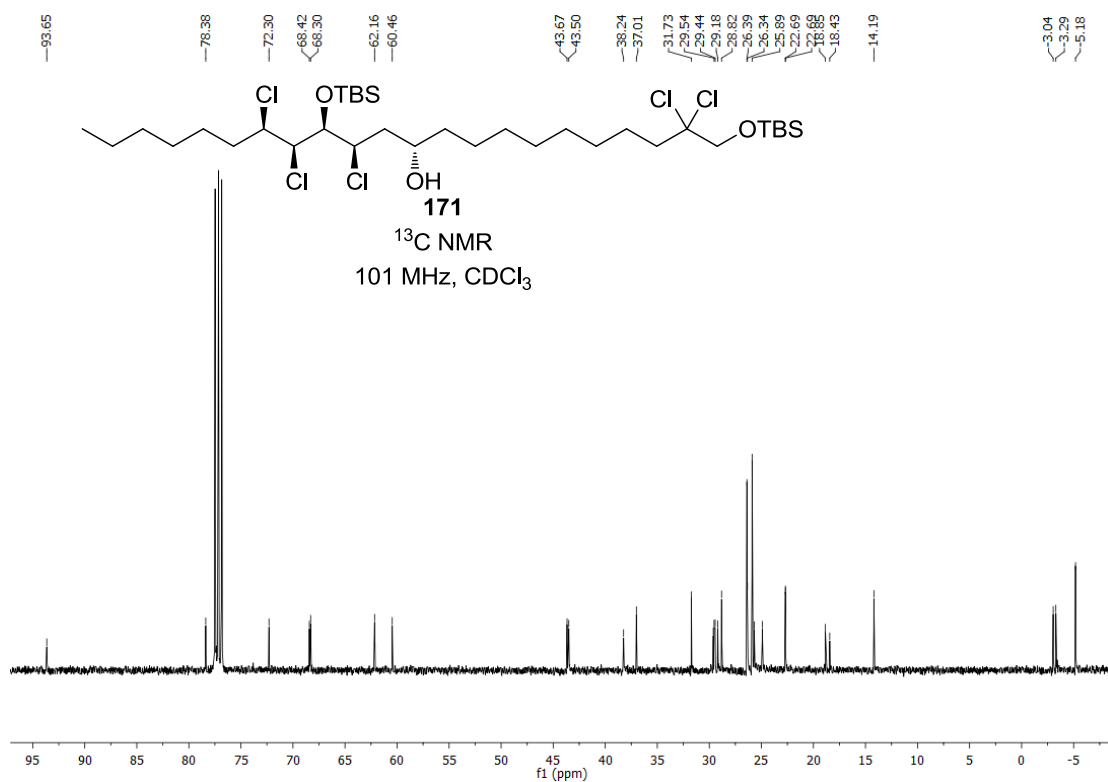
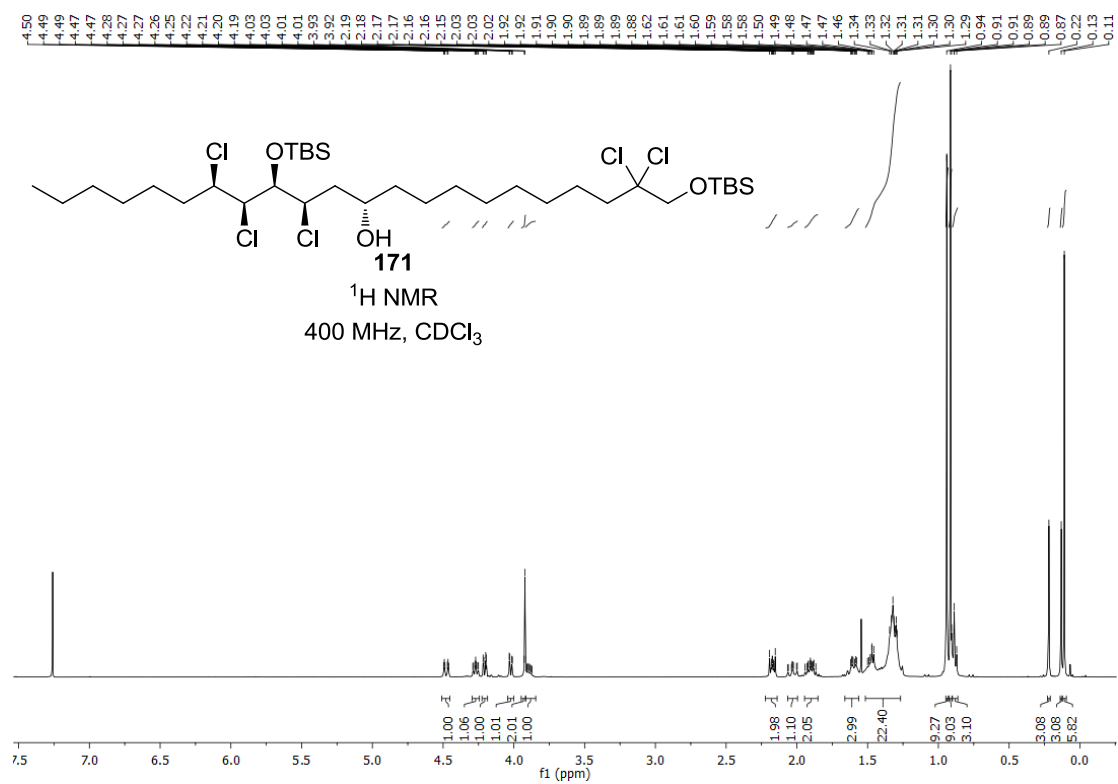


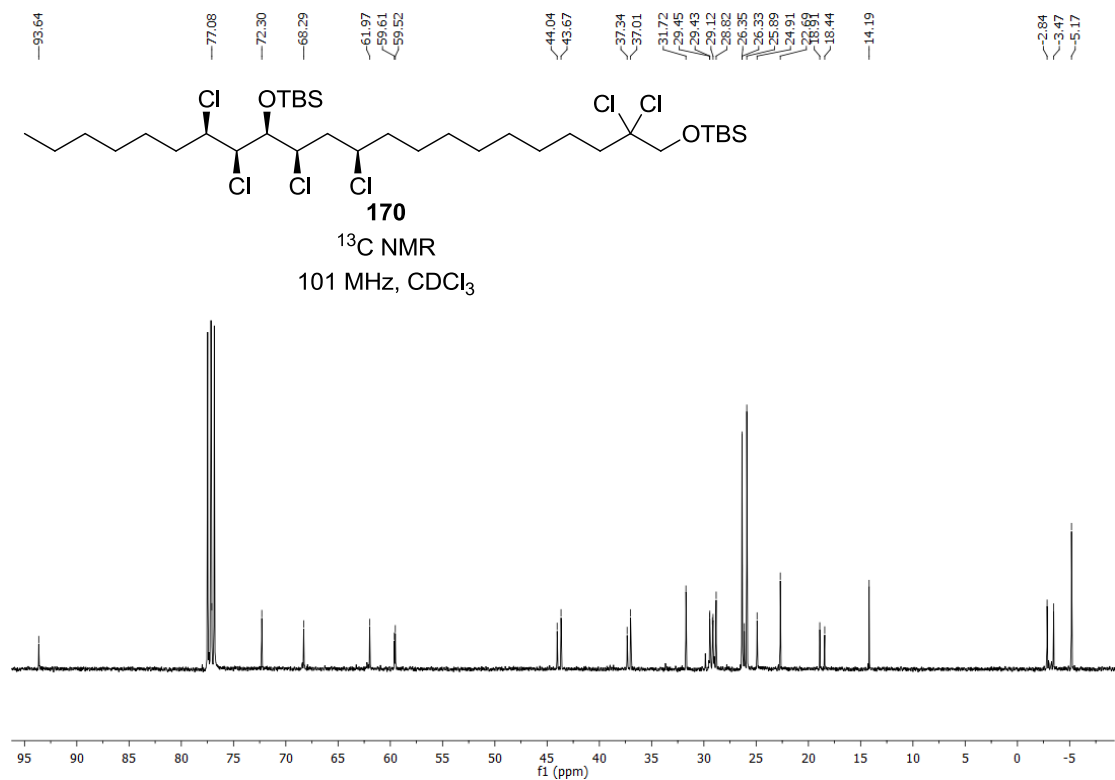
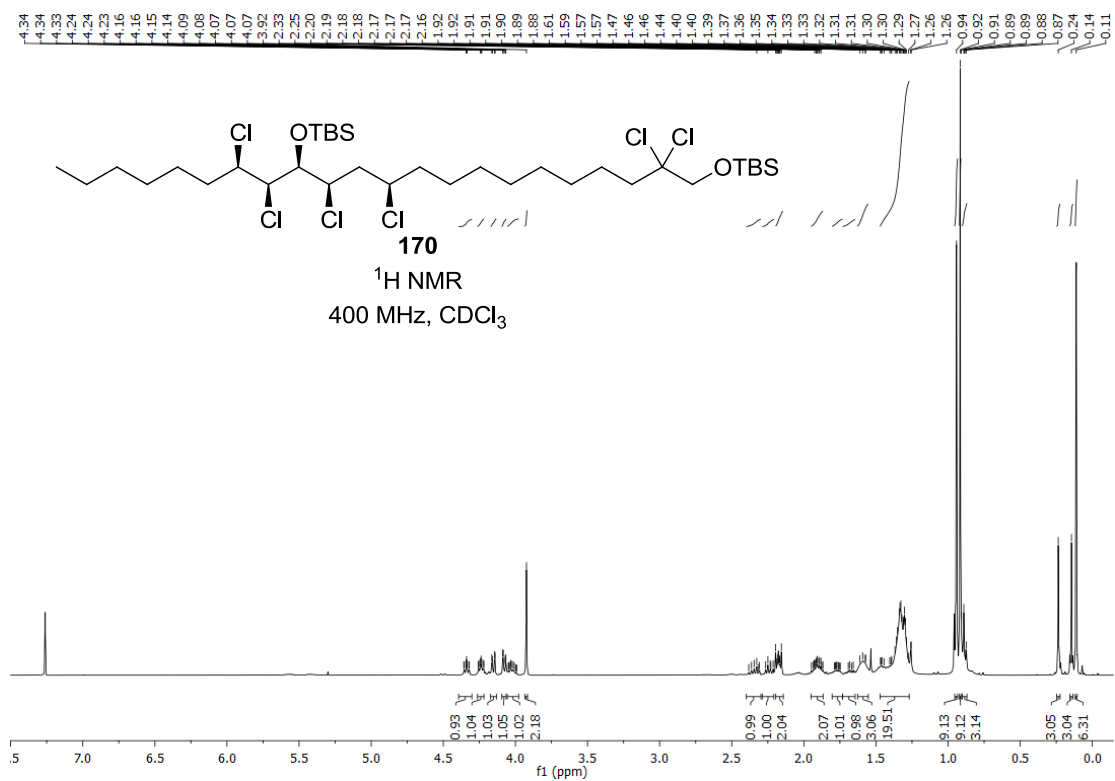
Appendix

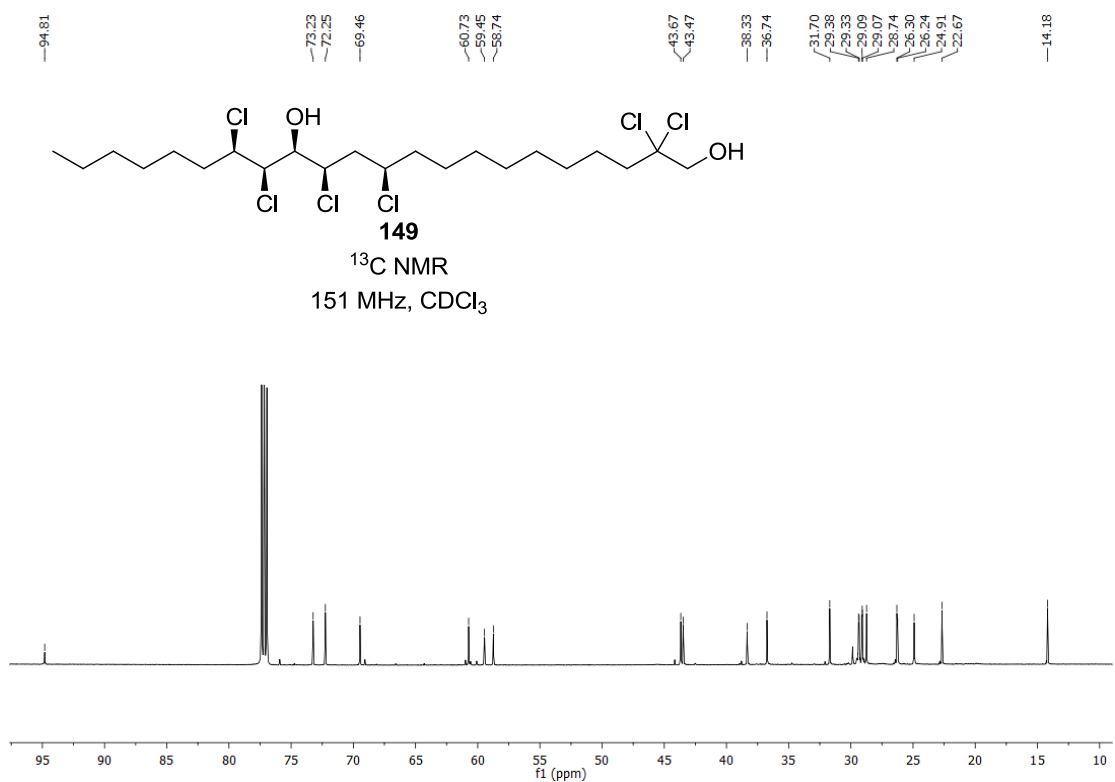
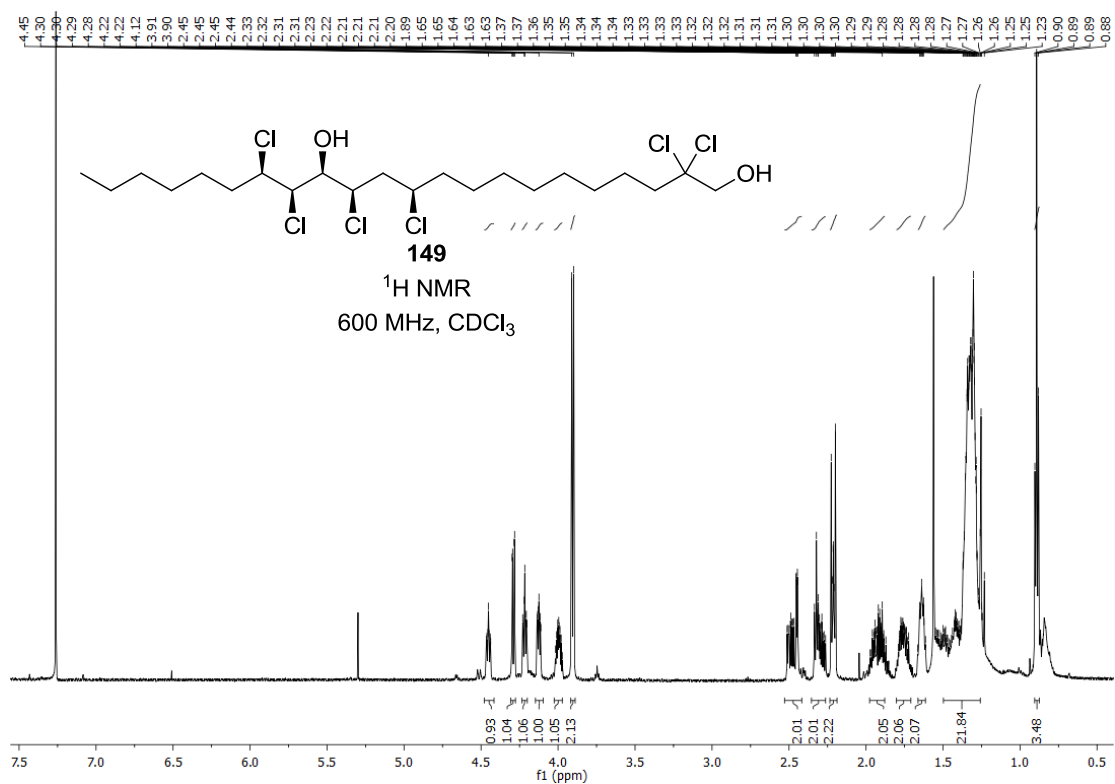


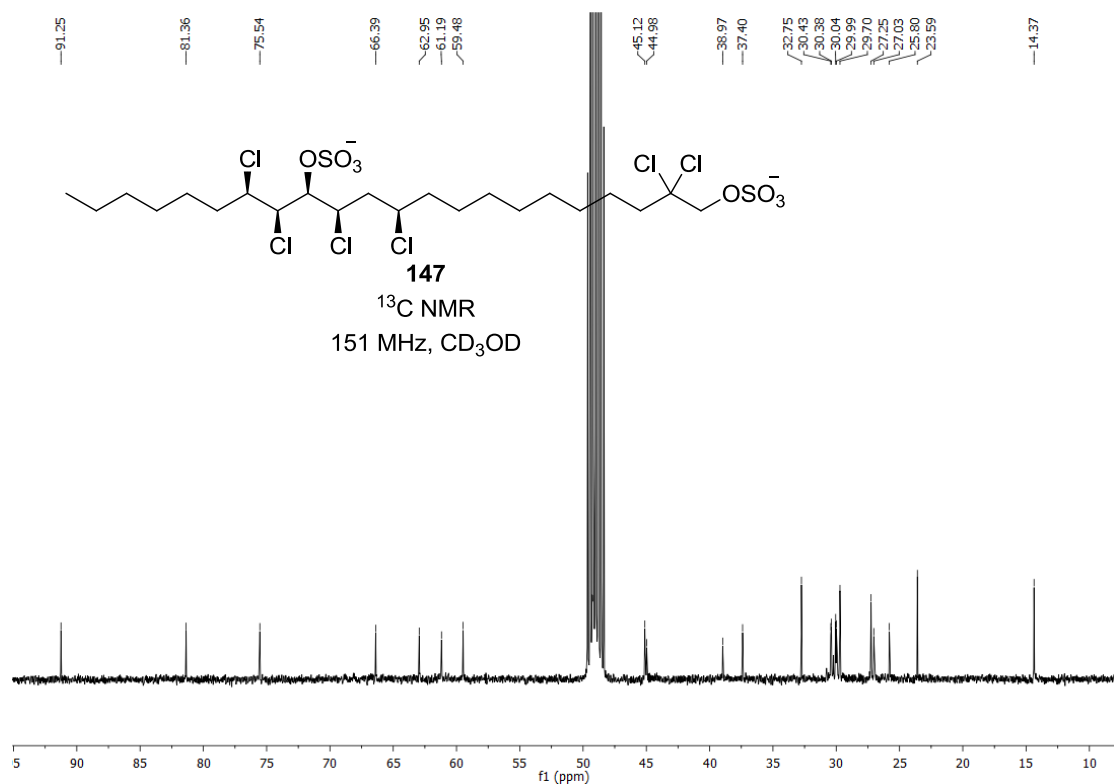
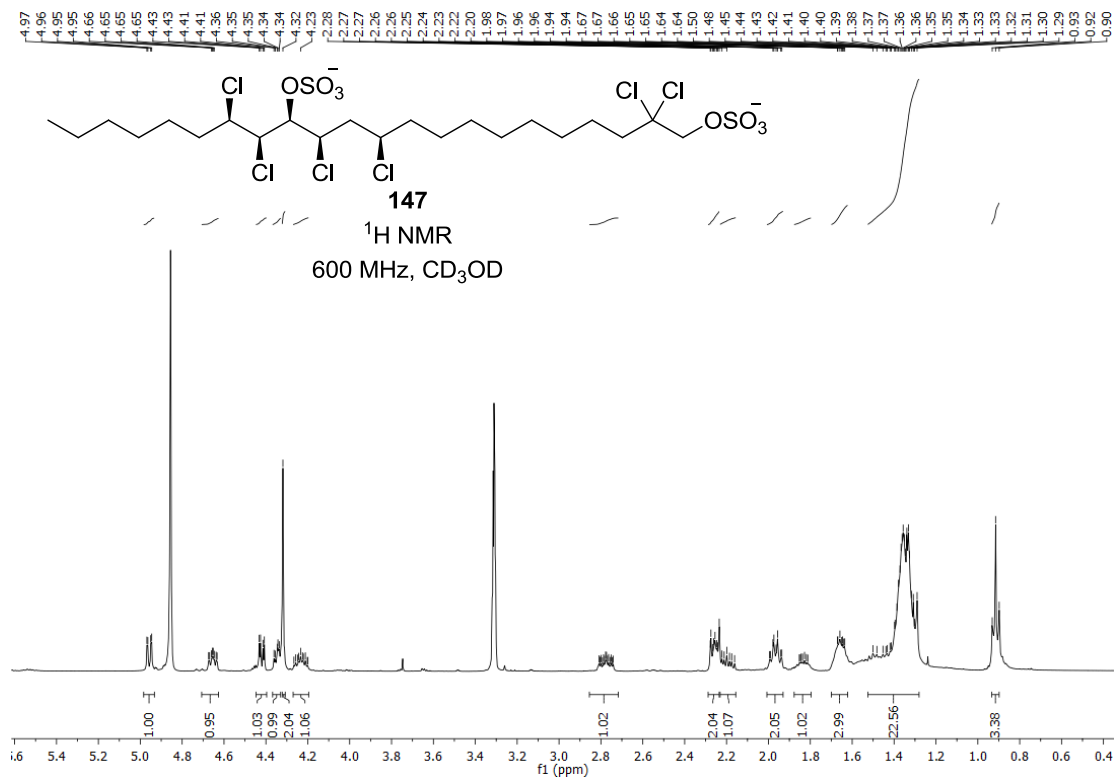


Appendix



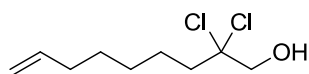






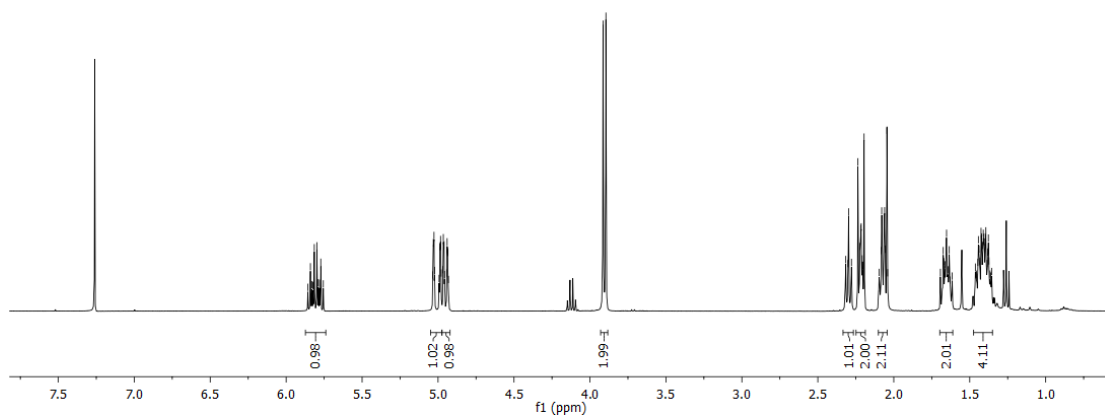
Appendix

5.84
5.81
5.80
5.77
5.03
5.02
4.99
4.98
4.97
4.96
4.94
4.94
4.94
4.93
3.91
3.90
2.32
2.30
2.28
2.24
2.22
2.22
2.21
2.21
2.20
2.20
2.10
2.08
2.08
2.08
2.06
2.06
2.04
2.04
1.69
1.67
1.67
1.67
1.66
1.66
1.65
1.64
1.64
1.63
1.46
1.46
1.45
1.44
1.44
1.43
1.43
1.42
1.41
1.41
1.40
1.40
1.39
1.38
1.38
1.38
1.37
1.36

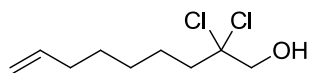


E8

¹H NMR
400 MHz, CDCl₃

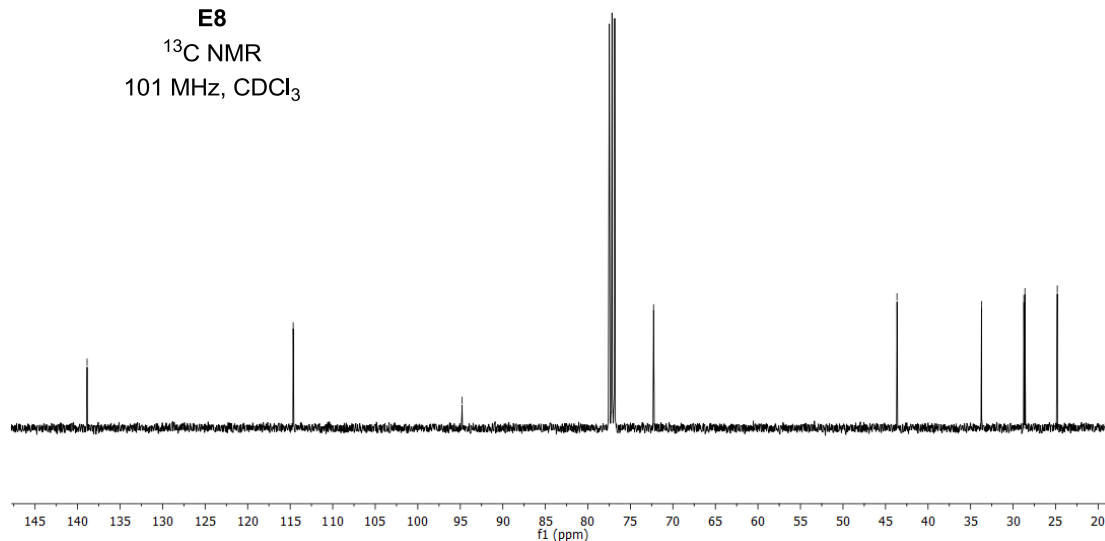


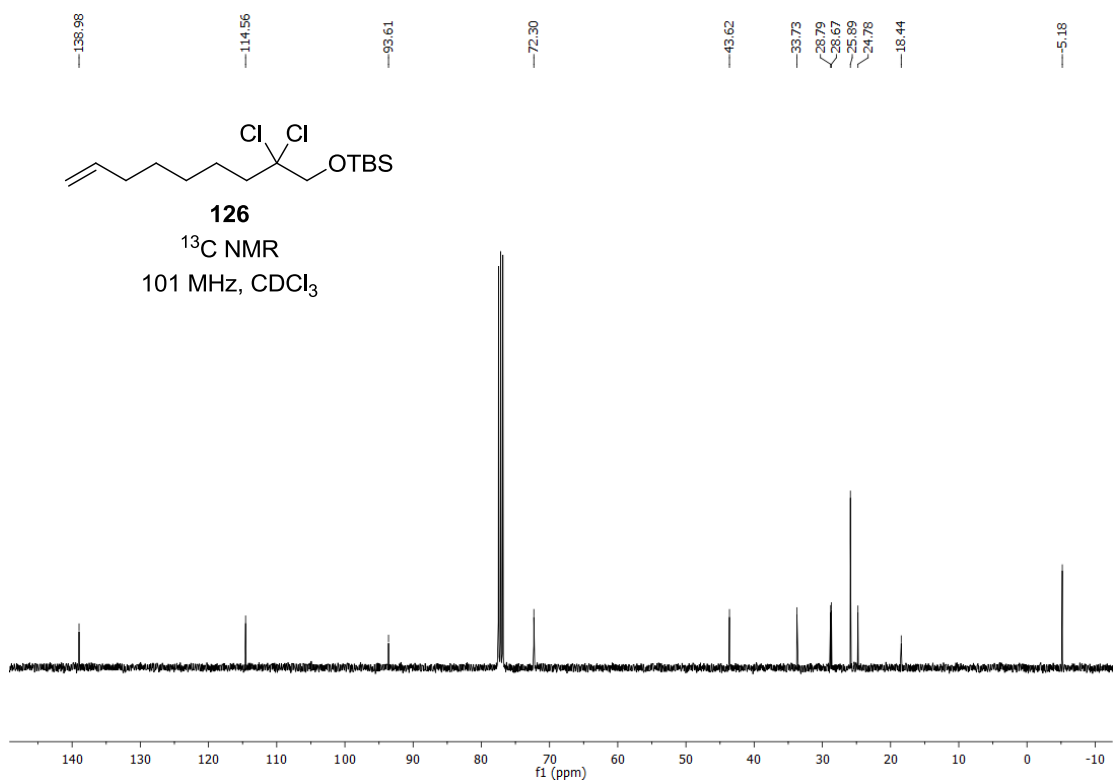
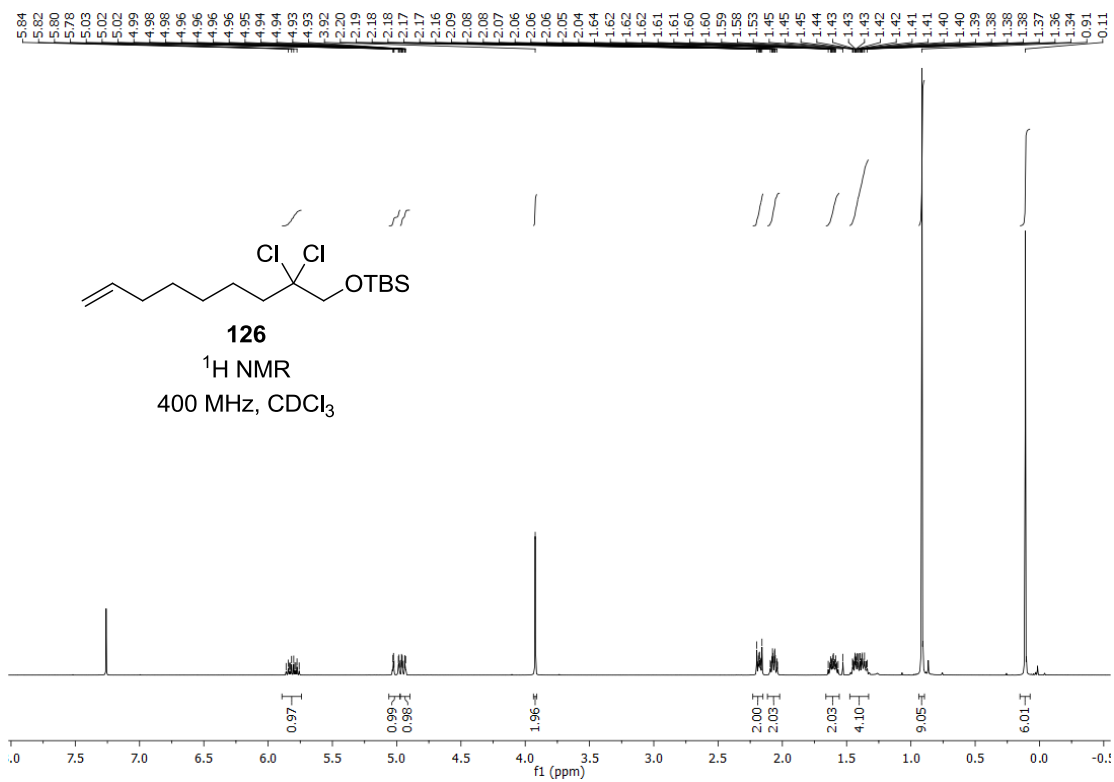
138.88
114.65
94.78
72.27
43.65
33.71
28.74
28.61
24.81

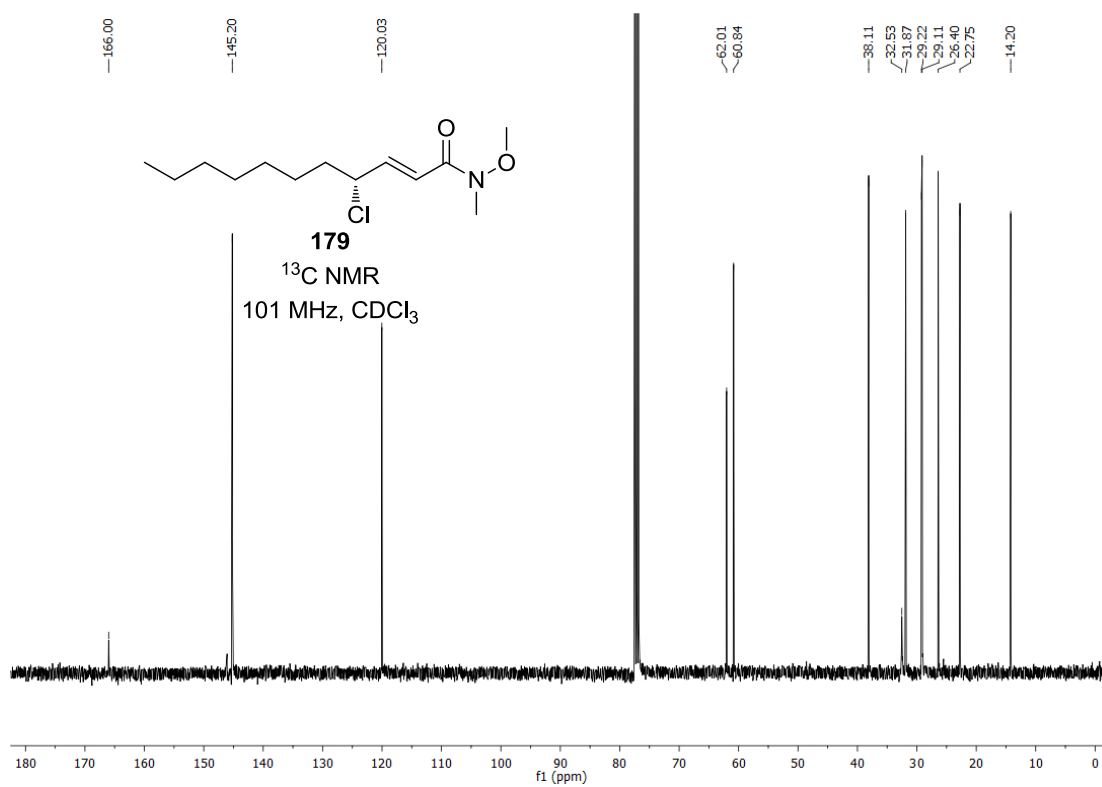
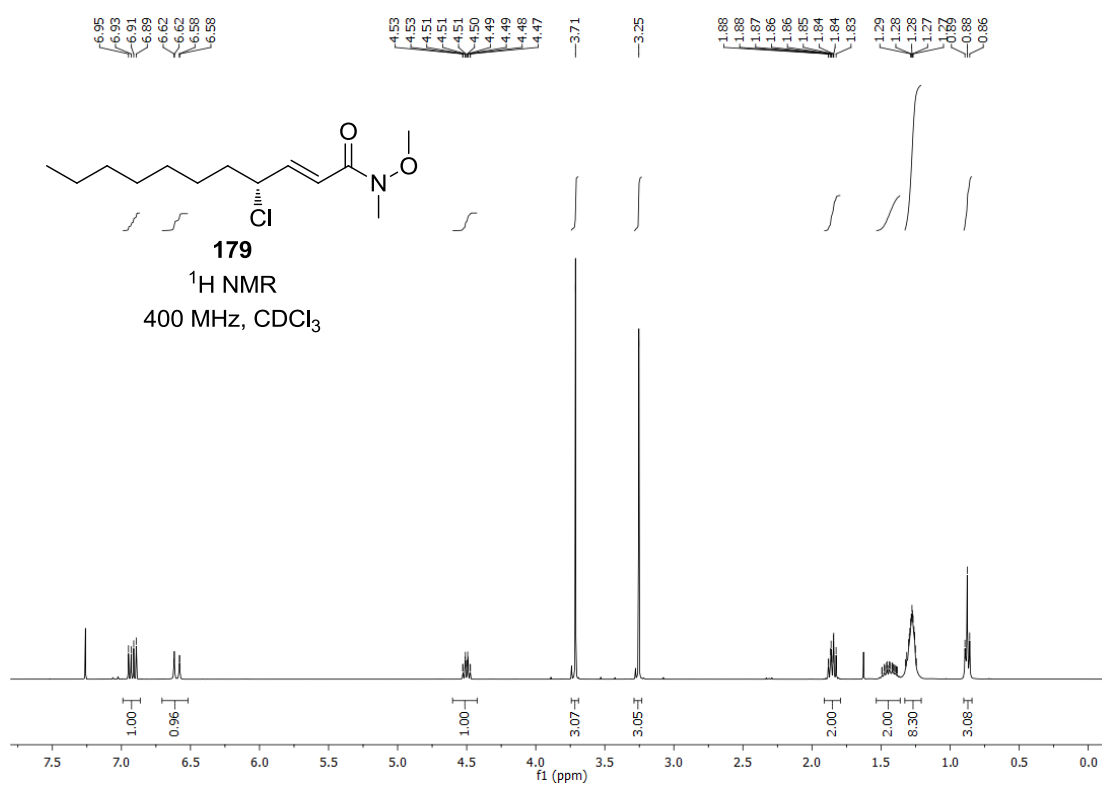


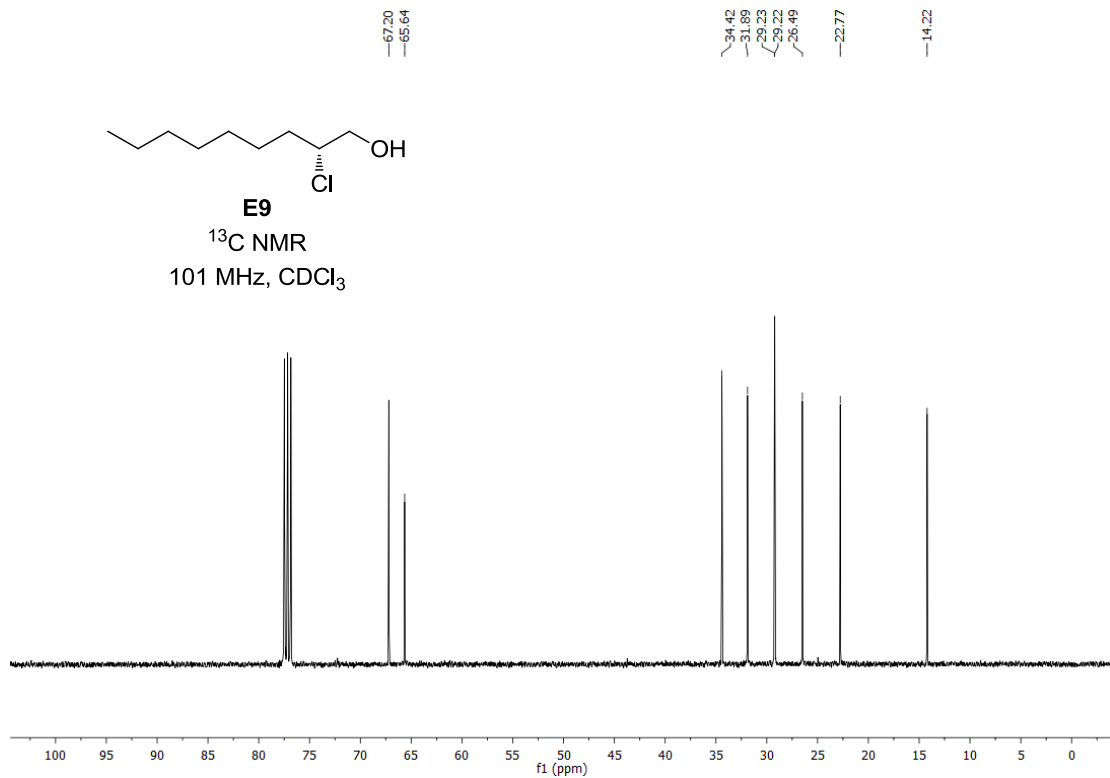
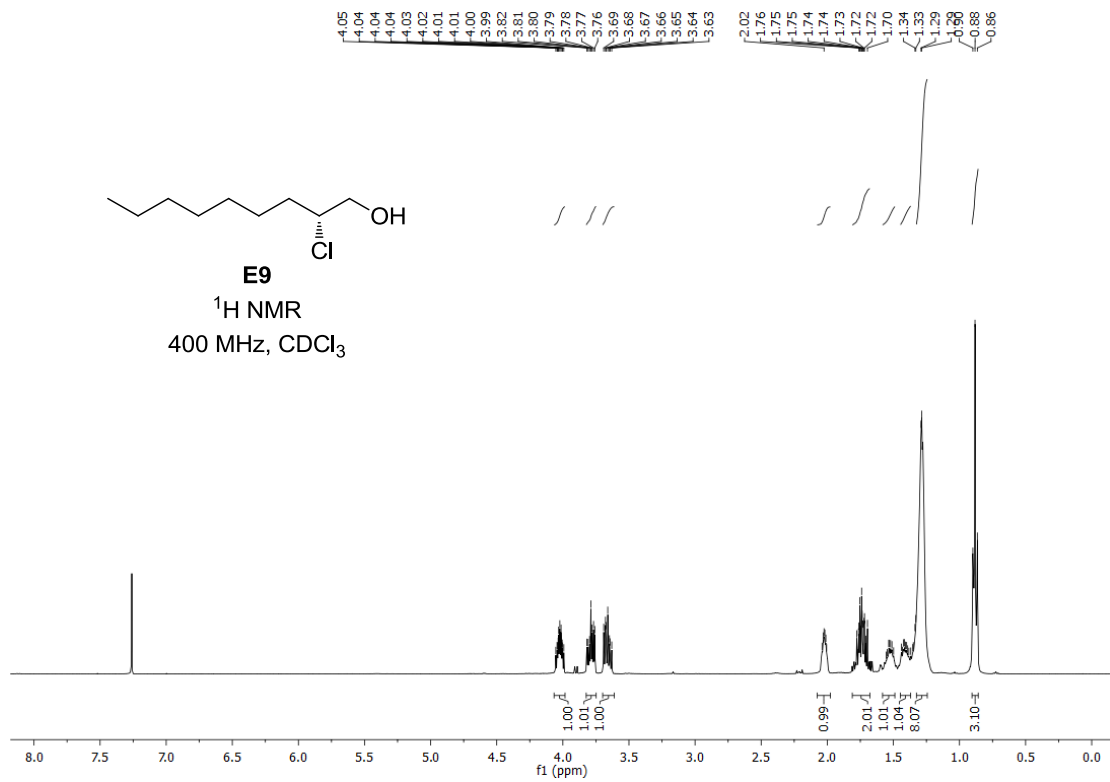
E8

¹³C NMR
101 MHz, CDCl₃

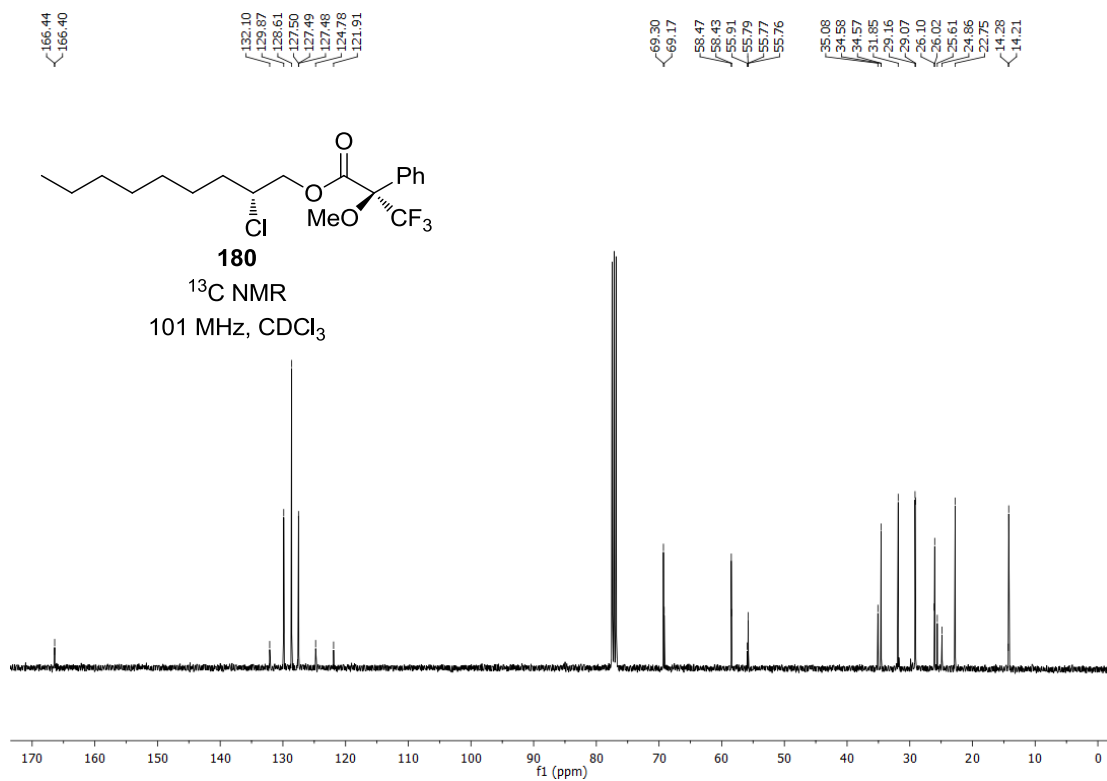
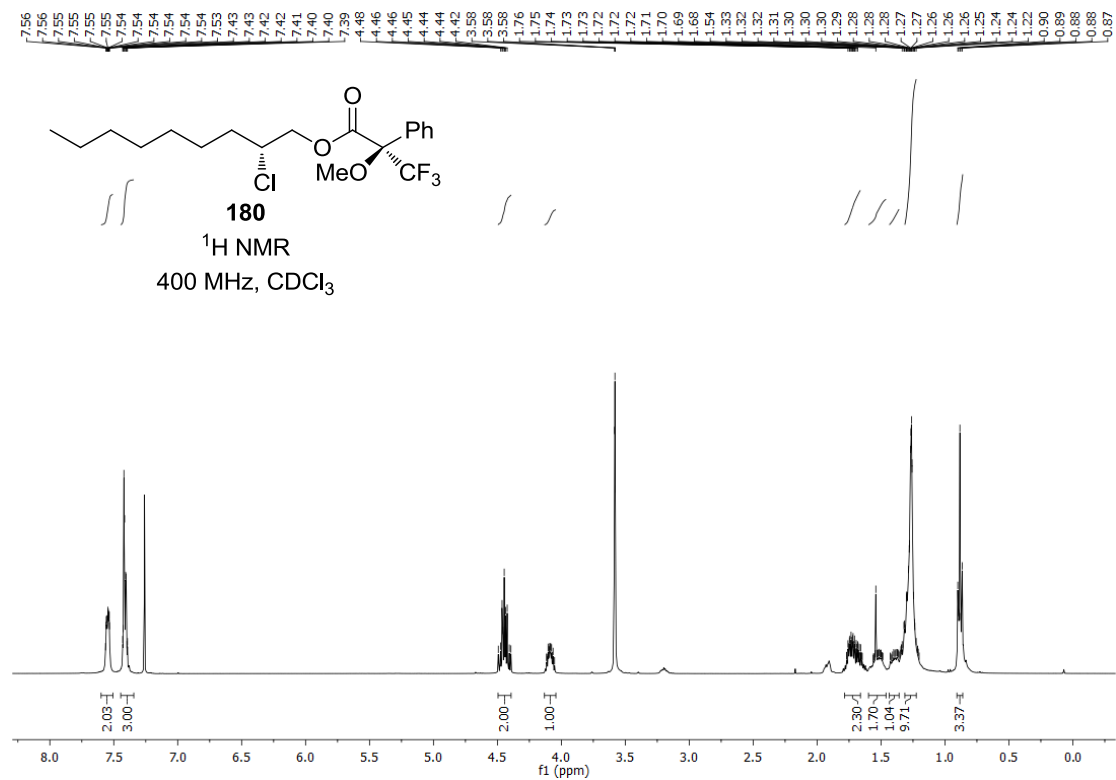


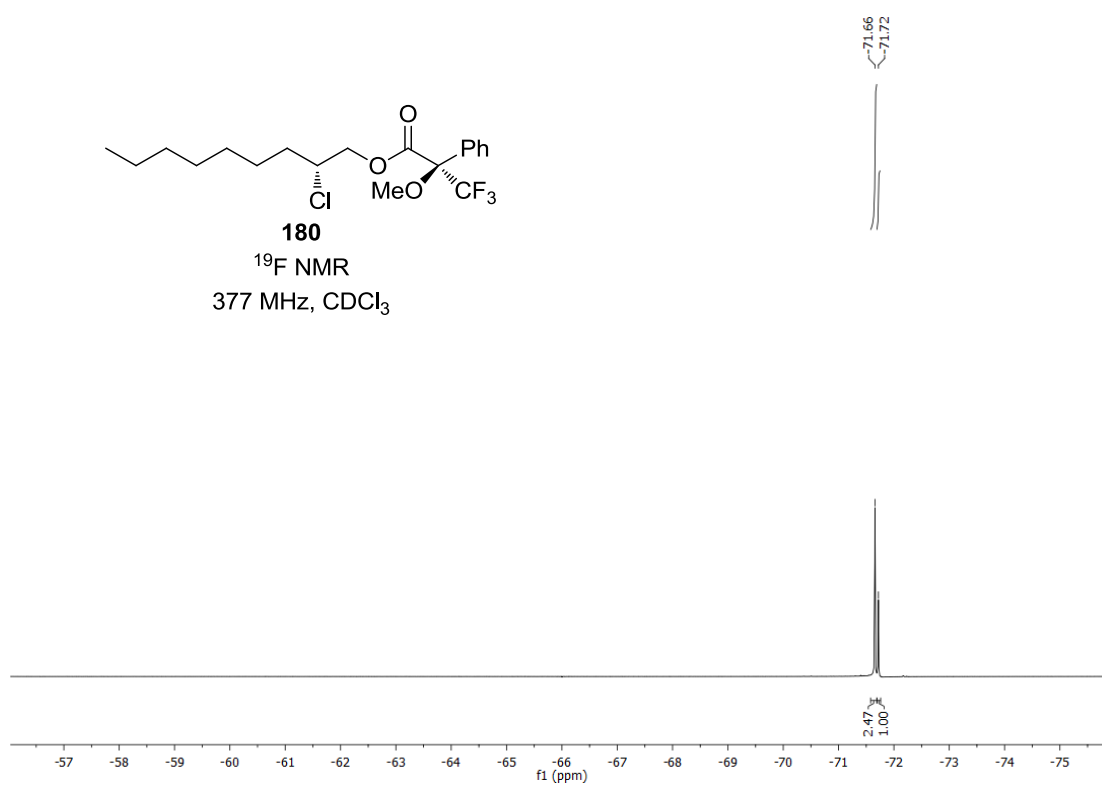


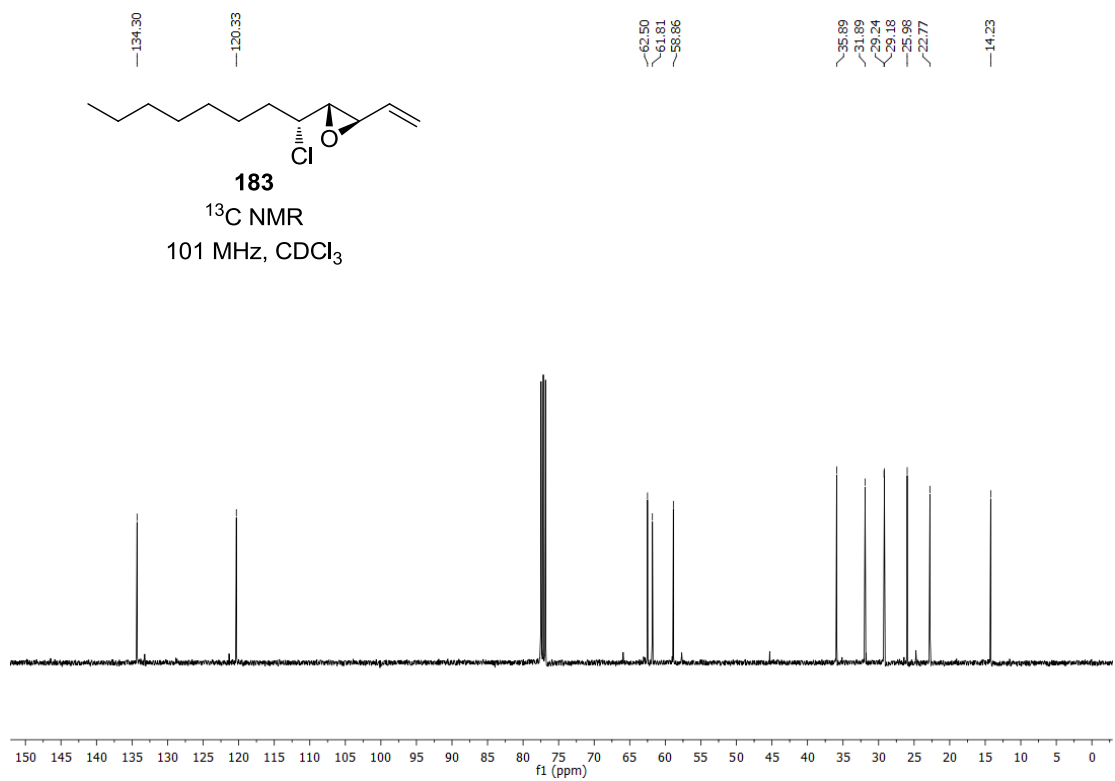
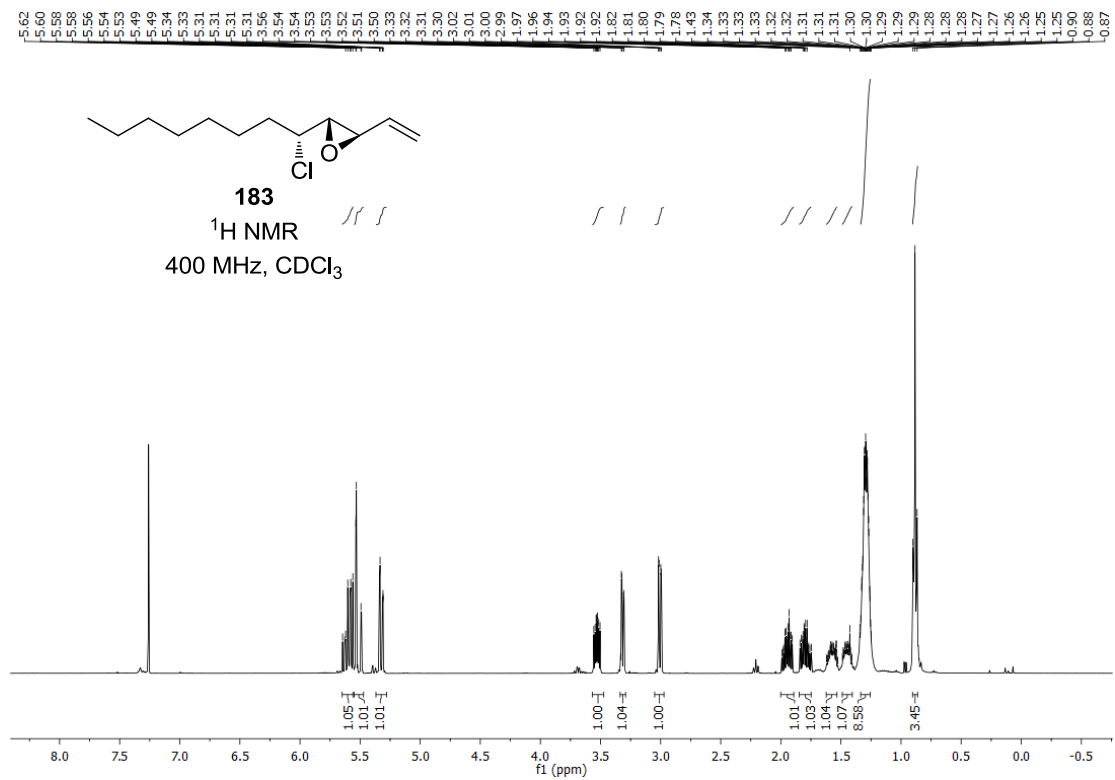


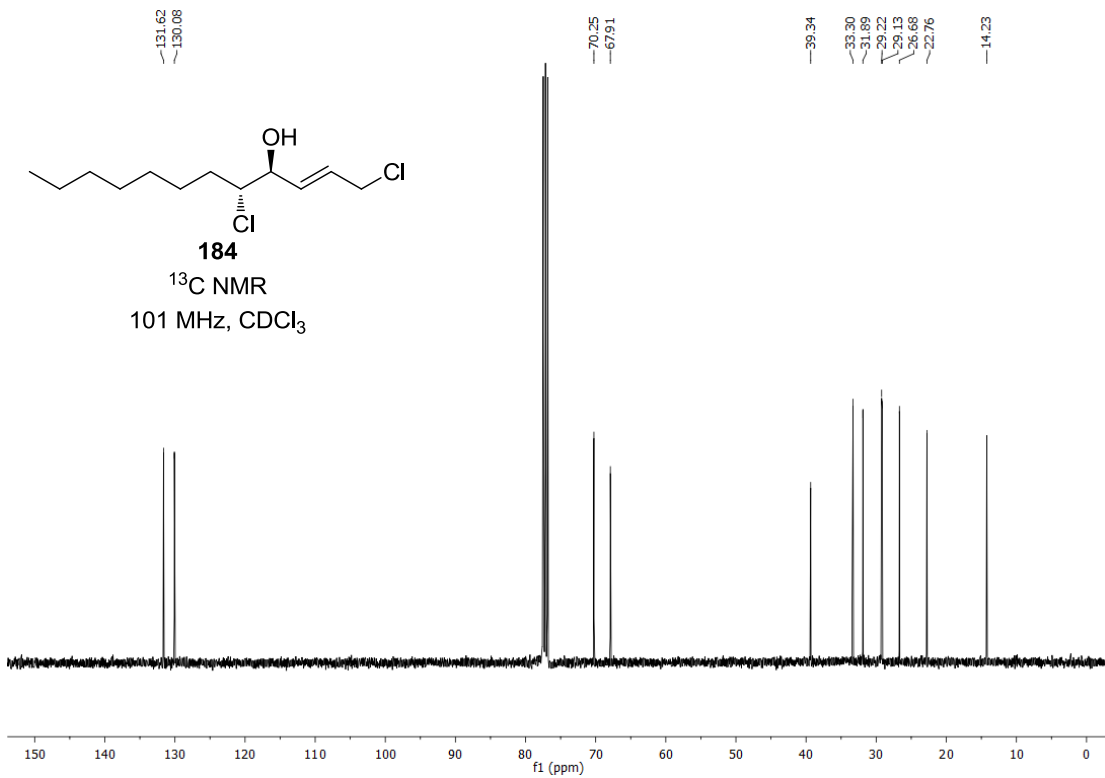
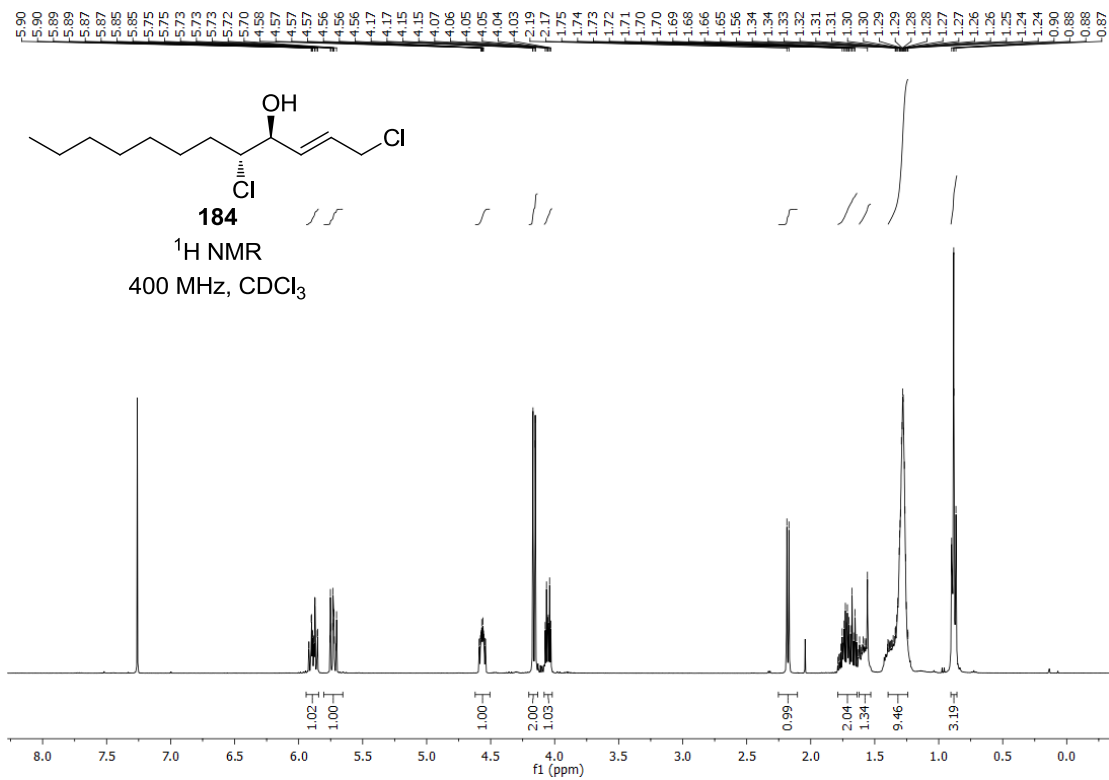


Appendix

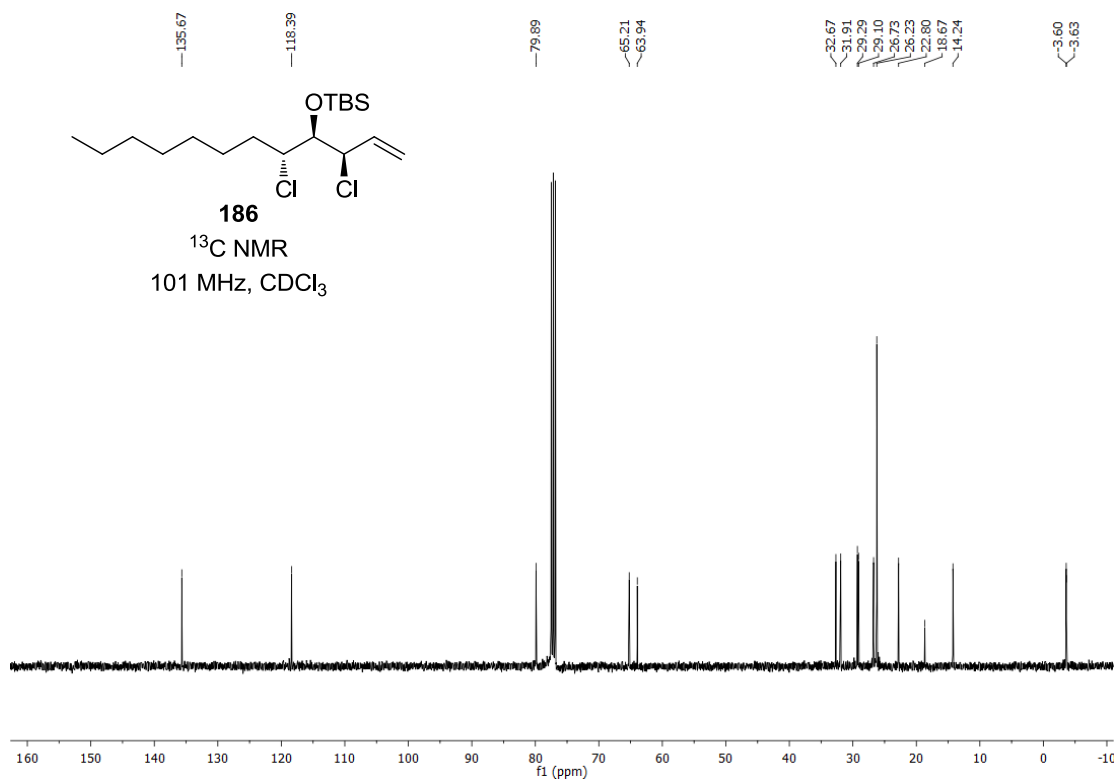
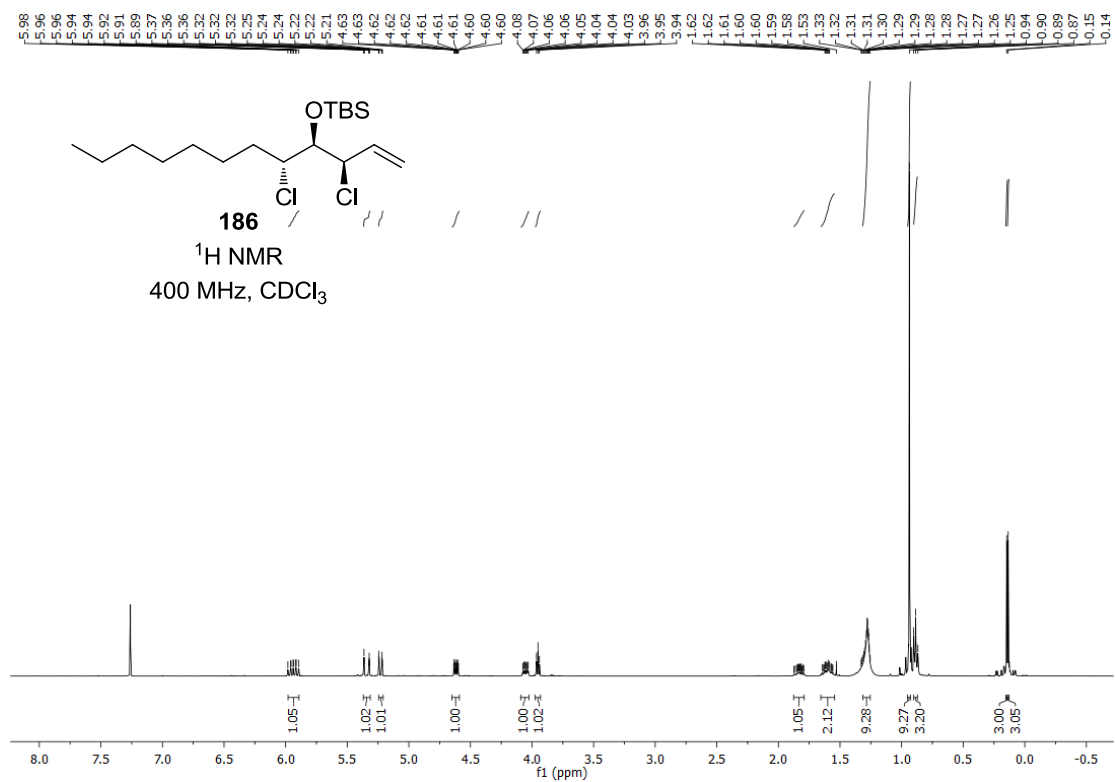


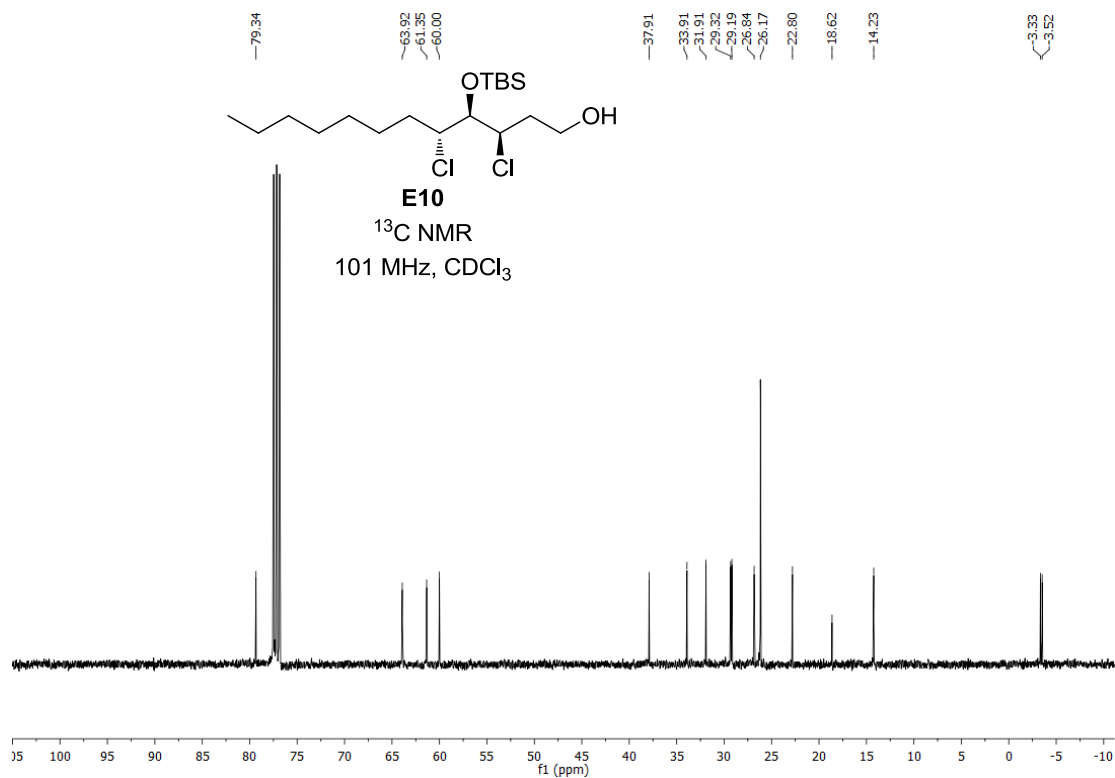
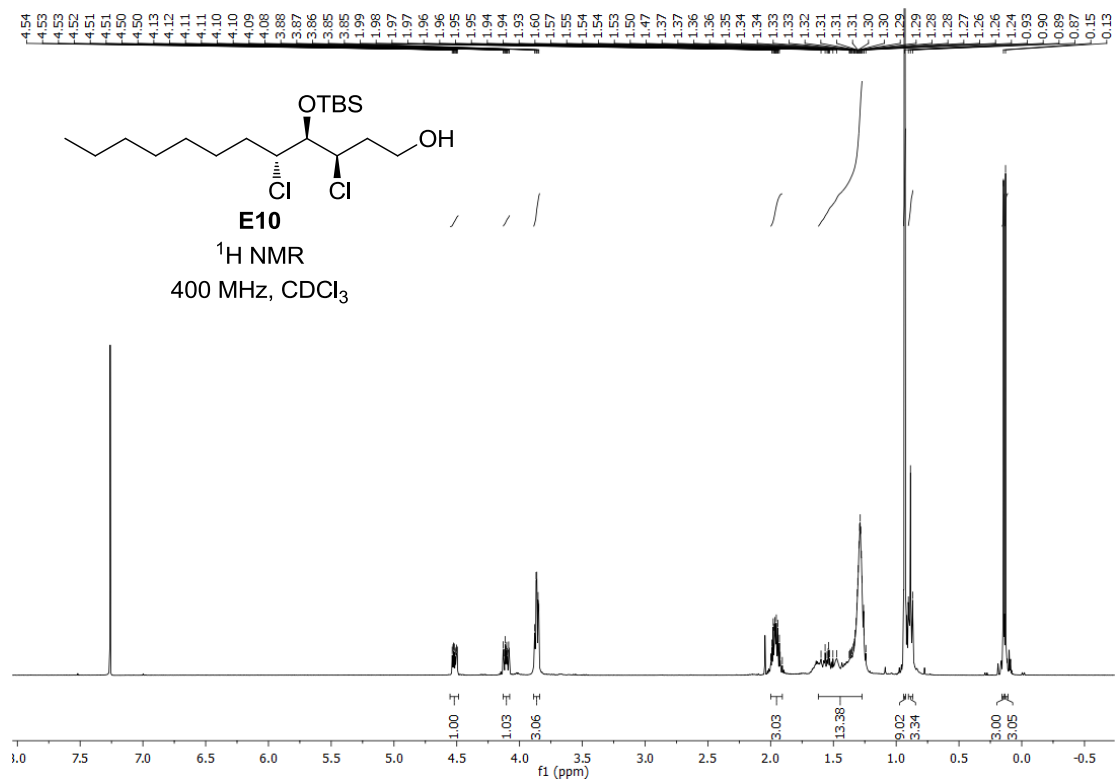




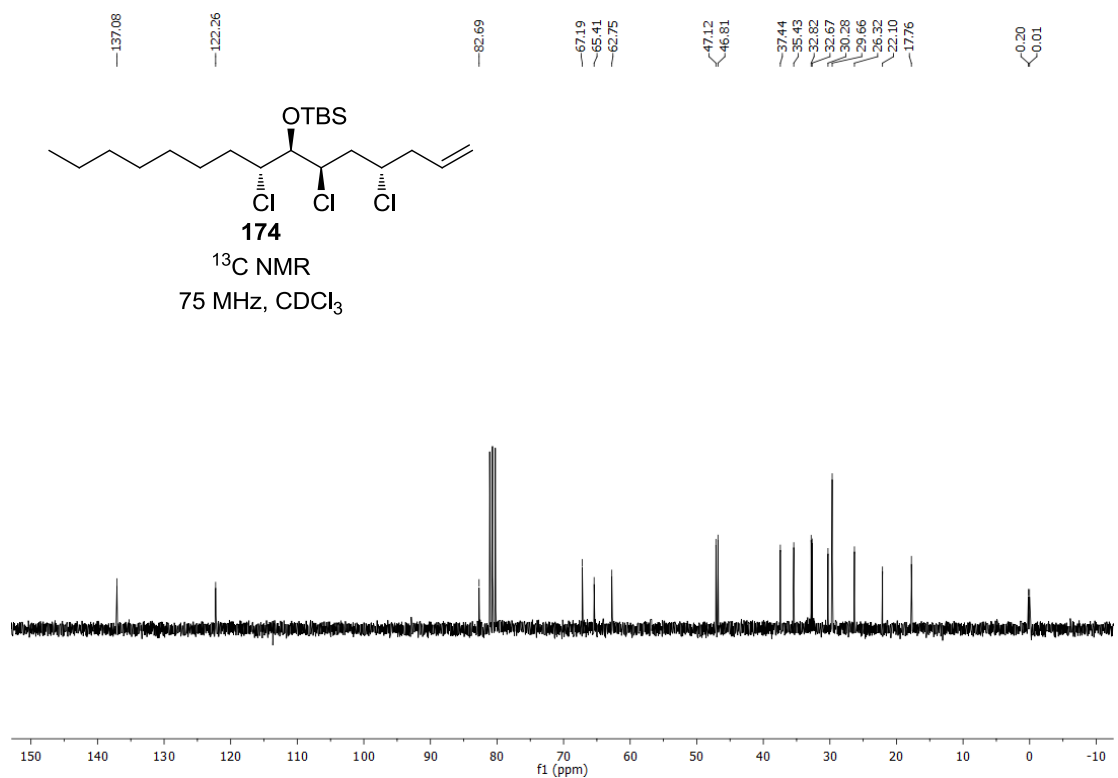
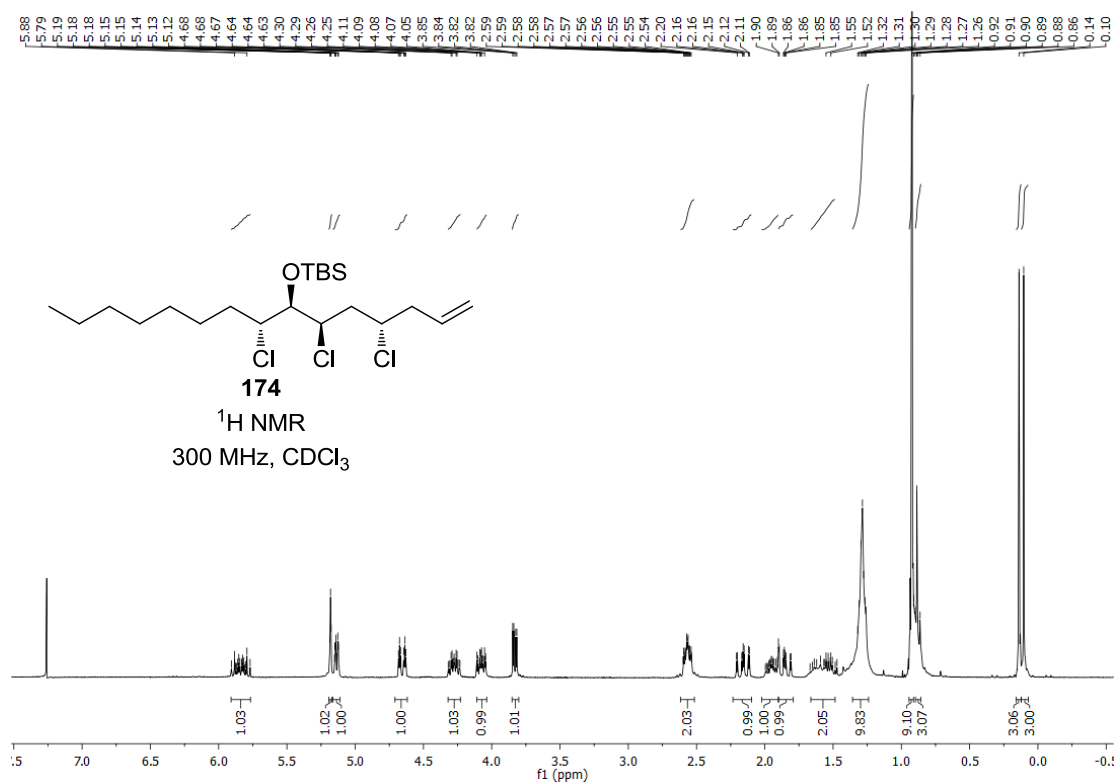


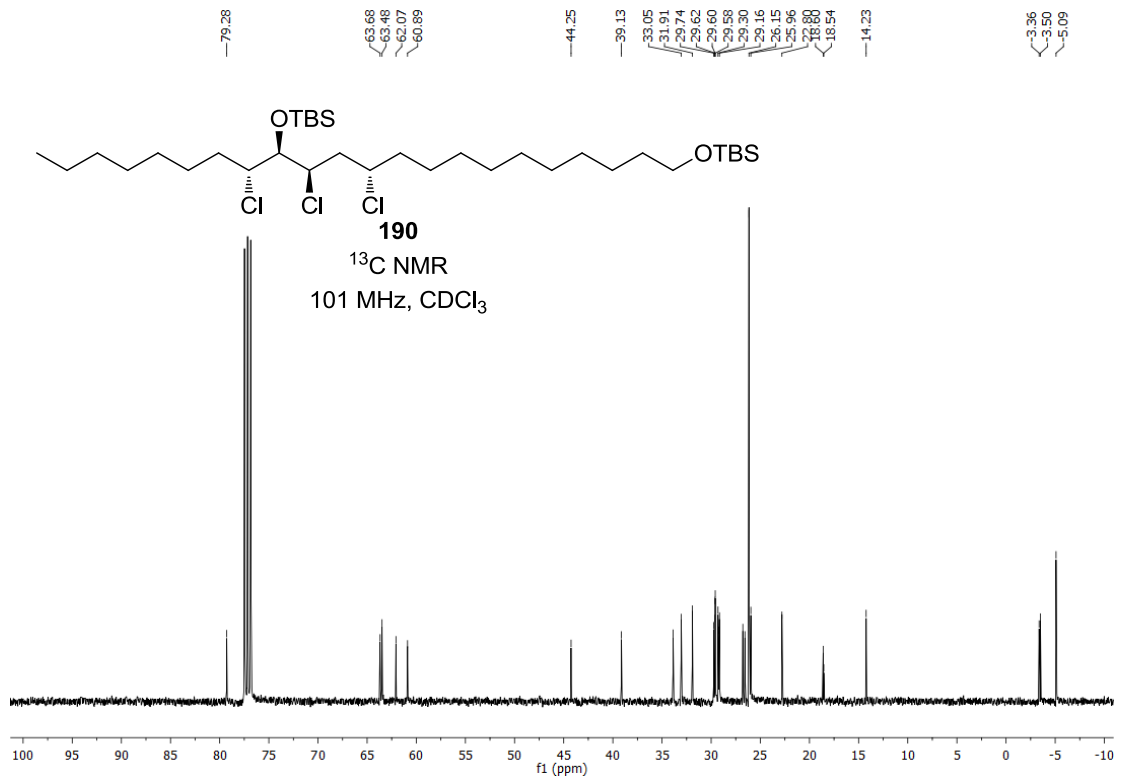
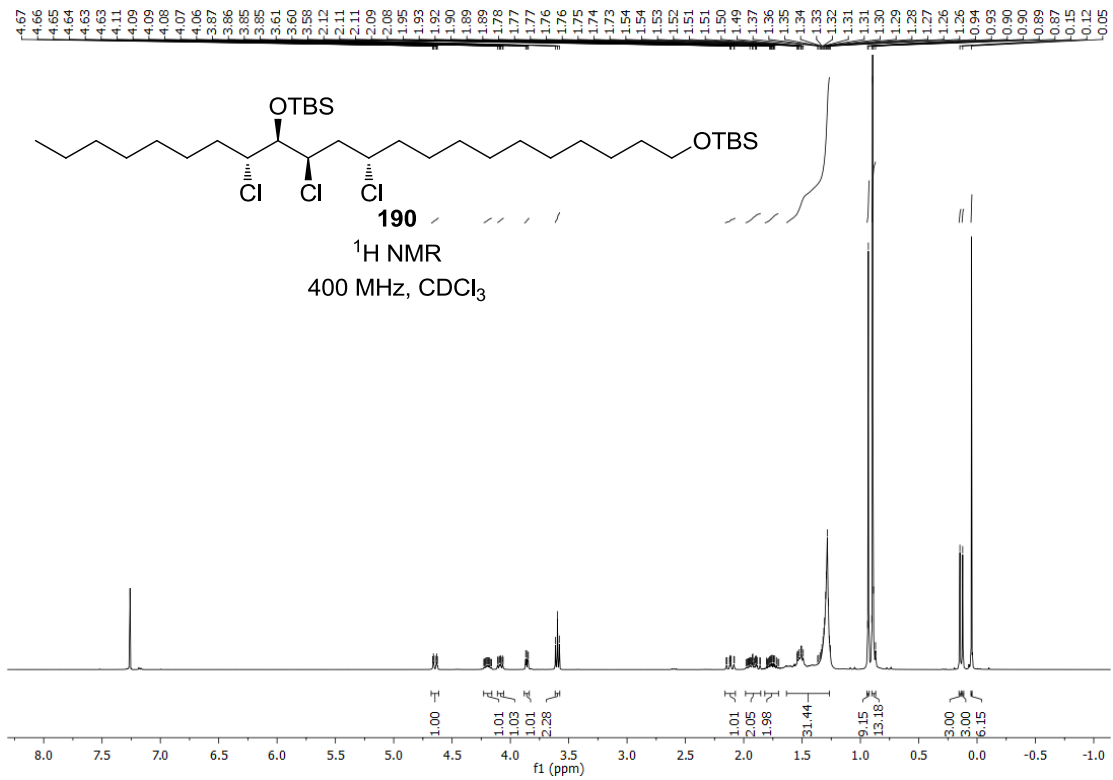
Appendix



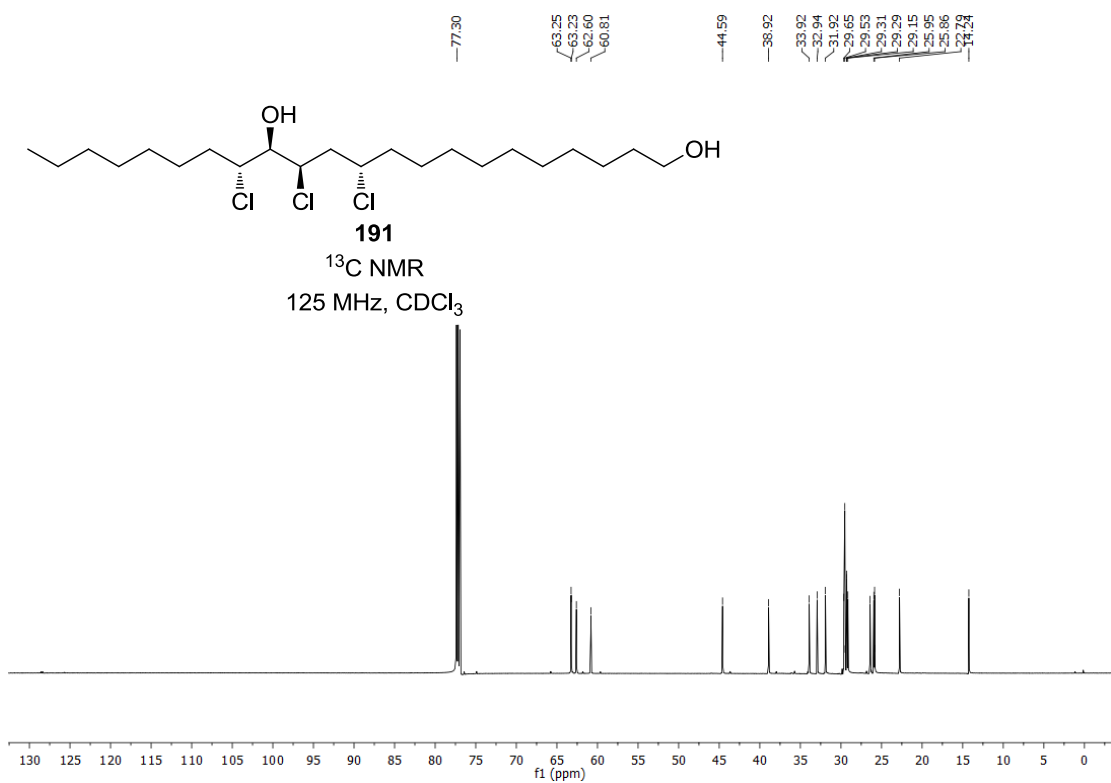
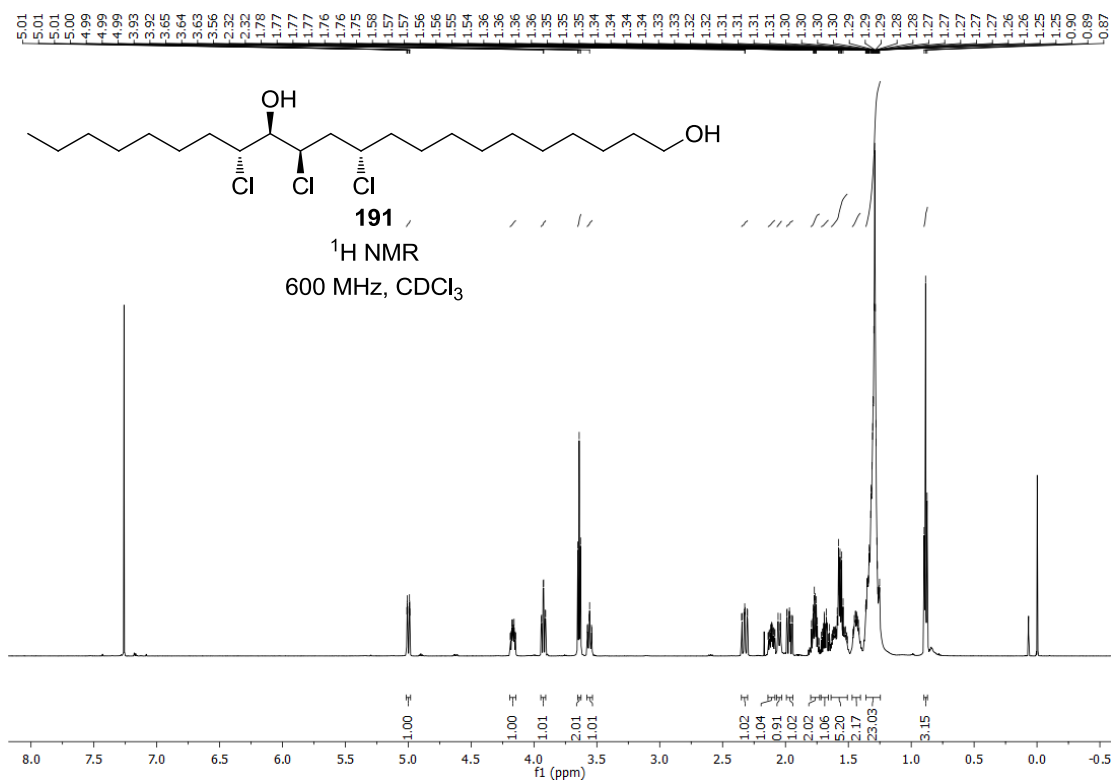


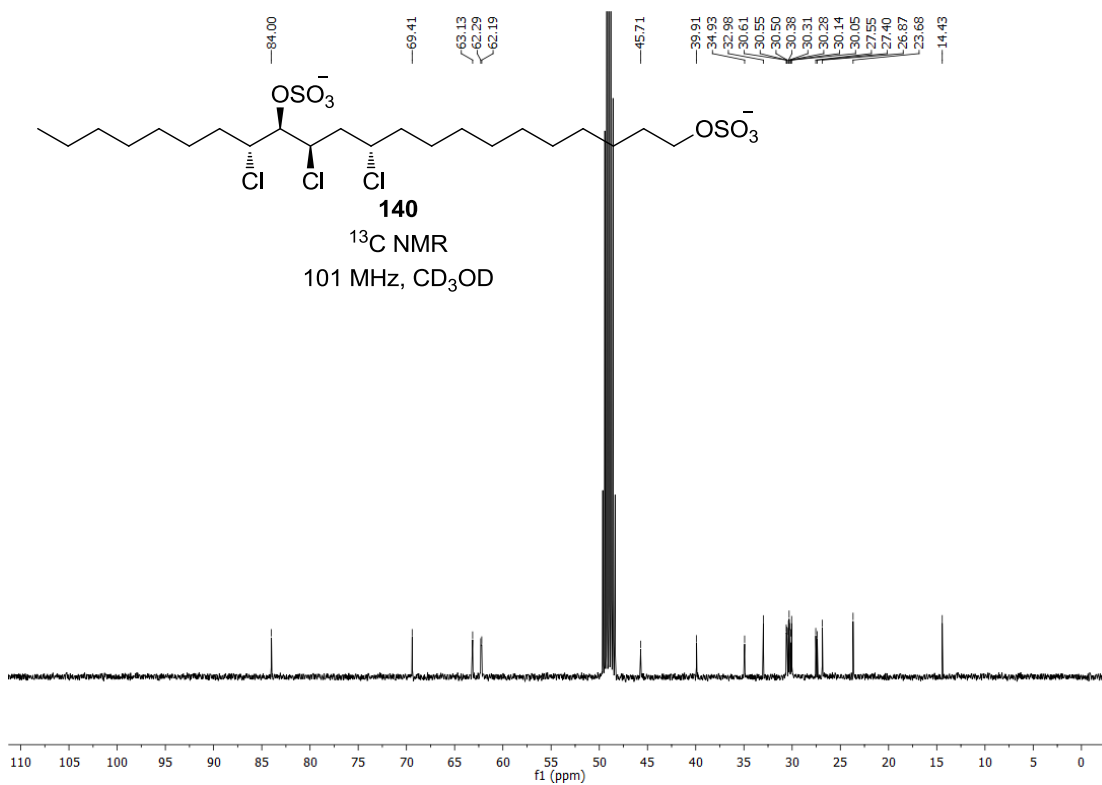
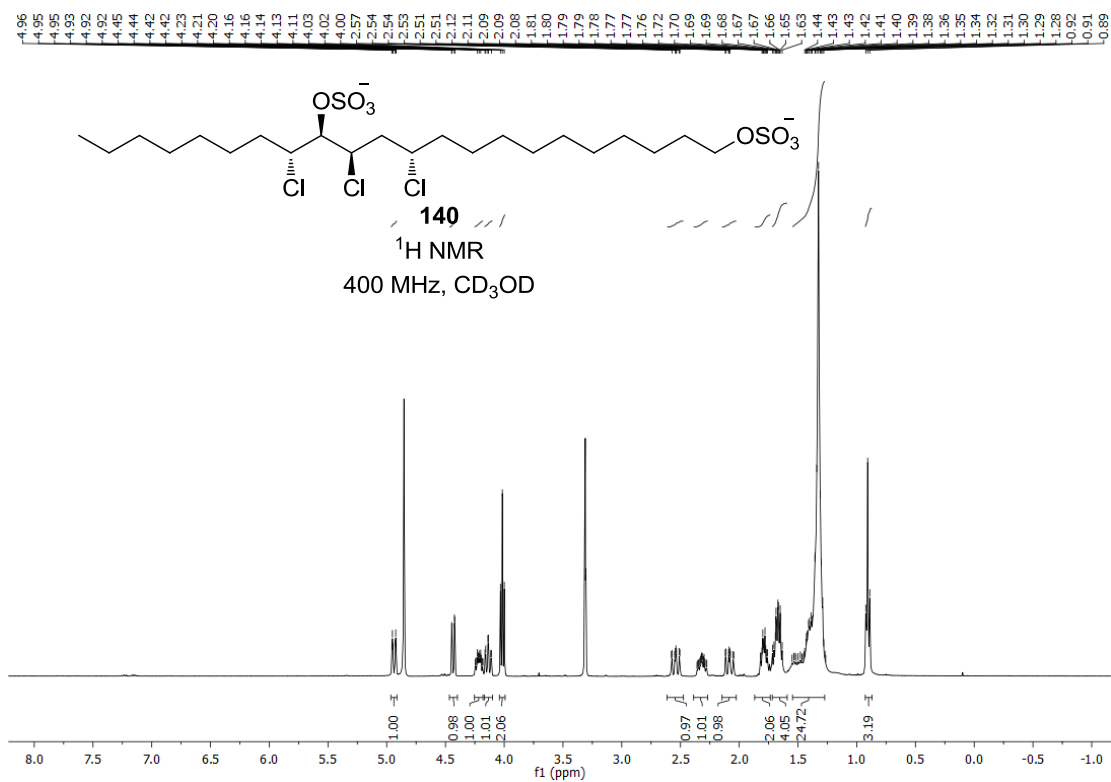
Appendix



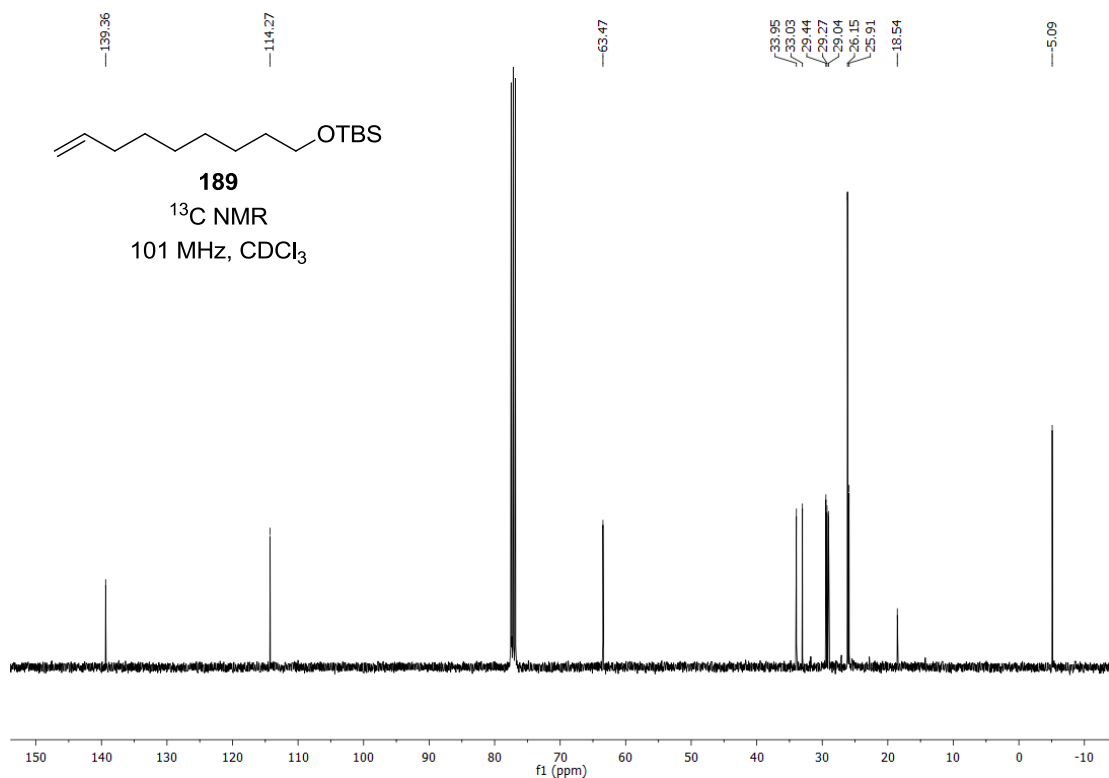
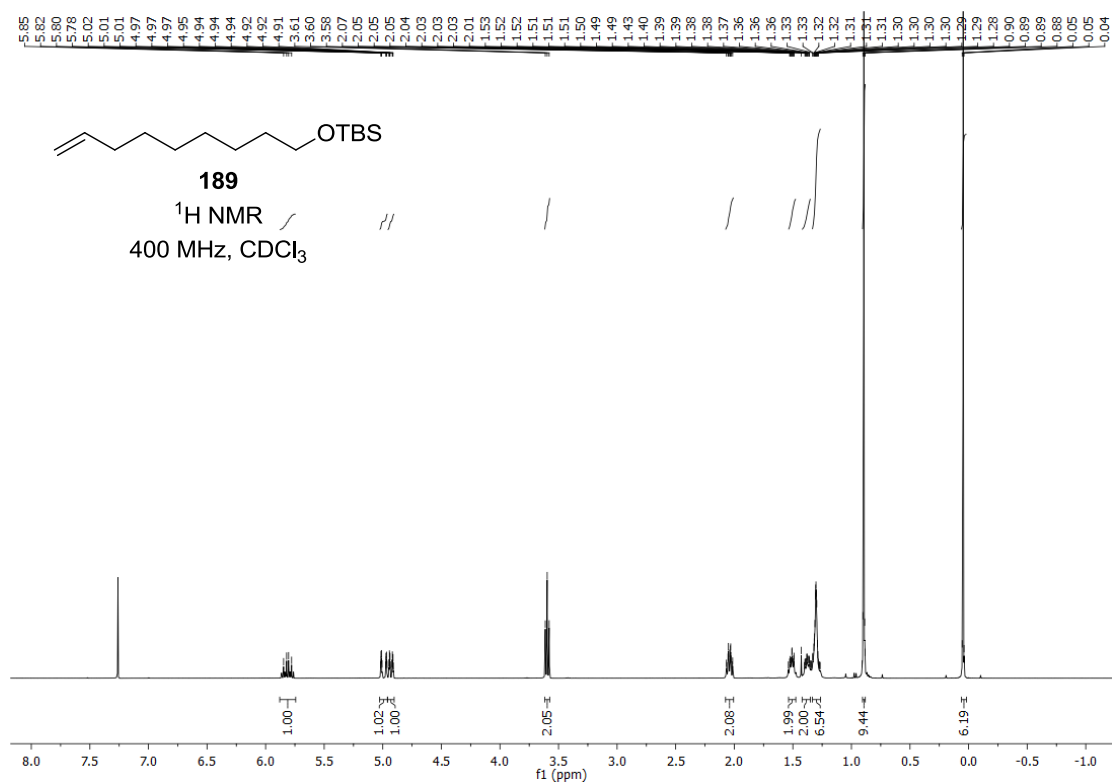


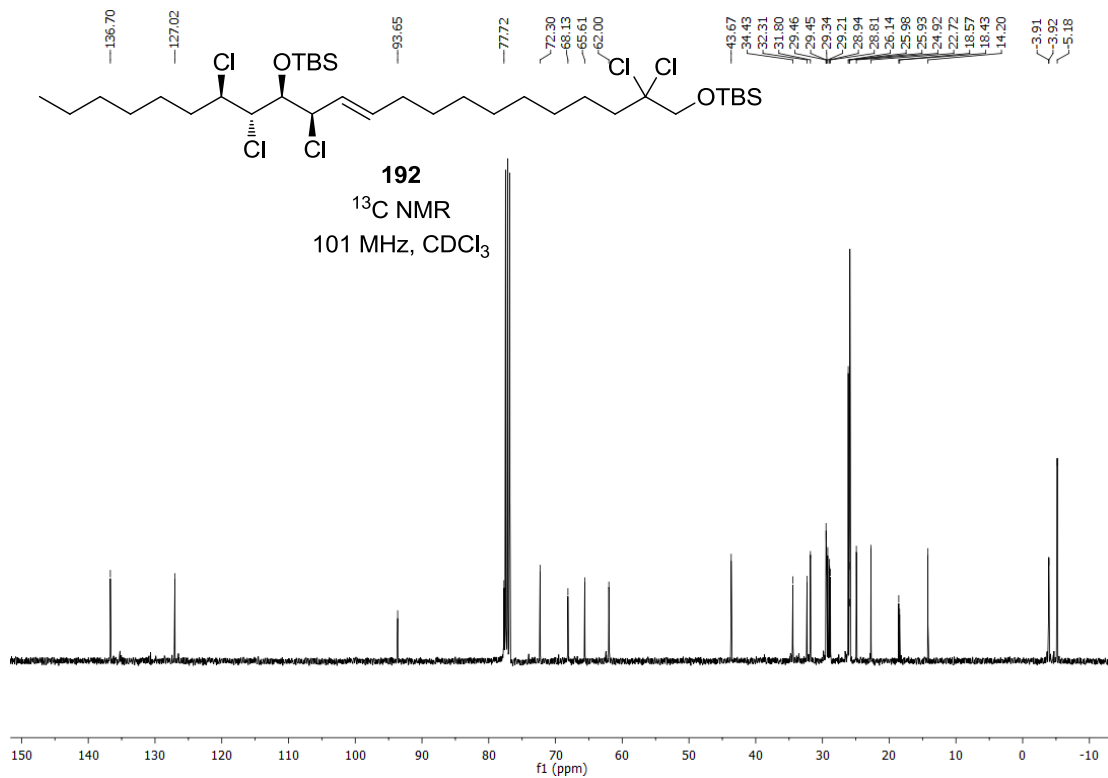
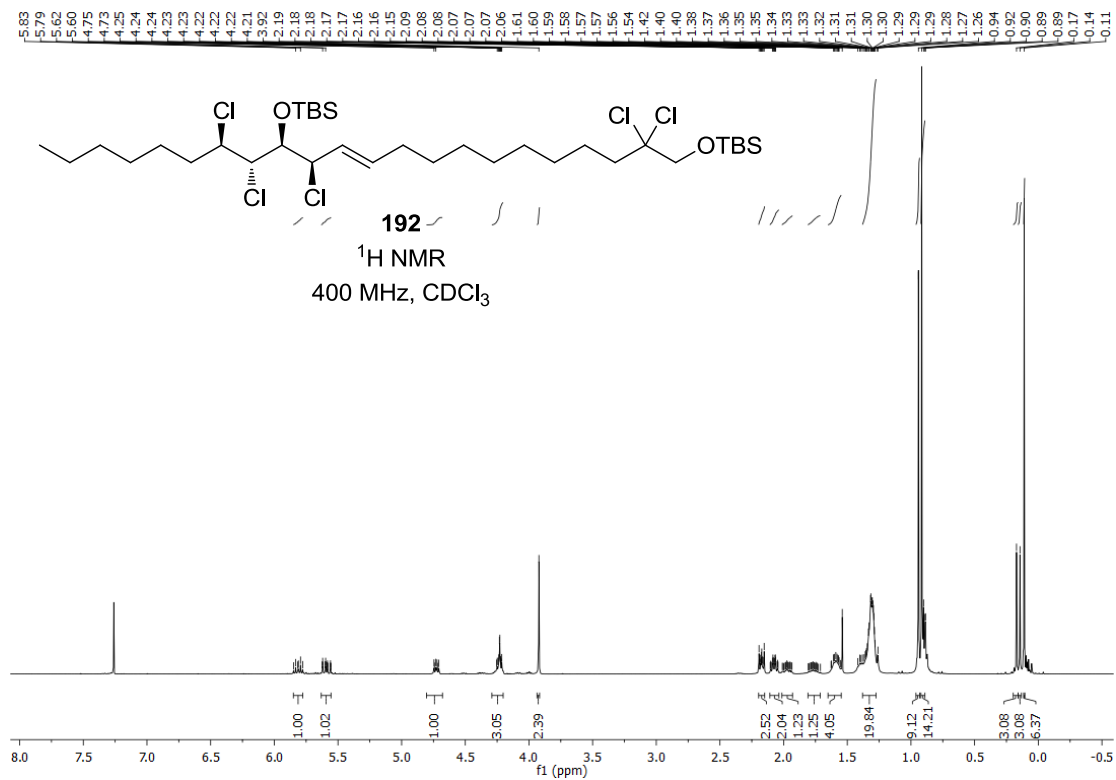
Appendix

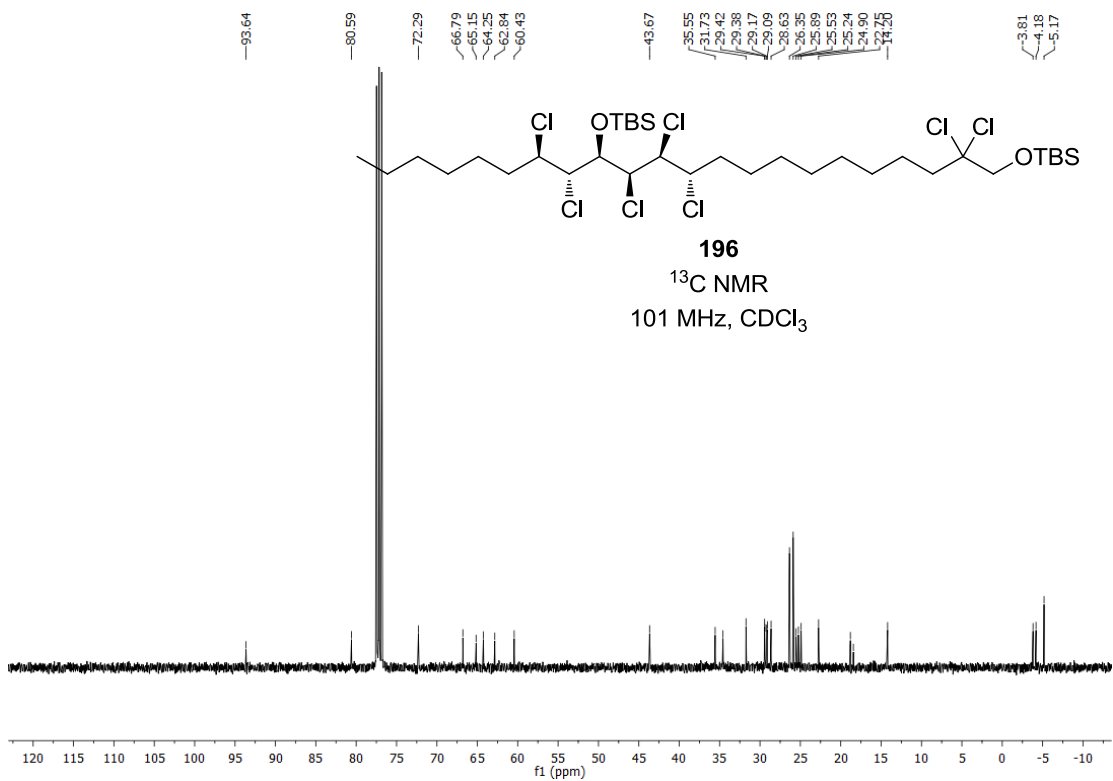
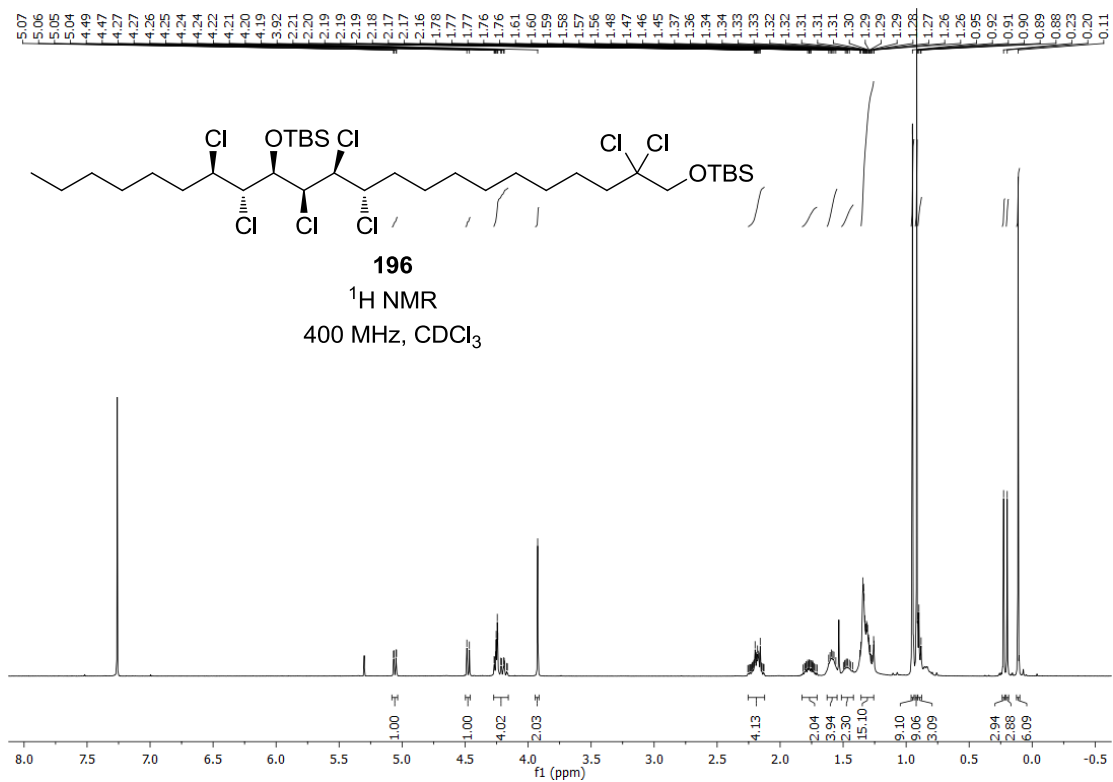


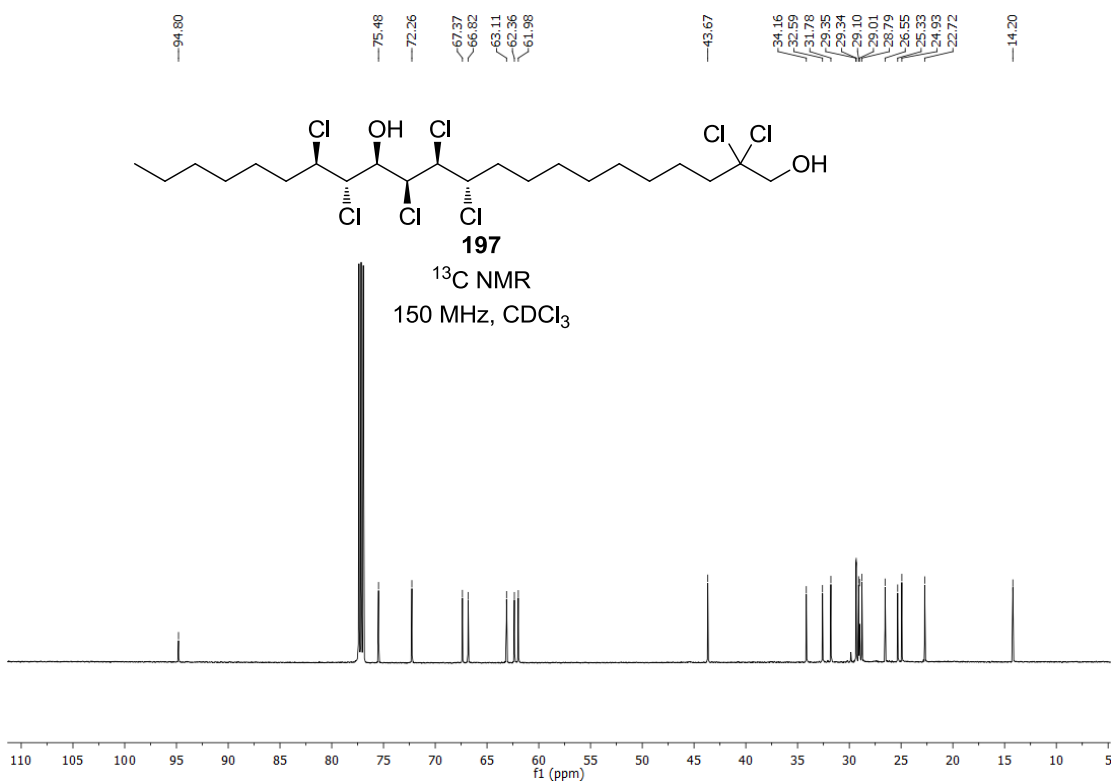
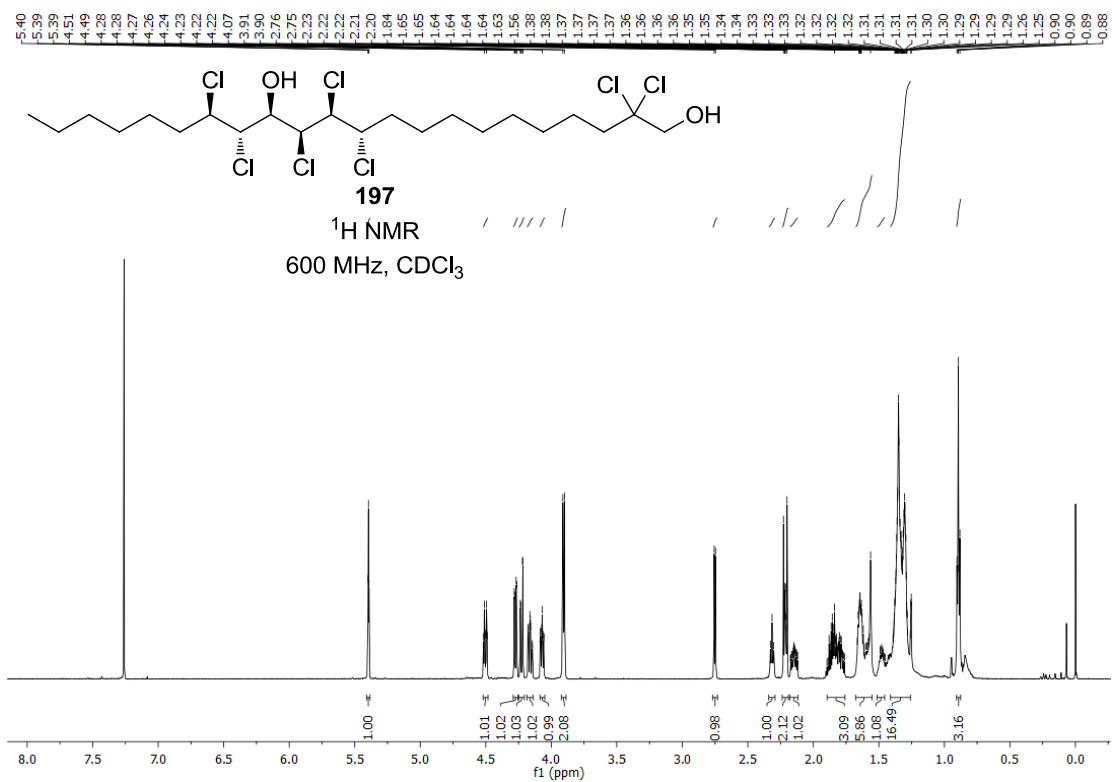


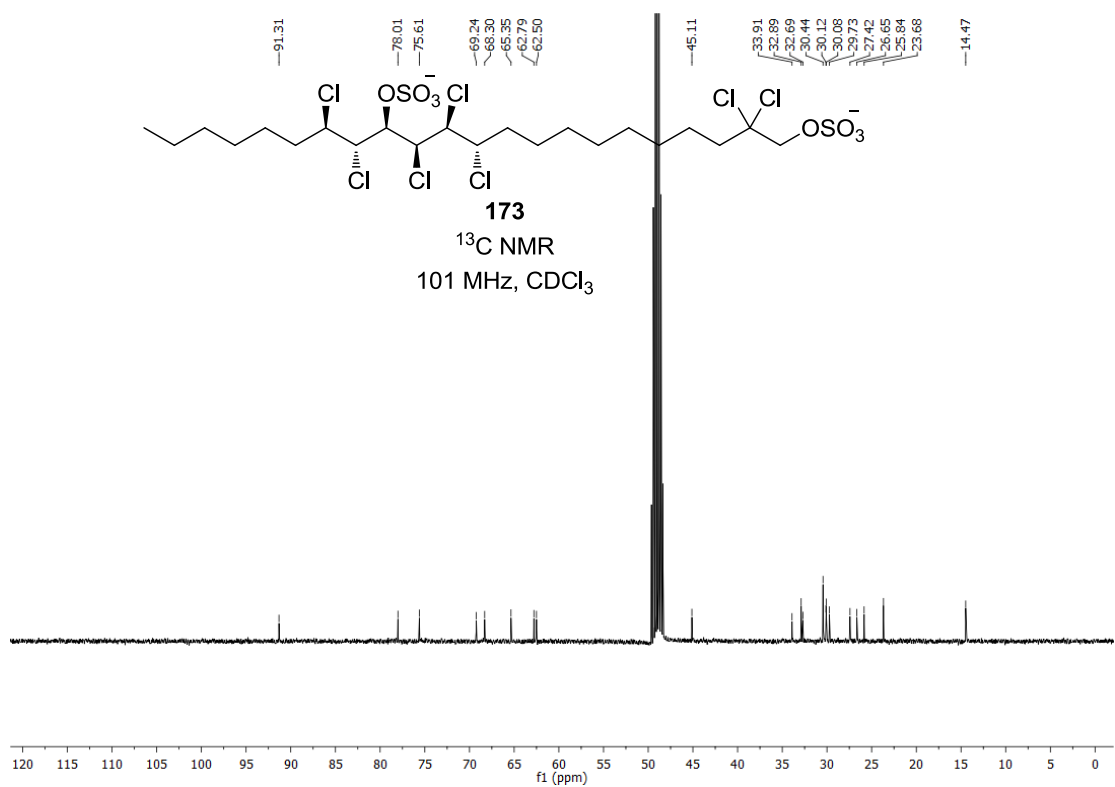
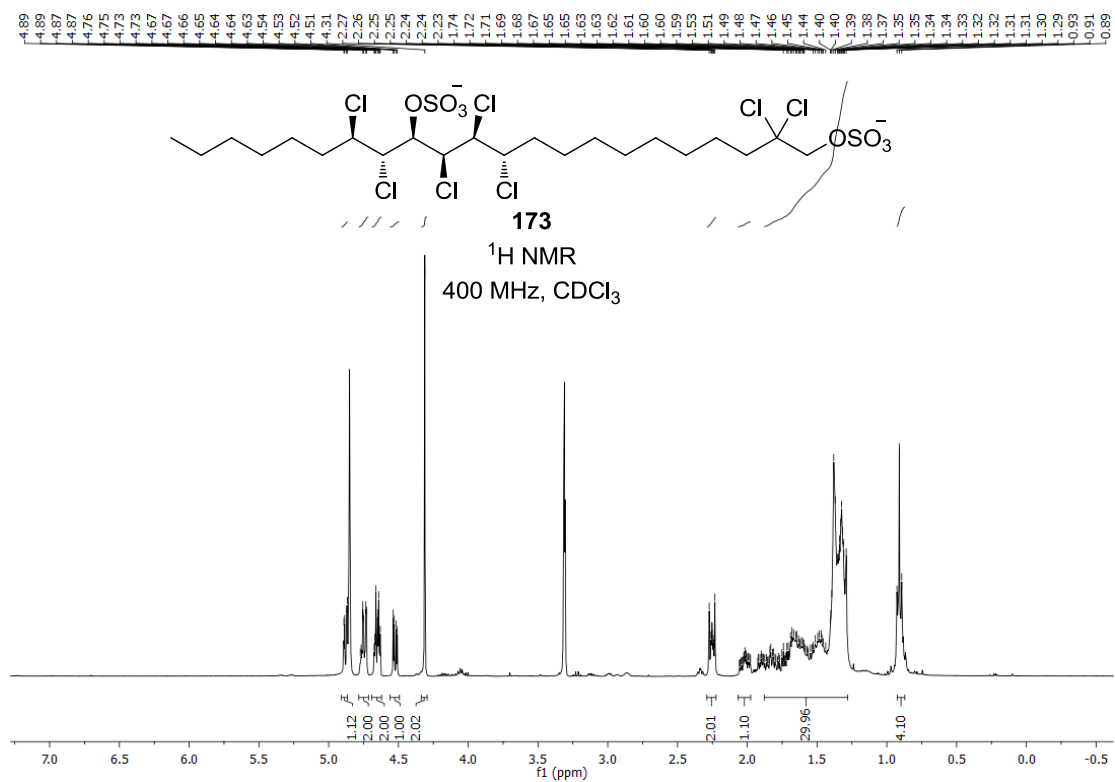
Appendix

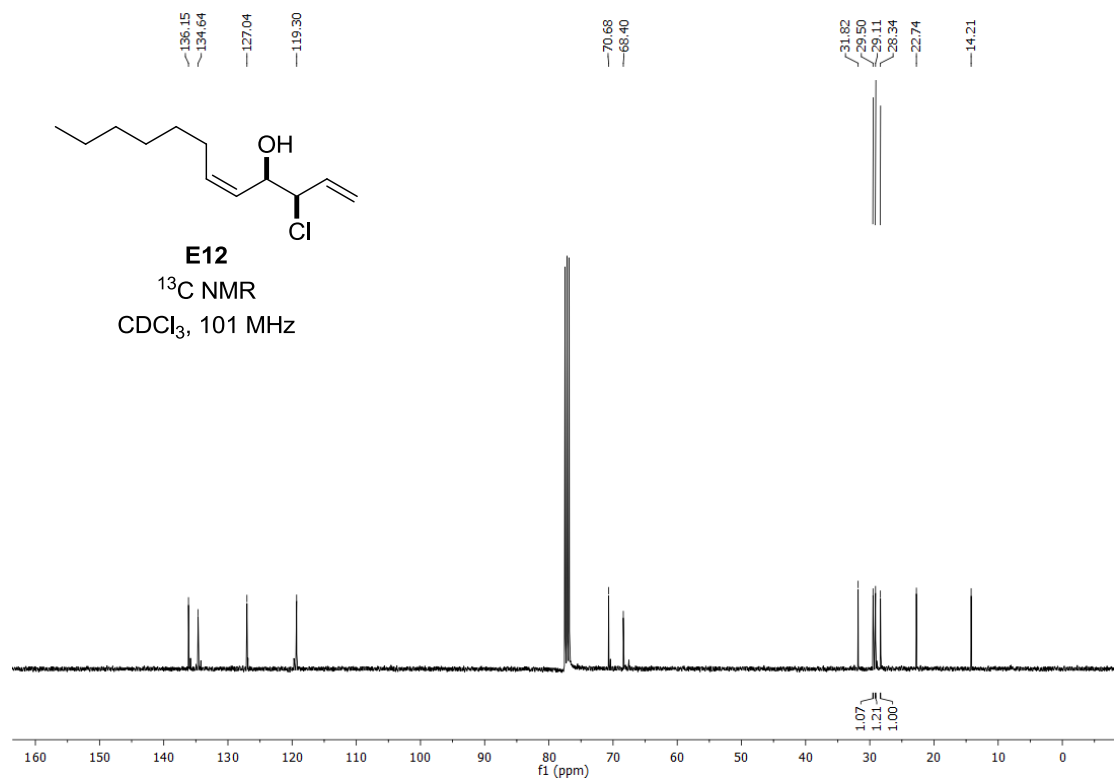
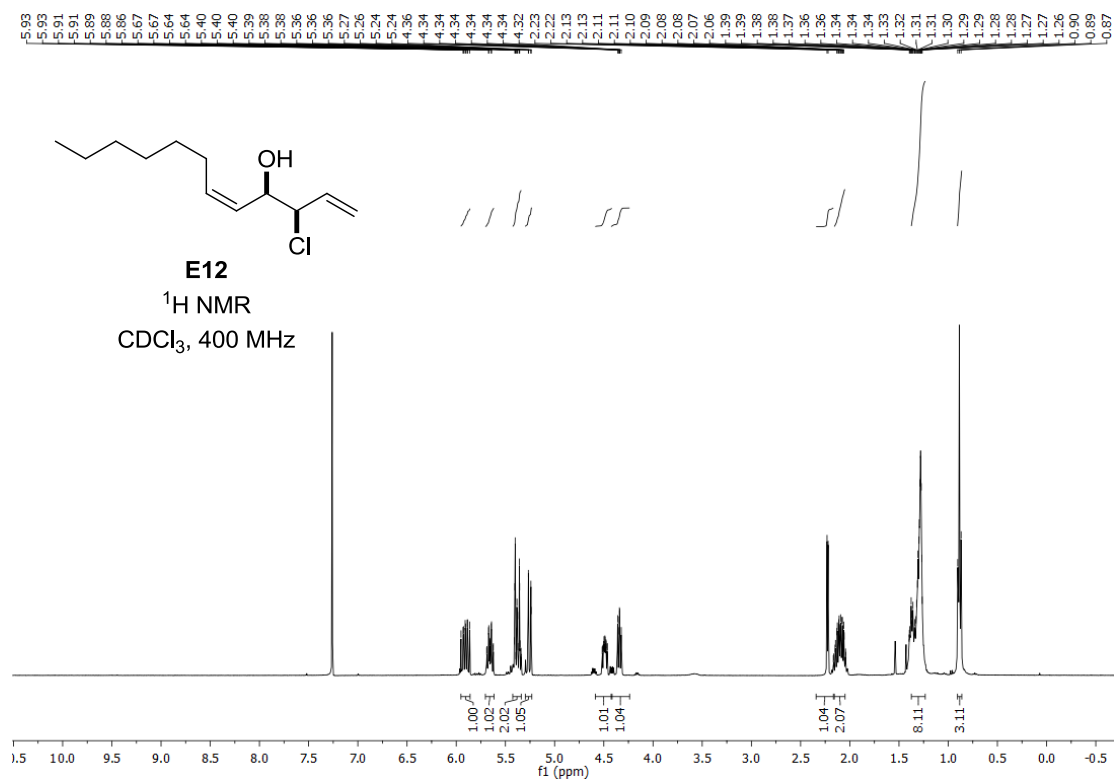


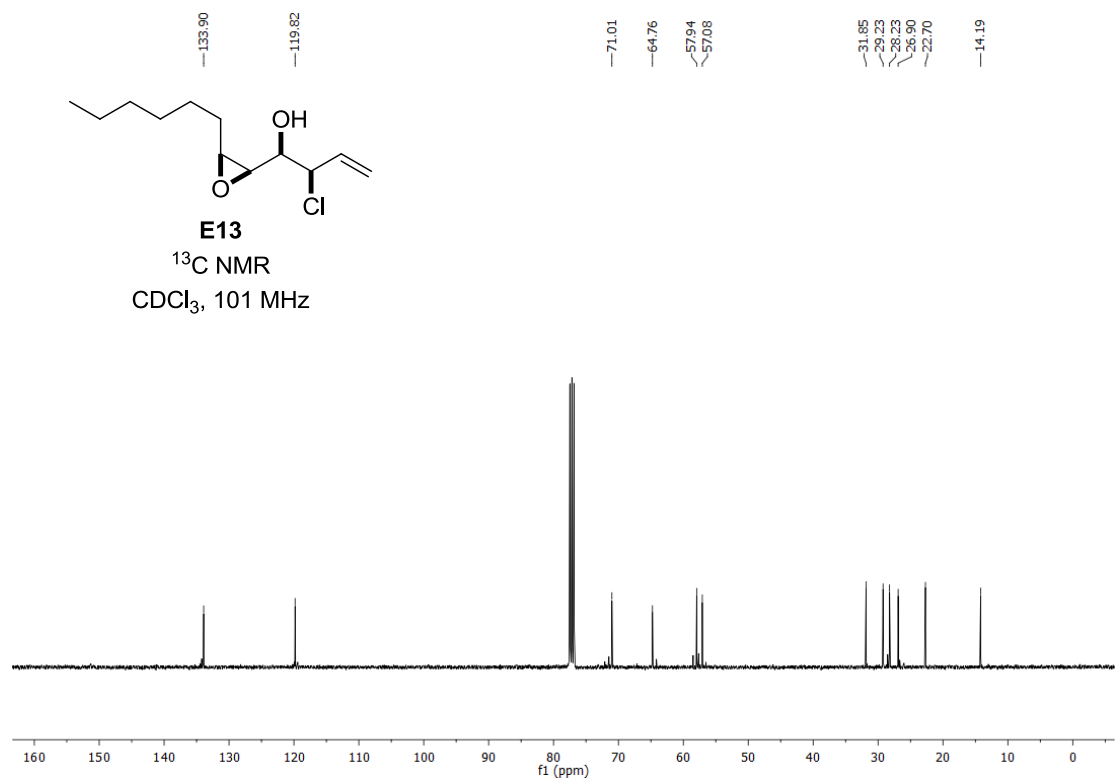
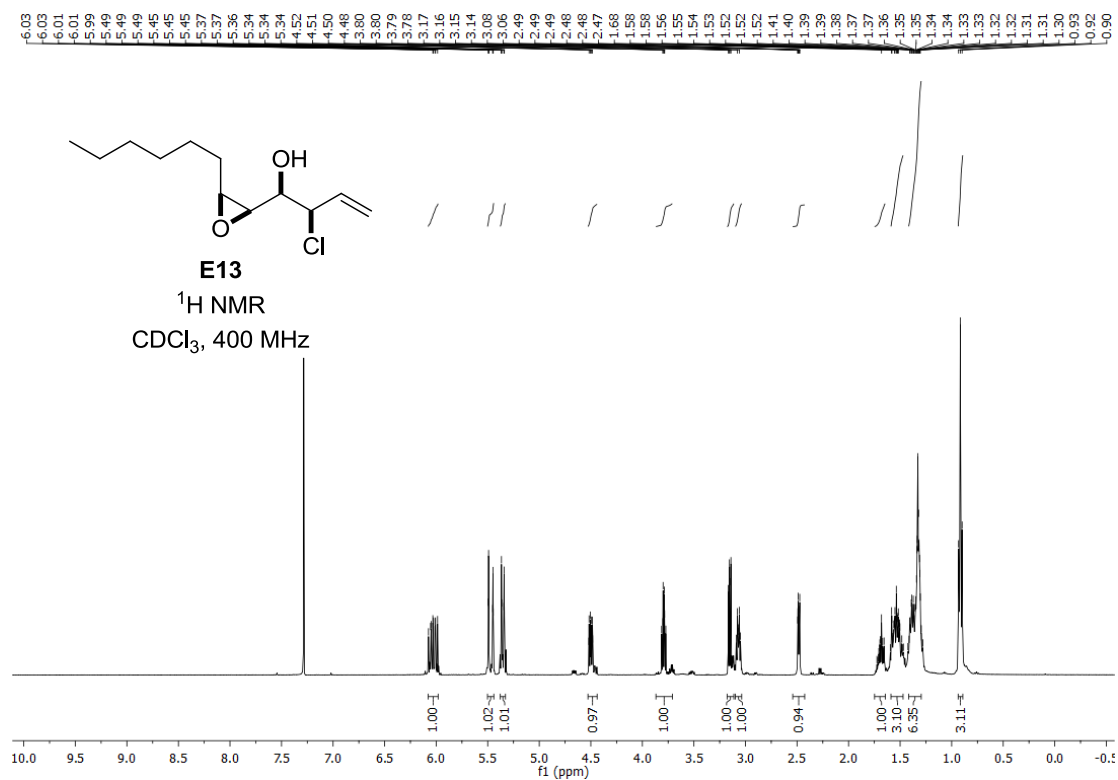


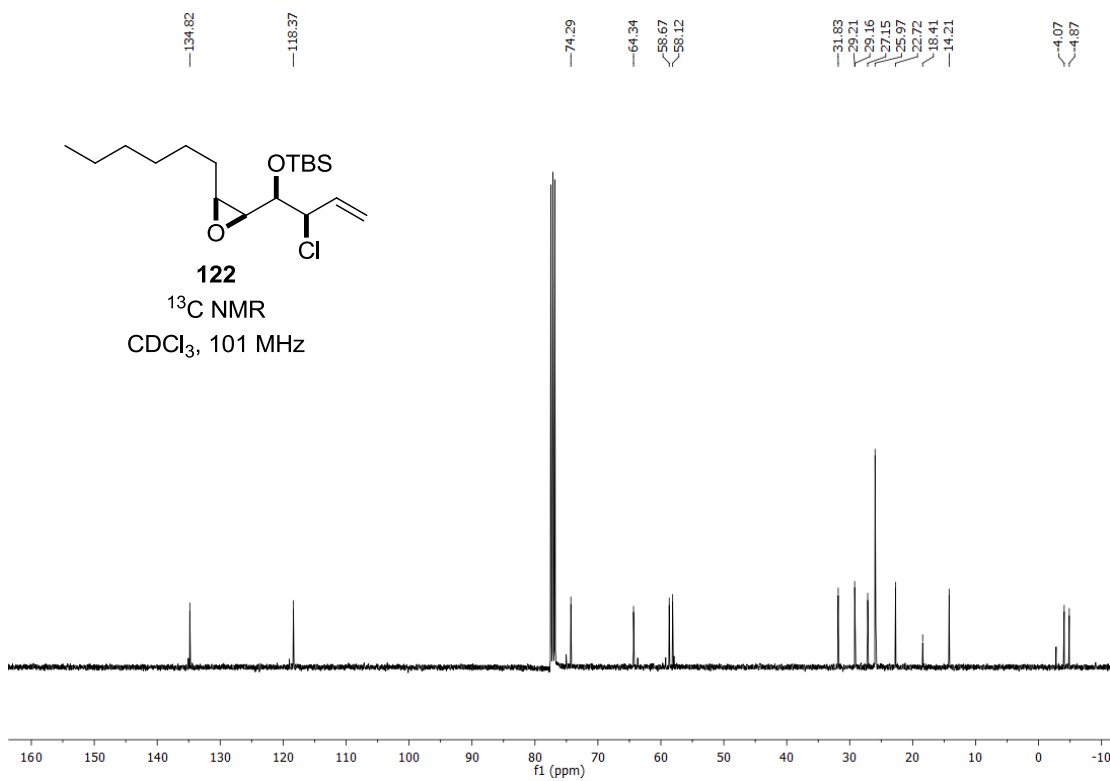
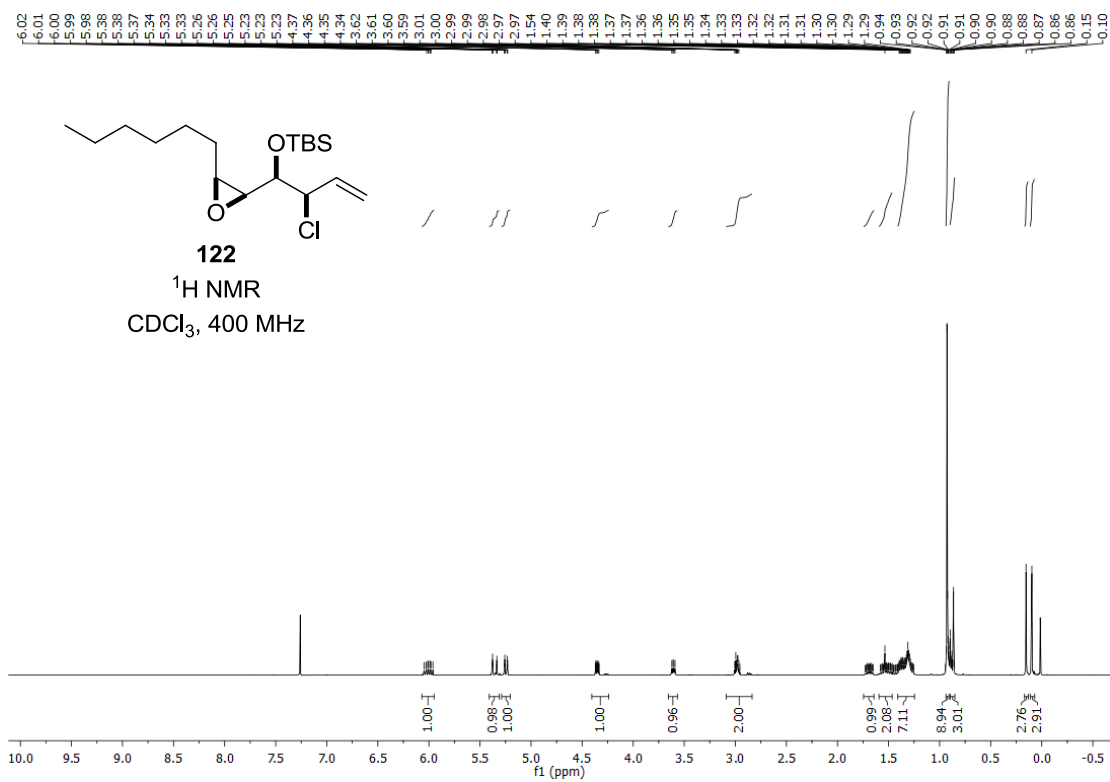


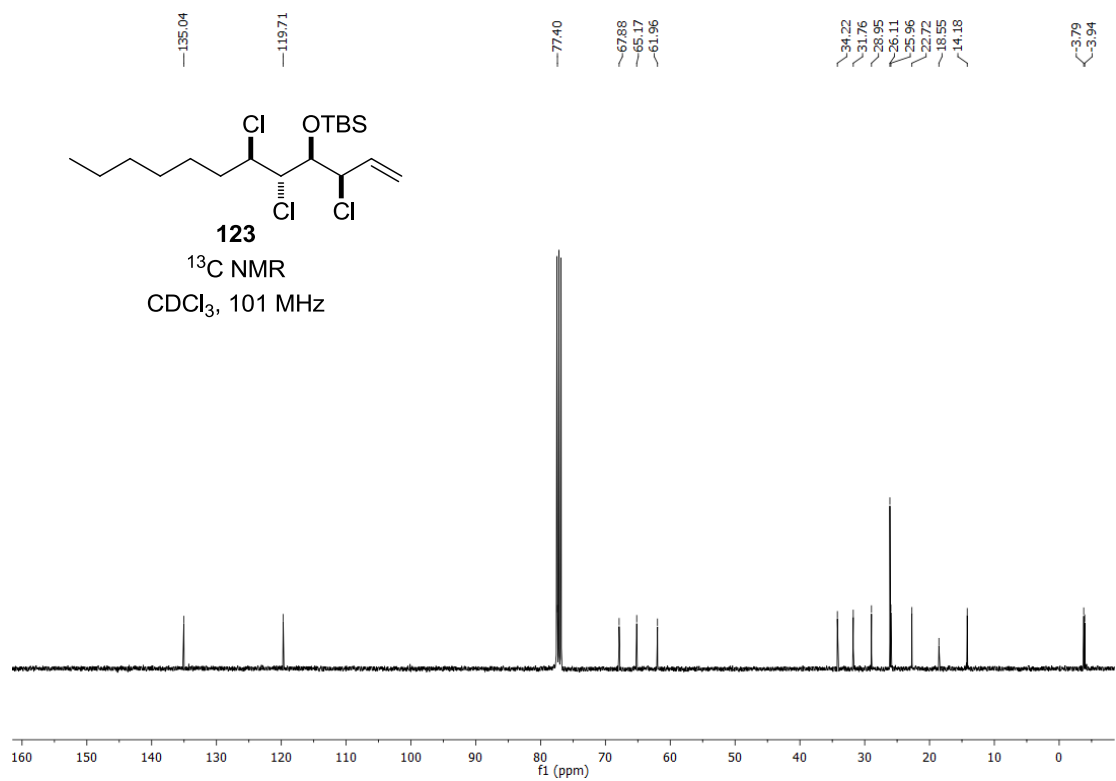
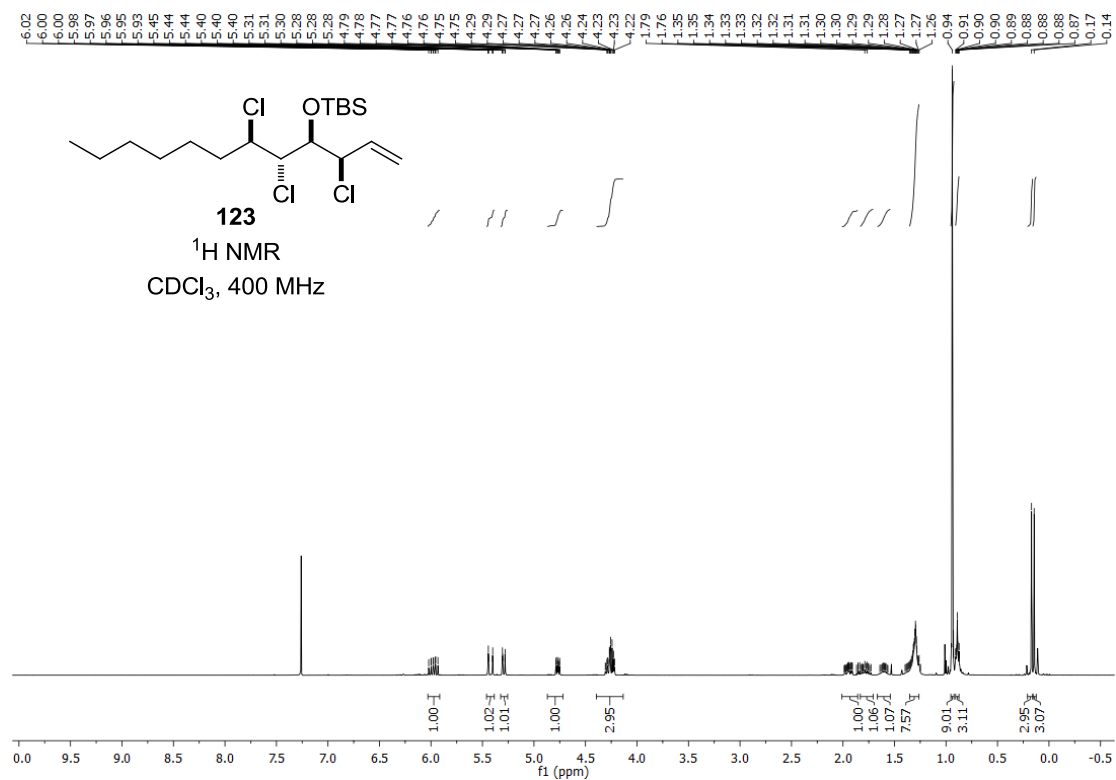


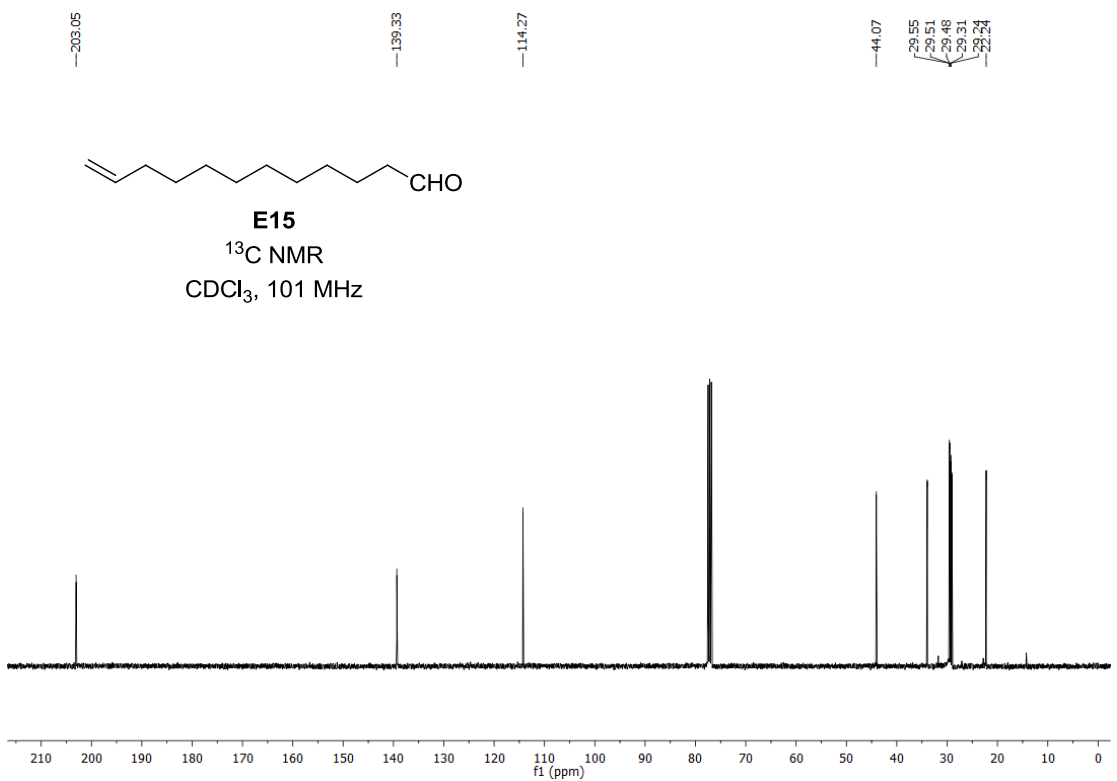
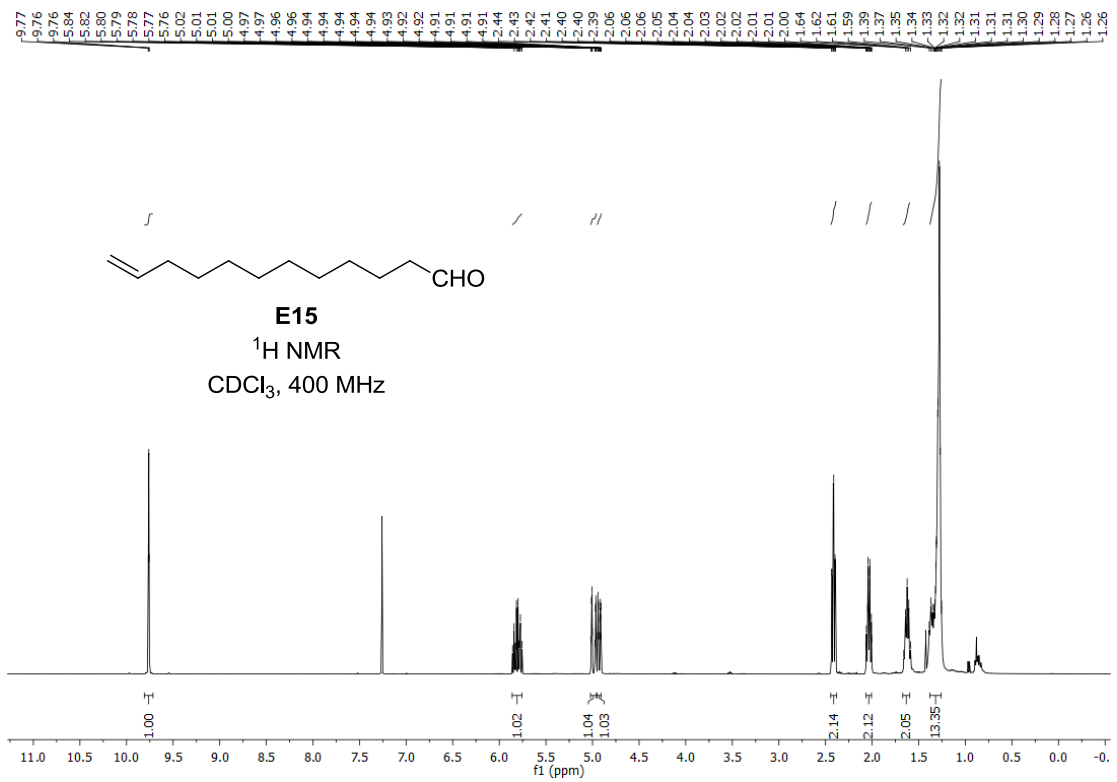




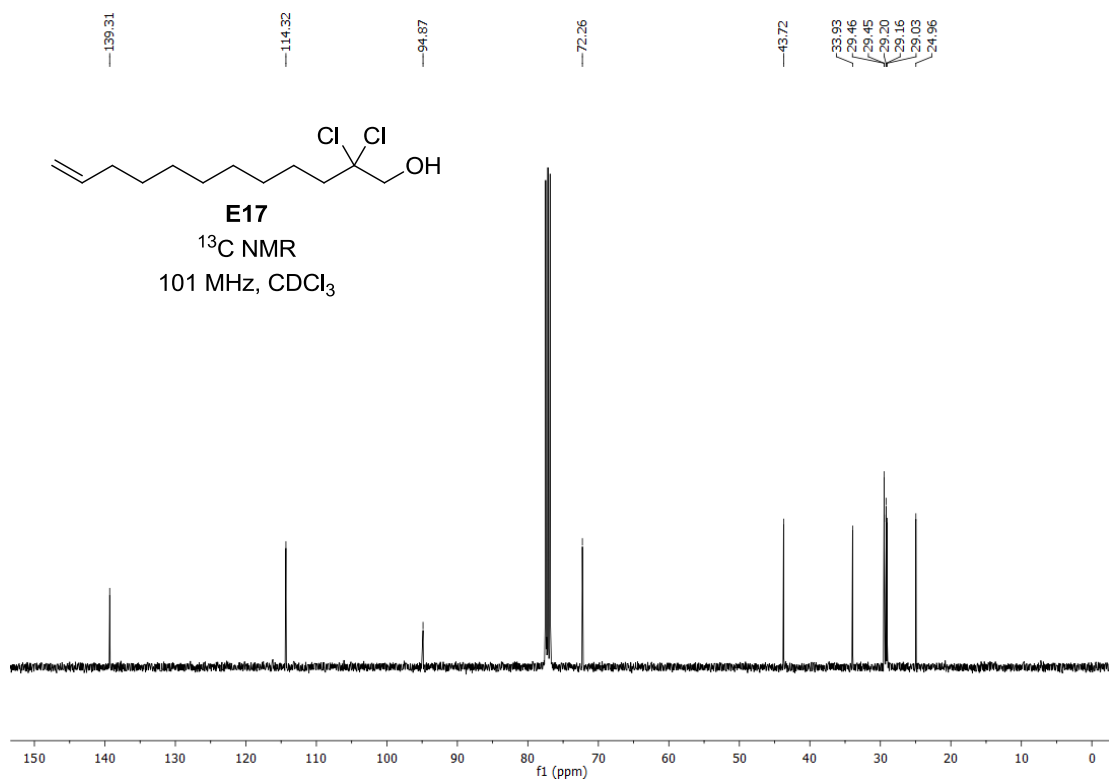
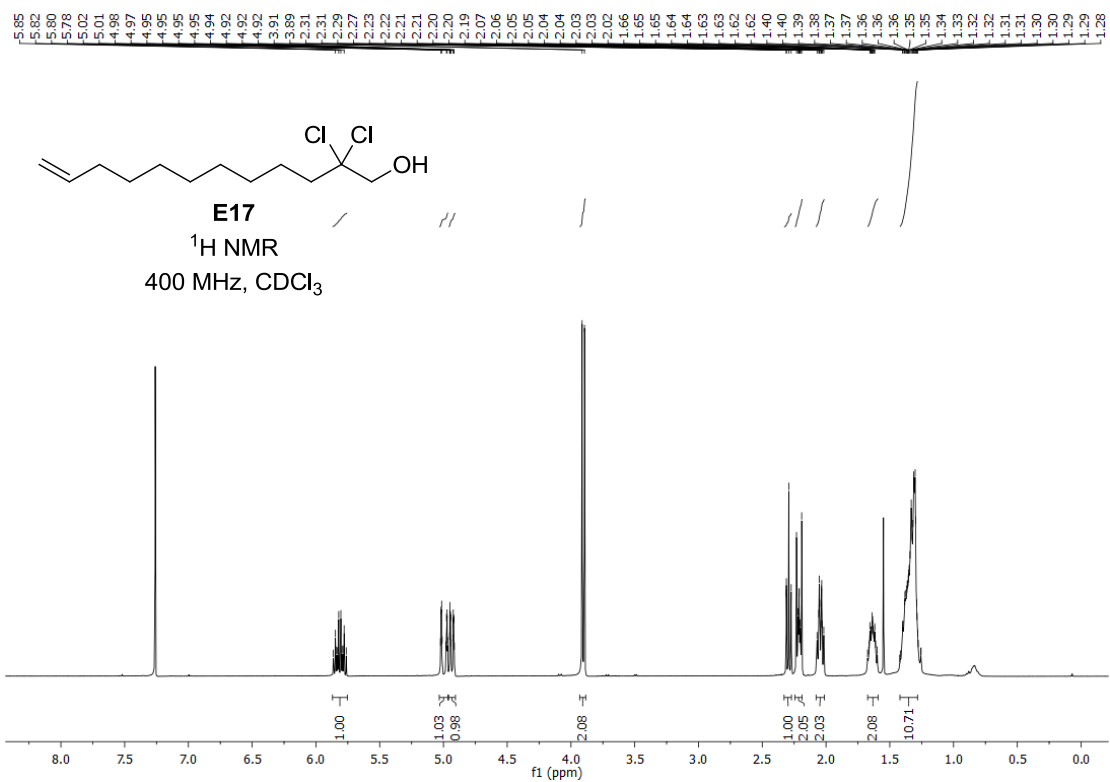


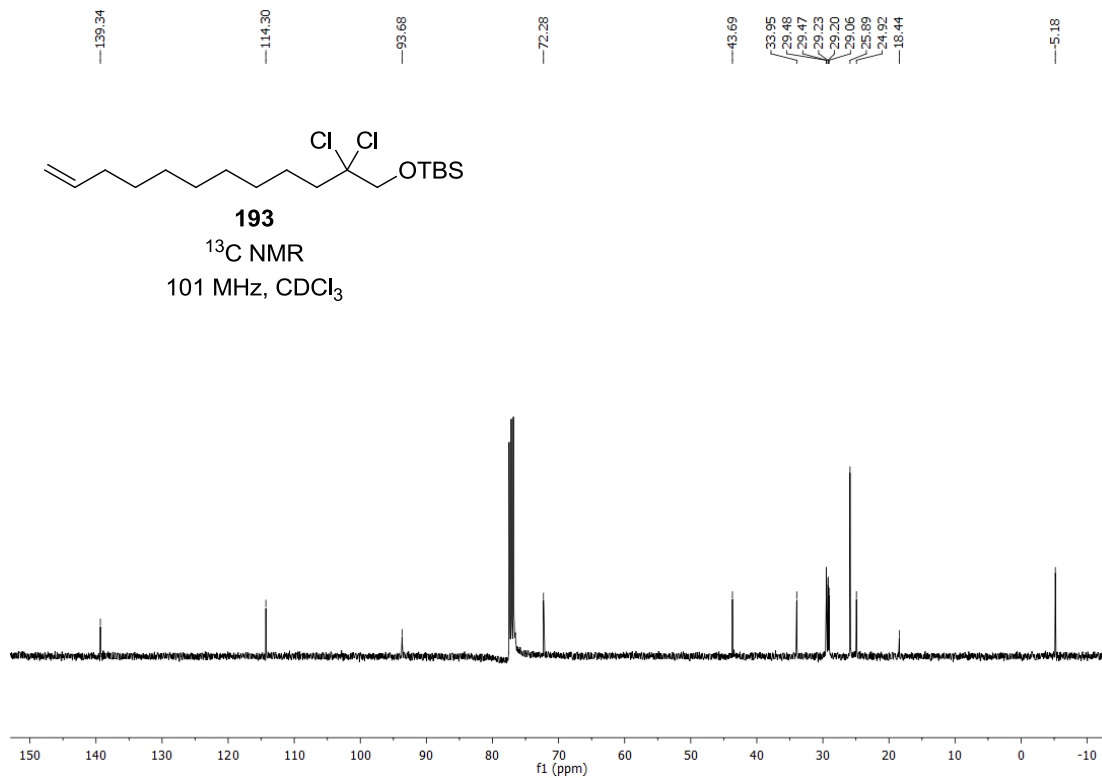
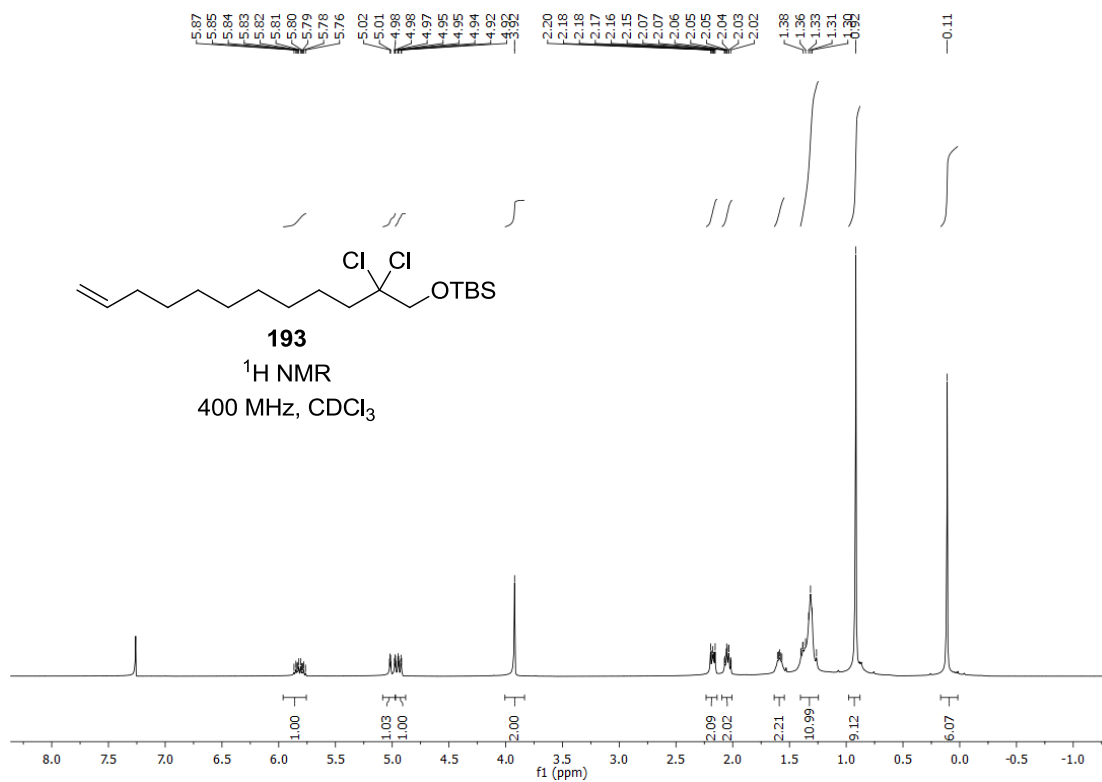


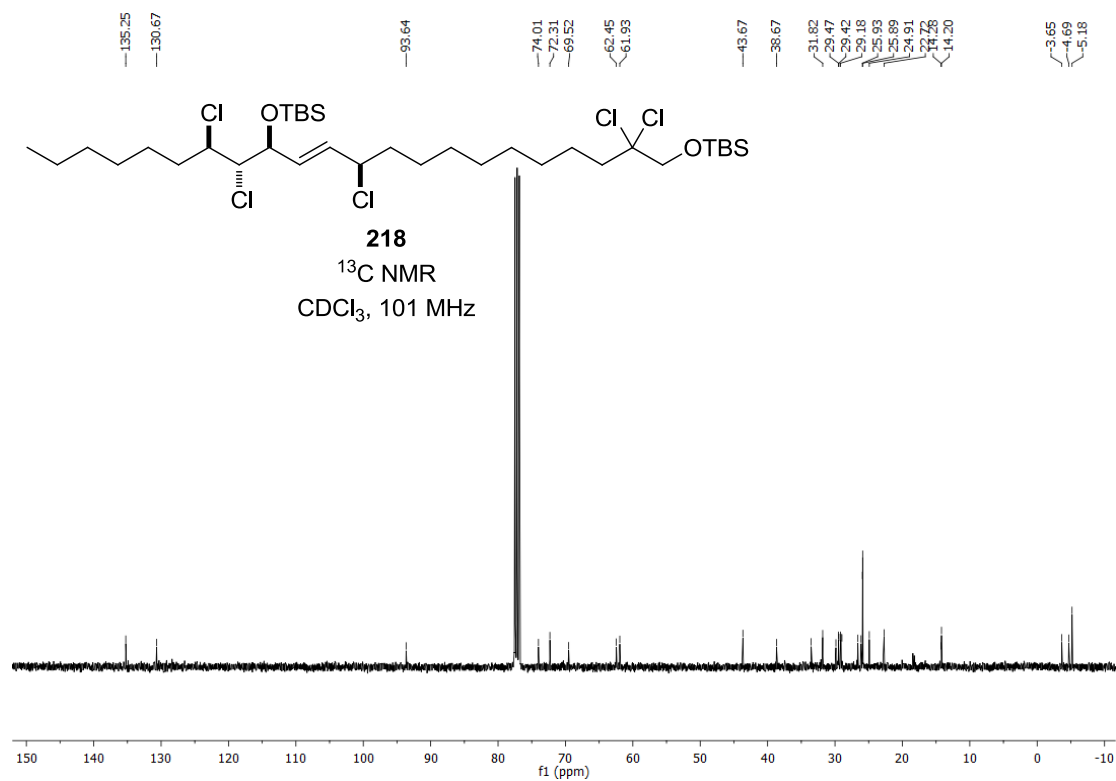
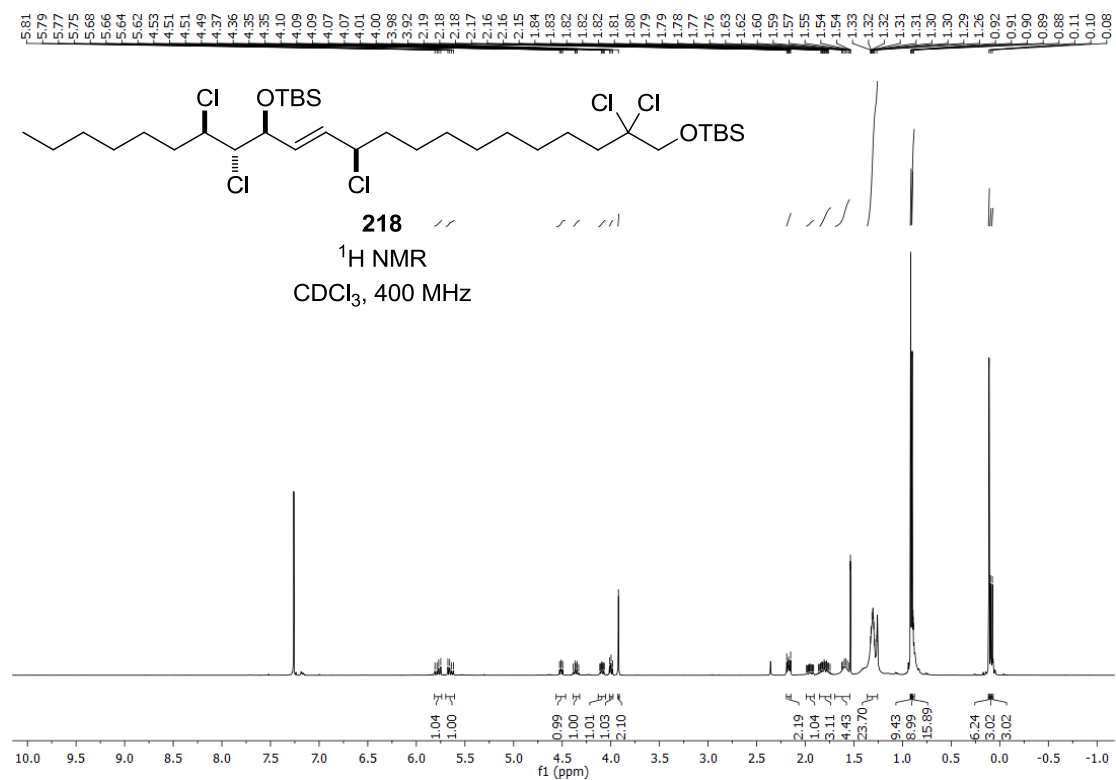


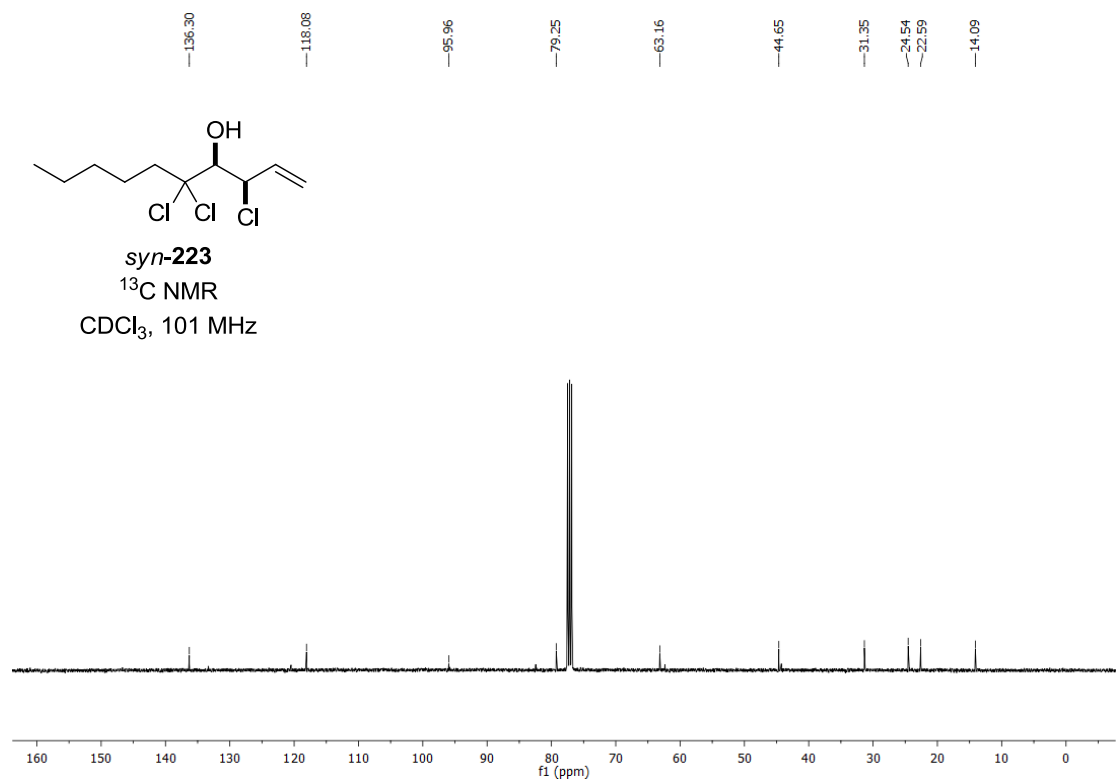
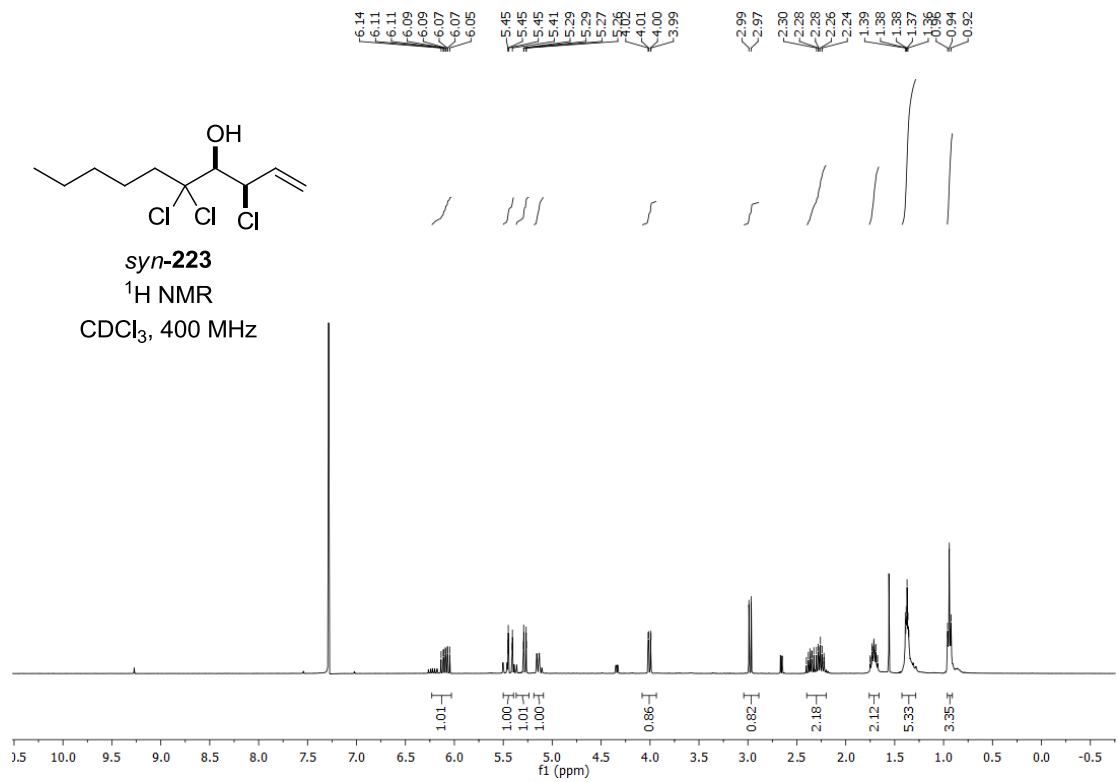


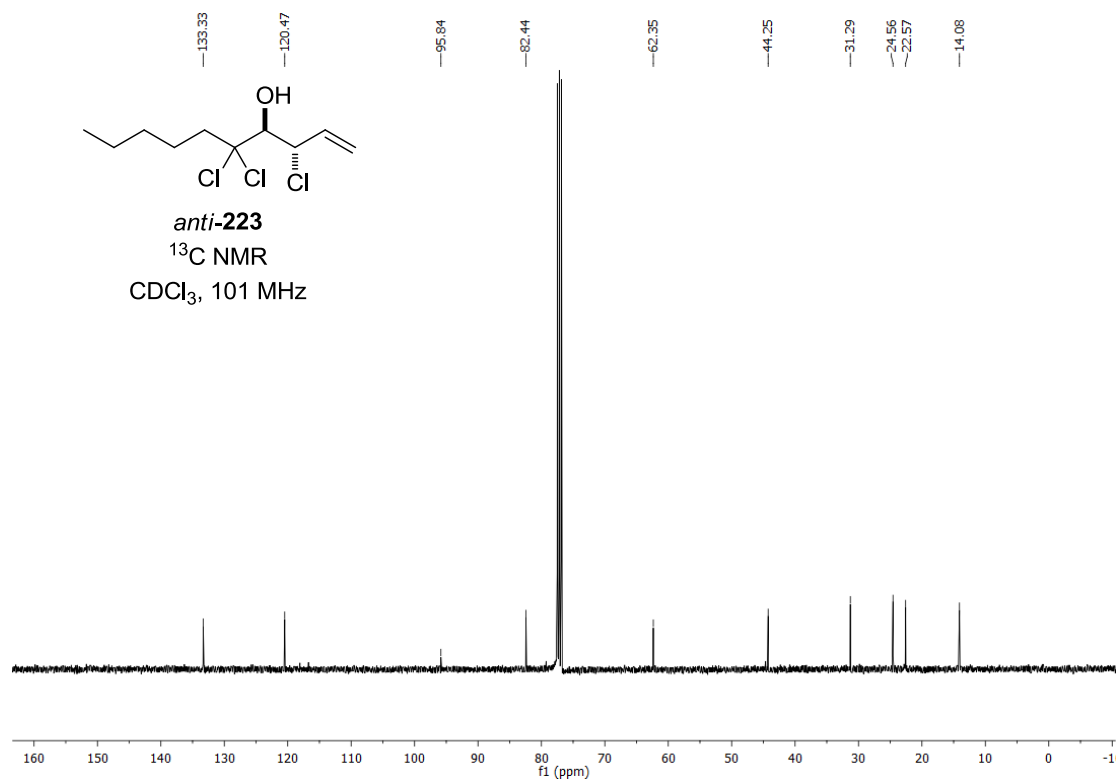
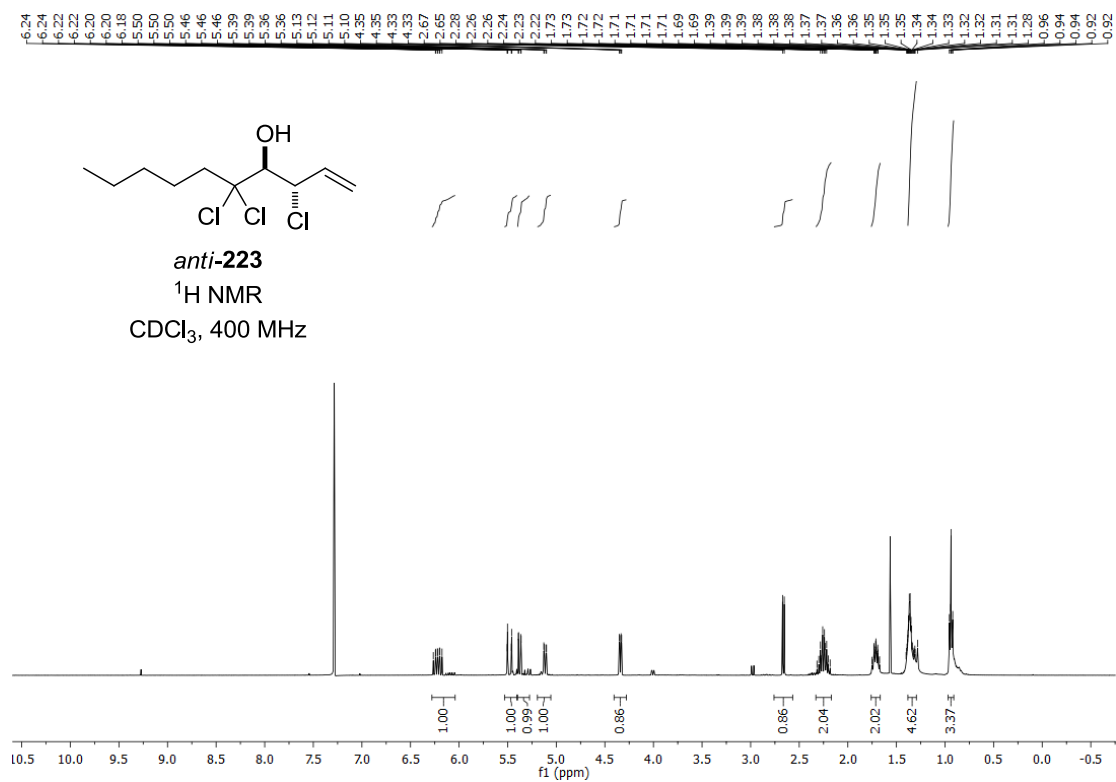
Appendix

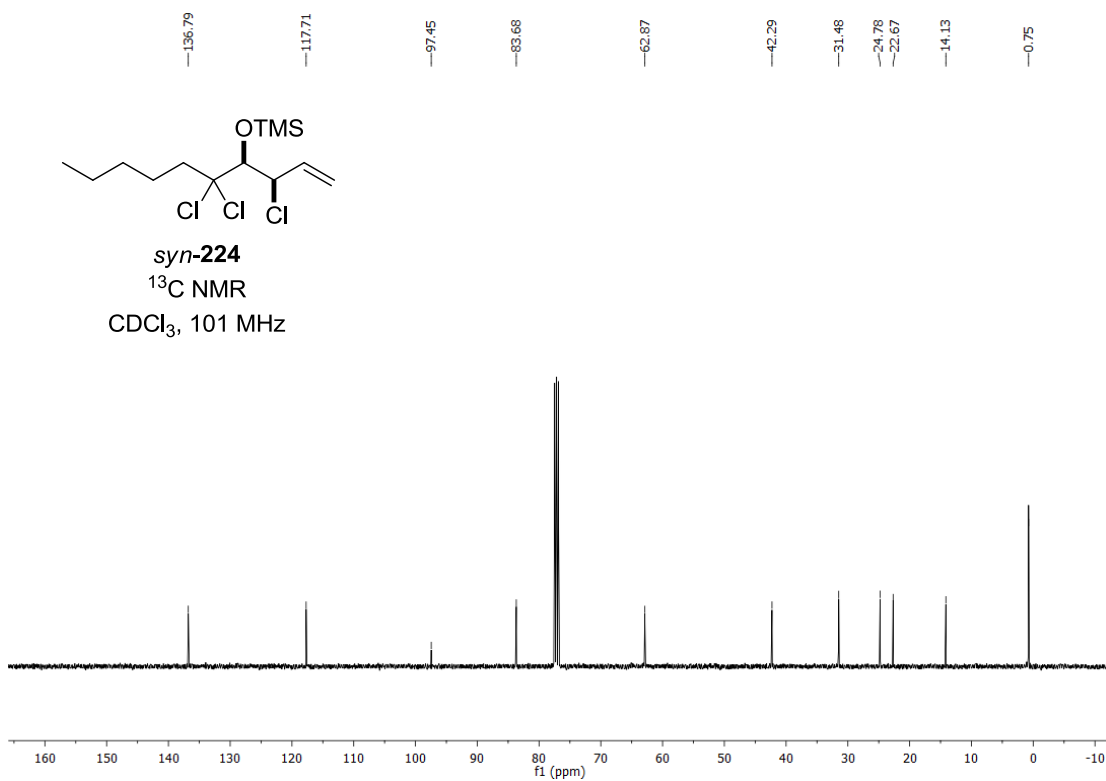
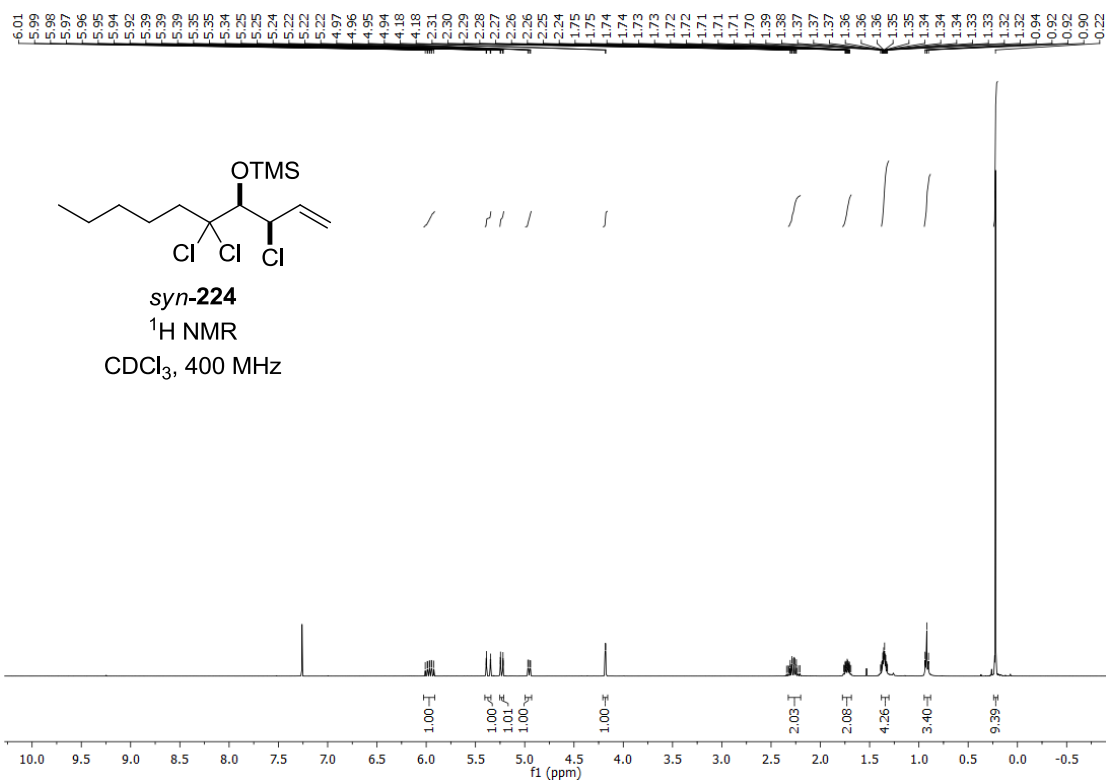


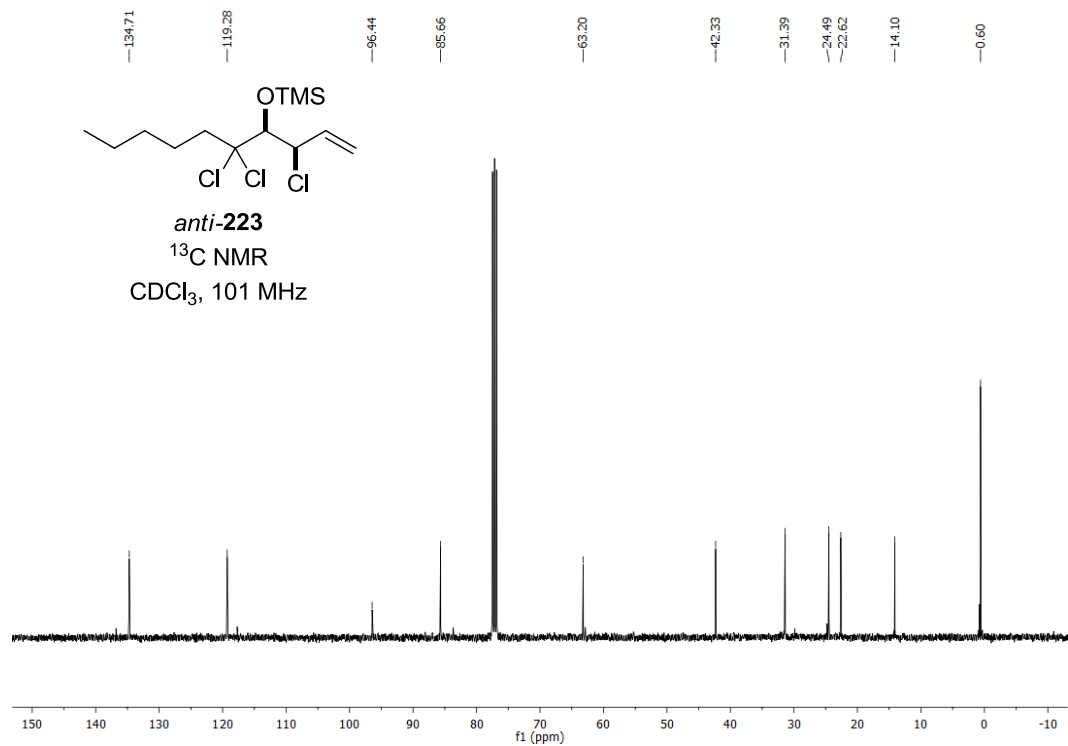
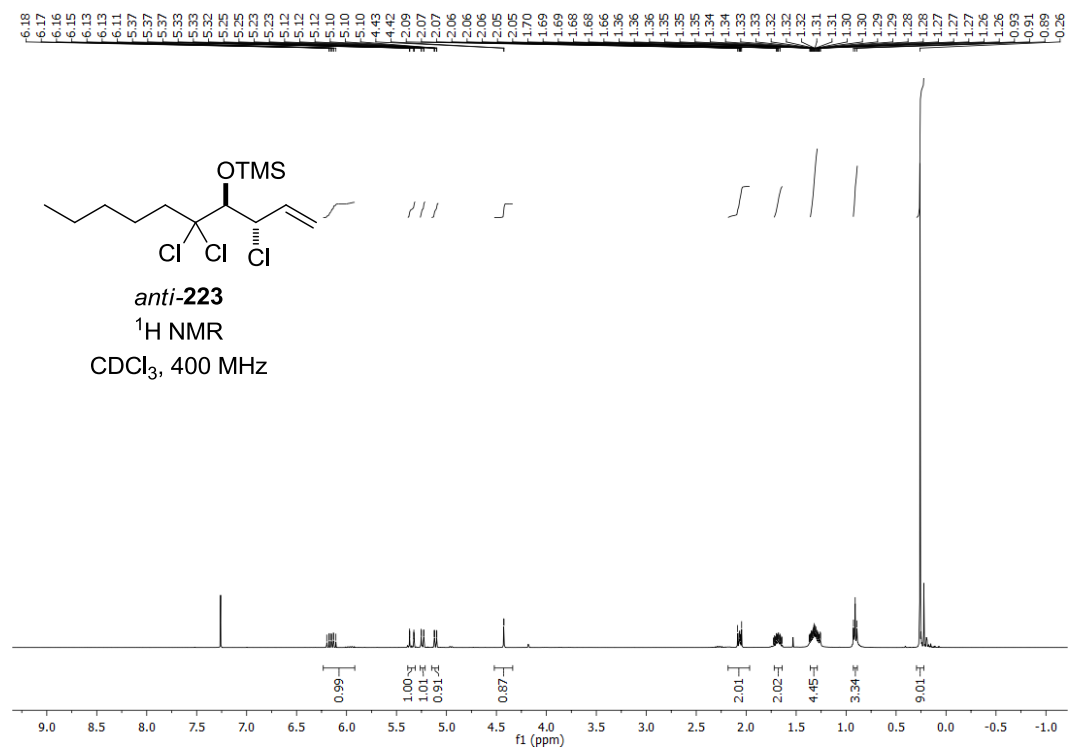


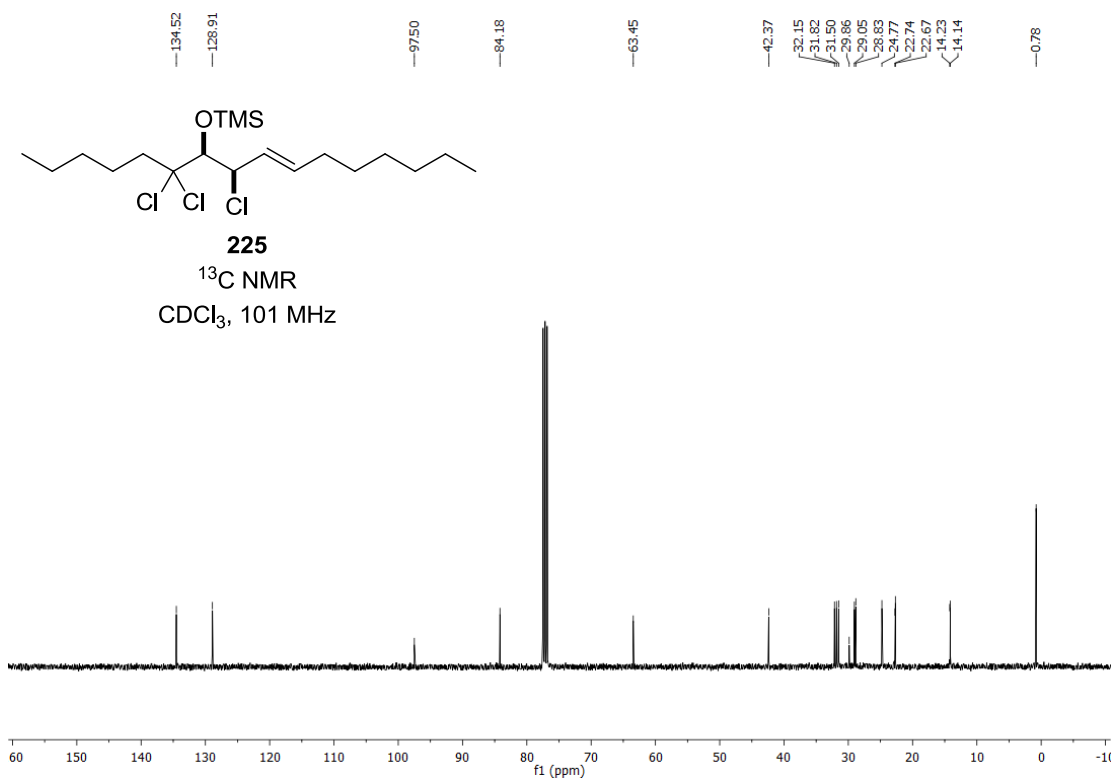
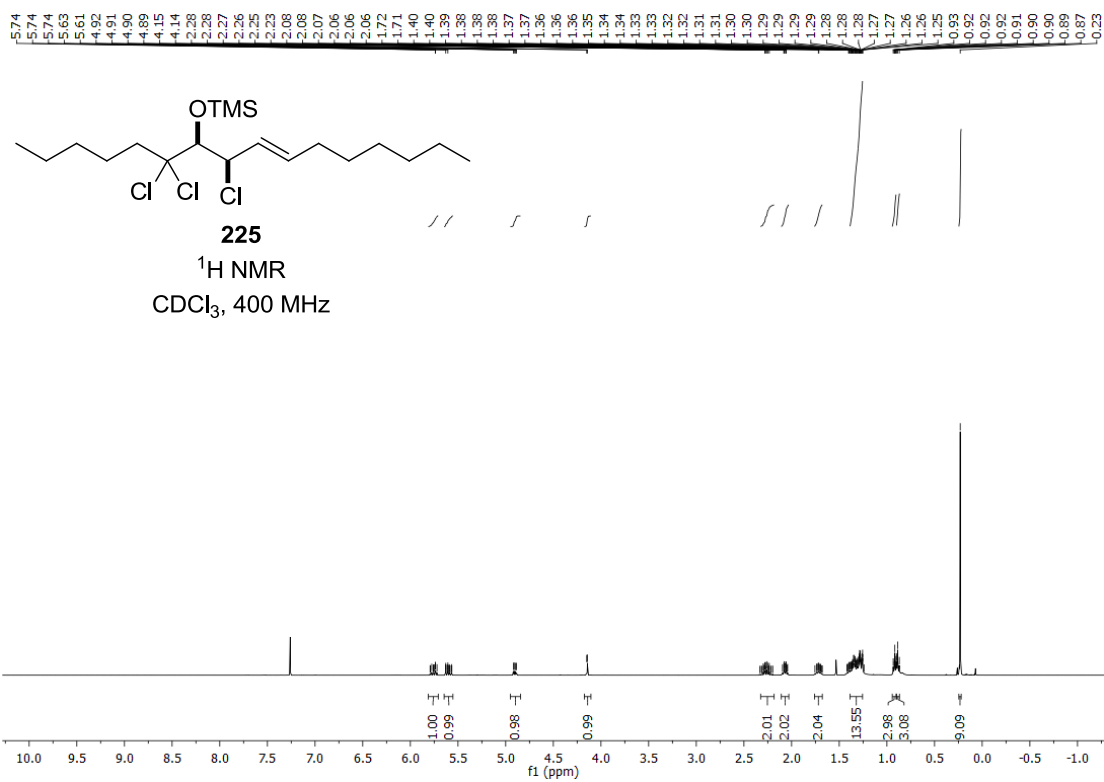




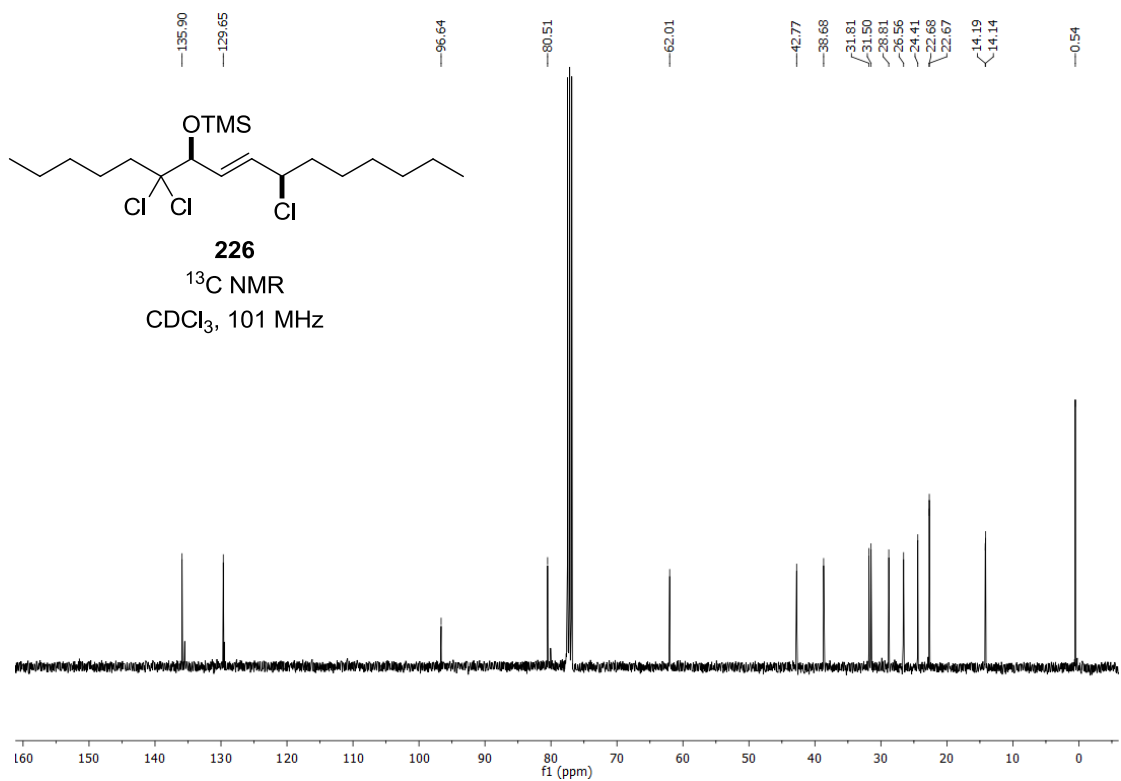
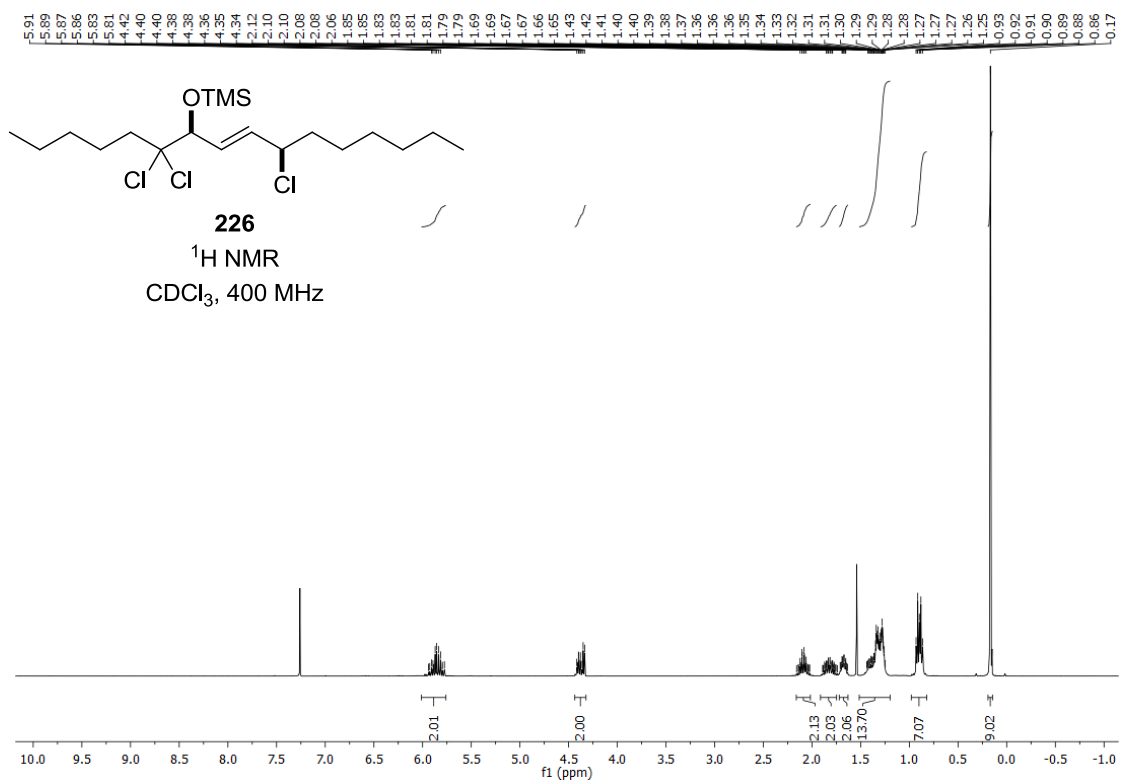


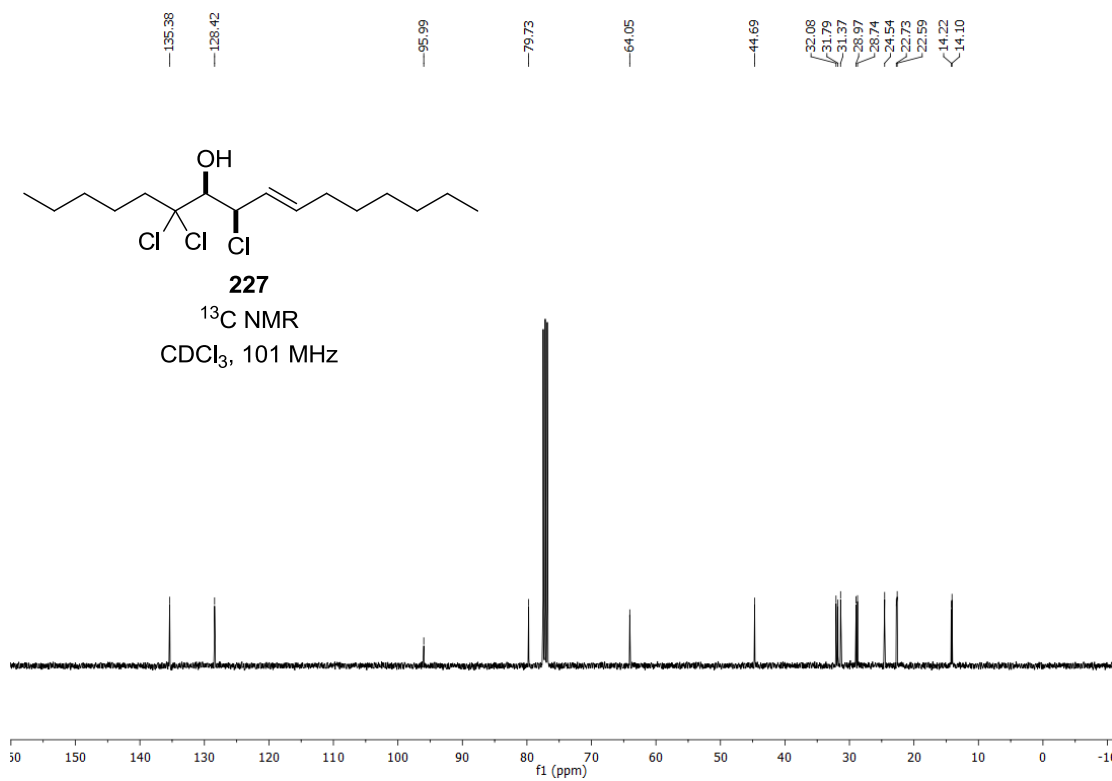
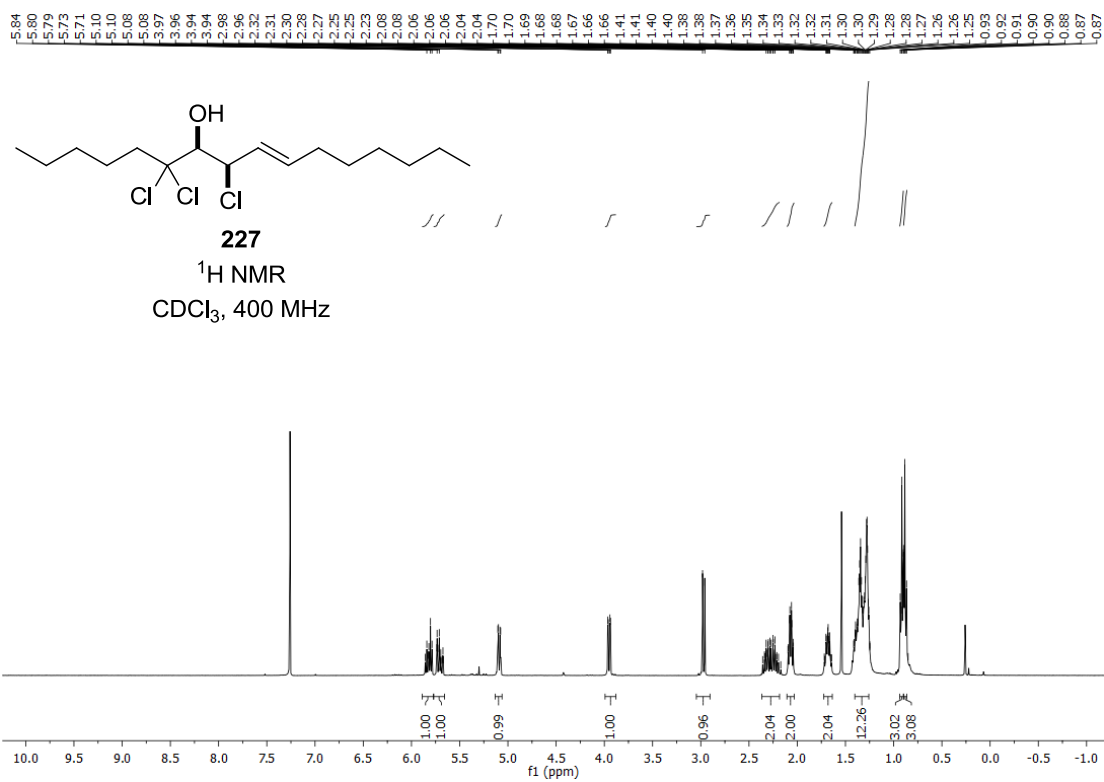


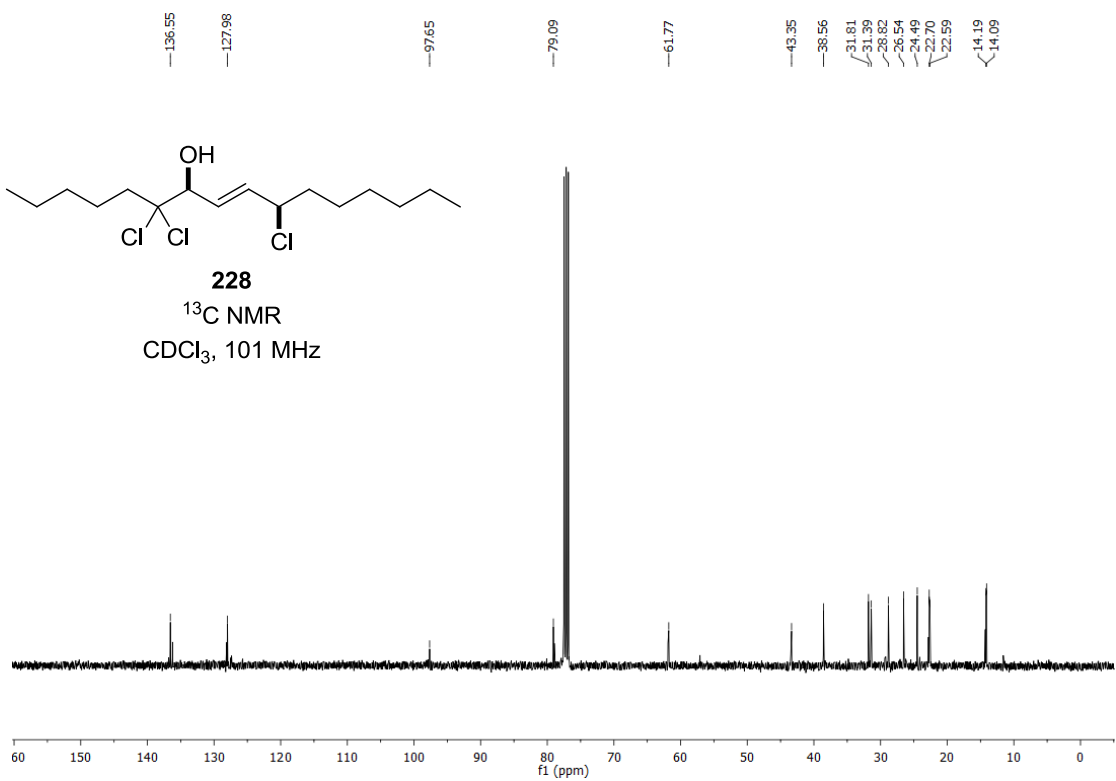
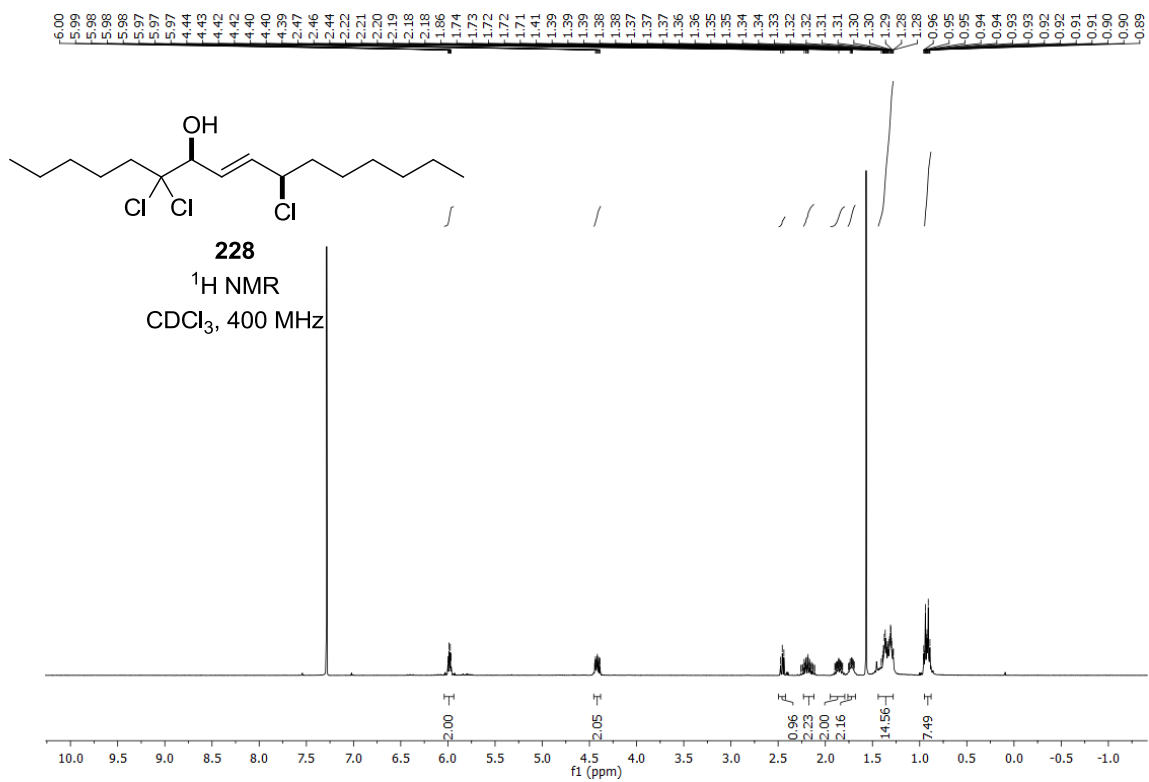


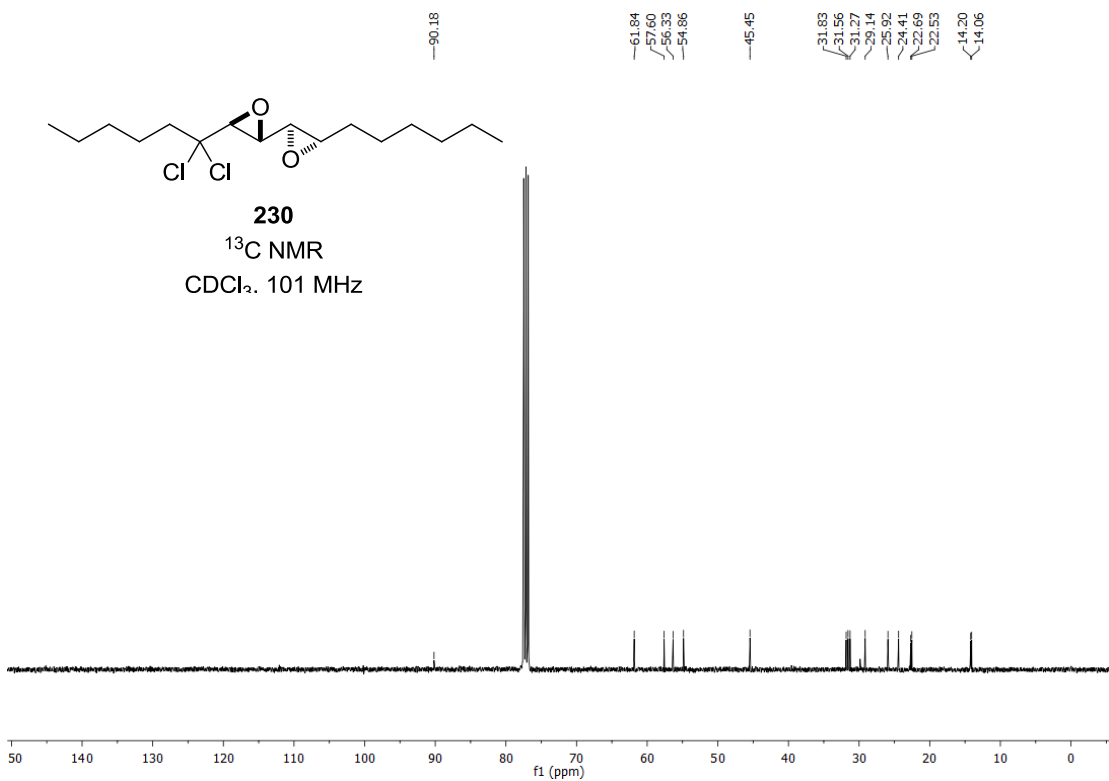
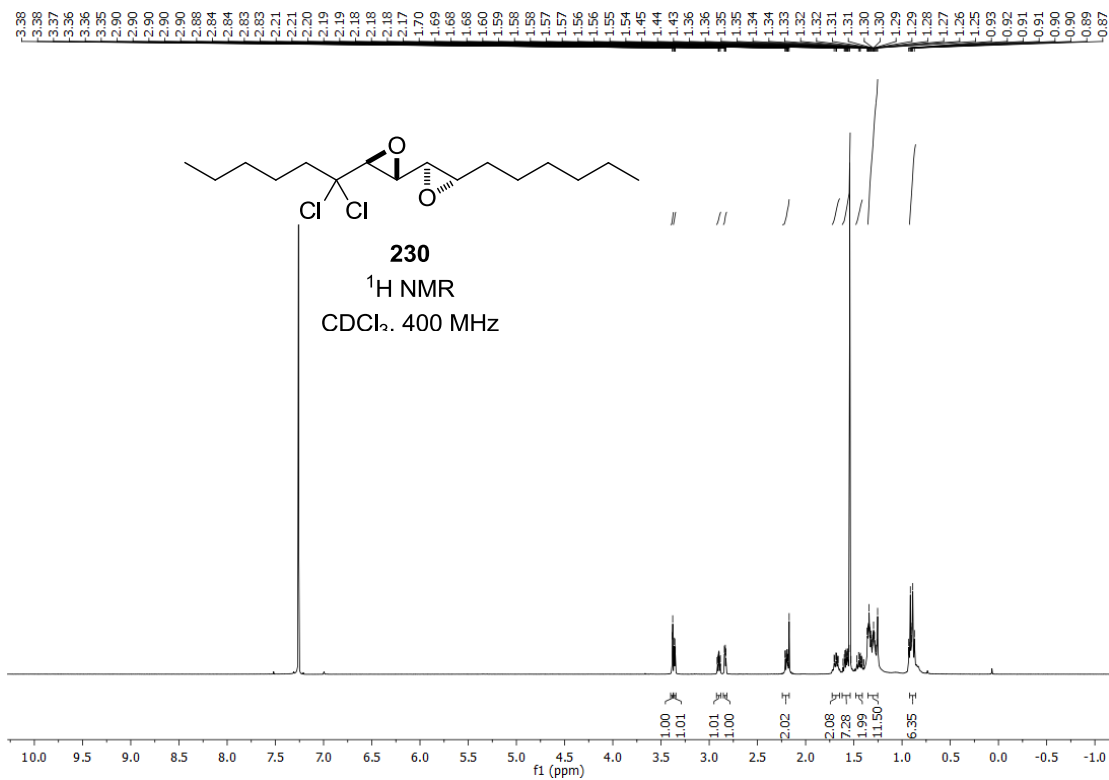


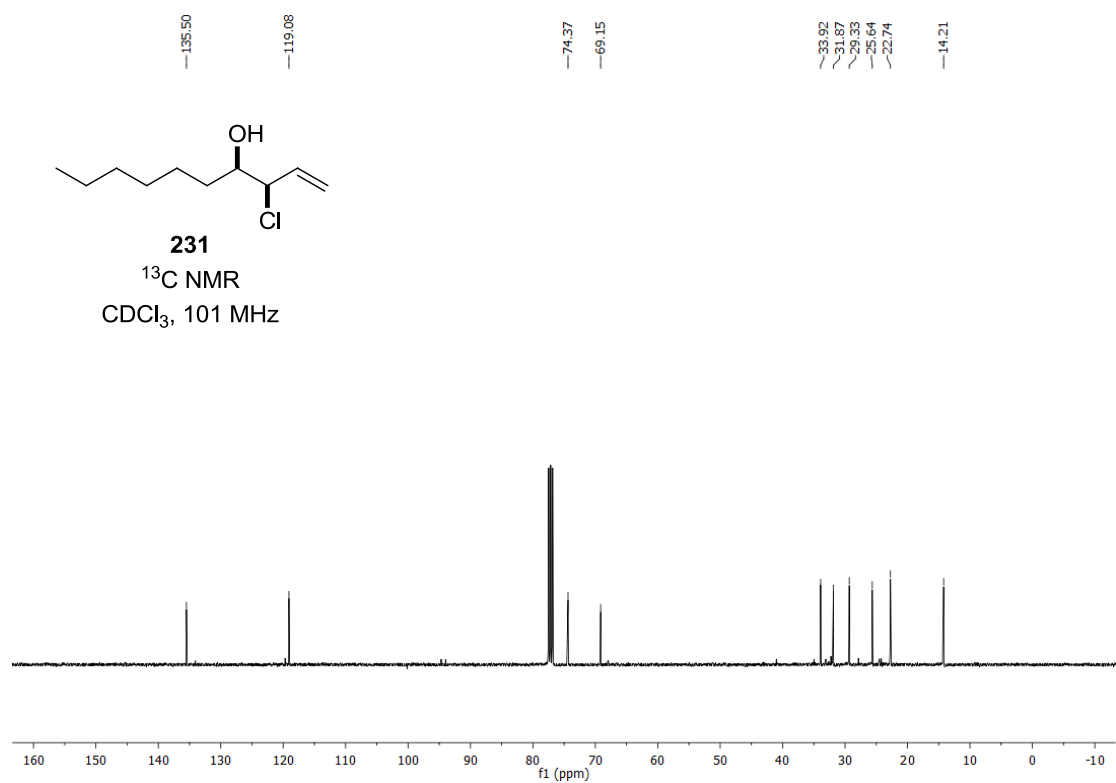
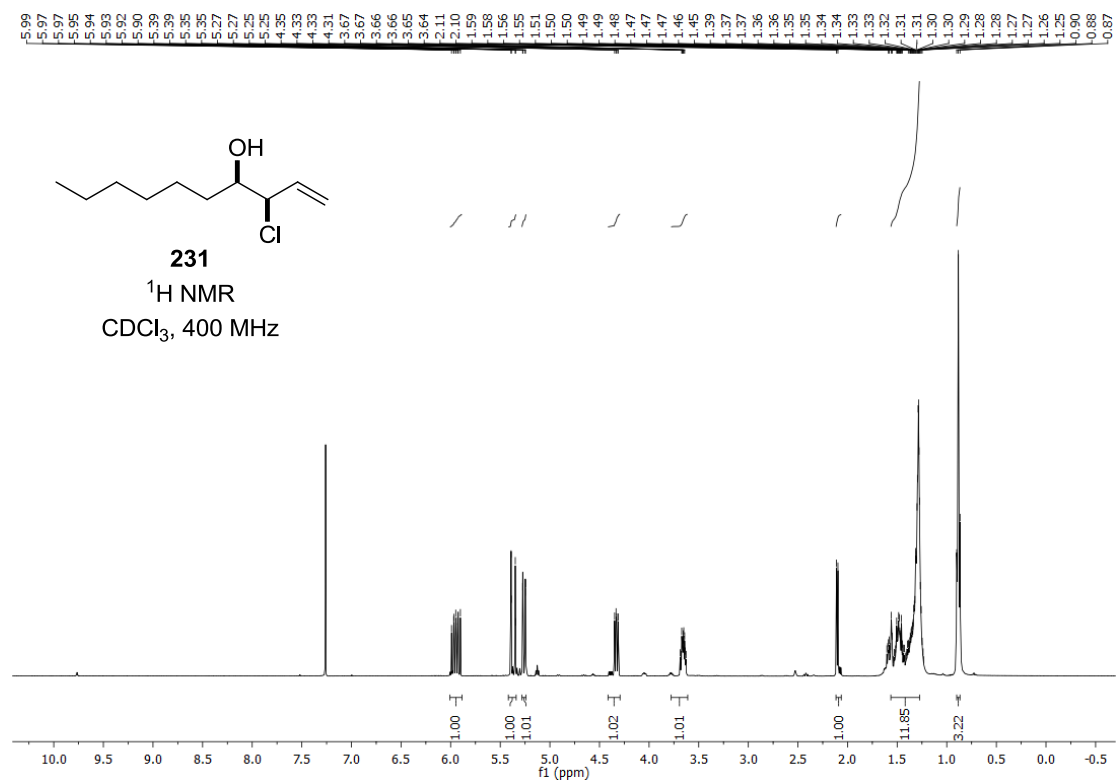
Appendix

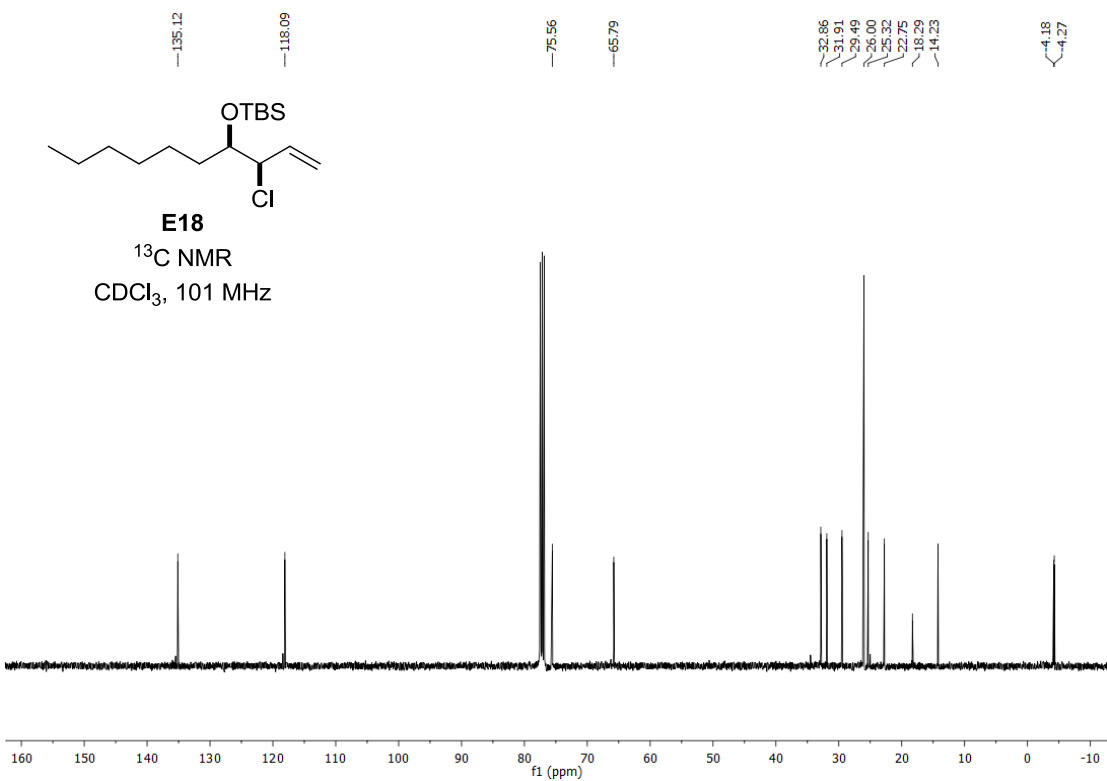
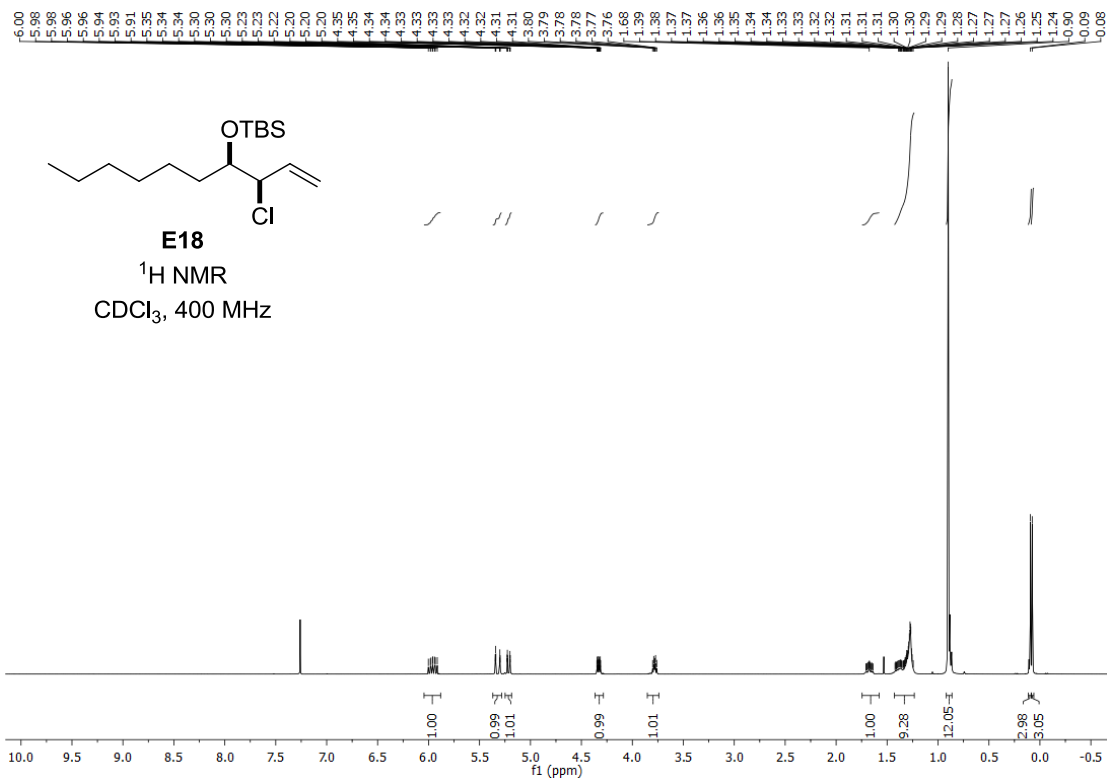


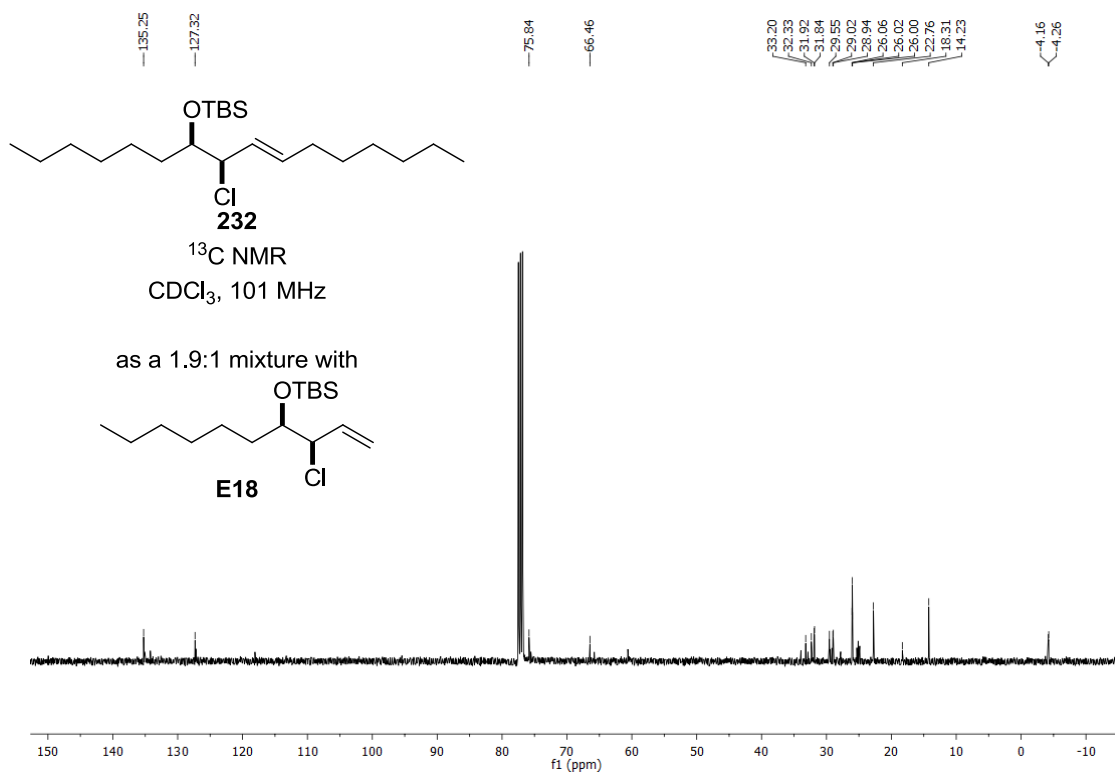
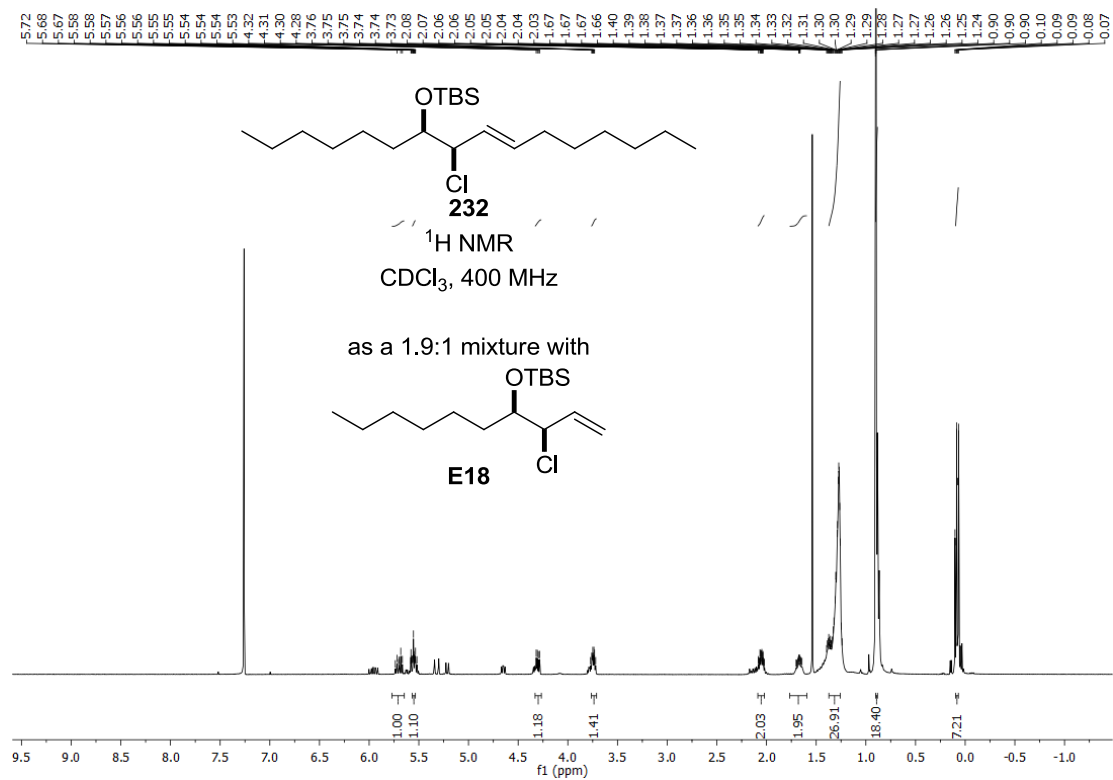


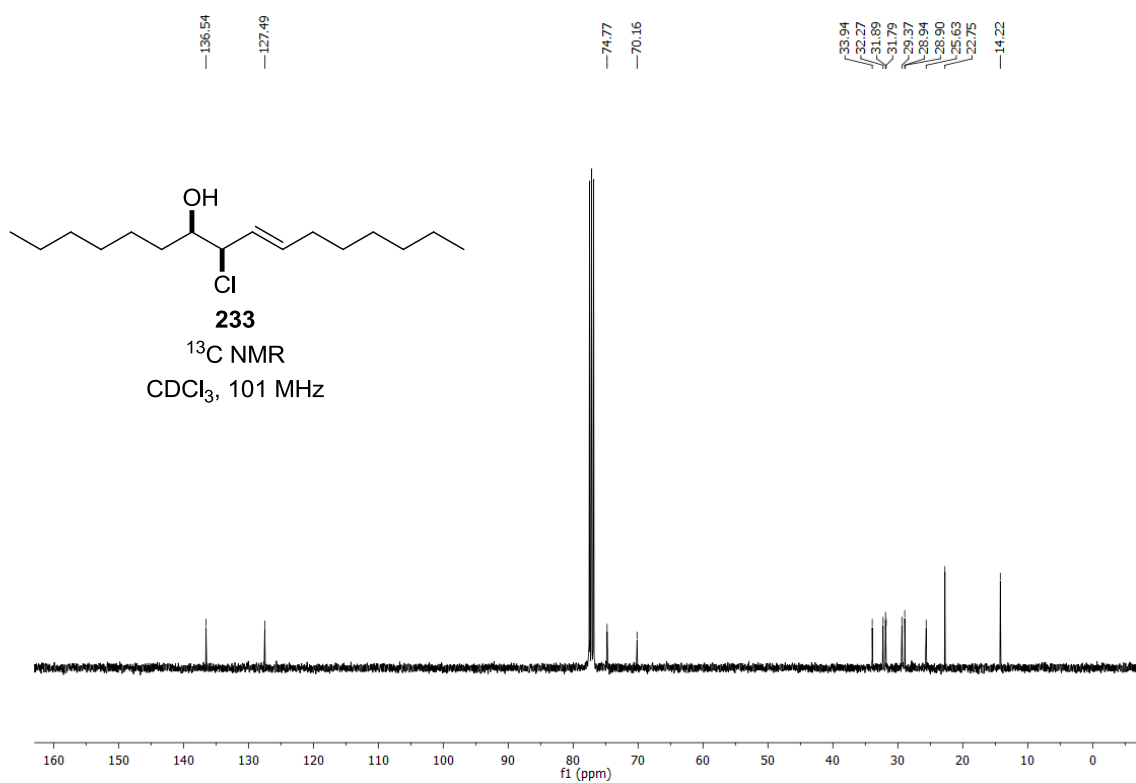
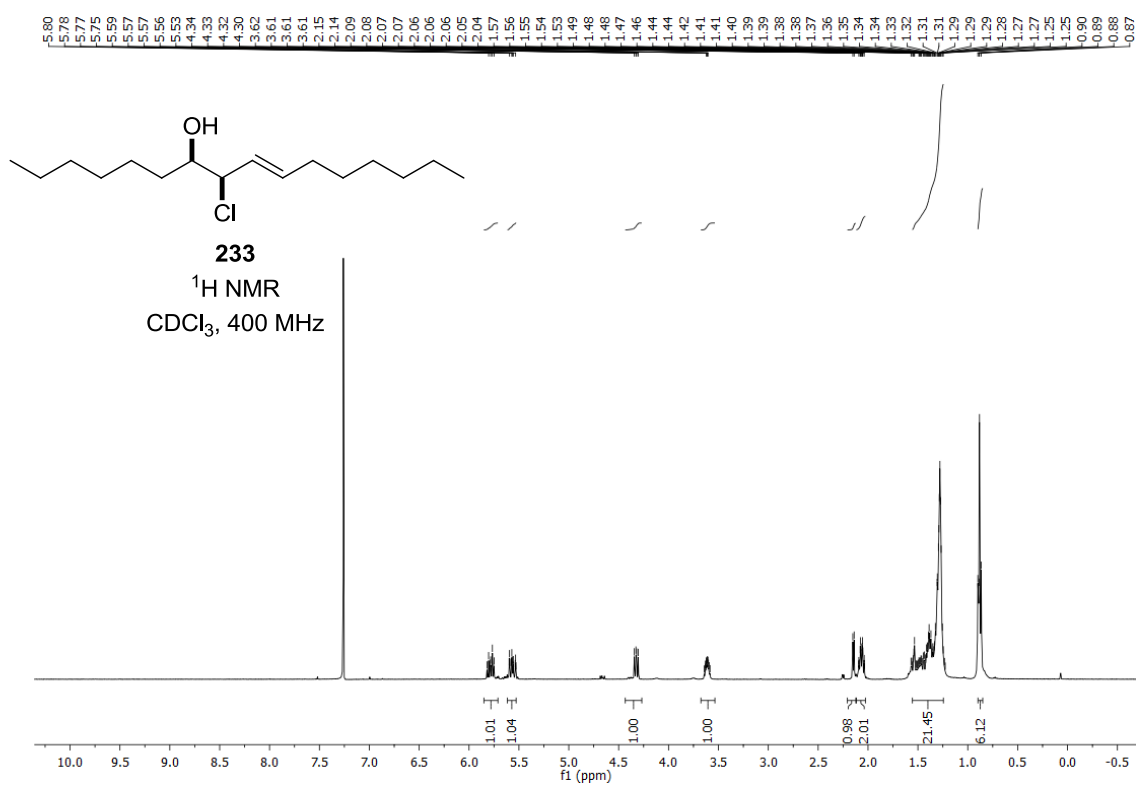


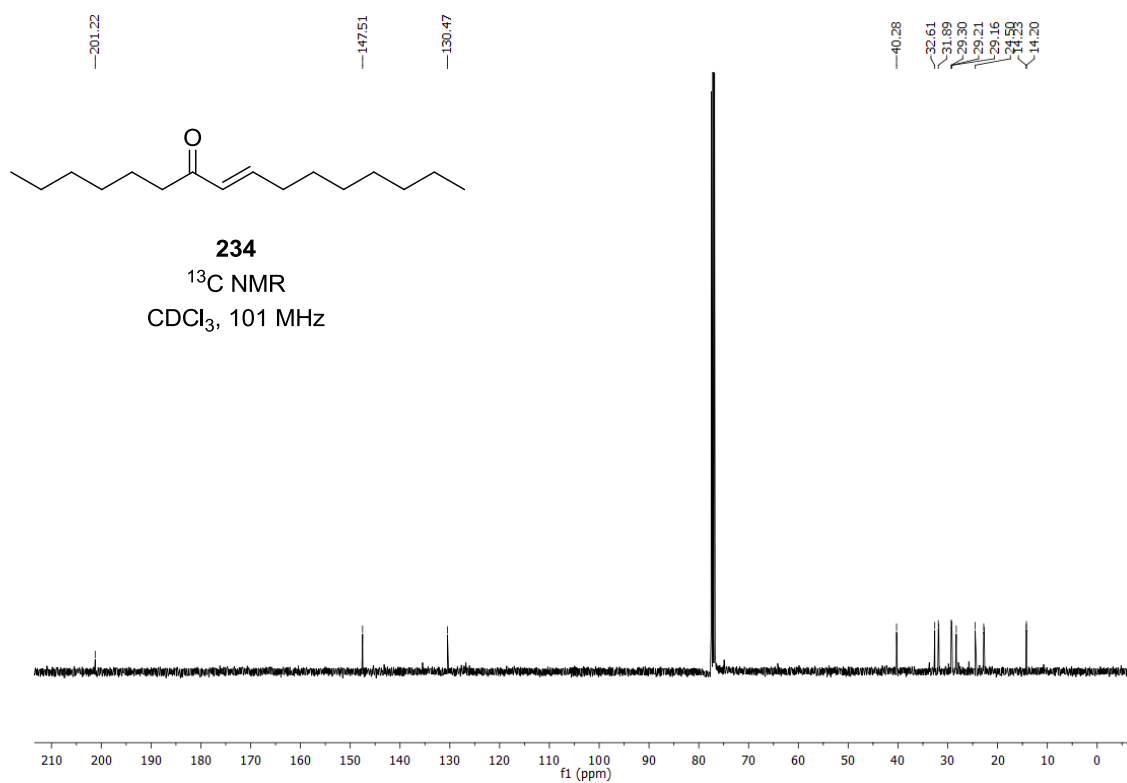
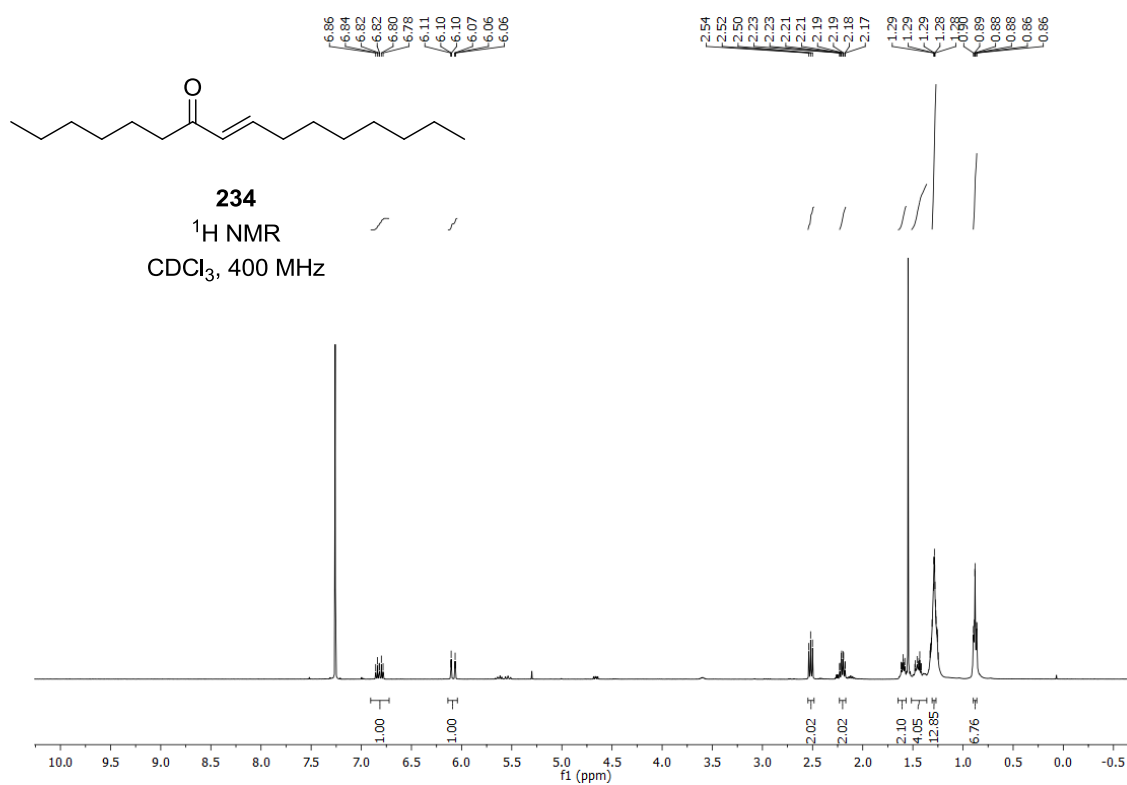


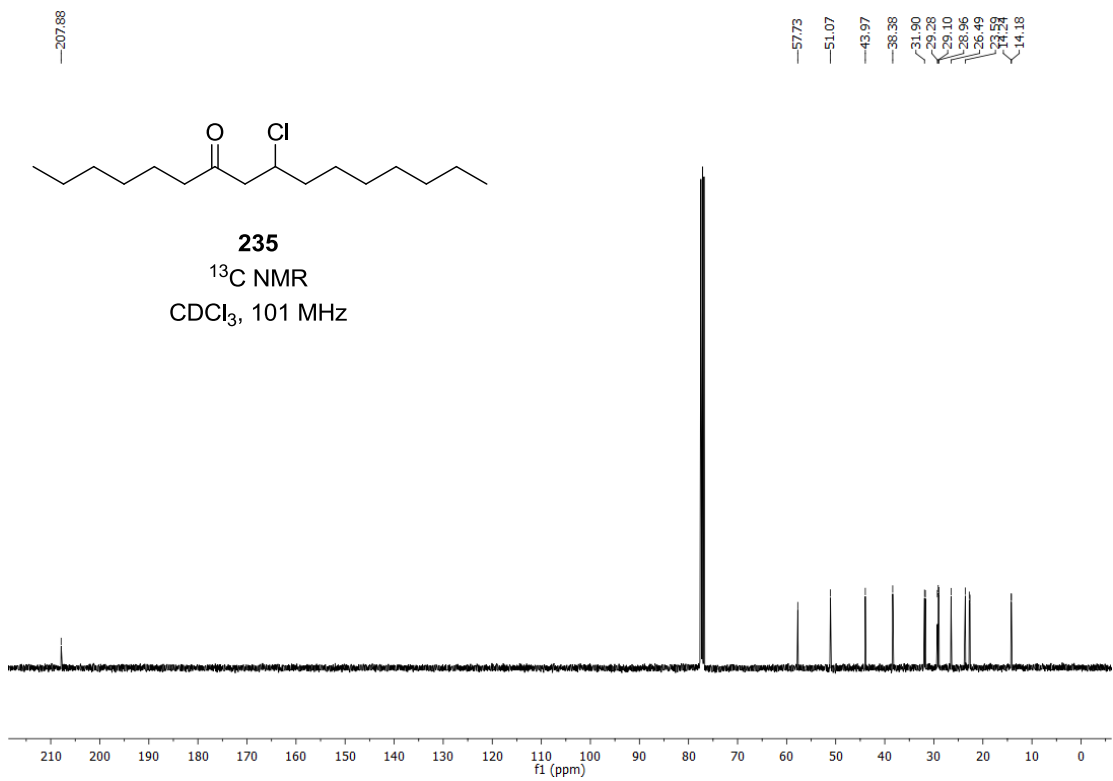
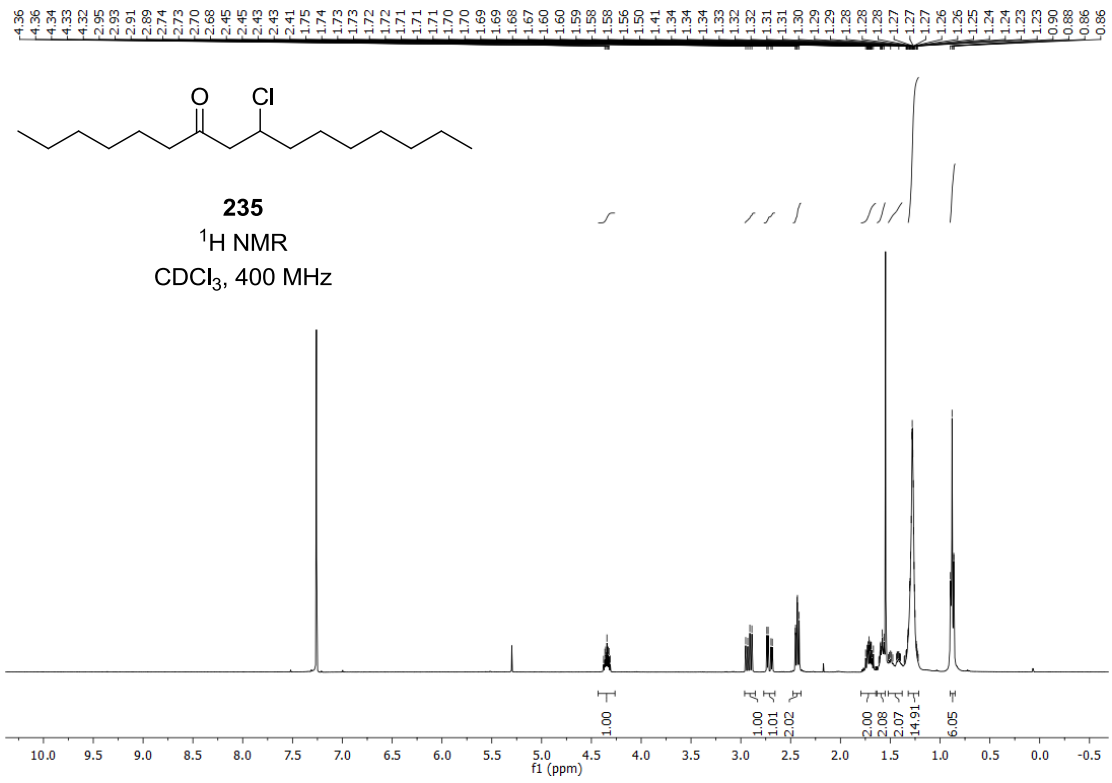




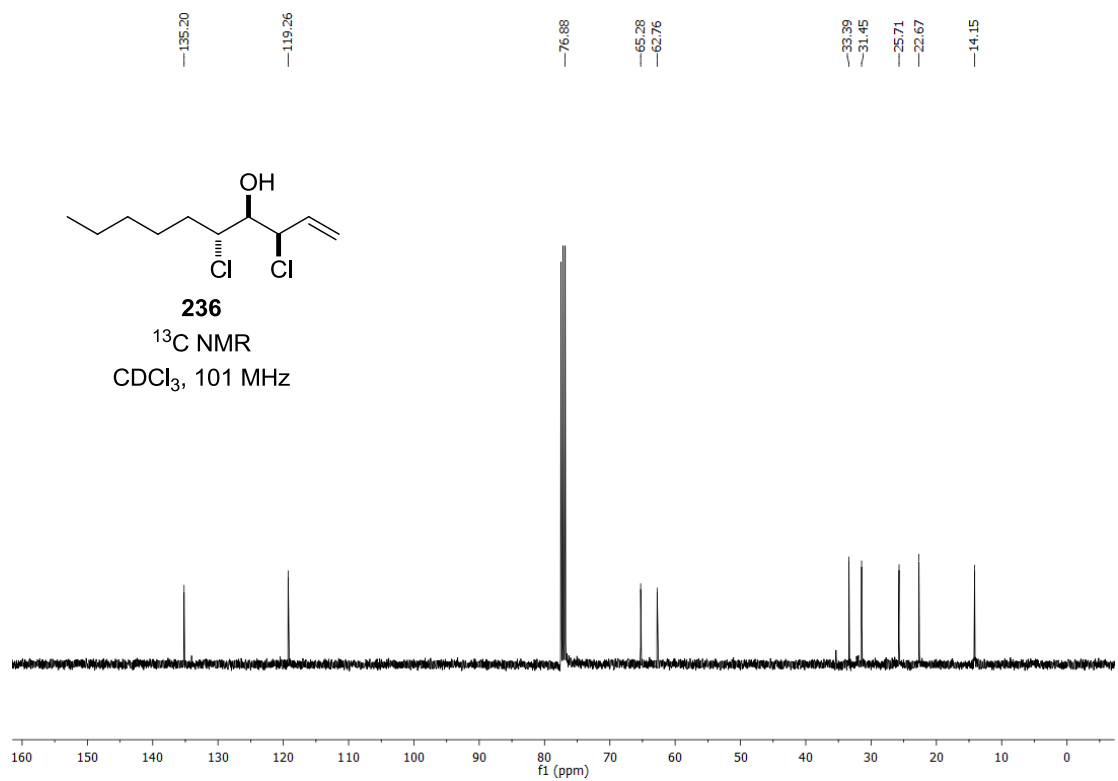
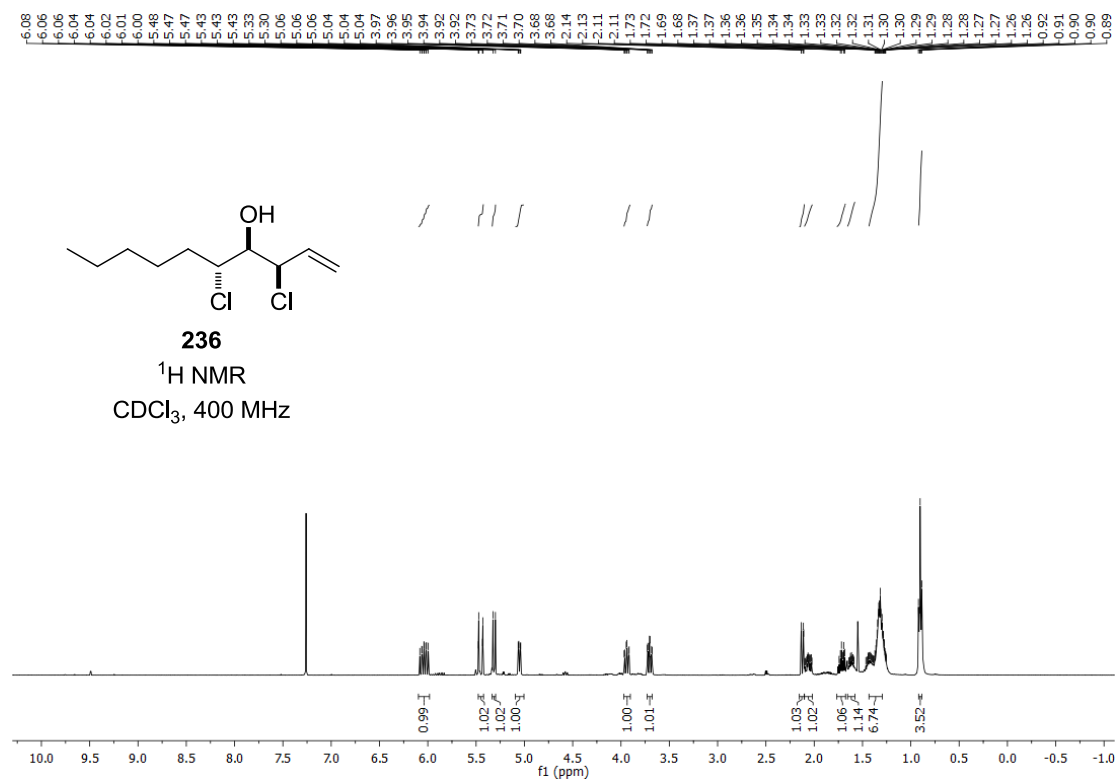


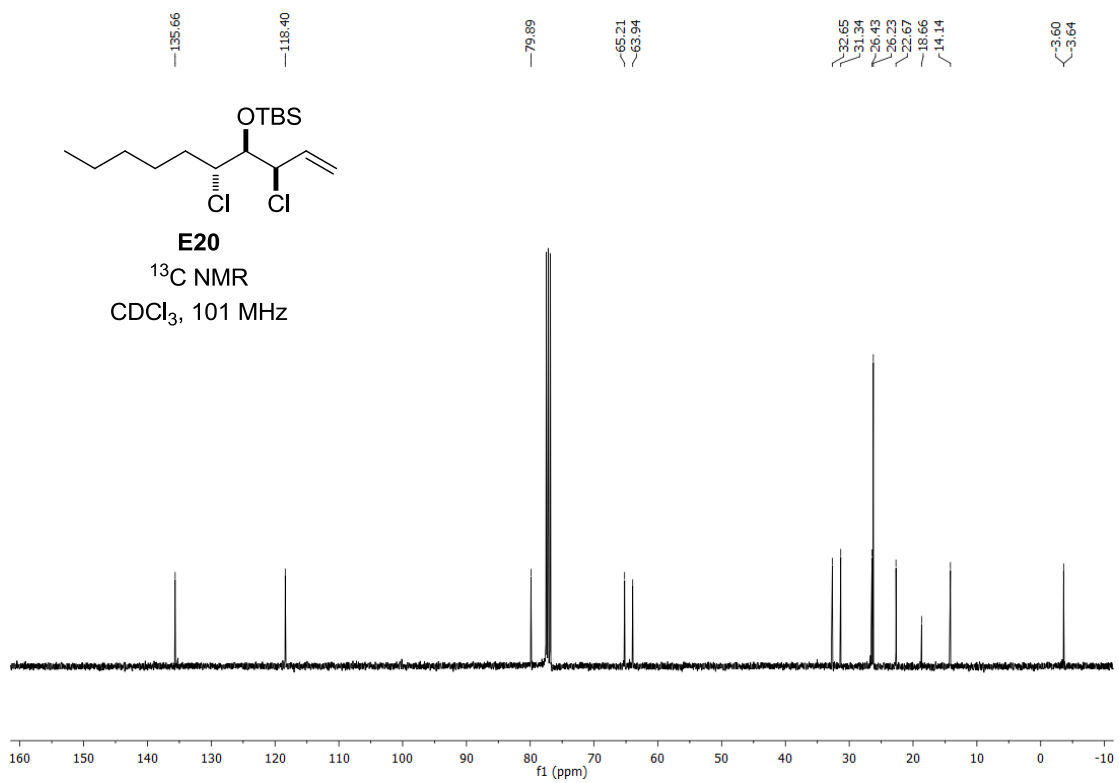
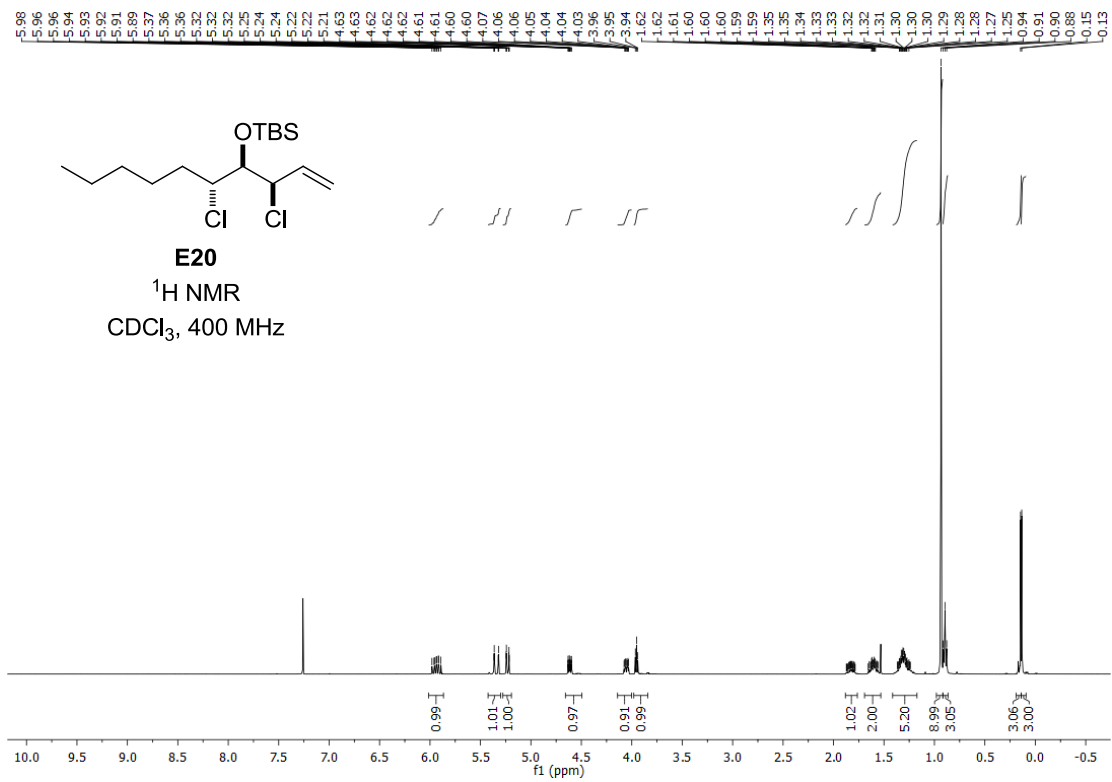


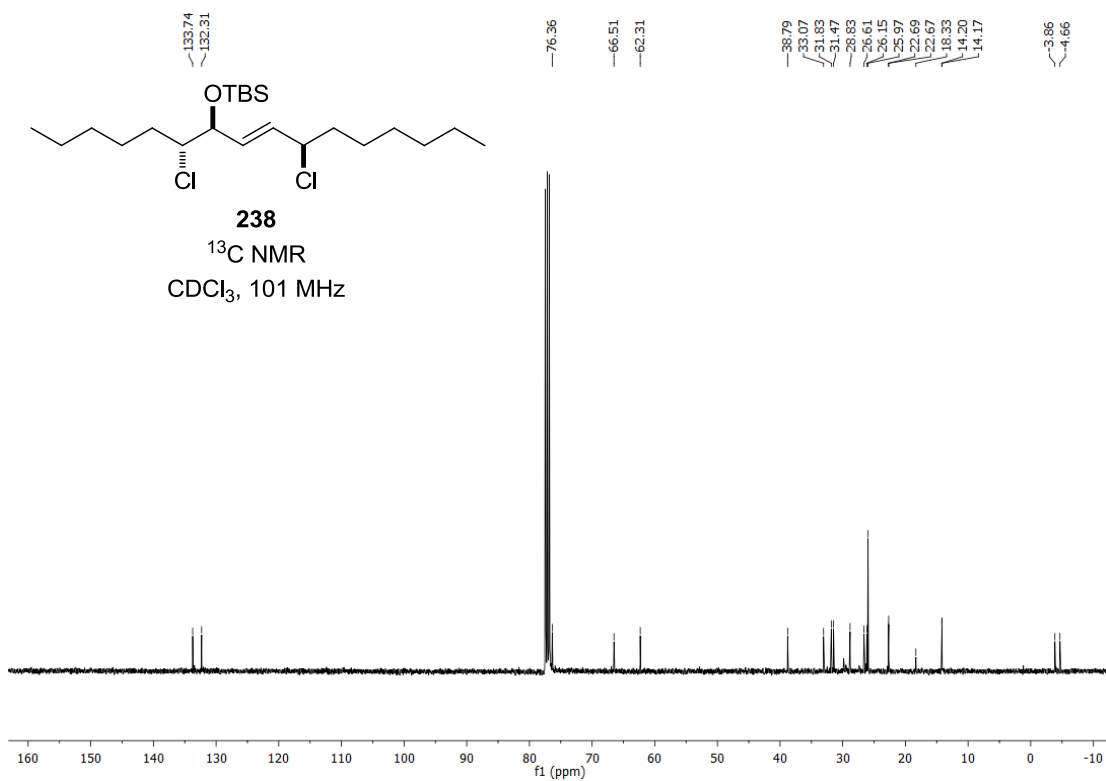
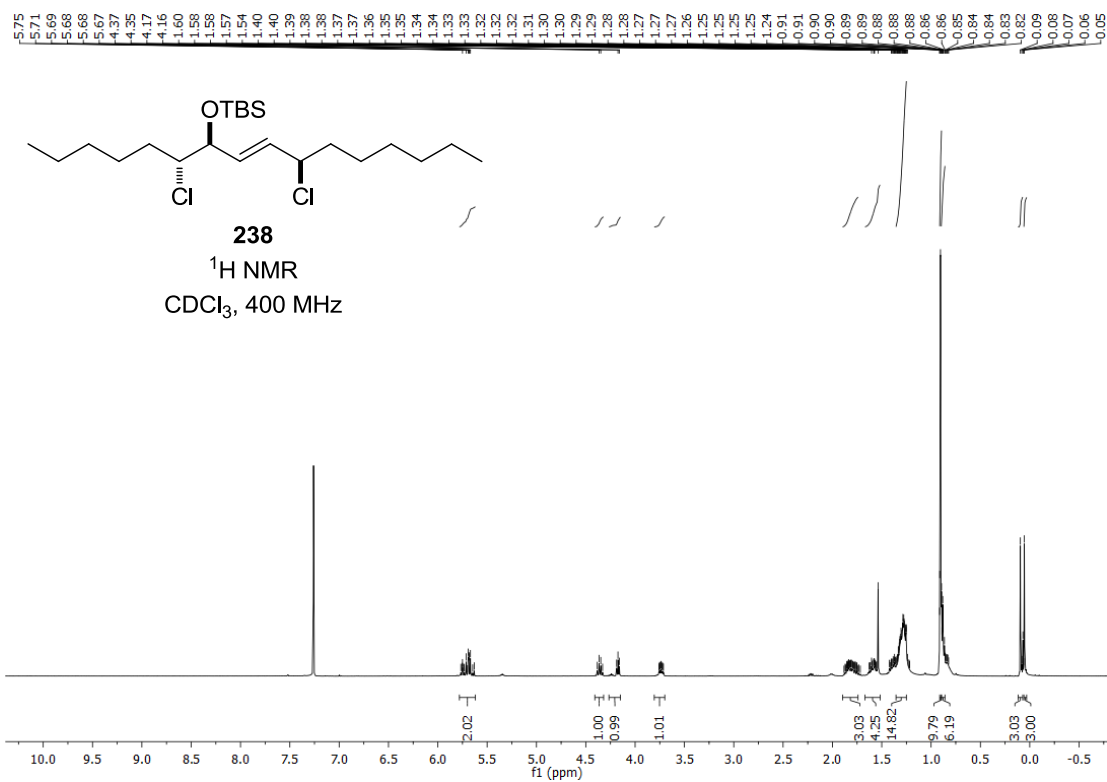




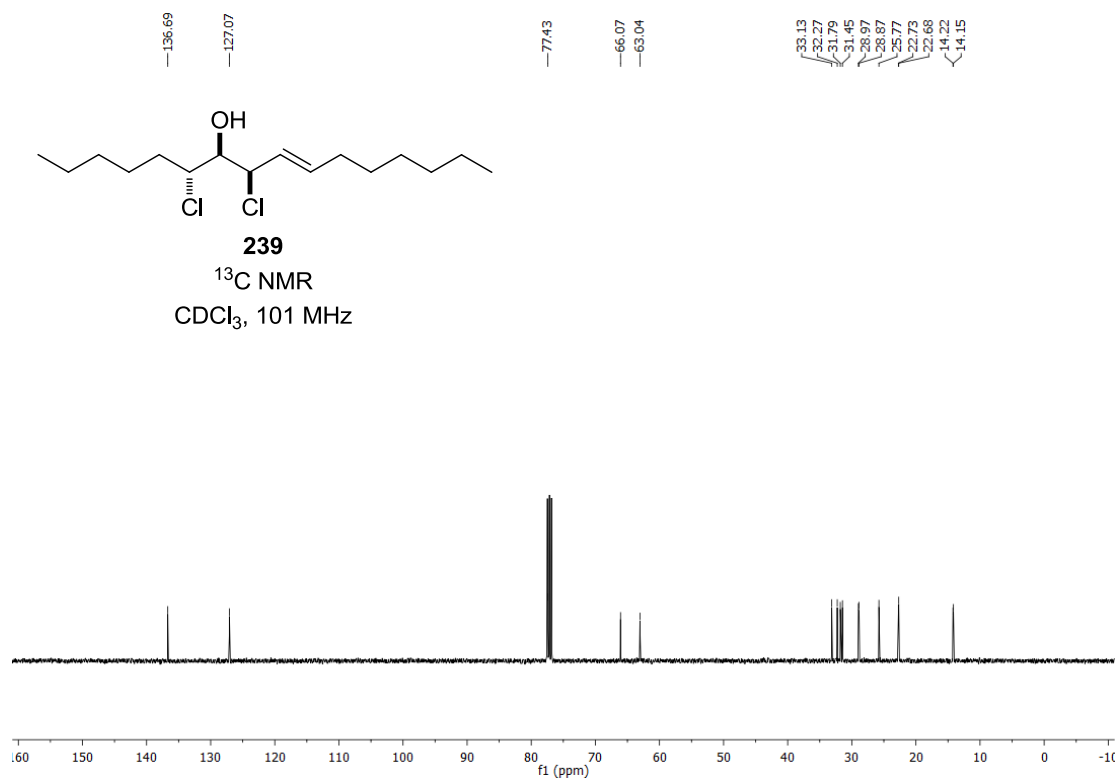
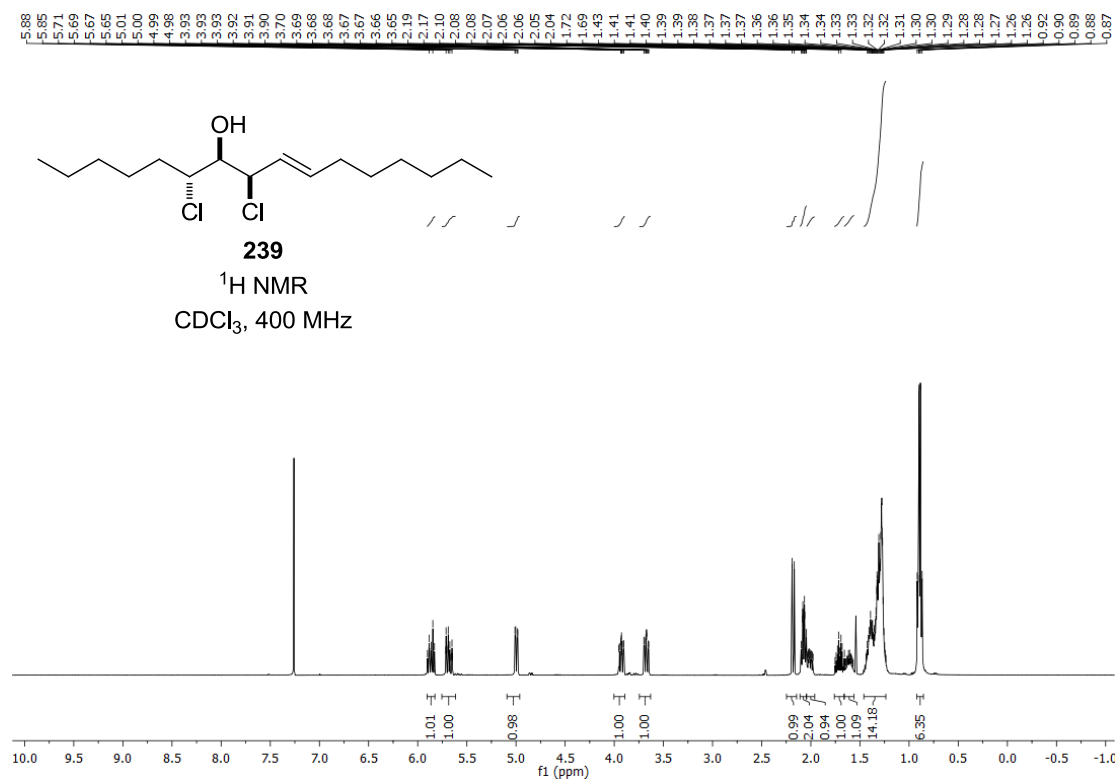
Appendix

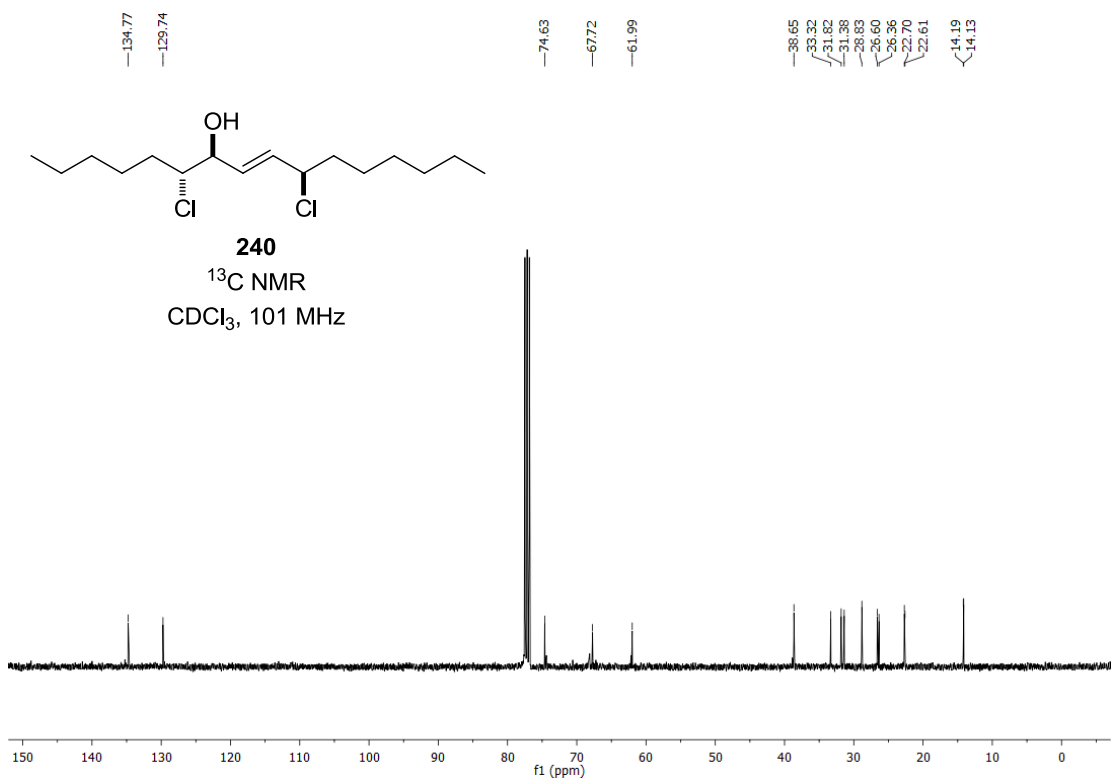
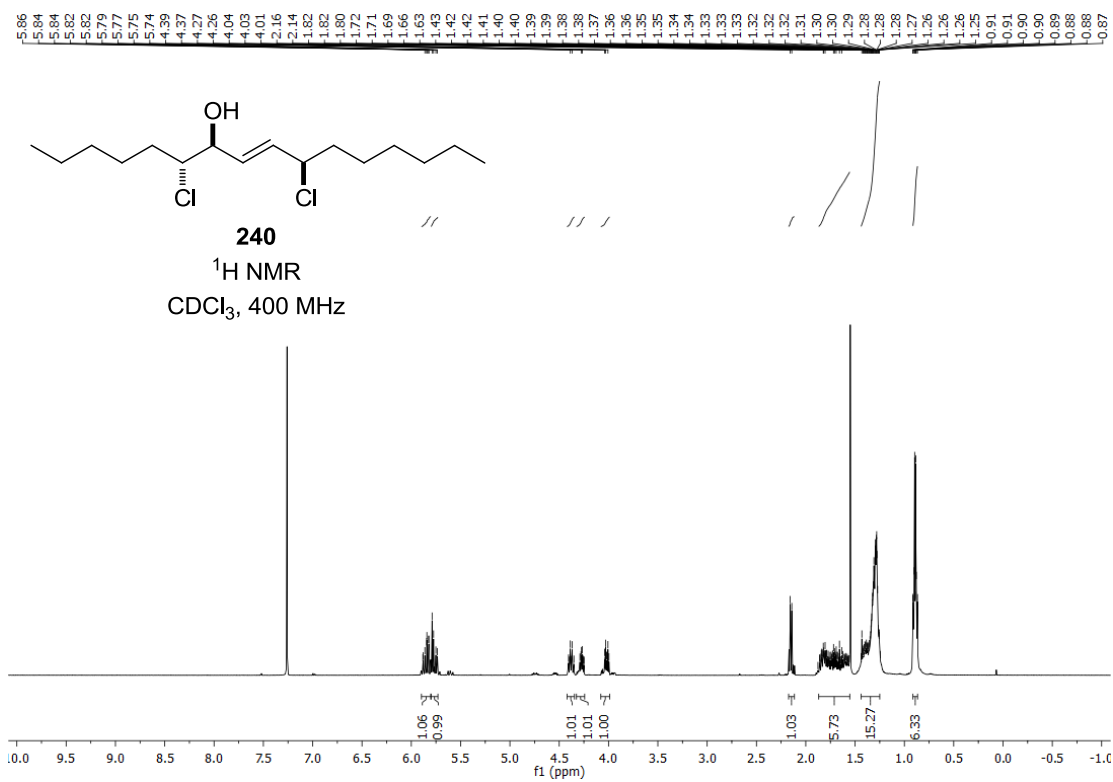




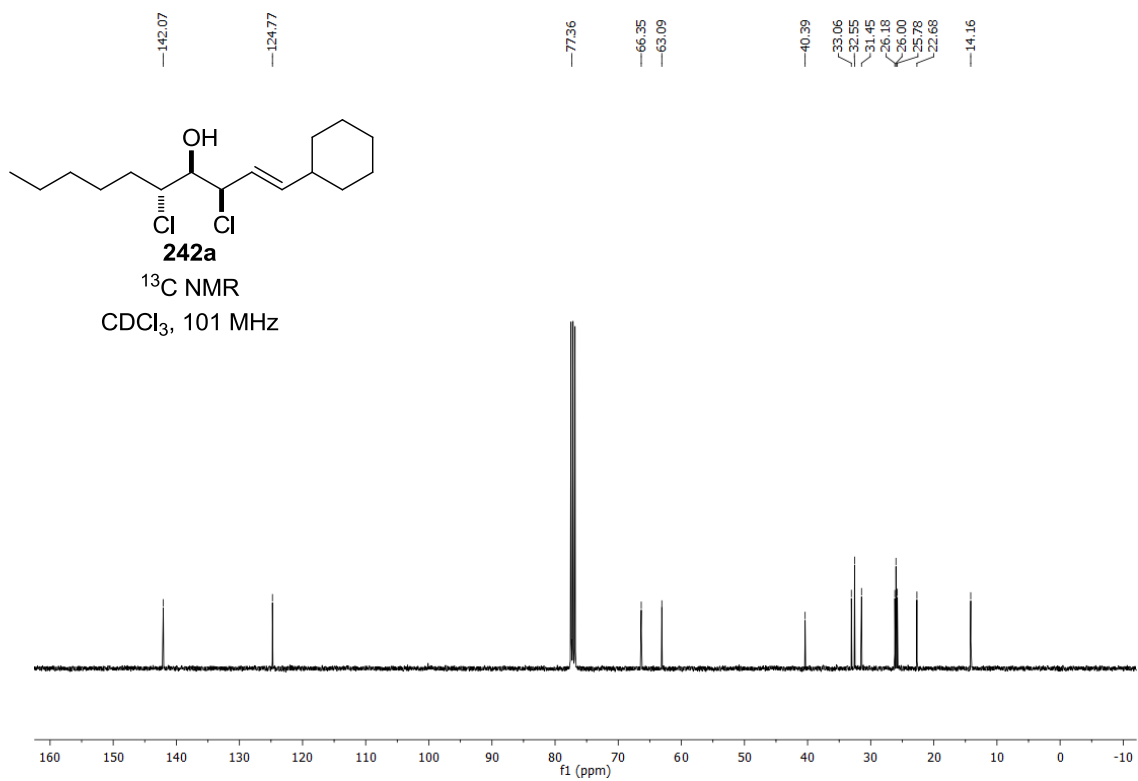
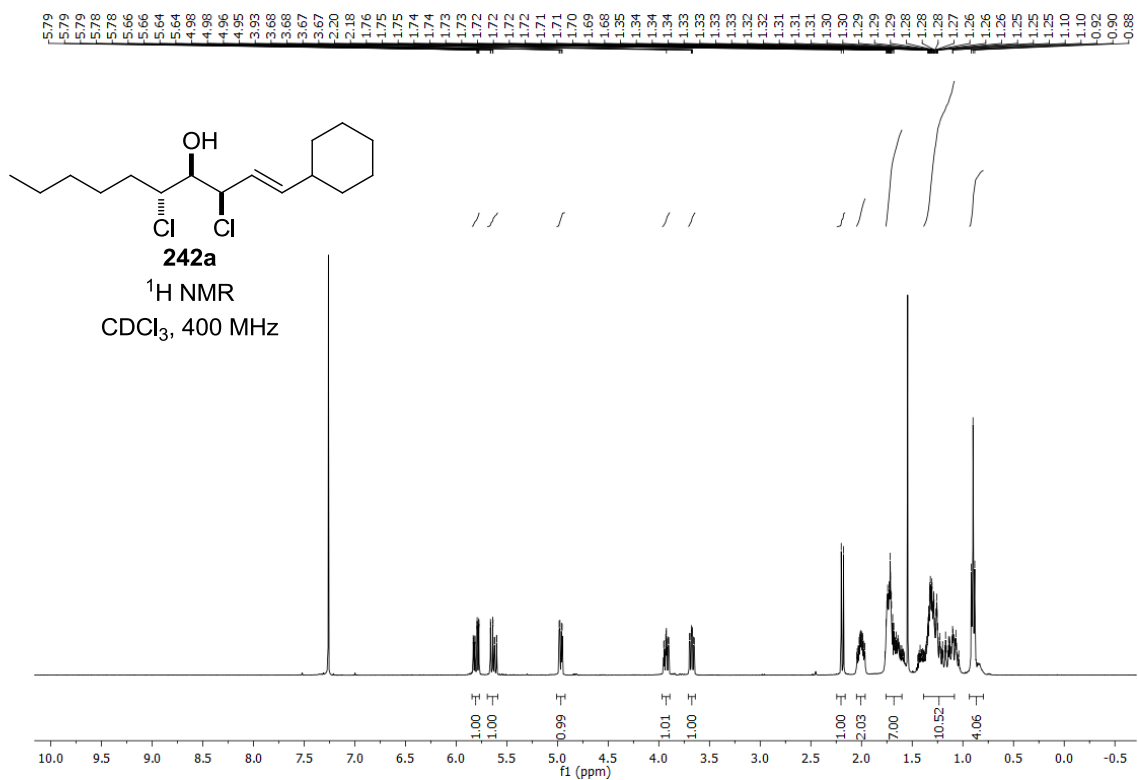


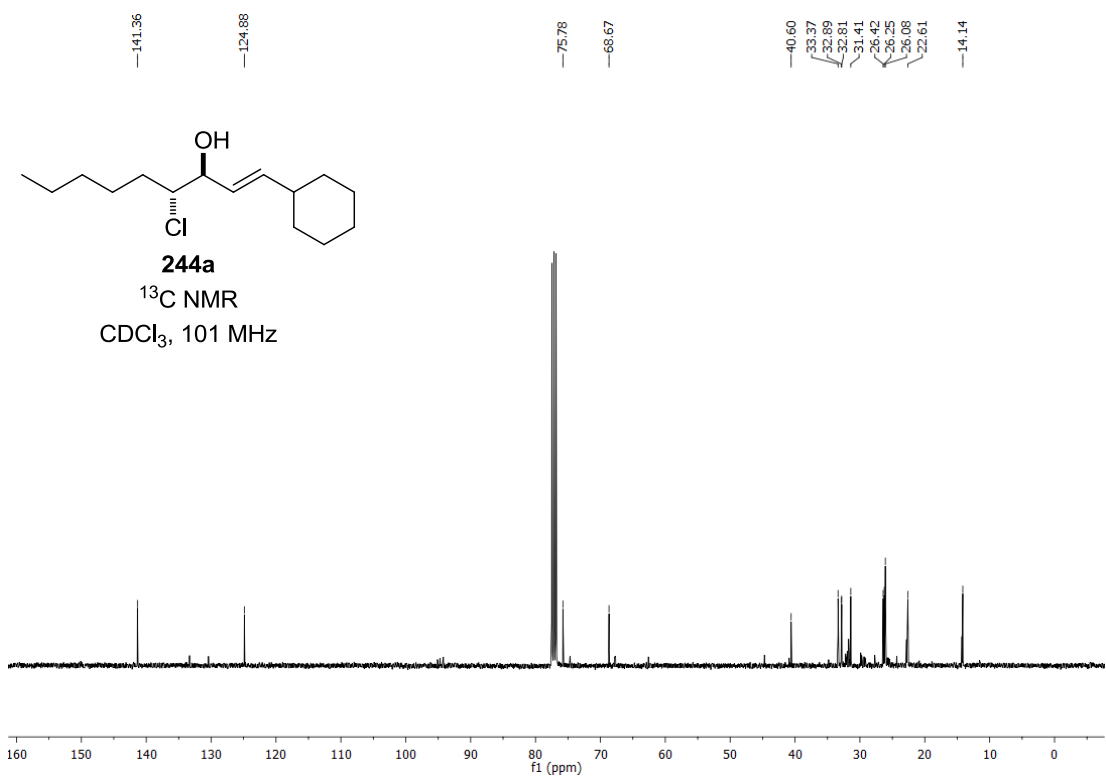
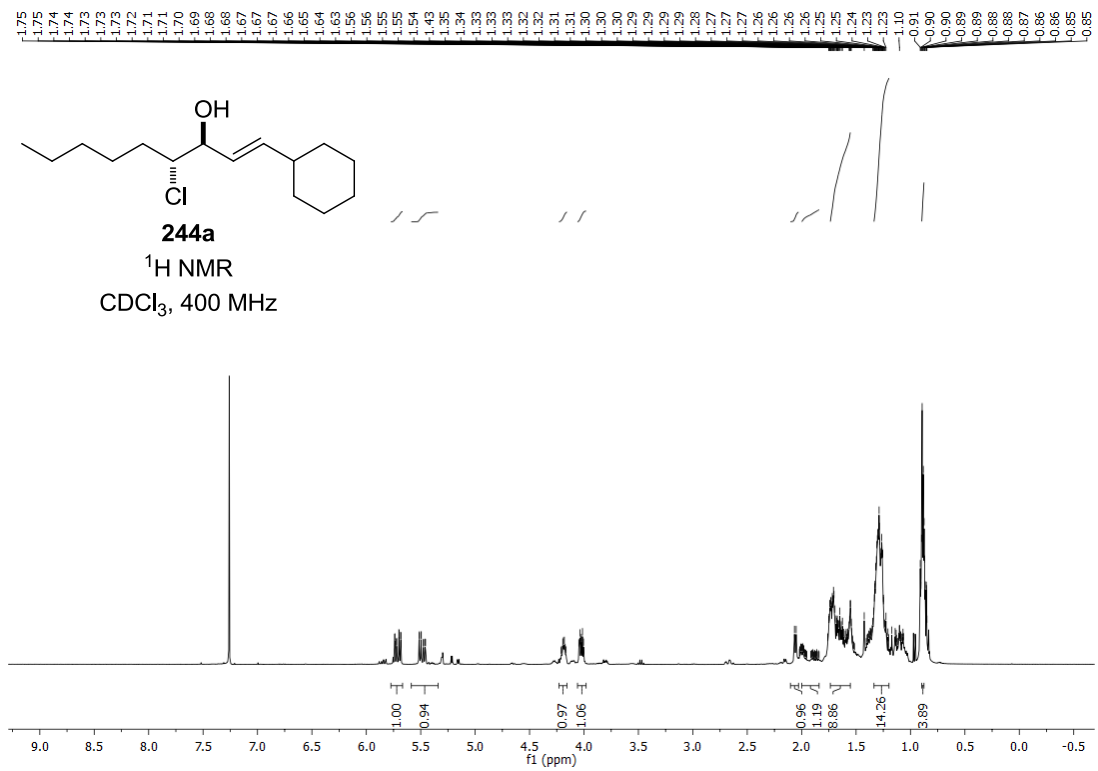
Appendix



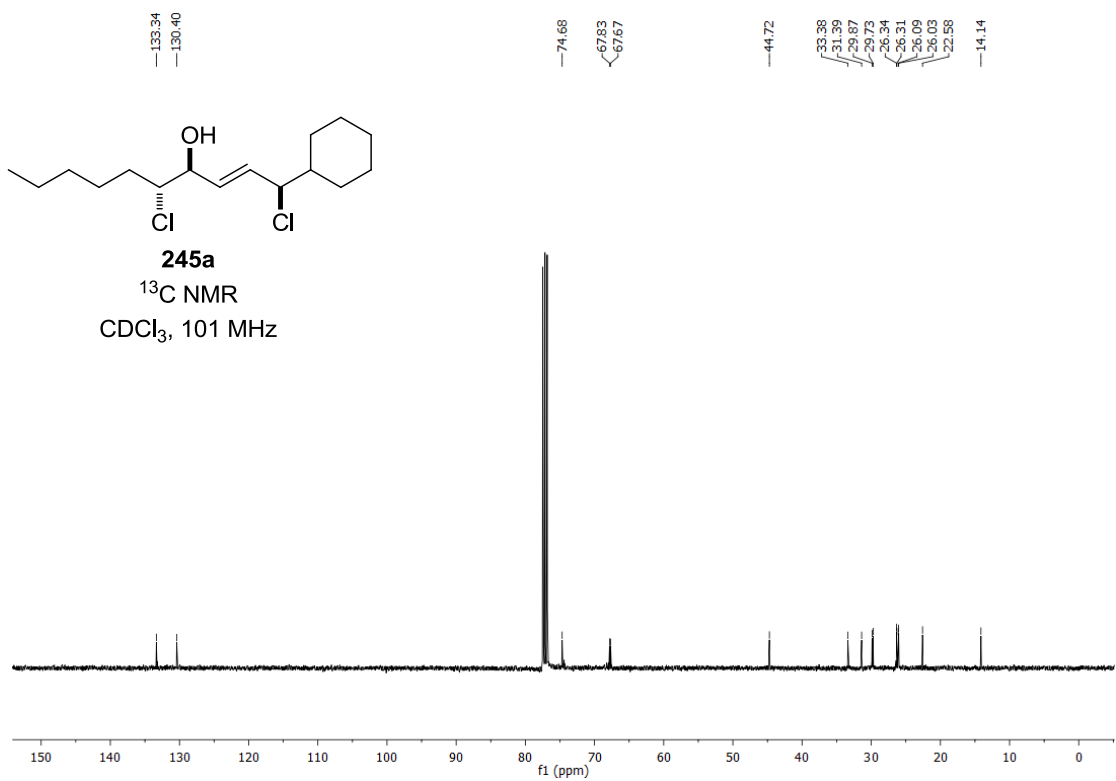
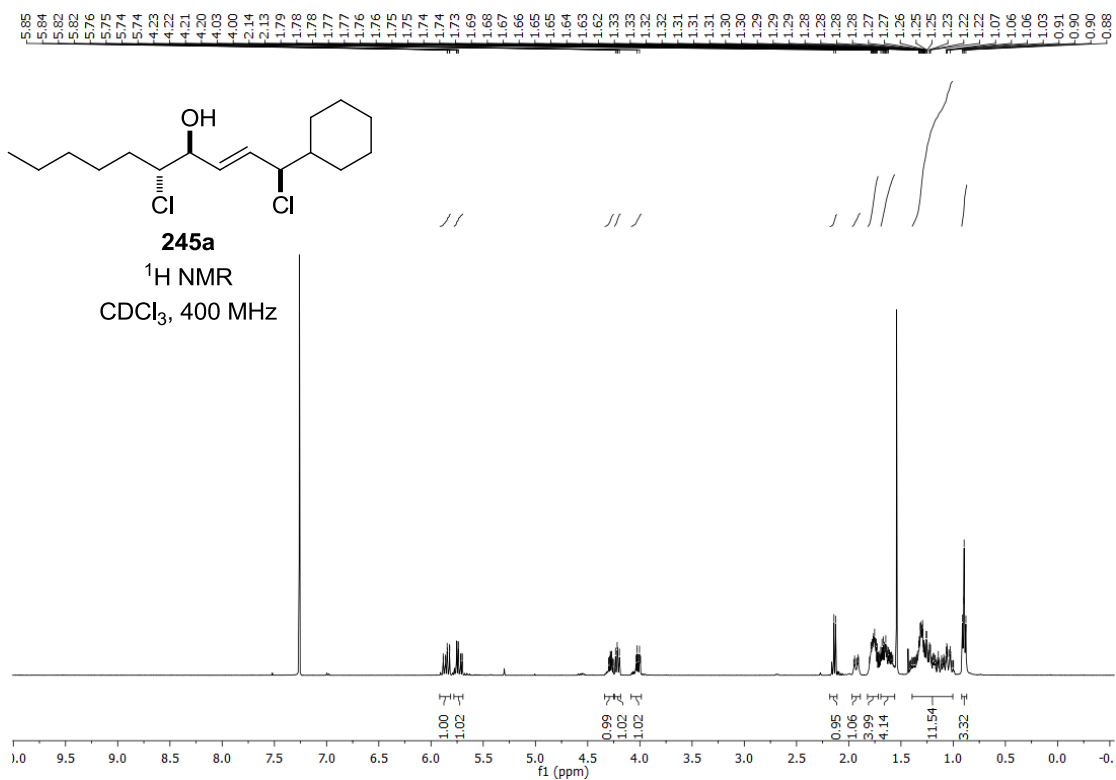


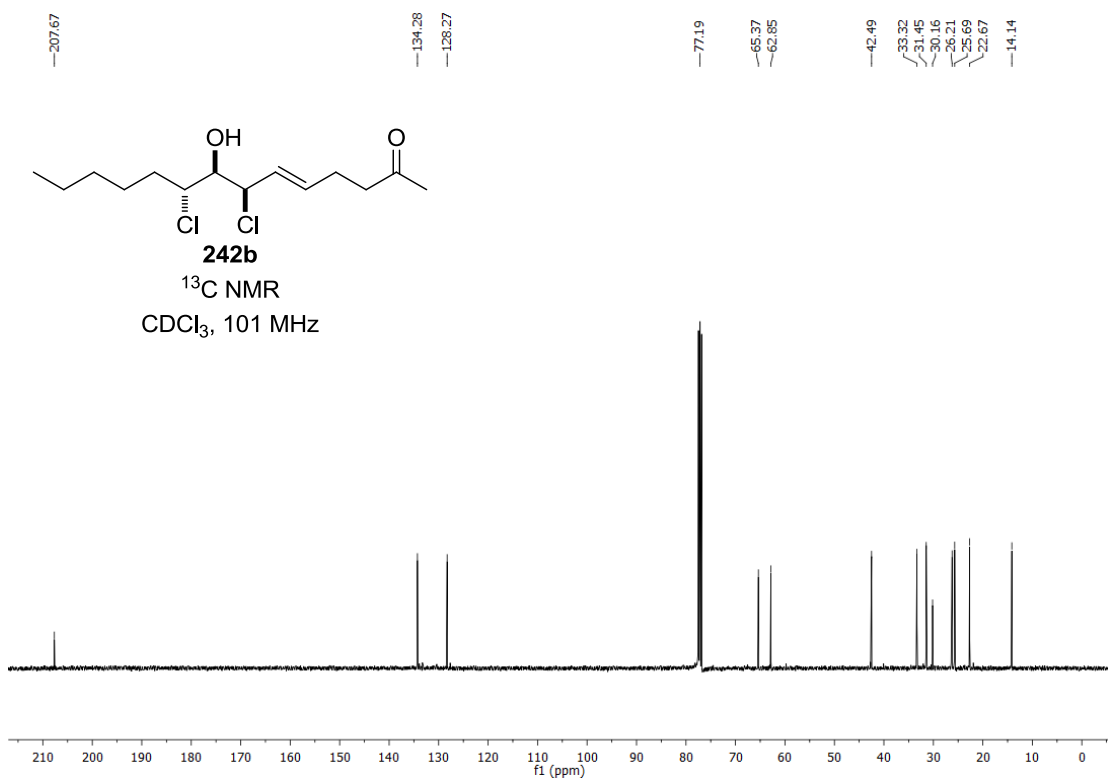
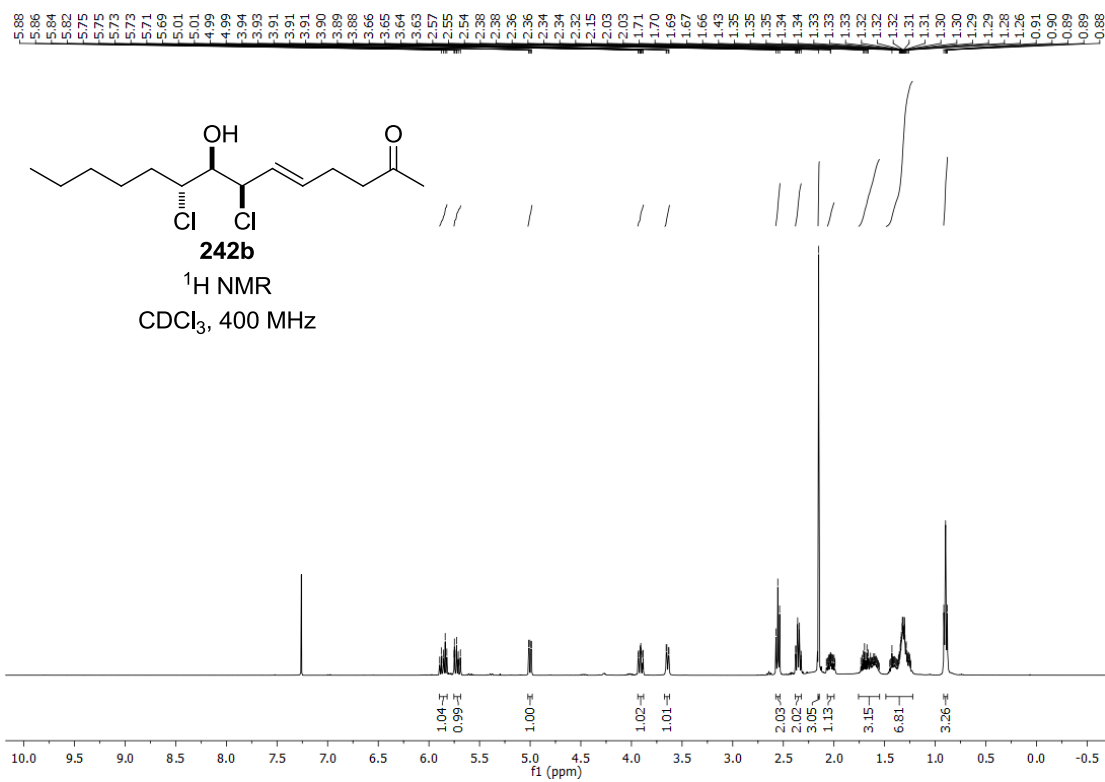
Appendix

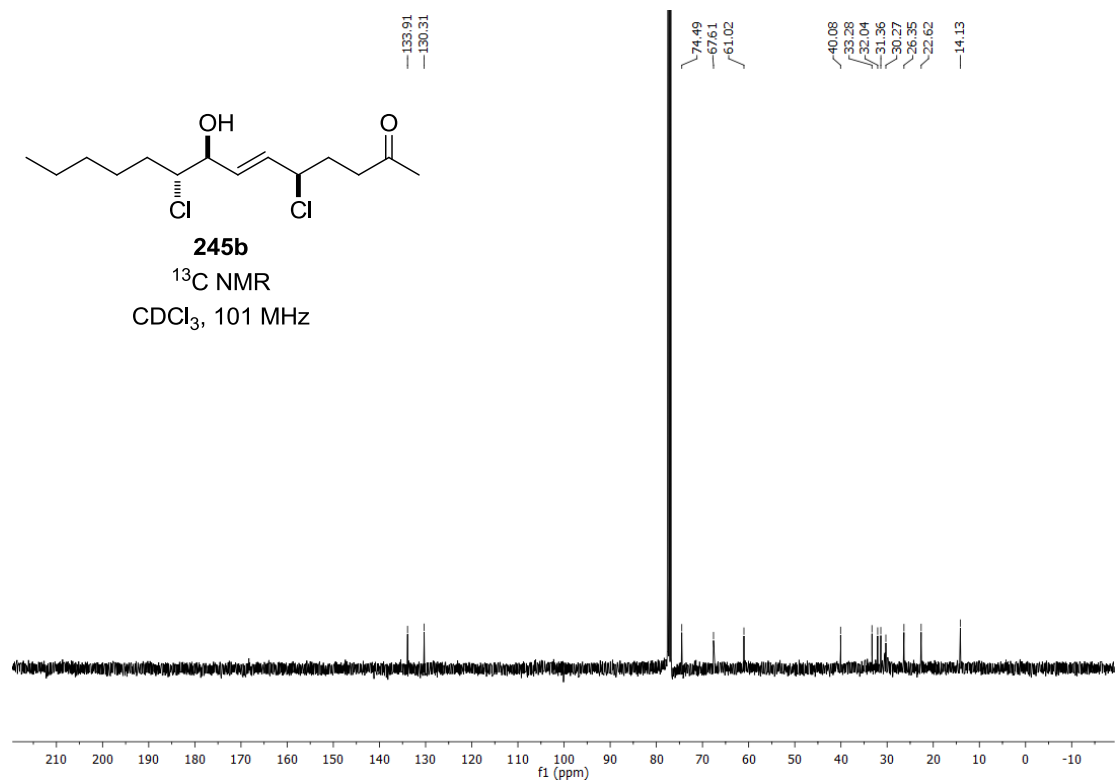
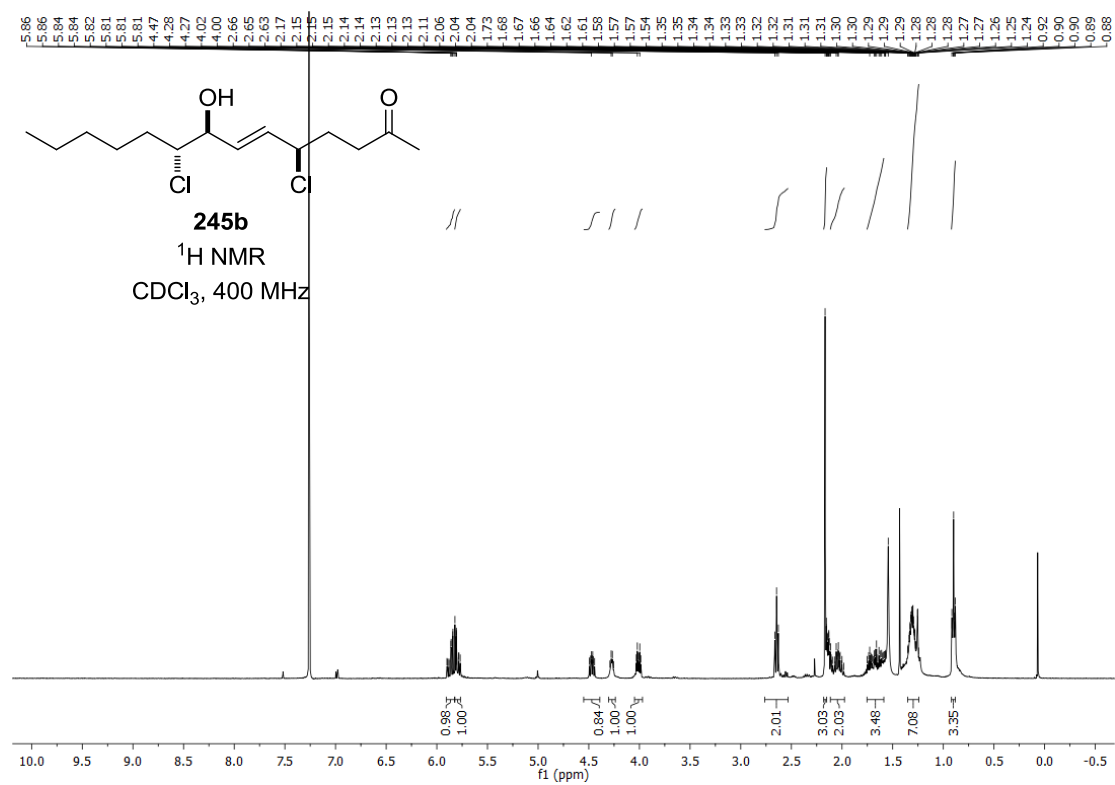


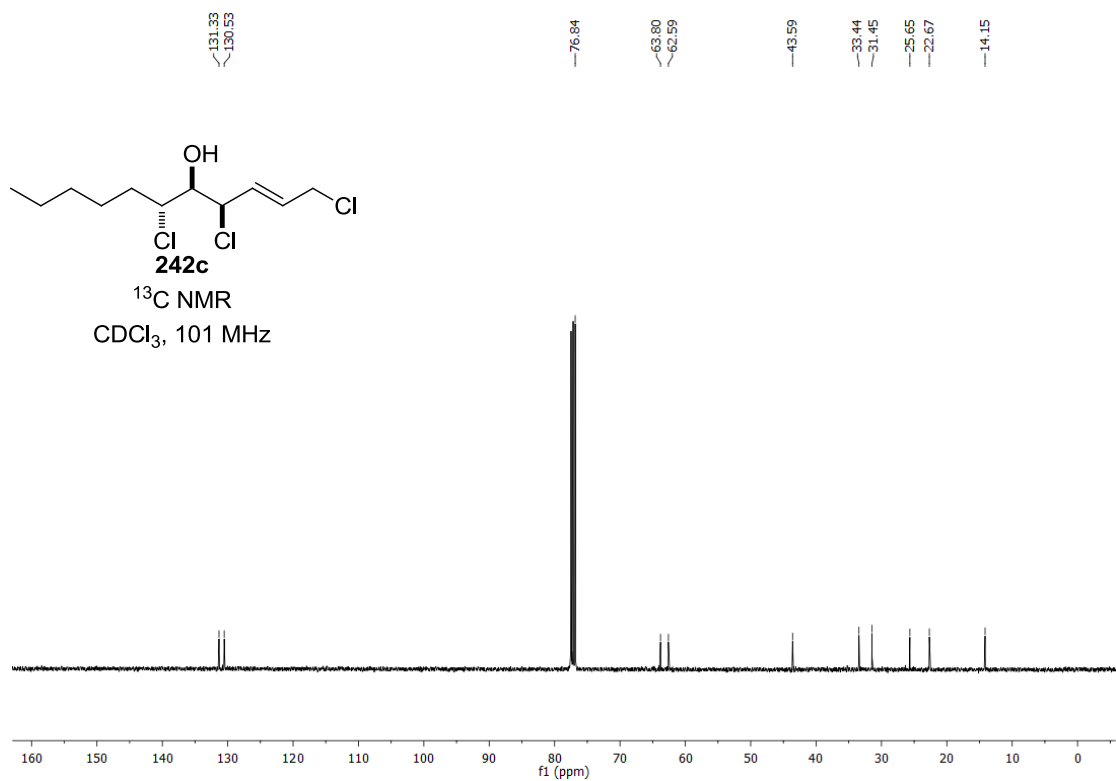
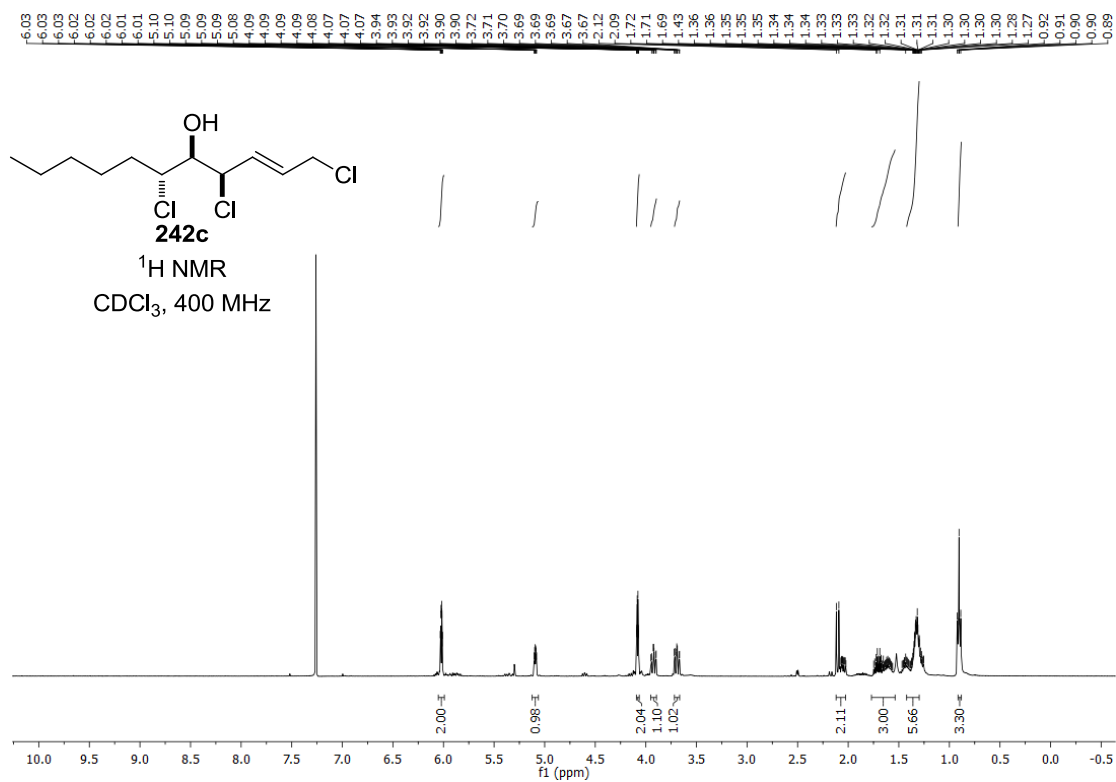


Appendix

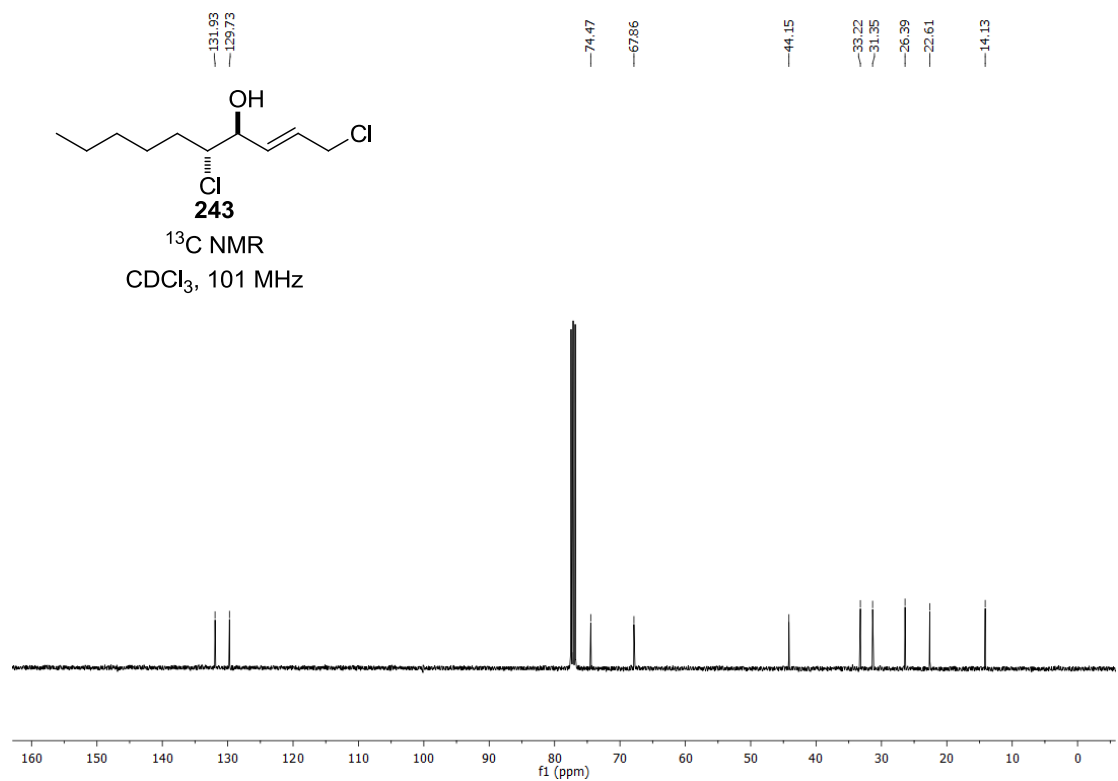
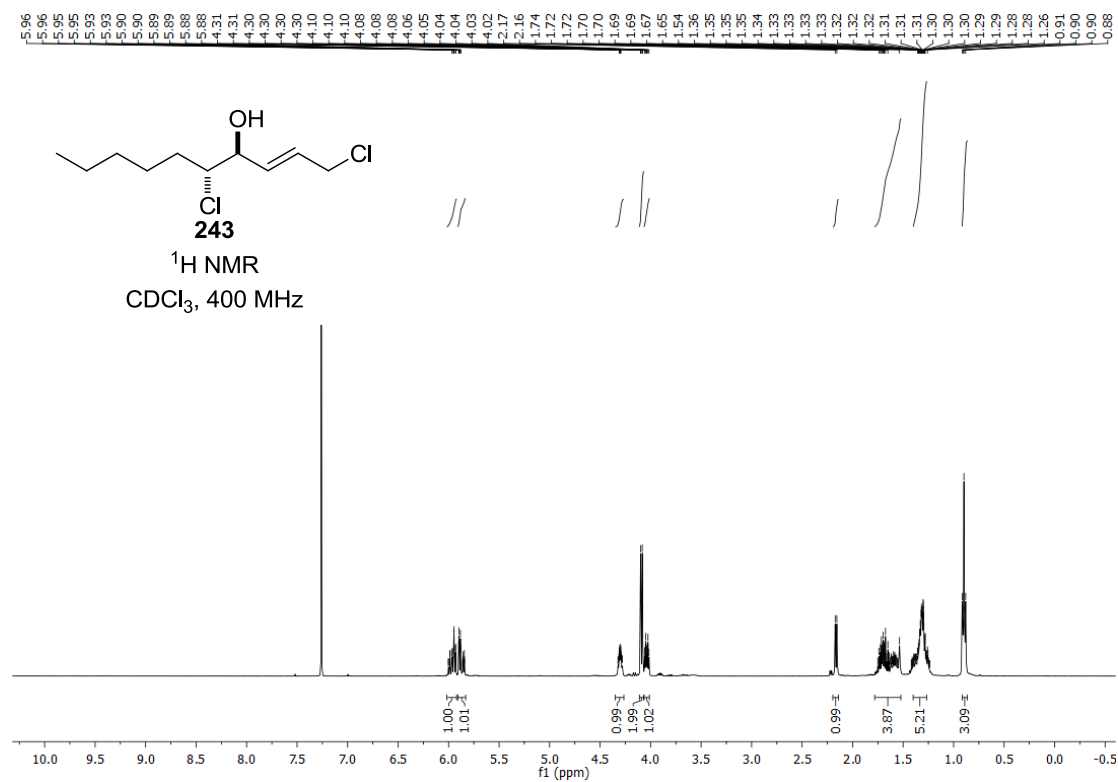


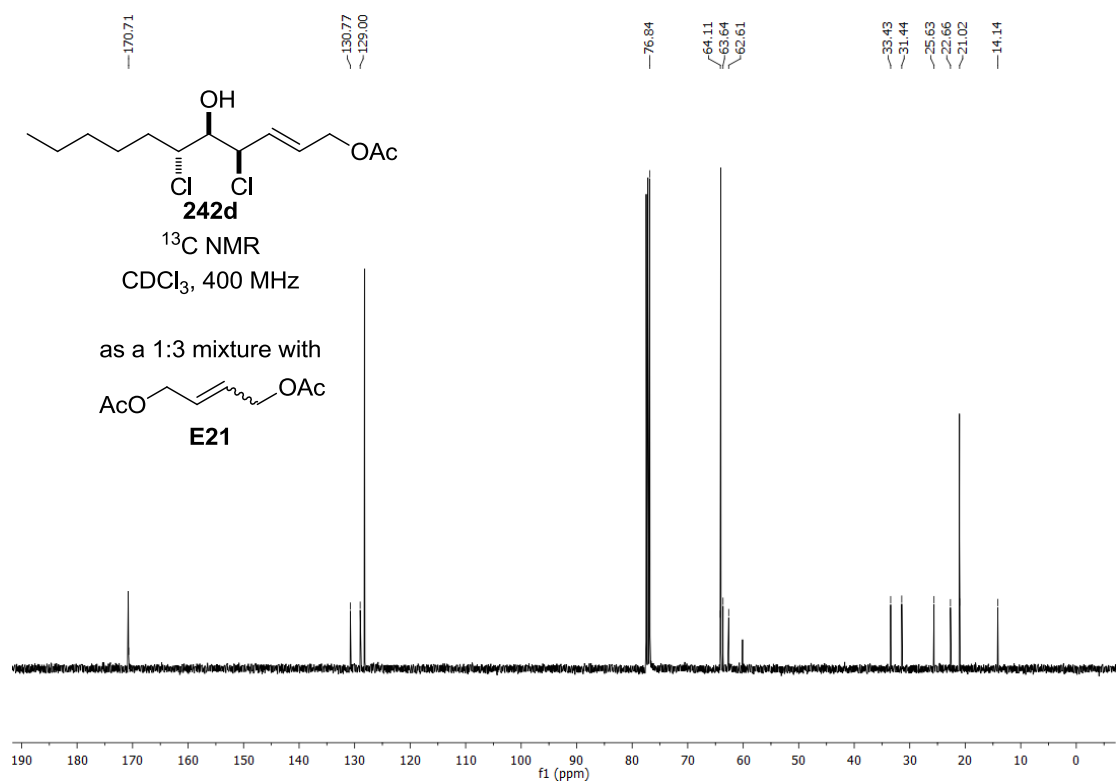
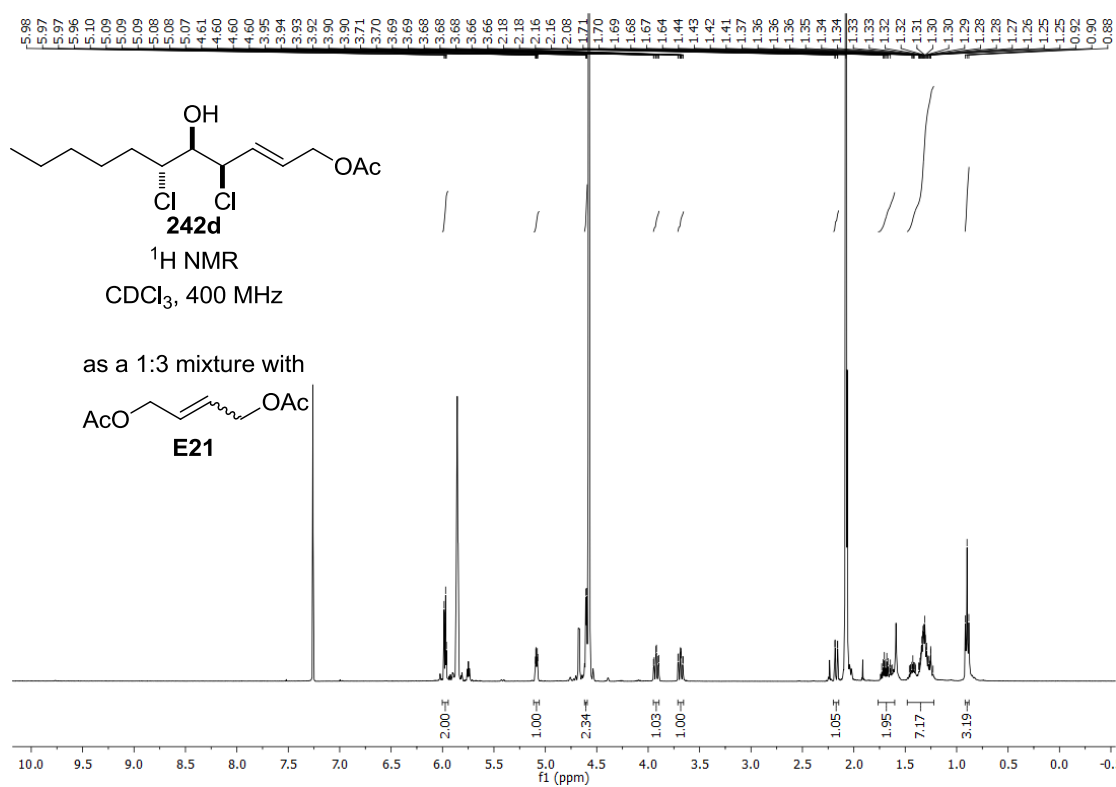


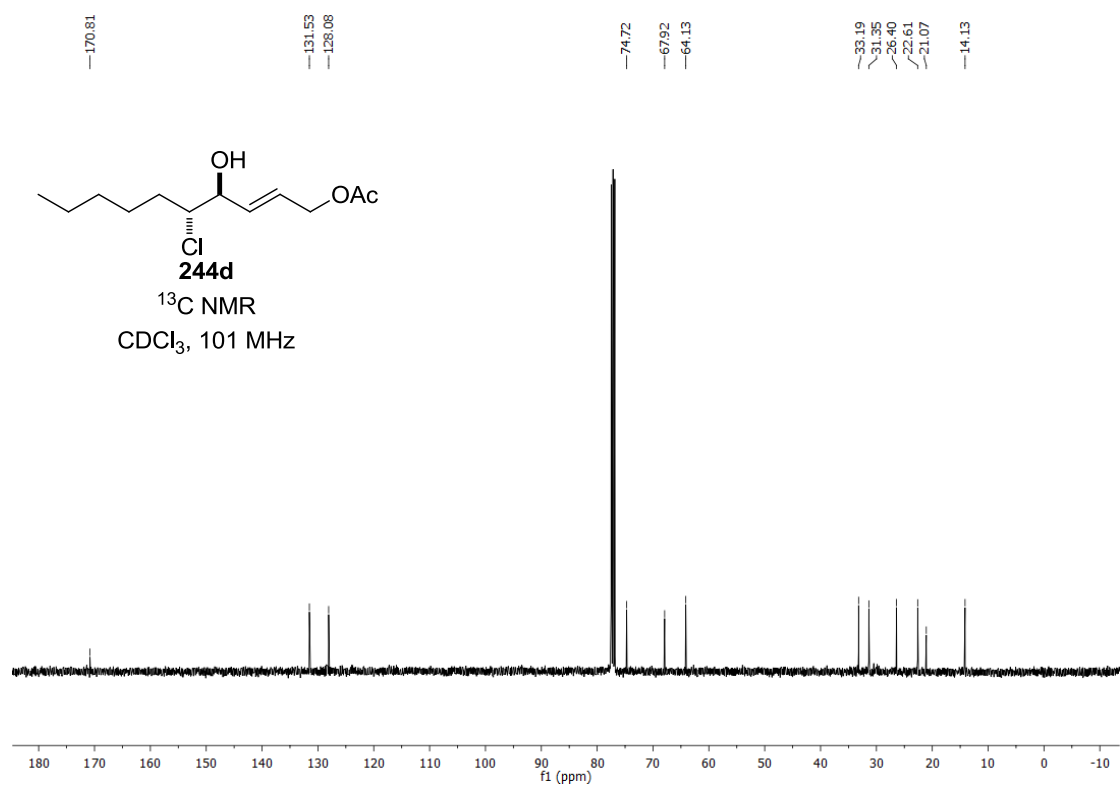
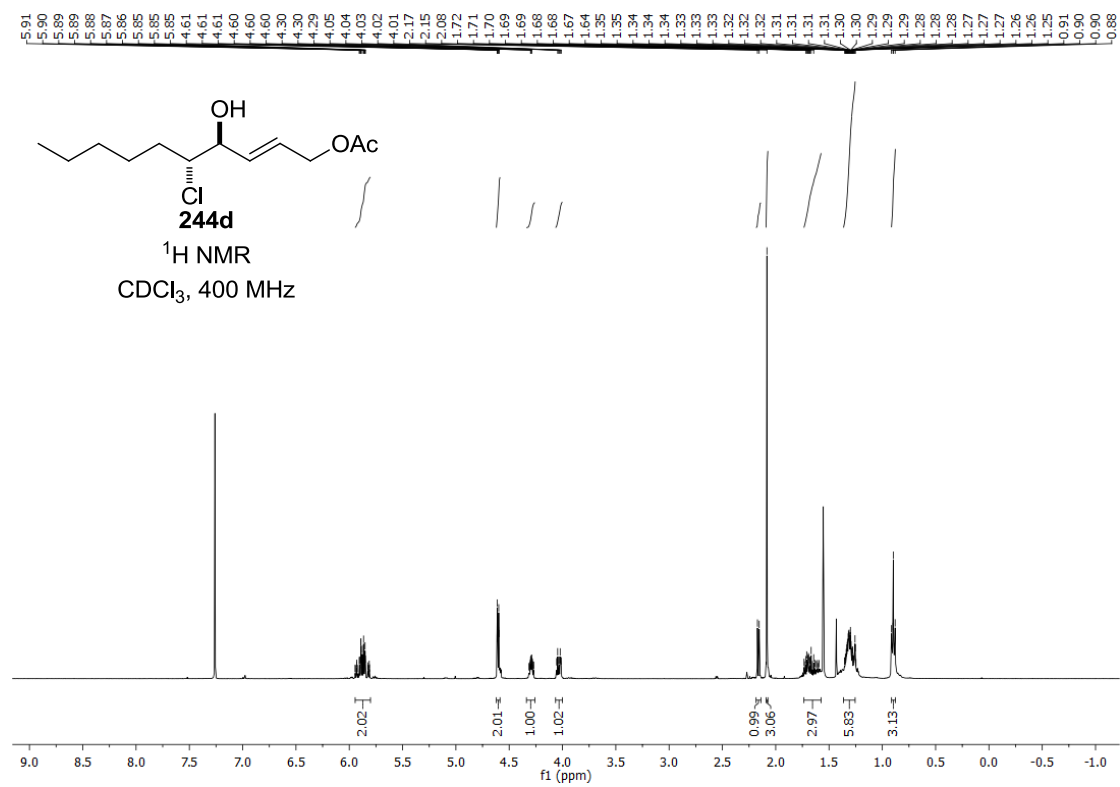


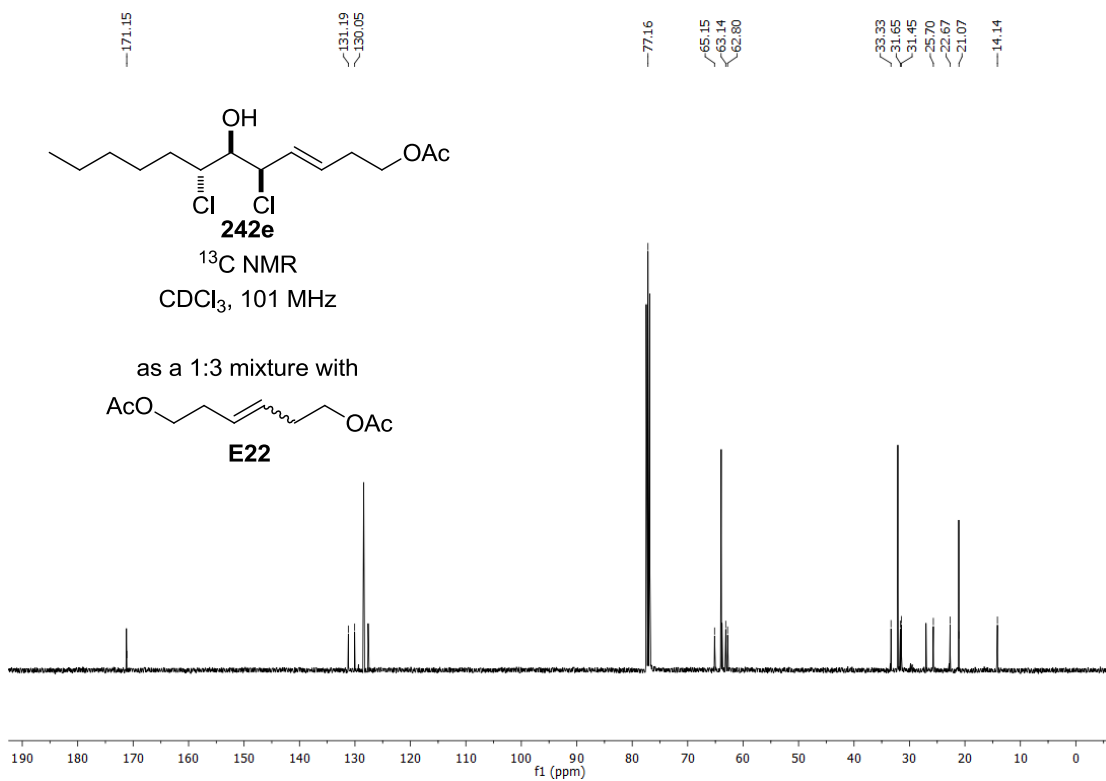
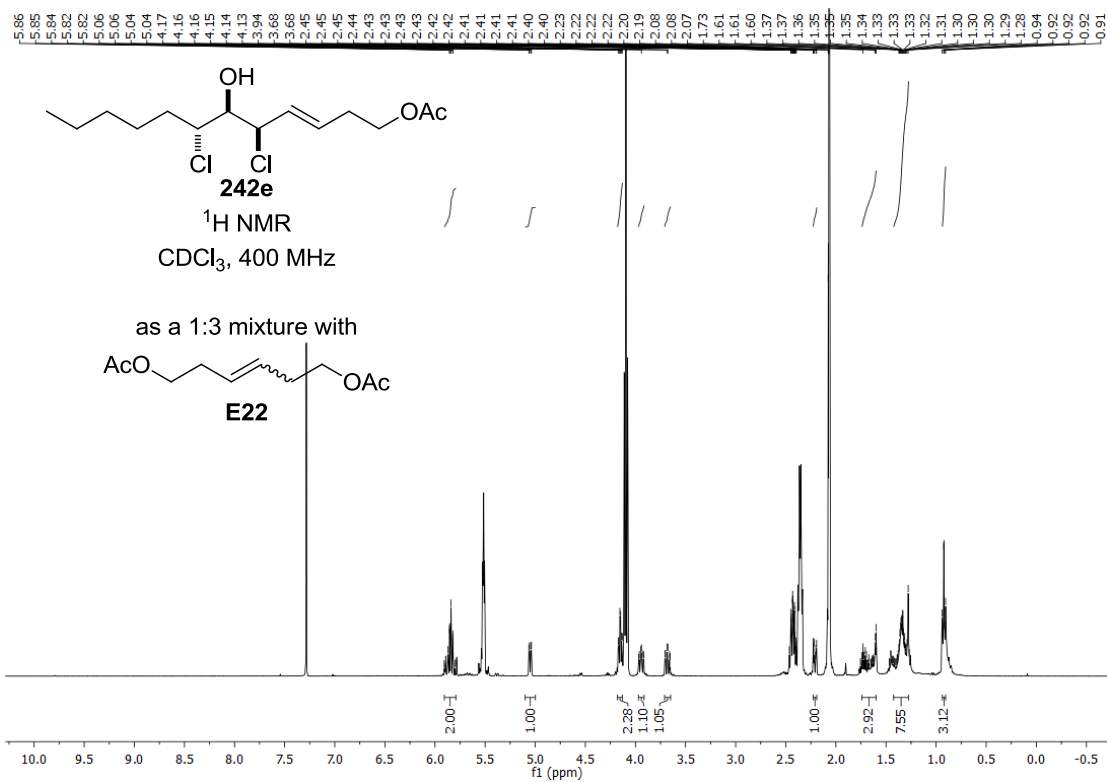


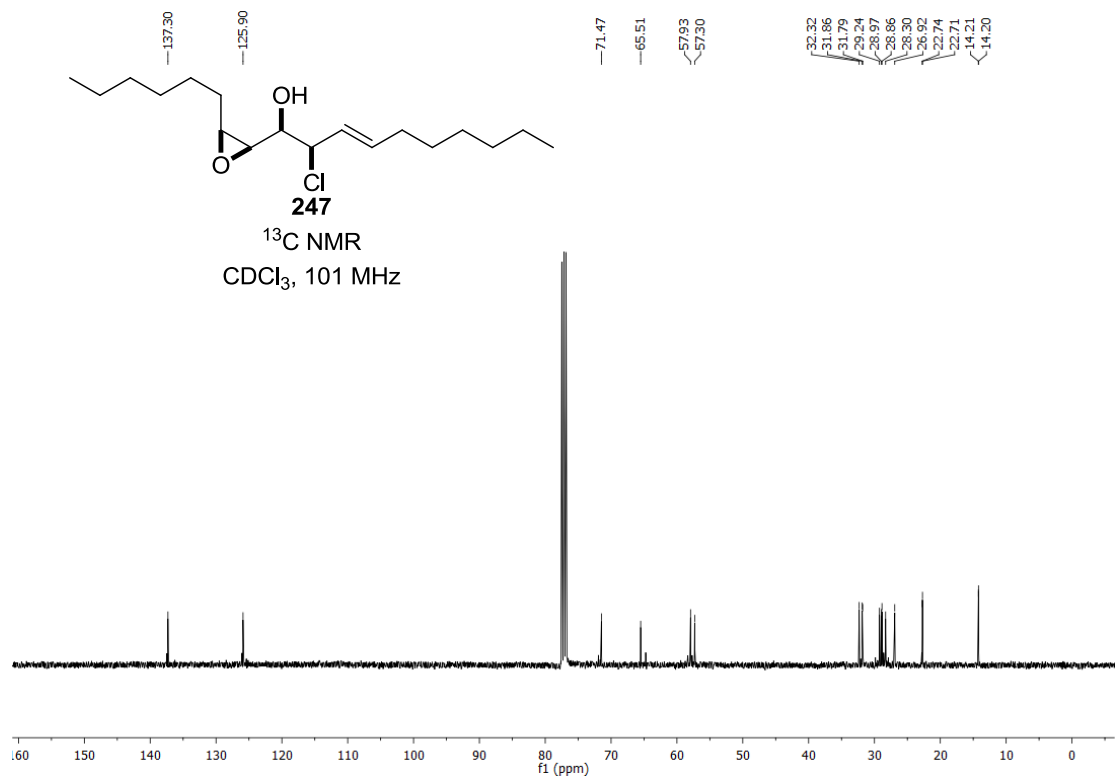
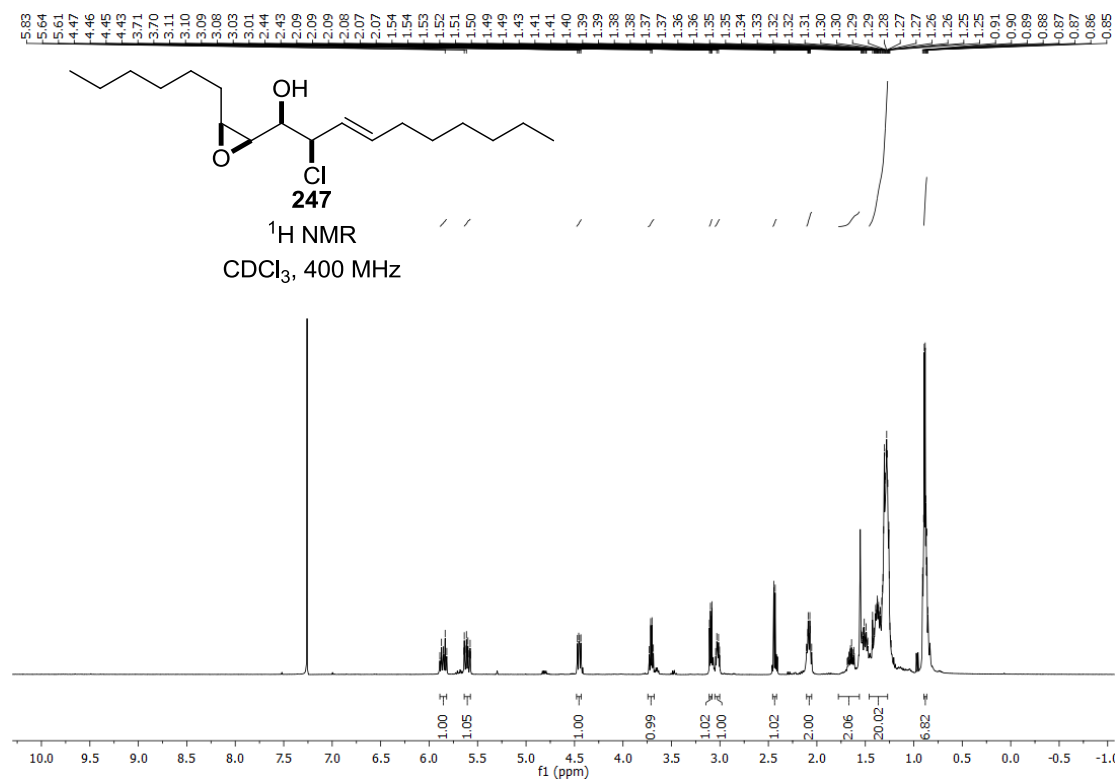
Appendix

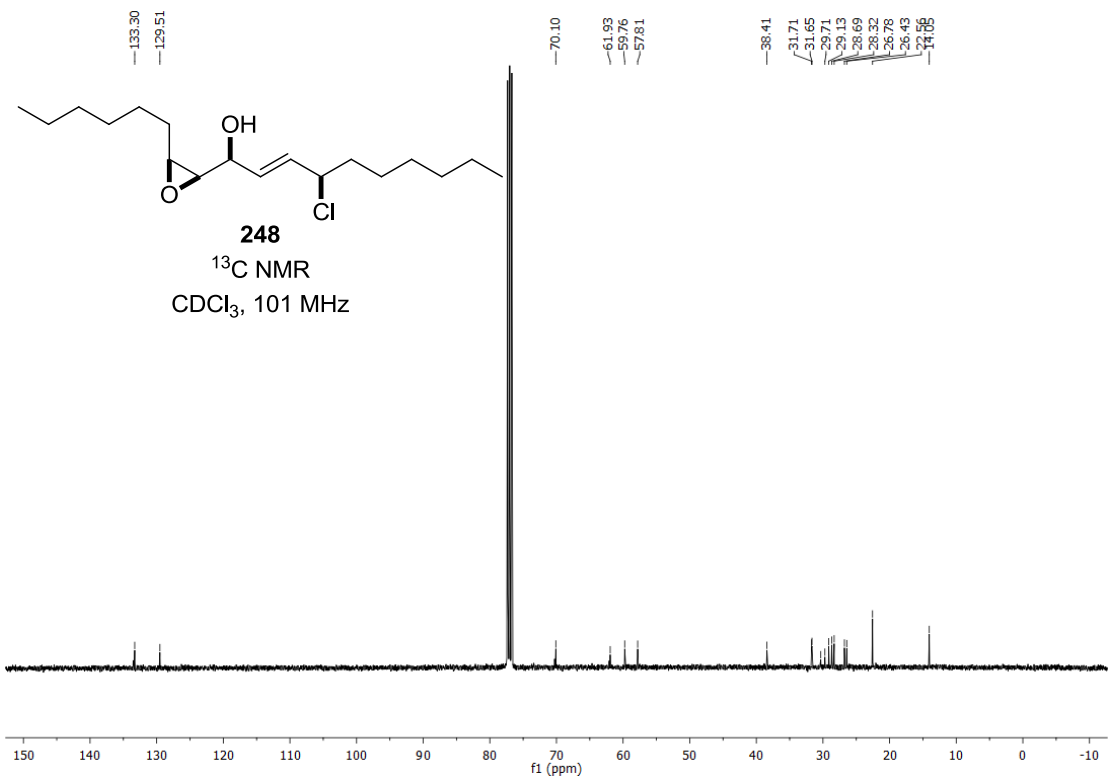
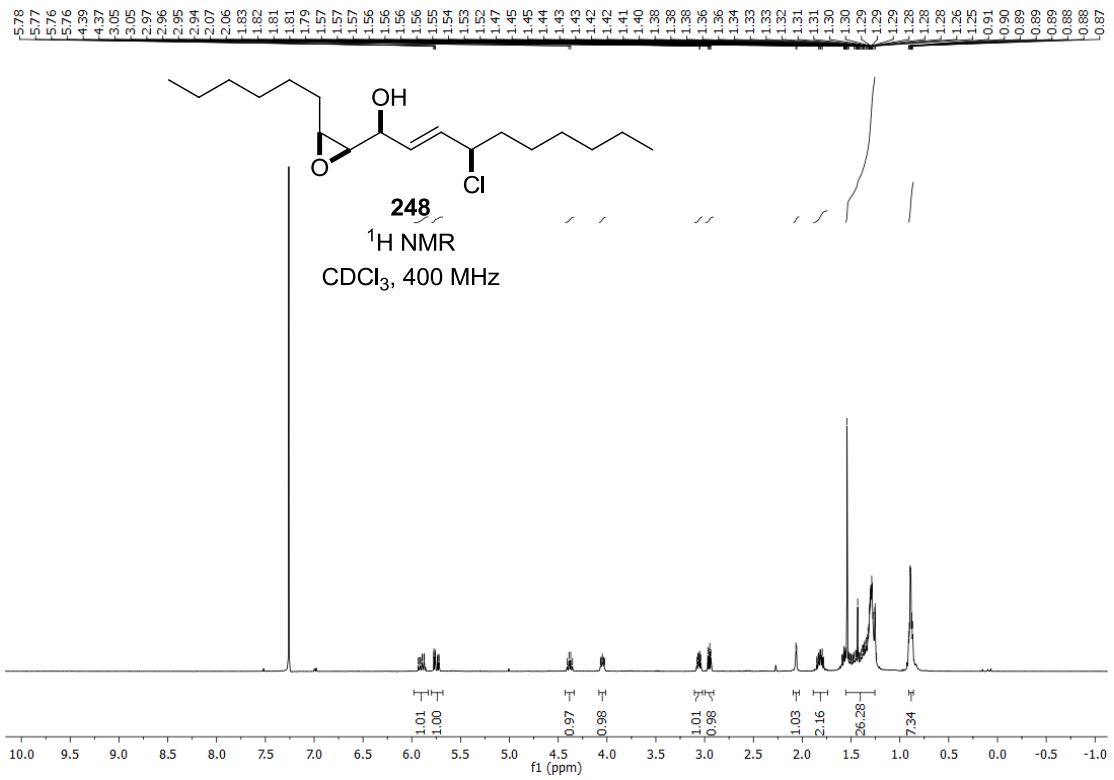


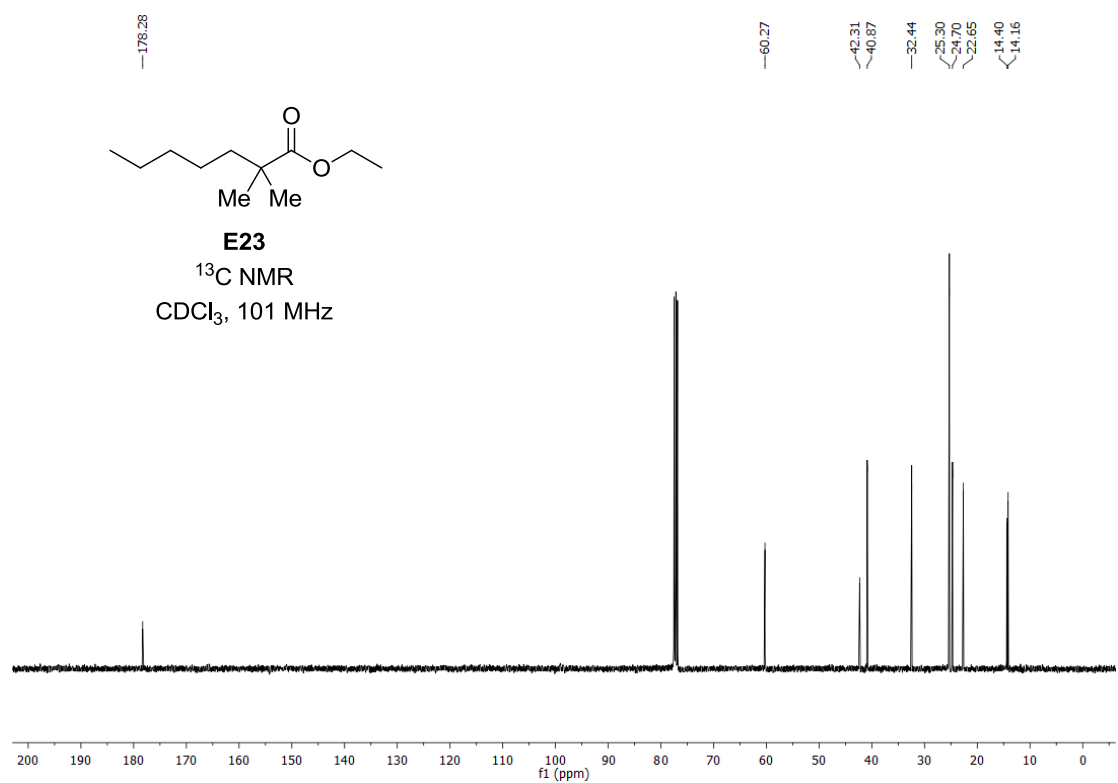
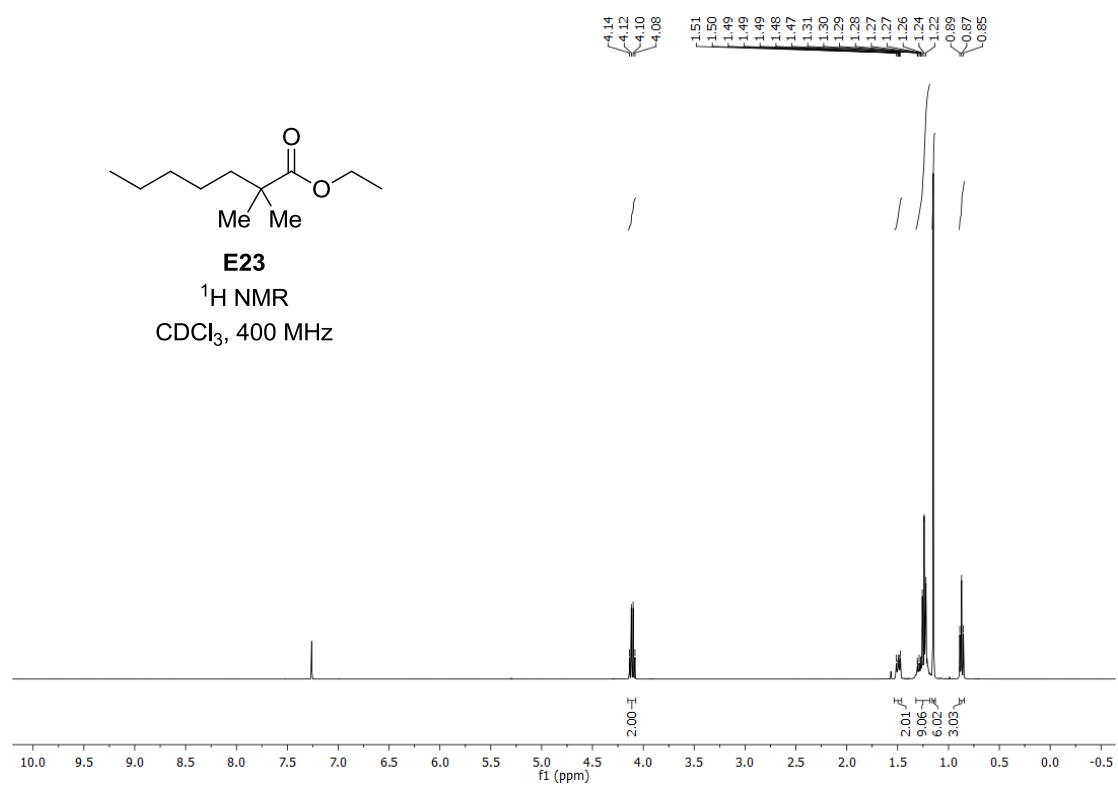


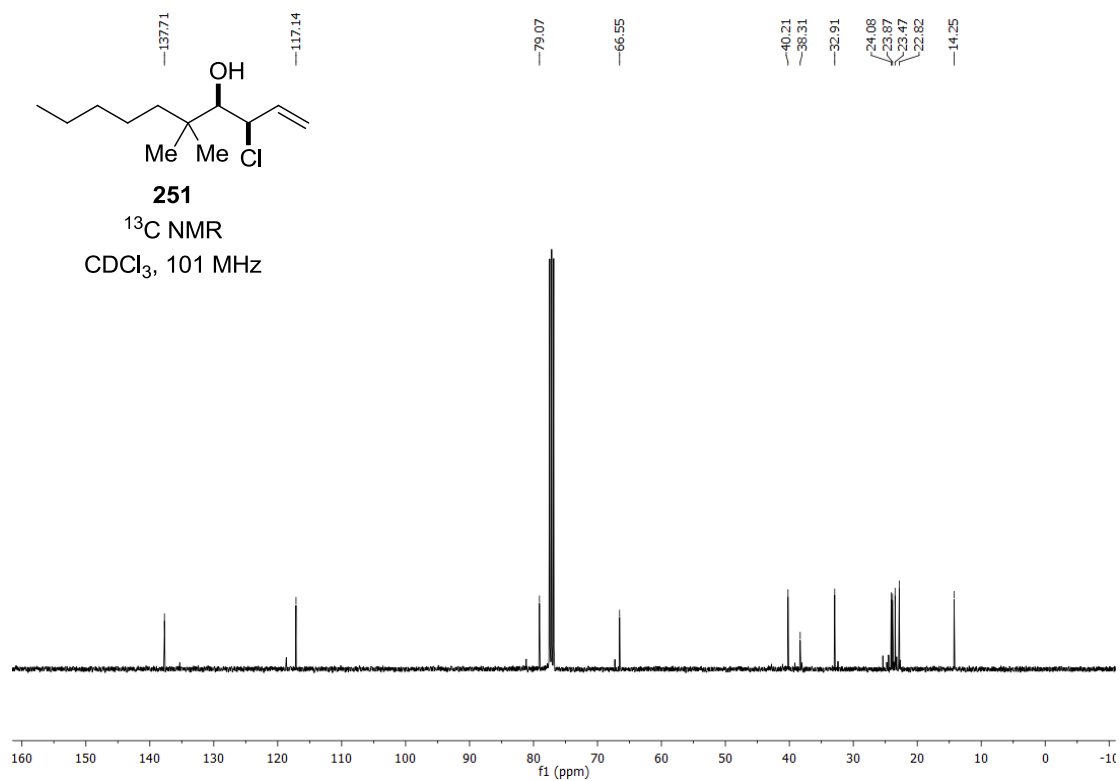
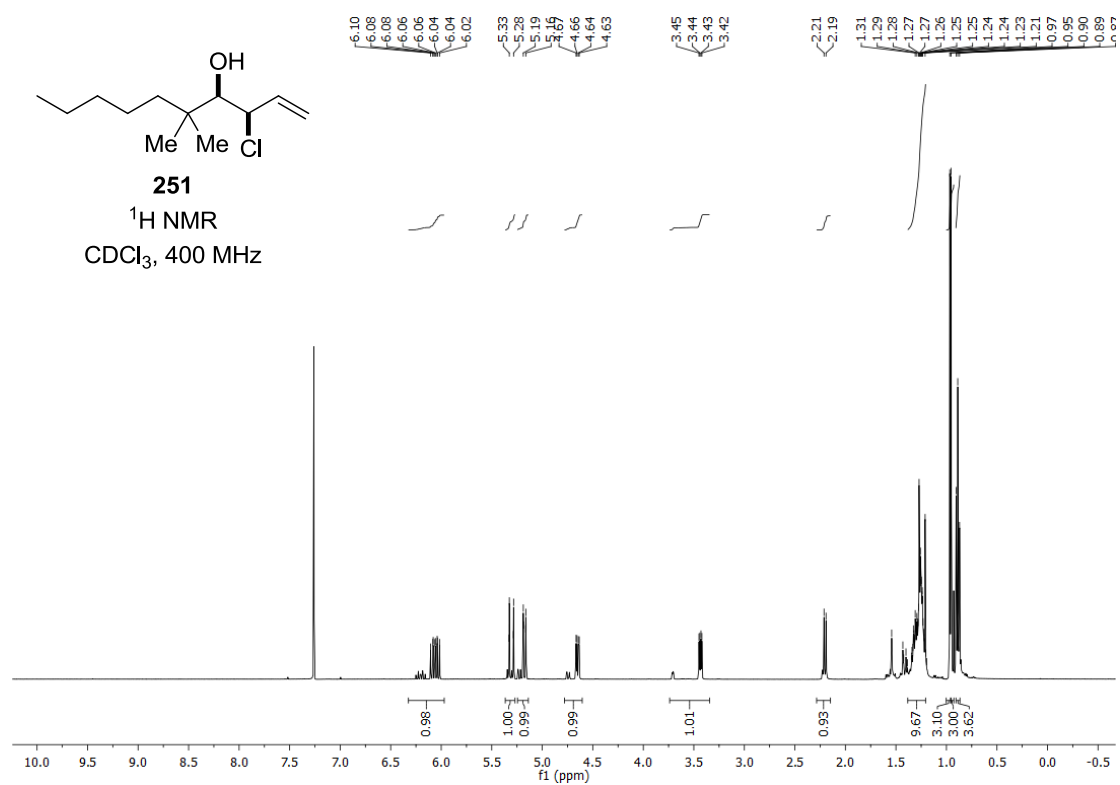


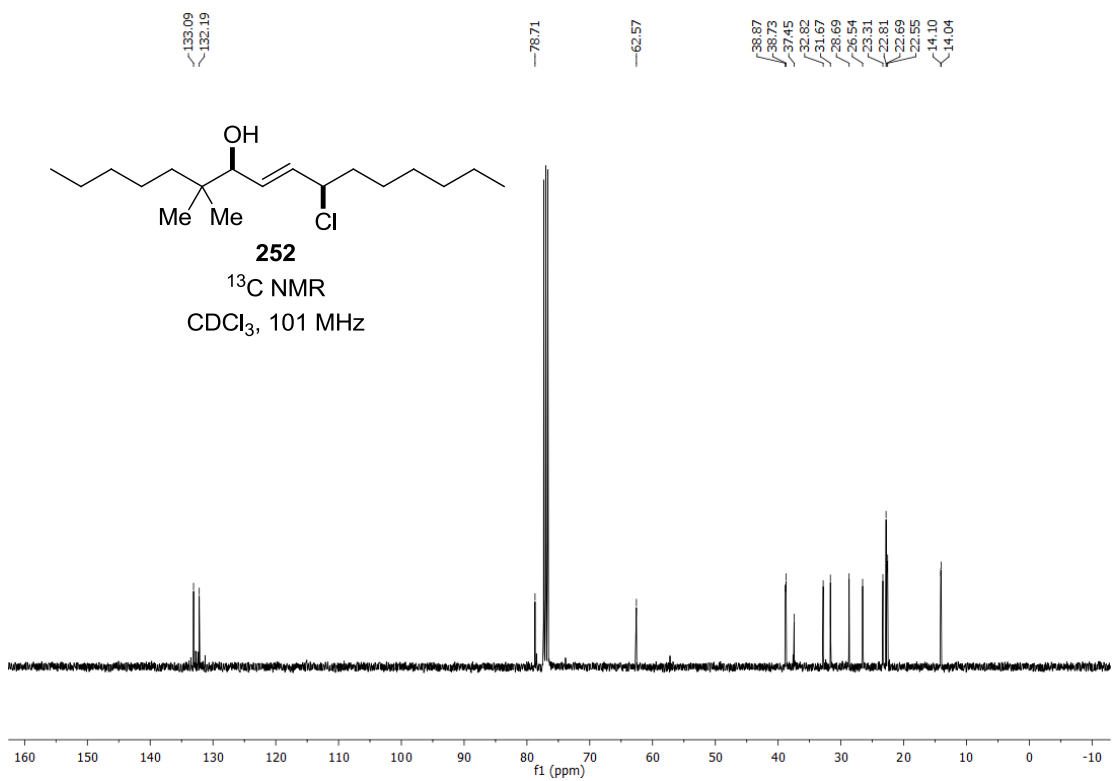
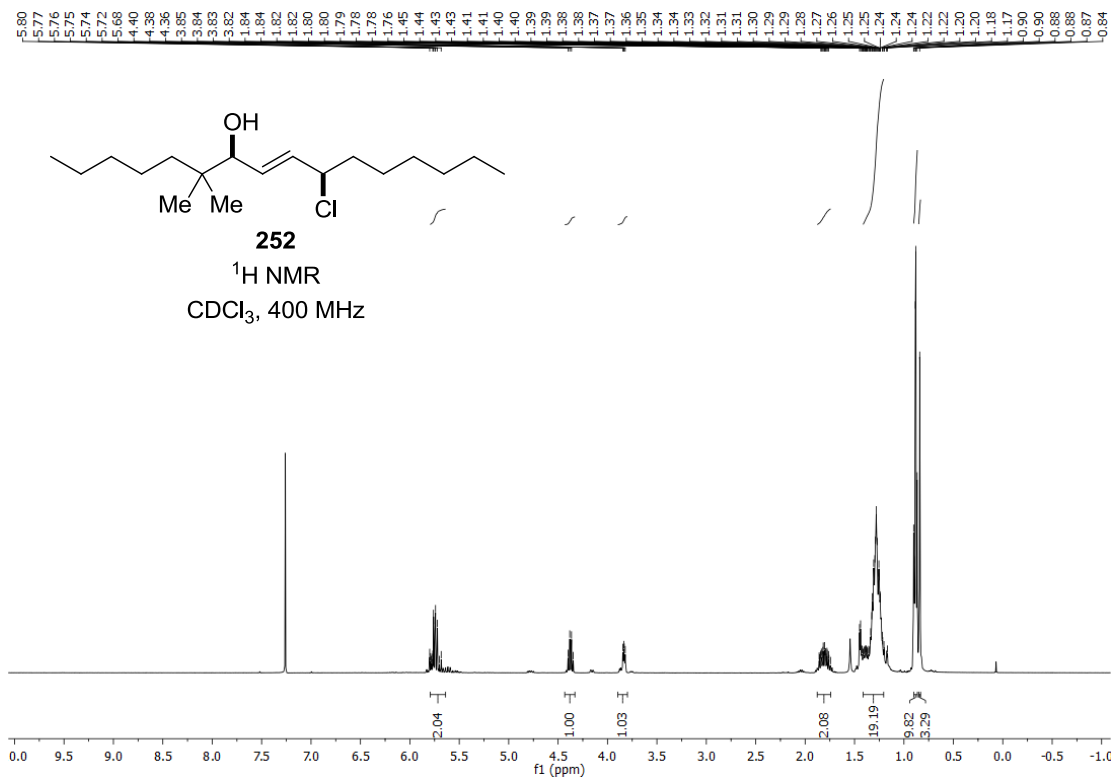


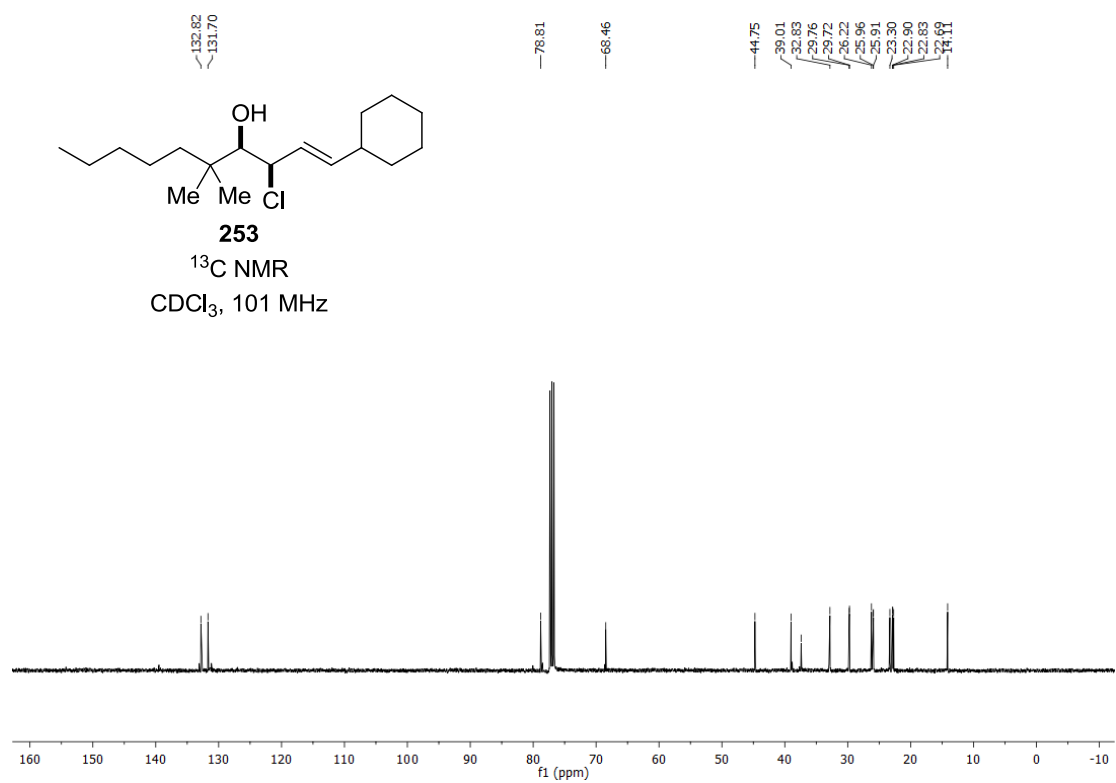
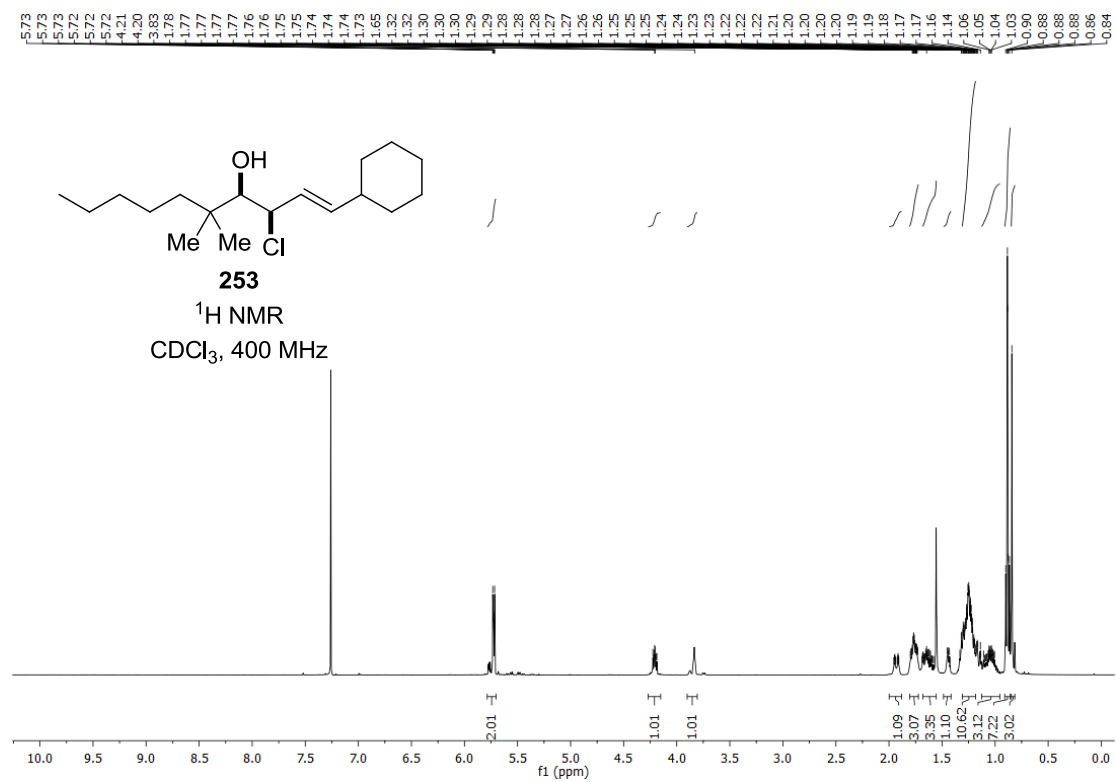


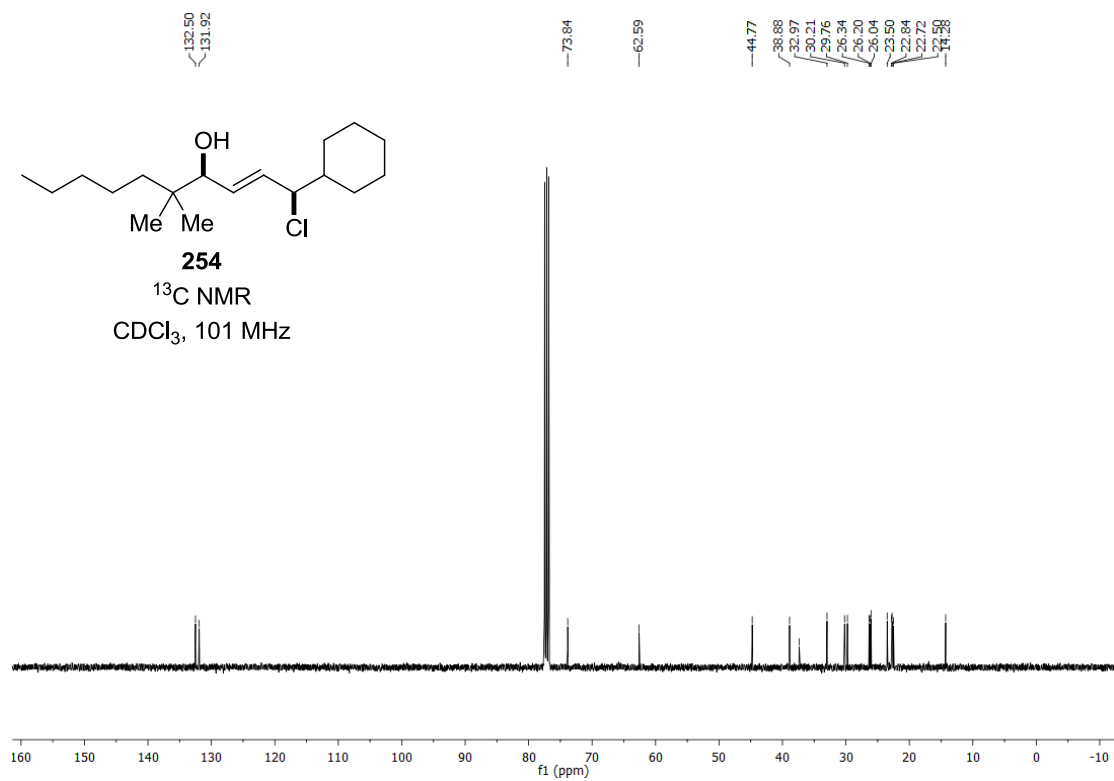
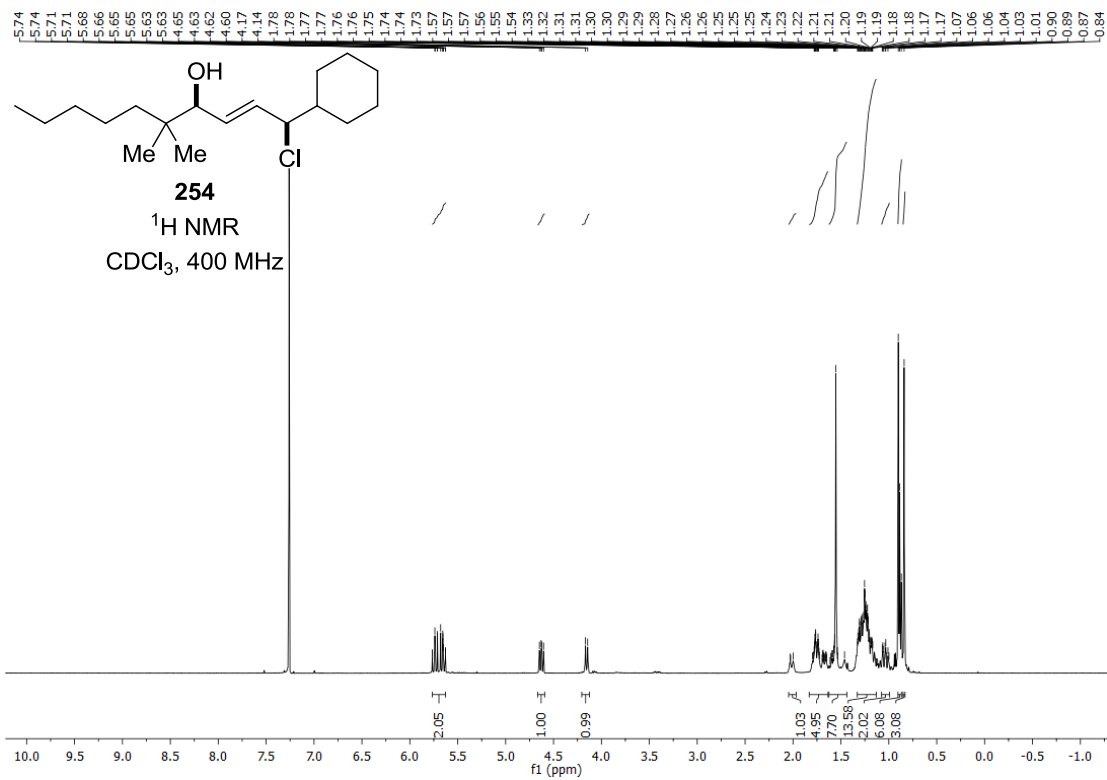


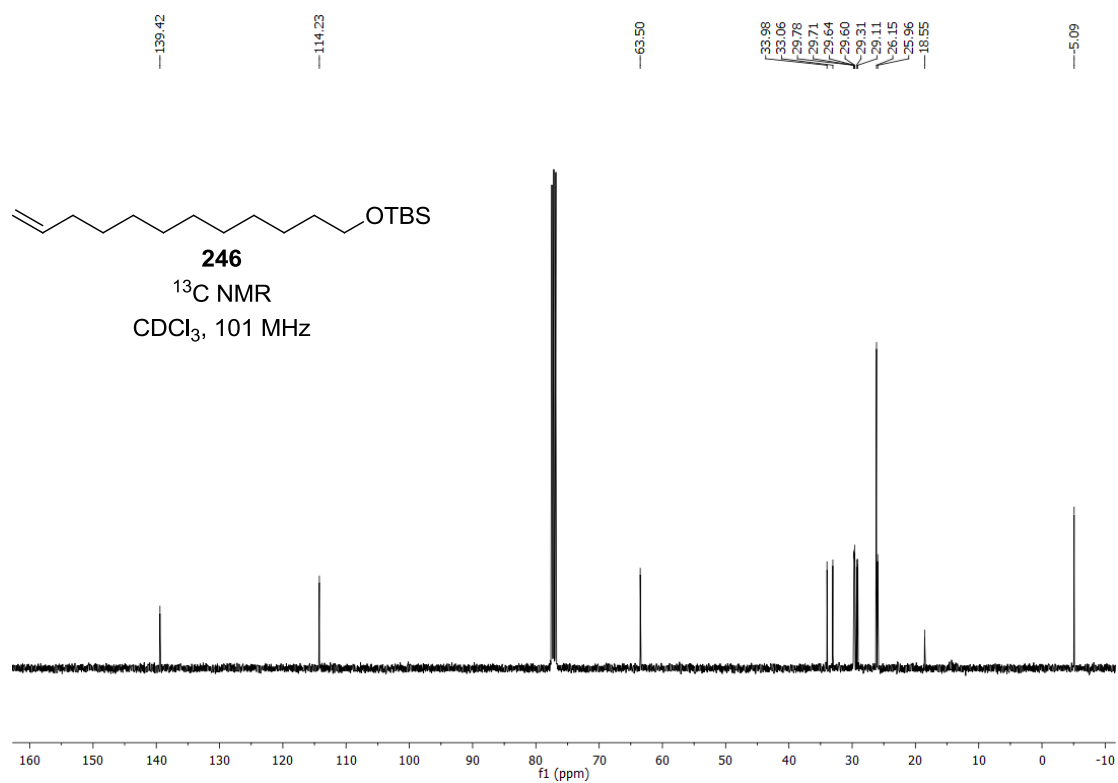
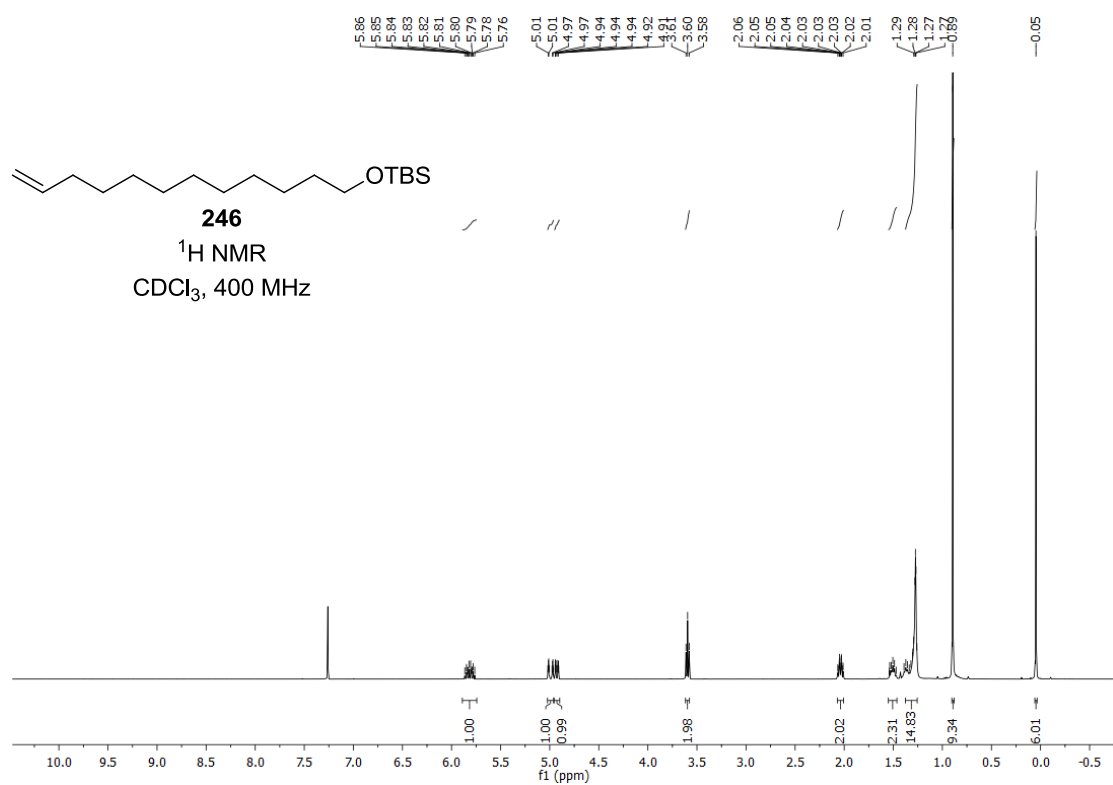


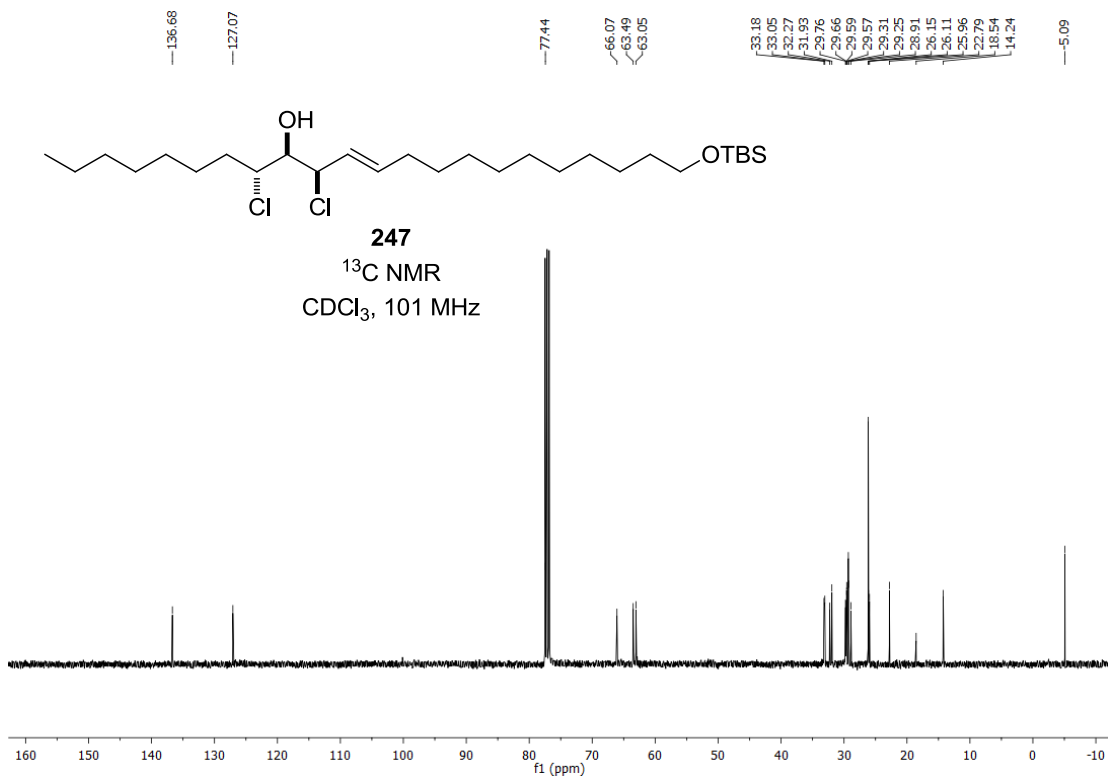
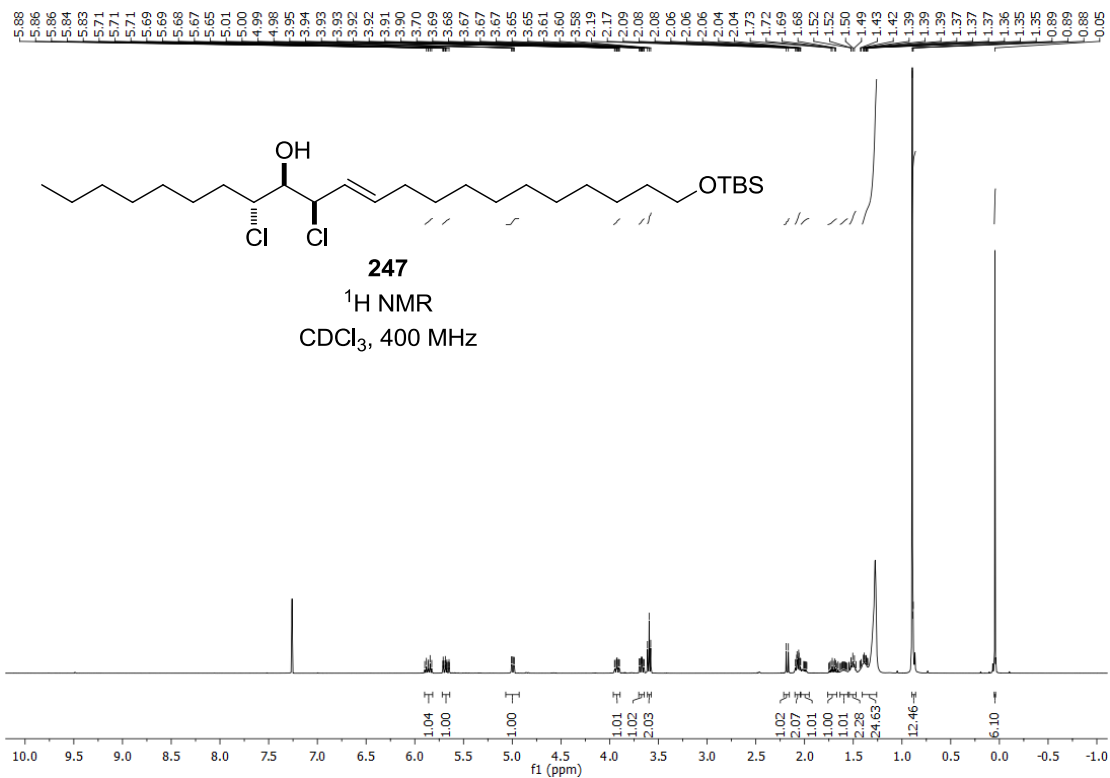


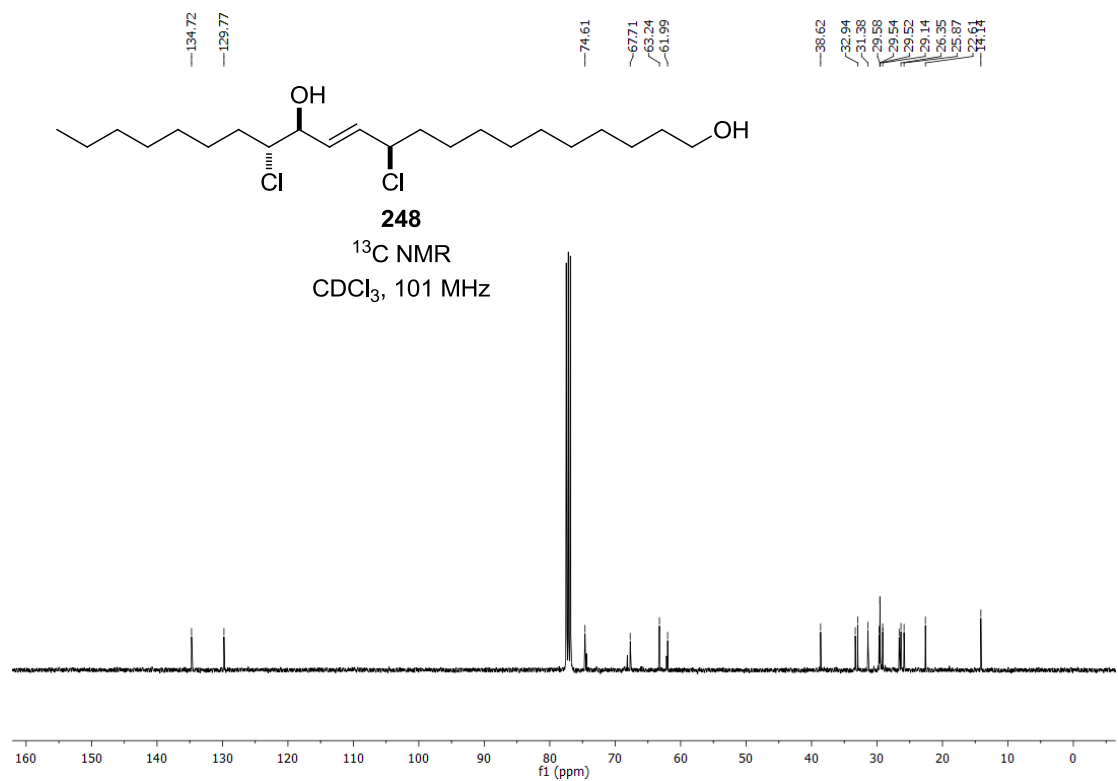
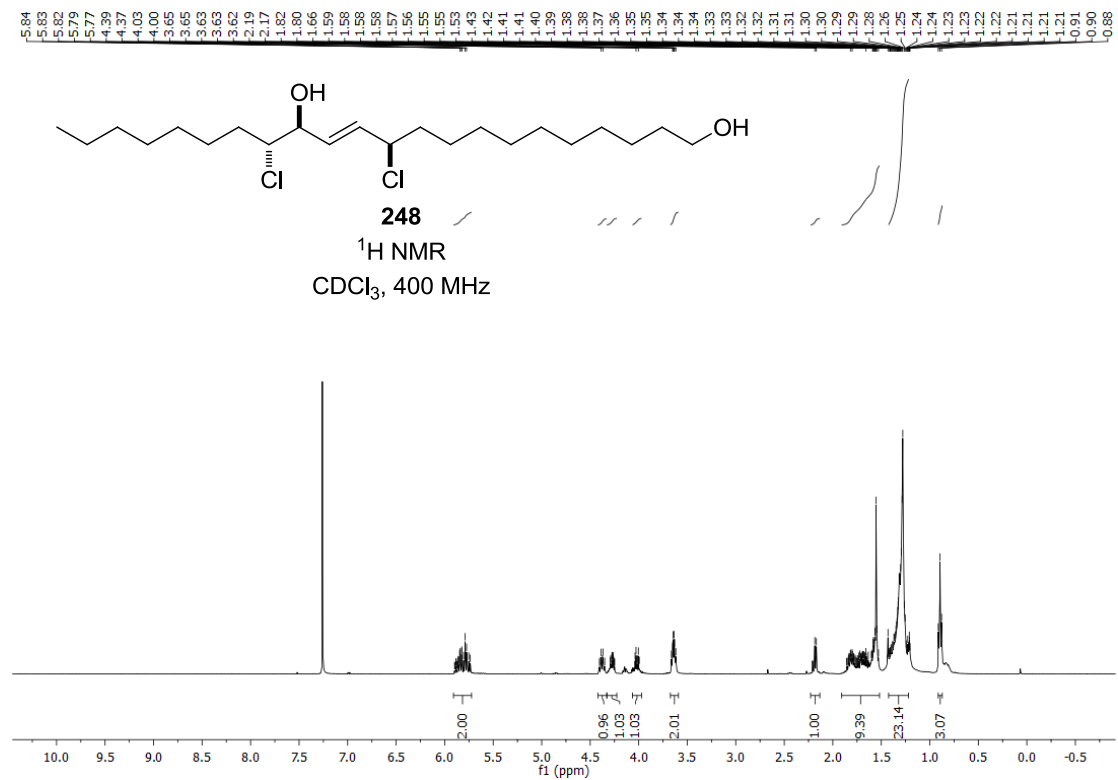


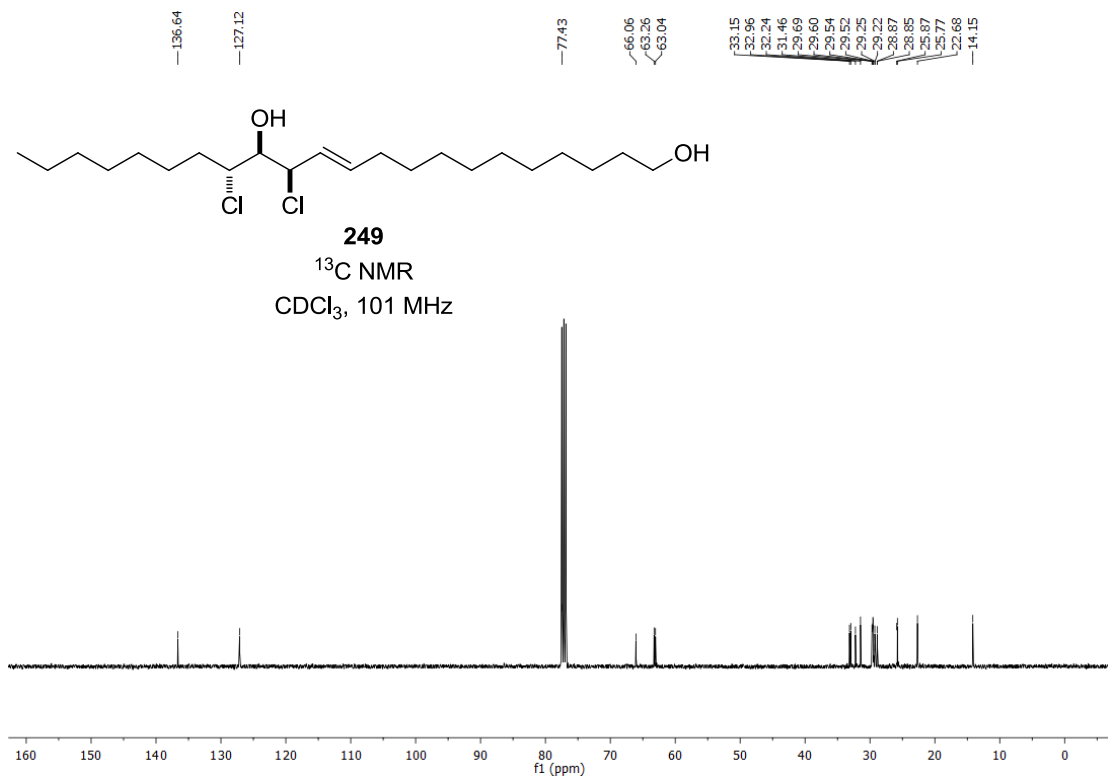
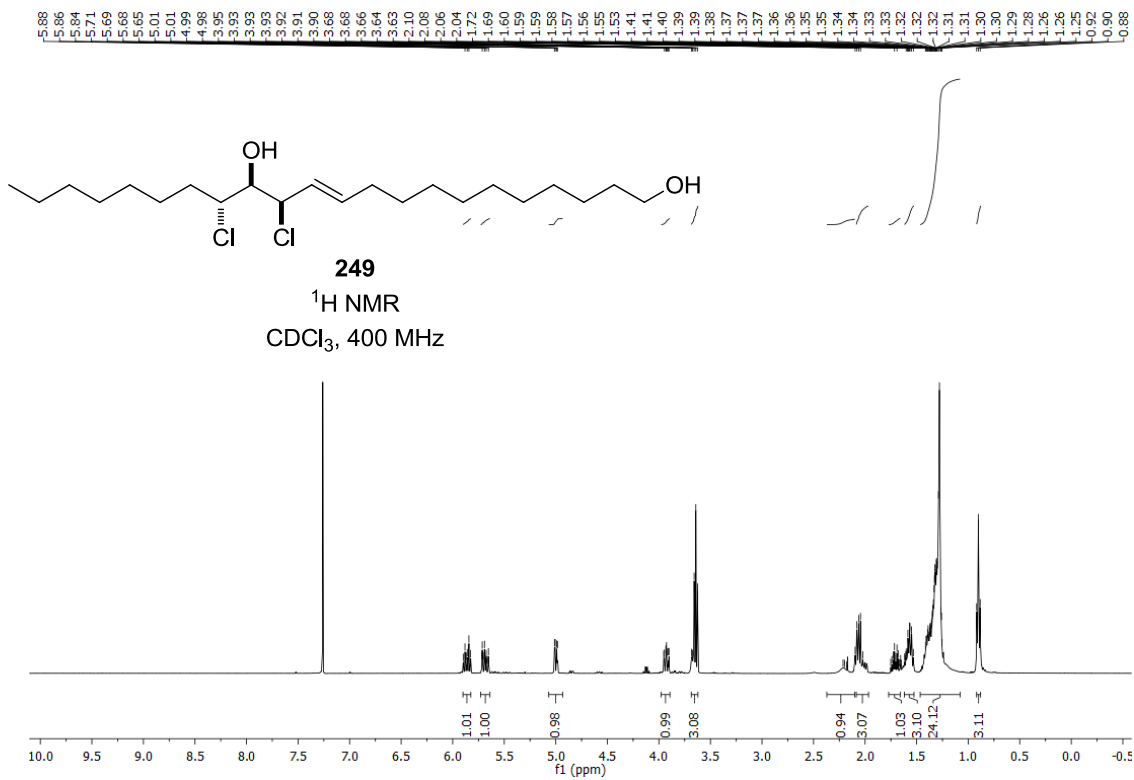


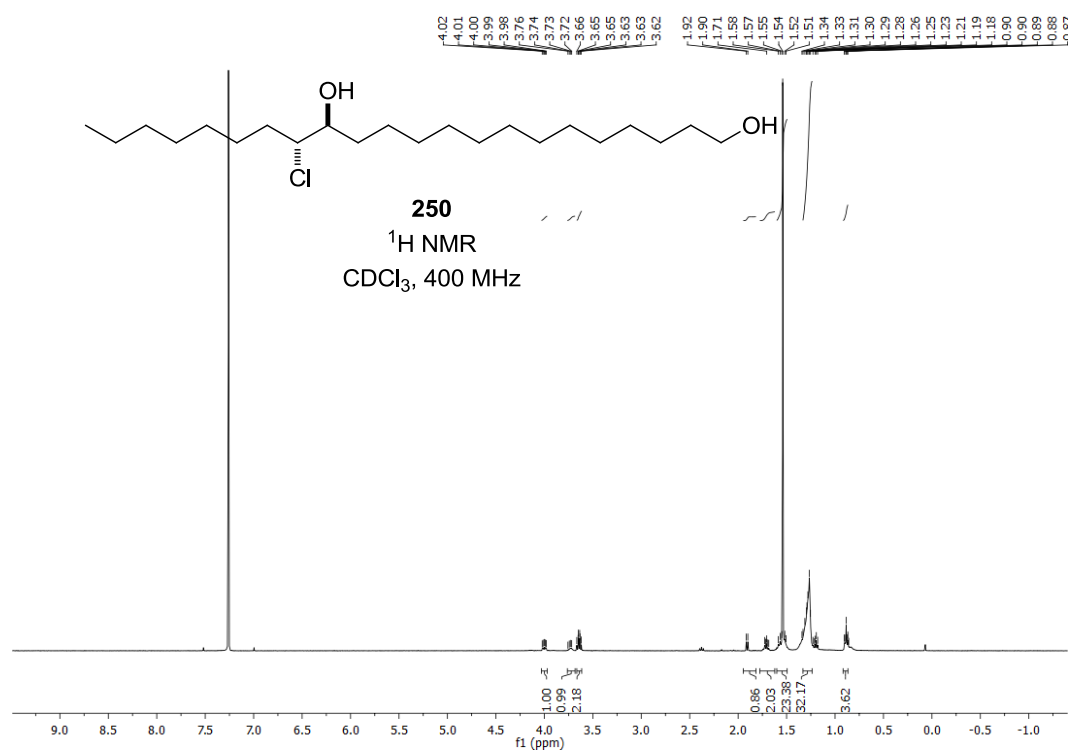


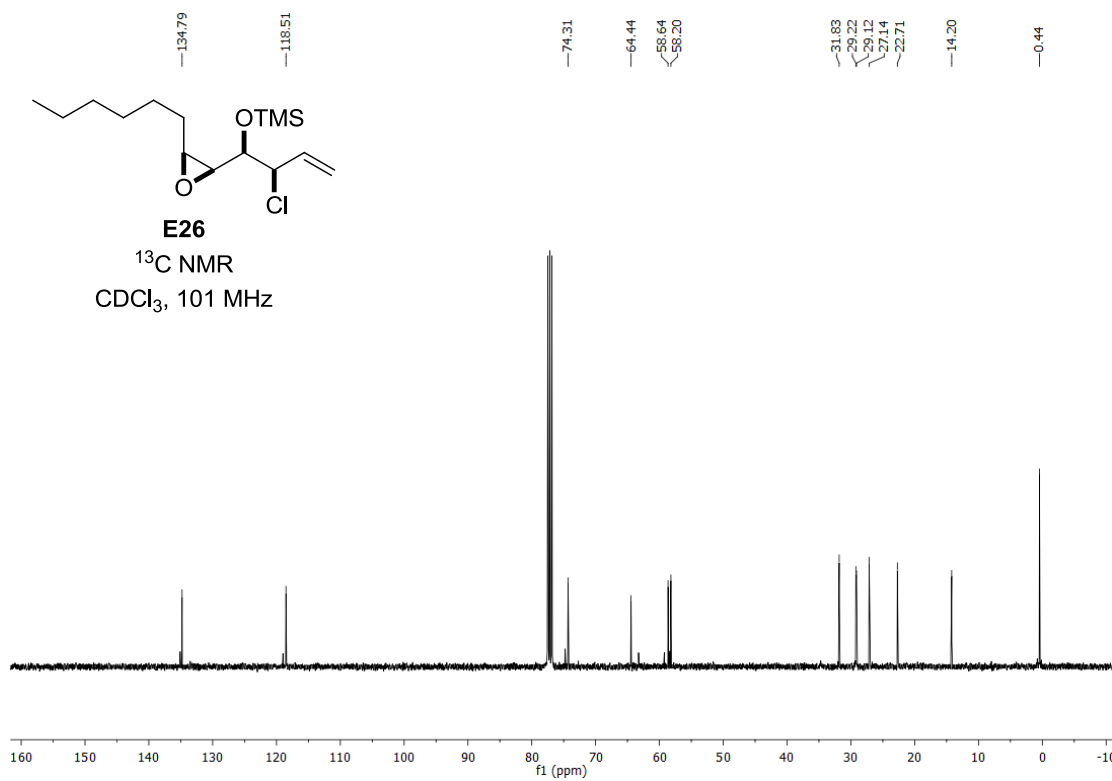
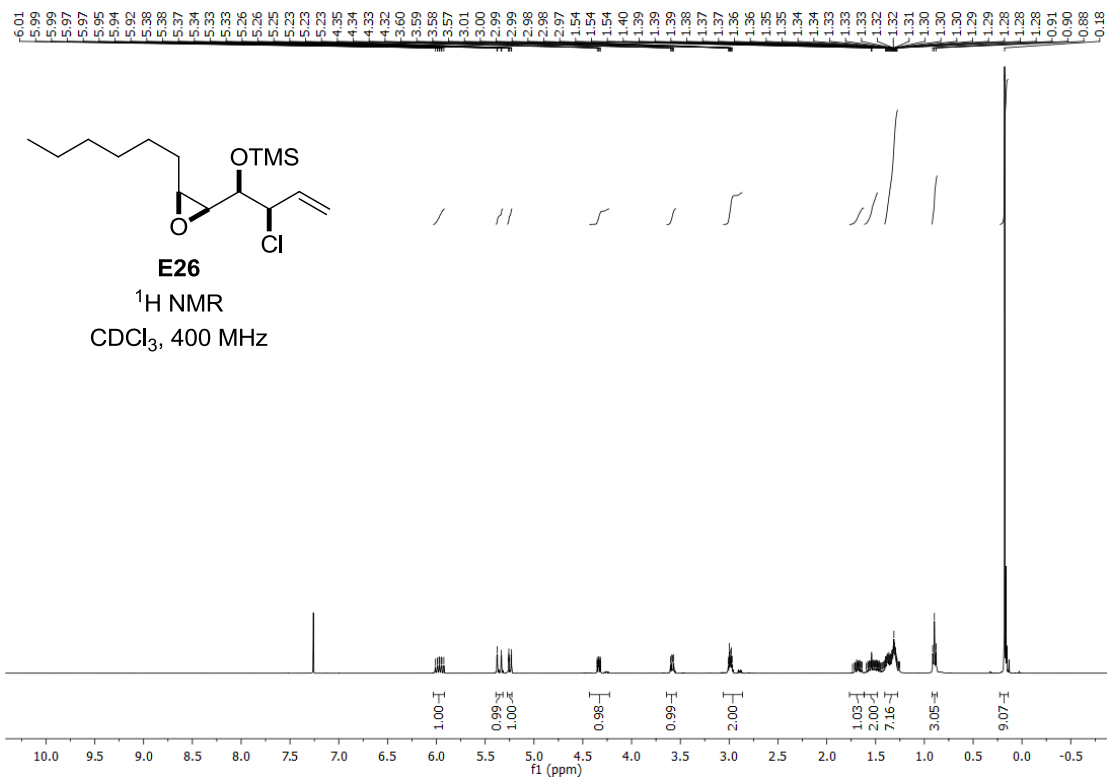




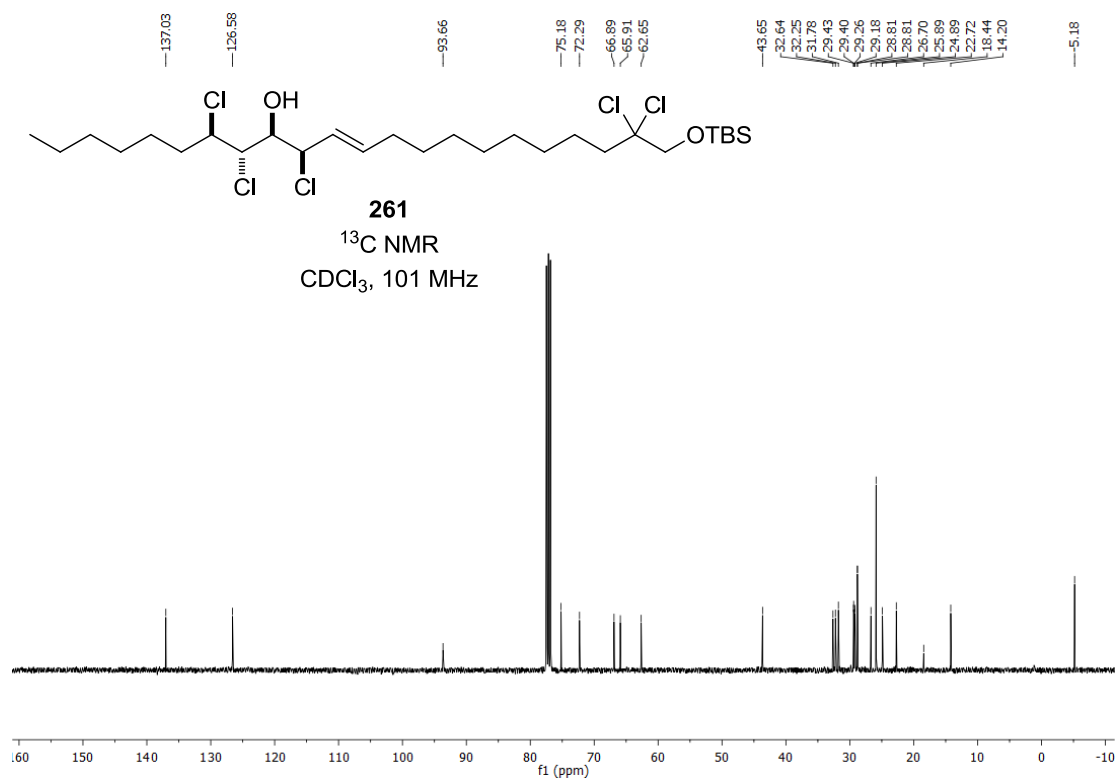
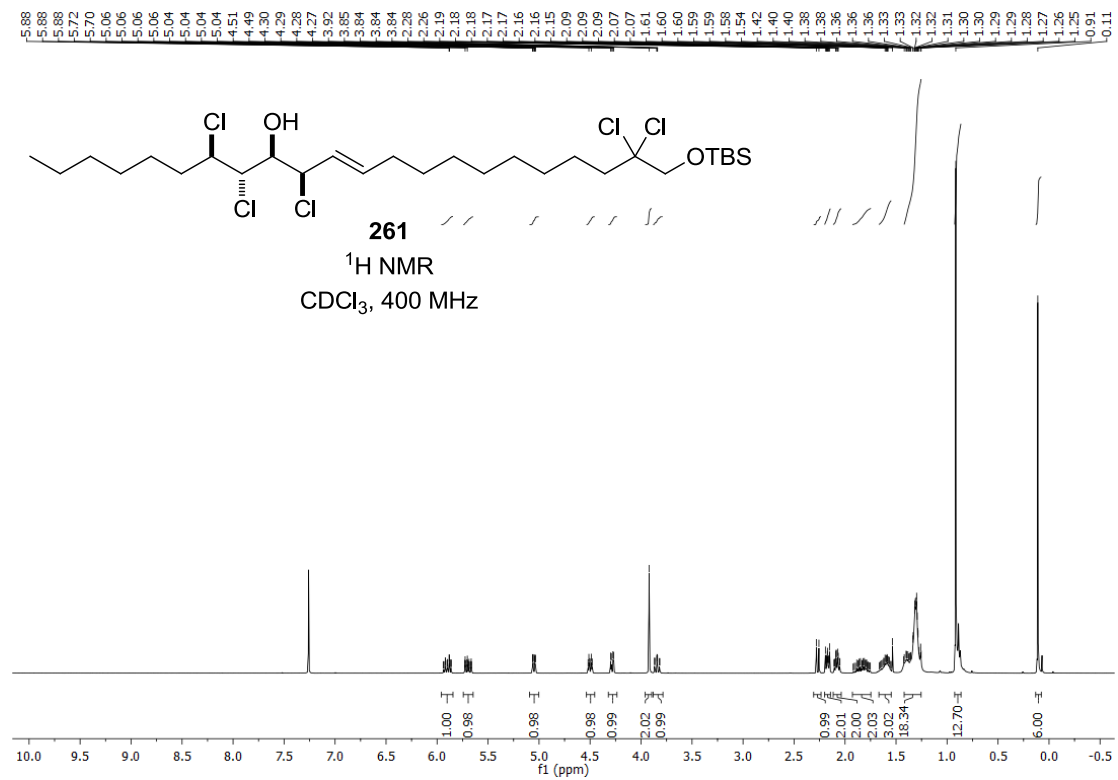


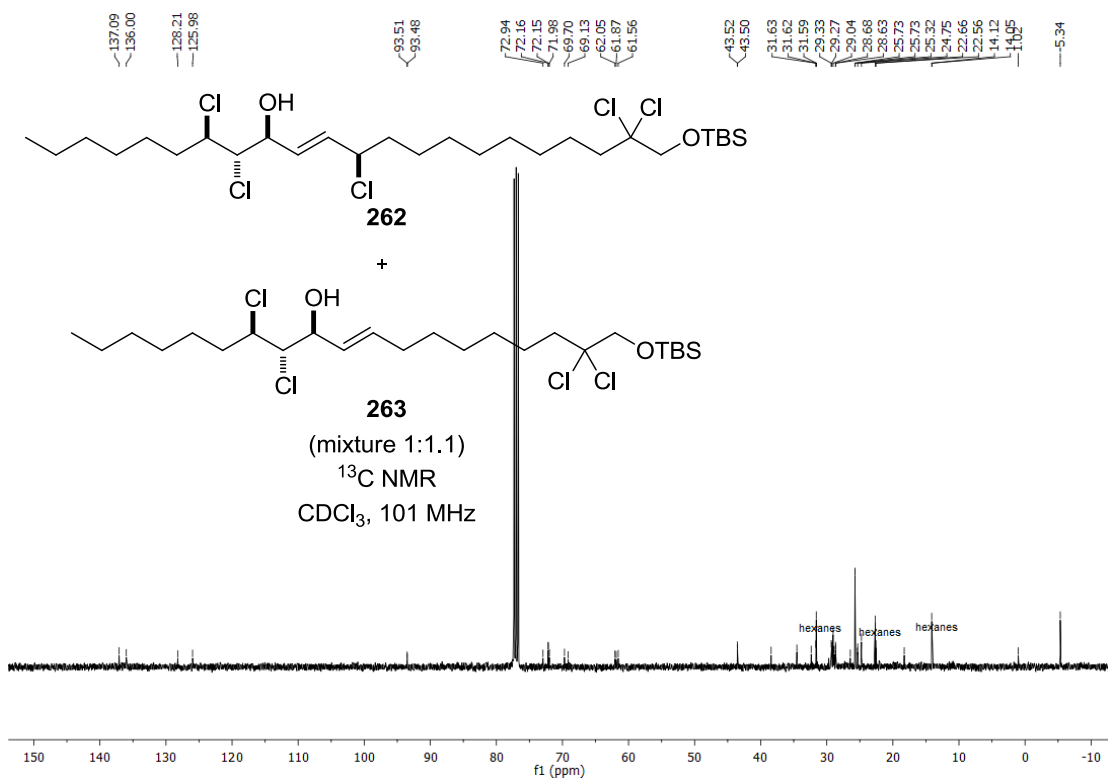
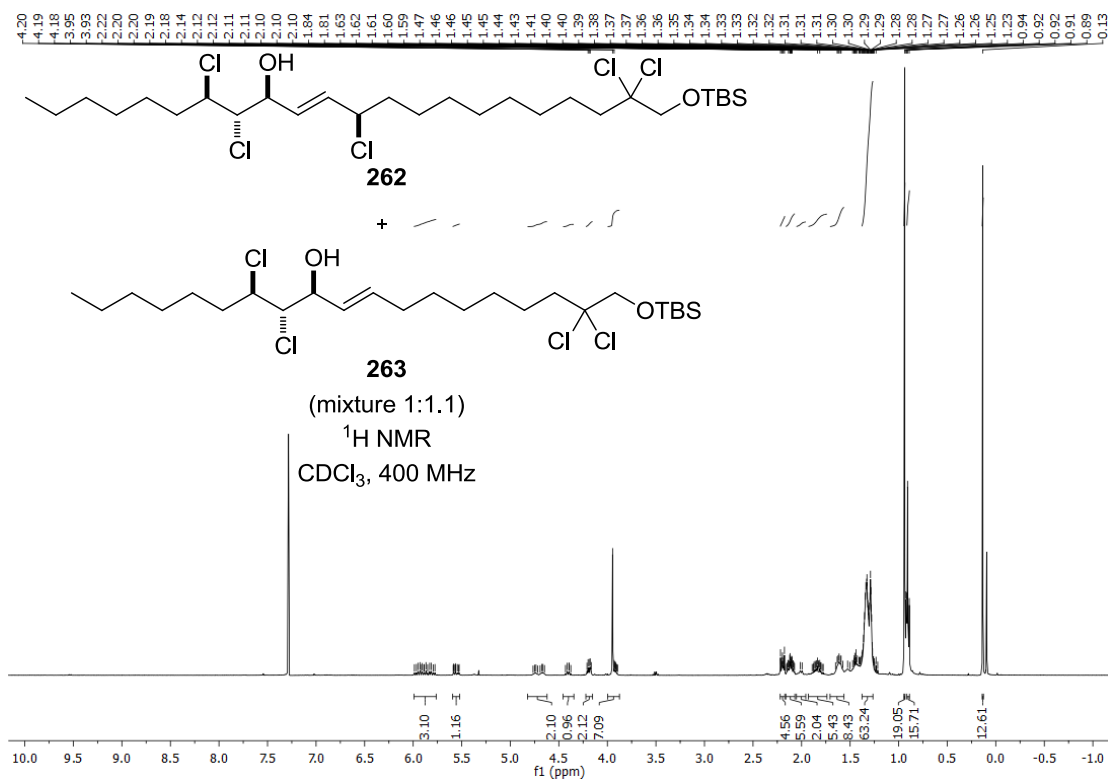






Appendix





Curriculum Vitae

born April 11th, 1989 in Erfurt, Germany

Education:

- 01/2014 – present *Doctor of Sciences ETH* in organic chemistry
ETH Zurich, Switzerland
Thesis: “Investigating the Chemistry and Biology of Danicalipin A and its Analogs”
Supervisor: Prof. Dr. Erick M. Carreira
- 09/2012 – 12/2013 *Master of Sciences ETH in Chemistry*
ETH Zurich, Switzerland
Thesis at Harvard University, Cambridge, MA, USA: “Employing Stannylenes as Ligands in Transition Metal Catalysis – Towards Olefin Hydroalkoxylation and Polymerization”
Supervisor: Prof. Dr. Tobias Ritter
- 09/2009 – 09/2012 *Bachelor of Sciences ETH in Chemistry*
ETH Zurich, Switzerland
- 09/1999 – 07/2008 *Abitur*
Kepler Gymnasium Ulm, Germany

Teaching Experience:

- 01/2014 – present Supervision of four undergraduate students during their Master thesis, Bachelor thesis, or research projects
- 07/2016 – 02/2017 Head teaching assistant for the undergraduate course “*Organic Chemistry III: Introduction to Asymmetric Synthesis*”
- 09/2014 – 12/2014 Teaching assistant of a laboratory course in organic synthesis for undergraduate students
- 09/2011 – 02/2016 Teaching assistant for five different undergraduate chemistry courses

Fellowship:

Student Fellowship from the Swiss-American Society for the Master’s thesis

